Towards a sustainable synthesis of aromatic isocyanates : by the palladium diphosphane catalyzed reduction of nitrobenzene; a first step

Mooibroek, T.J.

Towards a sustainable synthesis of aromatic isocyanates

by the palladium diphosphane catalyzed reduction of nitrobenzene; a first step

PROEFSCHRIFT

Ter verkrijging van
de graad van Doctor aan de Universiteit Leiden,
op gezag van Rector Magnificus Prof. Mr. P. F. van der Heijden,
volgens besluit van het College voor Promoties
te verdedigen op donderdag 22 december 2011
klokke 13.45 uur

door

Tiddo Jonathan Mooibroek
Geboren te Delft
In 1982

Samenstelling promotiecommissie

Promotores	Prof. Dr. E. Drent
	Prof. Dr. E. Bouwman
Overige leden	Prof. Dr. J. Reedijk
	Prof. Dr. C. J. Elsevier (Universiteit van Amsterdam)
	Prof. Dr. P.W.N.M. van Leeuwen (ICIQ, Tarragona, Spain)
	Prof. Dr. F. Ragaini (Università di Milano, Italy)
	Prof. Dr. J. Brouwer

This research was financially supported by the Dutch Organization for Scientific Research NWO (OND 1325300) and the printing of this thesis was made possible by a kind donation from Screening Devices B. V.

Printed by: Wöhrmann Print Service, Zutphen, The Netherlands

The whole is more than the sum of its parts
Aristotle, Metaphysica, 384-322 BC

Seek not to understand that you may believe, but believe that you may understand
Saint Augustine, Civitate Dei, 426 AC

voor mijn ouders,
voor Lauranne

Table of contents

List of abbreviations

AC	autoclave
ax	axial
Azo	azobenzene
Azoxy	azoxybenzene
bipy	bipyridine
BP	Becke Perdew functional
bpap	1,3–bis(1,3,5,7–tetramethyl–4,6,8–trioxa–2–phospha-amantyl)propane
br	broad (in NMR)
Bu	butyl
cal	Calories (1 cal = 4.184 Joule)
COD	1,4-cyclo-octadiene
COSY	correlation spectroscopy
CPCam	*p*-cresyl phenyl carbamate
CSD	Cambridge Structural Database
d	doublet (in NMR)
dba	dibenzylidene acetone
dd	double doublet (in NMR)
DFT	density functional theory
DMAN	1,8–bis(dimethylamino)naphthalene (Proton Sponge®)
DMC	dimethyl carbonate
DME	dimethyl ether
DMM	dimethoxy methane
DMO	dimethyl oxalate
DMPU	*N,N′*–di(3-methylphenyl) urea
DPC	diphenyl carbonate
DPO	*N,N′*–diphenyl oxalimide
dppb	1,4–bis(diphenylphosphanyl)butane
dppbz	1,2–bis(diphenylphosphanyl)benzene
dppe	1,2–bis(diphenylphosphanyl)ethane
dppe	1,2–bis(diphenylphosphanyl)ethane
dppm	bis(diphenylphosphanyl)methane
dppp	1,3–bis(diphenylphosphanyl)propane
DPU	*N,N′*–diphenyl urea
EA	elemental analysis
eq	equatorial
Eq(s).	Equation(s)
ESI	electron spray ionization
Et	ethyl
Exp.	experiment
F_5–L2	1,2–bis(di–pentafluorophenylphosphanyl)ethane
FID	free inductive decay (NMR) or flame ionization detector (GC)
FT	fourier transform
GLC	gas liquid chromatography
h	hour(s)

HOTs	*p*-toluenesulfonic acid
HPLC	high performance liquid chromatography
i (or *iso*)	iso
IR	infra red
J	coupling constant (in Hertz)
L2	1,2–bis(diphenylphosphanyl)ethane
L3	1,3–bis(diphenylphosphanyl)propane
L3X	2,2–dimethyl–1,3–bis(diphenylphosphanyl)propane
L4	1,4–bis(diphenylphosphanyl)butane
L4X	4,5–bis(diphenylphosphanylmethyl)–2,2–dimethyl–1,3–dioxolane
L5Fc	1,1'-bis(diphenylphosphanyl)ferrocene
LD50	lethal dose, whereby 50% of a given population dies
M	metal
m	multiplet (in NMR)
m	*meta*
MBA	*N*-methylene benzenamine
MDA	4,4'–methylene dianiline
MDI	4,4'–methylene diphenyl diisocyanate
Me	methyl
MEG	mono ethylene glycol
Mes	mesitylene
MF	methyl formate
MMFF	Merck molecular force field
MOF	metal organic framework
MPC	methyl phenylcarbamate
MPPU	3–methylphenyl phenylurea
MS	mass spectrometry
napht	naphtalene
NMR	nuclear magnetic resonance
o	*ortho*
OAc	acetate
oEtO-L2	1,2–bis(di–*o*–ethoxyphenylphosphanyl)ethane
oEtO-L3	1,3–bis(di–*o*–ethoxyphenylphosphanyl)propane
oEtO-L3X^2	2,2–diethyl–1,3–bis(di–*o*–ethoxyphenylphosphanyl)propane
oEtO-L4	1,4–bis(di–*o*–ethoxyphenylphosphanyl)butane
oMe-L3	1,3–bis(di–*o*–methylphenylphosphanyl)propane
oMeO-L2	1,2–bis(di–*o*–methoxyphenylphosphanyl)ethane
oMeO-L3	1,3–bis(di–*o*–methoxyphenylphosphanyl)propane
oMeO-L3X	2,2–dimethyl–1,3–bis(di–*o*–methoxyphenylphosphanyl)propane
oMeO-L3X^2	2,2–diethyl–1,3–bis(di–*o*–methoxyphenylphosphanyl)propane
oMeO-L3X^R	5,5–bis(di–*o*–methoxyphenylphosphanylmethyl)–2–cyclohexyl–1,3–dioxane
oMeO-L4	1,4–bis(di–*o*–methoxyphenylphosphanyl)butane
oMeO-L4X	4,5–bis(di–*o*–methoxyphenylphosphanylmethyl)–2,2–dimethyl–1,3–dioxolane
oMeO-L5Fc	1,1'-bis(di–*o*–methoxyphenylphosphanyl)ferrocene
P	pressure in bar
p	*para*

pbq	parabenzoquinone
Ph	phenyl
phen	1,10–phenanthroline
p*K*a	–log (ionisation constant (*K*a))
pMeO-L3	1,3–bis(di–*p*–methoxyphenylphosphanyl)propane
pMeO-L4	1,4–bis(di–*p*–methoxyphenylphosphanyl)butane
PPA	phenylphosphonic acid
ppm	parts per million
Pr	propyl
rpm	revolutions per minute
s	singlet (in NMR)
Sym.	simulation
t	triplet (in NMR)
TDI	2,4–toluene diisocyanate
tert	*tertiary*
TFE	2,2,2–trifluoroethanol
TLV	threshold limit value (in mg/kg)
TMBA	2,4,6–trimethylbenzoic acid
tmof	Trimethyl orthoformate
TMS	tetramethylsilane
TOF	turn over frequency (moles substrate / moles catalyst × unit of time)
TON	turn over number (moles substrate / moles catalyst)
TPB	*N*,*N*′,*N*″–triphenylbiurea
UHV	ultra high vacuum
UV	ultra violet
ΔH_f°	heat of formation

Chapter 1

General Introduction

Abstract. In this chapter the chemistry for the synthesis of aromatic isocyanates is reviewed and discussed. First, the industrially applied route to the polymer precursors MDI and TDI is discussed and the drawbacks are emphasized. Several alternative routes to aromatic isocyanates are considered with an emphasis on catalytic alternatives. The prior art in one of these routes, namely the Pd-catalyzed reductive carbonylation of nitro aromatic compounds, is reviewed and some mechanistic proposals are discussed. Finally, a description of the aim of the research and the contents of this thesis is given.

1.1. The industrial synthesis of aromatic isocyanates

1.1.1. Isocyanates, carbamates and ureas

Aromatic isocyanates, carbamates and ureas are related compounds (Scheme 1.1). Carbamates can be considered as 1:1 adducts of isocyanates and alcohols, and thermal cracking of the carbamate results in the related isocyanate and alcohol. Analogously, thermal cracking of a urea yields the related isocyanate and amine. These molecules find their application both in organic synthesis and in industry.[1] Initially, the discovery of isocyanates in 1849 by Wurtz,[2] did not lead to an application, although afterwards this class of compounds was thoroughly studied by the academic community. The discovery of polyurethanes by Bayer in 1937, triggered the interest in isocyanates and eventually resulted in the application of mono- and diisocyanates in a variety of polyurethane (flame-retarding) foams,[3-8] (bio-degradable) plastics,[9-12] pesticides,[13-17] adhesives,[18-20] and coatings.[14, 21-25] Carbamates and ureas are intermediates for the preparation of pesticides and fertilizers.[26, 27] The market for these molecules is vast (several million tons/year) and increasing,[28] since economies like Japan, China and India are expanding at an incredible rate.[29-32] Commercially, isocyanates are the most important class of these compounds, and in particular toluenediisocyanate (TDI) and 4,4'-diphenylmethanediisocyanate (MDI) are of great interest to industry.[33, 34]

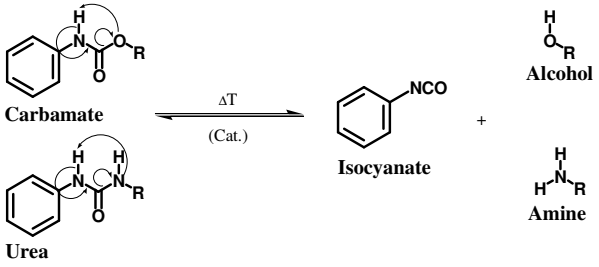

Scheme 1.1. Isocyanates, carbamates and ureas are related compounds.

1.1.2. Traditional route towards isocyanates

The traditional (and currently used) route to make TDI and MDI, as well as a variety of other isocyanates is often referred to as the 'phosgene route' (Scheme 1.2). This route roughly involves three relatively simple organic reactions, wherein a nitro-substituted substrate is first reduced to the corresponding amine

with a Ni or Pd catalyst in 98-99% yield.[35] The amine is then treated with phosgene to yield the intermediate carbamoyl chloride, which is subsequently dehydrochlorinated almost quantitatively above 50 °C, into the corresponding isocyanate. In order to minimize the formation of ureas in the second step, this process is carried out at high dilution (20%) and with an excess of phosgene (50-200%).

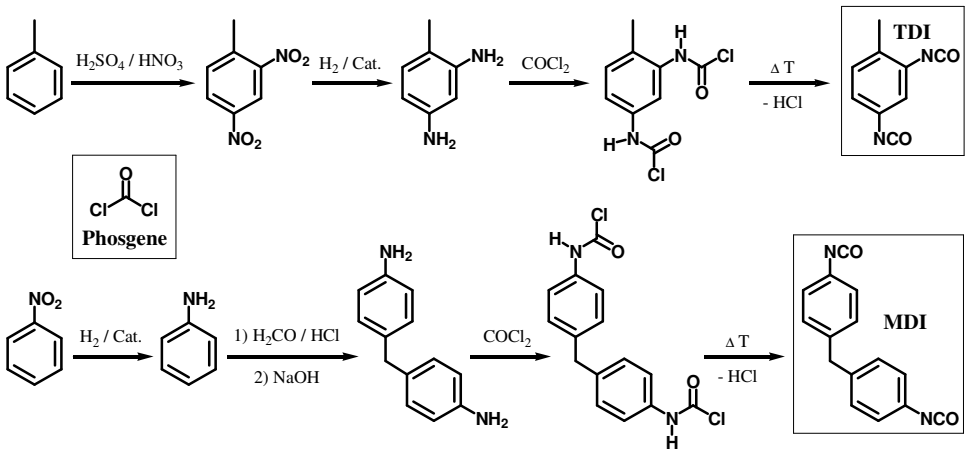

Scheme 1.2. Traditional synthetic pathway to toluenediisocyanate (TDI) and 4,4'-diphenylmethane-diisosyanate (MDI); the 'phosgene route'.

1.1.3. Major drawbacks of the phosgene route

Despite the high yields and good selectivity obtained with the phosgene route, there are essentially four major drawbacks. The first and most pronounced is the extreme toxicity (see Table 1.1) and flammability of phosgene and isocyanates, which make these chemicals extremely difficult to handle in bulk quantities and give them a high ranking in government lists of pollutants and eagerly forbidden chemicals. Phosgene was used as a chemical weapon in World War I, and around 36,600 tonnes of the gas were manufactured during this war, out of a total of 190,000 tonnes for all chemical weapons (19%), making it second only to chlorine gas (93,800 tonnes) in the quantity manufactured.[36] In total around 1.3 million people were injured and over 90,000 killed by the use of poisonous gases,[37] of which phosgene is acknowledged to have claimed most deaths.[38] A tragic methylisocyanate leaking accident in the night of 2nd/3rd December 1984 in a Union Carbide plant in Bhopal, India, clearly stressed the drawback of working with toxic chemicals on an industrial scale. Thousands of people were gassed to

death and more than 150,000 people were left severely disabled - of whom 22,000 have since died of their injuries - in a disaster now widely acknowledged as the world's worst-ever industrial disaster. More than two decades after the disaster, at least 50,000 people in Bhopal are too ill to work for their living, and the drinking water of at least 20,000 people is still contaminated.[39, 40]

The second major drawback in this reaction is that per mole of nitro group, two moles of corrosive hydrochloric acid are formed, rendering the medium very aggressive with time, thus allowing other side reactions to occur and to result in reactor degradation. The high dilution in which the reaction is carried out is the third limiting factor, since ideally concentrations should be high and volumes as low as possible, thus avoiding recycling and concentration costs. The final drawback is the unavoidable inclusion of chloride-containing compounds in the final product which can be detrimental for the further processing of the isocyanate.[3, 41]

Table 1.1. LD50 data (Lethal dose (mg/kg) at which 50% of a population dies) of phosgene, some isocyanates and some carbamates

Chemical	**LD_{50}**
Phosgene	1.8 (mice)[42] 1.4 (rats)[42] 1.3 (guinea pigs)[42] 1.0 (rabbits)[42, 43] 0.1 (TLV,[a] humans)[44]
Carbon Monoxide	3000 (mice)[45] 2000 (rats)[45] 6500 (guinea pigs)[45] 50 (TLV,[a] humans)[44]
MDI	5.8 (rats)[2]
TDI	> 31.6 (rats)[2]
Methylisocyanate	71 (rats)[2]
Phenyl isocyanate	940 (rats)[2]
Propham (iso-propyl N-phenylcarbamate)	9000 (rats)[2]
Chloropropham (iso-propyl N-(3-chlorophenyl)carbamate)	5000 – 7000 (rats)[2]

[a] Threshold Limited Value in mg/kg.

1.1.4. Requirements for an alternative isocyanate synthesis

Despite the disadvantages, the phosgene route is still the most lucrative and thus industrially applied procedure to date. In order to replace this procedure, a number of requirements can be thought of in the ideal scenario. First of all, readily accessible chemicals (cheap, large quantity) should be used and second, they should be as harmless as possible. A high overall yield, purity, and selectivity (atom economy) are also obvious requirements. What is more, a reaction

temperature of about 100 °C will be ideal as heat energy is a major waste product in many industrial processes.[46-50] The absence of over- and/or under-pressures and an easy product separation (from the solvent, starting materials and side products) is also logically favored. Finally, a one step (or one pot) synthetic procedure will be the route par excellence.

Most of these requirements could in theory be met by an efficient catalytic system, wherein additional requirements would be: the use of a cheap, fast (a Turn Over Frequency (TOF) in the order of 10^4 mol/mol.h^{-1} or higher), robust (a Turn Over Number (TON) in the order of 10^6 mol/mol or above)[51] and easily recycled catalyst. Naturally, the required TON and TOF strongly depend on the metal involved, since for instance Pd is about 5000 times more expensive than Cu.[52]

1.2. Alternative synthesis of isocyanates

1.2.1. Various organic synthetic pathways to isocyanates

Alternative ways to prepare isocyanates have been studied thoroughly for decades. Innumerable reports such as patents, reviews,[53, 54] and books[55, 56] were published already some decades ago, and more than 22 methods have been reported for the preparation of isocyanates by organic reactions. Although abundant in number, none of these methods is a serious alternative for the current phosgene route, as either stoichiometric quantities of salt or acid are produced, or the starting products are too intricate molecules (i.e. expensive) for this specific purpose. Furthermore, most of the reported pathways are inaccessible when aiming for isocyanates like MDI or TDI, and not all reactions can be conducted in high yields.

1.2.2. Various catalytic synthetic pathways to isocyanates

A promising approach is to synthesize TDI or DMI catalytically, by converting a nitro or amine compound into the corresponding isocyanate (Scheme 1.3). Considerable efforts have been made in studying the oxidative carbonylation[43, 57-63] (Scheme 1.3f) and carboalkoxylation[3, 4, 64-66] (Scheme 1.3g) of aniline, and especially the oxidative carbonylation has been studied with various catalytic systems.[67-85] However, aniline must first be synthesized by hydrogenation of nitrobenzene (Scheme 1.3e), thus the most attractive strategy involves the reaction

of a nitro compound with carbon monoxide, to yield the isocyanate directly. This conversion is thermodynamically favored ($\Delta H_f^\circ \approx$ -128.8 kcal/mol for nitrobenzene to phenyl isocyanate),[86, 87] but only proceeds in the presence of a metal catalyst.

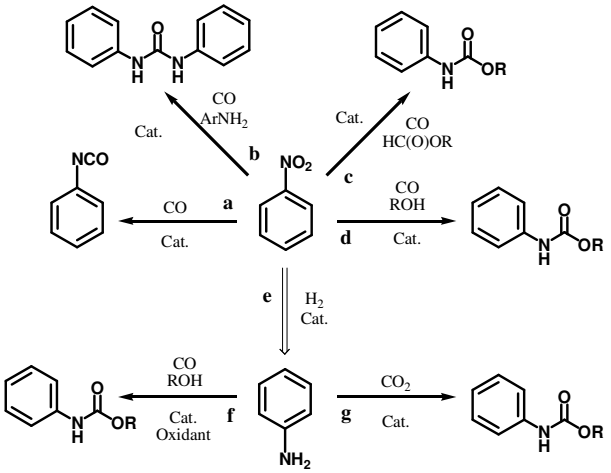

Scheme 1.3. Catalytic pathways toward isocyanates, starting from nitrobenzene (a-d) or aniline (f-g) which is made from nitrobenzene (e).

1.2.3. The reductive carbonylation of nitro compounds

There are two related pathways in which the reductive carbonylation of nitro compounds can lead to isocyanates, which are commonly referred to as the direct and the indirect method, as depicted in Scheme 1.4(a-b) respectively. In the direct method, a catalyst activates the nitro group and carbon monoxide to form the isocyanate with liberation of carbon dioxide. In the indirect method, the isocyanate is trapped by an additional reagent (alcohol or amine, which can be used as solvent) to form the related carbamate or urea. Thermal cracking then leads to the isocyanate and alcohol or amine, which can thus be recycled.

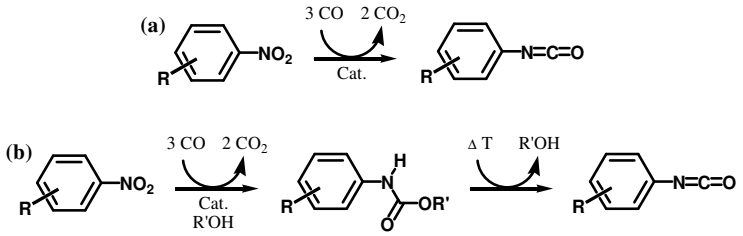

Scheme 1.4. (a) the direct, and (b) the indirect method for the reductive carbonylation of nitro compounds.

Initially, a variety of elements were investigated as catalyst for the conversion of nitroaromatic compounds to isocyanates, such as sulfur, tellurium and especially selenium, which was reported to be very efficient.[88] However, these derivatives seem to be far too toxic to be applied in industry,[89-91] and it appears difficult to separate the catalyst from the final product.[92, 93] Alternatively, group 8 – 10 metal compounds can be applied, and in 1967, Hardly and Bennett were the first to report the generation of isocyanates from nitro compounds using rhodium, palladium or other noble metal salts as catalyst with a Lewis acid promoter.[94]

Regarding the direct carbonylation of mono- or dinitroaromatic compounds, it has been reported that heterogeneous catalyst precursors such as Pd/C or Rh/C,[95] as well as inorganic polymeric precursors like $PdCl_2$ and $RhCl_3$ give poor results. Although addition of a Lewis acid promoter (such as $MoCl_5$, VCl_4, $FeCl_3$, etc.) strongly increases both the rate and selectivity of the reaction towards isocyanates,[96-101] the catalyst is quite rapidly deactivated, resulting in poor TONs ranging from 5[102] to a maximum of about 150,[103] the selectivity being 52 and 15% respectively. The addition of an aromatic nitrogen base such as pyridine is known to have a positive effect with most metal chlorides.[68, 92, 99, 101, 104-118] Polymetallic carbonyl precursors like $Ru_3(CO)_{12}$ or $[HRu_3(CO)_{12}]^-$ were reported to be virtually inactive.[97, 118, 119] The most active catalytic systems to date however, involve Pd-based catalysts. In one of these ([Pd]/phen/H^+), a chelating diimine ligand like phenanthroline is bound to a homogeneous Pd^{II} precursor and the reaction is co-catalyzed by non-coordinating acids such as 2,4,6-trimethylbenzoic acid.[120]

It must be pointed out, however, that these systems work better for the indirect carbonylations, and (consequently) in the last decades, research has been focused almost exclusively on the indirect carbamate/isocyanate route. One additional advantage is the reduced toxicity of carbamates with respect to isocyanates (Table 1.1), which makes them more viable candidates from a governmental and environmental point of view. Moreover, part of the carbamates produced could be used for other purposes than isocyanate production. For the indirect reductive carbonylation, very similar methods could be employed: solid supported metals in the presence of ligands,[121-125] MCl_n/ligand/Lewis acid (M = Pd, Ru, n = 2,3),[13, 124] or the more active polynuclear precursors like carbonyl clusters of Rh or

Ru[126] in the presence of a co-catalyst like NEt_4Cl.[119, 127] Especially chelating ligands were found to improve the catalytic activity, and both N-[26, 92, 120, 121, 127-165] and P-[166-172] donor ligands have been found to improve this catalytic activity. Since these homogeneous systems comprise the most potential of all, they will be discussed in more detail.

1.3. The indirect reductive carbonylation of nitro compounds using Pd^{II}–catalysts stabilized by P or N donor ligands

1.3.1. Phosphorus and nitrogen as donor atoms

Both phosphorus and nitrogen ligands with the general formula YR_3 (Y = P, N) (called phosphanes and amines respectively) can be described as sp^3 hybrids in a (close to) tetrahedral geometry, having a lone pair on the central atom, capable of donating its electron density to an empty (transition) metal d-orbital. Amines are more electronegative than their phosphane analogues, so one would expect them to bind stronger to a metal. However, unlike amines, phosphanes can act as a π acid with their σ^* orbitals, so they can be involved in π-backbonding (provided that the metal ion has available d-electrons), rendering the overall bond strength larger than would be expected intuitively (Figure 1.1). So, the overall metal-phosphate bond strength is determined by an interplay of σ donation and π backbonding, the first having an increasing contribution when electropositive / donating substituents are employed, the latter when electronegative / withdrawing substituents are used.[51]

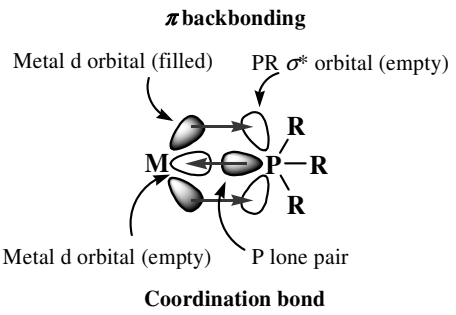

Figure 1.1. Schematic representation of the two factors governing the bond strength in a M-P bond: the donation of a lone pair (regular coordination bond), and the π backbonding of metal d electrons into PR σ^* orbitals. Shading represents orbital occupation.

1.3.2. Mono- and bidentate phosphane ligands

Due to their π backbonding capability, phosphanes (PR_3) are a very important class of ligands, as they can stabilize redox metal catalysts in high and low oxidation states. Especially zero-valent d^{10}-metals such as nickel and palladium

are known to bind strongly with phosphane ligands and not at all with amines. In addition, phosphanes constitute one of the few series of ligands in which both electronic and steric properties can be altered systematically. A useful classification of the electronic (υ_{CO})[173] and steric (θ)[174] nature for a series of monodentate phosphane ligands was described by Tolman, and selected examples are shown in Table 1.2.

The electronic parameter was defined using the carbonyl stretching frequency (υ_{CO} in cm^{-1}) of a 0.05 M solution of $Ni(CO)_3(PR_3)$ in CH_2Cl_2.[173] When R in PR_3 is electron donating, the electron density on nickel is increased, and some of the electron density is donated to the COs by back-donation. As a result, the υ_{CO} is lowered. Likewise, the use of electron withdrawing R-groups results in a higher υ_{CO}. Tolman defined the steric parameter of a monodentate phoshane ligand as the so-called cone angle (θ in º). This angle was obtained from space-filling models of a $M(PR_3)$ group with M–P distances fixed at 2.28 Å (Figure 1.2). The angle of the cone that just fits all atoms of the ligand is the cone angle (the metal is at the apex of the cone).

Table 1.2. Electronic and steric properties of monodentate phosphane ligands according to Tolman. [173, 174]

Ligand	ν_{CO} (cm^{-1})	$\Delta\nu$	θ (º)
P(*t*-Bu)$_3$	2056.1	0.0	182
P(*o*-MeOPh)$_3$	2058.3	2.7	-
PMe_3	2064.1	3.7	118
P(*p*-MeOPh)$_3$	2066.1	10.2	-
PPh_3	2068.9	12.9	145
$P(OEt)_3$	2076.6	20.4	109
PF_3	2110.8	54.6	104

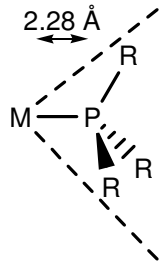

Figure 1.2. Schematic representation of the cone angle as defined by Tolman.[174]

A possible drawback of monodentate phosphane ligands is the lack of control over cis coordination, which is of the utmost importance in some catalytic reactions.[51, 175] This can be overcome by using a backbone spacer between two phosphorus donors thus ensuring a cis-coordination. In addition, fine-tuning the length of the backbone will enforce a specific geometry to the complex, as reflected in the P–M–P angle. This geometric parameter can be seen as a compromise between the metal preferred angle (for example 90º in a square planar Pd^{II} complex) and the ligand preferred angle[176, 177] (or bite-angle, β). Thus,

for a series of $Pd^{II}(ligand)Cl_2$ complexes with cis-coordinated bis(diphenylphosphane) ligands, the P–Pd–P angle increases from 72.7º to 85.8º to 90.6º for using a methylene (dppm), ethylene (dppe), or propylene backbone (dppp).[178] When the backbone is further extended to a butylene spacer in $Pd^{II}(dppb)(C_6F_5)_2$, the P-Pd-P angle is 96.8º.[179]

The effect of the P-M-P angle is both steric (size of the catalyst pocket) and electronic (M-P orbital overlap) in nature. In both cases, the effect is the stabilization or destabilization of intermediates and transition states in a catalytic cycle. The effect of ligand bite-angles on catalytic reactions such as the hydroformylation, CO-ethene copolymerization, allylation and C-C bond forming reactions is widely acknowledged, as reflected in several (review) articles on the topic.[175, 176, 180-183]

1.3.3. Catalytic systems based on phosphorus ligands

There are basically five research groups that have reported on the use of phosphorus ligands in the catalytic reduction of nitrobenzene, both in the patent and in the academic literature. Table 1.3 provides an overview of the ligands and metals reported, as well as their highest TOF (mol/mol.h^{-1}) and carbamate or urea selectivity (%) achieved. In 1982, Drent and van Leeuwen[92] patented the use of divalent Pd salts in combination with some mono- and bidentate phosphorus ligands (as well as some N-donating ligands, see next section) in the presence or absence of an acid as co-catalyst in the indirect carbonylation of nitro compounds to the corresponding carbamates or ureas. Relatively good results were obtained: TOFs up to 400 mol/mol.h^{-1} and selectivities for carbamate or urea of up to 95% were reported.

Thereafter, in 1986, Grate, Hamm, and Valentine[184] first patented their own catalytic systems with similar monodentate ligands, but with Ru^0 compounds in stead of Pd^{II} salts and only employing an amine as co-reagent, thus exclusively producing urea. Only moderate results were obtained: TOFs up to 30 mol/mol.h^{-1} and the selectivity for urea of less than 80%. Application of bidentate ligands and an alcohol improved performance, ensuing TOFs of up to 72 mol/mol.h^{-1} and carbamate selectivities of about 88%.[167, 185] In their third patent that year, they claimed ethanol to be a better reagent than methanol (obtaining a TOF of 41 mol/mol.h^{-1} and a carbamate selectivity of 74% with ethanol and none with

methanol). Finally, they extended their phosphane/Ru^0 library, claiming them in a 1987 WO patent,[186] only improving the TOF to about 72 mol/mol.h^{-1}. None of these patents reported on the addition of a Brønsted acid as co-catalyst, but Lewis acids were found to quench the reactivity.

Table 1.3. Schematic representation of (a) monodentate and (b) bidentate, or chelating phosphorus ligands that were used by several groups in the past decades, together with the highest turn over frequencies (TOF's) in h^{-1} and the highest selectivity in carbamate or urea in percentages (depending whether the indirect method involved an alcohol or amine respectively). Please note that these values are not necessarily derived from identical experiments. See text for comments and references.

(a) **(b)**

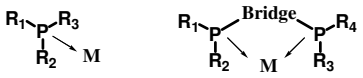

Ligands used	Reported by:	Max. TOF (h^{-1})	Max. carbamate or urea selectivity (%)
R_{1-4} = Me, CF_3, Et, Pr, Bu, Ph, C_6F_5, Ph(Me) **Bridge =** $(CH_2)_n$, C_2H_2, C_6H_4 **M =** Pd(II)	Drent *et al.* 1982	400	95
R_{1-4} = Me, Pr, Ph, o-Ph(Cl), p-Ph(OMe), C_6H_{11} **Bridge =** C_2H_4, C_3H_6, C_6H_4 **M =** Ru(0)	Grate *et al.* 1986/1987	70	88
R_{1-4} = Ph **Bridge =** CH_2, C_2H_4, C_3H_6, **M =** Ru(0)	Cenini and Ragaini *et al.* 1988	70	67
R_{1-4} = Me, Ph, o-Ph(Me), Bz, C_6H_{11} (only b) **Bridge =** CH_2, C_2H_4 **M =** Ru(0)	Gladfelter *et al.* 1991-1997	10	60
R_{1-4} = Ph (only b) **Bridge =**CH_2, C_2H_4, C_3H_6, C_4H_8, C_6H_4, Napht **M =** Pd(II)	Wehman *et al.* 1995	70	78
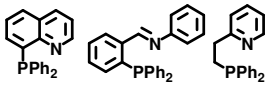 + Pd(II)	Wehman *et al.* 1995	20	66

After these reports, the academic world ensued these initial findings, and especially Gladfelter *et al*. spent a considerable amount of research on the Ru/P catalytic system in the 1990s. [168, 169, 171, 172, 187-192] Initially they reported some catalytic data concerning the Ru_2(bis(dimethylphosphanyl)methane)$_2(CO)_5$ dimer as catalyst (TOF of 7 mol/mol.h^{-1}, carbamate selectivity of 60%),[187] in their later studies they focused solely on the mechanistic aspects of the alcohol-assisted indirect carbonylation of nitro compounds. These studies mainly involved the

complex Ru(1,2-bis(diphenylphosphanyl)ethane)$(CO)_3$ as catalyst precursor,[168, 169, 171, 172, 188-190, 192] but other ligands/catalyst systems were also investigated.[168, 187, 191]

In 1988, Cenini and Ragaini *et al*. also reported on the use of almost identical Ru^0/P catalytic systems, resulting in similar TOFs and selectivities.[193] In the same paper, they also reported on the use of chelating N-donor ligands with which they continued their work (see section 1.3.3).

Notably, in 1995 Wehman *et al*. [194] reported on the use of some bidentate phosphane / Pd^{II} catalysts as well as on some bidentate P and N / Pd^{II} catalysts.[194, 195] She found that the use of bis(diphenylphosphanyl) ligands with a flexible bridge gave more efficient catalyst systems than their rigid counterparts, resulting in a TOF of about 68 mol/mol.h^{-1} and a carbamate selectivity of about 78% for the propylene-bridged ligand. The catalytic systems with P/N ligands showed almost no activity (TOF <20 mol/mol.h^{-1}, carbamate selectivity <65%).

1.3.4. Catalytic systems based on nitrogen ligands

The catalytic systems based on ligands with nitrogen-donor atoms have been intensively studied by essentially five groups. In Table 1.4, an overview is presented regarding the ligands and metals used by these groups, as well as the highest TOF (mol/mol.h^{-1}) and carbamate or urea selectivity (%) achieved. Since there are many papers on the topic, dealing with different aspects of the reaction, in this section only the molecular components of the applied catalytic system are mentioned together with their best achievements.

Similar to the research focused on phosphane ligands, the venture was initiated by the pioneering work of Drent and van Leeuwen in their 1982 patent,[92] mentioned earlier. They claimed the use of a variety of bidentate N-donor ligands wherein the amine/imine donors are bridged by different spacers.

Markedly, the use of 2,2'-bipyridine and 1,10-phenanthroline was preferred, the latter of which was found to result in one of the best catalytic systems to date (!), when combined with a strong Brønsted acid such as para-toluene sulfonic acid as co-catalyst (TOF = 1980 mol/mol.h^{-1}, carbamate selectivity = 95%). Five years

later, Drent patented a similar catalytic system,[131, 142] wherein the 1,10-phenanthroline/Pd^{II} was combined with a Lewis acid such as $Cu(PhSO_3)_2$, $Cu(ClO_4)_2$, or $VOSO_4$ as the co-catalyst. The use of $VOSO_4$ was found to result in the most active system of the series tested (TOF = 490 mol/mol.h^{-1}, carbamate selectivity = 88%).

Table 1.4. Schematic representation of (a) bidentate, or chelating, and (b) dipyridine / phenanthroline ligands that were used by several groups in the past decades, together with the highest turn over frequencies (TOFs) in h^{-1} and the highest selectivity in carbamate or urea in percent (depending whether the indirect method involved an alcohol or amine respectively). * Indicates that dinitrotoluene was used as substrate in stead of nitrobenzene. Please note that these values are not necessarily derived from identical experiments. See text for comments and references.

(a) **(b)**

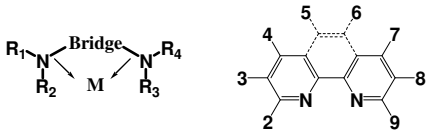

Catalyst systems used:	Reported by:	Max. TOF (h^{-1})	Max. carbamate or urea selectivity (%)
R_{1-4} = Me, Et, t-Bu, Ph **Bridge =** $(CH_2)_n$ n = 1-4 **(b) =** 2,2'-bipyridine and 1,10-phenentroline **M =** Pd(II) **Acid =** Brønsted or Lewis	Drent *et al.* 1982/1987	2000	95
(b) = (4,7-Me_2, 4,7-$(OMe)_2$, 4,7-Ph_2, 3,4,7,8-Me_4) 1,10-phenentroline **M =** Pd(II) or Pd/C(5%) **Acid =** None or Brønsted	Mestroni *et al.* 1984-1987 1999	130 260*	97 82*
(b) =(4,7-Cl_2, Me_2, OMe_2, $(NMe_2)_2$) 1,10-phenantroline, (4,4'-CF_3, Cl, Me, OMe, NMe_2) 2,2'-bipyridine **M =** Pd(II) **Acid =** None or Brønsted	Wehman and van Leeuwen *et al.* 1994-1996	380 180*	92 31*
(b) =(2,9Me_2, 4,7Me_2, 3,4,7,8-Me_4) 1,10-phenantroline, 2,2'-bipyridine **M =** Pd(II) or Pd/C(5%) **Acid =** None or Brønsted	Cenini and Ragaini *et al.* 1988-present	7900 580*	88 78*

From that time on, the academic world showed interest to fundamentally explore these remarkable findings, in order to improve these catalysts, and four groups worked on the subject in the past three decades. The group of Paul (who wrote a review on the topic in 2000)[196] and Osborn only reported on mechanistic studies.[153-155, 197] Other groups active in the field are the groups of Mestroni,[26, 120, 130, 135, 152, 156, 159, 198-205] Cenini and Ragaini,[120, 150, 157, 160-165, 193, 206-212] and van

Leeuwen,[144-146, 194, 195] the first of whom was the initial group to study similar N-donor based systems.

In the early eighties, Mestroni *et al*. worked for some time on a reaction closely related to the catalytic reductive carbonylation of nitroaromatics, i.e., the catalytic reduction of nitrobenzene to aniline in the presence of water and carbon monoxide. In these studies Ir, Rh or Os salts were used in combination with bipyridine or phenanthroline and KOH as the catalytic system.[198-200] Since this system is similar to the ones used for the reductive carbonylation of nitroaromatics, they employed their catalytic system also for this reaction.[26, 130, 135, 202] The metal mainly used was Pd, either immobilized on carbon or as Pd^{II} salt, and a bulky Brønsted acid was added (2,4,6-trimethylbenzoic acid (TMBA)). Remarkably, identical results were obtained for 3,4,7,8-tetramethyl-1,10-phenanthroline/Pd/C(5%)/TMBA[130] and [Pd(3,4,7,8-tetramethyl-1,10-phenanthroline)$_2$](PF_6)$_2$,[26] namely a TOF of 125 mol/mol.h^{-1} and a carbamate selectivity of 97%. After a 'break' of about twelve years, they reported the reductive carbonylation of 2,4-dinitrotoluene leading to TDI to proceed in high conversion (100%), selectivity (82%), and fair TOF (260 mol/mol.h^{-1}). In this study the cationic complex [Pd(1,10-phenanthroline)$_2$](PF_6)$_2$ was used with an excess of free ligand, hexafluoridophosphoric acid as co-catalyst, and a substrate/Pd ratio of 520. [152]

Van Leeuwen and Wehman[194] systematically studied the influence of electron donating or withdrawing substituents on the 4,4'-positions of 2,2'-bipyridine (R = CF_3, Cl, H, CH_3, OCH_3, $N(CH_3)_2$); it was found that electron donating substituents rendered [Pd(R_2bipy)$_2$](CF_3SO_3)$_2$–type catalysts more reactive whereas electron withdrawing substituents resulted in an inactive catalyst. Moreover, it was shown that replacement of one of the triflate anions by a chloride anion inhibited the catalytic reaction and, additionally, the presence of water reduced the selectivity for carbamate.[144] A selectivity of more than 99% for carbamate was achieved, but only a very low TOF of 28 mol/mol.h^{-1} was reached, using the preformed compound [Pd((NMe_2)$_2$bipy)$_2$](CF_3SO_3)$_2$ as catalyst precursor. Subsequently, a similar study was conducted for a series of 4,7-disubstituted 1,10-phenanthroline ligands (R = Cl, H, CH_3, OCH_3, $N(CH_3)_2$), confirming the benefit of electron-donating substituents.[145] Furthermore, they compared two non-coordinating anions in the preformed catalyst (CF_3SO_3 and

BF_4) and found a subtle balance in activity when using a certain ligand together with a certain anion. The best results in this paper were reported for the $[Pd(Me_2phen)_2](CF_3SO_3)_2$ catalytic system: a TOF of 311 mol/mol.h^{-1} and a carbamate selectivity of 84%. After this, the electronic and steric properties of the nitroaromatic substrate was systematically explored using in a series of p-substituted nitrobenzenes (R = CF_3, Cl, Br, H, CH_3, OCH_3, $N(CH_3)_2$), and the abovementioned catalyst.[194] It was found that electron-donating substituents decreased the conversion and increased the selectivity to carbamate. Introduction of (bulky) o-substituents (R = H, Cl, Me, Ph CF_3, OCH_3, $CH(CH_3)_2$, $C(CH_3)_3$) proved detrimental for both conversion and selectivity. Noteworthy, no acid co-catalyst was added during these studies. However, in another study, they reported on the influence of aromatic carboxylic acids as co-catalyst in this $[Pd(Me_2phen)_2](CF_3SO_3)_2$ system.[146] Although the pK_a-value of the acid used did not seem to make a difference, its concentration was found to be of the utmost importance for both the conversion of the substrate and the selectivity towards carbamate. Furthermore, the anion of the acid was found affect the results: weakly coordinating benzoate anions were believed to stabilize various palladium intermediates. However, if the concentration or the coordinating ability of the anions becomes too high, a negative effect was observed. The acid yielding the best results was found to be 2,4,6-trichlorobenzoic acid, yielding a TOF of 378 mol/mol.h^{-1} and a selectivity to carbamate of 92%. Moreover, they also found the presence of aniline to have a promoting effect on the TOF. Finally, the catalytic system ($[Pd(phen)_2](CF_3SO_3)_2$/4-chlorobenzoic acid) was tested with some commercially more interesting aromatic dinitro compounds, wherein TOFs of 73-183 mol/mol.h^{-1} and carbamate selectivities of 30 to 100% were achieved.[194]

The best results to date have been reported by Cenini and Ragaini *et al*., who started in the mid 1980s with a $Ru_3(CO)_{12}/H^+$ catalytic system.[119, 127] Thereafter they too added some bidentate ligands (N and P, see previous section), obtaining only poor results.[193] Subsequently, in 1990, it was reported that Pd and Rh supported on alumina (which are inactive as such) could be 'activated' by the addition of chelating N-donor ligands like 2,2'-bipyridine, 1,10-phenanthroline (and derivatives thereof) with or without a Brønsted acid (TMBA). The system Pd/Al_2O_3/bipy/H^+ was studied for the direct route, giving very poor results (TOF = 21 mol/mol.h^{-1}, isocyanate selectivity = 65%). The Rh/Al_2O_3/phen catalyst was studied for the indirect route, also resulting in poor results (TOF = 45 mol/mol.h^{-1},

carbamate selectivity = 68%). Since it was evidenced that a homogeneous catalyst, formed in situ from the heterogeneous precursor, was the active species, they continued their efforts by solely studying homogeneous systems. After a period of thirteen years (i.e. in 2003), they reported a study of the reaction involving the $[Pd(phenanthroline)_2](BF_4)_2$ system, co-catalyzed by an aromatic carboxylic acid (by then known to yield the best results). Moreover, since aniline had been reported to enhance the reactivity, they found that combining the two promoters (e.g. benzoic acid and aniline) in the molecule 2-NH_2PhCOOH, had a positive effect when compared to benzoic acid alone, resulting in a TOF of about 1400 mol/mol.h^{-1} and a carbamate selectivity of about 70%.[161] In the same year, they reported a TOF of roughly 6000 mol/mol.h^{-1} and a carbamate selectivity of 88%, using $[Pd(phenanthroline)_2][BF_4]_2$ as catalyst and H_3PO_4 (85%) and aniline as co-catalysts and working at temperatures as high as 170 ºC.[160, 162] These high values were obtained by increasing the CO pressure up to 100 bar, whereas the initially used CO pressure of 60 bar gave a TOF of 'only' 4130 mol/mol.h^{-1} and a selectivity for carbamate of 87%. In fact, a linear trend wherein the conversion is dependant in the CO pressure, without loss of selectivity, was disclosed. It is worth mentioning that analytically pure H_3PO_4 gave significantly poorer results than the cheaper 85% variant and other phosphorus acids, for reasons still not known.[162] Furthermore, they made use of the reactive drying agent 2,2-dimethoxypropane, that is known to be beneficial in similar reactions.[139, 140, 151, 152] How it is possible that these two reagents together (i.e. 85% H_3PO_4 and a drying agent) can be beneficial, is not clear. Nonetheless, it seems to work, and in the year after, this catalytic system was studied for the conversion on 2,4-dinitrotoluene instead of the model compound nitrobenzene, and some distinct parameters were optimized. The best acid co-catalysts for the reductive carbonylation of this molecule seemed to be phenylphosphonic or 4-tolylphosphonic acid. Furthermore, the addition of the aniline analogue of the substrate was found to be beneficial as well, and again the CO pressure was found to be an important parameter. Moreover, they reported an important 'extra feature' concerning the isolation of the carbamates involved: they precipitate from the solvent (methanol) when cooled to 0 °C, and after one recrystallization the 99% pure product could be isolated. Under their optimized conditions, they obtained unprecedented (for 2,4-dinitrotoluene) results, expressed in a TOF of 580 mol/mol.h^{-1} with 78% selectivity for the corresponding dicarbamate. Also in the year 2005, they reported on the indirect method using aniline as co reactant

for the production of ureas, and studied the effect of chloride anions on this reaction.[211] Although some positive effects of Cl^- were found for the conversion of nitrobenzene, an inhibiting effect was observed for the conversion of 2,4-dinitrotoluene. In both cases only poor results were obtained, however (TOF ~50 mol/mol.h^{-1}, urea selectivity ~50-98%). It is important to note, however, that these results were obtained using CO pressures of only 40 bar, whereas their previous (outstanding) results were obtained applying CO pressures up to 100 bar.[162, 163] The highest TOF reported to date, namely 7900 mol/mol.h^{-1} at 100 bar (5710 mol/mol.h^{-1} at 60 bar), has been reported very recently (2010) by using the unsymmetrical ligand 4-methoxyphenanthroline.[213]

1.4. Mechanistic considerations

1.4.1. Frequently reported side-products

Frequently reported side-product in the transition-metal catalyzed reductive carbonylation of nitrobenzene in methanol are azobenzene, azoxybenzene, aniline, isocyanate oligomers, metallacyclic compounds, *N,N'*-diphenylurea (DPU) and Pd^0 or palladium black (Figure 1.3). Although never isolated, nitrosoaromatic compounds (Ph-NO) are sometimes believed to be intermediate species for other side products since they are easily further deoxygenated.[53, 214, 215] Azo- and azoxyaromatic compounds are common byproducts and have been reported to poison the catalyst when present in high enough concentrations.[151] Aniline was first thought to be a mere side product,[119, 144, 146, 216] but has also been reported to act as co-catalyst.[160] Isocyanate oligomers are well known to be formed through either assisted or spontaneous self-coupling reactions.[214, 217-219] Metallacyclic compounds can be seen as either reaction intermediates (for the product or a byproduct) or a way to deactivate the catalyst; if the species is too stable it removes the metal from the catalytic cycle.

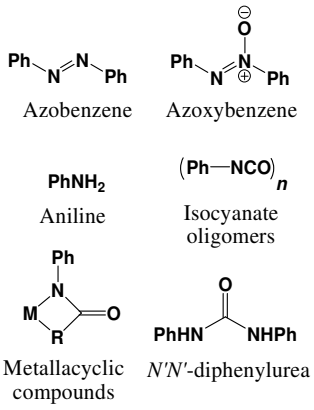

Figure 1.3. Frequently reported side-products in the reductive carbonylation of nitrobenzene.

Paul *et al.* elegantly proved that in non-alcoholic conditions phenylisocyanate reacts with a metallacyclic intermediate Pd species thus poisoning the catalyst.[155] This is schematically shown in Figure 1.4, wherein (a) is a reaction intermediate, (b) proved to be a very stable compound and (c) and (d) decomposed into

N,N',N''-triphenylbiurea (TPB) and DPU respectively, with liberation of the active species. Alternatively, these compounds can be formed by reacting aniline with isocyanate and the thus formed urea with (again) isocyanate, thus forming the diurea. However, in the presence of an alcohol, the corresponding carbamate is favored on thermodynamic grounds, thus ureas are only rarely isolated in high yields. The same reaction sequence may occur in the indirect pathway, but, since the concentration of isocyanate is low, catalyst degradation will be much slower via this route, thus allowing for relatively higher TON and TOF values to be reached, as is generally observed.

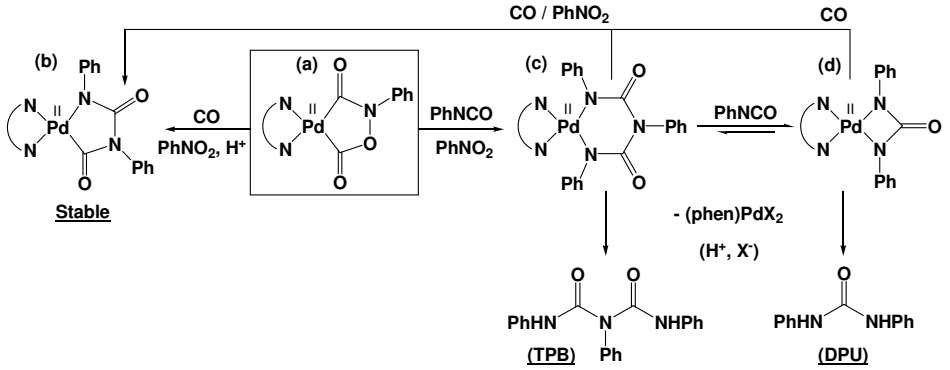

Figure 1.4. Palladacyclic structures studied by F. Paul *et al.*.[155] (a) is believed to be a key intermediate in the Pd/Phen/H^+ catalyzed reductive carbonylation of nitrobenzene, and (b) is a very stable species that can be formed thereof, thus poisoning the catalyst. (c) and (d) can also form from (a) and decompose into the active species and one of the byproducts often detected. See reference for exact reaction conditions and stoichiometry.

1.4.2. Interrelated proposals of the mechanism, in a historical context

1.4.2.1. Introduction

Although several papers have claimed otherwise,[150, 220, 221] the catalytic system in the carbonylation reaction of nitrobenzene is usually a homogeneous one. Even when a 'heterogeneous' catalyst is used, the active species is generally believed to be homogeneous,[120, 123, 124, 134] almost without exceptions.[222] The mechanism was initially (1970s) thought to proceed via a similar mechanism as the direct carbonylation, with subsequent reaction of the isocyanate with the alcohol employed. This idea was abandoned in the mid 1980s, as evidence suggesting a different mechanism was found,[119, 223-227] in which the alcohol is interacting with

the catalyst. Though the carbonylation reaction was discovered more than 50 years ago, still no clear-cut mechanism has been proposed so far. In fact, it seems likely to assume that different mechanisms may be operative in different catalytic systems. It lies outside the scope of this introductory chapter to discuss all mechanistic proposals in great detail; only some key-proposals will be briefly discussed.

Five groups have proposed a mechanism for the reductive carbonylation of nitrobenzene, and in an important review by Paul in 2000,[196] the proposed mechanisms are summarized of both the direct and indirect reductive carbonylation of nitro aromatics of all catalyst systems of which the mechanism have been studied. The five proposals for the Pd/phen/H^+ system by the different groups are provided in chronological order (the most recent proposal of each group is given).

1.4.2.2. The Pd/phen/H^+ mechanism

In nearly all proposed catalytic cycles, palladacyclic intermediates (see e.g. Figure 1.5a) play a crucial role and the active species that enters the catalytic cycle is believed to be a zeo-valent palladium complex (see e.g. **1** in Figure 1.6, hence rationalizing the similar activity when employing Pd/C and phen, as was done in the early days).[26, 130] Furthermore, the palladium compounds **2** – **4** (see Figure 1.6) were all characterized crystallographically (see Figure 1.5a-c) and form the basis of all proposed mechanisms. The first of these intermediate palladacyclic structures was isolated and characterized already in 1990 by Leconte *et al.*[153] (Figure 1.5a, see also **2** in Figure 1.6 and).

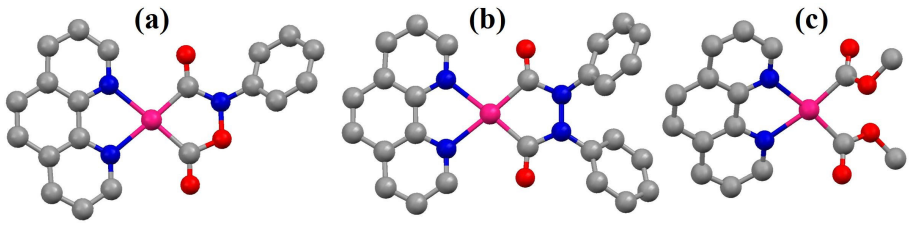

Figure 1.5. Perspective views of the crystal structures that are believed to be intermediates in the catalytic reductive carbonylation of nitro aromatic compounds based on the Pd/phen catalytic system. Their molecular structure is also shown in Figure 1.6 as compounds (2) – (4) respectively. Carbon is grey, nitrogen is blue, oxygen is red, palladium is pink, and hydrogen and solvent molecules are omitted for clarity.

Based on these structural data, the knowledge of the promoting influence of an acid and their own observations concerning the formation of aniline, Wehman *et al*. proposed the catalytic cycle as depicted in the top left of Figure 1.6. Despite the attractive simplicity of this cycle, empirical evidence for this proposal was minimal.[146]

The catalytic cycle proposed by Mestroni *et al*.[159] (top right in Figure 1.6) is based on their crystallographically characterized metallacycle **3**, which they proposed to be a key-intermediate in the catalytic cycle. In this proposal, azo- and azoxybenzene are considered to be formed as intermediates. However, they had no empirical evidence to prove this, nor did they explain the initial formation of azoxybenzene or the role of aniline in the process.

Another proposal was brought forth by Paul *et al*.[3, 16, 155, 196] (bottom left in Figure 1.6) and also involved a series of stepwise deoxygenation/carbonylation steps. This proposal is very similar, but more complicated than the one proposed by Wehman *et al*., forming the carbamate by a (stepwise) proton-catalyzed alcoholysis of **2**. Although one could argue in favor of the stability of the different metallacycles proposed here, as well as the likelihood of certain individual steps, here too the empirical evidence is lacking and it does not account for the formation/role of aniline or other byproducts/intermediates.

In their latest proposal[211] (centre right in Figure 1.6), which is partially based on their own crystallographically characterized Pd intermediate **4**,[208] Cenini *et al*. 'divide' the catalytic cycle into two distinct pathways: 1) the initial formation of a (metallacyclic) intermediate and the subsequent (proton-catalyzed) liberation of phenyl isocyanate and the active species (**2** and **1** in the Figure respectively); 2) a catalytic cycle involving the intermediate production of aniline and the acyl complex **4**, from which nucleophilic attack of aniline on **4** is thought to produce phenyl isocyanate and methanol. In both cases, phenyl isocyanate is thought to react with aniline to *N,N'*-diphenylurea, which is then converted to the carbamate to release aniline. This does seem to explain the promoting role of aniline[160] and merges the routes which can be envisaged with the two intermediary Pd structures **2** and **4**. However, here too, little evidence was brought forth to verify this experimentally, and no detailed mechanism was provided for the formation of aniline or other side-products.

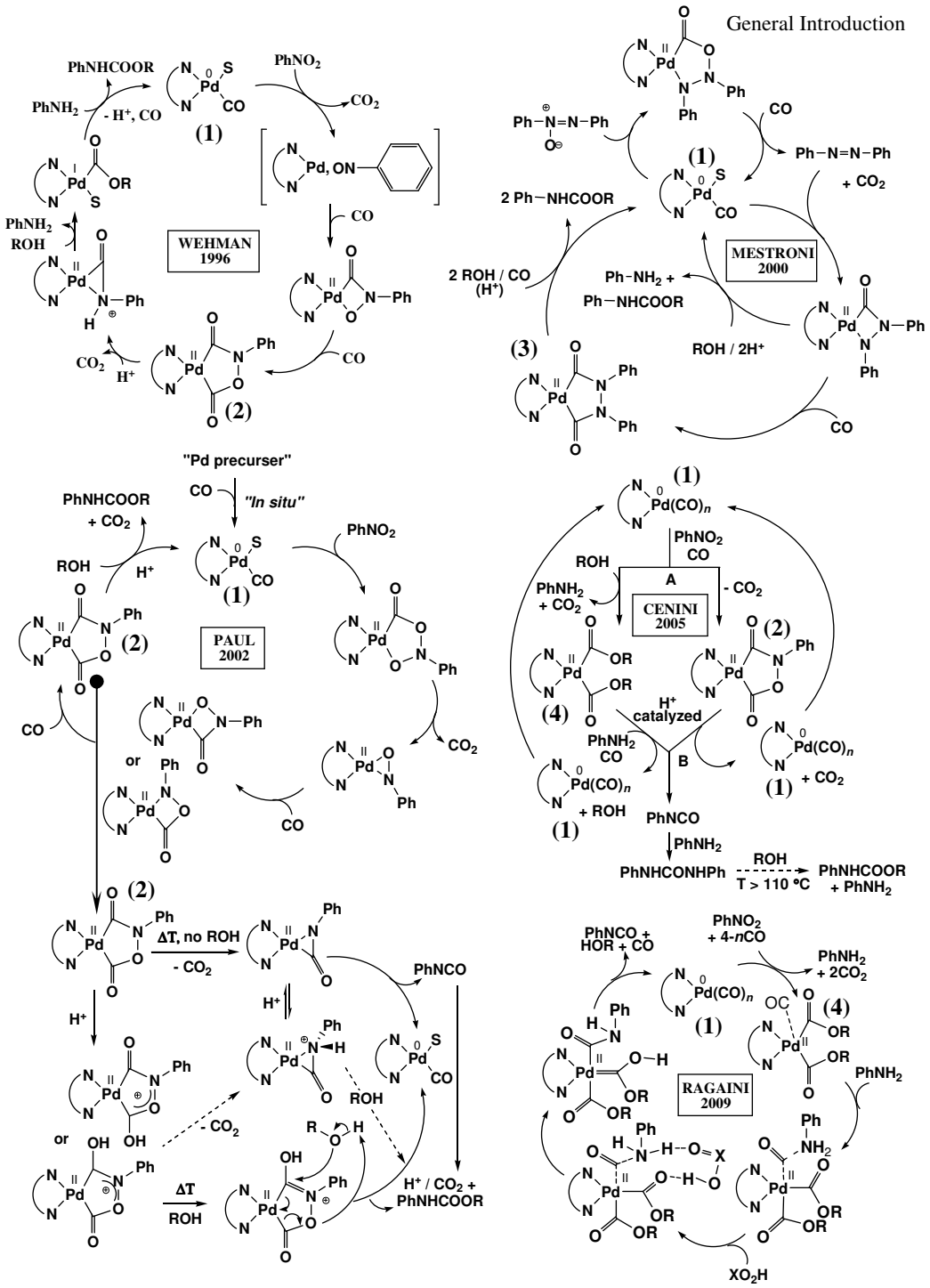

Figure 1.6. Different interrelated catalytic cycles for the Pd/phen/H^+ catalytic system as proposed by Wehman in 1996 (top left), Mestroni in 2000 (top right), Paul in 2002 (bottom left), and Cenini in 2005 (bottom right). The structures 2 – 4 were all characterized crystallographically (see Figure 1.5a-c). (1) is believed to be the active species and 2 – 4 are believed to be key-intermediates. S = solvent molecule. See text for further explanation.

Finally, Ragaini and co-workers very recently put forward a (bottom right in Figure 1.6) which shows strong resemblance to the mechanism proposed by Gladfelter *et al*. [168, 169, 171, 172, 187-190, 192] for the almost inactive (max. TOF of 7 h^{-1}) Ru/diphosphane catalytic system (not discussed further in this chapter). Like the proposal of Cenini, the palladium-diacyl complex **4** is also thought to be formed first, while reducing nitrobenzene to aniline. Aniline is then thought to attack on a CO molecule that is associating with Pd via one of the axial coordination sites, where after a carbonic acid (RO_2H) works as a co-catalyst to assist proton transfer from aniline to one of the acyl ligands, resulting in a carbene species. The carbene ligand in this pentacoordinate Pd-complex is thought to decompose to CO_2 and methanol, and then further to phenyl isocyanate, methanol, and the starting zero-valent palladium compound **1**. What is unclear however, is again how aniline is formed first, how exactly nitrobenzene is deoxygenated, and again very little experimental evidence has been put forth to verify this proposal; e.g. the proposed carbene intermediate is a formal Pd^{II} species surrounded by two anionic acyl-type ligands and three strong sigma-donor atoms (two phen-N and one carbene-C); clearly a situation that will not be favorable for a d^8 palladium complex.

1.4.3. Opportunities to generate mechanistic insight

Overall, the above mechanistic proposals rationalize the formation of carbonylation products such as phenyl isocyanate, methyl phenylcarbamate and *N,N'*-diphenylurea, and most of them rationalize the co-catalytic effect of added acid. There is however, not one unified and generally accepted mechanism to explain the formation of all these products, or of other observed products such as azo(xy)benzene and aniline. Moreover, the mechanism for nitrobenzene reduction/de-oxygenation is not well-understood, it is generally *assumed* to proceed by a series of carbonyation/decarboxylation steps to palladacycles such as **2** (see Scheme 1.5). However, a complete deoxygenation of nitrobenzene may also result in an imido-complex ('L_2Pd=NPh', see Scheme 1.5), from which products may then evolve.

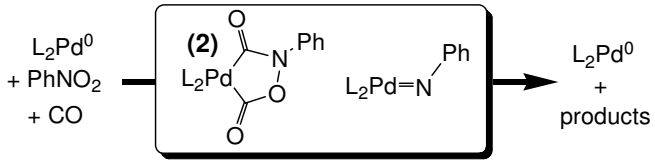

Scheme 1.5. Proposed crucial intermediates in the reductive carbonylation of nitrobenzene discussed in this thesis: a palladacyclic compound and a palladium-imido compound.

Speculations concerning the intermediacy of palladium–imido compounds in catalytic reactions have been put forward in literature of the 1960's and 1970's. The existence of such imido compounds has been postulated in the context of nitrobenzene reduction to aniline with CO/H_2O,[228, 229] in the carbonylation of nitrobenzene to phenyl isocyanate,[103, 230] and also speculatively proposed in the palladium/phen/H^+ catalyzed nitrobenzene carbonylation in methanol as the reaction medium.[146, 147] It has also been proposed that the palladium-catalyzed reduction of functionalized nitroarenes with CO proceeds via a palladium–imido intermediate to yield N-heterocyclic compounds.[231, 232] Moreover, a series of bidentate phosphane stabilized Ni–imido complexes has been isolated, characterized crystallographically, and were shown to react with CO to form isocyanates.[233-235]

Despite these indications, Pd-imido complexes are not generally considered as intermediates in the reductive carbonylation of nitrobenzene in an alcoholic solvent. This clearly presents an opportunity for further research, especially by applying diphosphane ligands to stabilize the palladium catalyst. Not only have Pd/diphosphane catalytic systems been scarcely studied, the steric and electronic properties of phosphane ligands are much easier to fine-tune than those of 1,10-phenanthroline (see also section 1.3.1.). This allows for a correlation to be established between the catalyst performance and its structure; allowing valuable information to be gained into the mechanism of the title reaction. Such knowledge is long overdue and clearly a prerequisite for the further rational development of new, possibly more active and selective, catalyst system for the alternative synthesis of aromatic isocyanates as outlined in section 1.2.

1.5. Aim and outline of this thesis

As discussed in detail in this chapter, the current industrially applied route to prepare aromatic isocyanates has several drawbacks, and alternative –phosgene free– strategies have been explored to replace this dangerous process. In particular strategies involving transition metal catalysts have arisen as potential alternatives. The most promising of these is the palladium-catalyzed indirect reductive carbonylation of nitro aromatic compounds, where the palladium metal is stabilized by phosphorus or nitrogen donor ligands. In particular the Pd/phen/H^+ catalytic system has been extensively studied over the years.

Despite these efforts, a clear, unified, and generally agreed upon mechanism for this reaction has still to emerge, yet such understanding is critical for the development of catalysts of optimal performance.

The aim of the research described in this thesis is therefore to gain understanding into the molecular mechanism of the palladium(/diphosphane) catalyzed reductive carbonylation of nitrobenzene in methanol. It is expected that such molecular understanding will –in the long run– allow the design of catalyst structures for optimal performance. In particular, the molecular connection between the steric and electronic properties of the catalyst complexes and their respective catalytic performances needs to be revealed. The research described in the subsequent chapters of this thesis is aimed at acquiring this knowledge.

The catalytic reactions reported in this thesis (but also in many other studies) are performed using in situ synthesized catalyst precursor complexes. It is known however, that this (Ligand)Pd(Anion)$_2$ complex formation process is not always straightforward, sometimes resulting in the formation of inactive complexes.[236] This process has therefore been studied in depth using palladium salts and various bidentate diarylphosphane ligands in methanol, acetone and dichloromethane, and the findings of these studies are condensed in **Chapter 2** of this thesis. Also presented in this chapter are the structural characteristics of selected complexes in the solid state and in solution.

Chapter 3 reports on selected catalytic nitrobenzene carbonylation experiments and a thorough qualification and quantification of the products formed. These products not only comprise the expected nitrobenzene reduction products, but also large amounts of methanol oxidation products. Based on these data, and partially on other carefully chosen catalytic experiments, a comprehensive conceptual analysis is given of the likely molecular processes that underlie the formation of the various products observed. This analysis leads to the postulation of a palladium-imido complex ('P_2Pd=NPh') as the central intermediate species in an unprecedented complex network of catalytic reactions. This hypothesis not only allows the rationalization of the products formed, but moreover allows for an accurate simulation of the observed product distributions and –to some extent– relate the catalyst performance to the structure of the catalyst as imposed by that of the ligand.

In the studies described in **Chapter 4**, a more comprehensive library of functionalized phosphane ligands has been applied in the title reaction, together with variations in reaction conditions. It is shown that the 'imido-hypothesis' as developed in Chapter 3 can indeed explain, on the molecular level, the effects that the catalyst structure and reaction conditions may have on the conversion of nitrobenzene and the observed selectivities. Moreover, additional spectroscopic evidence for the existence of this proposed 'P_2Pd=NPh' complex is presented. As an alternative intermediate for the production of nitrobenzene carbonylation products, a palladacyclic intermediate (see Scheme 1.5) was considered. It appeared however, that when supported by phosphane ligands, the palladacycle decomposes not to give carbonylation products but yielding a variety of –mainly unidentified– products via the palladium-imido complex. These data thus also point strongly into the direction of a 'P_2Pd=NPh' complex as centrally important product-releasing intermediate.

In **Chapter 5**, the mechanistic knowledge gained in the foregoing two chapters is applied to understand the evolution of methanol oxidation products during the nitrobenzene reduction process. In particular, the chapter focuses on the evolution of the useful methanol oxidative carbonylation products dimethyl carbonate (DMC) and dimethyl oxalate (DMO). Based on the effects that different functionalized phosphane ligands and different reaction conditions have on the activity and selectivity for DMC / DMO production, a more detailed molecular mechanism is proposed for their formation, involving –besides the P_2Pd=NPh complex– the dimethoxido complex $P_2Pd(OCH_3)_2$ and the acyl complex $[PdC(O)OCH_3]^+$.

Chapter 6 reports on a (catalytic and DFT) comparative study between palladium catalysts stabilized by the N-donor ligand phen and those stabilized by bidentate P-donor ligands, in particular one that displays a nearly identical selectivity for the nitrobenzene reduction products as the phen-supported system. The similarities and differences between these two catalytic systems could all be rationalized using the mechanism developed in Chapters 3–5. For example, also for the Pd/phen catalytic system the palladacyclic intermediate (Scheme 1.5) is most likely not a product releasing species. Our hypothesis centered around the Pd=NPh intermediate thus seems to provide a mechanistic understanding of the

title reaction that is generally applicable, irrespective of the supporting ligand. Under acidic conditions however, the palladacycle may become a product-releasing species in the Pd/phen/H^+ system, whereas this is not likely to be the case in Pd/diphosphane/H^+ systems.

The application of other nucleophiles than methanol (i.e. *p*-cresol, *i*-propanol, 2,2,2,-trifluoroethanol (TFE), and aniline) in the title reaction is explored in **Chapter 7**. Here too, it seems that the mechanism developed in chapters 3–5 can be applied to understand the experimental data. Moreover, TFE will be highlighted as a very promising nucleophile and solvent.

Finally, in **Chapter 8** is presented a detailed summary of the most important findings established in this thesis, together with some general conclusions and an outlook.

Parts of this thesis have been published,[237-239] have been submitted for publication,[240] or are soon to be submitted.[241, 242]

References

[1] R. H. Richter, R. D. Priester, *in: J.L. Kroschmitz, M. Howe-Grand (Eds.), Kirk-Othmer Encyclopedia of Chemical Technology, Vol. 14*, Wiley, New York, **1995**.
[2] H. Ulrich, *Ullmann's Encyclopedia of Industrial Chemistry, Vol. A14*, VCH publishers, New York, **1989**.
[3] S. Fukuoka, M. Chono, M. Kohno, *Chemtech* **1984**, *14*, 670.
[4] S. Fukuoka, M. Chono, M. Kohno, *J. Chem. Soc.-Chem. Commun.* **1984**, 399.
[5] S. V. Levchik, E. D. Weil, *J. Fire Sci.* **2006**, *24*, 345.
[6] S. V. Levchik, E. D. Wei, Recent progress in flame retardancy of polyurethane and polyisocyanurate foams in *Fire And Polymers Iv: Materials And Concepts For Hazard Prevention, Vol. 922*, Am. Chem. Soc., Washington, **2006**, pp. 280.
[7] J. Q. Wang, W. K. Chow, *J. Appl. Polym. Sci.* **2005**, *97*, 366.
[8] E. D. Weil, S. V. Levchik, *J. Fire Sci.* **2004**, *22*, 183.
[9] Y. Zheng, E. K. Yanful, A. S. Bassi, *Crit. Rev. Biotechnol.* **2005**, *25*, 243.
[10] K. K. Maniar, *Polym.-Plast. Technol. Eng.* **2004**, *43*, 427.
[11] G. T. Howard, *Int. Biodeterior. Biodegrad.* **2002**, *49*, 245.
[12] P. Antony, S. K. De, *J. Macromol. Sci.-Polym. Rev* **2001**, *C41*, 41.
[13] V. I. Manovyuvenskii, B. K. Nefedov, K. O. Khoshdurdyev, *Bull. Acad. of Sci. of USSR Div. Chem. Sci.* **1982**, *31*, 1176.
[14] R. L. Metcalf, *in: J.L. Kroschmitz, M. Howe-Grand (Eds.), Kirk-Othmer Encyclopedia of Chemical Technology, Vol. 14*, Wiley, New York, **1995**.
[15] T. Kato, K. Suzuki, J. Takahashi, K. Kamoshita, *J. Pestic. Sci.* **1984**, *9*, 489.
[16] N. N. Melinkov, *Chemistry of Pesticides*, Springer Verlag, Berlin, **1971**.
[17] G. S. Hertley, *Chemicals for Pest Control*, Pergamon, New York, **1969**.
[18] M. Jayabalan, P. P. Lizymol, *J. Polym. Mater.* **2000**, *17*, 9.

[19] R. Tout, *Int. J. Adhes. Adhes.* **2000**, *20*, 269.
[20] K. C. Frisch, *Polimery* **1996**, *41*, 257.
[21] G. A. Howarth, *Surf. Coat. Int. Pt. B-Coat. Trans.* **2003**, *86*, 111.
[22] J. Huybrechts, P. Bruylants, A. Vaes, A. De Marre, *Prog. Org. Coat.* **2000**, *38*, 67.
[23] G. A. Howarth, *JOCCA-Surf. Coat. Int.* **1999**, *82*, 460.
[24] K. Abate, *JOCCA-Surf. Coat. Int.* **1991**, *74*, 136.
[25] R. Heath, *J. of Coat. Fab.* **1985**, *15*, 78.
[26] A. Bontempi, E. Alessio, G. Chanos, G. Mestroni, *J. Mol. Catal.* **1987**, *42*, 67.
[27] J. Paetsch, *in "Ullmann's Encyclopaedia of Industrial Chemistry", Vol. 9*, VCH publishers, New York, **1975**.
[28] D. Randall, S. Lee (Eds.), *The Polyurethanes Book*, John Wiley & Sons, **2002**.
[29] B. M. Fleisher, *China Econ. Rev.* **2006**, *17*, 237.
[30] V. Kelkar, *Econ. Polit. Week.* **1999**, *34*, 2326.
[31] D. R. Khatkhate, *World Dev.* **1997**, *25*, 1551.
[32] I. Peng, *Soc. Policy Adm.* **2000**, *34*, 87.
[33] K. C. Fritsch, D. Klempner, *in: G. Allen, J.C. Bevington (eds.), Comprehensive Polymer Science, Vol. 5*, Pergamon, New York, **1989**.
[34] A. J. Ryan, J. L. Stanford, *in: G. Allen, J.C. Bevington (eds.), Comprehensive Polymer Science, Vol. 5*, Pergamon, New York, **1989**.
[35] K. Weisermel, H. J. Arpe, *Industrielle Organische Chemie*, VCH Verslagsgesellschaft GmbH, Weinheim, Germany, **1988**.
[36] http://en.wikipedia.org/wiki/Phosgene, **November 2011**
[37] http://www.firstworldwar.com/weaponry/gas.htm, **November 2011**
[38] UK Department of health, (Phosgene: guidelines for action in the event of a deliberate release), **Feb. 4th 2004**.
[39] http://en.wikipedia.org/wiki/Bhopal_disaster, **November 2011**
[40] http://www.bhopal.net, **November 2011**
[41] H. J. Twitchet, *Chem. Soc. Rev.* **1974**, *3*, 209.
[42] *Registry of Toxic Effects of Chemical Substances (RTECS, online database)*, United States Department of Health and Human Services (National Toxicology Information, National Library of Medicine), Bethesda, MD, **1993**.
[43] M. Aresta, E. Quaranta, *Chemtech* **1997**, *27*, 32.
[44] R.C. Weast (Ed.), *Handbook of Chemistry and Physics*, D-110, 58 ed., CRC Press Inc., Cleveland, **1977-1978**.
[45] C. S. Rose, R. A. Jones, L. J. Jenkins, J. Siegel, *Toxicol. Appl. Pharmacol.* **1970**, *17*, 752.
[46] N. Ozalp, *J. Energ. Res. Tech. Tans. Asme* **2009**, *131*
[47] J. P. Lange, *ChemSusChem* **2009**, *2*, 587.
[48] M. Neelis, M. Patel, K. Blok, W. Haije, P. Bach, *Energy* **2007**, *32*, 1104.
[49] R. F. Dunn, M. M. El-Halwagi, *J. Chem. Tech. & Biotech.* **2003**, *78*, 1011.
[50] T. A. Kantyka, *Chem. & Indust.* **1979**, 571.
[51] R. H. Crabtree, *The organometallic chemistry of the transition metals*, 4th ed., Wiley-Interscience, New Jersey (USA), **2005**.
[52] B. Cornils, W. A. Hermann (Ed.), *Applied homogeneous catalysis with organometallic compounds, Vol. I*, VCH Verslagsgesellschaft GmbH, Weinheim (Germany), **1996**.
[53] S. Ozaki, *Chem. Rev.* **1972**, *72*, 457.
[54] J. H. Saunders, R. J. Slocombe, *Chem. Rev.* **1948**, *43*, 203.
[55] J. H. Saunders, K. C. Frisch, *"Polyurethanes, Chemistry and Technology. Part I. Chemistry"*, Interscience, New York, **1962**.
[56] R. Vieweg, A. Hochtlen, *"Kunststoff Bandbuch. Band VII. Polyurethane."*, Carl Hander Verlag, München, **1966**.
[57] M. Aresta, A. Dibenedetto, E. Quaranta, *J. Chem. Soc.-Dalton Trans.* **1995**, 3359.
[58] C. Bruneau, P. H. Dixneuf, *J. Mol. Catal.* **1992**, *74*, 97.
[59] W. D. McGhee, D. P. Riley, M. E. Christ, K. M. Christ, *Organometallics* **1993**, *12*, 1429.

[60] W. D. McGhee, D. P. Riley, *Organometallics* **1992**, *11*, 900.
[61] T. Tsuda, H. Washita, K. Watanabe, M. Miwa, T. Saegusa, *J. Chem. Soc.-Chem. Commun.* **1978**, 815.
[62] M. Aresta, E. Quaranta, *Tetrahedron* **1991**, *47*, 9489.
[63] W. McGhee, D. Riley, K. Christ, Y. Pan, B. Parnas, *J. Org. Chem.* **1995**, *60*, 2820.
[64] A. A. Kelkar, D. S. Kolhe, S. Kanagasabapathy, R. V. Chaudhari, *Ind. Eng. Chem. Res.* **1992**, *31*, 172.
[65] U. Kiiski, T. Venalainen, T. A. Pakkanen, O. Krause, *J. Mol. Catal.* **1991**, *64*, 163.
[66] F. J. Waller, *J. Mol. Catal.* **1985**, *31*, 123.
[67] S. A. R. Mulla, C. V. Rode, A. A. Kelkar, S. P. Gupte, *J. Mol. Catal. A-Chem.* **1997**, *122*, 103.
[68] S. B. Halligudi, K. N. Bhatt, N. H. Khan, R. I. Kurashy, K. Venkatsubramanian, *Polyhedron* **1996**, *15*, 2093.
[69] I. Pri-Bar, J. Schwartz, *J. Org. Chem.* **1995**, *60*, 8124.
[70] V. L. K. Valli, H. Alper, *Organometallics* **1995**, *14*, 80.
[71] F. W. Hartstock, D. G. Herrington, L. B. McMahon, *Tetrahedron Lett.* **1994**, *35*, 8761.
[72] S. A. R. Mulla, S. P. Gupte, R. V. Chaudhari, *J. Mol. Catal.* **1991**, *67*, L7.
[73] B. M. Choudary, K. R. Kumar, M. L. Kantam, *J. Catal.* **1991**, *130*, 41.
[74] P. Giannoccaro, C. F. Nobile, G. Moro, A. Laginestra, C. Ferragina, M. A. Massucci, P. Patrono, *J. Mol. Catal.* **1989**, *53*, 349.
[75] S. P. Gupte, R. V. Chaudhari, *J. Catal.* **1988**, *114*, 246.
[76] H. Alper, G. Vasapollo, F. W. Hartstock, M. Mlekuz, D. J. H. Smith, G. E. Morris, *Organometallics* **1987**, *6*, 2391.
[77] P. Giannoccaro, *Inorg. Chim. Acta* **1988**, *142*, 81.
[78] H. Alper, F. W. Hartstock, *J. Chem. Soc.-Chem. Commun.* **1985**, 1141.
[79] J. J. Lindberg, B. Malm, L. Suomi, *Finnish Chem. Lett.* **1980**, 153.
[80] E. Bolzacchini, S. Meinardi, M. Orlandi, B. Rindone, *J. Mol. Catal. A-Chem.* **1996**, *111*, 281.
[81] T. W. Leung, B. D. Dombek, *J. Chem. Soc.-Chem. Commun.* **1992**, 205.
[82] F. Benedini, M. Nali, B. Rindone, S. Tollari, S. Cenini, G. Lamonica, F. Porta, *J. Mol. Catal.* **1986**, *34*, 155.
[83] M. M. T. Khan, S. B. Halligudi, S. Shukla, Z. A. Shaikh, *J. Mol. Catal.* **1990**, *57*, 301.
[84] J. E. McCusker, J. Logan, L. McElwee-White, *Organometallics* **1998**, *17*, 4037.
[85] K. Kondo, S. Yokoyama, N. Miyoshi, S. Murai, N. Sonoda, *Angew. Chem.* **1979**, *18*, 692.
[86] V. D. Selivanov, I. I. Konstantinov, *Zhurnal Fiz. Khimii* **1975**, *49*, 1056.
[87] D. R. Stull, E. F. Westrum, G. C. Sinke, *in "The Thermodynamics of organic compounds"*, J. Wiley and sons, New York, **1969**.
[88] G. W. Parshall, S. D. Ittel, *Homogeneous Catalysis*, 2 ed., Wiley, New York, **1992**.
[89] V. Macho, L. Vojcek, M. Schmidtova, J. Terlandova, *Collect. Czech. Chem. Commun.* **1992**, *57*, 2605.
[90] V. Macho, M. Kucera, M. Kralik, *Collect. Czech. Chem. Commun.* **1995**, *60*, 514.
[91] V. Macho, M. Kralik, F. Halmo, *J. Mol. Catal. A-Chem.* **1996**, *109*, 119.
[92] E. Drent, P. W. N. M. van Leeuwen, EU 0086281A1, **1982**.
[93] M. Röper, *in "Industrial applications of homogeneous catalysis"*, D. Reidel publishing company, Dordrecht, **1988**.
[94] W. B. Hardy, R. P. Bennett, *Tetrahedron Lett.* **1967**, 961.
[95] H. M. Colquhoun, D. J. Thompson, M. V. Twigg, *Carbonylation-Direct Synthesis of Carbonyl Compounds*, Plenum Press, New York, **1991**.
[96] B. K. Nefedov, V. I. Manovyuvenskii, K. O. Khoshdurdyev, *Bull. Acad. of Sci. of USSR Div. Chem. Sci.* **1978**, *27*, 99.
[97] V. I. Manovyuvenskii, K. B. Petrovskii, A. L. Lapidus, *Bull. Acad. of Sci. of USSR Div. Chem. Sci.* **1984**, *33*, 2486.
[98] H. Tietz, K. Unverferth, K. Schwetlick, *Zeitschrift Fur Chemie* **1980**, *20*, 411.

[99] H. Tietz, K. Schwetlick, *Zeitschrift Fur Chemie* **1985**, *25*, 147.
[100] B. K. Nefedov, V. I. Manovyuvenskii, A. L. Chimishkyan, V. M. Englin, *Kinet. Catal.* **1978**, *19*, 861.
[101] H. Tietz, K. Unverferth, K. Schwetlick, *Zeitschrift Fur Chemie* **1980**, *20*, 295.
[102] K. Unverferth, R. Hontsch, K. Schwetlick, *J. Prakt. Chem.* **1979**, *321*, 86.
[103] F. J. Weigert, *J. Org. Chem.* **1973**, *38*, 1316.
[104] H. Tietz, K. Schwetlick, *Zeitschrift Fur Chemie* **1985**, *25*, 149.
[105] B. N. Nefedov, V. I. Manovyuvenskii, *Bull. Acad. of Sci. of USSR Div. Chem. Sci.* **1979**, *28*, 540.
[106] H. Tietz, K. Unverferth, K. Schwetlick, *Zeitschrift Fur Chemie* **1977**, *17*, 368.
[107] V. I. Manovyuvenskii, A. V. Smetanin, B. K. Nefedov, *Bull. Acad. of Sci. of USSR Div. Chem. Sci.* **1980**, *29*, 1813.
[108] S. P. Gupte, R. V. Chaudhari, *J. Mol. Catal.* **1984**, *24*, 197.
[109] H. Tietz, K. Unverferth, K. Schwetlick, *Zeitschrift Fur Chemie* **1978**, *18*, 217.
[110] H. Tietz, K. Unverferth, D. Sagasser, K. Schwetlick, *Zeitschrift Fur Chemie* **1979**, *19*, 304.
[111] G. A. Razuvaev, B. K. Nefedov, V. I. Manovyuvenskii, L. V. Gorbunova, N. N. Vavilina, A. L. Chimishkyan, A. V. Smetanin, *Bull. Acad. of Sci. of USSR Div. Chem. Sci.* **1978**, *27*, 2294.
[112] V. I. Manovyuvenskii, B. K. Nefedov, A. V. Smetanin, *Bull. Acad. of Sci. of USSR Div. Chem. Sci.* **1980**, *29*, 1817.
[113] S. S. Novikov, V. I. Manoviuvenskii, A. V. Smetanin, B. K. Nefedov, *Dokl. Akad. Nauk USSR* **1980**, *251*, 371.
[114] V. I. Manovyuvenskii, A. L. Lapidus, K. B. Petrovskii, *Bull. Acad. of Sci. of USSR Div. Chem. Sci* **1985**, *34*, 1561.
[115] H. Tietz, P. Neitzel, K. Schwetlick, R. Szargan, *Zeitschrift Fur Chemie* **1984**, *24*, 186.
[116] H. Tietz, K. Schwetlick, G. Kreisel, *Zeitschrift Fur Chemie* **1985**, *25*, 290.
[117] Y. Izumi, Y. Satoh, K. Urabe, *Chem. Lett.* **1990**, 795.
[118] E. Bolzacchini, R. Lucini, S. Meinardi, M. Orlandi, B. Rindone, *J. Mol. Catal. A-Chem.* **1996**, *110*, 227.
[119] S. Cenini, C. Crotti, M. Pizzotti, F. Porta, *J. Org. Chem.* **1988**, *53*, 1243.
[120] S. Cenini, F. Ragaini, M. Pizzotti, F. Porta, G. Mestroni, E. Alessio, *J. Mol. Catal.* **1991**, *64*, 179.
[121] V. L. K. Valli, H. Alper, *J. Am. Chem. Soc.* **1993**, *115*, 3778.
[122] C. V. Rode, S. P. Gupte, R. V. Chaudhari, C. D. Pirozhkov, A. L. Lapidus, *J. Mol. Catal.* **1994**, *91*, 195.
[123] B. K. Nefedov, V. I. Manovyuvenskii, V. A. Semikolenov, V. A. Likholobov, Y. I. Ermakov, *Kinet. Catal.* **1982**, *23*, 851.
[124] A. L. Lapidus, A. F. Lunin, S. D. Pirozhkov, N. B. Leonchik, P. Neittsel, K. Shvetlik, *Bull. Acad. of Sci. of USSR Div. Chem. Sci.* **1981**, *30*, 1068.
[125] B. M. Choudary, K. K. Rao, S. D. Pirozhkov, A. L. Lapidus, *J. Mol. Catal.* **1994**, *88*, 23.
[126] F. Ragaini, S. Cenini, *J. Mol. Catal. A-Chem.* **2000**, *161*, 31.
[127] S. Cenini, M. Pizzotti, C. Crotti, F. Porta, G. Lamonica, *J. Chem. Soc.-Chem. Commun.* **1984**, 1286.
[128] F. Ragaini, S. Cenini, F. Demartin, *Organometallics* **1994**, *13*, 1178.
[129] F. Shi, Y. D. He, D. M. Li, Y. B. Ma, Q. H. Zhang, Y. Q. Deng, *J. Mol. Catal. A-Chem.* **2006**, *244*, 64.
[130] E. Alessio, G. Mestroni, *J. Organomet. Chem.* **1985**, *291*, 117.
[131] E. Drent, EU 224292, **1987**.
[132] J. Stapersma, K. Steernberg, European pattent number 269.686, **1988**.
[133] E. Alessio, G. Mestroni, European pattent number 0169650, **1985**.
[134] H. Tietz, K. Unverferth, D. Sagasser, K. Schwetlick, *Zeitschrift Fur Chemie* **1978**, *18*, 141.

[135] E. Alessio, G. Mestroni, *J. Mol. Catal.* **1984**, *26*, 337.
[136] P. Gutlich, A. Hauser, H. Spiering, *Angew. Chem.-Int. Edit. Engl.* **1994**, *33*, 2024.
[137] R. Sieber, S. Decurtins, H. Stoeckli-Evans, C. Wilson, D. Yufit, J. A. K. Howard, S. C. Capelli, A. Hauser, *Chem.-Eur. J.* **2000**, *6*, 361.
[138] P. Leconte, F. Metz, EU 330.591, **1989**.
[139] R. Santi, A. M. Romano, P. Panella, G. Mestroni, IT MI96A 002072, **1996**.
[140] R. Santi, A. M. Romano, P. Panella, G. Mestroni, IT MI96A 000433, **1997**.
[141] E. I. du Pont, Nemour&Co, GB 991110, **1965**.
[142] E. Drent, EU 0231045A2, **1987**.
[143] E. Drent, *Pure Appl. Chem.* **1990**, *62*, 661.
[144] P. Wehman, G. C. Dol, E. R. Moorman, P. C. J. Kamer, P. W. N. M. van Leeuwen, J. Fraanje, K. Goubitz, *Organometallics* **1994**, *13*, 4856.
[145] P. Wehman, V. E. Kaasjager, W. G. J. de Lange, F. Hartl, P. C. J. Kamer, P. W. N. M. van Leeuwen, J. Fraanje, K. Goubitz, *Organometallics* **1995**, *14*, 3751.
[146] P. Wehman, L. Borst, P. C. J. Kamer, P. W. N. M. van Leeuwen, *J. Mol. Catal. A-Chem.* **1996**, *112*, 23.
[147] P. Wehman, L. Borst, P. C. J. Kamer, P. W. N. M. van Leeuwen, *Chem. Ber.-Recl.* **1997**, *130*, 13.
[148] P. Wehman, H. M. A. van Donge, A. Hagos, P. C. J. Kamer, P. W. N. M. van Leeuwen, *J. Organomet. Chem.* **1997**, *535*, 183.
[149] P. Wehman, P. C. J. Kamer, P. W. N. M. van Leeuwen, *Chem. Commun.* **1996**, 217.
[150] F. Ragaini, S. Cenini, *J. Mol. Catal. A-Chem.* **1996**, *109*, 1.
[151] R. Santi, A. M. Romano, F. Panella, C. Santini, *J. Mol. Catal. A-Chem.* **1997**, *127*, 95.
[152] R. Santi, A. M. Romano, F. Panella, G. Mestroni, A. Sessanti, A. S. o Santi, *J. Mol. Catal. A-Chem.* **1999**, *144*, 41.
[153] P. Leconte, F. Metz, A. Mortreux, J. A. Osborn, F. Paul, F. Petit, A. Pillot, *J. Chem. Soc.-Chem. Commun.* **1990**, 1616.
[154] F. Paul, J. Fischer, P. Ochsenbein, J. A. Osborn, *Angew. Chem.* **1993**, *32*, 1638.
[155] F. Paul, J. Fischer, P. Ochsenbein, J. A. Osborn, *C. R. Chim.* **2002**, *5*, 267.
[156] A. S. o Santi, B. Milani, G. Mestroni, E. Zangrando, L. Randaccio, *J. Organomet. Chem.* **1997**, *546*, 89.
[157] N. Masciocchi, F. Ragaini, S. Cenini, A. Sironi, *Organometallics* **1998**, *17*, 1052.
[158] F. Paul, J. Fischer, P. Ochsenbein, J. A. Osborn, *Organometallics* **1998**, *17*, 2199.
[159] A. S. o Santi, B. Milani, E. Zangrando, G. Mestroni, *Eur. J. Inorg. Chem.* **2000**, 2351.
[160] F. Ragaini, C. Cognolato, M. Gasperini, S. Cenini, *Angew. Chem.* **2003**, *42*, 2886.
[161] M. Gasperini, F. Ragaini, S. Cenini, E. Gallo, *J. Mol. Catal. A-Chem.* **2003**, *204*, 107.
[162] F. Ragaini, M. Gasperini, S. Cenini, *Adv. Synth. Catal.* **2004**, *346*, 63.
[163] M. Gasperini, F. Ragaini, C. Cazzaniga, S. Cenini, *Adv. Synth. Catal.* **2005**, *347*, 105.
[164] F. Ragaini, M. Gasperini, S. Cenini, L. Arnera, A. Caselli, P. Macchi, N. Casati, *Chem. Eur. J.* **2009**, *15*, 8064.
[165] F. Ragaini, *Dalton Trans.* **2009**, 6251.
[166] J. D. Gargulak, A. J. Berry, M. D. Noirot, W. L. Gladfelter, *J. Am. Chem. Soc.* **1992**, *114*, 8933.
[167] J. H. Grate, D. R. Hamm, D. H. Valentine, WO 86/05178, **1986**.
[168] S. J. Sherlock, D. C. Boyd, B. Moasser, W. L. Gladfelter, *Inorg. Chem.* **1991**, *30*, 3626.
[169] J. D. Gargulak, M. D. Noirot, W. L. Gladfelter, *J. Am. Chem. Soc.* **1991**, *113*, 1054.
[170] N. G. Gaylord, J. H. Crowdle, *Chem. Ind.* **1955**, 145.
[171] J. D. Gargulak, W. L. Gladfelter, *J. Am. Chem. Soc.* **1994**, *116*, 3792.
[172] S. J. Skoog, J. P. Campbell, W. L. Gladfelter, *Organometallics* **1994**, *13*, 4137.
[173] C. A. Tolman, *J. Am. Chem. Soc.* **1970**, *92*, 2953.
[174] C. A. Tolman, *Chem. Rev.* **1977**, *77*, 313.
[175] E. Zuidema, P. W. N. M. van Leeuwen, C. Bo, *Organomet.* **2005**, *24*, 3703.
[176] P. Dierkes, P. W. N. M. van Leeuwen, *J. Chem. Soc. Dalton Trans.* **1999**, 1519.

[177] C. P. Casey, G. T. Whiteker, *Isr. J. Chem.* **1990**, *30*, 299.
[178] W. L. Steffen, G. J. Palenik, *Inorg. Chem.* **1976**, *15*, 2432.
[179] T. Koizumi, A. Yamazaki, T. Yamamoto, *Dalton Trans.* **2008**, 3949.
[180] P. W. N. M. van Leeuwen, M. A. Zuideveld, B. H. G. Swennenhuis, Z. Freixa, P. C. J. Kamer, K. Goubitz, J. Fraanje, M. Lutz, A. L. Spek, *J. Am. Chem. Soc.* **2003**, *125*, 5523.
[181] M. N. Birkholz, Z. Freixa, P. W. N. M. van Leeuwen, *Chem. Soc. Rev.* **2009**, *38*, 1099.
[182] S. Pascual, P. de Mendoza, A. A. C. Braga, F. Maseras, A. M. Echavarren, *Tetrahedron* **2008**, *64*, 6021.
[183] P. W. N. M. van Leeuwen, P. C. J. Kamer, J. N. H. Reek, P. Dierkes, *Chem. Rev.* **2000**, *100*, 2741.
[184] J. H. Grate, D. R. Hamm, D. H. Valentine, US 4.600.793, **1983**.
[185] J. H. Grate, D. R. Hamm, D. H. Valentine, US 4.603.216, **1986**.
[186] J. H. Grate, D. R. Hamm, D. H. Valentine, WO 85/01285, **1985**.
[187] J. D. Gargulak, R. D. Hoffman, W. L. Gladfelter, *J. Mol. Catal.* **1991**, *68*, 289.
[188] J. D. Gargulak, W. L. Gladfelter, *Abstr. Pap. Am. Chem. Soc.* **1992**, *204*, 38.
[189] J. D. Gargulak, W. L. Gladfelter, *Inorg. Chem.* **1994**, *33*, 253.
[190] J. D. Gargulak, W. L. Gladfelter, *Organometallics* **1994**, *13*, 698.
[191] B. Moasser, C. Gross, W. L. Gladfelter, *J. Organomet. Chem.* **1994**, *471*, 201.
[192] S. J. Skoog, W. L. Gladfelter, *J. Am. Chem. Soc.* **1997**, *119*, 11049.
[193] S. Cenini, M. Pizzotti, C. Crotti, F. Ragaini, F. Porta, *J. Mol. Catal.* **1988**, *49*, 59.
[194] P. Wehman, PhD thesis, University of Amsterdam (UvA) (chapter 7), **1995**.
[195] P. Wehman, R. E. Rulke, V. E. Kaasjager, P. C. J. Kamer, H. Kooijman, A. L. Spek, C. J. Elsevier, K. Vrieze, P. W. N. M. van Leeuwen, *J. Chem. Soc.-Chem. Commun.* **1995**, 331.
[196] F. Paul, *Coord. Chem. Rev.* **2000**, *203*, 269.
[197] L. Barloy, R. M. Gauvin, J. A. Osborn, C. Sizun, R. Graff, N. Kyritsakas, *Eur. J. Inorg. Chem.* **2001**, 1699.
[198] E. Alessio, G. Zassinovich, G. Mestroni, *J. Mol. Catal.* **1983**, *18*, 113.
[199] G. Mestroni, G. Zassinovich, C. Delbianco, A. Camus, *J. Mol. Catal.* **1983**, *18*, 33.
[200] E. Alessio, F. Vinzi, G. Mestroni, *J. Mol. Catal.* **1984**, *22*, 327.
[201] E. Alessio, G. Clauti, G. Mestroni, *J. Mol. Catal.* **1985**, *29*, 77.
[202] G. Clauti, G. Zassinovich, G. Mestroni, *Inorg. Chim. Acta* **1986**, *112*, 103.
[203] B. Milani, A. Anzilutti, L. Vicentini, A. S. o Santi, E. Zangrando, S. Geremia, G. Mestroni, *Organometallics* **1997**, *16*, 5064.
[204] B. Milani, G. Corso, E. Zangrando, L. Randaccio, G. Mestroni, *Eur. J. Inorg. Chem.* **1999**, 2085.
[205] B. Milani, A. Marson, E. Zangrando, G. Mestroni, J. M. Ernsting, C. J. Elsevier, *Inorg. Chim. Acta* **2002**, *327*, 188.
[206] F. Ragaini, T. Longo, S. Cenini, *J. Mol. Catal. A-Chem.* **1996**, *110*, L171.
[207] F. Ragaini, M. Macchi, S. Cenini, *J. Mol. Catal. A-Chem.* **1997**, *127*, 33.
[208] E. Gallo, F. Ragaini, S. Cenini, F. Demartin, *J. Organomet. Chem.* **1999**, *586*, 190.
[209] F. Ragaini, A. Ghitti, S. Cenini, *Organometallics* **1999**, *18*, 4925.
[210] M. Gasperini, F. Ragaini, S. Cenini, *Organometallics* **2002**, *21*, 2950.
[211] M. Gasperini, F. Ragaini, C. Remondini, A. Caselli, S. Cenini, *J. Organomet. Chem.* **2005**, *690*, 4517.
[212] A. Maldotti, R. Amadelli, L. Samiolo, A. Molinari, A. Penoni, S. Tollari, S. Cenini, *Chem. Commun.* **2005**, 1749.
[213] F. Ferretti, F. Ragaini, R. Lariccia, M. Gallo, S. Cenini, *Organometallics* **2010**, *29*, 1465.
[214] D. P. N. Satchell, R. S. Satchell, *Chem. Soc. Rev.* **1975**, *4*, 231.
[215] R. G. Arnold, J. A. Nelson, J. J. Verbanc, *Chem. Rev.* **1957**, *57*, 47.
[216] S. Cenini, M. Pizzotti, F. Porta, G. Lamonica, *J. Organomet. Chem.* **1975**, *88*, 237.
[217] M. Spirkova, M. Kubin, P. Spacek, I. Krakovsky, K. Dusek, *J. Appl. Polym. Sci.* **1994**, *53*, 1435.
[218] R. P. Tiger, L. I. Sarynina, S. G. Entelis, *Uspekhi Khimii* **1972**, *41*, 1672.

[219] A. K. Zhitinkina, N. A. Shibanova, O. G. Tarakanov, *Uspekhi Khimii* **1985**, *54*, 1866.
[220] S. Cenini, C. Crotti, M. Pizzotti, *in: R. Ugo (Ed.), Aspects in Homogeneous Catalysis, Vol. 6*, Dordrecht, **1988**.
[221] B. K. Nefedov, V. I. Manoviuvenskii, S. S. Novikov, *Dokl. Akad. Nauk SSSR* **1977**, *234*, 1343.
[222] B. Elleuch, Y. Bentaarit, J. M. Basset, J. Kervennal, *Angew. Chem.* **1982**, *21*, 687.
[223] S. Bhaduri, H. Khwaja, N. Sapre, K. Sharma, A. Basu, P. G. Jones, G. Carpenter, *J. Chem. Soc.-Dalton Trans.* **1990**, 1313.
[224] C. H. Liu, C. H. Cheng, *J. Organomet. Chem.* **1991**, *420*, 119.
[225] S. Bhaduri, H. Khwaja, K. Sharma, P. G. Jones, *J. Chem. Soc.-Chem. Commun.* **1989**, 515.
[226] H. Alper, K. E. Hashem, *J. Am. Chem. Soc.* **1981**, *103*, 6514.
[227] G. Mestroni, G. Zassinovich, E. Alessio, M. Tornatore, *J. Mol. Catal.* **1989**, *49*, 175.
[228] K. Nomura, *J. Mol. Catal. A*. **1998**, *130*, 1.
[229] J. E. Yanez, A. B. Rivas, J. Alvarez, M. C. Ortega, A. J. Pardey, C. Longo, R. P. Feazell, *J. Coord. Chem.* **2006**, *59*, 1719.
[230] T. Kajimoto, J. Tsuji, *Bul. Chem. Soc. Jpn.* **1969**, *42*, 827.
[231] Smolinsk.G, B. I. Feuer, *J. Org. Chem.* **1966**, *31*, 3882.
[232] M. Akazome, T. Kondo, Y. Watanabe, *J. Org. Chem.* **1994**, *59*, 3375.
[233] R. Waterman, G. L. Hillhouse, *J. Am. Chem. Soc.* **2008**, *130*, 12628.
[234] R. Waterman, G. L. Hillhouse, *J. Am. Chem. Soc.* **2003**, *125*, 13350.
[235] D. J. Mindiola, G. L. Hillhouse, *J. Am. Chem. Soc.* **2001**, *123*, 4623.
[236] A. Marson, A. B. van Oort, W. P. Mul, *Eur. J. Inorg. Chem.* **2002**, *11*, 3028.
[237] T. J. Mooibroek, E. Bouwman, M. Lutz, A. L. Spek, E. Drent, *Eur. J. Inorg. Chem.* **2010**, 298.
[238] T. J. Mooibroek, M. Lutz, A. L. Spek, E. Bouwman, **2010**, *39*, 11027.
[239] T. J. Mooibroek, L. Schoon, E. Bouwman, E. Drent, *Chem. Eur. J.* **2011**, DOI: 10.1002/chem.201100923.
[240] T. J. Mooibroek, E. Bouwman, E. Drent, *Organometallics* **2011**, submitted.
[241] T. J. Mooibroek, W. Smit, E. Bouwman, E. Drent, **2011**, to be submitted.
[242] T. J. Mooibroek, E. Bouwman, E. Drent, **2011**, to be submitted.

Chapter 2

Complex formation and structure

Abstract: In this chapter the synthetic pathways towards Pd^{II} complexes of functionalized bidentate diphenylphosphane ligands of the type [Pd(ligand)(anion)$_2$] and [Pd(ligand)$_2$](anion)$_2$ is described. Eighteen different ligands have been used in combination with strongly (acetate, OAc^-) or weakly (tosylate, OTs^-) coordinating anions. Of some representative complexes the solid state structure was determined with X-ray crystallography. It is shown that the solid state structures are fully retained in solution. The formation of [Pd(ligand)(anion)$_2$]-type complexes was studied in detail using ^{1}H- and ^{31}P-NMR spectroscopy.
Depending on the ligand structure the complex is formed instantaneously, *via* a polynuclear intermediate or is not formed at all. Complex formation is demonstrated to depend on the length and rigidity of the ligand backbone, and on the steric bulk at the ortho position of the phenyl rings on phosphorus. It was also found that the coordinating ability of the anions can alter the structure of the kinetic and/or the thermodynamic product.

2.1 Introduction

For some decades, Pd^{II}-diphosphane catalytic systems have enjoyed much attention, both from academia and industry. Especially the copolymerization of CO and ethene has been widely studied[1, 2] and applied (Carilon®(Shell) and Ketonex® (BP)) using such catalytic systems. A reaction, in which these palladium catalysts are relatively poorly studied, is the carbonylation of nitroaromatic molecules to aromatic isocyanates.[3-8] For this reaction most endeavours involve catalysts of the type $[Pd^{II}(1,10\text{-phenanthroline})_2](anion)_2$,[4-8, 10-19] and only few involve catalysts of the type P_2Pd^{II}.[4, 17, 20, 21] Since there is no fundamental reason why N_2Pd^{II} complexes should perform better than P_2Pd^{II} complexes, in the present thesis the focus lies on studying these palladium-phosphane complexes in the carbonylation of nitrobenzene. In many catalytic studies the catalyst is often formed *in situ* by mixing a palladium^{II} salt with a diphosphane ligand in methanol, assuming that the desired [Pd(diphosphane)$(anion)_2$]-type complexes are actually formed. However, complex formation is not always a trivial process. For example, for the copolymerization of CO and ethene it has been reported that the catalytic performance of *in situ* formed catalysts may be inferior to that of the preformed catalysts.[23]

It has also been reported that when $[Pd(OAc)_2]$ and an equimolar amount of dppe (1,2-bis(diphenylphosphanyl)ethane) are dissolved in CD_3OD, initially the catalytically inactive complex $[Pd(dppe)_2](OAc)_2$ is formed; only after standing for about 24 hours, the catalytically active species $[Pd(dppe)(OAc)_2]$ is obtained.[24]

To the best of my knowledge, there is no simple way to predict the exact kinetic pathway *via* which a certain ligand will or will not form the desired [Pd(diphosphane)$(anion)_2$]-type complex. Therefore, the present chapter describes a study to determine the influence of the bridging groups and substituents in chelating diphosphane ligands (see Table 2.1) on the kinetics and the result of complex formation. Furthermore, the role of the anion in the complex formation process was investigated by using acetate (strongly coordinating) and tosylate (weakly coordinating) anions. Prior to this, however, the synthesis of this type of complexes is reported, followed by their structural characteristics in the solid phase and in solution.

Table 2.1. Schematic representation of the ligands used in this study. The inset figures show the general structures.

Code	X	R	Schematic drawing
L2	H		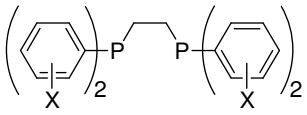
oMeO-L2	*o*-MeO		
oEtO-L2	*o*-EtO		
L3	H	H	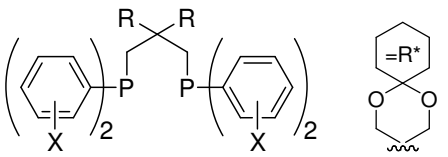
L3X	H	CH_3	
oMe-L3	*o*-Me	H	
oMeO-L3	*o*-MeO	H	
oEtO-L3	*o*-EtO	H	
pMeO-L3	*p*-MeO	H	
oMeO-L3X	*o*-MeO	CH_3	
oMeO-L3X[2]	*o*-MeO	CH_2CH_3	
oEtO-L3X[2]	*o*-EtO	CH_2CH_3	
oMeO-L3X[R]	*o*-MeO	R*	
L4	H	H	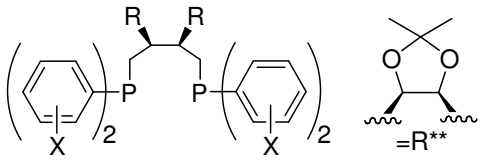
oMeO-L4	*o*-MeO	H	
oEtO-L4	*o*-EtO	H	
pMeO-L4	*p*-MeO	H	
L4X	H	R**	
oMeO-L4X	*o*-MeO	R**	

2.2 Results and discussion

2.2.1. Complex synthesis

Starting from crystalline $[Pd_3(OAc)_6]$,[25] four solvents were employed in the complex synthesis. In order of increasing polarity these are: $CHCl_3$, CH_2Cl_2, $(CH_3)_2CO$ and CH_3OH. The methods by which the desired complexes can successfully be obtained are summarized schematically in Figure 2.1. However, some difficulties were encountered in the synthesis and isolation of these complexes. Dry and degassed solvents must be used as too much water generally hampered the isolation due to the formation of an oil and partial oxidation of the ligand. Furthermore, the flasks were wrapped in foil; the absence of light in most cases prevented plating of Pd^0. The choice of the solvent appeared to be most important. $CHCl_3$ must be avoided since severe plating was usually observed when working with this solvent. CH_2Cl_2 and $(CH_3)_2CO$ were best suited for the synthesis of the monochelate [Pd(ligand)(anion)$_2$]–type complexes. Methanol is the only solvent in which the bischelate [Pd(ligand)$_2$](OAc)$_2$–type complexes can

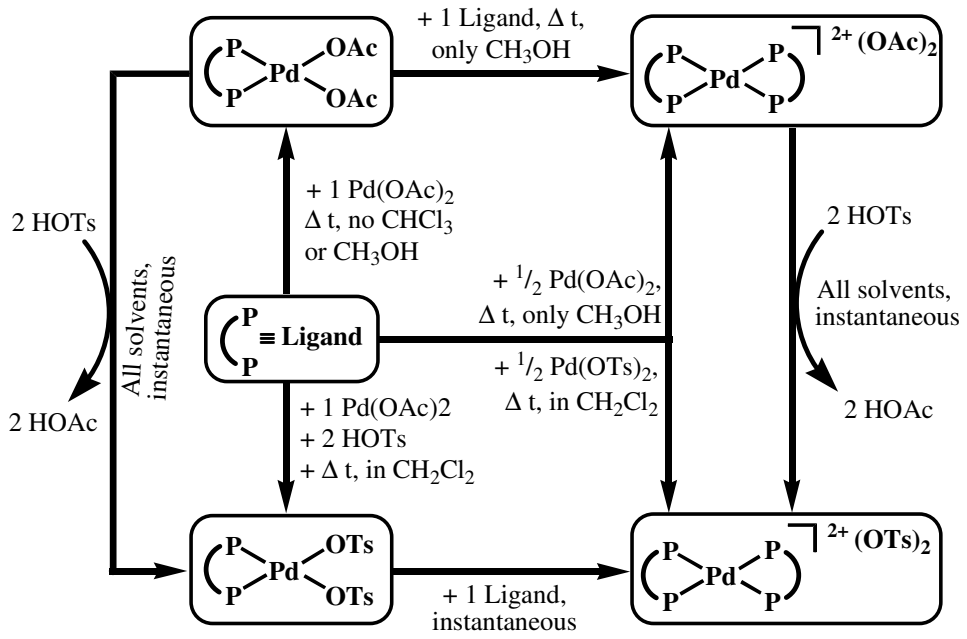

Figure 2.1. Schematic overview of the synthetic methods to form the monochelate complex [Pd(ligand)(anion)$_2$] or the bischelate complex [Pd(ligand)$_2$](anion)$_2$ with acetate or tosylate anions.

be synthesized; the other solvents are not polar enough to sufficiently dissociate the OAc^- anions. The bischelate complexes [Pd(ligand)$_2$](OTs)$_2$ can be prepared in all four solvents.

Not all complexes form instantaneously. Indeed, in some cases the desired complex is formed only after several hours (see complex formation studies for details). Therefore, depending on the ligand, the reaction mixture should stand for an appropriate amount of time (usually overnight), as otherwise a mixture of species may be isolated.

Once the monochelate or bischelate complex had been formed with the acetate anions, addition of two equivalents of *p*-toluenesulfonic acid resulted in the quantitative replacement of the anions in any of the solvents, as evidenced by the appearance of a peak around 1.0 ppm for acetic acid.
The 1,4-butyl bridged ligands present a special case. When applying the procedure of Mul and co-workers,[24] the unsubstituted ligand L4 yielded the monochelate complex. This was not the case for oMeO-L4 and oEtO-L4. When a

solution of $Pd(OAc)_2$ was added to oMeO-L4, a clear yellow solution was formed immediately. However, after standing for two minutes, a yellow precipitate formed, which turned red-brown over time. The isolated solid proved to be insoluble in a vast variety of different solvents, indicating that this solid is a coordination polymer. When a solution of $Pd(OAc)_2$ was added to oEtO-L4, a mixture of species was formed (several ^{31}P-resonances), which did not change over time. No attempts were made to further characterize these compounds.

Not all complexes were isolated and fully characterized; some were only detected in situ during the NMR studies. Nevertheless, for convenience, in Table S1 the proton and phosphorus resonances of all the palladium complexes that could be measured are summarized. The monochelate complexes are indicated as M(x)A or M(x)T with ligand x and coordinating acetate or tosylate anions, respectively, whereas the bischelate complexes are indicated as B(x)A or B(x)T with ligand x and non-coordinating acetate or tosylate anions.

2.2.2. Complex structures in the solid state

Light yellow transparent single crystals of the compounds $[Pd(oMeO\text{-}L2)(OAc)_2]$ (M(oMeO-L2)A), $[Pd(MeO\text{-}L3)(OAc)_2]$ (M(MeO-L3)A), $[Pd(MeO\text{-}L3X)(OAc)_2]$ (M(MeO-L3X)A), $[Pd(MeO\text{-}L3X^R)(OAc)_2]$ (M(MeO-L3X^R)A), and $[Pd(MeO\text{-}L3X)_2](OTs)_2$ (B(oMeO-L3X)T) were obtained using the solvent diffusion technique. The crystal structures were determined by X-ray diffraction; crystallographic data and details of the structure refinement are given in Table **2.2**. Perspective views of the molecular structures of M(oMeO-L3X)A and B(oMeO-L3X)T in the crystal are shown in Figure 2.2. Since the global structures of the monochelate complexes are very similar, projections of the complexes

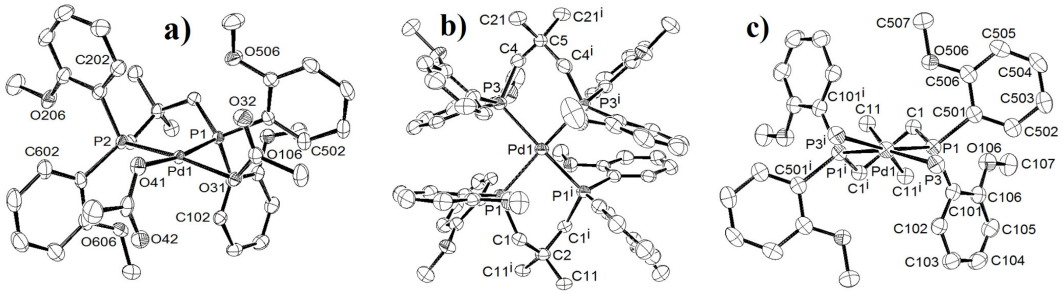

Figure 2.2. Displacement ellipsoid plots (50% probability level). a: $[Pd(oMeOL3X)(OAc)_2]$ (front view); b: cation of $Pd(oMeOL3X)_2](OTs)_2$ (top view); c: cation of $[Pd(oMeOL3X)_2](OTs)_2$ (front view along the twofold axis, one ligand omitted, except for the phosphorus atoms). Hydrogen atoms, uncoordinated anions and uncoordinated solvent molecules are omitted for clarity. Symmetry operation i: 1-*x*, *y*, 0.5-*z*.

M(oMeO-L2)A, M(oMeO-L3)A and M(oMeO-L3X^R)A can be found in the Supporting Information. Selected bond distances, angles and torsion angles are listed in

Table 2.2. Selected interatomic distances, angles, and other relevant geometric data for complexes M(oMeO-L2)A, M(oMeO-L3)A, M(oMeO-L3X)A, M(oMeO-L3X^R)A, and B(oMeO-L3X)T.

Complex:	**M(oMeO-L2)A***	**M(oMeO-L3)A**	**M(oMeO-L3X)A**	**M(oMeO-L3X^R)A**	**B(oMeO-L3X)T***	
	(pseudo) coordination [Å]					
$Pd_1 – P_1$	2.2177(6)	2.2223(6)	2.2366(6)	2.2341(8)	2.4091(8)	
$Pd_1 – P_2$		2.2273(5)	2.2305(5)	2.2254(8)		
$Pd_1 – P_3$					2.3938(9)	
$Pd_1 – O_{31}$	2.0984(14)	2.1112(14)	2.0891(13)	2.047(2)		
$Pd_1 – O_{41}$		2.0946 (13)	2.0936(15)	2.064(2)		
$Pd_1 – O_{32}$	2.9169(17)	2.8662(19)	3.1771(16)	3.099(2)		
$Pd_1 – O_{42}$		2.8067(19)	3.0718(16)	3.153(2)		
	*anagostic interactions [Å]***					
$Pd_1 \cdots H_{102}$	2.75	2.72	2.87	2.82	3.03	
$Pd_1 \cdots H_{202}$		2.69	2.75	2.71		
$Pd_1 \cdots H_{302}$					3.06	
	*C-H•••π interactions [Å]***					
$H_{502} \cdots C_{101}$	2.57	2.70	2.53	2.59	2.66	
$H_{502} \cdots C_{106}$	2.77	2.82	2.53	2.72	2.63	
$H_{602/702} \cdots C_{201/301}$		2.61	2.55	2.54	2.67	
$H_{602/702} \cdots C_{206/306}$		2.59	2.66	2.68	2.82	
	Angles [°]					
$P_3 – Pd_1 – P_{3'}$					86.04(3)	
$P_1 – Pd_1 – P_3$					95.71(3)	
$P_1 – Pd_1 – P_{3'}$					166.56(3)	
$P_1 – Pd_1 – P_{2/1'}$	85.98(3)	95.497(19)	90.62(2)	92.22(3)	85.69(4)	
$O_{31} – Pd_1 – O_{41/31'}$	92.22(8)	87.03(5)	92.20(6)	94.97(9)		
$P_1 – Pd_1 – O_{41}$	90.91(5)	90.78(4)	90.38(4)	87.00(6)		
$P_2 – Pd_1 – O_{42}$		87.14(4)	87.70(4)	86.24(6)		
$P_1 – Pd_1 – O_{41/31'}$	176.69(4)	174.80(4)	170.96(4)	172.80(6)		
$P_2 – Pd_1 – O_{31}$		171.72(4)	174.09(4)	176.36(6)		
$Pd_1 – O_{31} – C_{31}$	111.28(14)	108.29(13)	121.81(13)	117.90(18)		
$Pd_1 – O_{41} – C_{41}$		107.86(12)	117.96(14)	120.6(2)		
$Pd_1 – O_{32} – C_{31}$	73.80(14)	74.79(14)	68.60(12)	67.53(18)		
$Pd_1 – O_{42} – C_{41}$		75.65(14)	70.89(13)	68.40(18)		
	Dihedral angles between the PdP_2 and the PdX_2 planes [°]					
$PdP_2 – PdX_2$ (dihedral)	1.56(7), X = O	7.22(8), X = O	10.46(6), X = O	7.63(9), X = O	19.78(5), X = P	
	*Cremer-Pople ring puckering parameters for the PdP_2C_2 and PdP_2C rings****					
					Ring 1	Ring 2
Q_2 [Å]	0.492(2)	0.5247(19)	0.8588(17)	0.812(2)	0.906(3)	0.898(3)
Q_3 [Å]		0.3266(19)	-0.0369(16)	0.051(2)	0.000(2)	0.000(3)
θ [°]		58.09(18)	92.46(11)	86.42(14)	90.00(13)	90.00(19)
φ_2 [°]	270.00(12)	156.4(2)	266.99(11)	82.57(16)	270.00(14)	270.00(14)
	Torsion angles [°]					
$Pd_1 – P_1 – C_{101} – C_{102}$	-7.1(2)	-4.95(18)	-1.38(18)	11.5(3)	6.1(3)	
$Pd_1 – P_2 – C_{201} – C_{202}$		-5.67(19)	-1.8(2)	8.3(3)		
$Pd_1 – P_3 – C_{301} – C_{302}$					13.0(3)	
$Pd_1 – P_1 – C_{501} – C_{502}$	102.30(18)	-104.51(18)	105.15(18)	-113.0(3)	120.0(3)	
$Pd_1 – P_2 – C_{601} – C_{602}$		-102.44(17)	104.54(17)	-108.1(3)		
$Pd_1 – P_3 – C_{701} – C_{702}$					101.7(3)	

[*] Coordination rings are located on twofold axis. [**] Hydrogen atoms were introduced in calculated positions based on a C-H distance of 0.95 Å. [***] Cremer-Pople ring puckering parameters for the PdP_2C_2 and PdP_2C rings.[22]

Table **2.2**.
Complexes M(oMeO-L2)A and B(oMeO-L3X)T are located on twofold rotation axes, respectively, running through the palladium centre and the central carbon atom(s) of the ligand backbone. Hence, M(oMeO-L2)A has only one unique phosphorus atom, and B(oMeO-L3X)T only two. The palladium centers in the complexes M(oMeO-L2)A, M(oMeO-L3)A, M(oMeO-L3X)A, M(oMeO-L3X^R)A, and B(oMeO-L3X)T are in distorted square-planar geometries with *cis*-P_2O_2 donor sets for the monochelate complexes and a P_4 donor set for the bischelate complex. The Pd–P and Pd–O distances can be considered as normal.[26] Although the acetate anions are coordinated in a monodentate fashion, they may be considered pseudo-chelating with their second O-atom at distances to Pd ranging between 2.8067(19) (M(oMeO-L3)A) and 3.1771(16) (M(oMeO-L3X)A) Å, and Pd–O–C angles ranging between 67.53(18)° (M(oMeO-L3X^R)A) and 75.65(14)° (M(oMeO-L3X)A). The magnitude of the distortion from the ideal square-planar geometry varies considerably. The dihedral angle between the P–Pd–P and X–Pd–X (X = P or O) planes range from 1.56(7)° in M(oMeO-L2)A, to 7.22(8)-10.46(6)° in M(oMeO-L3)A, M(oMeO-L3X)A, and M(oMeO-L3X^R)A, and is 19.78(5)° in the bischelate complex B(oMeO-L3X)T. The large tetrahedral distortion in B(oMeO-L3X)T is due to the presence of large steric bulk of two ligands around the palladium centre; there are no other intermolecular or intramolecular contacts responsible for this distortion. The ligand bite angles also vary considerably. The ethylene bridged ligand oMeO-L2 in M(oMeO-L2)A has a bite angle of 85.98(3)°, whereas the propylene bridged ligand L7 in M(oMeO-L3)A has a bite-angle of 95.497(19)°. This angle is slightly compressed by the addition of steric bulk to the backbone, resulting in 90.62(2)° in M(oMeO-L3X)A and 92.22(3)° in M(oMeO-L3X^R)A. In the bischelate complex B(oMeO-L3X)T, the angle is compressed even further to a mere 85.69(4)°. The six-membered PdP_2C_2 coordination rings in M(oMeO-L3X)A, M(oMeO-L3X^R)A, and B(oMeO-L3X)T have a twist-boat and in M(oMeO-L3)A a screw-boat conformation, while the five-membered PdP_2C ring in M(oMeO-L2)A has a half-chair conformation.

It is possible to distinguish the two aryl rings on each phosphorus atom as oriented either axially (for the NMR discussion denoted as rings 100, 200, 300, and 400) or equatorially (rings 500, 600, 700, and 800) with respect to the chelate ring of the bidentate ligand (see for example rings 100 and 500 in Figure 2a and 2c). The axial phenyl rings are held in place by Pd···H interactions between its

ortho proton and the filled palladium d_z^2 orbital. Similar interactions have been reported for related nickel and palladium complexes.[27, 28] These interactions have been described as anagostic,[29] and are characterized by a Pd–P–C–C torsion angle close to 0°. The Pd···H distances (between 2.71 (M(oMeO-L3X^R)A) and 3.06 Å (B(oMeO-L3X)T)), and the Pd–P–C–C torsion angles (between 1.38(18)° (M(oMeO-L3X)A) and 11.5(3)° (M(oMeO-L3X^R)A)) of the observed anagostic interactions, can be considered as normal.[28] Furthermore, relatively strong intramolecular C-H···π interactions between the *ortho* protons of the equatorial rings (H502, H602, H702) and one π-bond of the axial rings (C101/C106, C201/C206, C301/C306) are observed.[30] The various H···C distances, ranging between 2.527 (for M(oMeO-L3X)A) and 2.817 (for M(oMeO-L3)A) Å, are well within the sum of the van der Waals radii of H and C (2.90 Å).

The structures of the complexes [Pd(L2)OAc$_2$],[31] [Pd(oMeO-L2)Cl$_2$] and [Pd(oMeO-L3)Cl$_2$],[32] as well as of the analogous nickel^{II} complexes [Ni(oMeO-L3)I$_2$][27] and [Ni(oMeO-L3)Cl$_2$][33] have been published; the reported distances, angles and Pd···H or Ni···H interactions are comparable to those described above.

2.2.3. Complex structures in solution

As typical examples, the ^{1}H-NMR-spectra of the monochelate complexes M(oMeO-L3X^R)A and M(oMeO-L3X^R)T are shown in Figure 2.3a and 2.3c respectively (in $(CD_3)_2CO$)). In the solid-state structures, the two phenyl rings on each phosphorus atom are distinct with respect to their orientation to the plane of coordination and have been labelled as axial or equatorial. In solution at room temperature, however, only one set of resonances is observed, as is shown in Figure 2.3a for M(oMeOL3X^R)A. The observation that the two phenyl rings appear to be equivalent in solution is due to dynamic flipping of the backbone.[27] When this flipping is frozen at low temperature, the axial and equatorial protons become inequivalent; two sets of proton resonances are observed in ^{1}H-NMR spectra (Figure 2.3b). The proton resonances of the axial phenyl rings are relatively deshielded due to the Pd···H interactions, whereas the proton resonances of the equatorial phenyl rings are shielded due to the H···Cπ interactions.

For the monochelate complex M(oMeO-L3X^{R})T with the weakly-coordinating OTs^{-} anions (Figure 2.3c) a different phenomenon is observed upon cooling; the peaks are not split, but broadened (Figure 2.3d). It suggests that the weakly-coordinating OTs^{-} anions are displaced with solvent molecules; the Pd^{II} ion is in a [Pd(ligand)(solvent)$_2$]$^{2+}$ coordination sphere and even at low temperatures the coordinated solvent ligands are quickly exchanged with other solvent molecules, thus decreasing the steric hindrance for the flipping of the backbone. Further cooling should result in a complete splitting into two sets of protons. In contrast, the presence of relatively strongly coordinating OAc^{-} anions in M(oMeO-L3X^{R})A makes the overall complex more rigid at lower temperature, thereby hindering the dynamic flipping of the backbone. In the case of the crowded [Pd(ligand)$_2$](anion)$_2$ complexes, two sets of proton resonances are observed at all temperatures. Their spectra resemble the one shown in Figure 2.3b.

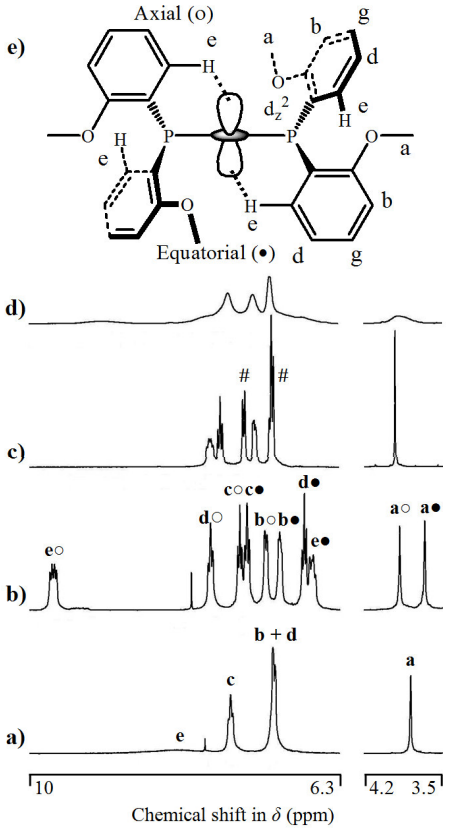

Figure 2.3. ^{1}H-NMR spectra of monochelate complexes in $(CD_3)_2CO$: a) M(oMeO-L3X^{R})A at 23 °C; b) M(oMeO-L3X^{R})A at –60 °C; c) M(oMeO-L3X^{R})T at 23 °C; d) M(oMeO-L3X^{R})T at –60°C; e) schematic view of the interactions and labeling of the H atoms. An '●' indicates that the resonance belongs to an equatorially aligned ring, 'o' indicates that the resonance belongs to an axially aligned ring, and '#' indicates a resonance from a tosylate anion.

2.2.4. Complex formation studies

2.2.4.1 General

NMR-studies were performed to explore the kinetics of formation of the palladium complexes of different types of ligands in more detail. Using $Pd(OAc)_2$, the complex formation was studied in the deuterated solvents CD_2Cl_2, $(CD_3)_2CO$, and CD_3OD. When using $Pd(OTs)_2$ the only suitable solvent is a

Table 2.3. Overview of complex formation studies, monitored with ^{1}H and ^{31}P NMR spectroscopy.[a]

Entry	Ligand	$Pd(OAc)_2$ CD_3OD	$Pd(OAc)_2$ $(CD_3)_2CO$	$Pd(OAc)_2$ CD_2Cl_2	$Pd(OTs)_2$ CD_2Cl_2[b]
1	L2	b→m (0.44)	m	m	(b in CD_3OD)[9]
2	oMeO-L2	m + b	m	m	
3	oEtO-L2	m + b	m	m	
4	L3	m	m	m	b→m (6.23)
5	L3X	m	m	m	
6	oMe-L3	i	p→m (1.03)	m	
7	oMeO-L3	p→m (0.07)[b]	p→m (0.49)	p→m (0.53)	b→m (0.01)[c]
8	oEtO-L3	i	p→m (0.25)	p→m (1.00)	
9	pMeO-L3	m	m	m	
10	oMeO-L3X	m	m	m	
11	oMeO-L3X^2	m	m	m	
12	oEtO-L3X^2	m	m	m	
13	oMeO-L3X^R	i	m	m	
14	L4			p→m (1.07)	m
15	oMeO-L4	i	i	p→x (1.26)	
16	oEtO-L4	i	i	p→x (0.58)	
17	pMeO-L4			p→m (1.15)	
18	L4X			m	
19	oMeO-L4X			m	

[a] $[Pd(OAc)_2]$ or [Ligand] = 16 mM. The values between parentheses represent a reaction constant (k' in h^{-1}, see experimental section) for the observed conversion. m = monochelate complex; b = bischelate complex; p = polynuclear complex; x = unidentified complex(es); i = ligand or complex is insoluble. See text for further explanation. [b] 17% ($^{v}/_{v}$) of $(CD_3)_3CO$ in CD_2Cl_2 was actually used due to solubility problems. [c] the complex formation was accompanied by plating over time.

mixture of $(CD_3)_2CO$ in CD_2Cl_2 (17% *v/v*); $Pd(OTs)_2$ is immediately reduced in CD_3OD, HOTs and $Pd(OTs)_2$ are insoluble in pure CD_2Cl_2, and most $[Pd(ligand)_2](OTs)_2$-type complexes are insoluble in $(CD_3)_2CO$. An overview of the results of selected complex formation studies is presented in Table 2.3. During these studies a variety of complexes were observed *in situ*, but were not isolated. Nonetheless, an overview of the ^{1}H- and ^{31}P-NMR data of all the detected complexes is given in Appendix I.

2.2.4.2. Ethylene-bridged ligands

Use of the ethylene-bridged ligands (L2, oMeO-L2, and oEtO-L2) directly results in the formation of the monochelate complex [Pd(ligand)(OAc)2] when the reaction is performed in $(CD_3)_2CO$ or CD_2Cl_2 (entries 1-3). In CD_3OD however, as reported by Mul and co-workers,[24] L2 initially forms the bischelate complex (δ_P = 58.7 ppm) as the kinetic product, which converts to the thermodynamically

more stable monochelate complex (δ_P = 63.7 ppm) over time (k' = 0.44 h^{-1}). In the case of the sterically more demanding ligands oMeO-L2 and oEtO-L2, in CD_3OD the monochelate complex is formed directly as the major species (~ 70%). The other product is the bischelate complex (~ 30%). The composition of this mixture did not change over time (eight hours), nor upon addition of another 0.2 equivalents of $Pd(OAc)_2$. This indicates that the oMeO moieties on the ligand shield the palladium in the bischelate complex from OAc^- coordination. It thus appears that ethylene-bridged ligands directly form the monochelate complex, except in a relatively polar solvent. Only then the OAc^- anions may dissociate from Pd^{II} to allow a second ligand to coordinate, thus forming the bischelate complex. Indeed, it has been reported that by employing the weakly-coordinating OTs^- anions, the bischelate complex is formed exclusively.[24]

2.2.4.3. Propylene-bridged ligands

For the ligands with an unsubstituted propylene backbone (entries 4 and 6-9) different behaviour is observed when starting from $Pd(OAc)_2$. In the case of L3, the monochelate complex is formed immediately in all solvents. However, the *ortho*-methoxy analogue of this ligand (oMeO-L3) forms the monochelate complex *via* an intermediate species, as is illustrated in Figure 2.4 (in CD_2Cl_2).

This intermediate is not the usual bischelate complex, since the characteristic resonances of the axial and equatorial (*ortho*) protons are not observed. In the NMR spectra of this intermediate, no free ligand ^{31}P resonance is observed at −37 ppm, and several resonances are observed for the *ortho*-methoxy protons (3.3 – 3.9 ppm). The resonances around 1.8 and 0.6 ppm are indicative of different types of OAc^- anions. These observations suggest the formation of a polynuclear species, which could be either a polymeric compound $[Pd(oMeO\text{-}L3)(OAc)_2]_n$ in which the ligand is monodentate and bridging, or a dinuclear complex $[\{Pd(oMeO\text{-}L3)(OAc)\}_2(oMeO\text{-}L3)](OAc)_2$. The intermediate species could be isolated, but a mass higher than that of the monochelate complex could not be detected using ESI mass spectroscopy.

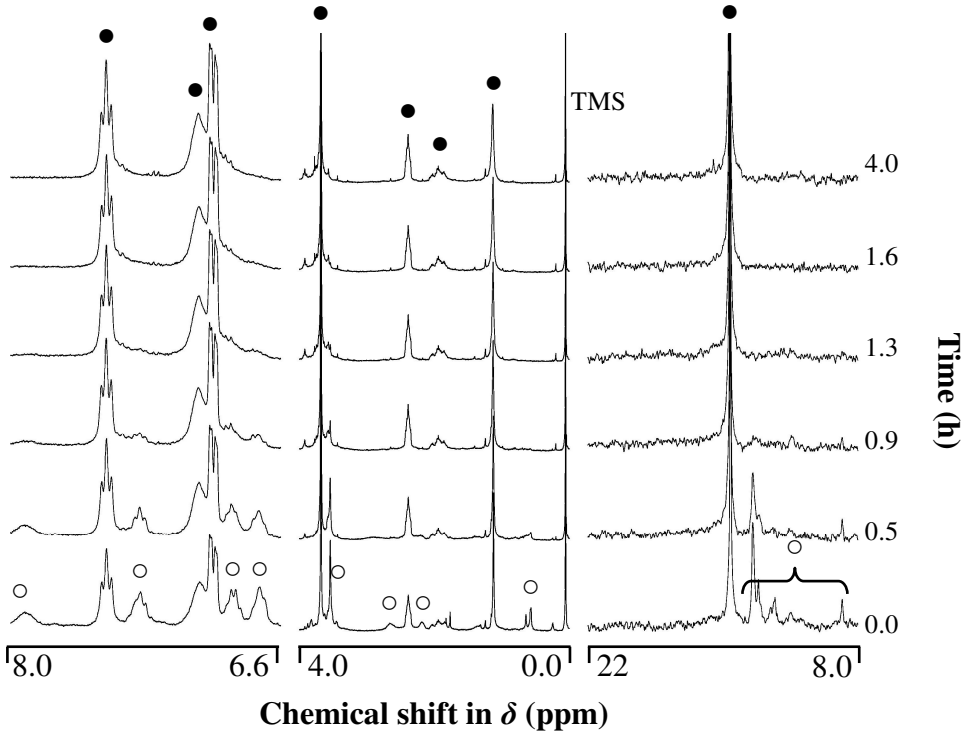

Figure 2.4. Complex-forming study followed by ^{1}H- and ^{31}P-NMR; [Pd(OAc)$_2$] in CD_2Cl_2 added to **oMeO-L3**. ● = resonance of the (thermodynamic) monochelate complex; ○ = resonance of the (kinetic) intermediate.

To investigate whether the difference in behaviour of the ligands L3 and oMeO-L3 is due to steric or electronic reasons, a series with increased steric bulk on the *ortho* position was studied; L3 (H), oMe-L3 (Me), oMeO-L3 (MeO), and oEtO-L3 (EtO). The same type of intermediate is observed for these ligands (entries 6-8) in $(CD_3)_2CO$; the conversion to the monochelate complex follows approximate first-order kinetics (see Figure 2.5). An increase in steric bulk results in a lower p → m conversion rate, with *k'* = 1.03, 0.49, and 0.25 h^{-1} for oMe-L3, oMeO-L3, and oEtO-L3, respectively. Apparently, in the proposed intermediate polynuclear species, the larger steric '*ortho*-bulk' of the ligand shields the palladium d_z^2 orbital (see also Figure 2.3e) for the approach of a phosphane (in the case of [Pd(L)(OAc)$_2$]$_n$) or an acetate anion (in the case of [{Pd(L)(OAc)}$_2$L](OAc)$_2$).

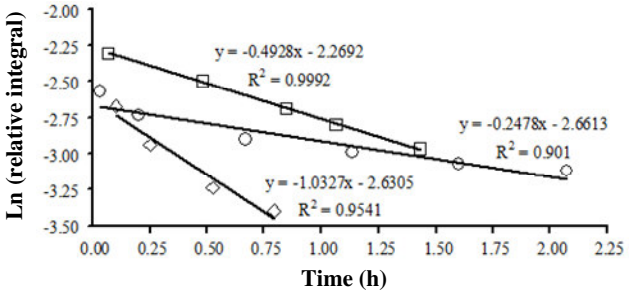

Figure 2.5. Effect of the steric bulk on monochelate complex formation with propylene-bridged ligands in acetone; Plot of ln(relative integral) versus time (h), at 23 °C with linear trend lines. ◇ = oMe-L3 @ δ = 8.1 ppm; ○ = oEtO-L3 @ δ = 7.4 ppm; □ = oMeO-L3 @ δ = 7.3 ppm.

This is illustrated in Figure 2.6. To confirm that the effect is purely based on sterical grounds the experiment was repeated with pMeO-L3 (entry 9). This ligand indeed showed the immediate formation of the monochelate complex in all three solvents.

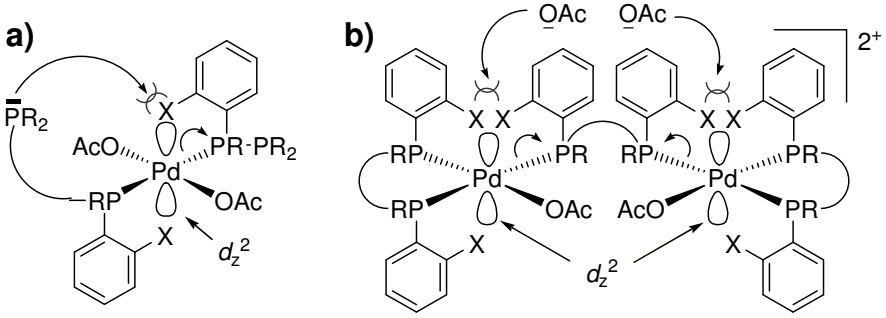

Figure 2.6. Illustration of the ligand induced steric hampering that retards the formation of [Pd(**L**)(OAc)$_2$]–type complexes. The steric bulk of the *ortho*-moieties (X) of the ligand shields the palladium d_z^2 orbital from ligand approach in [Pd(L)(OAc)$_2$]$_n$ (a), or from acetate coordination in [{Pd(L)(OAc)}$_2$(L)](OAc)$_2$ (b).

Interestingly, when the propylene backbone is more rigid by the *gem*-dialkyl substitution of the central carbon atom in the bridge (oMeO-L3X, oMeO-L3X^2 oEtO-L3X^2, and oMeO-L3X^R, entries 10-13), no intermediate species is observed. In these cases the monochelate complex is immediately formed, even for ligand oEtO-L3X^2, which comprises the larger oEtO substituent on the phenyl rings. This observation is attributed to the so-called 'Thorpe-Ingold' effect;[34, 35] due to

the presence of the two substituents on the central carbon atom in the backbone, the two phosphorus atoms are pre-oriented and more likely to form a chelate on palladium. In line with this, L3X also forms the monochelate complex immediately.

2.2.4.4. Butylene-bridged ligands

With the butylene-bridged ligands L4 and pMeO-L4 (entries 14 and 17) the monochelate complex is formed only *via* an intermediate species; several ^{31}P resonances around 12 ppm disappear over time. The approximate first order reaction constants of these conversions are of the same magnitude (in CD_2Cl_2 *k'* = 1.07 and 1.15 h^{-1} for L4 and pMeO-L4, respectively). This difference in behaviour between the unsubstituted C3 and C4-bridged ligands is ascribed to the increased

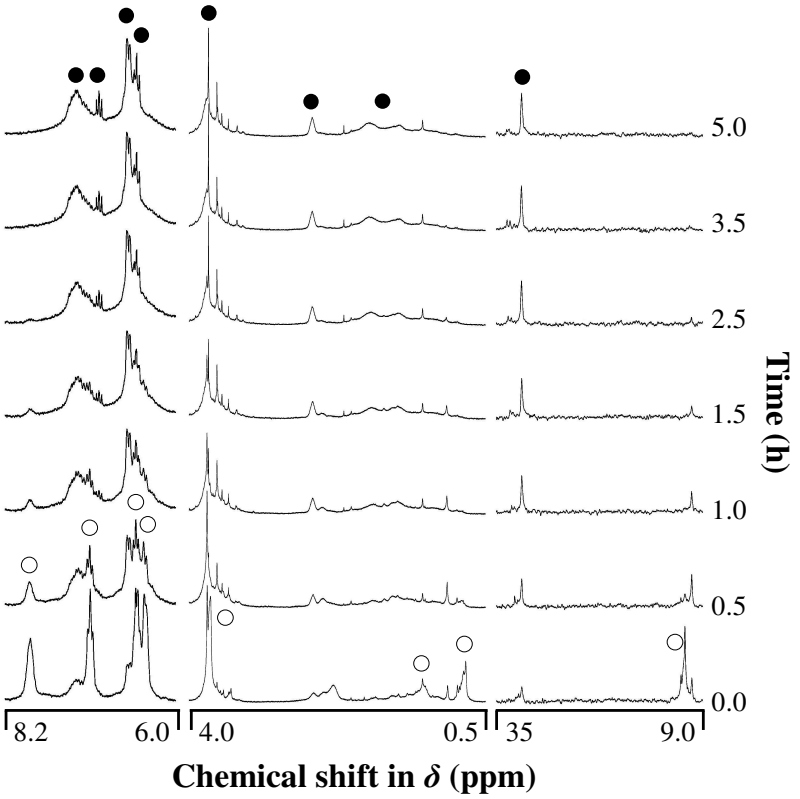

Figure 2.7. Complex formation for oMeO-L4 monitored by ^{1}H- and ^{31}P-NMR; $[Pd(OAc)_2]$ in CD_2Cl_2 added to oMeO-L4. ● = resonance of thermodynamic product; ○ = resonance of the kinetic intermediate.

flexibility of the butylene backbone. This renders the ligand a weaker chelate thus favoring the initial formation of a polynuclear species. In agreement with this hypothesis, using a ligand with a more rigid backbone (L4X, entry 18) the monochelate complex is formed immediately.

A different thermodynamic species is observed when steric bulk is added to the *ortho* position in the flexible butylene-bridged ligands (oMeO-L4 and oEtO-L4). This is exemplified for ligand oMeO-L4 in Figure 2.7. The kinetic product is rather similar to those formed for L4 (*o*-H4) and pMeO-L4 analogues. A number of resonances is observed in ^{31}P NMR around 11 ppm, and in ^{1}H NMR around 3.75 ppm for the methoxy group. Especially the aromatic resonance around 7.9 ppm is very characteristic for this type of intermediate. However, for oMeO-L4 and pMeO-L4 the nature of the thermodynamic product is unclear; it is most certainly not the desired monochelate complex, or the bischelate complex. The rate of conversion again depends on the size of the steric bulk; k' = 1.26 (oMeO-L4) and 0.58 (oEtO-L4). Since pMeO-L4 eventually forms the monochelate complex, the formation of the unidentified species is ascribed to steric influences. When the backbone is made more rigid (oMeO-L4X), the monochelate complex is formed immediately and none of the other species were detected.

2.2.4.5. The role of the coordinating strength of the anions

Not only the steric bulk and (the rigidity of) the ligand backbone are important for the course and rate of the complex formation. The coordination strength of the anions was also found to be an important factor. For L2 (ethylene backbone) it is known that when employing the weakly coordinating $CF_3C(O)O^-$ anions in CD_3OD, the bis-chelate complex is both the kinetic and thermodynamic species.[24]

For the propylene bridged ligands, it was found that the more polar the solvent, the more dissociated the OAc^- anions become, and hence the slower the conversion to the monochelate complex. This is most prominently reflected in the series performed with oMeO-L3. As can be seen from entry 7 in Table 2.3, the monochelate complex is formed more rapidly in CD_2Cl_2 (k' = 0.53) than in $(CD_3)_2CO$ (k' = 0.49), and only very slowly in CD_3OD (k' = 0.07). Similar trends were observed with ligands oMe-L3 and oEtO-L3 (entries 6 and 8). That these

observations are due to the coordinating ability of the anions is confirmed by employing weakly-coordinating OTs^- anions. Instead of a polynuclear species, oMeO-L3 now forms the bischelate complex as kinetic product (entry 7). Evidently, OTs^- anions are highly dissociated (even in the relatively apolar CD_2Cl_2) to allow the formation of a cationic species with a P_4 donor set. The conversion to the monochelate complex is extremely slow (k' = 0.01 h^{-1}), because the oMeO moieties shield the palladium d_z^2 orbitals from anion coordination (see Figure 2.6). Evidently, OTs^- anions coordinate so weakly that they can hardly overcome this steric repulsion induced by the oMeO moieties. When working with L3 (*o*-H, entry 4), the bischelate complex was also formed as intermediate. However, due to the smaller *ortho*-bulk the conversion to the monochelate complex proceeds very rapidly (k' = 6.23 h^{-1}).

The coordinating ability of the anions also influences the course of the complex formation with butylene-bridged ligands. As can be seen in entry 14 (L4, *o*-H), when employing OTs^- anions the monochelate complex is formed immediately, whereas with OAc^- anions it proceeds *via* some intermediate. This can be rationalized as follows. When OAc^- anions are used, the monochelate complex (P_2O_2 donor set) is formed *via* a PO_3 donor set. This is due to the strongly-coordinating nature of the OAc^- anions (perhaps in a bridging manner). When the anions are weakly-coordinating (OTs^-) the P_2O_2 donor set is formed immediately. That the ligand L4 does not form the bischelate complex (e.g., a P_4 donor set like its propylene bridged analogue L3) is ascribed to its larger bite-angle ($\beta \approx 99°$ *versus* 94°).[36] This imposes a sterical constraint on the adjacent coordination sites,[37, 38] thus disfavouring bischelate complex formation.

2.3. Conclusions

A variety of palladium complexes with substituted bidentate diphenylphosphane ligands has been synthesized using straightforward synthetic procedures. More specifically, monochelate and bischelate complexes with strongly (OAc^-) or weakly (OTs^-) coordinating anions have been obtained, and structures of representative complexes have been described. Using variable temperature NMR studies it was shown that the solid state structure of this type of complexes is fully retained in solution.

It was shown that three ligand-dependent factors play a crucial role in the formation of [Pd(ligand)(anion)$_2$]-type complexes: the length of the bridge between the phosphorus donors; the steric bulk at the *ortho* position of the phenyl rings; and the rigidity of the backbone. The coordinating ability of the anions was also found to be an important factor in the complex forming process.

Depending on these factors, the desired [Pd(ligand)(anion)$_2$] complex is formed instantaneously, *via* some intermediate, or not at all. Notably, when making the ligand bridge more rigid, the desired [Pd(ligand)(anion)$_2$] complex is formed directly in all cases studied.

It is thus concluded that it is important to realize that the formation of [Pd(ligand)(anion)$_2$]-type complexes is not always instantaneous or successful. Thus, when performing catalytic reactions with *in situ* formed complexes, one should make sure that the desired complex will actually form. With this study I hope to have provided a significant contribution to the fundamental understanding which ligand parameters determine whether the desired catalyst will indeed be formed.

2.4. Experimental Section

2.4.1. Materials

Solvents and chemicals were commercially available as A.R. grade and used as received, unless stated otherwise. The ligand and complex syntheses were performed under an inert atmosphere of argon and the purifications were commonly performed in air, unless stated otherwise. A schematic overview of the ligands used in this study is presented in Table 2.1. The ligands L2, L3, L4, and pMeO-L4 are commercially available and were used as received. The ligands L3X, oMeO-L4, and oEtO-L4 have been synthesized according to literature procedures.[39-42] The other ligands were obtained as a gift from Shell International Chemicals B.V., where they were prepared according to literature procedures.[43-51] All ligand molecular data are summarized in Appendix I.

2.4.2. Physical methods

Common analytical techniques

^{1}H- and ^{31}P{^{1}H}-NMR spectra were recorded using a DPX Bruker instrument operating at 300 or 400 MHz. Chemical shifts are reported in δ (parts per million); the proton resonances are given relative to the solvent peak (CD_3OD = 3.33, $(CH_3)_2SO$ = 2.50, $(CH_3)_2CO$ = 2.06, $CDCl_3$ = 7.26, CD_2Cl_2 = 5.30 ppm) or tetramethylsilane (TMS, 0 ppm). The phosphorus resonances are given relative to the external standard H_3PO_4 (85%, 0 ppm). C, H, and N analyses were carried out using an automatic Perkin-Elmer 2400 Series II CHNS/O microanalyzer. ESI Mass Spectroscopy was carried out using a Finnigan Aqua Mass Spectrometer equipped with an electrospray ionisation (ESI) source. Sample solutions (10 μL of a 1 mg/mL solution) were introduced in the ESI source by using a Dionex ASI-100 automated sampler injector and an eluent running at 0.2 ml/min.

X-ray crystal structure determinations

X-ray intensities were measured on a Nonius KappaCCD diffractometer with rotating anode (graphite monochromator, λ = 0.71073 Å) at a temperature of 150(2) K. Data were integrated with the HKL2000[52] ([Pd(oMeO-L2)$(OAc)_2$], [Pd(oMeO-L3X)$(OAc)_2$], [Pd(oMeO-L3X)]$(OTs)_2$) or EvalCCD[53] ([Pd(oMeO-L3)$(OAc)_2$], [Pd(oMeO-L3X^{R})$(OAc)_2$]) software. The structures were solved with Direct Methods using the programs SIR-97[54] ([Pd(oMeO-L2)$(OAc)_2$], [Pd(oMeO-L3X)]$(OTs)_2$) and SHELXS-97[55] ([Pd(oMeO-L3X)$(OAc)_2$]) or with automated Patterson Methods using the program DIRDIF-99[56] ([Pd(oMeO-L3)$(OAc)_2$], [Pd(oMeO-L3X^{R})$(OAc)_2$]). The structures were refined with SHELXL-97[55]. Non-hydrogen atoms were refined with anisotropic displacement parameters. Hydrogen atoms were located in difference-Fourier maps ([Pd(oMeO-L2)$(OAc)_2$], [Pd(oMeO-L3X)$(OAc)_2$]) or introduced in calculated positions ([Pd(oMeO-L3)$(OAc)_2$], [Pd(oMeO-L3X^{R})$(OAc)_2$], [Pd(L10)]$(OTs)_2$) and refined with a riding model. Drawings, structure calculations and checking for higher symmetry were performed with the PLATON software[57]. Further experimental details are given in Table 2.4.

CCDC 748839-748843 contain the supplementary crystallographic data for this chapter. These data can be obtained free of charge from The Cambridge Crystallographic Data Centre via www.ccdc.cam.ac.uk/data_request/cif.

[Pd(oMeO-L2)$(OAc)_2$]: The $CHCl_3$ solvent molecule was refined with a disorder model. [Pd(oMeO-L3)$(OAc)_2$]: Hydrogen atoms of the water molecule were refined freely with isotropic displacement parameters. [Pd(oMeO-L3X)$(OAc)_2$]: Hydrogen atoms of the water molecules were kept fixed at the positions located in difference Fourier maps. The methyl groups of the acetate ligands were refined with two conformations, respectively. [Pd(oMeO-L3X)]$(OTs)_2$: The crystal structure contains solvent accessible voids (1046 $Å^3$ / unit cell) filled with disordered solvent molecules. Their contribution to the structure factors was secured by back-Fourier transformation using the SQUEEZE routine of the program PLATON[57] resulting in 307 e^- / unit cell.

Table 2.4. Details of the X-ray crystal structure determinations.

complex formula	[Pd(oMeO-L2)$(OAc)_2$]	[Pd(oMeO-L3)$(OAc)_2$]	[Pd(oMeO-L3X)$(OAc)_2$]	[Pd(oMeO-L3X^R)$(OAc)_2$]	[Pd(oMeO-L3X)$_2$]$(OTs)_2$
CCDC refcode	748839	748840	748841	748842	748843
emperical formula	$C_{34}H_{38}O_8P_2Pd \cdot 2CHCl_3$	$C_{35}H_{40}O_8P_2Pd \cdot H_2O$	$C_{37}H_{44}O_8P_2Pd \cdot 3H_2O$	$C_{43}H_{52}O_{10}P_2Pd$	$[C_{66}H_{76}O_8P_4Pd](C_7H_7O_3S)_2$
fw	981.72	775.03	839.11	897.19	1569.92
crystal colour	colourless	yellow	colourless	yellow	yellow
crystal size [mm^3]	0.21x0.15x0.12	0.24x0.18x0.15	0.30x0.12x0.08	0.66x0.12x0.12	0.30x0.12x0.12
crystal system	monoclinic	monoclinic	monoclinic	monoclinic	monoclinic
space group	C2/c (no. 15)	$P2_1/c$ (no. 14)	$P2_1/c$ (no. 14)	$P2_1/c$ (no. 14)	C2/c (no. 15)
***a* [Å]**	21.3571(2)	13.9845(3)	13.7552(1)	10.8518(4)	26.4819(3)
***b* [Å]**	11.0576(1)	16.2664(4)	14.2919(1)	26.8681(11)	14.1198(2)
***c* [Å]**	19.5445(2)	20.0199(3)	20.0689(2)	15.5000(7)	24.7120(3)
β [°]	116.1887(4)	130.991(2)	96.4044(4)	113.881(3)	118.1165(6)
***V* [Å^3]**	4141.78(7)	3437.47(16)	3920.68(6)	4132.4(3)	8149.85(18)
Z	4	4	4	4	4
d_{calc} [g/cm^3]	1.574	1.498	1.422	1.442	1.279
μ [mm^{-1}]	0.961	0.687	0.612	0.584	0.417
(sin θ/λ)$_{max}$ [Å^{-1}]	0.65	0.65	0.65	0.65	0.60
refl. (meas./unique)	33907 / 4746	58871 / 7906	55912 / 8984	136182 / 9451	37289 / 7346
abs. corr.	multi-scan	multi-scan	multi-scan	multi-scan	multi-scan
abs. corr. range	0.85-0.89	0.75-0.90	0.92-0.96	0.60-0.93	0.74-0.96
param. / restraints	270 / 66	438 / 0	470 / 0	511 / 0	464 / 0
***R*1/*wR*2 [*I*>2σ(*I*)]**	0.0299 / 0.0731	0.0257 / 0.0579	0.0314 / 0.0722	0.0409 / 0.0745	0.0463 / 0.1129
***R*1/*wR*2 [all refl.]**	0.0436 / 0.0793	0.0400 / 0.0637	0.0470 / 0.0797	0.0676 / 0.0856	0.0685 / 0.1222
S	1.100	1.044	1.067	1.152	1.031
$\Delta\rho_{min/max}$ [eÅ^{-1}]	-0.54 / 0.51	-0.43 / 0.60	-0.68 / 0.84	-0.71 / 0.57	-0.59 / 0.95

2.4.3. NMR complex formation studies

Preparation of the samples, using $Pd(OAc)_2$

12.8 μmol of the ligand was weighed into an NMR tube and put under argon. In another tube, 3.59 mg (16 μmol) of $Pd(OAc)_2$ was dissolved in 1 ml of solvent under an argon atmosphere. Of this solution, 0.8 ml (12.8 μmol of Pd) was added to the ligand using a 1 ml syringe, which was dry and flushed with argon. The thus obtained mixture (16 mM) was thoroughly mixed using a vortex mixer

until a clear solution was obtained. When no clear solution was obtained within ten minutes of mixing, the sample was considered to be insoluble and was discarded.

Preparation of the samples, using $Pd(OTs)_2$

12.8 μmol of the ligand was weighed into an NMR tube and put under argon. In another tube, 3.59 mg (16 μmol) $Pd(OAc)_2$ and 5.51 mg (32 μmol) HOTs were dissolved in 1 ml $(CD_3)_2CO$ in CD_2Cl_2 (17% v/v), under an argon atmosphere. Of this solution, 0.8 ml (12.8 μmol of Pd) was added to the ligand using a 1 ml syringe, which was dry and flushed with argon. The thus obtained mixture (16 mM) was thoroughly mixed using a vortex mixer until a clear solution was obtained. When no clear solution was obtained within ten minutes of mixing, the sample was considered to be insoluble and was discarded.

NMR kinetic measurements

The clear solutions were monitored with ^{1}H- and ^{31}P{^{1}H}-NMR spectroscopy, over a period of about four to fourteen hours. All measurements of the same experiment (e.g. a specific complex formation study) were recorded with an identical number of free inductive decays (FIDs). For a typical proton measurement, the number of FIDs was 16. For the phosphorus NMR spectra the number of FIDs was typically 40.

Data Analysis

For the data analysis of the complex formation studies, the integral of an isolated aromatic resonance of the intermediate species was taken relative to the total integral of all aromatic protons. The natural logarithm of this number was plotted against time, which always resulted in a hyperbolically shaped curve. Of the initial linear part, the best fit was calculated with the least-squares method. These are the graphs that are given in this paper. The slopes of these linear functions reflect the (presumed first order) reaction constant (*k*'), not in absolute, but in relative sense. This was done because the exact nature of the disappearing species is (in most cases) unknown.

Low temperature NMR experiments

Some of the obtained complexes were characterized by ^{1}H- and ^{31}P-NMR spectroscopy, both at room temperature (20 °C) and at low temperature (–60 °C). This was typically done by monitoring the ^{1}H- and ^{31}P-NMR resonances of a 16 mM solution during cooling at 20, 0, –20, –40, and –60 °C. Before a spectrum at a specific temperature was recorded, it was ensured that the cooling apparatus was stable with an error of about 1 °C. When this was achieved, a waiting period of about ten minutes was applied to ensure that the sample had acquired the temperature as indicated by the cooling apparatus.

2.4.4. General methods for the synthesis of the complexes

Method A. For [Pd(Ligand)$(OAc)_2$]

A 74 mM solution of $Pd(OAc)_2$ in CH_2Cl_2 was prepared and filtered. A 25 ml round-bottomed flask filled with argon was charged with 10 ml of this solution and a magnetic stirring rod. To the stirred solution, 0.74 mmol of the solid ligand was added and the reaction mixture was stirred overnight (wrapped in aluminium foil), where after the solvent volume was reduced to about 5 ml. The complex was precipitated with Et_2O/*n*-hexane, collected by filtration over a glass frit (P4), washed with Et_2O/*n*-hexane and dried *in vacuo*.

Method B. For [Pd(Ligand)(OTs)$_2$]

A 74 mM solution of $Pd(OAc)_2$ in CH_2Cl_2 was prepared and filtered. A 25 ml round-bottomed flask filled with argon was charged with 10 ml of this solution and a magnetic stirring rod. To the stirred solution, 0.74 mmol of the solid ligand was added and the reaction mixture was stirred overnight (wrapped in aluminium foil). Then, *para*-toluene sulfonic acid (1.5 mmol, 0.26 g) was added and the solvent volume was reduced to about 5 ml. The complex was precipitated with Et_2O/*n*-hexane, collected by filtration over a glass frit (P4), washed with Et_2O/*n*-hexane and dried *in vacuo*.

Method C. For [Pd(Lidand)$_2$](OAc)$_2$

A 25 ml round-bottomed flask filled with argon was charged with 15 ml MeOH, 1 mmol of the ligand, and a stirring rod. The resulting suspension was stirred, and 2 ml of a filtered $Pd(OAc)_2$ solution (0.25 M in CH_2Cl_2) was added. After overnight stirring (wrapped in aluminium foil), the solvent volume was reduced to about 5 ml. The complex was precipitated with Et_2O/*n*-hexane, collected by filtration over a glass frit (P4), washed with Et_2O/*n*-hexane and dried *in vacuo*.

Method D. For [Pd(Ligand)$_2$](OTs)$_2$

A 25 ml round-bottomed flask filled with argon was charged with 15 ml MeOH, 1 mmol of the ligand, and a stirring rod. In another round-bottomed flask, 2 mmol (0.35 g) of *para*-toluene sulfonic acid was added to 4 ml of a 0.25 M solution of $Pd(OAc)_2$ in CH_2Cl_2. From this solution, 2 ml were added to the ligand/MeOH suspension. After overnight stirring (wrapped in aluminium foil), the solvent volume was reduced to about 5 ml. The complex was precipitated with Et_2O/*n*-hexane, collected by filtration over a glass frit (P4), washed with Et_2O/*n*-hexane and dried *in vacuo*.

2.4.5. Complex data

[Pd(L2)(OAc)$_2$] (M(L2)A) was prepared following method A. The product was obtained as a yellow powder, with an isolated yield of 97% (447 mg). The compound was recrystallized by layering a solution of the complex in dichloromethane with diethyl ether. ^{1}H NMR (300 MHz, CH_3OH): δ 7.80 (q, 8H, *m*-Ph-*H*), 7.52 (m, 4H, *p*-Ph-*H*), 7.45 (t, 8H, *o*-Ph-*H*), 2.50 (m, 4H, PCH_2), 1.49 (s, 6H, OC(O)CH_3) ppm; ^{31}P NMR (300 MHz, CH_3OH): δ 63.66 ppm. Elemental analyses for [Pd(L2)(OAc)$_2$], $C_{30}H_{30}O_4P_2Pd$ (622.92) • 0.75 CH_2Cl_2: calcd. C 53.79, H 4.62; found C 53.58, H 4.65. ESI Mass Spectroscopy, m/z found (calcd): $[M^- OAc]^+$ = 562.66 (563.05).

[Pd(L2)(OTs)$_2$] (M(L2)T) was prepared following method B. The product was obtained as a yellow powder, with an isolated yield of 89% (558 mg). The compound was recrystallized by layering a solution of the complex in dichloromethane with *n*-hexane. ^{1}H NMR (300 MHz, $OC(CH_3)_2$): δ 7.95 (q, 8H, *m*-Ph-*H*), 7.76 (m, 4H, *p*-Ph-*H*), 7.63 (m, 8H, *o*-Ph-*H*), 7.51 (d, 4H, *o*-OTs-*H*), 7.11 (d, 4H, *m*-OTs-*H*), 3.08 (m, 4H, PCH_2), 2.32 (s, 6H, *p*-OTs-CH_3) ppm; ^{31}P NMR (300 MHz, $OC(CH_3)_2$): δ 74.26 ppm. Elemental analyses for [Pd(L2)(OTs)$_2$], $C_{40}H_{38}O_6P_2PdS_2$ (847.22) • 0.5 CH_2Cl_2 • 0.25 C_6H_{14}: calcd. C 54.24, H 5.08, S 5.88; found C 54.24, H 5.00, S 5.91. ESI Mass Spectroscopy, m/z found (calcd): $[M - OTs]^+$ = 674.70 (675.05).

[Pd(L2)$_2$](OTs)$_2$ (B(L2)T) was prepared following method D. The product was obtained as a yellow powder, with an isolated yield of 92% (573 mg). The compound was recrystallized by layering a solution of the complex in dichloromethane with *n*-hexane. ^{1}H NMR (300 MHz, $CHCl_3$): δ 8.08 (d, 4H, *o*-OTs-*H*), 7.46 (m, 20H, *m*-Ph-*H* + *m*-OTs-*H*), 7.26 (m, 20H, *o*-Ph-*H* + *p*-Ph-*H*), 3.16 (m, 8H, PCH_2), 2.39 (s, 6H, *p*-OTs-CH_3) ppm; ^{31}P NMR (300 MHz, $CHCl_3$): δ 56.74 ppm. Elemental analyses for [Pd(L2)$_2$](OTs)$_2$, $C_{66}H_{62}O_6P_4PdS_2$ (1245.64) • 2 CH_2Cl_2 • C_6H_{14}: calcd. C

59.19, H 5.37, S 4.05; found C 59.26, H 5.25, S 3.94. ESI Mass Spectroscopy, m/z found (calcd): $[M - OTs]^+$ = 1072.73 (1073.19).

[Pd(oMeO-L2)(OAc)$_2$] (M(oMeO-L2)A) was prepared following method A. The product was obtained as a yellow powder, with an isolated yield of 81% (445 mg). Single crystals suitable for X-ray crystallography were obtained by layering a solution of the complex in dichloromethane with *n*-hexane. ^{1}H NMR (300 MHz, $CDCl_3$): δ 8.04 (q, 4H, *o*-Ph-*H*), 7.50 (t, 4H, *p*-Ph-*H*), 7.04 (t, 4H, OC=C-*H*), 6.92 (q, 4H, *m*-Ph-*H*), 3.72 (s, 12H, OCH_3), 2.63 (d, 4H, PCH_2), 1.36 (s, 6H, OC(O)CH_3) ppm; ^{31}P NMR (300 MHz, $CDCl_3$): δ 60.91 ppm. Elemental analyses for [Pd(oMeO-L2)(OAc)$_2$], $C_{34}H_{38}O_8P_2Pd$ (743.03) • 0.3 H_2O: calcd. C 54.52, H 5.20; found C 54.99, H 5.65. ESI Mass Spectroscopy, m/z found (calcd): $[M - OAc]^+$ = 682.75 (683.98).

[Pd(oMeO-L2)(OTs)$_2$] (M(oMeO-L2)T) was prepared following method B. The product was obtained as a yellow powder, with an isolated yield of 68% (487 mg). The compound was recrystallized by layering a solution of the complex in dichloromethane with diethyl ether. ^{1}H NMR (300 MHz, $OC(CH_3)_2$): δ 7.65 (m, 4H, *p*-Ph-*H* + *o*-Ph-*H*), 7.50 (d, 4H, *o*-OTs-*H*), 7.24 (t, 4H, OC=C-*H*), 7.09 (m, 8H, *m*-Ph-*H* + *m*-OTs-*H*), 3.80 (s, 12H, OCH_3), 3.05 (m, 4H, PCH_2), 2.29 (s, 6H, *p*-OTs-CH_3) ppm; ^{31}P NMR (300 MHz, $OC(CH_3)_2$): δ 57.50 ppm. Elemental analyses for [Pd(oMeO-L2)(OTs)$_2$], $C_{44}H_{46}O_{10}P_2PdS_2$ (967.33) • 1 CH_2Cl_2 • 0.25 $O(C_2H_3)_2$: calcd. C 51.60, H 4.75, S 2.97; found C 51.67, H 4.64, S 2.82. ESI Mass Spectroscopy, m/z found (calcd): $[M - OTs]^+$ = 794.77 (796.13).

[Pd(oMeO-L2)$_2$](OAc)$_2$ (B(oMeO-L2)A) was prepared following method C. The product was obtained as a yellow powder, with an isolated yield of 73% (460 mg). The compound was recrystallized by layering a solution of the complex in dichloromethane with diethyl ether. ^{1}H NMR (300 MHz, $CDCl_3$): δ 8.14 (br, 4H, *o*-Ph-*H*(ax)), 7.80 (t, 4H, *p*-Ph-*H*(ax)), 7.54 (m, 4H, *m*-Ph-*H*(ax)), 7.35 (m, 4H, *m*-Ph-*H*(eq)), 7.11 (d, 4H, OC=C-*H*(ax)), 6.88 (d, 4H, OC=C-*H*(eq)), 6.46 (t, 4H, *p*-Ph-*H*(eq)), 5.88 (br, 4H, *o*-Ph-*H*(eq)), 3.68 (s, 12H, OCH_3(ax)), 3.59 (s, 12H, OCH_3(eq)), 3.20 (m, 8H, PCH_2), 2.02 (s, 6H, OC(O)CH_3) ppm; ^{31}P NMR (300 MHz, $CDCl_3$): δ 55.83 ppm. Elemental analyses for [Pd(oMeO-L2)$_2$](OAc)$_2$, $C_{64}H_{70}O_{12}P_4Pd$ (1261.55) • 1 $O(C_2H_3)_2$ • 3 H_2O: calcd. C 52.63, H 5.70; found C 52.35, H 5.93. ESI Mass Spectroscopy, m/z found (calcd): $[M - 2\ OAc]^{2+}$ = 571.72 (571.73).

[Pd(oMeO-L2)$_2$](OTs)$_2$ (B(oMeO-L2)T) was prepared following method D. The product was obtained as a yellow powder, with an isolated yield of 30% (223 mg). The compound was recrystallized by layering a solution of the complex in dichloromethane with diethyl ether. ^{1}H NMR (300 MHz, $CDCl_3$): δ 8.08 (br, 4H, *o*-Ph-*H*(ax)), 7.89 (d, 4H, *o*-OTs-*H*), 7.81 (t, 4H, *p*-Ph-*H*(ax)), 7.50 (t, 4H, *m*-Ph-*H*(ax)), 7.26 (t, 4H, *m*-Ph-*H*(eq)), 7.12 (d, 4H, *m*-OTs-*H*), 6.97 (d, 4H, OC=C-*H*(ax)), 6.82 (d, 4H, OC=C-*H*(eq)), 6.56 (t, 4H, *p*-Ph-*H*(eq)), 5.84 (br, 4H, *o*-Ph-*H*(eq)), 3.67 (s, 12H, OCH_3(ax)), 3.52 (s, 12H, OCH_3(eq)), 3.03 (m, 8H, PCH_2), 2.33 (s, 6H, *p*-OTs-CH_3) ppm; ^{31}P NMR (300 MHz, $CDCl_3$): δ 55.95 ppm. Elemental analyses for [Pd(oMeO-L2)$_2$](OTs)$_2$, $C_{74}H_{78}O_{14}P_4PdS_2$ (1485.85) • 2 CH_2Cl_2 • 2 $O(C_2H_3)_2$: calcd. C 55.93, H 5.70, S 3.63; found C 56.04, H 5.88, S 3.80. ESI Mass Spectroscopy, m/z found (calcd): $[M - OTs]^+$ = 1072.73 (1073.19).

[Pd(L3)(OAc)$_2$] (M(L3)A) was prepared following method A. The product was obtained as a yellow powder, with an isolated yield of 93% (438 mg). The compound was recrystallized by layering a solution of the complex in dichloromethane with diethyl ether. ^{1}H NMR (300 MHz, $CHCl_3$): δ 7.72 (m, 8H, *m*-Ph-*H*), 7.34 (m, 12H, *o*-Ph-*H* + *p*-Ph-*H*), 2.51 (m, 4H, PCH_2), 2.15 (m, 2H, PCH_2CH_2), 1.34 (s, 6H, OC(O)CH_3) ppm; ^{31}P NMR (300 MHz, $CHCl_3$): δ 9.74 ppm. Elemental analyses for [Pd(L3)(OAc)$_2$], $C_{31}H_{32}O_4P_2Pd$ (636.95) • 0.5 CH_2Cl_2 • 0.5 $O(C_2H_3)_2$: calcd. C 56.16, H 5.35; found C 56.64, H 5.33. ESI Mass Spectroscopy, m/z found (calcd): $[M - OAc]^+$ = 576.65 (577.91).

[Pd(L3)(OTs)$_2$] (M(L3)T) was prepared following method B. The product was obtained as a yellow powder, with an isolated yield of 78% (497 mg). The compound was recrystallized by layering a solution of the complex in dichloromethane with diethyl ether. ^{1}H NMR (300 MHz, $CHCl_3$): δ 7.67 (q, 8H, *o*-Ph-*H*), 7.41 (m, 8H, *p*-Ph-*H* + *o*-OTs-*H*), 7.26 (t, 8H, *m*-Ph-*H*), 6.86 (d, 4H, *m*-OTs-*H*), 2.83 (m, 4H, PCH_2), 2.25 (m, 2H, PCH$_2$CH_2), 2.31 (s, 6H, *p*-OTs-CH_3) ppm; ^{31}P NMR (300 MHz, $CHCl_3$): δ 15.88 ppm. Elemental analyses for [Pd(L3)(OTs)$_2$], $C_{41}H_{40}O_6P_2PdS_2$ (861.25) • 1.3 H_2O: calcd. C 55.63, H 4.86, S 5.15; found C 55.73, H 4.79, S 5.51. ESI Mass Spectroscopy, m/z found (calcd): $[M - OTs]^+$ = 688.71 (689.07).

[Pd(L3X)(OAc)$_2$] (M(L3X)A) was prepared following method A. The product was obtained as a yellow powder, with an isolated yield of 96% (472 mg). The compound was recrystallized by layering a solution of the complex in dichloromethane with diethyl ether. ^{1}H NMR (300 MHz, $CHCl_3$): δ 7.90 (m, 8H, *o*-Ph-*H*), 7.44 (m, 12H, *m*-Ph-*H* + *p*-Ph-*H*), 2.29 (d, 4H, PCH_2), 0.91 (s, 6H, CCH_3), 1.44 (s, 6H, OC(O)CH_3) ppm; ^{31}P NMR (300 MHz, $CHCl_3$): δ 16.35 ppm. Elemental analyses for [Pd(L3X)(OAc)$_2$], $C_{33}H_{36}O_4P_2Pd$ (665.00) • 0.25 CH_2Cl_2 • 0.5 O(C_2H_3)$_2$: calcd. C 58.62, H 5.65; found C 58.66, H 5.57. ESI Mass Spectroscopy, m/z found (calcd): $[M - OAc]^+$ = 604.77 (605.10).

[Pd(L3X)(OTs)$_2$] (M(L3X)T) was prepared following method B. The product was obtained as a yellow powder, with an isolated yield of 83% (546 mg). The compound was recrystallized by layering a solution of the complex in dichloromethane with diethyl ether. ^{1}H NMR (300 MHz, CH_3OH): δ 7.88 (d, 4H, *o*-OTs-*H*), 7.58 (br, 8H, *o*-Ph-*H*), 7.29 (m, 16H, *m*-Ph-*H* + *p*-Ph-*H* + *m*-OTs-*H*), 2.59 (br, 4H, PCH_2), 2.38 (s, 6H, *p*-OTs-CH_3), 0.26 (s, 6H, CCH_3) ppm; ^{31}P NMR (300 MHz, CH_3OH): δ 6.72 ppm. Elemental analyses for [Pd(L3X)(OTs)$_2$], $C_{43}H_{44}O_6P_2PdS_2$ (889.30) • CH_2Cl_2 • 1.25 O(C_2H_5)$_2$: calcd. C 55.29, H 5.30, S 4.52; found C 55.37, H 5.19, S 4.69. ESI Mass Spectroscopy, m/z found (calcd): $[M - OTs]^+$ = 688.71 (689.07).

[Pd(L3X)$_2$](OTs)$_2$ (B(L3X)T) was prepared following method D. The product was obtained as a yellow powder, with an isolated yield of 92% (612 mg). The compound was recrystallized by layering a solution of the complex in dichloromethane with diethyl ether. ^{1}H NMR (300 MHz, CH_3OH): δ 8.00 (d, 4H, *o*-OTs-*H*), 7.60 (br, 16H, *o*-Ph-*H*), 7.26 (m, 28H, *m*-Ph-*H* + *p*-Ph-*H* + *m*-OTs-*H*), 2.62 (br, 8H, PCH_2), 2.38 (s, 6H, *p*-OTs-CH_3), 0.26 (s, 12H, CCH_3) ppm; ^{31}P NMR (300 MHz, CH_3OH): δ 5.63 ppm. Elemental analyses for [Pd(L3X)$_2$](OTs)$_2$, $C_{72}H_{74}O_6P_4PdS_2$ (1329.80) • 1.25 CH_2Cl_2 • O(C_2H_3)$_2$: calcd. C 63.83, H 6.00, S 4.33; found C 63.73, H 6.24, S 4.62. ESI Mass Spectroscopy, m/z found (calcd): $[M - OTs]^+$ = 1156.91 (1157.28).

[Pd(oMeO-L3)(OAc)$_2$] (M(oMeO-L3)A) was prepared following method A. The product was obtained as a yellow powder, with an isolated yield of 87% (487 mg). Single crystals suitable for X-ray crystallography were obtained by layering of *n*-hexane with a solution of the complex in dichloromethane. ^{1}H NMR (300 MHz, $CDCl_3$): δ 8.25 (br, 4H, *o*-Ph-*H*), 7.50 (t, 4H, *p*-Ph-*H*), 7.08 (br, 4H, *m*-Ph-*H*), 6.94 (d, 4H, OC=C-*H*), 3.76 (s, 12H, OCH_3), 2.44 (m, 4H, PCH_2), 1.95 (m, 2H, PCH$_2$CH_2), 1.26 (s, 6H, OC(O)CH_3) ppm; ^{31}P NMR (300 MHz, CDCl3): δ 14.50 ppm. Elemental analyses for [Pd(oMeO-L3)(OAc)$_2$], $C_{35}H_{40}O_8P_2Pd$ (757.05) • CH_2Cl_2: calcd. C 54.35, H 6.08; found C 54.18, H 6.21. ESI Mass Spectroscopy, m/z found (calcd): $[M - OAc]^+$ = 698.62 (698.01).

[Pd(oMeO-L3)$_2$](OAc)$_2$ (B(oMeO-L3)A) was prepared following method C. The product was obtained as a yellow powder, with an isolated yield of 94% (606 mg). The compound was recrystallized by layering a solution of the complex in dichloromethane with diethyl ether. ^{1}H NMR (300 MHz, CH_3OH): δ 8.59 (br, 4H, *o*-Ph-*H*(ax)), 7.74 (t, 4H, *m*-Ph-*H*(ax)), 7.46 (t, 4H, *p*-Ph-*H*(ax)), 7.30 (t, 4H, *p*-Ph-*H*(eq)), 7.05 (m, 8H, OC=C-*H*(ax + eq)), 6.61 (t, 4H, *m*-Ph-*H*(eq)), 5.91 (br, 4H, *o*-Ph-*H*(eq)), 4.23 (s, 12H, OCH_3(ax)), 3.42 (s, 12H, OCH_3(eq)), 2.90 (m, 4H, PCH_2(ax)), 2.38 (m, 4H, PCH_2(eq)), 1.95 (m, 2H, PCH$_2$CH_2), 1.87 (s, 6H, OC(O)CH_3) ppm; ^{31}P NMR (300 MHz, CH_3OH): δ 5.56 ppm. Elemental analyses for [Pd(oMeO-L3)$_2$](OAc)$_2$, $C_{66}H_{74}O_{12}P_4Pd$

(1289.60) • CH_2Cl_2: calcd. C 55.96, H 6.58; found C 55.91, H 6.58. ESI Mass Spectroscopy, m/z found (calcd): $[M - 2\ OAc]^{2+}$ = 584.83 (585.15).

[Pd(oMeO-L3)$_2$](OTs)$_2$ (B(oMeO-L3)T) was prepared following method D. The product was obtained as a yellow powder, with an isolated yield of 72% (545 mg). The compound was recrystallized by layering a solution of the complex in dichloromethane with diethyl ether. ^{1}H NMR (300 MHz, $CHCl_3$): δ 8.51 (br, 4H, *o*-Ph-*H*(ax)), 7.96 (d, 4H, *o*-OTs-*H*), 7.73 (t, 4H, *m*-Ph-*H*(ax)), 7.64 (t, 4H, *p*-Ph-*H*(ax)), 7.20 (m, 8H, *p*-Ph-*H*(eq) + *m*-OTs-*H*), 6.99 (d, 4H, OC=C-*H*(ax)), 6.83 (d, 4H, OC=C-*H*(eq)), 6.47 (t, 4H, *m*-Ph-*H*(eq)), 5.82 (br, 4H, *o*-Ph-*H*(eq)), 4.33 (s, 12H, OCH_3(ax)), 3.38 (s, 12H, OCH_3(eq)), 2.85 (m, 4H, PCH_2(ax)), 2.36 (s, 6H, *p*-OTs-CH_3), 2.25 (m, 4H, PCH_2(eq)), 1.52 (br, 4H, PCH$_2$CH_2) ppm; ^{31}P NMR (300 MHz, $CHCl_3$): δ 4.81 ppm. Elemental analyses for [Pd(oMeO-L3)$_2$](OTs)$_2$, $C_{76}H_{82}O_{14}P_4PdS_2$ (1513.90) • 0.25 CH_2Cl_2 • 0.25 O(C_2H_3)$_2$: calcd. C 59.72, H 5.52, S 3.96; found C 59.48, H 5.87, S 3.96. ESI Mass Spectroscopy, m/z found (calcd): $[M - OTs]^+$ = 1340.53 (1341.30).

[Pd(oMeO-L3X)(OAc)$_2$] (M(oMeO-L3X)A) was prepared following method A. The product was obtained as a yellow powder, with an isolated yield of 96% (558 mg). Single crystals suitable for X-ray crystallography were obtained by layering of *n*-hexane with a solution of the complex in dichloromethane. ^{1}H NMR (300 MHz, $CDCl_3$): δ 8.15 (br, 4H, *o*-Ph-*H*), 7.51 (t, 4H, *m*-Ph-*H*), 7.07 (m, 4H, *p*-Ph-*H*), 6.92 (d, 4H, OC=C-*H*), 3.86 (s, 12H, OCH_3), 2.58 (d, 4H, PCH_2), 1.20 (s, 6H, OC(O)CH_3), 0.33 (s, 6H, CCH_3) ppm; ^{31}P NMR (300 MHz, CDCl3): δ 20.84 ppm. Elemental analyses for [Pd(oMeO-L3X)(OAc)$_2$], $C_{37}H_{44}O_8P_2Pd$ (785.11) • CH_2Cl_2 • 0.7 C_6H_{12}: calcd. C 54.51, H 6.01; found C 54.39, H 5.96. ESI Mass Spectroscopy, m/z found (calcd): $[M - OAc]^+$ = 724.77 (726.06).

[Pd(oMeO-L3X)$_2$](OAc)$_2$ (B(oMeO-L3X)A) was prepared following method C. The product was obtained as a yellow powder, with an isolated yield of 97% (653 mg). The compound was recrystallized by layering a solution of the complex in dichloromethane with diethyl ether. ^{1}H NMR (300 MHz, CH_3OH): δ 8.36 (br, 4H, *o*-Ph-*H*(ax)), 7.64 (t, 4H, *m*-Ph-*H*(ax)), 7.30 (m, 8H, *p*-Ph-*H*(ax) + *p*-Ph-*H*(eq)), 7.11 (d, 4H, OC=C-*H*(ax)), 6.92 (d, 4H, OC=C-*H*(eq)), 6.70 (t, 4H, *m*-Ph-*H*(eq)), 6.48 (br, 4H, *o*-Ph-*H*(eq)), 4.26 (s, 12H, OCH_3(ax)), 3.41 (s, 12H, OCH_3(eq)), 2.78 (d, 4H, PCH_2(ax)), 2.44 (d, 4H, PCH_2(eq)), 1.88 (s, 6H, OC(O)CH_3), 0.22 (s, 12H, CCH_3) ppm; ^{31}P NMR (300 MHz, CH_3OH): δ 10.88 ppm. Elemental analyses for [Pd(oMeO-L3X)$_2$](OAc)$_2$, $C_{70}H_{82}O_{12}P_4Pd$ (1345.71) • 2.5 CH_2Cl_2 • 2.5 O(C_2H_3)$_2$: calcd. C 57.28, H 6.44; found C 56.97, H 6.90. ESI Mass Spectroscopy, m/z found (calcd): $[M - 2\ OAc]^{2+}$ = 613.43 (613.18).

[Pd(oMeO-L3X)$_2$](OTs)$_2$ (B(oMeO-L3X)T) was prepared following method D. The product was obtained as a yellow powder, with an isolated yield of 89% (699 mg). Single crystals suitable for X-ray crystallography were obtained by layering of hexane with a solution of the complex in acetone. ^{1}H NMR (300 MHz, $CDCl_3$): δ 8.29 (br, 4H, *o*-Ph-*H*(ax)), 7.95 (d, 4H, *o*-OTs-*H*), 7.56 (m, 8H, *p*-Ph-*H*(ax) + *m*-Ph-*H*(ax)), 7.16 (m, 8H, *p*-Ph-*H*(eq) + *m*-OTs-*H*), 7.07 (d, 4H, OC=C-*H*(ax)), 6.68 (d, 4H, OC=C-*H*(eq)), 6.53 (t, 4H, *m*-Ph-*H*(eq)), 6.34 (br, 4H, *o*-Ph-*H*(eq)), 4.38 (s, 12H, OCH_3(ax)), 3.38 (s, 12H, OCH_3(eq)), 2.70 (d, 4H, PCH_2(ax)), 2.36 (s, 6H, *p*-OTs-CH_3), 2.30 (d, 4H, PCH_2(eq)), 0.12 (s, 12H, CCH_3) ppm; ^{31}P NMR (300 MHz, $CDCl_3$): δ 10.10 ppm. Elemental analyses for [Pd(oMeO-L3X)$_2$](OTs)$_2$, $C_{80}H_{90}O_{14}P_4PdS_2$ (1570.01) • 0.25 CH_2Cl_2 • 0.5 C_6H_{14}: calcd. C 58.87, H 5.79, S 3.92; found C 58.40, H 5.99, S 3.51. ESI Mass Spectroscopy, m/z found (calcd): $[M - OTs]^+$ = 1396.47 (1396.37).

[Pd(oMeO-L3X^R)(OAc)$_2$] (M(oMeO-L3X^R)A) was prepared following method A. The product was obtained as a yellow powder, with an isolated yield of 94% (624 mg). Single crystals suitable for X-ray crystallography were obtained by layering of *n*-hexane with a solution of the complex in acetone. ^{1}H NMR (300 MHz, $CDCl_3$): δ 8.50 (br, 4H, *o*-Ph-*H*), 7.52 (br, 4H, *m*-Ph-*H*), 7.08 (br, 4H, *p*-Ph-*H*), 6.94 (d, 4H, OC=C-*H*), 3.88 (s, 12H, OCH_3), 3.09 (s, 4H, CCH_2O), 2.68 (s, 4H, PCH_2),

1.57 (m, 4H, OCCH_2), 1.37 (m, 6H, OCCH$_2$CH_2 + OCCH$_2$CH$_2$CH_2), 1.21 (s, 6H, OC(O)CH_3) ppm; ^{31}P NMR (300 MHz, $CDCl_3$): δ 18.05 ppm. Elemental analyses for [Pd(oMeO-L3X^R)(OAc)$_2$], $C_{43}H_{52}O_{10}P_2Pd$ (897.23): calcd. C 57.56, H 5.84; found C 57.00, H 6.16. ESI Mass Spectroscopy, m/z found (calcd): [M –OAc]$^+$ = 836.82 (838.19).

[Pd(oMeO-L3X^R)$_2$](OAc)$_2$ (B(oMeO-L3X^R)A) was prepared following method C. The product was obtained as a yellow powder, with an isolated yield of 70% (550 mg). The compound was recrystallized by layering a solution of the complex in dichloromethane with *n*-hexane. ^{1}H NMR (300 MHz, CH_3OH): δ 8.35 (br, 4H, *o*-Ph-*H*(ax)), 7.34 (t, 4H, *p*-Ph-*H*(ax)), 7.29 (t, 4H, *p*-Ph-*H*(eq)), 7.14 (d, 4H, OC=C-*H*(ax)), 6.97 (d, 4H, OC=C-*H*(eq)), 6.78 (t, 4H, *m*-Ph-*H*(ax)), 6.72 (t, 4H, *m*-Ph-*H*(eq)), 6.48 (br, 4H, *o*-Ph-*H*(eq)), 4.30 (s, 12H, OCH_3(ax)), 3.42 (s, 12H, OCH_3(eq)), 2.88 (d, 4H, PCH_2(ax)), 2.56 (m, 12H, PCH_2(eq) + CCH_2O), 1.88 (s, 6H, OC(O)CH_3), 1.37 (m, 8H, OCCH_2), 1.23 (m, 12H, OCCH$_2$CH_2 + OCCH$_2$CH$_2$C*H*2) ppm; ^{31}P NMR (300 MHz, CH_3OH): δ 8.82 ppm. Elemental analyses for [Pd(oMeO-L3X^R)$_2$](OAc)$_2$, $C_{82}H_{98}O_{16}P_4Pd$ (1569.96) • 0.5 CH_2Cl_2 • 0.5 C_6H_{14}: calcd. C 62.03, H 6.45; found C 62.00, H 6.46. ESI Mass Spectroscopy, m/z found (calcd): [M – 2 OAc]$^{2+}$ = 725.15 (725.23).

[Pd(oMeO-L3X^R)$_2$](OTs)$_2$ (B(oMeO-L3X^R)T) was prepared following method D. The product was obtained as a yellow powder, with an isolated yield of 63% (565 mg). The compound was recrystallized by layering a solution of the complex in dichloromethane with *n*-hexane. ^{1}H NMR (300 MHz, $CHCl_3$): δ 8.28 (br, 4H, *o*-Ph-*H*(ax)), 8.00 (d, 4H, *o*-OTs-*H*), 7.60 (m, 8H, *p*-Ph-*H*(ax) + *m*-Ph-*H*(ax)), 7.17 (m, 20H, OC=C-*H*(ax) + *p*-Ph-*H*(eq) + *m*-OTs-*H*), 6.74 (d, 4H, OC=C-*H*(eq)), 6.54 (t, 4H, *m*-Ph-*H*(eq)), 6.34 (br, 4H, *o*-Ph-*H*(eq)), 4.44 (s, 12H, OCH_3(ax)), 3.40 (s, 12H, OCH_3(eq)), 2.73 (d, 4H, PCH_2(ax)), 2.44 (m, 18H, PCH_2(eq) + CCH_2O + *p*-OTs-CH_3), 1.42 (br, 8H, OCCH_2), 1.23 (br, 12H, OCCH$_2$CH_2 + OCCH$_2$CH$_2$CH_2) ppm; ^{31}P NMR (300 MHz, $CHCl_3$): δ 8.03 ppm. Elemental analyses for [Pd(oMeO-L3X^R)$_2$](OTs)$_2$, $C_{92}H_{106}O_{18}P_4PdS_2$ (1794.26) • 0.33 CH_2Cl_2: calcd. C 60.84, H 5.90, S 3.50; found C 60.84, H 5.90, S 3.02. ESI Mass Spectroscopy, m/z found (calcd): [M – 2 OTs]$^{2+}$ = 726.50 (725.94).

[Pd(L4)(OAc)$_2$] (M(L4)A) was prepared following method A. The product was obtained as a yellow powder, with an isolated yield of 96% (463 mg). The compound was recrystallized by layering a solution of the complex in dichloromethane with diethyl ether. ^{1}H NMR (300 MHz, CH_3OH): δ 7.63 (q, 8H, *o*-Ph-*H*), 7.47 (t, 4H, *p*-Ph-*H*), 7.34 (t, 8H, *m*-Ph-*H*), 2.44 (br, 4H, PCH_2), 1.93 (m, 4H, PCH$_2$CH_2), 1.32 (s, 6H, OC(O)CH_3) ppm; ^{31}P NMR (300 MHz, CH_3OH): δ 28.56 ppm. Elemental analyses for [Pd(L4)(OAc)$_2$], $C_{32}H_{34}O_4P_2Pd$ (650.98) • 1.5 CH_2Cl_2: calcd. C 51.69, H 4.79; found C 51.88, H 4.93. ESI Mass Spectroscopy, m/z found (calcd): [M – OAc]$^+$ = 590.73 (591.08).

[Pd(L4)(OTs)$_2$] (M(L4)T) was prepared following method B. The product was obtained as a yellow powder, with an isolated yield of 92% (596 mg). The compound was recrystallized by layering a solution of the complex in dichloromethane with diethyl ether. ^{1}H NMR (300 MHz, $CHCl_3$): δ 7.70 (t, 8H, *p*-Ph-*H*), 7.54 (t, 8H, *m*-Ph-*H*), 7.40 (m, 8H, *o*-Ph-*H* + *o*-OTs-*H*), 6.93 (d, 4H, *m*-OTs-*H*), 2.58 (br, 4H, PCH_2), 2.31 (s, 6H, *p*-OTs-CH_3), 2.15 (m, 4H, PCH$_2$CH_2) ppm; ^{31}P NMR (300 MHz, $CHCl_3$): δ 32.80 ppm. Elemental analyses for [Pd(L4)(OTs)$_2$], $C_{42}H_{42}O_6P_2PdS_2$ (875.28) • 1.25 CH_2Cl_2 • 1.25 O(C_2H_3)$_2$: calcd. C 54.08, H 5.13, S 5.02; found C 54.22, H 5.00, S 5.13. ESI Mass Spectroscopy, m/z found (calcd): [M – OTs]$^+$ = 702.62 (703.08).

References

[1] E. Drent, P. H. M. Budzelaar, *Chem. Rev.* **1996**, *96*, 663.
[2] C. Bianchini, A. Meli, *Coord. Chem. Rev.* **2002**, *225*, 35.
[3] F. Paul, *Coord. Chem. Rev.* **2000**, *203*, 269.
[4] E. Drent, P. W. N. M. van Leeuwen, EU 0086281A1, **1982**.
[5] E. Drent, EU 0231045A2, **1987**.
[6] F. Ragaini, C. Cognolato, M. Gasperini, S. Cenini, *Angew. Chem.* **2003**, *42*, 2886.
[7] E. Drent, *Pure Appl. Chem.* **1990**, *62*, 661.
[8] P. Wehman, L. Borst, P. C. J. Kamer, P. W. N. M. van Leeuwen, *J. Mol. Catal. A-Chem.* **1996**, *112*, 23.
[9] A. Marson, A. B. van Oort, W. P. Mul, *Eur. J. Inorg. Chem.* **2002**, 3028.
[10] E. Drent, EU 224292, **1987**.
[11] A. Bontempi, E. Alessio, G. Chanos, G. Mestroni, *J. Mol. Catal.* **1987**, *42*, 67.
[12] S. Cenini, F. Ragaini, M. Pizzotti, F. Porta, G. Mestroni, E. Alessio, *J. Mol. Catal.* **1991**, *64*, 179.
[13] R. Santi, A. M. Romano, F. Panella, G. Mestroni, A. Sessanti, A. S. o Santi, *J. Mol. Catal. A-Chem.* **1999**, *144*, 41.
[14] P. Leconte, F. Metz, A. Mortreux, J. A. Osborn, F. Paul, F. Petit, A. Pillot, *J. Chem. Soc.-Chem. Commun.* **1990**, 1616.
[15] P. Wehman, V. E. Kaasjager, W. G. J. de Lange, F. Hartl, P. C. J. Kamer, P. W. N. M. van Leeuwen, J. Fraanje, K. Goubitz, *Organometallics* **1995**, *14*, 3751.
[16] P. Wehman, G. C. Dol, E. R. Moorman, P. C. J. Kamer, P. W. N. M. van Leeuwen, J. Fraanje, K. Goubitz, *Organometallics* **1994**, *13*, 4856.
[17] P. Wehman, PhD thesis, University of Amsterdam (UvA) **1995**.
[18] F. Ragaini, M. Gasperini, S. Cenini, *Adv. Synth. Catal.* **2004**, *346*, 63.
[19] F. Ragaini, *Dalton Trans.* **2009**, 6251.
[20] J. H. Grate, D. R. Hamm, D. H. Valentine, US 4.603.216, **1986**.
[21] P. Wehman, R. E. Rulke, V. E. Kaasjager, P. C. J. Kamer, H. Kooijman, A. L. Spek, C. J. Elsevier, K. Vrieze, P. W. N. M. van Leeuwen, *J. Chem. Soc.-Chem. Commun.* **1995**, 331.
[22] D. Cremer, J. A. Pople, *J. Am. Chem. Soc.* **1975**, *97*, 1354.
[23] C. Bianchini, A. Meli, W. Oberhauser, *Dalton Trans.* **2003**, 2627.
[24] A. Marson, A. B. van Oort, W. P. Mul, *Eur. J. Inorg. Chem.* **2002**, *11*, 3028.
[25] F. A. Cotton, S. Han, *Rev. De Chim. Min.* **1983**, *20*, 496.
[26] A. G. Orpen, L. Brammer, F. H. Allen, O. Kennard, D. G. Watson, R. Taylor, *J. Chem. Soc. Dalton Trans.* **1989**, S1.
[27] I. M. Angulo, E. Bouwman, M. Lutz, W. P. Mul, A. L. Spek, *Inorg. Chem.* **2001**, *40*, 2073.
[28] C. Bianchini, A. Meli, W. Oberhauser, A. M. Segarra, C. Claver, E. J. G. Suarez, *J. Mol. Catal. A-Chem.* **2007**, *265*, 292.
[29] M. Brookhart, M. L. H. Green, G. Parkin, *Proc. Natl. Acad. Sci. U. S. A.* **2007**, *104*, 6908.
[30] J. F. Malone, C. M. Murray, M. H. Charlton, R. Docherty, A. J. Lavery, *J. Chem. Soc, Faraday Trans.* **1997**, *93*, 3429.
[31] C. Bianchini, H. M. Lee, A. Meli, W. Oberhauser, M. Peruzzini, F. Vizza, *Organometallics* **2002**, *21*, 16.
[32] C. Bianchini, P. Bruggeller, C. Claver, G. Czermak, A. Dumfort, A. Meli, W. Oberhauser, E. J. G. Suarez, *Dalton Trans.* **2006**, 2964.
[33] I. M. Angulo, E. Bouwman, R. van Gorkum, S. M. Lok, M. Lutz, A. L. Spek, *J. Mol. Catal. A-Chem.* **2003**, *202*, 97.
[34] M. E. Jung, *J. Am. Chem. Soc.* **1991**, *113*, 224.
[35] P. V. R. Schleyer, *J. Am. Chem. Soc.* **1961**, *83*, 1368.
[36] T. Hayashi, M. Konishi, Y. Kobori, M. Kumada, T. Higuchi, K. Hirotsu, *J. Am. Chem. Soc.* **1984**, *106*, 158.

[37] R. J. van Haaren, K. Goubitz, J. Fraanje, G. P. F. van Strijkdonk, H. Oevering, B. Coussens, J. N. H. Reek, P. C. J. Kamer, P. W. N. M. van Leeuwen, *Inorg. Chem.* **2001**, *40*, 3363.
[38] A. G. Avent, R. B. Bedford, P. A. Chaloner, S. Z. Dewa, P. B. Hitckcock, *J. Chem. Soc., Dalton Trans.* **1996**, 4633.
[39] L. Brandsma, H. D. Verkruijsse, *Synth. Commun.* **1990**, *20*, 2273.
[40] P. H. M. Budzelaar, J. A. van Doorn, N. Meijboom, *Recl. Trav. Chim. Pays-Bas-J. Roy. Neth. Chem. Soc.* **1991**, *110*, 420.
[41] J. A. van Doorn, PhD thesis, University of Amsterdam (UvA) **1991**.
[42] W. Hewertson, H. R. Watson, *J. Chem. Soc.* **1962**, 1490.
[43] F. Bickelhaupt, US 4874897, **1989**.
[44] W. Eilenberg, EU 364046, **1991**.
[45] J. A. van Doorn, US 4994592, **1991**.
[46] R. van Ginkel, US 6548708, **2003**.
[47] E. Drent, US 5091587, **1992**.
[48] C. F. Hobbs, US 4120901, **1987**.
[49] P. W. Clark, B. J. Mulraney, *J. Organomet. Chem.* **1981**, *217*, 51.
[50] J. M. Brown, B. A. Murrer, *Tetrahedron Lett.* **1980**, *21*, 581.
[51] R. L. Wife, A. B. van Oort, J. A. van Doorn, P. W. N. M. van Leeuwen, *Synthesis* **1983**, *1*, 71.
[52] Z. Otwinowski, W. Minor, *Methods in Enzymology, Vol. 276*, Academic press, **1997**.
[53] A. J. M. Duisenberg, L. M. J. Kroon-Batenburg, A. M. M. Schreurs, **2003**, *36*, 220.
[54] A. Altomare, M. C. Burla, M. Camalli, G. L. Cascarano, C. Giacovazzo, A. Guagliardi, A. G. G. Moliterni, G. Polidori, R. Spagna, *J. Appl. Cryst.* **1999**, *32*, 115.
[55] G. M. Sheldrick, *Acta Cryst.* **2008**, *A64*, 112.
[56] P. T. A. Beurskens, G.; Beurskens, G.; Bosman, W. P.; Garcia-Granda, S.; Gould, R. O.; Smith, J. M. M.; Smykalla, C., *The DIRDIF97 program system: Technical report of the Crystallography Laboratory; University of Nijmegen, The Netherlands* **1997**
[57] A. L. Spek, *J. Appl. Cryst.* **2003**, *36*, 7.

Chapter 3

An unexpectedly complex network of catalytic reactions, centred around a Pd-imido intermediate.

Abstract: The reactivity of palladium compounds of bidentate diaryl-phosphane ligands has been studied in the reaction of nitrobenzene with CO in methanol. Careful analysis of the reaction mixtures revealed that besides the frequently reported reduction products of nitrobenzene (methyl phenylcarbamate (MPC), *N,N'*-diphenylurea (DPU), aniline, azobenzene (Azo) and azoxybenzene (Azoxy)), large quantities of oxidation products of methanol were co-produced as well (dimethyl carbonate (DMC), dimethyl oxalate (DMO), methyl formate (MF), H_2O, and CO). From these observations, it is concluded that several catalytic processes operate simultaneously, and are coupled *via* common catalytic intermediates.

Starting from an *in situ* formed P_2Pd^0 compound, oxidation to a palladium-imido compound 'P_2Pd^{II}=NPh', can be achieved by the de-oxygenation of nitrobenzene (a) with two molecules of CO, (b) with two molecules of CO and the acidic protons of two methanol molecules, or (c) with all four hydrogen atoms of one methanol molecule. Reduction of P_2Pd^{II}=NPh to P_2Pd^0 makes the overall process catalytic, while at the same time forming Azo(xy), MPC, DPU, and aniline. It is proposed that the Pd-imido species is the central key-intermediate species that can link together all reduction products of nitrobenzene and all oxidation products of methanol in one unified mechanistic scheme. The relative occurrence of the various catalytic processes is shown to be dependent on the characteristics of the catalysts, as imposed by the ligand structure.

3.1. Introduction

Replacing wasteful and dangerous industrial processes by more environmentally friendly and safer ones is one of the challenges in current day catalysis. For example the large scale reduction of nitro aromatic compounds to their corresponding carbamates, ureas, or isocyanates is of great significance to society. Carbamates and ureas are used on a large scale as pesticides, fertilizers and dyes.[1] Aromatic isocyanates are used in the preparation of (flame-retarding) foams,[2, 3] (bio-degradable) plastics,[4, 5] pesticides,[6, 7] adhesives[8-10] and coatings.[6, 11, 12] In particular the polymer precursors MDI and TDI[13, 14] (Figure 3.1) are of great importance, and are annually produced on the megaton scale.[15]

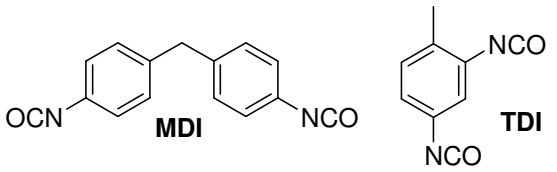

Figure 3.1. Two industrially-produced aromatic isocyanates.

Starting from nitroarenes, the synthesis of both MDI and TDI involves the usage of an excess of the highly toxic[16, 17] phosgene, and produces two moles of hydrochloric acid per mole of product.[18, 19] The most viable alternative for these processes having emerged so far, is the catalytic reductive carbonylation of nitroarenes.[20] In the presence of an alcohol or an amine, a carbamate or urea is formed (equations 1a and 1c). Both molecules can be pyrolyzed to yield the isocyanate with the recovery of the alcohol or amine employed (equations 1b and 1d).

$$PhNO_2 + CH_3OH + 3\ CO \rightarrow PhNH(CO)OCH_3 + 2\ CO_2 \quad (1a)$$

$$PhNH(CO)OCH_3 + \Delta T \rightarrow PhNCO + CH_3OH \quad (1b)$$

$$PhNO_2 + PhNH_2 + 3\ CO \rightarrow PhNH(CO)NHPh + 2\ CO_2 \quad (1c)$$

$$PhNH(CO)NHPh + \Delta T \rightarrow PhNCO + PhNH_2 \quad (1d)$$

In the 1980s it was discovered that palladium supported by bidentate N- or P-ligands afforded catalysts for this reaction in methanol (~500 turnover numbers).[21-23] In particular, the use of the ligand 1,10-phenanthroline (phen), in

the presence of an acid co-catalyst, proved to result in quite active catalysts (turnover numbers in the order of 10^3). Thus far, most scientific endeavors have been concentrated on the $[Pd(phen)_2]X_2$ / H^+ catalytic system in methanol,[24-35] leaving the Pd-phosphorus-based systems virtually unstudied.[31, 36-39] However, since it is commonly accepted that Pd^0 species function as intermediate in the catalytic cycle,[20, 32, 40-42] it was envisaged that catalysts with bidentate P-ligands could well perform differently from those with N-based ligands; due to their π-backbonding capability they could give improved stabilization of the Pd^0 intermediates.

Therefore, the palladium-catalyzed carbonylation of nitrobenzene in methanol was studied, using bidentate diarylphosphane ligands. During these studies it was found through careful quantitative analysis of the reaction mixtures that a number of reactions must be operating simultaneously. The aim of the present study has therefore been to explore which reactions take place and to propose a reaction network comprising these reactions.

3.2. Results

3.2.1. General considerations

In the catalytic carbonylation reactions the catalyst precursor complexes were formed *in situ* from $Pd(OAc)_2$ and 1.5 equivalents of ligand, as shown in Chapter 2, the palladium-ligand complex formation in methanol is instantaneous with the bidentate ligands used in this study.[43] As a control, the activity of several pre-formed precursor complexes was also tested, and identical results were obtained. Care was taken that the carbonylation experiments were carried out under strictly anhydrous conditions (< 100 ppm H_2O), using pre-dried reagents (see Appendix II, section 2).

The products observed in the carbonylation experiments are collected in Scheme 3.1 and full analytical details of all these products as found in these catalytic experiments are given in Table AII.1 in Appendix II. The commonly observed products of nitrobenzene carbonylation are methylphenylcarbamate (MPC) and N,N'-diphenylurea (DPU) with methanol and aniline as the nucleophilic reagent, respectively. Commonly reported side products are azobenzene (Azo),

azoxybenzene (Azoxy) and aniline.[20] The formation of aniline (and the related DPU) is usually attributed to the presence of water, either in the reagents or formed in situ, e.g. *via* acid-catalyzed etherification of methanol. Unexpectedly, analysis of the carefully prepared water-free reaction system (see section 2 of Appendix II) revealed that with most of the palladium-diphosphane catalyst systems significant amounts of dimethylcarbonate (DMC), dimethyloxalate (DMO) and to a lesser extent methyl formate (MF) were also produced. Even more surprisingly, significant amounts of water appeared to be formed as a reaction product (see section 3 of Appendix II). However, neither dimethyl ether (DME), nor dimethoxy methane (DMM) was observed as a reaction product, thus excluding methanol self-etherification or etherification with any possibly formed free formaldehyde under reaction conditions as a source of water. It is noteworthy that DMM is commonly observed in cationic palladium-catalyzed olefin hydrocarbonylation experiments involving methanol as the H-donor substrate.[44]

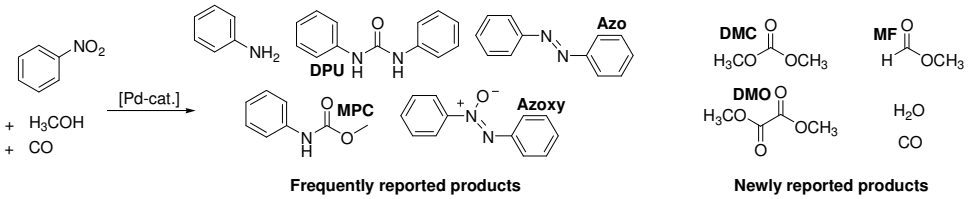

Scheme 3.1. Reaction products found in the catalytic carbonylation of nitrobenzene in methanol using palladium-diphosphane catalysts.

In the initial screening studies a large number of diphosphane ligands have been used, with variations in the length and flexibility of the backbone spacer as well as in the substituents on the phenyl rings. It appeared that not only the activity, but in particular the selectivity of the catalysts for the formation of the various products was highly dependent on the ligand structure. The observed trends in different reactivities and selectivities will be illustrated using the ligands shown in Figure 3.2. These bidentate phosphane ligands have either a rigid C3 (L3X) or a rigid C4 backbone (L4X), while the aryl rings can be functionalized with methoxy moieties in the ortho position (oMeO-L3X and oMeO-L4X). It has been shown in Chapter 2 that these ligands readily form stable complexes with $Pd(OAc)_2$ in methanol.[43] The results of the catalytic nitrobenzene carbonylation experiments using these complexes are summarized in Table 1. Results obtained with a more extended range of ligands are subject of Chapter 4 of this thesis.[45]

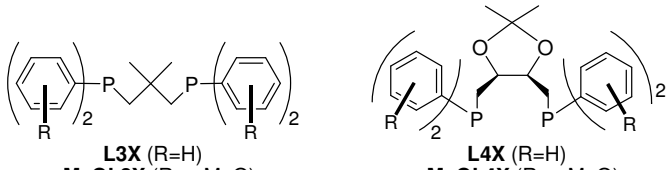

L3X (R=H)
oMeOL3X (R=*o*-MeO)

L4X (R=H)
oMeOL4X (R=*o*-MeO)

Figure 3.2. Overview of the ligands used in this study.

3.2.2. Ligand effects on the reduction products of nitrobenzene

Analysis of the reaction mixtures was carried out using GLC techniques; most products were quantified using calibration lines made with authentic samples using decane as internal standard and are reported in Table 1 in mmol produced. The appropriateness in time of the calibration lines was ensured by regular analysis of known quantities of analytes. The solid DPU was isolated and its quantity determined by weight.

Table 3.1. Results of the catalytic reaction of nitrobenzene in methanol using palladium-diphosphane catalysts.[a]

Entry	Ligand	$PhNO_2$	$PhNH_2$	DPU[b]	MPC	Azo	Azoxy	$\Sigma_{\varnothing}$	DMC	DMO	MF	H_2O[c]
1	L3X	8.1	8.3	0.8	5.3	0.1	0.4	24.3	4.2	3.1	0.2	3.4
2	oMeO-L3X	0.6	5.7	3.1	11.6	0.1	0.1	24.5	0.4	0.4	1.1	0.7
3	L4X	11.8	1.9	0.5	0.5	0.1	4.5	24.4	2.3	5.9	0.2	10.0
4	oMeO-L4X	2.4	10.5	1.9	5.6	0.5	0.6	24.5	2.1	7.3	0.6	8.7

[a] Reaction conditions: $Pd(OAc)_2$: Ligand : nitrobenzene = 0.05 : 0.075 : 24.4 mmol, in 25 ml methanol. Reaction mixtures were heated for four hours at 110 ºC under a CO atmosphere of 50 bar (initial pressure). Quantities are reported in mmol. See also Table AII.1. [b] quantified by weight. [c] quantified using a reaction with trimethylorthoformate (see Appendix II, sections 2 and 3).

The accuracy of the quantitative analysis of the phenyl-containing products is excellent as demonstrated by the observed conservation of aryl rings (column $\Sigma_{\varnothing}$). The activity of the palladium catalysts with the four different ligands is good to high, with conversions of $PhNO_2$ varying between 50-100% (column $PhNO_2$). With L3X as the supporting ligand a reasonably active catalyst is obtained; 67% conversion of nitrobenzene was reached in 4 hours (entry 1). The main reaction product is aniline, while selectivity to MPC is only 33%. The catalyst with ligand L4X showed a slightly lower activity, but a drastically different selectivity was observed; the major product is azoxybenzene (entry 3). The highest activity is obtained with catalysts containing ortho-methoxy substituted ligands (entries 2

and 4) with >90% nitrobenzene conversion. The use of these ligands also results in significantly higher selectivity for the product MPC; considerably lower amounts of the coupling products azo- and azoxybenzene are produced.

3.2.3. Ligand effects on the oxidation products of methanol and the hydrogen mass-balance

Although the mass conservation of phenyl rings appeared to be excellent for the products derived from nitrobenzene, a closer look at the hydrogen atom conservation revealed that the products aniline and DPU contain hydrogen atoms that can only be derived from methanol. Indeed, quantitative analysis of all (with GLC detectable) reaction products in the liquid phase showed that in all experiments significant amounts of the methanol-derived oxidation products dimethyl carbonate (DMC) and dimethyl oxalate (DMO) are formed, products which are known to be formed from methanol in the presence of an oxidant.[46-49] Methyl formate (MF) is also produced, albeit to a lesser extent. Clearly, these products are formed from a H-donating methanol carbonylation process (DMC, DMO) liberating two 'hydrogen atoms' or an oxidative dehydrogenation process (MF) liberating four 'hydrogen atoms' (eq. 2a-b; n = 1 or 2).[50] The produced hydrogen atoms are transferred to nitrobenzene *via* a mechanism postulated below, thus forming aniline and thereby also DPU as secondary product (eq. 2c).[51]

$$2\ CH_3OH + n\ CO \rightarrow H_3CO(CO)_nOCH_3 + \text{'2H'} \quad (2a)$$

$$2\ CH_3OH \rightarrow HC(O)OCH_3 + \text{'4H'} \quad (2b)$$

$$PhNO_2 + 2\ CO + \text{'2H'} \rightarrow PhNH_2 + 2\ CO_2 \quad (2c)$$

This implies that nitrobenzene is reduced while functioning as the oxidant for the oxidative carbonylation and oxidative dehydrogenation of methanol. Interestingly, the presence of o-MeO moieties on the ligands has an influence on the relative amounts of DMC, DMO, and MF formed in the reactions; the catalysts with the unsubstituted ligands L3X or L4X produce relatively more DMC and DMO, whereas the catalysts with the methoxy-substituted ligands oMeO-L3X or oMeO-L4X produce relatively higher amounts of MF.

H-atom conservation of all products requires that the sum of the hydrogen-releasing compounds (DMC + DMO + 2MF) must equal the sum of the hydrogen-consuming products ($PhNH_2$ + DPU). Although the hydrogen mass-balance is partly restored when taking the formation of DMC, DMO and MF into account, the hydrogen balance still appeared to be significantly uneven. Further investigations revealed that water is co-produced (see section 3 of Appendix II for the experimental procedure for determination of the quantity of water), suggesting that the stoichiometries described by equations 3a-b may also play an important role.

$$PhNO_2 + CO + \text{‘4H’} \rightarrow PhNH_2 + CO_2 + H_2O \quad (3a)$$

$$PhNO_2 + \text{‘6H’} \rightarrow PhNH_2 + 2\,H_2O \quad (3b)$$

However, the hydrogen balance appears still uneven when H_2O production is taken into account (i.e., DMC + DMO + 2MF = $PhNH_2$ + DPU + H_2O). Interestingly, when using the ligands with a C4 backbone (entries 2 and 4) large amounts of water were detected, whereas for ligands with a C3 backbone (entries 1 and 2) relatively small amounts of water were detected. This could be due to the concurrent production and consumption of water. Note however that the consumption of water should not affect the hydrogen mass-balance, as the H-atoms would end up in $PhNH_2$ or DPU.

3.2.4. Hydrogen mass-balance; complete dehydrogenation of methanol

The hydrogen mass-balance involving all of the products detected in the liquid phase of the reaction mixture is shown schematically in Figure 3.3.

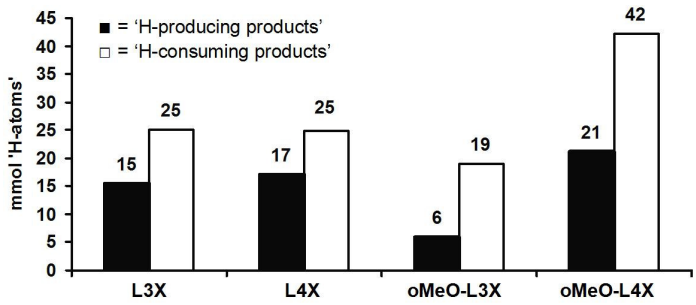

Figure 3.3. Visualization of the hydrogen mass-balance for the products reported in Table 3.1, 2(DMC + DMO + 2MF) =(■) and 2(H_2O + $PhNH_2$ + DPU)= (□).

As can be seen from this figure, for each of the catalysts significantly more 'hydrogen-consuming' products (H_2O, $PhNH_2$, and DPU) than 'hydrogen-releasing' compounds (DMC, DMO, and MF) are observed. This suggests that there must be an as yet unknown additional source of hydrogen atoms. Because the CO used was more than 99% pure, the option was considered that the H-atoms originate from impurities (H_2O/H_2) in this reactant. However, traces of water (20 vpm according to the manufacturer)[52] could account only for a maximum of ~6 μmol H-atoms. Similarly, even if it is assumed that the CO contains 1% H_2 and this, as an unlikely event, would be totally consumed as reductant for nitrobenzene, the maximum amount of H-atoms from this source can be only 4 mmol (2 mmol H_2), whereas for the ligand oMeO-L4X 21 mmol too many H-atoms are observed. This leaves as a surprising conclusion that methanol itself can be the only plausible source of hydrogen atoms, meaning that methanol can also be *fully* dehydrogenated to CO. Apparently, in addition to the production of DMC/DMO (eq. 2a) or MF (eq. 2b), CO production can liberate four 'H-atoms', as shown in equation 4.

$$CH_3OH \rightarrow CO + \text{'4H'} \qquad (4)$$

To verify this possible reaction, the gas phase of an autoclave experiment in which a catalytic reaction was conducted in the presence of methanol containing 4% $^{13}CH_3OH$ (v/v) and using only 5 bar CO was analyzed by mass spectroscopy (see Table S2 for details). A catalyst system with oMeO-L3X as supporting ligand was chosen, as with this catalyst the H-mass conservation is significantly violated. This resulted in a significant increase of 15% of ^{13}C-enriched CO, which must originate from full methanol dehydrogenation.[53] Moreover, it appeared to be possible to even out the hydrogen mass balance for this experiment, as the amount of fully dehydrogenated methanol can be estimated.[54] When repeating this experiment under an argon atmosphere (in the absence of CO) CO_2 was produced (see Figure S2) with the co-production of some nitrobenzene reduction products. This also proves that methanol must have been fully stripped of H-atoms to function as the reductant of nitrobenzene.

3.2.5. Methanol as transfer hydrogenation reagent

As the above observations imply that methanol can act as a transfer hydrogenation reagent, it was tested if a better transfer hydrogenation donor, i.e. *iso*-propanol,

would give similar results. Indeed, using (oMeO-L3X)$Pd^{II}(OAc)_2$ as catalyst precursor, a reaction of nitrobenzene in *iso*-propanol using 50 bar CO resulted almost exclusively in the formation of aniline, with the co-production of a large quantity of acetone. In contrast with acetone as the stable transfer hydrogenation end-product, palladium-bound formaldehyde (formed after the first dehydrogenation of CH_3OH) can be further stripped from H-atoms under reaction conditions to give CO. To further test if formaldehyde could be an intermediate, 0.30 g of para-formaldehyde (about 9 mmol $(O=CH_2)_n$, assuming that 10% of the weight consists of water 'end groups') was suspended in a methanol/nitrobenzene mixture and allowed to react for four hours at reaction temperature (110 ºC), in the presence of an active catalyst.

The result is shown in entry 1 of Table 2; surprisingly, in this reaction MF was formed almost exclusively. When this experiment was repeated in the absence of a catalyst and nitrobenzene (entry 2) dimethoxymethane (DMM) was, as expected, exclusively formed instead. When aniline was also present in a reaction mixture (entry 3), formaldehyde was again reacted to MF, but now also a significant amount of N-methylenebenzenamine ($PhN=CH_2$, MBA) was formed. MBA can be seen as a condensation product of formaldehyde and aniline and is sometimes also detected in small amounts after a normal catalytic experiment. This confirms that in the presence of the catalyst, formaldehyde can react to MF and to MBA rather than to DMM. Thus, when methanol dehydrogenation proceeds *via* a Pd-formaldehyde intermediate, this suggests that the formaldehyde molecule does not dissociate from the catalyst, as otherwise DMM would be produced instead.

Table 3.2. Reactivity of *para*-formaldehyde with methanol and aniline in the presence or absence of an active catalyst. Quantities are reported in mmol.[a]

Entry	Catalyst	P_{CO}	Additives	MF	DMM	MBA
1	Yes	50	~9 $(H_2CO)_n$ 24.4 $PhNO_2$	7.8	trace	trace
2	No	50	~9 $(H_2CO)_n$	trace	3.7	-
3[b]	Yes	5	~9 $(H_2CO)_n$ 10 $PhNH_2$ 4.9 $PhNO_2$	3.0	-	1.6

[a] Reaction mixtures were heated for four hours at 110 ºC in 25 ml methanol. The catalyst is Pd(oMeO-L3X)$(OAc)_2$ synthesized *in situ* from 0.05 mmol $Pd(OAc)_2$ and 0.075 mmol oMeO-L3X. See also Table S1 for a full analysis of the reaction mixtures. [b] the CO pressure and nitrobenzene concentration were lowered to suppress the carbonylation reaction.

3.2.6. Ligand effects in the consumption of water

As for some catalysts large amounts of water were detected (Table 3.1) and almost no water was observed for other catalysts, it was investigated if perhaps water could also be consumed during the reaction. Thus, the reactions as shown in Table 3.1 were repeated, but now water was deliberately added to the system (Table , see also section 4 of Appendix II for experimental details). When employing catalysts containing the ligands with a C3 backbone (entries 1 and 3), it appears that water is largely consumed during the reaction; only some residual water was detected when 12 mmol water was added prior to the catalytic run (entries 1-2 and 3-2). However, when using ligands with a C4 backbone, large amounts of water were already detected after a normal catalytic experiment (entries 2-1 and 4-1). When 12 mmol water was added prior to a catalytic run (entries 2-2 and 4-2) this amount is found back after the experiment, in addition to the amount formed during the reaction. It thus appears that water is formed but only partly consumed when using catalysts comprising the ligands L4X and oMeO-L4X, but added water appears to be largely consumed when using catalysts with the ligands L3X and oMeO-L3X.

Water may be consumed by replacing methanol as a reagent in equation 1a, the combination of 2a+2c, or the combination of 4+(2×2c).

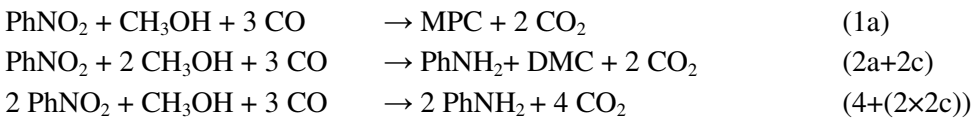

$PhNO_2 + CH_3OH + 3\ CO \rightarrow MPC + 2\ CO_2$ (1a)

$PhNO_2 + 2\ CH_3OH + 3\ CO \rightarrow PhNH_2 + DMC + 2\ CO_2$ (2a+2c)

$2\ PhNO_2 + CH_3OH + 3\ CO \rightarrow 2\ PhNH_2 + 4\ CO_2$ (4+(2×2c))

When water replaces methanol in the formation of MPC (eq. 1a), phenylcarbamic acid (PhNHC(O)OH) will be formed, which decomposes into aniline and CO_2, thus leading to the stoichiometry shown in equation 1a*. When water replaces one methanol molecule in the formation of DMC (eq. 2a), methyl hydrogen carbonate ($CH_3OC(O)OH$) will be formed, which will readily decompose into methanol and CO_2. This will lead to the stoichiometry given by equation 2a*, which is effectively the water-gas-shift reaction. When combining equation 2a* with equation 2c (aniline formation), the net overall stoichiometry also amounts to equation 1a*. Similarly, stoichiometry 1a* results when (two) water molecules replace methanol in equation 4, and this reaction is combined with the production of aniline (2×eq. 2c).

$PhNO_2 + H_2O + 3\ CO \rightarrow PhNH_2 + 3\ CO_2$ (1a*)

$H_2O + CO \rightarrow CO_2 + \text{'2H'}$ (2a*)

From the above it follows that, when water is consumed, either the amount of MPC (cq. DPU) must decrease while increasing the amount of aniline accordingly, or the amount of DMC (or DMO) must decrease while keeping the amount of aniline constant. This is indeed reflected in the change in product distributions for the reactions with and without added water, as can be seen in Table 3 (see note for a detailed calculation).[55]

Table 3.3. Catalytic carbonylation reactions using in situ synthesized $Pd(Ligand)(OAc)_2$ catalyst precursors with and without added water present.[a]

Entry	Ligand	H_2O added[b]	H_2O detected[c]	DMC+ DMO	MPC+ DPU	$PhNH_2$+ DPU
1-1	L3X	-	3.4	7.3	6.1	9.1
1-2	``	12	7.4	3.5	4.0	11.1
		Cons:[d]	8.0	Δ[e] = –3.8	Δ = –2.1	Δ = 2.0
2-1	L4X	-	10.0	8.2	1.0	2.4
2-2	``	12	22.3	7.8	0.9	2.3
		Cons:	–0.3	Δ = –0.4	Δ = –0.1	Δ = –0.2
3-1	oMeO-L3X	-	0.7	0.8	14.7	8.8
3-2	``	12	1.9	0.2	9.3	14.0
		Cons:	10.8	Δ = –0.6	Δ = –5.4	Δ = 5.2
4-1	oMeO-L4X	-	8.7	9.4	7.5	12.4
4-2	``	12	18.8	9.6	6.6	13.3
		Cons:	1.9	Δ = 0.2	Δ = –0.9	Δ = 0.9

[a] Reaction conditions: $Pd(OAc)_2$: Ligand : nitrobenzene = 0.05 : 0.075 : 24.4 mmol, in 25 ml methanol. Reaction mixtures were heated for four hours at 110 ºC under a CO atmosphere of 50 bar (initial pressure). Quantities are reported in mmol. See also Table S1. [b] before the catalytic reaction; [c] after the catalytic reaction. [d] mmol water consumed, as calculated by (12+entry X-1) – entry X-2; [e] Difference between entry (X-2) – (entry X-1). See also section 4 of the Appendix II.

3.2.7. *In situ* trapping experiments

As the formation of *all* observed products may very well be explained by postulating a palladium imido species "Pd=NPh" as the key-intermediate species (as is discussed below), it was attempted to obtain evidence for its existence under reaction conditions. Attempts were thus undertaken to trap this species by adding cyclohexene[56] during a catalytic experiment (Scheme 3.2).

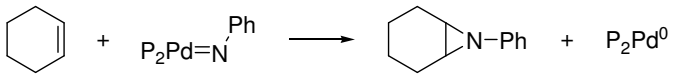

Scheme 3.2. Proposed trapping reaction of an imido complex with cyclohexene.

When adding 25 mmol cyclohexene during a catalytic run indeed the formation of the corresponding aziridine was observed when employing Pd^{II}(L4X) or Pd^{II}(oMeO-L3X) as catalyst precursor. In Figure 3.4, the mass and defragmentation pattern are shown of the peak in the GLC-MS spectrum that was assigned to this trapping product; both the mass and the defragmentation pattern are consistent with the structure of 7-phenyl-7-aza-bicyclo[4.1.0]heptane.

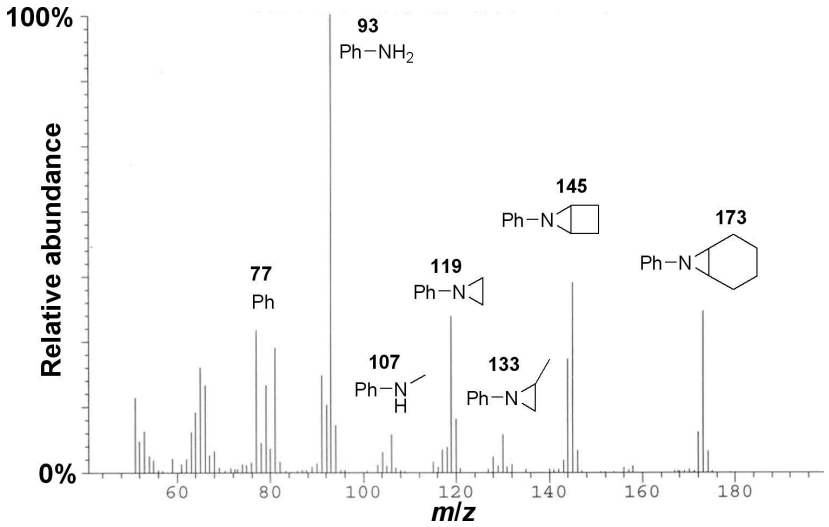

Figure 3.4. Mass spectrum of a compound detected with GLC-MS analysis of a reaction mixture to which cyclohexene was added.

3.3. Discussion

3.3.1. Coupling oxidation of methanol with reduction of nitrobenzene

In the studies on the carbonylation of nitrobenzene in methanol to form methylphenylcarbamate, the usually reported side-products only comprise the phenyl-containing compounds aniline, DPU, Azo and Azoxy, depending on the reaction conditions and additives.[20] In general, the mechanistic proposals

(Scheme 3.3) for the reaction catalyzed by Pd–1,10-phenanthroline systems start with oxidative coupling of CO and $PhNO_2$ at an (*in situ* generated) Pd^0 species to form a Pd^{II} species.[20, 32, 57] During the proposed catalytic cycle the catalyst remains in the Pd^{II} oxidation state; in the final MPC-generating step Pd^0 is regenerated from a palladacyclic intermediate such as the one shown in Scheme 3.3.[28, 40]

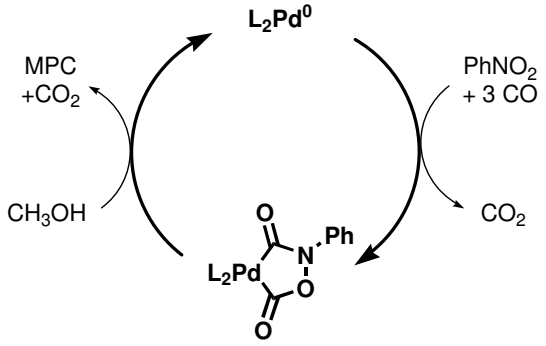

Scheme 3.3. Generally accepted mechanistic proposal for the reductive carbonylation of nitrobenzene, wherein the bidentate ligand (L_2) is 1,10-phenanthroline.

The most remarkable observation applying bidentate diarylphosphanes as ligands in the catalyst is the formation –under mild reaction conditions– of substantial amounts of products that are derived from oxidative reactions involving methanol as well as products derived from reduction of nitrobenzene. Clearly, the carbonylation of methanol to DMC (or DMO) must be accompanied by a reduction of Pd^{II} to Pd^0; conversely, the oxidant nitrobenzene will oxidize Pd^0 to Pd^{II} while being reduced to aniline, DPU, MPC and Azo(xy). These elementary process steps must form the basis for product formation shown in Table 1. Dictated by the hydrogen mass-balance, the transfer of 'H-atoms' from methanol (eq. 2a, 2b, 4) to nitrobenzene (eq. 2c, 3a, 3b) must play an important role in these reactions. A palladacyclic intermediate such as the one shown in Scheme 3.3 cannot be used to rationalize the formation of oxidation products of methanol, nor the H-transfer from methanol to nitrobenzene. Therefore, an alternative catalytic intermediate must be proposed that can link the reduction of nitrobenzene with the oxidation of methanol.

3.3.2. Reduction of nitrobenzene; a palladium-imido complex as key intermediate

Central in understanding the Pd-phosphane catalysts systems is the central hypothesis of this thesis, namely that the $PhNO_2$ reduction process is modified in the sense that a Pd-imido intermediate is formed (see also Scheme 3.4 and 5, and further details below).[32, 57, 58] Such a species will allow a catalytic connection to be made between the reductive processes involving nitrobenzene and oxidative processes involving methanol. Thus, with Pd-phosphane systems, a nitrobenzene reduction stoichiometry is proposed with CO as the reductant, as given in equation (5a).

$$P_2Pd^0 + PhNO_2 + 2\ CO \rightarrow P_2Pd^{II}{=}NPh + 2\ CO_2 \qquad (5a)$$

However, as clearly evidenced by the significant *formation* of H_2O with some of the catalysts, 'H-atoms' from methanol obviously also act as a direct reductant for nitrobenzene, to eventually form the same Pd-imido intermediate. A reasonable way to achieve this is *via* stoichiometry (5b), wherein the acidic hydrogen atoms of two methanol molecules and two CO molecules act as reductant for nitrobenzene. Note that the second molecule of CO is not directly used to de-oxygenate nitrobenzene, but is merely used to form DMC.

$$P_2Pd^0 + PhNO_2 + 2\ CO + 2\ CH_3OH \rightarrow P_2Pd^{II}{=}NPh + DMC + H_2O + CO_2 \qquad (5b)$$

Furthermore, as evidenced by the gas phase enrichment of ^{13}CO from $^{13}CH_3OH$, it must be concluded that methanol can be *fully* stripped of H-atoms, e.g. *via* stoichiometry (5c).

$$P_2Pd^0 + PhNO_2 + CH_3OH \rightarrow P_2Pd^{II}{=}NPh + 2\ H_2O + CO \qquad (5c)$$

In the latter stoichiometry, CO could also act as a co-reductant together with two instead of four H-atoms of methanol thus forming $H_2C{=}O$. However, formaldehyde was never detected, nor its methanol condensation product DMM. On the other hand, MF was always detected which may be seen as resulting from a modified version of equation 5c, wherein two molecules of methanol react to give MF instead of CO (see also eq. 2b).

The proposed Pd-imido intermediate can thus be formed in three ways: de-oxygenation of nitrobenzene with two equivalents of CO only (eq. 5a), with the acidic protons of two molecules of CH_3OH and with two CO (eq. 5b), and with all four H-atoms of one CH_3OH (eq. 5c).

3.3.3. A palladium-imido complex as key intermediate; mechanistic considerations

The reductive cyclization of (*ortho*) functionalized aromatic nitro compounds has been proposed to proceed *via* a palladium-imido compound.[59] Additionally, using deuterium labelling experiments the intermediacy of a palladium-imido species was demonstrated in the reductive N-heterocyclization of various 2-nitrostyrene and N-(2-nitrobenzylidene)amine derivatives to the corresponding indole and 2*H*-indazole derivatives.[60] A Pd–imido compound has never been reported and only once claimed to be spectroscopically (IR) detected.[61] However, a series of bidentate phosphane stabilized Ni–imido complexes has been isolated. Upon reaction with CO these complexes formed phenylisocyanate and upon reaction with ethene the corresponding aziridine could be obtained.[62-64] Inspired by these reports, cyclohexene was during a catalytic run with the aim to trap the nitrene ligand of the possible P_2Pd^{II}=NPh intermediate. GLC-MS analysis after these runs indeed revealed the presence of the corresponding aziridine. These observations lend credibility to the postulation of a Pd-imido complex as important intermediate for the reduction reactions of nitrobenzene.[32, 57, 58] Synthetic efforts aimed at formation and spectroscopic characterization of (diphosphane)Pd-imido complexes give further evidence of their existence; the synthesis and reactivity of these complexes is part of Chapter 4 of this thesis.

At this stage, an experimentally proven, direct evidence for the intermediacy of a palladium-imido species in the above proposed reactions (eq. 5a-c) cannot yet be given. However, it is considered highly useful to further elaborate on the molecular mechanistic basis underlying these proposed stoichiometries. Such a consideration will provide for the construction of the appropriate framework to rationalize how the nitrobenzene reduction process is linked with the oxidation of methanol. Also, the experimentally observed product compositions can then be

related to the P_2Pd^{II} complexes in terms of their structural and electronic properties (*vide supra*).

The commonly proposed pathway to reduce nitrobenzene with CO alone is shown in the top of Scheme 3.4. An oxidative coupling of CO and nitrobenzene at Pd^0 involves formal oxidation of Pd^0 (**C1**) to give the palladacyclic species (**C2a**). This can be followed by further de-oxygenation *via* successive CO_2 extrusion / carbonylation / CO_2 extrusion (*via* **C3a** and **C4a**) to give the palladium-imido intermediate. This sequence would account for the stoichiometry given in equation (5a). Note that CO insertion into the Pd-N bond of (**C4a**) can also occur; this would afford the palladacycle generally proposed and observed for Pd-1,10-phenanthroline nitrobenzene reduction systems.[28, 40]

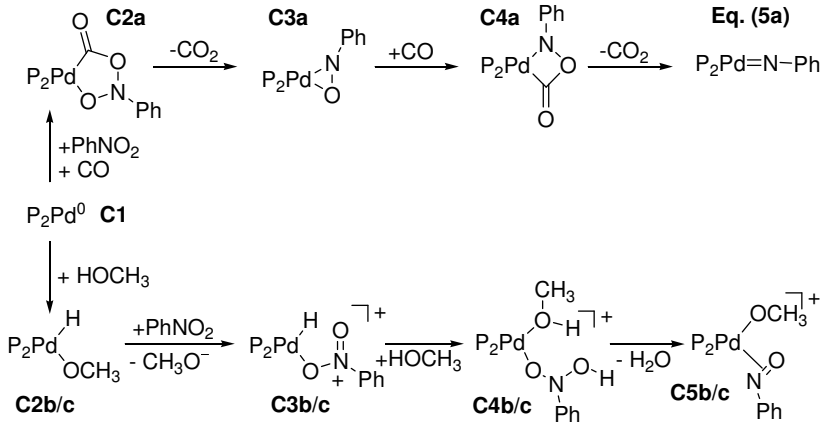

Scheme 3.4. Mechanistic proposals for nitrobenzene reduction with CO as only reductant (top, forming P_2Pd^{II}=NPh *via* eq. 5a), and the initial steps with CH_3OH as reductant (bottom).

Alternatively, the reduction of nitrobenzene must be achieved by H-atoms from methanol eventually leading to equations (5b) and (5c). This transfer hydrogenation process most likely involves palladium hydride chemistry, without involvement of 'free' H_2, as methanol dehydrogenation to H_2 and DMC, MF, or CO is endothermic by about +21, +48, and +44 kcal.mol^{-1}, respectively.[65-67] First, Pd-hydride formation might take place by oxidative addition of methanol onto P_2Pd^0 to give (**C2b/c**), as is shown at the bottom of Scheme 3.4. Displacement of a CH_3O^- anion by nitrobenzene gives the cationic Pd-hydride

(**C3b/c**). Migration of the hydride to the coordinated nitrobenzene then yields (**C4b/c**) in which the nitrobenzene fragment has become anionic, i.e. $[ON(Ph)OH]^-$. Nucleophilic attack of the anionic $[ON(Ph)OH]^-$ fragment on the acidic proton of methanol in (**C4b/c**) forms palladium-bound nitrosobenzene (**C5b/c**) and liberates H_2O, thus completing the first reduction step.[68]

As is shown in Scheme 3.5, it is thought that the different pathways to the stoichiometries given in equations (5b) or (5c) are determined in complex (**C5b/c**). Thus, CO insertion (top) into the Pd–OCH_3 bond of (**C5b/c**) affords (**C6b**), from which DMC can be formed, thus yielding the Pd^0-nitrosobenzene complex (**C3a**) (nitrosobenzene was indeed experimentally observed in trace amounts). From here, just as in the 'CO-only' reduction route (top in Scheme 3.4), the Pd-imido complex can be formed by a carbonylation/CO_2 extrusion, thus leading to the overall stoichiometry given by equation (5b).

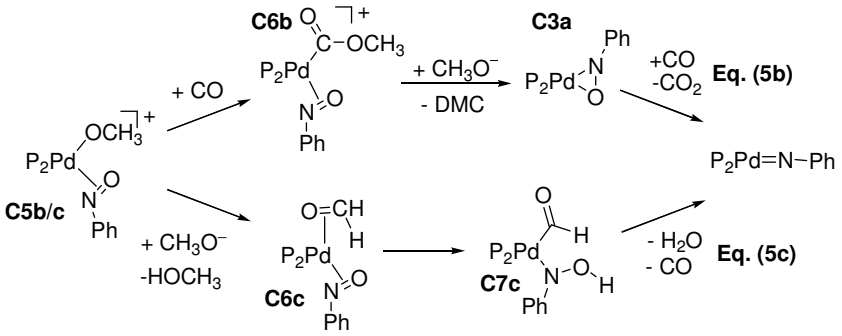

Scheme 3.5. Mechanistic proposals for nitrobenzene reduction to P_2Pd^{II}=NPh with either CH_3OH/CO as co-reductants (top, using only the -OH proton of methanol, eq. 5b) or with only CH_3OH as reductant (bottom, also using the -CH_3 protons of methanol, eq. 5c).

Alternatively (bottom), nucleophilic attack of the uncoordinated CH_3O^- anion in (**C5b/c**) on a H-atom of the coordinated CH_3O^- anion (i.e., a net β-H abstraction) will liberate methanol and form a zero-valent palladium-formaldehyde / nitrosobenzene complex (**C6c**). In a subsequent reaction involving intramolecular H-transfer (presumably *via* the Pd centre) from formaldehyde to nitrosobenzene, palladium can be oxidized to (**C7c**). This clearly is a hypothetical reaction, but may be viewed as bearing resemblance with oxidative coupling of CO with nitrobenzene at Pd^0 in the formation of a palladacycle (**C2a**, Scheme 3.4). The last

H-atom can then be transferred by nucleophilic attack of the $[N(Ph)OH]^-$ anion on the Pd-C(O)H proton, thus forming the Pd-imido complex, H_2O, and CO. This results in the overall stoichiometry given by equation (5c). Note that reaction of (**C7c**) with methanol could also lead to MF, water and the imido-intermediate (not shown in Scheme 3.5).

While there is no *a priori* way to estimate the respective contributions of nitrobenzene reduction by two CO (eq. 5a), two CH_3OH and two CO (eq. 5b), or one CH_3OH alone (eq. 5c), the above mechanistic basis provides a rationale for the generation of H_2O, DMC/DMO, CO, and MF by an oxidative dehydrogenation of methanol with nitrobenzene as the oxidant. All these proposed reactions result in the same P_2Pd^{II}=NPh intermediate (as summarized in Scheme 3.6) as a centrally important intermediate species in a complex network of catalytic cycles that links *all* the oxidation products of methanol with *all* the reduction products of nitrobenzene, as is discussed below.

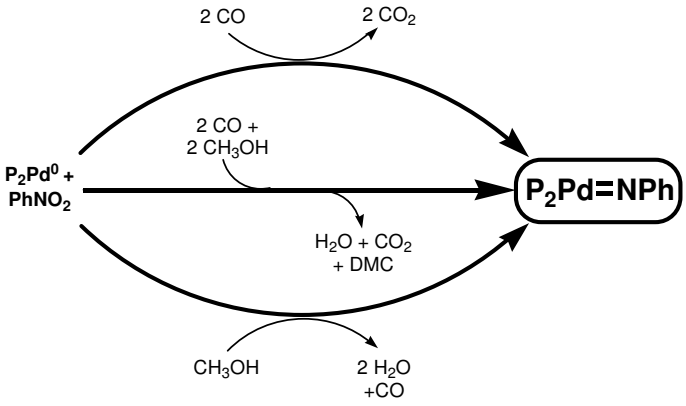

Scheme 3.6. Three competing pathways for the reduction of nitrobenzene to a Pd^{II}-imido intermediate, using two CO (top), one CO and the acidic protons of two methanol (centre) or all H-atoms of one methanol (bottom) as de-oxygenating agent.

3.3.4. Protonation of the palladium-imido complex; formation of aniline

To sustain coupled *catalytic* cycles for production of both the methanol oxidation products as well as the nitrobenzene reduction products, a product-releasing species of the one cycle must be an initiating intermediate species in the complementary product catalytic cycle. Thus, it is appropriate to consider how the

palladium-imido species could account for the formation of the aryl-containing products while being reduced to Pd^0 to sustain such reactions catalytically.

Because the imido nitrogen is formally dianionic and thus expected to be basic, protonation by methanol may readily occur. This will generate aniline and a dimethoxide species, $P_2Pd^{II}(OCH_3)_2$, as shown in equation 6.

$$P_2Pd^{II}{=}NPh + 2\ HOCH_3 \rightarrow PhNH_2 + P_2Pd^{II}(OCH_3)_2 \quad (6)$$

Once this dimethoxido-Pd^{II} complex is formed, carbonylation can reduce Pd^{II} to Pd^0 and generate DMC or DMO, as shown by equations (7a) and (7b).

$$P_2Pd^{II}(OCH_3)_2 + CO \rightarrow OC(OCH_3)_2 + P_2Pd^0 \quad (7a)$$
$$P_2Pd^{II}(OCH_3)_2 + 2\ CO \rightarrow (OC)_2(OCH_3)_2 + P_2Pd^0 \quad (7b)$$

Carbonylation reactions (7) are thought to proceed *via* displacement of the anionic CH_3O^- moiety by CO coordination and subsequent nucleophilic attack of methoxide on coordinated CO forming $P_2Pd(COOCH_3)(OCH_3)$ (I); reductive elimination of DMC then regenerates the P_2Pd^0 compound. When CO succeeds in displacing the CH_3O^- moiety in (I), subsequent nucleophilic attack of CH_3O^- on coordinated CO gives the dicarbomethoxide compound, $P_2Pd(COOCH_3)_2$ (II) which again gives P_2Pd^0 upon reductive elimination of DMO. It is thus thought that DMC and DMO are formed *via* related elementary reaction steps. Their respective yields will depend on the relative abundance of species (I) and (II), which is determined by the competition between CO and CH_3O^- for a coordination site at the palladium centre in (I). Further details of this methanol carbonylation process and factors that influence the rate and selectivity of these reactions will be subject of a separate publication.[45] As far as the present discussion concerns, it suffices to notice that DMC and DMO can be regarded as one product, providing two H-atoms.

Thus, a *catalytic* coupling can be established between two sets of half reactions: one set (eq. 5a-c) wherein nitrobenzene is being reduced while P_2Pd^0 is oxidized to a P_2Pd^{II}=NPh intermediate (producing CO_2/H_2O/DMC/DMO/CO/MF); and one complementary series of reactions (eq. 6 and 7a-b) wherein the P_2Pd^{II}=NPh

intermediate is reduced to P_2Pd^0 *via* the $P_2Pd^{II}(OCH_3)_2$ complex, thereby producing $PhNH_2$, but also DMC/DMO.

3.3.5. "Disproportionation" of nitrobenzene with the palladium-imido complex; formation of azo(xy)benzene

When using $P_2Pd(L4X)$ as the catalyst, significant amounts of azoxybenzene were produced, apparently at the expense of aniline and MPC (Table 1). It seems likely that when employing $P_2Pd(L4X)$, the Pd-imido-intermediate is also formed, but this species then does not react with methanol to produce DMC/DMO and aniline (eq. 6), but instead undergoes attack by nitrobenzene giving a "disproportionation"-type reaction to form azoxybenzene and formally a '$P_2Pd{=}O$' complex (eq. 8a). The possible existence of such a compound has been proposed before in the form of '$(Ph_3P)_2PdO$'.[69] Furthermore, $((t\text{-}Bu)_3P)_2Pd$ has been reported to react with dioxygen to give a deep-red compound analyzed as $[(t\text{-}Bu)_3P)PdO]_n$. The IR spectrum of this compound did not show a ν(O–O) band that is expected for a side-on O_2 coordination.[70] The hypothetical '$P_2Pd{=}O$' species will be readily de-oxygenated by CO to form CO_2, thus regenerating the zero-valent palladium species (eq. 8b). Alternatively, the '$P_2Pd{=}O$' complex can be protonated with methanol to form water and $P_2Pd^{II}(OCH_3)_2$ (eq. 8c), which can also regenerate P_2Pd^0 (eq. 7). This sequence couples azoxybenzene formation to catalytic nitrobenzene reduction, either directly *via* P_2Pd^0 (eq. 8b), or indirectly *via* $P_2Pd(OCH_3)_2$ (eq. 8c). The considerably less pronounced formation of azobenzene can be seen as a similar process involving attack of nitrosobenzene (as intermediate product in nitrobenzene de-oxygenation, Scheme 3.4) on the same Pd-imido intermediate (eq. 8d). Indeed, trace amounts of nitrosobenzene are sometimes observed.

$$P_2Pd^{II}{=}NPh + PhNO_2 \rightarrow PhN(O)NPh + 'P_2Pd^{II}{=}O' \quad (8a)$$

$$'P_2Pd^{II}{=}O' + CO \rightarrow CO_2 + P_2Pd^0 \quad (8b)$$

$$'P_2Pd^{II}{=}O' + 2\ HOCH_3 \rightarrow H_2O + P_2Pd^{II}(OCH_3)_2 \quad (8c)$$

$$P_2Pd^{II}{=}NPh + PhNO \rightarrow PhNNPh + 'P_2Pd^{II}{=}O' \quad (8d)$$

It thus appears that also the formation of reductive self-coupling products of nitrobenzene (to give azoxy- and azobenzene) can be linked into the network of P_2Pd^{II}/P_2Pd^0 catalytic cycles centered around the Pd-imido intermediate (eq. 5-8).

3.3.6. Carbonylation of nitrobenzene; MPC, DPU, and CO_2

The nitrobenzene carbonylation products MPC and DPU can also be linked to the imido-intermediate. Mono-protonation of P_2Pd^{II}=NPh (eq. 9a) by methanol, followed by CO insertion (eq. 9b) and reductive elimination (eq. 9c), leads to MPC while regenerating P_2Pd^0. When in this sequence of reactions methanol is replaced by aniline, DPU will be formed instead of MPC. Likewise, when water replaces methanol, phenyl carbamic acid will be produced. MPC and DPU can interconvert into each other under reaction conditions by trans-esterification, and can thus be considered as essentially the same nitrobenzene carbonylation products. Phenylcarbamic acid will decompose (eq. 9d) into aniline and CO_2, which is formally also a carbonylation product of nitrobenzene.

$$P_2Pd^{II}{=}NPh + HOCH_3 \rightarrow P_2Pd^{II}(OCH_3)NHPh \quad (9a)$$

$$P_2Pd^{II}(OCH_3)NHPh + CO \rightarrow Pd^{II}C(O)OCH_3(NHPh) \quad (9b)$$

$$Pd^{II}C(O)OCH_3(NHPh) \rightarrow P_2Pd^0 + MPC \quad (9c)$$

$$PhNHC(O)OH \rightarrow PhNH_2 + CO_2 \quad (9d)$$

Such a sequence of reactions bears strong mechanistic resemblance to those of olefin carbonylation reactions catalyzed by similar P_2Pd^{II} catalysts; in the presence of methanol, aniline or water, esters, amides or carboxylic acids are produced respectively.[71]

Alternatively, CO coordination and migration of the imido-moiety towards coordinated CO could yield P_2Pd^0 and phenylisocyanate, which can be trapped by methanol, aniline or water to produce MPC, DPU, or aniline and CO_2 (phenylcarbamic acid) as well. Note, however, that both pathways involve the complete de-oxygenation of nitrobenzene, followed by (methoxy)carbonylation of the Pd-imido intermediate. Thus, the combination of both sets of half-reactions, represented by equations 5 and equations 9, naturally leads to the full catalytic cycles for reductive carbonylation of nitro aromatics to products like carbamates and ureas.

One particularly attractive point of the above proposed nitrobenzene carbonylation mechanism appears that even this carbonylation cycle involves – and competes for– the Pd-imido intermediate. This Pd-imido complex thus not only rationalizes the observed catalytic connection between nitrobenzene

reduction chemistry and methanol oxidation chemistry, but also provides the link with reductive carbonylation of nitrobenzene as well as with reductive self-coupling of nitrobenzene. The connection between nitrobenzene carbonylation chemistry, azo(xy)benzene formation and methanol carbonylation is schematically depicted in Scheme 3.7.

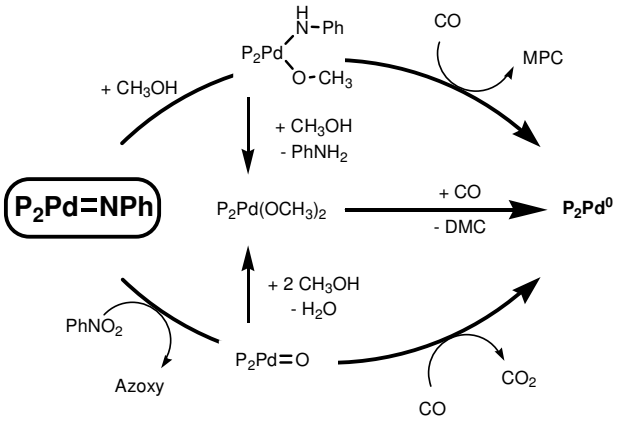

Scheme 3.7. Competing reactions for the Pd-imido intermediate, with: methanol and CO (top), or nitrobenzene and CO (bottom). Both pathways can also lead to $P_2Pd(OCH_3)_2$ by reaction with methanol (centre). In all cases, P_2Pd^0 is formed.

3.3.7. A complex network of catalytic cycles, centred around the Pd-imido complex

As the above discussion makes clear, it seems that when using the palladium-diphosphane catalysts for the carbonylation of nitrobenzene in methanol, an unexpectedly complex network of several catalytic reactions are simultaneously operative. A prime hypothesis in this thesis is that these reactions encompass competing processes for the reaction of P_2Pd^0 to the P_2Pd^{II}-imido complex, as well as competing processes for the reaction of the P_2Pd^{II}-imido complex to P_2Pd^0. A catalytic scheme that links together all these processes is condensed in the working hypothesis shown in Scheme 3.8, which reveals the P_2Pd^{II}=NPh complex as the central intermediate species.

The *in situ* formed P_2Pd^0 complex can be seen as entry point for all catalytic processes (left). The first competing processes are the net oxidation of P_2Pd^0 to the P_2Pd^{II}-imido complex with either only two CO (top left, eq. 5a), two $CH_3O\mathit{H}$

and two CO (centre left, eq. 5b), or only one C*H*$_3$O*H* (bottom left, eq. 5c) as de-oxygenating reagents for nitrobenzene.

Formation of the imido intermediate can be followed (right) by a protonation to form $P_2Pd^{II}(OCH_3)NHPh$ (top right, eq. 9a) or a "disproportionation" to form Azo(xy) and 'P_2Pd=O' (bottom right, eq. 8a). Both intermediates can be carbonylated to form respectively, MPC (top right, eq. 9b/c) or CO_2 (bottom right, eq. 8b) and re-form the initial P_2Pd^0 species to make these reactions catalytic. Alternatively, both intermediates can be protonated to form $P_2Pd^{II}(OCH_3)_2$ and aniline (top right, eq. 6) or water (bottom right, 8c). Carbonylation of this $P_2Pd^{II}(OCH_3)_2$ complex will produce DMC/DMO and regenerate P_2Pd^0 (centre right, eq. 7), allowing these reactions to proceed catalytically as well.

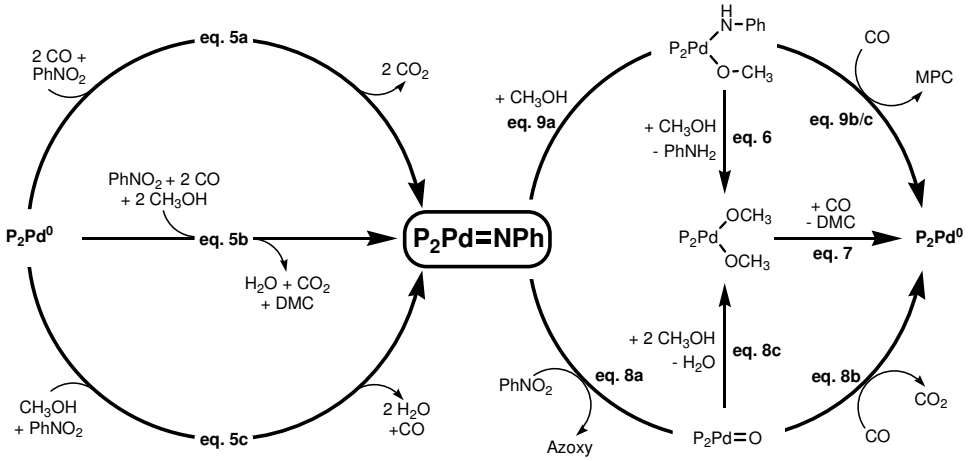

Scheme 3.8. Working hypothesis of the interrelated catalytic cycles operating in the P_2Pd catalyzed reaction of nitrobenzene with CO in methanol, rationalizing all the products observed.

3.3.8. Simulation of reaction stoichiometries

From the complex network of reactions unfolded above, it follows that a combination of the half-reactions that oxidize P_2Pd^0 to P_2Pd^{II}=NPh with the half-reactions that reduce P_2Pd^{II}=NPh to P_2Pd^0 will result in all possible overall stoichiometries being catalytic in both P_2Pd^0 and P_2Pd=NPh. The exercise to derive all possible catalytic stoichiometries is shown in section 5 of Appendix II (see especially Scheme AII.1). For simplification, DMO is counted as DMC, MF

is counted as CO, and DPU is counted both as aniline and as MPC. Also, the very small amount of azobenzene is taken with azoxybenzene as 'Azoxy'.

Thus, the possible overall stoichiometries are given by equations 10 – 18, all of which are highly exothermic (ΔH_f^o varies from –95 to –175 kcal.mol^{-1}, see table AII.5 for details). In equations 10 – 12, CO is the only de-oxygenating agent, while for equations 13 – 15 two CO and two acidic H-atoms from methanol function as de-oxygenating reagents. In equations 16 – 18, all four H-atoms from methanol are used to de-oxygenate one nitrobenzene. The equations marked with '*' are reactions wherein one methanol molecule is substituted for a water molecule (see Appendix II for details).

$PhNO_2 + CH_3OH + 3\ CO$	$\rightarrow MPC + 2\ CO_2$	(10)
$PhNO_2 + 2\ CH_3OH + 3\ CO$	$\rightarrow PhNH_2 + 2\ CO_2 + DMC$	(11)
$2\ PhNO_2 + 3\ CO$	$\rightarrow Azoxy + 3\ CO_2$	(12)
$PhNO_2 + 3\ CH_3OH + 3\ CO$	$\rightarrow MPC + CO_2 + H_2O + DMC$	(13)
$PhNO_2 + 4\ CH_3OH + 3\ CO$	$\rightarrow PhNH_2 + CO_2 + H_2O + 2\ DMC$	(14)
$2\ PhNO_2 + 2\ CH_3OH + 3\ CO$	$\rightarrow Azoxy + 2\ CO_2 + H_2O + DMC$	(15)
$PhNO_2 + 2\ CH_3OH$	$\rightarrow MPC + 2\ H_2O$	(16)
$PhNO_2 + 3\ CH_3OH$	$\rightarrow PhNH_2 + 2\ H_2O + DMC$	(17)
$2\ PhNO_2 + CH_3OH$	$\rightarrow Azoxy + 2\ H_2O + CO_2$	(18)
$PhNO_2 + H_2O + 3\ CO$	$\rightarrow PhNH_2 + 3\ CO_2$	(10/11*)
$PhNO_2 + 2\ CH_3OH + 3\ CO$	$\rightarrow PhNH_2 + 2\ CO_2 + DMC$	(13/14*)
$PhNO_2 + CH_3OH$	$\rightarrow PhNH_2 + CO_2 + H_2O$	(16/17*)

The sum of weighted contributions of each of these catalytic reactions will ultimately determine the experimentally observed product composition in the liquid phase (note: the gaseous product CO_2 was not quantitatively determined).

The experimental parameters obtainable from the observed product compositions, i.e. the H-atom balance, the aryl product distribution, product ratios, water production and the effect of water addition on product composition, were used to extract the weighted contribution of the various possible reactions given in

equations 10-18 and 10/11*-16/17*, and thus to simulate the product compositions as a function of the catalyst (see Appendix II). The results of this simulation are summarized in Table 3.2. By grouping reactions together according to their underlying nitrobenzene de-oxygenation pathway, it can be seen that the actual reaction pathways catalysed by a specific catalyst appear to depend strongly on its structure, which is primarily determined by the supporting ligand. It is shown that of the catalysts tested, all three de-oxygenation pathways contribute, but that there exist significant differences between catalysts. Remarkably, de-oxygenation by full methanol dehydrogenation (column 'CH_3OH') is less dependent on the catalyst structure, while the DMC (DMO) producing '$2CO/2CH_3OH$' de-oxygenation pathway is strongly suppressed by *o*-methoxy substitution of the aryl groups in the diphosphane ligand. In contrast, the 'CO' de-oxygenation pathway appears to be enhanced by this substitution.

Table 3.2. Simulations of the experimental data, using equations 10 – 18 (see Appendix II for details).

		Product distribution						De-oxygenation pathway (%)		
Ligand	**Data**	**MPC**	**$PhNH_2$**	**Azoxy**	**DMC**	**H_2O**	**Water 'cons.'[a]**	CO[b]	$2CO/2CH_3OH$[c]	CH_3OH[d]
L3X	Exp.	6.1	9.1	0.5	7.3	3.4	100%	37%	46%	17%
	Sim.	6.1	9.1	0.5	7.2	3.5				
oMeO-L3X	Exp.	14.7	8.8	0.2	0.8	0.7	100%	78%	3%	18%
	Sim.	14.7	8.8	0.2	0.8	0.7				
L4X	Exp.	1.0	2.4	4.6	8.2	10.0	24%	9%	66%	24%
	Sim.	1.0	2.4	4.6	8.6	9.6				
oMeO-L4X	Exp.	7.5	12.4	1.1	9.4	8.7	24%	72%	0%	28%
	Sim.	7.5	12.4	1.1	9.4	8.7				

[a] Sum of weighted contributions of the three 'water-consuming' reactions given in equations 10/11*, 13/14* and 16/17* as fraction of the total sum of weighted contributions of the reaction given by equations 10, 11, 13, 14, 16, 17, and 10/11*, 13/14* ,16/17*. [b] Sum of weighted contributions equations 10 – 12. [c] Sum of weighted contributions equations 13 – 15. [d] Sum of Weighted contributions equations 16 – 18. See SI for more details. 'MPC' = MPC+DPU; 'Azoxy' = Azoxy + Azo; . '$PhNH_2$' = $PhNH_2$ + DPU; and 'DMC' = DMC+DMO.

A larger backbone length of the diphosphane ligand (L4X *vs*. L3X), which affects the ligand's bite-angle, is leading towards a larger contribution (from 46% to 66%) of the '$2CO/2CH_3OH$' de-oxygenation pathway. Remarkably, when *o*-methoxy substitution in the L4X ligand is introduced, the situation completely

changes toward a strong contribution of the 'CO' de-oxygenation pathway (9% for L4X and 72% for oMeO-L4X).

Finally, a noteworthy difference between catalysts with C3 and C4 backbone ligands appears their reactivity towards water as nucleophilic reagent (column 'water cons.'): whereas the Pd^{II}(L3X) catalysts are very reactive towards water, the Pd^{II}(L4X) catalysts appear much less sensitive towards water (see also Table 3).

Complete rationalization of the catalyst performance as judged from its product slate, in terms of molecular details of these catalysts, can, of course, not easily be achieved. To come to a fully detailed molecular rationalization of catalyst performance will certainly require in-depth further organometallic studies on possible catalytic intermediates. One such a study, involving the synthesis and study of the reactivity patterns of P_2Pd^{II}-imido complexes is reported in Chapter 4 of this thesis. Nevertheless, it is considered worthwhile as a first attempt to discuss some of the most prominent observations from the product simulations in terms of the molecular characteristics of proposed catalytic Pd intermediates. The discussion presented below, will provide some guidance for the further (organometallic) mechanistic studies described in Chapters 4, 5, and 6.

3.3.9. Ligand effects; 2CO *versus* 2CO / $2CH_3OH$ *versus* CH_3OH deoxygenation

The first remarkable observation from the product simulations shown in Table 3.2, concerns the significant effect of o-MeO substituents of the ligands (entries oMeO-L3X and oMeO-L4X) on the nitrobenzene de-oxygenation pathway. The relative contribution of the reactions in which CO is the only reductant ('CO') (eq. 10 – 12) is largest for catalysts bearing the o-MeO-functionalized ligands (~75%). For catalysts comprising the unfunctionalized ligands L3X and L4X on the other hand, the reactions in which two CO and the acidic H-atoms of methanol ('2CO/2CH_3O*H*') function as co-reductant (eq. 13 – 15) is dominant (~50-70%). The catalyst structure is of less importance for the reactions wherein full methanol dehydrogenation ('C*H*$_3$O*H*') drives nitrobenzene de-oxygenation (eq. 16 – 18). The contribution of equations 16 – 18 hardly alters when the ligands bear the *o*-MeO-functionality and only slightly (7-10%) when the longer butylene backbone

is employed. The modest increase of the 'CH_3OH' de-oxygenation pathway due to *o*-MeO substituents in the ligands might seem somewhat surprising. One would expect the electron-donating *o*-MeO substituents to enhance the basicity of the palladium centre in P_2Pd^0, thereby facilitating the oxidative addition of methanol on P_2Pd^0 (i.e., protonation at the basic metal centre), thus rendering the '$2CO/2CH_3OH$' and 'CH_3OH' pathways (Scheme 3.4 and Scheme 3.5) more probable. This suggests that electronic effects are counteracted by steric effects of the *o*-MeO substituents. On the other hand, the data also suggest that in the competition of oxidative addition of methanol and the oxidative coupling of CO and nitrobenzene on P_2Pd^0 (Scheme 3.4), a more basic metal catalyst (o-MeO-groups) is more involved in the oxidative CO coupling reaction with nitrobenzene. This is in line with the general notion that using the even more basic N-donor ligand 1,10-phenanthroline as the supporting ligand, CO reduction is the only de-oxygenation pathway.[20-35] The observations presented in this chapter with various Pd-phenanthroline catalyst systems confirm this as well. A comprehensive performance comparison under various conditions between N_2Pd and P_2Pd catalyst systems is given in Chapter 6 of this thesis.[45]

For the nitrobenzene de-oxygenation pathways that start with oxidative addition of methanol ('$2CO/2CH_3OH$' and 'CH_3OH') to P_2Pd^0 (Scheme 3.4), the *o*-MeO-functionalized catalysts are much more selective (~85-100%) *via* the full dehydrogenation pathway of methanol ('CH_3OH') relative to the '$2CO/2CH_3OH$' de-oxygenation pathway. This can be understood by the steric hindrance that the *o*-MeO-substituents impose on the axial positions of the Pd centre in the catalyst, effectively shielding the d_z^2 orbitals of palladium.[43, 72, 73]

Thus, after the formation of **C5b/c** (see Scheme 3.4 and Scheme **3.5**), the coordination of CO on the axial position is sterically hampered, thus also hampering a (temporarily) associative displacement of a nitroso ligand required for the formation of **C6b** (left in Scheme 3.9), and thus also the '$2CO/2CH_3OH$' de-oxygenating pathway. Instead, the CH_3O^- anion present outside the first coordination sphere of the P_2Pd^{II} centre in **C5b/c** will deprotonate the coordinated CH_3O^- to form methanol and palladium-bound formaldehyde (right in Scheme 3.9), eventually leading to the full dehydrogenation of methanol (shown in Scheme 3.5).

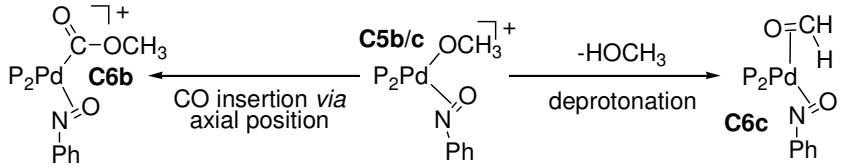

Scheme 3.9. Mechanistic scheme rationalizing the selectivity that the o-MeO-functionality induces on the de-oxygenation with one CO and two CH_3OH (left) versus one CH_3OH (right).

3.3.10. Ligand effects; DMC/DMO *versus* MPC/DPU *versus* $PhNH_2/CO_2$

Another important observation from the product simulation is that for L3X and oMeO-L3X it appears that all aniline produced can be formed *via* the 'water consuming reactions' given by equations 10/11*, 13/14* and 16/17*. For the catalysts comprising the ligands with a butylene backbone, these reactions only contribute about 25% (see column 'Water 'cons.'' in Table 3.2). This is in line with the findings that especially with Pd^{II}(L3X) and Pd^{II}(oMeO-L3X) added water could quite effectively replace methanol as reactant to give aniline instead of MPC (or DPU) and DMC (or DMO). Also remarkable is the observation that the *o*-methoxy substituents render the catalyst more selective towards MPC (DPU), clearly at the expense of DMC/DMO formation.

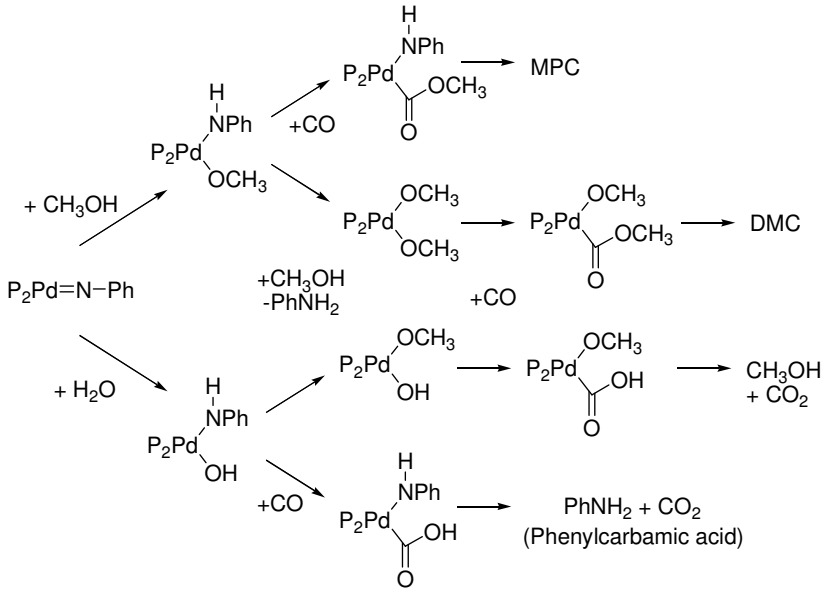

Scheme 3.10. Mechanistic scheme showing the related production of MPC, DMC, and aniline/CO_2.

These observations can be rationalized schematically as is illustrated in Scheme 3.10. First, the imido nitrogen of the P_2Pd^{II}=NPh intermediate can be protonated by a CH_3OH molecule (top in Scheme 3.10) that is approaching the Pd-centre *via* the (not so sterically crowded) equatorial positions, thus forming $P_2Pd^{II}NHPh(OCH_3)$. As this species is sterically more crowded in the equatorial positions, a second CH_3OH molecule will first associate with the Pd-centre *via* its axial positions, resulting in the formation of aniline and a $P_2Pd^{II}(OCH_3)_2$ complex. As the *o*-MeO-substituents on the ligands shield the axial positions of Pd,[43, 72, 73] these *o*-MeO groups will hamper this second protonation step, thus also hampering DMC formation. Instead, MPC is then formed by the sequence: associative displacement of CH_3O^- by the smaller and neutral CO molecule, followed by nucleophilic attack by CH_3O^- at the coordinated CO molecule and reductive elimination of MPC (Scheme 3.10, upper pathway).

Alternatively, water can replace methanol in the first protonation step (bottom in Scheme 3.10, although formally also in a later stage) to open up two analogous reaction pathways that result in the formation of aniline instead of MPC (top) or DMC (bottom). As it appears from the data (Tables 3 and 4), the amount of aniline (DPU) formed *via* such 'water-consuming' reactions is not so large when using catalysts of a ligand with a C4 backbone (weighted contribution 24%), but when the supporting ligand has a C3 backbone, all aniline is formed in this way. This is counterintuitive from a steric point of view, because water is smaller than methanol and because a C4-backbone could induce more steric constraint in the equatorial coordination positions of the catalyst (larger bite-angle). The effect must therefore be of a combined electronic and steric origin.

Indeed, P_2Pd^{II} complexes in which the ligand has a C3-backbone typically have a P-Pd-P angle close to the ideal 90º, whereas the steric constraints imposed by a longer C4-backbone result in a P-Pd-P angle of typically 96º.[74] As a result, orbital overlap will be less, thus hampering the electron flow from the aryl rings to palladium, which results in a less basic palladium centre (in e.g. P_2Pd^{II}=NPh).

3.3.11. Ligand effects; Azoxy *vs.* $PhNH_2$/MPC

Interestingly, from the working hypothesis shown in Scheme 3.8, it can be predicted that the phenyl moiety in the imido-intermediate can end up either in azoxy (disproportionation, bottom right in Scheme 3.8, eq. 8a) or in aniline / MPC (protonation, top right in Scheme 3.8, eq. 6 and eq. 9b/c). From the catalytic data shown in Table 3.2, it appears that when using Pd^{II}(L4X), the disproportionation route dominates (4.6 mmol Azo(xy) and 3.4 mmol '$PhNH_2$'/'MPC'), but for Pd^{II}(L3X) the protonation route becomes dominant (0.5 mmol Azo(xy) and 15.6 mmol '$PhNH_2$'/'PhNCO').

This difference in selectivity must be related to the different ligand bite-angle,[75] which is about 90º in L3X and 96º in L4X.[74] As is illustrated in Scheme 3.11, one N-O bond in nitrobenzene is formally completely polarized, whereas the O-H bond in methanol is charge neutral. As a result, and because the imido complex is also polarized, nitrobenzene is thought to associate stronger to the Pd=N bond than methanol.

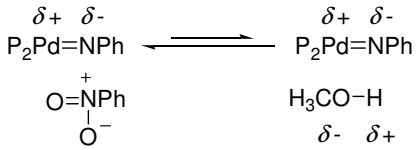

Scheme 3.11. Competition for association with the Pd-imido intermediate between nitrobenzene and methanol.

This effect may be similar in catalysts with either ligand L3X or L4X. However, as the bite-angle is larger in L4X, this might well enforce a kind of disproportionation reaction between the imido-intermediate and nitrobenzene by forcing them together and thus lowering the activation barrier for this reaction. It is indeed well-known that reaction between cis-coordinated fragments (e.g. reductive elimination) opposite to a bidentate phosphane ligand is expedited by enlarging the bite angle of the ligand.[75-79] What is more, the observation that azoxybenzene formation can be suppressed when equipping the ligand with *o*-MeO-phenyl rings, is in line with such a mechanistic proposal; the electron-donating methoxy groups can render the imido intermediate more basic, thus allowing an easier reaction with the (abundantly present) methanol. The o-MeO-groups might also (concurrently) prevent the approach of the larger nitrobenzene to the axial positions of Pd, in favor of the smaller methanol.

3.3.12. Ligand effects; activity *vs.* o-MeO-groups

It is important to note that the overall activity is significantly higher when employing *o*-MeO-functionalized ligands: the conversions increase from 67% using L3X to 98% using oMeO-L3X and from 52% using L4X to 90% using oMeO-L4X. This probably implies that the methanol carbonylation cycle to DMC (DMO) is rate determining in the combined nitrobenzene reduction – methanol carbonylation cycle. With *o*-MeO-modified ligands, the overall catalytic cycle can take a short-cut to MPC formation which results in an overall higher rate of reductive carbonylation. It is furthermore likely that the 'CO' de-oxygenation route is faster than the two de-oxygenation routes involving methanol. As the *o*-MeO-functionalized catalysts are mostly involved in this 'CO' de-oxygenation pathway (~75%), these catalysts thus can lead to higher nitrobenzene conversion rates.

3.4. Conclusions

It was shown that a number of unexpected products is formed when performing the carbonylation of nitrobenzene in methanol with P_2Pd-based catalysts. Furthermore, it was postulated that nitrobenzene can oxidize P_2Pd^0 to the imido species 'P_2Pd^{II}=NPh'. In this process nitrobenzene is reduced; this can be done not only by two CO molecules, but also by two CO in combination with the acidic protons of two methanol molecules, or by using all four H-atoms of one molecule of methanol. During these processes, CO_2, H_2O, DMC/DMO, CO, and MF are formed. Starting from the P_2Pd^{II}=NPh intermediate, the formation of Azo(xy), MPC/DPU, and aniline is accompanied by the regeneration of P_2Pd^0, thus making these reactions catalytic.

Although many of the (organometallic) details of the catalytic pathways are still largely unknown, the first aim has been to unravel all catalytic organic reactions that proceed in the palladium-diphosphane catalyzed carbonylation of nitrobenzene in methanol. A network of coupled catalytic cycles containing common intermediate catalytic species has been developed, which all point towards a P_2Pd^{II}=NPh complex as the key-intermediate species. Indeed, using this imido-intermediate it is possible to connect a complex network of catalytic reactions, both for the oxidation of methanol as well as for the reduction of nitrobenzene. What is more, when cyclohexene was added during a catalytic run

the corresponding aziridine was observed, which strongly suggests the presence of a P_2Pd^{II}=NPh intermediate. Based on the analysis of the observed product distribution in combination with the possible reactions involving the hypothetical P_2Pd^{II}=NPh key-intermediate species, it was possible to accurately simulate the relative weight of the reactions taking place and –to some extent– relate the performance of the catalysts with structural parameters of the catalyst complexes.

Regarding the original aim of the selective reductive carbonylation of nitrobenzene, it was found that P_2Pd^{II}(oMeO-L3X) is the most active (98% conversion) and selective (62% carbonylation) one of the catalysts tested. The catalytic carbonylation of methanol to DMC and DMO can have important technological implications, as both DMC and DMO are industrially important molecules. DMC has been proposed to replace phosgene as carbonylating agent,[80-84] while DMO can serve as intermediate in a syngas based route to monoethyleneglycol (MEG).[85] Obviously, the catalysts described in this paper that catalytically produce DMC or DMO are worth investigating further in this respect.

The present work provides a basis for a two-way further development of optimal catalyst systems suitable for either the effective and selective reductive carbonylation of nitro aromatics to give carbamate esters or ureas, or to optimal catalysts systems for the selective oxidative carbonylation of alcohols to give difunctional esters such as carbonate or oxalate esters, and in which nitro aromatics can serve as the oxidant, thus co-producing aromatic amines. Further catalytic and organometallic research into the reductive carbonylation of nitro aromatics as well as the oxidative carbonylation of alcohols thus is imminent.

3.5. Experimental

3.5.1. General remarks

All ligands were generously provided by Shell Global Solutions Amsterdam b.v., where they were synthesized according to literature procedures.[86-94] All other solids were purchased from Acros organics and used as received. Methanol, nitrobenzene and aniline were all of analytical reagent purity, and were distilled under an argon atmosphere over the appropriate drying agent.[95] After the distillation, these liquids were saturated with argon. It was ensured that no water was present using an analytical reaction with trimethylorthoformate according to a modified literature procedure[96] (see below and also Appendix II). Carbon monoxide (> 99% pure)[52] was purchased from Linde gas Benelux B.V. and used as received. ^{1}H–, and ^{13}C–NMR spectra were recorded on a Bruker DPX300 (300 MHz) or a Bruker DMX400 (400 MHZ) machine. High pressure catalysis experiments were conducted in stainless steel autoclaves (100 ml) equipped with two inlet/outlet valves, a burst disc, a pressure sensor, and a thermocouple. The autoclaves were heated by a HEL© polyBLOCK electrical heating system. Temperatures and pressures where measured with probes connected to a computer interface making it possible to record these parameters throughout the course of the reaction. GLC-MS measurements were performed on a Hewlett Packard series 2 type 5890 gas chromatograph equipped with a Hewlett Packard 5971 mass selective detector. Depending on the analyte, a polar or an apolar column was used. Technical details and settings are identical to those used for the quantitative GLC-FID measurements (see below). Mass spectroscopic spectra of the gas phase were recorded with a Spectra MicroVision plus 24 VDC series K64764, coupled to a computer for digital readout. Data points were collected with a resolution of 0.25 m/z in the range of m/z = 3 to 50.

3.5.2. Catalytic / high pressure reactions

In a typical catalytic experiment, 0.05 mmol $Pd(OAc)_2$ and 0.075 mmol ligand (and if relevant another additive) were weighed and transferred into an autoclave, together with a magnetic stirring rod. The autoclave was tightly closed and subsequently filled with argon using a Schlenk-system that was connected to the one of the valves of the autoclave. Through the other valve was added 2.50 ml (24.4 mmol) dried and degassed nitrobenzene, under a continuous flow of argon. In a similar fashion, 25.0 ml dried and degassed methanol was then added. This reaction mixture was allowed to stir at 500 rpm for about 15 minutes to ensure that complex formation was complete.[43] The autoclave was then inserted into the heating block and pressurized with 50 bar carbon monoxide gas. The reaction mixture was heated to 110 ºC (within 30 minutes) under stirring at 500 rpm. After standing for four hours at this temperature, the autoclave was cooled to room temperature in about one hour. The autoclave was then slowly vented to atmospheric pressure and the reaction mixture was analyzed as described below. To check reproducibility, all catalytic reactions were performed in quadruplet; the relative standard deviation was always less than 5% for all products.

3.5.3. Trapping experiments with cyclohexene

Using standard Schlenk techniques, 2.7 ml (25 mmol) cyclohexene (passed through an alumina column and saturated with argon) was transferred into a piece of stainless steel tubing (5 ml) that was closed on both sides by two valves. This piece of tubing was mounted on one of the gas inlet/outlet valves of an autoclave that was prepared for a normal high pressure catalytic reaction (see above). The catalytic reaction was then started as normal. After the decline in pressure inside the autoclave was about halfway of what is usually observed when using a specific catalyst, cyclohexene was added to the reaction mixture with a small overpressure of CO. The reaction was then allowed to continue for a total of the usual four hours. After cooling and venting, the reaction mixture was analyzed with GLC-FID and GLC-MS analysis.

3.5.4. Quantitative GLC-FID analysis of reaction mixtures

Prior to the work-up of N,N'-diphenylurea (see below), a 0.5 ml sample (diluted with 1.0 ml methanol) was taken to quantify the other analytes with GLC-FID analysis. GLC-FID analysis was done using an apolar and a polar column, and decane as internal standard.

For the apolar column, a Hewlett Packard 6890 series gas chromatograph equipped with an auto sampler was used. An AT™-1 column (length: 30 m; diameter: 0.25 mm; film thickness: 1.00 μm) was used as stationary phase with helium as mobile phase. The injector and detector were operated at 250 ºC. An injection volume of 1 μl was taken with a split ratio of 10:1. After injection the column was heated at 120 ºC for five minutes, where after it was heated to 175 ºC (10 ºC/min.) and then to 325 ºC (50 ºC/min.) for four minutes. This method was used to quantify the following products (t_R in minutes): dimethylcarbonate (4.1), dimethyloxalate (5.9), nitrosobenzene (7.8), aniline (8.5), decane (9.7), methylene-benzenamine (10.2) nitrobenzene (11.0), methylphenylcarbamate (13.4), azobenzene (14.8), and azoxybenzene (15.7).

For the polar column, a Varian star 3400 CX gas chromatograph equipped with a Shimadzu integrator was used. A Varian WCOT fused silica CP-wax 58 (FFAP) column (length: 25 m; diameter: 0.32 mm; film thickness: 1.20 μm) was used as stationary phase with helium as mobile phase. The injector and detector were operated at 250 ºC. An injection volume of 0.5 μl was taken with a split ratio of 10:1. The temperature of the column was maintained at 40 ºC throughout the 10 minute elution time. This method was used to quantify of the products (t_R in minutes): dimethoxymethane (1.5), methyl formate (1.9), acetone (2.4), decane (6.4), and trimethylorthoformate (7.3). Water was analyzed by adding an amount of freshly prepared 0.55 M HOTs in trimethylorthoformate to the reaction mixture, heating to 70 ºC for 120 minutes followed by cooling to laboratory temperature and thereafter analyzing the amount of methyl formate that is formed. See Appendix II information for more details.[96]

3.5.5. Quantification of N,N'-diphenylurea

Since N,N'-diphenylurea (DPU) is a solid and poorly soluble in methanol, this compound was quantitatively analyzed by isolation and determination of its weight. First, a sample was taken for GLC-FID analysis (see above). Then, 10 ml *n*-hexane was added to the reaction mixture to ensure that all DPU precipitated. The reaction mixture was then stirred and carefully filtered using a weighed paper filter and a Büchner funnel. The resulting solid was washed five times with 2 ml portions of *n*-hexane and dried overnight in a vacuum oven at 50 ºC. The amount of DPU could then be determined by weight. For each isolated batch, ^{1}H- and ^{13}C-NMR spectroscopic analysis was used to verify the purity of DPU.

3.5.6. Mass spectroscopic analysis of the gas phase

The gas phase mass spectroscopic analysis was carried out with the setup shown in Figure 3.5. For a background measurement, valves B, C, D, and E were opened and valves A, F, and G were closed, so that the gas phase in the tubing from the autoclave until the mass spectrometer could be measured. Before measuring the gas phase inside the autoclave, it was ensured that a steady flow of about one bubble per second was obtained by closing valve E, opening valve A and then D and regulating the flow with valve B. Then valve D and E were opened so that the gas out of the autoclave could flow into the mass spectrometer. The pressure was then regulated with valve G to ensuring a strong signal on the mass spectrometer. When the signal was stable, five mass spectra were recorded in the *m*/*z* range of 3 – 50 with a resolution of 0.25 *m*/*z*. From these spectra the average integrals and standard deviations of a specific mass (for example; mass 28 = Σ 27.5 to 28.5) could be calculated. A column (∅ = 0.5 cm, 35 cm long) filled with anhydrous $Ni(SO_4)$ was used to avoid the interference of methanol (see supporting information for details).

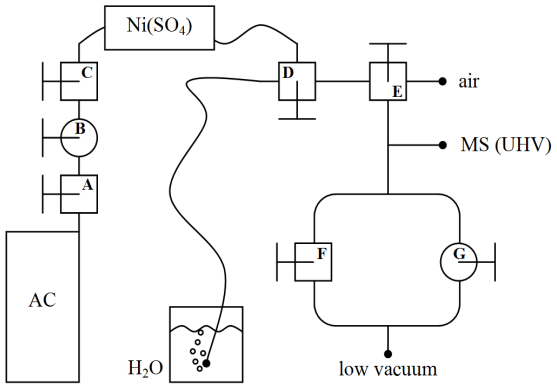

Figure 3.5. Schematic representation of the experimental setup used for the mass spectroscopic analysis of the gas phase inside an autoclave (AC). Valves A, C, D, E, and F are ball valves; and valves B and G are needle valves. MS = mass spectrometer, UHV = ultra high vacuum (~10^{-8} bar). Low vacuum was about 10^{-5} bar.

References

[1] J. Paetsch, *in "Ullmann's Encyclopaedia of Industrial Chemistry", Vol. 9*, VCH publishers, New York, **1975**.

[2] S. Fukuoka, M. Chono, M. Kohno, *J. Chem. Soc.-Chem. Commun.* **1984**, 399.

[3] J. Q. Wang, W. K. Chow, *J. Appl. Polym. Sci.* **2005**, *97*, 366.

[4] Y. Zheng, E. K. Yanful, A. S. Bassi, *Crit. Rev. Biotechnol.* **2005**, *25*, 243.

[5] K. K. Maniar, *Polym.-Plast. Technol. Eng.* **2004**, *43*, 427.

[6] R. L. Metcalf, *in: J.L. Kroschmitz, M. Howe-Grand (Eds.), Kirk-Othmer Encyclopedia of Chemical Technology, Vol. 14*, Wiley, New York, **1995**.

[7] N. N. Melinkov, *Chemistry of Pesticides*, Springer Verlag, Berlin, **1971**.

[8] M. Jayabalan, P. P. Lizymol, *J. Polym. Mater.* **2000**, *17*, 9.

[9] R. Tout, *Int. J. Adhes. Adhes.* **2000**, *20*, 269.

[10] K. C. Frisch, *Polimery* **1996**, *41*, 257.

[11] G. A. Howarth, *Surf. Coat. Int. Pt. B-Coat. Trans.* **2003**, *86*, 111.

[12] J. Huybrechts, P. Bruylants, A. Vaes, A. De Marre, *Prog. Org. Coat.* **2000**, *38*, 67.

[13] A. J. Ryan, J. L. Stanford, *in: G. Allen, J.C. Bevington (eds.), Comprehensive Polymer Science, Vol. 5*, Pergamon, New York, **1989**.

[14] K. Weisermel, H. J. Arpe, *Industrielle Organische Chemie*, VCH Verslagsgesellschaft GmbH, Weinheim, Germany, **1988**.

[15] www.gem-chem.net/capacity.html, **November 2011**

[16] *Registry of Toxic Effects of Chemical Substances (RTECS, online database)*, United States Department of Health and Human Services (National Toxicology Information, National Library of Medicine), Bethesda, MD, **1993**.

[17] R.C. Weast (Ed.), *Handbook of Chemistry and Physics*, D-110, 58 ed., CRC Press Inc., Cleveland, **1977-1978**.

[18] R. H. Richter, R. D. Priester, *in: J.L. Kroschmitz, M. Howe-Grand (Eds.), Kirk-Othmer Encyclopedia of Chemical Technology, Vol. 14*, Wiley, New York, **1995**.

[19] H. Ulrich, *Ullmann's Encyclopedia of Industrial Chemistry, Vol. A14*, VCH publishers, New York, **1989**.

[20] F. Paul, *Coord. Chem. Rev.* **2000**, *203*, 269.
[21] E. Drent, P. W. N. M. van Leeuwen, EU 0086281A1, **1982**.
[22] E. Drent, EU 224292, **1987**.
[23] E. Drent, EU 0231045A2, **1987**.
[24] E. Drent, *Pure Appl. Chem.* **1990**, *62*, 661.
[25] A. Bontempi, E. Alessio, G. Chanos, G. Mestroni, *J. Mol. Catal.* **1987**, *42*, 67.
[26] S. Cenini, F. Ragaini, M. Pizzotti, F. Porta, G. Mestroni, E. Alessio, *J. Mol. Catal.* **1991**, *64*, 179.
[27] R. Santi, A. M. Romano, F. Panella, G. Mestroni, A. Sessanti, A. S. o Santi, *J. Mol. Catal. A-Chem.* **1999**, *144*, 41.
[28] P. Leconte, F. Metz, A. Mortreux, J. A. Osborn, F. Paul, F. Petit, A. Pillot, *J. Chem. Soc.-Chem. Commun.* **1990**, 1616.
[29] P. Wehman, V. E. Kaasjager, W. G. J. de Lange, F. Hartl, P. C. J. Kamer, P. W. N. M. van Leeuwen, J. Fraanje, K. Goubitz, *Organometallics* **1995**, *14*, 3751.
[30] P. Wehman, G. C. Dol, E. R. Moorman, P. C. J. Kamer, P. W. N. M. van Leeuwen, J. Fraanje, K. Goubitz, *Organometallics* **1994**, *13*, 4856.
[31] P. Wehman, PhD thesis, University of Amsterdam (UvA) **1995**.
[32] P. Wehman, L. Borst, P. C. J. Kamer, P. W. N. M. van Leeuwen, *J. Mol. Catal. A-Chem.* **1996**, *112*, 23.
[33] F. Ragaini, C. Cognolato, M. Gasperini, S. Cenini, *Angew. Chem.* **2003**, *42*, 2886.
[34] F. Ragaini, M. Gasperini, S. Cenini, *Adv. Synth. Catal.* **2004**, *346*, 63.
[35] F. Ragaini, *Dalton Trans.* **2009**, 6251.
[36] E. Drent, P. E. Prillwitz, EU ZA8609251 (A), **1985**.
[37] J. H. Grate, D. R. Hamm, D. H. Valentine, US 4.603.216, **1986**.
[38] P. Wehman, R. E. Rulke, V. E. Kaasjager, P. C. J. Kamer, H. Kooijman, A. L. Spek, C. J. Elsevier, K. Vrieze, P. W. N. M. van Leeuwen, *J. Chem. Soc.-Chem. Commun.* **1995**, 331.
[39] P. Wehman, H. M. A. van Donge, A. Hagos, P. C. J. Kamer, P. W. N. M. van Leeuwen, *J. Organomet. Chem.* **1997**, *535*, 183.
[40] A. S. o Santi, B. Milani, E. Zangrando, G. Mestroni, *Eur. J. Inorg. Chem.* **2000**, 2351.
[41] F. Paul, J. Fischer, P. Ochsenbein, J. A. Osborn, *C. R. Chim.* **2002**, *5*, 267.
[42] M. Gasperini, F. Ragaini, C. Remondini, A. Caselli, S. Cenini, *J. Organomet. Chem.* **2005**, *690*, 4517.
[43] T. J. Mooibroek, E. Bouwman, M. Lutz, A. L. Spek, E. Drent, *Eur. J. Inorg. Chem.* **2010**, *2*, 298.
[44] R. I. Pugh, E. Drent, *Adv. Synth. Catal.* **2002**, *344*, 837.
[45] T. J. Mooibroek, E. Bouwman, E. Drent, *Organometallics* **2011**, submitted.
[46] E. Amadio, G. Cavinato, A. Dolmella, L. Toniolo, *Inorg. Chem.* **2010**, *49*, 3721.
[47] S. P. Current, *J. Org. Chem.* **1983**, *48*, 1779.
[48] D. M. Fenton, Steinwan.Pj, *J. Org. Chem* **1974**, *39*, 701.
[49] S. Uchiumi, K. Ataka, T. Matsuzaki, *J. Orgmet. Chem.* **1999**, *576*, 279.
[50] D. M. Pearson, R. M. Waymouth, *Organometallics* **2009**, *28*, 3896.
[51] Note that DPU can be formed by the reaction of nitrobenzene, CO and (*in situ* generated) aniline, but also by the transesterification of MPC with aniline. In both cases, aniline is formed first and DPU is thus derived from aniline.
[52] customer.linde.com/FIRSTspiritWeb/linde/LGNL/media/datasheets/NL-PIB-0024.pdf, **November 2011**
[53] Using our experimental setup, for pure CO before the catalytic run, the natural abundance of mass 29 (relative to mass 28) was determined to be 1.27 ± 0.03% (n=5). After the catalytic run using 4% $^{13}CH_3OH$ (v/v), 1.46 ± 0.02% (n=5) of m/z = 29 CO was detected.
[54] For the initial 15.1 mmol CO (5 bar, ~ 75 ml) to become enriched (from 1.27%) to 1.46% ^{13}CO from $^{13}CH_3OH$ (4% v/v) dehydrogenation, about 0.72 mmol methanol could have been dehydrogenated to CO (15.1 mmol × (0.0146-0.0127) × (100/4)). This should result in 2.9 mmol H-atoms. In the liquid phase of this experiment, 1.3 mmol MF was found,

meaning that the total amount of hydrogen atoms produced should be 8.1 mmol (4×1.3+2.9). Also in the liquid phase, 1.8 mmol aniline and 2.1 mmol H_2O were detected, which corresponds with 7.8 mmol H-atoms. Thus, the hydrogen mass balance is now approximately even; 8.1 mmol H-atoms should have been produced by CO and MF formation from methanol, and 7.8 mmol H-atoms were measured in the form of $PhNH_2$ and H_2O: a difference well within the experimental error of about 5%.

[55] For Pd^{II}(L3X), 8.0 mmol H_2O has replaced CH_3OH in some way as H donating agent. The amount of MPC+DPU decreased with 2.1 mmol, which was accompanied by a corresponding increase in $PhNH_2$+DPU of 2.0 mmol, while at the same time the amount of DMC+DMO decreased with 3.8 mmol. Taken together, this amounts to (2.1+3.8=) 5.9 mmol of combined products from reactions in which water has replaced methanol as H-donor. The remaining (8.0-5.9=) 2.1 mmol water must then have (at least partially) replaced methanol in reactions that, otherwise in the absence of water, would involve complete stripping of H-atoms from methanol (to CO, analogous to eq. 4). Likewise, for Pd^{II}(oMeO-L3X), the 10.8 mmol water consumed replaced methanol in the production of MPC (5.4 mmol), DMC (0.6 mmol), and CO (10.8-0.6-5.4 = 4.8 mmol). For Pd^{II}(L4X), hardly any water was consumed, which is also reflected in the unchanged product distribution. For Pd^{II}(oMeO-L4X) a mere 1.9 mmol of water was consumed, which apparently has replaced methanol in the formation of MPC (0.9 mmol), DMC (0.2 mmol), and CO (1.9-0.2-0.9 = 0.8 mmol).

[56] Cyclohexene was chosen because it is easy to handle and because it is known that a P_2Ni=NR complex can react stoichiometrically with double bonds (see reference 63).

[57] P. Wehman, L. Borst, P. C. J. Kamer, P. W. N. M. van Leeuwen, *Chem. Ber.-Recl.* **1997**, *130*, 13.

[58] F. J. Weigert, *J. Org. Chem.* **1973**, *38*, 1316.

[59] Smolinsk.G, B. I. Feuer, *J. Org. Chem.* **1966**, *31*, 3882.

[60] M. Akazome, T. Kondo, Y. Watanabe, *J. Org. Chem.* **1994**, *59*, 3375.

[61] M. J. McGlinch, F. G. A. Stone, *Chem. Comm.* **1970**, 1265.

[62] R. Waterman, G. L. Hillhouse, *J. Am. Chem. Soc.* **2008**, *130*, 12628.

[63] R. Waterman, G. L. Hillhouse, *J. Am. Chem. Soc.* **2003**, *125*, 13350.

[64] D. J. Mindiola, G. L. Hillhouse, *J. Am. Chem. Soc.* **2001**, *123*, 4623.

[65] R. D. Lide (Ed.), *Handbook of Chemistry and Physics*, 88th ed., CRC Press Inc., Cleveland, **2007-2008**.

[66] H. K. Hall, J. H. Baldt, *J. Am. Chem. Soc.* **1971**, *93*, 140.

[67] W. V. Steele, R. D. Chirico, S. E. Knipmeyer, A. Nguyen, N. K. Smith, *J. Chem. Eng. Data* **1997**, *42*, 1037.

[68] It should be noted that complexes **C3b/c** through **C5b/c** are denoted as cationic palladium complexes. Of course, the methoxide anion generally cannot be regarded as non-coordinating anion to a P_2Pd^{II} centre. However, in methanol as solvent the methoxide anion can be comfortably accommodated by solvent methanol molecules around the palladium centre by spreading its negative charge over several methanol molecules via a (dynamic) hydrogen-bonding network.

[69] B. Marciniec, E. Mackowska, *J. Mol. Cat.* **1989**, *51*, 41.

[70] T. Yoshida, S. Otsuka, *J. Am. Chem. Soc.* **1977**, *99*, 2134.

[71] E. Drent, Chapters 2.3 and 3.3 in *Applied homogeneous catalysis with organometallic compounds, Vol. 3* (Eds.: B. Cornils, W. A. Hermann), Wiley-VCH, **2002**.

[72] I. M. Angulo, E. Bouwman, M. Lutz, W. P. Mul, A. L. Spek, *Inorg. Chem.* **2001**, *40*, 2073.

[73] A. Marson, A. B. van Oort, W. P. Mul, *Eur. J. Inorg. Chem.* **2002**, *11*, 3028.

[74] T. Hayashi, M. Konishi, Y. Kobori, M. Kumada, T. Higuchi, K. Hirotsu, *J. Am. Chem. Soc.* **1984**, *106*, 158.

[75] P. Dierkes, P. W. N. M. van Leeuwen, *J. Chem. Soc. Dalton Trans.* **1999**, 1519.

[76] P. W. N. M. van Leeuwen, P. C. J. Kamer, J. N. H. Reek, P. Dierkes, *Chem. Rev.* **2000**, *100*, 2741.
[77] R. J. van Haaren, K. Goubitz, J. Fraanje, G. P. F. van Strijkdonk, H. Oevering, B. Coussens, J. N. H. Reek, P. C. J. Kamer, P. W. N. M. van Leeuwen, *Inorg. Chem.* **2001**, *40*, 3363.
[78] E. Zuidema, P. W. N. M. van Leeuwen, C. Bo, *Organomet.* **2005**, *24*, 3703.
[79] M. N. Birkholz, Z. Freixa, P. W. N. M. van Leeuwen, *Chem. Soc. Rev.* **2009**, *38*, 1099.
[80] Y. Ono, *Pure & Appl. Chem.* **1996**, *68*, 367.
[81] Y. Ono, *Appl. Catal. A.* **1997**, *155*, 133.
[82] Y. Ono, *Catalysis Today* **1997**, *35*, 15.
[83] F. Rivetti, *CR Acad. Sci. II C* **2000**, *3*, 497.
[84] P. Tundo, M. Selva, *Acc. Chem. Res.* **2002**, *35*, 706.
[85] For example following the sequence: Ox. (an oxidant in general, in our case nitrobenzene) + 2 CO + 2 CH_3OH → 'H_2Ox.' + $H_3CO(CO)_2OCH_3$ (DMO); DMO + 4 H_2 → $HO(CH_2)_2OH$ (MEG) + 2 CH_3OH. This amounts to the net stoichiometry: Ox. + 2 CO + 4 H_2 → 'H_2Ox.' + $HO(CH_2)_2OH$ (MEG).
[86] F. Bickelhaupt, US 4874897, **1989**.
[87] W. Eilenberg, EU 364046, **1991**.
[88] J. A. van Doorn, US 4994592, **1991**.
[89] R. van Ginkel, US 6548708, **2003**.
[90] E. Drent, US 5091587, **1992**.
[91] C. F. Hobbs, US 4120901, **1987**.
[92] P. W. Clark, B. J. Mulraney, *J. Organomet. Chem.* **1981**, *217*, 51.
[93] J. M. Brown, B. A. Murrer, *Tetrahedron Lett.* **1980**, *21*, 581.
[94] R. L. Wife, A. B. van Oort, J. A. van Doorn, P. W. N. M. van Leeuwen, *Synthesis* **1983**, *1*, 71.
[95] W. L. F. Armarego, C. L. L. Chai, *Purification of laboratory chemicals*, 5th ed., Elsevier, Amsterdam, **2003**.
[96] J. Chen, J. S. Fritz, *Anal. Chem.* **1991**, *63*, 2016.

Chapter 4

Mechanistic study of the palladium–bidentate diarylphosphane catalysed carbonylation of nitrobenzene in methanol; a palladium-imido complex as the central product-releasing species.

Abstract: The L_2Pd^{II} catalyzed reduction of nitrobenzene with CO in methanol was studied using bidentate diphenyl phosphane ligands with different backbone spacers and aryl ring substituents. More carbonylation products (methylphenyl carbamate, diphenyl urea) are formed relative to hydrogenation products (aniline, diphenylurea) when using a ligand with smaller bite–angle (C_3–backbone) or equipping the ligand with *ortho*–methoxy groups. Up to 73% coupling products (azo(xy)benzene) were obtained when using a ligand with a larger bite–angle (C_4–backbone). Based on these observations and the dependencies of the product formation on reactant concentrations ($PhNO_2$, CO) it is proposed that all products compete for the same palladium–imido (P_2Pd^{II}=NPh) intermediate. Additional proof for the existence and reactivity of P_2Pd^{II}=NPh species comes from a $^{31}P\{^1H\}$NMR and ESI–MS analysis of a reaction of a P_2Pd^0 compound with mesityl azide, forming what appears to be a Pd-imido complex. This complex was shown to react with CO and methanol to give methyl mesityl carbamate under mild conditions.

The palladacycle **C7** '$P_2PdC(O)N(Ph)OC(O)$' was considered as an alternative carbonylation product releasing intermediate. However, ligand exchange reactions of the stable 'phen–**C7**' with diphosphane ligands (studied with $^{31}P\{^1H\}$–NMR and ESI-MS) indicate that the 5–membered 'P_2–**C7**' readily decomposes under mild conditions by loss of CO rather than CO_2, to eventually (presumably) form the P_2Pd^{II}=NPh intermediate instead of carbonylation products. DFT calculation indicate that steric repulsion causes the lower stability of a diphosphane–**C7** relative to phen–**C7**.

These combined catalytic and organometallic data thus all point strongly to a P_2Pd^{II}=NPh complex as *the sole most probable product-releasing* intermediate species.

4.1. Introduction

Aromatic isocyanates are useful molecules, and annually produced on the megaton scale.[1] In particular, the polymer precursors MDI and TDI[2, 3] (Figure 4.1) are produced from nitrobenzene in efficient but less–desirable processes.[4] These processes are generally referred to as the 'phosgene routes', as they are based on the usage of the highly toxic[5, 6] phosgene gas (~100 times more toxic than CO).

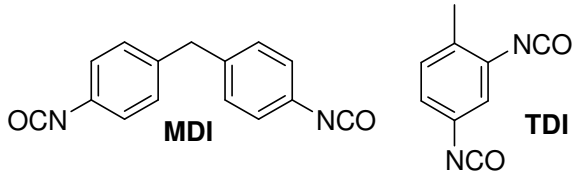

Figure 4.1. Two industrially produced aromatic isocyanates.

The most viable alternative that has emerged so far, is the reductive carbonylation of nitrobenzene with CO, producing only CO_2 as by–product.[7] The often reported aryl–containing side products that can be formed in this reaction comprise the self–coupling products azobenzene (Azo) and azoxybenzene (Azoxy). When this reaction is performed in methanol, methylphenylcarbamate (MPC) is usually the main product, with the co–production of Azo, Azoxy, aniline and/or N,N'–diphenylurea (DPU).[7, 8] MPC can be pyrolyzed to liberate the desired phenylisocyanate, recovering methanol.

It was discovered in the 1980s that palladium(II) stabilized with bidentate N– or P–ligands yields relatively active catalysts for this reaction (~500 turnover numbers, in methanol).[9-11] Most scientific studies have thus far concentrated on studying the $[Pd(phen)_2]X_2$ / H^+ catalytic system in methanol (phen = 1,10–phenanthroline),[8, 12-22] leaving the Pd–phosphorus–based systems virtually unstudied.[19, 23-26] In particular, mechanistic studies have not been reported for such a Pd–phosphorus based system.

Mechanistic proposals for the reaction catalyzed by Pd–phen systems generally start with oxidative coupling of CO and $PhNO_2$ at an (*in situ* generated) Pd^0 species to form a Pd^{II} species.[7, 20, 27] During the proposed catalytic cycle the catalyst remains in the Pd^{II} oxidation state, but in the final MPC–generating step

Pd^0 is regenerated from a palladacyclic intermediate such as the one shown in Figure 4.2a. [7, 16, 18, 20, 28, 29]

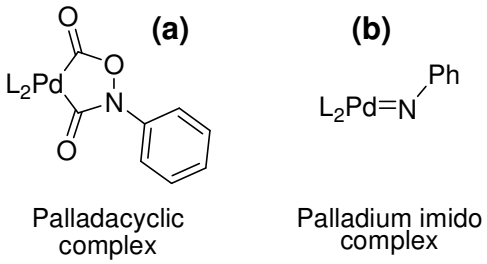

Figure 4.2. Two complexes that could be intermediates in the reductive carbonylation of nitrobenzene: (a) palladacyclic complex, and (b) palladium–imido complex. L_2 = chelating bidentate ligand.

Speculations about the intermediacy of palladium–imido compounds (see Figure 4.2b) in catalytic reactions have been put forward in literature of the 1960's and 1970's. Their existence has been postulated in the context of nitrobenzene reduction to aniline with CO/H_2O,[30, 31] in the carbonylation of nitrobenzene to phenylisocyanate,[32, 33] and also speculatively proposed in the palladium/phen/acid catalyzed nitrobenzene carbonylation in methanol as the reaction medium.[20, 27] It has been proposed that the palladium-catalyzed reduction of functionalized nitroarenes with CO proceeds *via* a palladium–imido intermediate to yield N-heterocyclic compounds.[34, 35] A series of bidentate phosphane stabilized Ni–imido complexes has been isolated, characterized crystallographically, and were shown to react with CO to form isocyanates.[36-38]

One of the most remarkable observations during the catalytic nitrobenzene carbonylation studies using Pd–bidentate diarylphosphane catalyst precursors (Chapter 3), concerned the significant co–production of various methanol oxidation products.[39] These products include dimethyl carbonate (DMC), dimethyl oxalate (DMO), methyl formate (MF), and even carbon monoxide (CO). The H–atoms that are liberated during these methanol oxidation processes are transferred to nitrobenzene and are found back in the products $PhNH_2$, DPU and H_2O. A palladacyclic species such as depicted in Figure 4.2a cannot be used to rationalize the formation of oxidation products of methanol, nor can it be used to explain the H–transfer process from methanol to nitrobenzene. It was therefore proposed (see also Chapter 3) that a Pd–imido complex (Figure 4.2b) must be a key–intermediate species in the catalytic system, as it allows for a clear catalytic connection to be made between the oxidation of methanol and the reduction of

nitrobenzene.[39] Starting from such an imido complex, the formation of *all* aryl–containing reaction products commonly observed (i.e., MPC, DPU, Azo(xy)benzene and $PhNH_2$) can be easily rationalized, whereas a palladacyclic species can only explain the formation of nitrobenzene carbonylation products (MPC and DPU, or 'PhNCO' in general). Some evidence for the intermediacy of palladium–imide complexes in the present catalytic system came from trapping experiments, which showed formation of 7–phenyl–7–aza–bicyclo[4.1.0]heptane when carbonylation of nitrobenzene was carried out in the presence of cyclohexene.[39]

In the present mechanistic study, a variety of bidentate diarylphosphane ligands have been used with variation in the length and rigidity of the backbone spacer, and with different substituents on the aryl rings with the aim to differentiate between electronic and steric effects of the ligands on the product distribution. Additional mechanistic information has been gathered from studying the effects of reaction conditions on the product composition. Finally, efforts were undertaken aimed at the development of synthetic routes to the proposed palladacyclic and palladium–imido complexes and to investigate their fate with NMR and ESI–MS characterization techniques, as well as with DFT calculations.

4.2. Results

4.2.1. General considerations

It was shown in Chapter 2 that complex formation of $Pd(OAc)_2$ with the ligands used in this study, yielding $P_2Pd(OAc)_2$, is instantaneous in methanol.[40] Therefore, the catalyst precursor $P_2Pd(OAc)_2$ in the catalytic studies was formed *in situ* from $Pd(OAc)_2$ and the bidentate ligand (1:1.5). The relatively small excess of ligand 'P_2' over the stoichiometric amount of Pd was applied to allow rapid quantitative formation of $P_2Pd(OAc)_2$. A small excess of ligand is also required to compensate for small amounts of mono–phosphane oxide impurities or the formation of small amounts of phosphane oxide during the reaction. Reproducible catalytic results with *in situ* formed catalysts, obtained at the ratio P_2/Pd=1.5, were found to be indistinguishable from those of preformed $P_2Pd(OAc)_2$ complexes.

The products that are formed during a catalytic experiment are shown in Scheme 4.1. The aryl-containing reduction products of nitrobenzene can be grouped in carbonylation products methylphenylcarbamate (MPC) and *N*,*N*'diphenylurea (DPU), coupling products azobenzene (Azo) and azoxybenzene (Azoxy), and hydrogenation products aniline ($PhNH_2$) and DPU.[41] The formation of $PhNH_2$ and DPU requires a source of H–atoms. In the present system methanol is the primary H–source by acting as transfer hydrogenation agent for nitrobenzene.[39] These methanol oxidation processes lead to the formation of the oxidative carbonylation products dimethyl carbonate (DMC), dimethyl oxalate (DMO), and to the formation of oxidative dehydrogenation products methyl formate (MF), water, and carbon monoxide.

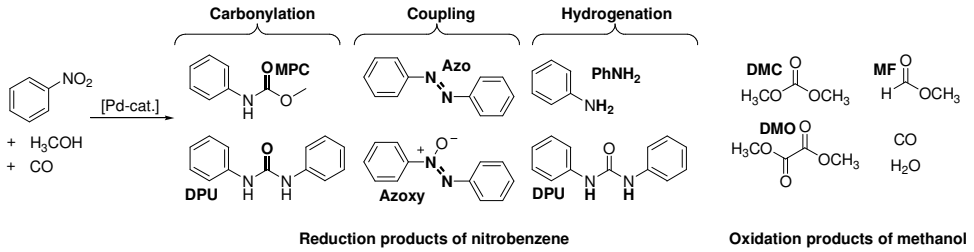

Scheme 4.1. Overview of the different products that are formed in the palladium–catalyzed carbonylation of nitrobenzene in methanol.

The stability of the aryl–containing reaction products was tested under standard catalytic conditions (Table AIII.2) and in all cases except one, these products were found to be inert. The exception is DPU, which reacts with methanol to form MPC and aniline with about 50% conversion (4 hours at 110 ºC). Note that DPU can thus be seen as consisting of 'phenylisocyanate' (carbonylation product) and 'aniline' (hydrogenation product). It is therefore best to view both MPC and DPU *together* as carbonylation products, and aniline and DPU *together* as hydrogenation products. The coupling products Azo and Azoxy were detected with most catalysts; Azoxy is always the major product with selectivity up to 70% while Azo is a minor product (<5%).

In the initial catalyst screening studies a large variety of diarylphosphane ligands has been used. The observed trends in the different reactivity and selectivities will be discussed using the ligands shown in Figure 4.3. These ligands have either a

propylene (L3) or a butylene (L4) backbone, which is in some cases made more rigid by substitution (indicated by 'X'). The aryl rings of the ligands were functionalized with methoxy groups in the *ortho* or *para* position (oMeO– or pMeO–) in order to differentiate between steric and electronic effects.

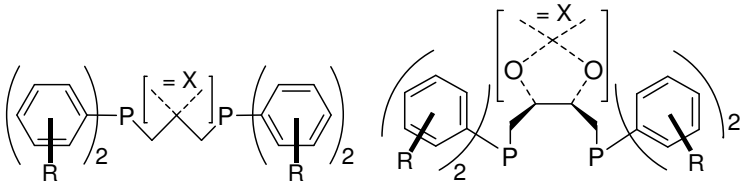

L3	(R=H)	**L4**	(R=H)
L3X	(R=H)	**L4X**	(R=H)
oMeO–L3	(R=*o*–MeO)		
oMeO–L3X	(R=*o*–MeO)	**oMeO–L4X**	(R=*o*–MeO)
pMeO–L3	(R=*p*–MeO)	**pMeO–L4X**	(R=*p*–MeO)

Figure 4.3. The ligands used in the catalytic experiments reported in this study.

The focus of the present chapter is the study of the influence of catalyst structure and carbonylation conditions on the formation of the various aryl–containing reduction products of nitrobenzene, and the possible role of a palladacyclic– and/or palladium imido–complex (Figure 4.2b) as intermediate in the formation of these products. Therefore, only the data of aryl–containing reaction products are shown in Table 4.1. A full analysis of the reaction mixtures was always performed however, and the data of the other reaction products are available in Table AIII.1. A general overview of all reactions that are operative has been reported in Chapter 2,[39] and the formation of oxidation products of methanol will be the focus Chapter5.[42]

4.2.2. General ligand effects in the reaction of nitrobenzene

The analysis of the reaction mixtures was carried out using gas–liquid chromatography (GLC); all products were quantified using calibration lines made from authentic samples. The accuracy of the quantitative analysis of the phenyl–containing products is excellent as confirmed by the sum of the aryl rings (column $\Sigma_{\varnothing}$ in Table 4.1, see also Table AIII.1). The conversions reached using the

palladium catalysts varies considerably with the ligand structure.[43] The conversion of nitrobenzene for all catalysts is moderate to high, ranging from 40 – 98%, corresponding to catalyst turnover numbers of 200–480.

Most catalysts containing a ligand with a propylene–backbone (entries 1, 3 – 5) are more selective towards carbonylation (~60%, column 'NCO') than towards hydrogenation (~40%, column 'NH'). For most catalysts containing a ligand with a butylene–backbone, this selectivity is reversed (~30% carbonylation and ~60% hydrogenation, entries 6, 8, and 9).

Table 4.1. Reactions of nitrobenzene with CO in methanol, catalyzed by a variety of Pd^{II}(ligand) complexes.[a]

		Conv.	Quantity (mmol)							Selectivity (%)[c]		
Entry	Ligand	(%)[b]	$PhNO_2$	MPC	DPU	$PhNH_2$	Azo	Azoxy	$\Sigma_{\varnothing}$	NCO	N=N	NH
1	L3	67	8.1	5.9	1.7	5.1	0.1	0.4	23.5	49	6	44
2	L3X	67	8.1	5.3	0.8	8.3	0.1	0.4	24.3	38	6	56
3	oMeO–L3	53	11.5	6.6	0.9	4.1	0.1	0.1	24.4	58	3	39
4	oMeO–L3X	98	0.6	11.6	3.1	5.7	0.1	0.1	24.5	62	2	37
5	pMeO–L3	54	11.3	5.2	1.9	3.9	0.0	0.1	24.4	55	1	45
6	L4	60	9.8	3.0	0.8	5.4	0.2	2.1	24.4	26	32	42
7	L4X	52	11.8	0.5	0.5	1.9	0.1	4.5	24.4	8	73	19
8	oMeO–L4X	90	2.4	5.6	1.9	10.5	0.5	0.6	24.5	34	10	56
9	pMeO–L4	40	14.7	2.6	0.0	5.9	0.0	0.3	23.8	29	7	65

[a] Reactions were heated for four hours at 110 ºC in 25.0 ml dry and degassed methanol under 50 bar CO pressure. The catalyst was generated *in situ* from 0.05 mmol $Pd(OAc)_2$. Mole ratios are: $Pd(OAc)_2$: Ligand : nitrobenzene = 1 : 1.5 : 488. [b] Conversion = $(24.4 - PhNO_2)/24.4 \times 100\%$. [c] Selectivity towards carbonylation products = (MPC + DPU) / $(\Sigma_{\varnothing} - PhNO_2) \times 100\%$; selectivity towards coupling products = (2×Azo + 2×Azoxy) / $(\Sigma_{\varnothing} - PhNO_2) \times 100\%$; Selectivity towards hydrogenation products = ($PhNH_2$ + DPU) / $\Sigma_{\varnothing} - PhNO_2) \times 100\%$.

Interestingly, the selectivity towards Azo(xy) coupling products (column 'N=N') appears to depend strongly on the ligand bite–angle (β). catalysts containing unsubstituted ligands with a propylene backbone ($\beta \approx 90º$)[44, 45] yield approximately 6% coupling products (entries 1 and 2), whereas this is 32 – 73% (entries 6 and 7) when using similar ligands with a butylene backbone ($\beta \approx 94º$). The formation of coupling products can be suppressed in favour of the carbonylation reaction by equipping the aryl rings of ligands with electron–donating methoxy groups either in the *ortho* (10% coupling, entry 8) or *para* (7% coupling, entry 9) position, indicating that this effect is predominantly electronic

in origin. A similar, although less pronounced effect is observed for the ligands with a propylene backbone (entries 1 – 5). The effect of a larger ligand bite angle and the effect of methoxy substituents in aryl phosphane ligands appears to be a general phenomenon, as several ligands with larger bite angles gave similar results.

4.2.3. The effects of reactants and additives

4.2.3.1 Effect of the concentration of CO and $PhNO_2$

Several experiments were conducted in which the concentration of a specific reactant was varied. Shown in Figure 4.4 are the selectivities observed for the carbonylation (white bars), coupling (black bars) and the hydrogenation reactions (grey bars), when increasing the CO pressure from 25 to 100 bar (see Table AIII.1).

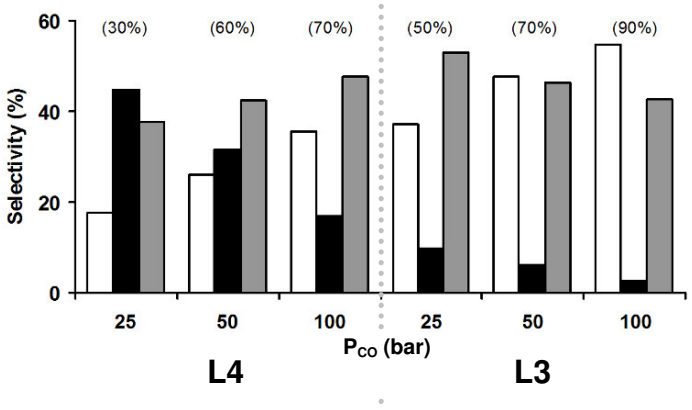

Figure 4.4. The selectivity of catalysts containing ligands L4 and L3 as a function of CO pressure (bar). Carbonylation products = □ = MPC + DPU; Coupling products = ■ = Azo + Azoxy; hydrogenation products = ■ = $PhNH_2$ + DPU. The conversion of nitrobenzene is given in parentheses.

Interestingly, for Pd^{II}(L4) as catalyst precursor, with increasing CO pressures the nitrobenzene conversion roughly doubles and the reaction becomes more selective towards both the carbonylation and hydrogenation products at the expense of the coupling products. When using Pd^{II}(L3) as catalyst precursor, the selectivity for

carbonylation products increases at the expense of both the coupling and the hydrogenation products.

Because of a higher–than–unity molecularity in nitrobenzene for the formation of Azo(xy) coupling products, the initial concentration of nitrobenzene was also varied. The catalyst precursor Pd^{II}(L4) was selected for investigation as for this catalytic system selectivity for coupling products is highest. As is shown in Figure 4.5 (see also Table AIII.1), the relative ratio of carbonylation (NCO) and hydrogenation (NH) products over coupling (N=N) products decreases significantly with increasing nitrobenzene concentrations, thus suggesting that the formation of Azo(xy) coupling products from nitrobenzene is competing with the carbonylation and hydrogenation reactions, but with higher order kinetics in nitrobenzene.

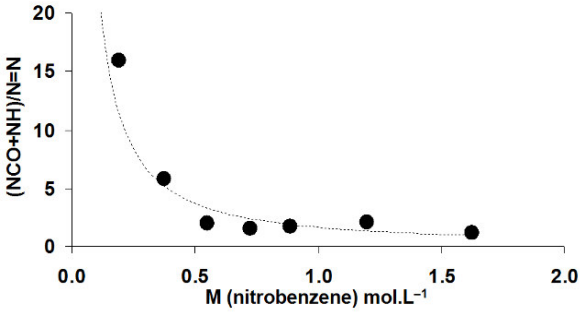

Figure 4.5. Plot of the ratio of (carbonylation (NCO) and hydrogenation (NH) products) relative to the amount of coupling products (N=N) as a function of the initial concentration of nitrobenzene in $mol.l^{-1}$, when using Pd^{II}(L4) as catalyst precursor. The line is added as an aid for the eye.

4.2.3.2 Effect of the acidity of the reaction medium

As is shown in Table AIII.1 and Figure 4.6 for Pd^{II}(L4X), upon addition of *para*–toluenesulfonic acid (HOTs) (pK_a = –2.7)[46] in sub–stoichiometric amounts on palladium the conversion of nitrobenzene increases from about 50% to a maximum of 84%, with a suppression of the coupling reaction (73 to 32%) in favor of the hydrogenation (15 to 49%) and carbonylation reactions (4 to 19%). When further increasing the acidity by adding an excess (4 eq.) of HOTs on palladium, the conversion decreases to 47%. At the same time however, the reaction becomes more selective towards hydrogenation (49 to 65%) and less selective towards coupling products (32 to 20%). The selectivity for carbonylation remains approximately constant.

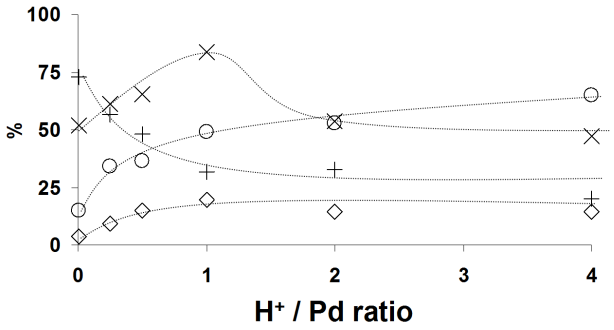

Figure 4.6. Plot of the conversion of nitrobenzene (×) and the selectivity towards coupling products (+, Azo(xy)), hydrogenation products (○, DPU + $PhNH_2$), and carbonylation products (◇, MPC + DPU) as a function of the amount of *p*–toluenesulfonic acid added (relative to Pd) when using the catalyst precursor Pd^{II}(L4X). The lines were added as an aid for the eye.

The addition of a base results in the reverse effect on conversion of nitrobenzene and selectivity for coupling products. The addition of only 2 eq. of a strong base ('Proton Sponge®', i.e. 1,8–bis(dimethylamino)naphthalene (DMAN)) on palladium leads to a decrease of the conversion to 20%. Azo(xy) coupling products are formed almost exclusively (94%), while carbonylation is totally suppressed. The effects of addition of strong base and acid on selectivity and conversion of the catalyst based on L4X are depicted in Figure 4.7.

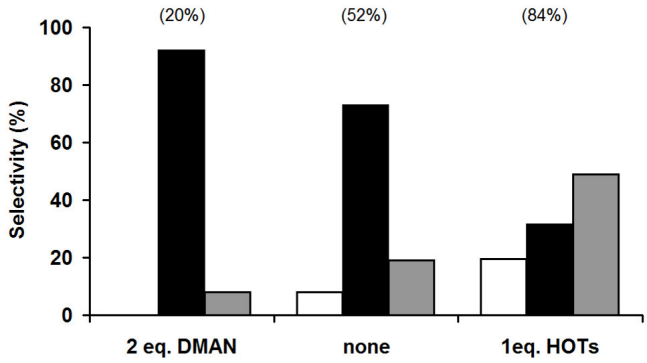

Figure 4.7. The selectivity when using Pd^{II}(L4X) and the indicated additive for: carbonylation products (□, MPC + DPU), coupling products (■, Azo + Azoxy), and hydrogenation products (■, $PhNH_2$ + DPU). The conversion of nitrobenzene is given in parentheses.

The effect of acidity on the system containing Pd^{II}(oMeO–L3X) as the catalyst precursor was also investigated, as this catalytic system is already very active in the absence of acid (96% conversion), while only producing ~2% coupling products. As can be seen in Figure 4.8, when adding up to four equivalents of

HOTs (on Pd), the conversion of nitrobenzene steadily decreases from 96 to 7%; at higher acid concentrations more hydrogenation products (40 to 70%) are produced at the expense of carbonylation products (60 to 30%).

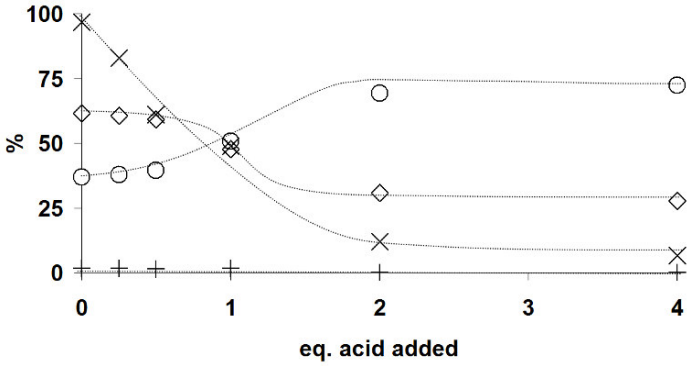

Figure 4.8. Plot of the conversion of nitrobenzene (×) and the selectivity towards coupling products (+, Azo + Azoxy), hydrogenation products (○, DPU + $PhNH_2$), and carbonylation products (◇, MPC + DPU) as a function of the amount of p–toluenesulfonic acid added (relative to Pd) when using the catalyst precursor Pd^{II}(oMeO–L3X). The lines are added as an aid for the eye.

Addition of a base 2 eq. of the base DMAN to the Pd^{II}(oMeO–L3X) catalytic system, results in a lower conversion of nitrobenzene, without a significant change in selectivity. The effects of addition of 2 equivalents of strong base or one equivalent of strong acid are compared in Figure 4.9, thus revealing that for this catalyst system the most significant effect is on conversion, which is lowered when adding either DMAN (from ~100 to 80%) or HOTs (from ~100 to 50%). The selectivity for coupling products remains very low in all instances.

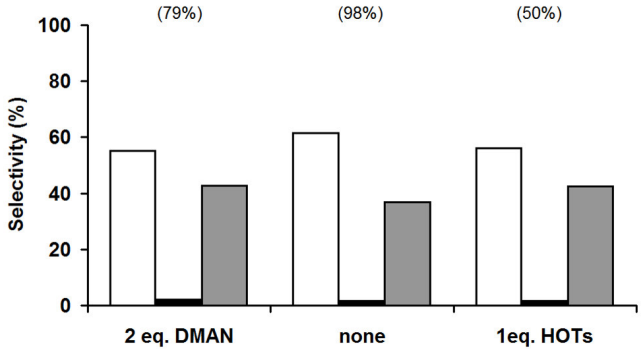

Figure 4.9. The selectivity when using oMeO–L3X and the indicated additive for: carbonylation products (□, MPC + DPU), coupling products (■, Azo + Azoxy), and hydrogenation products (■, $PhNH_2$ + DPU). The conversion of nitrobenzene is given in parentheses.

To assess if the effect on the catalytic activity is dependent on the anion in the acid employed, reactions were performed adding half an equivalent of TMBA (trimethylbenzoic acid; pK_a = 3.43).[46] As is shown for the Pd^{II}(L4X) catalytic system in Figure 4.10a, irrespective of the acid, the same trend is observed: the conversion is increased while the formation of coupling products is suppressed in favor of carbonylation and hydrogenation products. This effect is more pronounced for the stronger acid HOTs compared to the weaker acid TMBA, suggesting that the effect really depends on the available concentration of protons. For the series with the Pd^{II}(oMeO–L3X) catalytic system (Figure 4.10b), the conversion decreases but the selectivity changes only slightly, irrespective of the acid. In both cases, when the reaction medium becomes more acidic, relatively more hydrogenation products are produced.

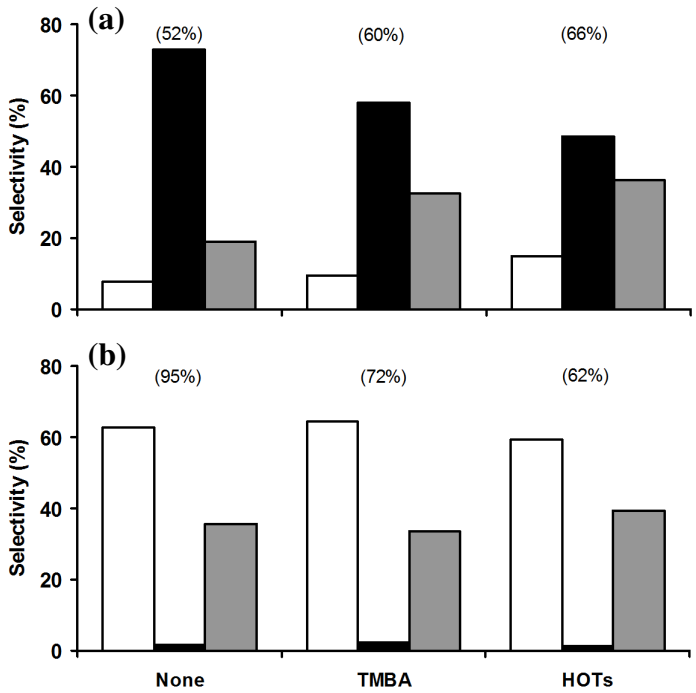

Figure 4.10. The product distribution in the carbonylation of nitrobenzene when using L4X (a) or oMeO–L3X (b), when adding 0.5 equivalent (on Pd) of the indicated acid. Carbonylation products = □ (MPC + DPU), coupling products = ■ (Azo + Azoxy) and hydrogenation products = ■, ($PhNH_2$ + DPU). The conversion of nitrobenzene is given in parentheses.

4.2.4. Investigations into the possible intermediacy of a palladacyclic complex

4.2.4.1 General considerations

The palladacyclic compound shown in Figure 2a, wherein L_2 = 1,10–phenanthroline (phen) has been characterized crystallographically. This complex can be synthesized under conditions very similar to those of catalytic experiments, and has been reported to be thermally stable to about 170 ºC.[16] Upon addition of an acid and heating to 90 °C in ethanol this complex decomposes to yield ethyl phenyl carbamate (80%).[16] The possible formation of such a palladacyclic compound in the diphosphane–based system was therefore investigated both experimentally and theoretically.

4.2.4.2 Attempted synthesis and DFT calculations

Attempts were undertaken to synthesize the diphosphane palladacyclic complexes with the ligands L3X and oMeO–L3X using the same procedure reported for the phen compound (ethanol, 60 °C).[16, 47] To verify whether a palladacyclic complex was formed at all, the reaction mixtures were analyzed with $^{31}P\{^{1}H\}$–NMR analysis, directly after the presumed reaction took place. Only for the ligand L3X the analysis revealed the presence –besides various other products– of an un–symmetric complex (two doublets around 3.8 and 5.8 ppm, J = 30 Hz) that might well be the anticipated 'L3X–palladacycle'. However, all attempts to isolate this species from the complex mixture of products were unsuccessful, leading to reaction mixtures in which the un–symmetric complex disappeared in the course of experimentation. This led us to investigate the stability of such complexes theoretically, using DFT calculations. As the solid state structure of the 'phen–palladacycle' has been reported (i.e., (phen)PdC(O)ON(Ph)C(O) • $PhNO_2$),[47] this complex was calculated in order to validate the computational method (Figure 4.11a). The structural characteristics of the DFT–optimized structure are indeed very similar to those of the X–ray structure (Table 4.2). The minor variations might be due to crystal packing forces and the lattice nitrobenzene molecule.

Also given in Table 4.2 are selected characteristics of the palladacyclic complexes containing the ligands oMeO–L3X and L3X; perspective views of the calculated structures are given in Figure 4.11a1–c1. As expected, the P1–Pd–P2 coordination angle is about 90º for both phosphorus ligands, whereas the N1–Pd–N2 angle for

phen is 76º. Note that as the dihedral angle between the L1–Pd–L2 and C1–Pd–C2 planes increases along the series (from 0.86º for phen to 21.47º for L3X, see also Figure 11a2–c2), the L–Pd and C–Pd distances are elongated. With these geometric changes, the enthalpy of formation of the P_2–palladacycle –relative to the phen–palladacycle– decreases with 13.3 kcal.mol^{-1} for the L3X complex. This suggests that when the P–Pd–P angle is larger, the palladacyclic complex becomes more distorted and as a result becomes less stable, thus lowering the barrier for decomposition.

Table 4.2. Selected data of some (calculated) 'Ligand–palladacyclic' complexes (see also Figure 4.11).

	X–ray	DFT (BP / 6–31G*)		
Complex (→):			**oMeO–**	
Parameter (↓):	**phen**	**phen**	**L3X**	**L3X**
L1 – Pd (Å)	2.128	2.203	2.434	2.438
L2 – Pd (Å)	2.130	2.203	2.429	2.423
C1 – Pd (Å)	1.939	1.973	2.024	2.027
C1 – Pd (Å)	1.927	1.987	2.040	2.037
L1 – Pd – L2 (º)	77.66	76.04	90.98	90.68
C1 – Pd – C2 (º)	82.02	82.00	81.36	80.93
LLPd/PdCC (º)	1.89	0.86	16.30	21.47
'ΔH' (kcal.mol^{-1})[a]	–	–75.4	–65.3	–62.1
'ΔH'$_{rel}$ (kcal.mol^{-1})[b]	–	0	10.1	13.3

[a] The enthalpy of formation was calculated from: Pd(Ligand)$(CO)_2$ + $PhNO_2$ + CO → Complex + CO_2. [b] relative to 'phen–palladacycle'.

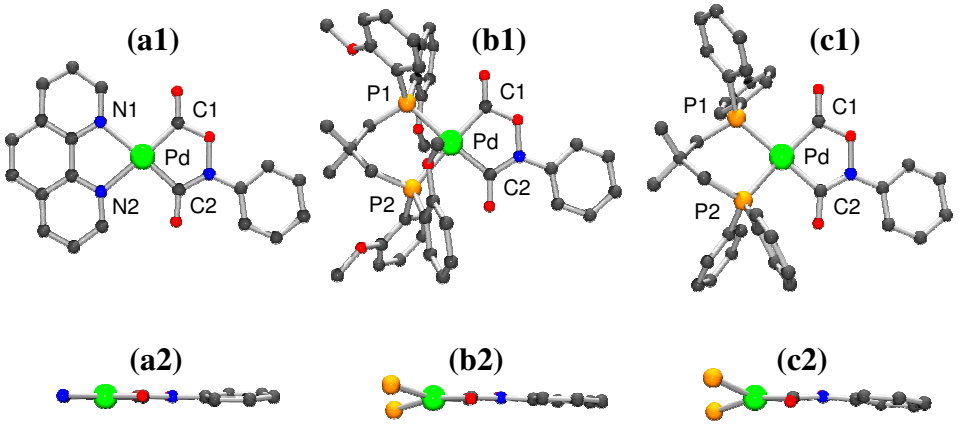

Figure 4.11. Perspective views of the calculated palladacyclic complexes with the ligands: (a1) phen (b1) oMeO–L3X; (c1) L3X. Side views for these complexes are shown in a2–c2, wherein only the donor–atoms of the ligands are shown for clarity. Color code: Pd (green), P (orange), N (blue), O (red), C (grey), H atoms are omitted for clarity.

4.2.4.3 L3X–palladacycle synthesis via ligand exchange

As attempts to isolate P_2–palladacycle complexes were unsuccessful and DFT calculation indicate that these complexes are less stable than their phen analogue, it was subsequently considered to monitoring phenanthroline ligand exchange by L3X of the synthetically well–proven phen–palladacycle complex (Scheme 4.2)[16, 47] in the hope of learning more about the stability of such 'L3X–palladacycle' (**II**).

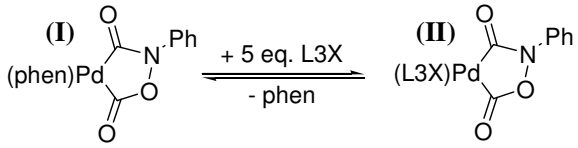

Scheme 4.2. Envisaged ligand exchange between 'phen–palladacycle' (**I**) and L3X to form 'L3X–palladacycle' (**II**).

An NMR experiment was conducted wherein (under an argon atmosphere) five equivalents of the free ligand L3X (dissolved in deuterated nitrobenzene) were added to one equivalent of the 'phen–palladacycle' (complex (**I**)). The yellow suspension was measured with $^{31}P\{^{1}H\}$–NMR, showing initially the resonance of ligand L3X around –25.1 ppm and only traces of a new complex around 4 – 6 ppm (Figure 4.12a), which was also observed in the reaction mixture of the attempt to synthesize (**II**) directly *via* nitrobenzene carbonylation.

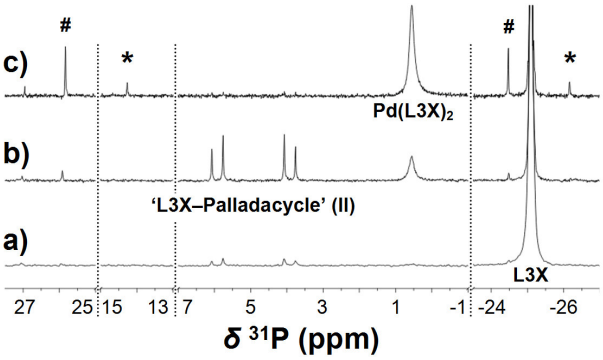

Figure 4.12. $^{31}P\{^{1}H\}$–NMR spectra for a solution containing 'phen–palladacycle' and 5 eq. of L3X in an argon atmosphere in nitrobenzene before heating (a), after heating to 60 ºC for about one minute and then cooled to room temperature (b), after standing for an additional two hours at room temperature (c). # = the mono–oxide of L3X; * = the mono–phosphazene of L3X.

After gentle heating to about 60 ºC for about one minute, a clear solution was obtained which was cooled to room temperature (~25 ºC), and measured with

$^{31}P\{^{1}H\}$–NMR. As can be seen in Figure 4.12b, an un–symmetric diphosphane complex was formed, characterized by two doublets centred around 3.8 and 5.8 ppm (J = 30 Hz). In the ^{1}H–NMR spectrum of this solution, an isolated resonance is observed around 9.1 ppm, characteristic for uncoordinated phen, suggesting a successful ligand exchange. Assuming that L3X replaces phen as ligand while keeping the palladacycle intact, the $^{31}P\{^{1}H\}$–NMR spectrum could thus tentatively be assigned to the un–symmetric 'L3X–palladacyle' complex (**II**).

The un–symmetric complex is unstable and disappears in about two hours at room temperature, while a new broad resonance around 0.5 ppm appears. This resonance belongs to the neutral bis–ligand complex $[Pd^{0}(L3X)_2]$, as verified by *in situ* synthesis of $[Pd^{0}(L3X)_2]$ from $[Pd_2(dba)_3]$ (dba = dibenzylidene acetone) and 10 equivalents of L3X in nitrobenzene (Figure AIII.1). After the *in situ* synthesis of $[Pd^{0}(L3X)_2]$, resonances due to some mono–oxidized ligand ('P=O'; 25.8 and –24.5 ppm) and some di–oxidized ligand ('O=PP=O'; 27.0 ppm) are present as well (Figure AIII.1). These same resonances are also found in the ligand exchange experiment (Figure 4.12), but two additional resonances are observed around 14.3 and –26.2 ppm (marked with '*' in Figure 4.12c). These resonances grow equally fast, indicating that they belong to the same species. Obviously, this species is not ligand mono–oxide, nor can this be a divalent palladium complex; $[Pd^{II}(L3X)(OAc)_2]$ is characterized by a sharp singlet around 16 ppm and $[Pd^{II}(L3X)_2](OTs)_2$ exhibits a broad resonance around 5 ppm.[40] This leaves as the only likely option the formation of a phosphazane ('P=NPh'), which must be formed during the decomposition of the initially formed un–symmetric 'L3X–palladacycle' complex (**II**). The presence of such a phosphazene was also observed with Electron Spray Ionization Mass Spectroscopy (*vide infra*).

To further characterize the decomposition pathway of the postulated 'L3X–palladacycle'complex (**II**), the ligand exchange experiment was repeated under an atmosphere of carbon monoxide. The kinetic data of this experiment are shown in Figure 4.13b, while Figure 4.13a shows the kinetic data for the reaction under argon. The rate of appearance of $[Pd^{0}(L3X)_2]$ (0.5 ppm, 0.0021 and 0.0004 min^{-1}) is about twice the rate of the disappearing $^{31}P\{^{1}H\}$–NMR signals at 3.8 and 5.8 ppm (–0.0011 and –0.0002 min^{-1}), which is consistent with the assignment of the disappearing compound to a compound containing one diphosphane ligand (two P–atoms, possibly 'L3X–palladacycle' (**II**)), and the appearing species to

$[Pd^0(L3X)_2]$ (four P–atoms). The decomposition of the presumed 'L3X–palladacycle' (**II**) is approximately five times slower for the reaction under carbon monoxide atmosphere (–0.0002 min^{-1}) compared the reaction in argon (–0.0011 min^{-1}). In a CO atmosphere less $[Pd^0(L3X)_2]$ is formed during the initial ligand exchange reaction (the intercept is 0.046 (CO) *versus* 0.074 (Ar)).

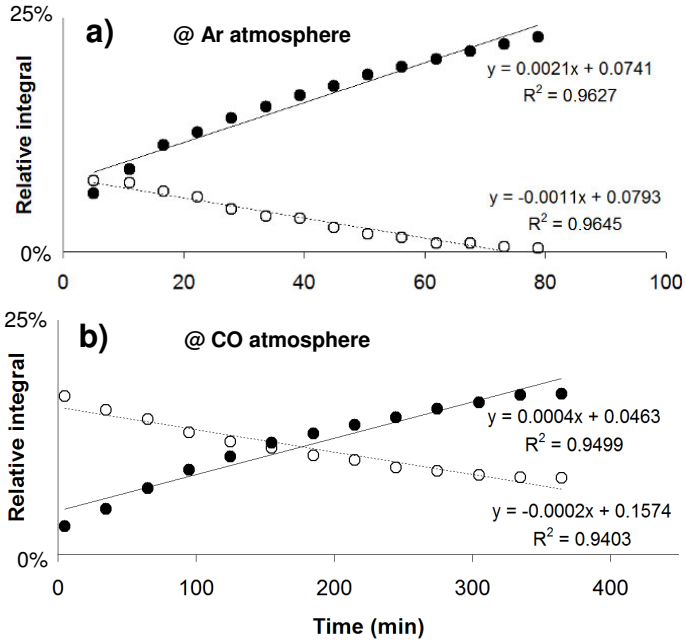

Figure 4.13. Plot of the $^{31}P\{^1H\}$–NMR integrals (relative to the ligand and the appearing and disappearing compounds) for the resonance of $[Pd^0(L3X)_2]$ around 0.5 ppm (●) and 'L3X–palladacycle' around 5 ppm (○) as a function of time; a) under an argon atmosphere; b) under an atmosphere of CO.

4.2.4.4 Ligand exchange experiment with 1 eq. L3X and ESI–MS analysis

The above data strongly suggest that the 'L3X–palladacycle' complex (**II**) formed from Phen–L3X exchange is unstable and decomposes at ambient temperatures (~25 ºC); the stabilizing effect of a CO atmosphere indicates that this proceeds *via* a reversible decarbonylation / carbonylation process. Apparently, extrusion of CO_2 from the 'L3X– palladacycle' (**II**) has a higher barrier than decarbonylation, as also judged from the fact that only traces of isocyanate are formed (*vide infra*). In an attempt to prevent the decomposition of 'L3X–palladacycle'(**II**) to $[Pd^0(L3X)_2]$, which possibly is accelerated by the presence of excess of L3X, and

in order to detect possible intermediate species in the presumed decarbonylation of 'L3X–palladacycle' (**II**), the ligand exchange experiment was repeated with only one equivalent of L3X. The resulting spectra are shown in Figure 4.14.

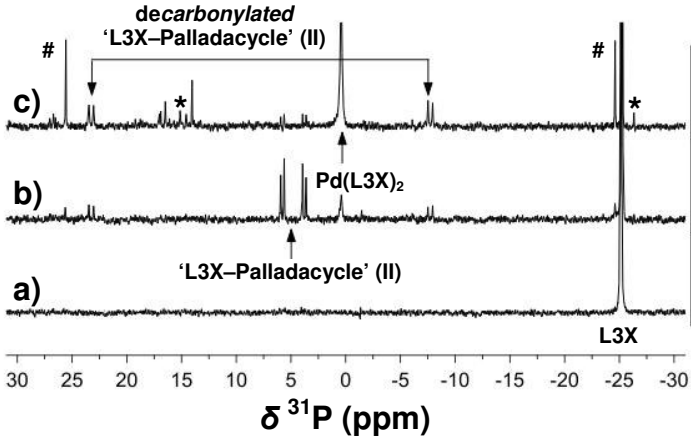

Figure 4.14. $^{31}P\{^{1}H\}$–NMR spectra for a solution containing 'phen–palladacycle' and 1 eq. of L3X in nitrobenzene before heating (a), after heating to 60 ºC for about one minute and cooling to room temperature (b), after standing for an additional 180 minutes at room temperature (c). # = the mono–oxide of L3X; * = the mono–phosphazene of L3X.

The $^{31}P\{^{1}H\}$–NMR spectrum of the yellow suspension obtained after mixing 'phen–palladacycle'(**I**) with one equivalent of L3X in nitrobenzene initially shows only pure ligand (–25 ppm, Figure 4.14a). The reaction mixture was then heated gently to about 60 °C for about one minute, and after cooling to room temperature the resulting clear orange solution was again measured with $^{31}P\{^{1}H\}$–NMR (Figure 4.14b). Besides the resonances of the anticipated un–symmetric species around 5.0 ppm and some $[Pd^{0}(L3X)_2]$ around 0.5 ppm, two additional weak doublet signals were observed around 23.9 and –7.1 ppm which evolved at the same rate and have an identical coupling constant (J = 42 Hz). This is consistent with the formation of another un–symmetric mono–chelate palladium complex, which may well be a de*carbonylated* 4–membered ring 'L3X–palladacycle' complex (**III**) with the proposed structure shown in Scheme 4.3 (see also next section). The formation of another decarbonylated 4–membered ring L3X–palladacycle complex (**IV**) was also considered (Scheme 4.3). However, the large difference in chemical shift (31 ppm) between the two phosphorus nuclei is

more consistent with palladacycle (**III**), as the Pd–C(O)O–moiety will cause severe deshielding (23.9 ppm), while the Pd–N(Ph)– moiety will cause significant shielding (–7.1 ppm). The weak resonances observed between 14–18 ppm may then perhaps arise from the 4–membered L3X–palladacycle complex (**IV**).

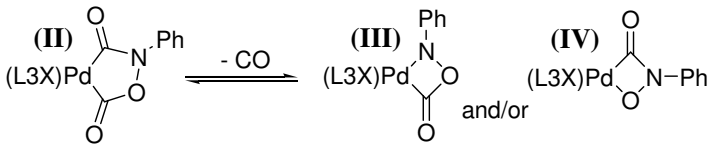

Scheme 4.3. Proposed structure of 4–membered ring 'L3X–palladacycle' complexes (**III**) and (**IV**) formed after decarbonylation of 5–membered ring 'L3X–palladacycle' complex (**II**).

After the solution was allowed to stand at room temperature for an additional 180 minutes (Figure 4.14c), the 'L3X–palladacycle' (**II**) is almost absent, while the (presumed) decarbonylated 4–membered 'L3X–palladacycle'(**III**) is still significantly present (~20% based on Pd;[48] see also Figure AIII.2). $[Pd^0(L3X)_2]$ has become the major species (33% based on Pd). Amongst the several unknown species that have evolved (resonances between 14 and 18 ppm; 25% based on Pd) the presence of L3X–palladacycle complex (**IV**) can neither be proven nor be ruled out. Some ligand mono–oxide is formed ('P=O'; 25.8 and –24.5 ppm), and some uncoordinated ligand (–25.1 ppm) is still present, thus suggesting that the ligand exchange reaction is not quantitative after 180 minutes; this is corroborated by ^{1}H–NMR showing that 'phen–palladacycle' (**I**) is also still present in approximately the same amount as uncoordinated L3X.[48]

These results strongly suggest the initial formation of 'L3X–palladacycle' (**II**) on ligand exchange of L3X with phen–palladacycle (**I**), while its subsequent disappearance seems to proceed *via* a decarbonylation process to give either 4–membered L3X–palladacycle complex (**III**) or (**IV**), or both. To obtain more evidence for the decarbonylation pathway, the ligand exchange experiment was repeated and after gentle heating the clear solution was now measured with electron spray ionization mass spectroscopy (ESI–MS). In the resulting mass spectrum (Figure 4.15), the highest observed mass (*m/z* 986.2) originates from $[Pd(L3X)_2]^+$ (exact mass = 986.3).

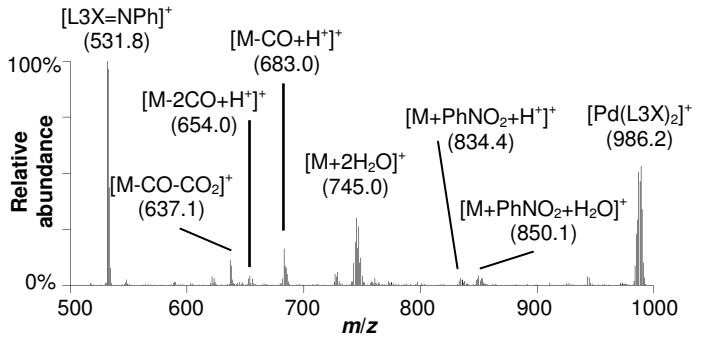

Figure 4.15. ESI mass spectrum of reaction mixture taken directly after the ligand exchange of phen-palladacycle (I) with one equivalent of L3X. M = 'L3X–palladacycle' (II) = [(L3X)PdC(O)ON(Ph)C(O)].

As the lower mass products observed are absent in an ESI–MS of pure $[Pd^0(L3X)_2]$ in nitrobenzene, these lower mass peaks must originate from other complexes formed in the exchange reaction. Although the exact mass (709.1) of the presumed 'L3X–palladacycle' (**II**) is not observed, various peaks and their isotope distributions are consistent with solvent adducts of 'L3X–palladacycle' (**II**), as is detailed in Figure 4.16.

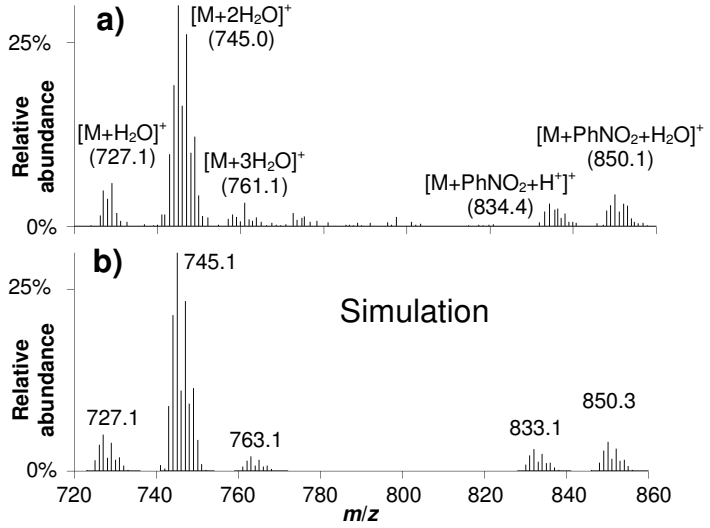

Figure 4.16. (a) Zoom–in and assignment of the ESI mass spectrum of reaction mixture from *in situ* synthesis of 'L3X–palladacycle' (**II**) (=M); (b) simulation.

In the ESI–MS of the reaction mixture (Figure 4.15) a small peak is present with a mass corresponding to the decarbonylated 'L3X–palladacycle' (**III**) or (**IV**) ([M–CO+H$^+$]$^+$; 683.0), whereas the mass of decarboxylated 'L3X–palladacycle' ([M–CO_2]$^+$; exact mass = 665.1) is not observed. The small peak at *m/z* 654.0 corresponds to [M–2CO+H]$^+$, i.e. nitrosobenzene bound to [(L3X)Pd^0]. Interestingly, the small feature at *m/z* 637.1 can be assigned to [M–CO–CO_2]$^+$, which corresponds to an imido complex '(L3X)Pd=NPh' (**V**). The presence of a (L3X)Pd(ONPh) and a (L3X)Pd=NPh (**V**) complex as fragmentation products of 'L3X–palladacycle' (**II**), is very likely reflecting its thermal decomposition pathway. The reaction product of (L3X)Pd=NPh with L3X (i.e. the phosphazene '[L3X=NPh]$^+$'; *m/z* 531.8) is clearly present as well (see also ^{31}P{^{1}H}–NMR above), while small quantities of aniline and nitrosobenzene are observed with GLC–MS.

These MS data are thus in agreement with the NMR data, and suggest that the initially formed 5–membered P_2–palladacycle may (at least partially) decompose to a P_2Pd–imido species, *via* (**III**), as is shown in Scheme 4.4. The imido complex (**V**) may then, at least partially, reacts with coordinated P_2 ligand to the observed phosphazene while liberating zero–valent palladium, which is trapped by uncoordinated L3X as [Pd^0(L3X)$_2$].

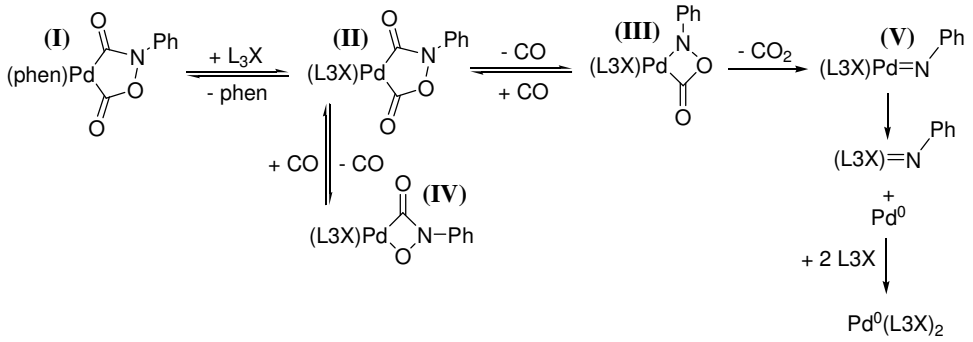

Scheme 4.4. Proposed reaction sequence of the ligand exchange between 'phen–palladacycle' (**I**) and the diphosphane ligand L3X, followed by decomposition of the 'L3X–palladacycle' (**II**).

4.2.4.5 Attempted identification and quantification of 'PhN'–containing products

The reaction sequence shown in Scheme 4.4 cannot be the entire story however, as the formation of 'L3X=NPh' is by no means quantitative with respect to the amount of 'PhN' that was initially present in the form of phen–palladacycle (**I**) (~10 μmol). The integrals of 'L3X=NPh' and [$Pd^0(L3X)_2$] by the end of the ligand exchange experiment (Figure 4.14c) indicate that merely ~0.4 μmol of the initial 'PhN' ends up in the L3X–phosphazene.[49] Likely products that may contain the remaining ~9.6 μmol of the 'PhN' fragment could be aniline, phenylisocyanate, nitrosobenzene and/or azo(xy)benzene. Because the ^{1}H–NMR resonances of all possible reaction products containing the 'PhN' moiety are obscured by the resonances of the abundantly present nitrobenzene, L3X, and [$Pd^0(L3X)_2$], the solution was analyzed with GLC–MS. However, using this technique it only proved possible to positively identify about 10% of the NPh fragment originally present in complex (**I**) as aniline, nitrosobenzene, phenyl isocyanate and L3X=NPh.

To obtain more unambiguous information about the fate of the 'PhN' moiety the NMR experiment was repeated in non–aromatic solvents such as CH_3NO_2 and CD_2Cl_2 (see Appendix III, section AIII.3.1) Although these experiments strongly suggest the formation of *various* 'PhN' containing products, neither a positive identification nor quantification could be achieved, mostly due to the interference of the aromatic resonances of L3X and $Pd^0(L3X)_2$. Experiments using a ligand with pentafluorophenyl groups were also inconclusive, but again showed the formation of various 'PhN'–containing products (see Appendix III, section AIII.3.2).

4.2.4.6 Ligand exchange experiment with a bulky phosphane ligand

In an attempt to stabilize a possible 'Pd=NPh' species, the ligand exchange experiment was repeated with 5 equivalents of the sterically very bulky[50] phosphane ligand 1,3–bis(1,3,5,7–tetramethyl–4,6,8–trioxa–2–phospha-amantane)propane (bpap, Figure 4.17). Unfortunately, the anticipated ligand exchange reaction was not observed when the yellow 'phen–palladacycle' (**I**) / bpap suspension in nitrobenzene was carefully heated; only the resonances of the free ligand were observed around –31.0 (*rac*) and –30.2 (*meso*) ppm.[51] When the

solution was heated for four hours at 100 °C, small peaks of various unidentified species evolved between 0 and 15 ppm (see Figure AIII.3 for $^{31}P\{^{1}H\}$–NMR spectrum). Most resonances lie around +28 and –30 ppm ('free' bpap), which most likely belong to ligand oxide or possibly also phosphane species such as 'bpap=NPh' or 'bpap(=NPh)$_2$'.

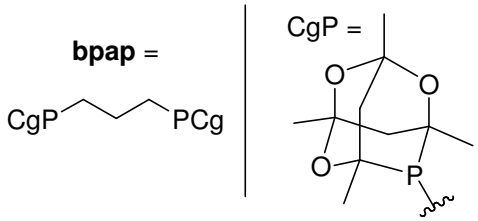

Figure 4.17. Drawing of 1,3–bis(1,3,5,7–Tetramethyl–4,6,8–trioxa–2–phosphaamantane)-propane (bpap), used as mixture of the *rac* (*αα*/*ββ*) and *meso* (*α*/*β*) diastereoisomers (1:0.3 ratio).

To investigate whether a 'Pd=NPh' species is present amongst the species observed by NMR, the reaction mixture was analyzed with ESI–MS spectroscopy; the resulting mass spectrum is shown in Figure 4.18. The largest peak around *m*/*z* = 687 and its isotope distribution (see inset figure) are in perfect agreement with $[(bpap)Pd{=}NPh{\cdot}H_2O]^+$ (which may also be written as $[(bpap)Pd(OH)NHPh]^+$). The second largest peak with mass around *m*/*z* 564 is consistent with the mono phosphazane of bpap, $[bpap{=}NPh{+}H]^+$ (exact mass of 564.3). The highest observed masses around *m*/*z* = 1051 and 1069 are relatively small and are consistent with $[Pd(bpap)_2{+}H]^+$ and $[Pd(bpap)_2{+}H_2O{+}H]^+$ (exact masses 1051.3 and 1069.3 respectively). These data thus again point to the palladium-imido complex as intermediate decomposition product of (**I**) via a ligand exchange as was shown in Figure 4.14.

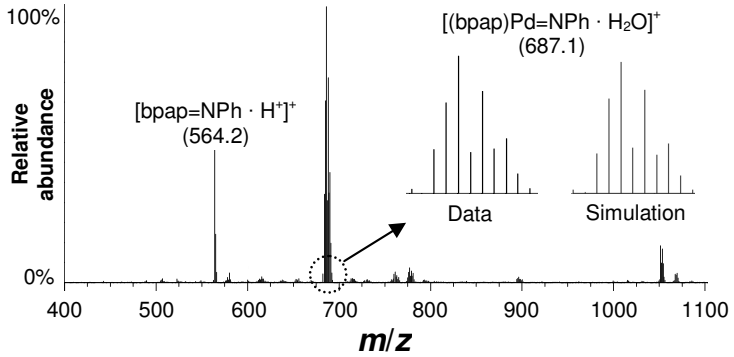

Figure 4.18. ESI mass spectrum of a solution containing 'phen–palladacycle'(**I**) and 5 eq. of bpap in nitrobenzene, after heating four hours at 100 °C. Inset: an enlargement of the indicated area, with a simulation of that mass.

These data are thus in agreement with the data obtained from ligand exchange and ESI-MS experiments with L3X in that an initially formed 5–membered P_2–palladacycle may (at least partially) decompose to a P_2Pd–imido species, *via* (**III**), as is shown in Figure 4.14. The imido complex (**V**) then, at least partially, reacts with coordinated P_2 ligand to the observed phosphazene while liberating zero–valent palladium, which is trapped by uncoordinated L3X as $[Pd^0(L3X)_2]$.

4.2.5. Investigations into the possible existence of di-phosphane palladium imido complexes

4.2.5.1 DFT calculations

As the above all points towards a palladium–imido intermediate as a species of crucial importance, DFT calculations were performed to gain insight into the geometric and electronic properties of diphosphane–palladium–imido complexes. As a means of validating the computation method, the structure of the reported Ni–imido compound 1,2–*bis*–(di–tert–butylphosphanyl)ethane)Ni=N(Mes)[38] was calculated (Figure 4.19a). As can be seen in Table 4.3, characteristic distances and angles for the DFT–optimized structure are almost identical to those of the crystal structure of the nickel–imido compound. The only noticeable difference is the Ni–N–C angle, which is 180º in the crystal structure and 178.7º in the calculated structure.

Table 4.3. Selected data of several (calculated) imido complexes.

Complex (→):	**Ni – Imido[a]**		**Pd – imido[b]**		
Parameter (↓):	**X–ray[38]**	**DFT**	**L4**	**pMeO–L4**	**L3X**
Distances (Å)					
M=N	1.703	1.707	1.885	1.888	1.878
M–L1	2.189	2.195	2.279	2.323	2.274
M–L2	2.181	2.183	2.323	2.279	2.322
Angles (º)					
P1 – M – P2	90.94	90.95	97.56	97.27	92.48
P1 – M – N	134.4	134.6	146.7	146.0	151.7
P2 – M – N	134.4	134.4	116.6	116.7	115.6
$Q(N)_{NPA}$			–0.817	–0.848	–0.833
***p*K_a[c]**			11.2	16.6	13.9
Azoxy selectivity	–	–	32%	7%	6%

[a] 1,2–*bis*–(di–tert–butylphosphanyl)ethane)Ni=N(mesityl).[38] [b] (ligand)Pd=NPh. [c] $pK_a = (Q(N)_{NPA} * -174) - 131$ ($R^2 = 0.983$)[52]

Considering the computational method valid, several P_2Pd^{II}=NPh complexes were calculated. As the catalyst system based on Pd^{II}(L4) produces significant amounts of azoxybenzene, and because azoxybenzene production can be suppressed by equipping the ligand aryl rings with electron–donating methoxy groups or by decreasing the bite angle, the series of Pd–imido complexes (L4)Pd^{II}=NPh, (pMeO–L4)Pd^{II}=NPh, and (L3X)Pd^{II}=NPh has been calculated. Characteristic data are listed in Table 4.3, and perspective views of the calculated structures are shown in Figure 4.19b–d.

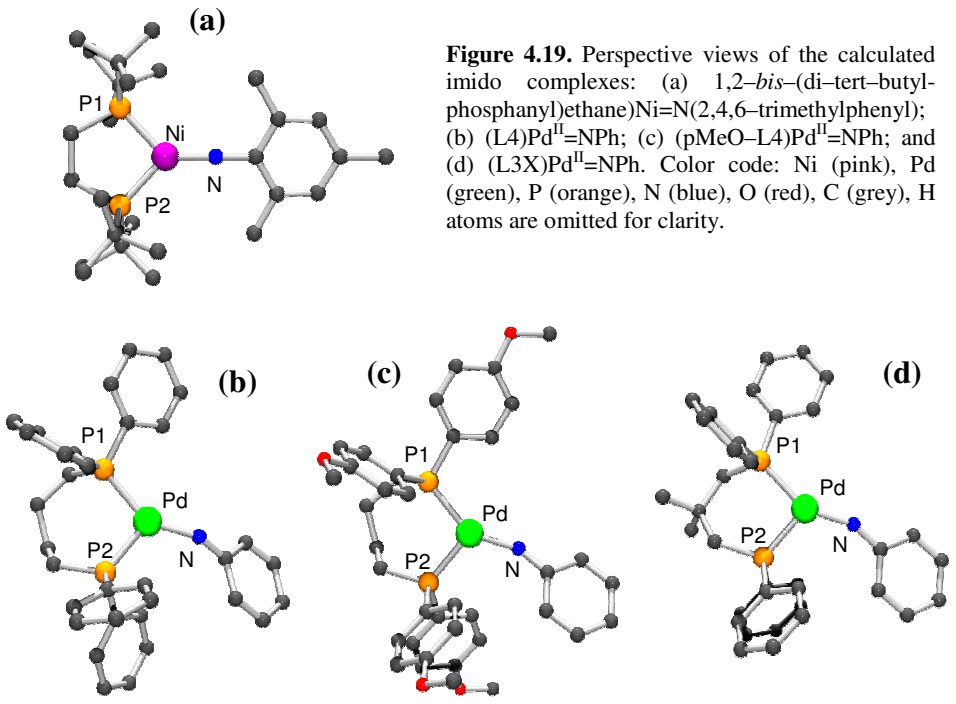

Figure 4.19. Perspective views of the calculated imido complexes: (a) 1,2–*bis*–(di–tert–butyl-phosphanyl)ethane)Ni=N(2,4,6–trimethylphenyl); (b) (L4)Pd^{II}=NPh; (c) (pMeO–L4)Pd^{II}=NPh; and (d) (L3X)Pd^{II}=NPh. Color code: Ni (pink), Pd (green), P (orange), N (blue), O (red), C (grey), H atoms are omitted for clarity.

As expected, the main geometric difference between these computed complexes is the P1–Pd–P2 angle, which is larger (97º) for the complexes bearing a ligand with a butylene backbone compared to the propylene–bridged analogue (92º). The angle P1–Pd=N is about 152º when using L4 and pMeO–L4, compared to 146º when using L3X, showing that these complexes are asymmetric, in contrast to the

Ni–imido complex (both P–Ni=N angles are 135º). This geometric difference between these Ni– and Pd– imido complexes is probably due to the bulkier phosphane ligand used in the nickel compound (i.e., forcing the symmetry). A practical consequence of this is that the equatorial position *cis* to P1 in the P_2Pd=NPh complexes is fairly open for incoming substrates.

When comparing the charge density on the imido–nitrogen atom based on the natural population analysis ($Q(N)_{NPA}$),[53] it appears that its basicity is smallest ($Q(N)_{NPA}$ = –0.817, pK_a = 11.2)[52] in (L4)Pd^{II}=NPh, which, from this series of catalyst precursors, is the most selective towards Azoxy formation (32%).[54] For the other two complexes, which are far less selective towards Azoxy, the $Q(N)_{NPA}$ and the related pK_a are larger.

4.2.5.2 *Synthesis of a palladium–imido complex and its reactivity with CO/CH_3OH*

Attempts were undertaken to synthesize a P_2Pd^{II}=NR complex and study its reactivity towards CO/CH_3OH. To the best of my knowledge, the synthesis of Pd–imidoaryl complexes has not been reported so far. Only in one instance has the detection of a particular class of group 10 metal (fluoro–alkyl) imido complexes been claimed, based solely on IR–spectroscopic measurements.[55] The synthesis of P_2Ni^{2+}=NR complexes has been reported, however.[36-38] These reports were therefore chosen as the starting point for synthetic investigations. Thus, the reaction of a P_2Pd^0(dba) complex with an aryl azide was envisaged to yield the corresponding imido complex with the extrusion of dinitrogen (Scheme 4.5). In order to protect and stabilize the supposedly reactive Pd=N–R bond the sterically crowded diphosphane ligand bpab and mesitylene (Mes) azide were used in this attempt.

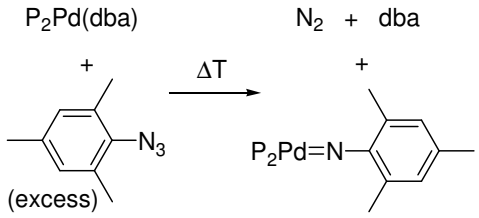

Scheme 4.5. Reaction scheme for the synthesis of a Pd–imido complex.

Selected $^{31}P\{^{1}H\}$–NMR spectra of reaction mixtures for the *in situ* formation of [(bpap)Pd^{II}=NMes] are shown in Figure 4.20. The $^{31}P\{^{1}H\}$–NMR spectrum of the starting compound [Pd^{0}(bpap)(dba)] in d^{8}–toluene shows two broad resonances around 2.5 and 5.0 ppm, due to the presence of *rac* (*αα*/*ββ*) and *meso* (*α*/*β*) diastereoisomers of bpap (Figure 4.20a).[51, 56] The small resonances around 28 and 29 ppm are due to the presence of a small amount of ligand oxide ('P=O'). No changes in the NMR are observed when an excess of mesitylene azide is added, not even after heating to 50 °C (not shown). The reaction mixture was therefore heated to 100 °C for about 30 minutes (Figure 4.20b) after which the reaction mixture was allowed to cool to room temperature (Figure 4.20c).

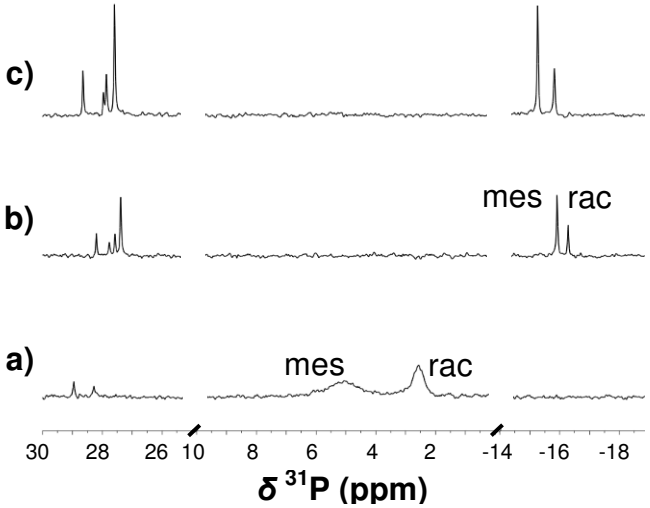

Figure 4.20. $^{31}P\{^{1}H\}$–NMR spectra of reaction mixtures for the *in situ* formation of of [(bpap)Pd=NMes] in d^{8}–toluene, from [Pd(bpap)(dba)] and mesitylene azide: (a) pure [Pd(bpap)(dba)]; (b) after mesitylene azide addition and heated at 100 °C; (c) after cooling to room temperature.

After heating to 100 °C all [Pd^{0}(bpap)(dba)] has reacted as is evidenced by the disappearance of the resonances around 2.5 and 5.0 ppm. The resonances that were assigned to ligand oxide ('P=O', 28.0 and 28.7 ppm) have grown somewhat and two new resonances appeared around 27.6 and 27.9 ppm, which are assigned to a phosphazene moiety ('P=NMes', also observed with mass spectroscopy, *vide infra*). In addition, two resonances are observed around –15.3 and –15.8 ppm.

These resonances cannot be due to uncoordinated mono–oxide or mono–phosphazene version of the ligand, as the $^{31}P\{^{1}H\}$–NMR resonances of the free ligand moiety are positioned around –31.0 (*rac*) and –30.2 (*meso*) ppm.[51] The resonances around –15.3 and –15.8 ppm may be assigned to the anticipated palladium–imido species [(bpap)Pd^{II}=NMes].[57] The DFT–calculations of such imido–complexes with phosphane ligands L4, L4X, and L3X (*vide infra*) suggest that these complexes are slightly asymmetric, and should thus appear as a double doublet in $^{31}P\{^{1}H\}$–NMR. The singularity of the observed resonances around –15.3 and –15.8 ppm may well be explained by a thermal equilibrium process, but also by the very bulky ligands surrounding Pd, hence forcing higher symmetry as is observed for similar P_2Ni^{2+}=NR complexes with bulky P_2 and NR ligands.[36-38]

The reaction mixture was diluted with CH_3CN and analyzed with ESI–MS; part of the resulting mass spectrum is shown in Figure 4.21a, while Figure 4.21b shows a simulation of the three most prominent features in the spectrum.

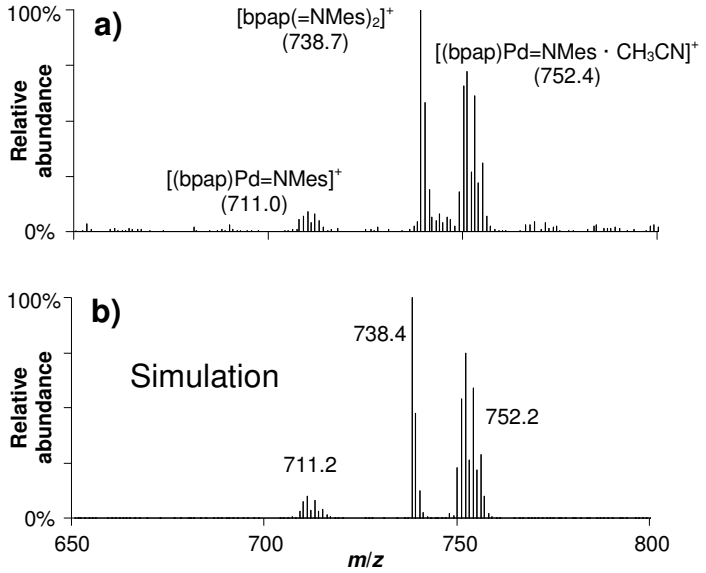

Figure 4.21. (a) ESI mass spectrum of diluted (CH_3CN) reaction mixture from *in situ* synthesis of [(bpap)Pd=NMes] from the NMR study; (b) simulation of the three most prominent MS peaks.

The highest mass (*m/z* 752.4) and its isotope distribution is in excellent agreement with a species [(bpap)Pd=NMes · CH_3CN]$^+$. The mass and isotope distribution at

m/*z* = 711.0 may be assigned to [(bpap)Pd^{II}=NMes]$^+$ (calc. = 711.2). The mass centred on *m*/*z* = 738.7 is assigned to the double phosphazane ('MesN=PP=NMes'; calc. = 738.4). Also present but not shown in the figure is a small peak belonging to bpap containing one phosphorus oxide and one phosphazane ('O=PP=NMes', *m*/*z* = 621.3). It is noteworthy that mono–phosphazene–phosphane ligand is not observed, consistent with the $^{31}P\{^1H\}$NMR spectra shown in Figure 19. The formation of the observed diphosphazane compounds may result from the Staudinger reaction of the azide with possibly uncoordinated phosphane ligand.[58] The formation of the diphosphazane could also imply however, that [(bpap)Pd^{II}=NMes] acts as the imidation agent for the diphosphane ligand. The NMR and ESI–MS results are both consistent with the formation of [(bpap)Pd^{II}=NMes] as shown in Scheme 4.5.

Finally, a new reaction mixture of (bpap)Pd^{II}=NMes was prepared as described above, whereafter CO was bubbled though the solution for about five minutes at 25 °C followed by the addition of CH_3OH. The addition of methanol may trap any possibly formed mesitylene isocyanate, or react with solvated CO and the imido complex to yield methyl mesityl carbamate. The resulting reaction mixture was analyzed with GLC–MS, clearly revealing the presence of methyl mesityl carbamate with a retention time t_R of 20.8 minutes (~20% peak intensity, indicating that it is formed from the metal–imido intermediate),[59] and an *m*/*z* of 193 (exact mass = 193.1; Figure AIII.11). The unlikely event[60] that methyl mesityl carbamate is formed by direct reaction between the excess of mesityl azide, CO and methanol –without involvement of the palladium complex– was also considered. However, when methanol is added to a CO saturated solution of mesityl azide, and the resulting solution is analyzed with GLC–FID, methyl mesityl carbamate is not observed.

It is thus concluded, both from spectroscopic evidence as well as from the observed reactivity of the complex with CO/Methanol, that a species has been synthesized that appears to be a first 'Pd=NAr' complex. It also demonstrates that such Pd=NPh species can be methoxy-carbonylated to produce carbamate (and a zero-valent Pd species) under mild conditions.

4.3. Discussion

4.3.1. A complex network of catalytic reactions centred around a P_2Pd^{II}=NPh complex

As explained in detail in Chapter 3, a remarkable observation when applying bidentate diarylphosphanes as ligands in the palladium catalyzed carbonylation of nitrobenzene is the formation of substantial amounts of methanol oxidation products such as DMC, DMO, MF, and CO.[39] During the formation of these products, H–atoms are liberated, which are transferred to nitrobenzene and are observed in the products $PhNH_2$, DPU and H_2O. Thus, apart from CO, methanol functions as a reductant and hydrogen transfer reagent for nitrobenzene. This provides very important mechanistic information; the oxidation of methanol is clearly coupled with the reduction of nitrobenzene involving Pd^0/Pd^{II} chemistry.

To sustain catalytic cycles for both the methanol oxidation products as well as for the nitrobenzene reduction products, a product–releasing species of the one cycle must be an initiating intermediate in the complementary product cycle. In Chapter 3 it was proposed that a Pd–imido species, (P_2Pd^{II}=NPh) is such a key intermediate to several product–generating catalytic cycles, as is briefly summarized below.[39]

Nitrobenzene reduction to the imido–complex involves oxidation of Pd^0 to Pd^{II}, and can be described by the three half–reactions given in Equations 1a–c. The nitrobenzene deoxygenating reagents are respectively two molecules of CO (1a), one CO and two acidic $CH_3O\mathit{H}$ H–atoms (1b), or all H–atoms from one CH_3OH molecule (1c). The formation of DMO can be seen as a modified version of Equation 1b (with 2 CO), and the formation of MF can be regarded as a modified version of Equation 1c (with 2 CH_3OH).

$$P_2Pd^0 + PhNO_2 + 2\ CO \rightarrow P_2Pd^{II}{=}NPh + 2\ CO_2 \quad (1a)$$

$$P_2Pd^0 + PhNO_2 + 2\ CO + 2\ CH_3OH \rightarrow P_2Pd^{II}{=}NPh + H_2O + CO_2 + DMC \quad (1b)$$

$$P_2Pd^0 + PhNO_2 + CH_3OH \rightarrow P_2Pd^{II}{=}NPh + CO + 2\ H_2O \quad (1c)$$

In order for these reactions to be catalytic in palladium, the P_2Pd^{II}=NPh complex must be reduced to P_2Pd^0, which can proceed as described by Equations 2a–c. This would then explain the formation of all aryl contain reduction products of

nitrobenzene; MPC (2a), aniline (2b), and Azoxy (2c). DPU formation is a modified version of Equation 2a ($PhNH_2$ instead of CH_3OH), and Azo formation can be seen as a modified version of Equation 2c (PhNO instead of $PhNO_2$), or may be the result of a further deoxygenation of azoxybenzene.

$$P_2Pd^{II}{=}NPh + CO + CH_3OH \rightarrow P_2Pd^0 + MPC \quad (2a)$$
$$P_2Pd^{II}{=}NPh + CO + 2\ CH_3OH \rightarrow P_2Pd^0 + PhNH_2 + DMC \quad (2b)$$
$$P_2Pd^{II}{=}NPh + CO + PhNO_2 \rightarrow P_2Pd^0 + Azoxy + CO_2 \quad (2c)$$

When water is formed (eq. 1b and 1c), water may replace methanol in the above reactions (eq. 2a and 2b), which will lead to phenyl carbamic acid (PhNHC(O)OH) instead of MPC in Equation 2a, or to methyl hydrogen carbonate ($CH_3OC(O)OH$) instead of DMC in Equation 2b; both are instable products and will readily decompose into $PhNH_2/CO_2$ and CH_3OH/CO_2 respectively. In both cases, this thus leads to the same stoichiometry, as is shown by Equation 2d.

$$P_2Pd^{II}{=}NPh + CO + H_2O \rightarrow P_2Pd^0 + PhNH_2 + CO_2 \quad (2d)$$

A combination of the half–reactions that oxidize Pd^0 to Pd^{II} (eqs. 1) with the half–reactions that reduce Pd^{II} to Pd^0 (eqs. 2), leads to the overall possible stoichiometries described in Chapter 3.[39] This allows the construction of a relatively simple and unifying catalytic scheme, rationalizing the formation of all methanol oxidation products and all nitrobenzene reduction products (Scheme 4.6).

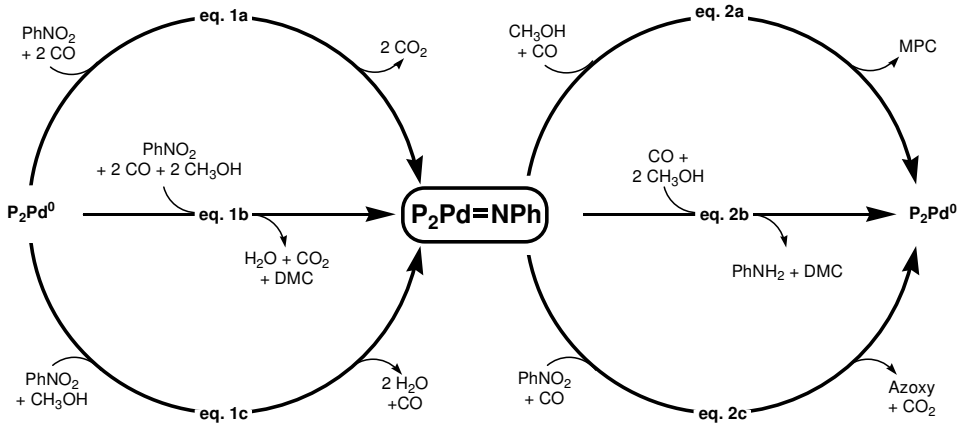

Scheme 4.6. Proposed reaction scheme for the catalytic processes in the P_2Pd-catalyzed carbonylation of nitrobenzene in methanol.

4.3.2. Nitrobenzene de–oxygenation mechanisms leading to a P_2Pd^{II}=NPh complex

4.3.2.1 MPC production via *Pd–imido complex* vs. *palladacyclic complex*

In the proposed reaction scheme condensed in Scheme 4.6, the formation of the nitrobenzene carbonylation products (MPC and DPU) does not require the palladacyclic intermediate shown in Figure 4.2 (i.e. (**II**) when L3X is the supporting ligand). However, the presence and involvement of such a species can not be excluded based on the above constructed hypothesis alone. A mechanistic pathway towards MPC that involves the palladium–imido complex (eq. 1a and 2a) cannot easily be distinguished from a mechanism involving the palladacyclic complex (eq. 3a and 3b): both amount to the same net stoichiometry as given by Equation 3c.

$$P_2Pd^0 + PhNO_2 + 3\ CO \rightarrow \text{'}P_2\text{–palladacycle'} + CO_2 \quad (3a)$$

$$\text{'}P_2\text{–palladacycle'} + CH_3OH \rightarrow P_2Pd^0 + MPC + CO_2 \quad (3b)$$

$$PhNO_2 + 3\ CO + CH_3OH \rightarrow MPC + 2\ CO_2 \quad (3c)$$

It is thus useful to elaborate on the molecular mechanistic basis underlying the proposed nitrobenzene deoxygenation pathways given in Equations 1a–c, and compare these with a possible deoxygenation pathway involving a palladacyclic complex (eq. 3a). Especially a comparison between the related deoxygenation pathways 1a and 3a (using only CO as deoxygenating reagent) will shed light on the likelihood of both pathways.

4.3.2.2 Proposed $PhNO_2$ deoxygenation pathways; CO–only

The commonly proposed pathway to reduce nitrobenzene with CO alone (see Scheme 4.7) when 1,10–phenanthroline is the supporting ligand, leads to the palladacycle 'phen–**C7**' (i.e. (**I**)) *via* the pathway **C1→C2→C3→C4→C7**. It is generally proposed that palladacycle 'phen–**C7**' is the direct precursor for the formation of isocyanates and carbamates.[7, 16, 18, 20, 28, 29]

The central thesis as established from the present work using bidentate diarylphosphane ligands (as P_2 in Scheme 4.7) in palladium-catalyzed nitrobenzene carbonylation, is that not only when methanol functions as deoxygenation agent, but also when the 'CO–only' deoxygenation pathway is

followed, the proposed Pd–imido complex **C5** is the most relevant intermediate instead of the palladacycle **C7**. The imido complex **C5** is not only necessary for a rational coupling of methanol oxidation chemistry with nitrobenzene reduction chemistry, but it is also a likely intermediate for the competing production of MPC, DPU, $PhNH_2$, and Azo(xy)benzene.

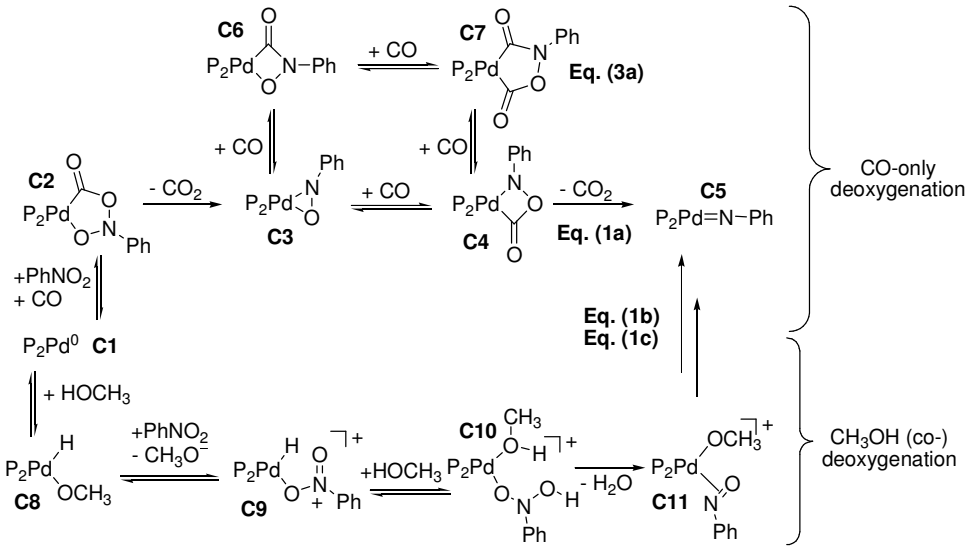

Scheme 4.7. Working hypothesis for the formation the palladacyclic intermediate (top) and the Pd–imido intermediate (centre and bottom), in the reduction of nitrobenzene.

In Scheme 4.7, the current understanding of the 'CO–only' deoxygenation pathway is summarized, including the new findings based on the NMR, ESI–MS and GLC–MS studies on the fate of a L3X–palladacycle complex (i.e., **C7** in Scheme 4.7). The first step towards the imido complex **C5** during actual catalysis is thought to involve oxidation of P_2Pd^0 (**C1**) to give species **C2**, by an oxidative coupling of CO and nitrobenzene at P_2Pd^0. Irreversible CO_2 extrusion will then lead to species **C3**, while this species under high CO pressure (carbonylation conditions) is in equilibrium with the interconvertible species, **C4**, **C6**, and **C7** *via* a series of reversible CO insertions/de-insertions (see also Scheme 4.4). In fact, it is a quite general phenomenon that in palladium-catalyzed carbonylations, e.g. of alkenes, alkynes, and alcohols, reversible carbonylation steps are involved. Escape from these equilibria can only occur by irreversible product-forming steps.[61]

The experimental studies and DFT calculations described above indicate that diphosphane–based palladacyclic complexes of the **C7**–type are considerably less stable than the corresponding phen–palladacyclic complexes; decarbo**n**ylation of the P_2–palladacyclic complexes takes place even at room temperature. Contrary to the initial expectations, CO_2 extrusion from the P_2-**C7** complex does not occur to a significant extent, apparently as a consequence of a higher activation barrier than decarbo**n**ylations to **C4** and/or **C6**. The CO_2 extrusion from the four-membered L3X–palladacycle **C4** to give Pd–imido species **C5** on the other hand, appears to be kinetically favourable as indicated by the NMR experiments showing an overall fast decomposition of **C7**, *via* **C4** to the several 'NPh' derived products. Only some 10% of the originally present 'NPh' fragment of the starting palladacycle in the ligand exchange experiments can be accounted for by specifically identified products, such as L3X=NPh, aniline, nitrosobenzene and phenyl isocyanate, but some 90% must thus have ended up in a variety other (possibly oligo–) aromatic compounds under the prevailing reaction conditions, with the concomitant appearance of neutral $[Pd^0(L3X)_2]$ species.

Apparently, the barrier for **C7** decarboxylation is significantly higher than the barrier for **C7** decarbonylation, thus preventing this palladacycle from being an important product-releasing species to the nitrobenzene carbonylation products MPC and DPU. In this respect, diphosphane–based catalysts could deviate from phen–based catalyst; decarboxylation of 'phen–**C7**' (i.e., complex (**I**)) has been proposed as the route to isocyanates/carbamates.[7, 16, 18, 20, 28, 29] The relative importance of decarbo**x**ylation *versus* decarbo**n**ylation of **C7** under actual carbonylation conditions will depend on the type of ligand applied in the catalyst, and on the relative activation barriers for these two processes. As discussed above, the combination of using diphosphane ligands and relatively mild reaction temperatures, likely causes the decarbo**x**ylation process not being able to compete with the lower barrier decarbo**n**ylation process, but it can, of course, not be excluded that at certain elevated temperatures and certain applied conditions the higher barrier process may also come into play. Under these circumstances an additional channel for production of carbamates will thus be opened. With diphosphanes as supporting ligands, formation of **C7** (see equations 3a,b) is, however, unlikely being a prerequisite for the formation of phenyl isocyanate or its derivative MPC. In fact, it was shown that a pre-synthesized 'Pd=NPh'

species, supported by the bpap ligand, reacts under mild conditions with CO and methanol to give the corresponding carbamate.

4.3.2.3 Proposed $PhNO_2$ deoxygenation pathways; CH_3OH (co–) reduction

The reduction of nitrobenzene can also be achieved by H–atoms from methanol, eventually leading to Equations (1b) and (1c). This transfer hydrogenation process most probably involves palladium hydride chemistry, without involvement of 'free' H_2 as is shown at the bottom of Scheme 4.7. The proposed mechanistic pathways for these stoichiometries have been described in Chapter 3,[39] and will be the focus of Chapter 5. For present purposes, it suffices to note that both deoxygenation pathways involving CH_3OH (eq. 1b and 1c) eventually will form *only* the imido intermediate of the **C5** type; so without any involvement of palladacyclic complexes such as **C7**.

Thus the catalytic and organometallic data presented in this chapter all point towards the P_2Pd^{II}=NPh complex **C5** as the most likely intermediate, not only as a key species to connect reduction of nitrobenzene with oxidation of methanol, but also as an important intermediate in the genesis of *all* the 'PhN' containing nitrobenzene reduction products, including carbonylation products.

The 5–membered palladacyclic compound **C7** on the other hand, most likely is not a significant MPC/DPU product releasing species. Instead, **C7** is thought to be part of several interconvertible (± CO) palladacycles (**C3**, **C4**, **C6**) that together act as temporary reservoir for the organic 'PhN' group. This formally fully reduced nitrobenzene fragment only escapes the reservoir species by the irreversible CO_2 extrusion from **C4** to form the imido-intermediate **C5**, from which the formation of all the nitrobenzene reduction products can be rationalized, including MPC and DPU.

4.3.3. Ligands effects in the reaction of P_2Pd^{II}=NPh

4.3.3.1 Azo(xy) formation vs. *carbonylation/hydrogenation*

The influence of the ligand structure on the nitrobenzene deoxygenation pathway has already been discussed in Chapter 3;[39] here the focus lies on the influence of the ligand structure on the subsequent reactivity of the P_2Pd–imido complex.

From the current mechanistic understanding summarized in Scheme 4.6, it follows that once the P_2Pd^{II}=NPh intermediate is formed, there is a competition between three different reactions: carbonylation (2a), hydrogenation (2b) and the coupling reaction (2c). The results described in Section 4.2.3.1 show that the selectivity for Azoxy depends on the concentration of nitrobenzene. This is in accordance with a mechanism in which nitrobenzene and methanol compete for a reaction with the same Pd–imido intermediate. This scheme also rationalizes the observation that an increase in CO pressure results in increasing contributions of carbonylation *and* hydrogenation reactions of nitrobenzene at the cost of the Azo(xy) forming coupling reactions, in agreement with the proposal that CO competes with nitrobenzene for reaction with the same Pd–imido intermediate.

When enlarging the bite-angle of the ligand considerably more Azoxy coupling products are formed (from 6% for L3 to 32% for L4, Table 1). When the ligand L4 is made more rigid (L4X), even more coupling products are produced (73%). This suggests that the steric property of the catalyst complex in the plane of coordination is an important parameter in determining the fate of the 'PhN' moiety. This effect bears resemblance with the observed strongly increased rate of the reductive elimination due to larger bite–angle P_2 ligands at a P_2Pd^{II} centre carrying two organic anionic groups.[44, 62-65] In the present system, the reductive elimination of azoxy– or azo– benzene from a [P_2Pd^{II}=NPh($PhNO_2$ / PhNO] moiety is apparently accelerated by enforcing close contact at the Pd centre, between the imido group and nitro– or nitroso group and therefore simultaneously forming azo(xy) benzene and a 'P_2Pd=O' species.[66] The latter 'Pd=O' complex can enter subsequent catalytic processes, such as carbomethoxylation (*via* protonation by methanol) or carbonylative de-oxygenation of nitrobenzene (by oxidation of CO).[39] It must, however, be noted that in the ligand exchange experiments described in section 4.2.4.3, most of which were carried out in nitrobenzene as the solvent, no azo(xy) benzene could be observed as a 'NPh' derived product during the decomposition of palladacycles: obviously, its formation is still an activated process, that does not occur to any appreciable extent under the low temperature conditions applied in these experiments.

The increased relative rate of azo(xy)benzene formation cannot, however, be purely steric in origin as the presence of electron–donating methoxy groups, *both*

in the ortho– *and* in the *para*–positions of the phenyl rings, significantly suppresses the coupling reaction (from 32% for L4 to 7% for pMeO–L4). A similar effect is observed when comparing L3 with pMeO–L3 (6% *vs*. 1%).

The bite angle of the ligand can also have an effect on the basicity of the imido–nitrogen of the corresponding P_2Pd^{II}=NPh complex. Palladium complexes of P_2-ligands with a C3–backbone are characterized by a P–Pd–P angle close to 90°, which is ideal for maximal orbital overlap. In complexes of P_2-ligands with a C4–backbone, this P–Pd–P angle typically is around 94°.[45] In these complexes there will thus be less orbital overlap, which in turn hampers the flow of electrons from the aryl rings to palladium. This is indeed reflected in the DFT–calculated basicity of the imido–nitrogen atom, which is higher for (L3X)Pd=NPh than for (L4)Pd=NPh. Thus, for electronic reasons (partially dictated by the steric properties of the ligand backbone), protonation (also leading to carbonylation, *vide supra*), is more easily achieved in the case of the L3–type ligands, whereas the 'disproportionation' reaction is relatively facilitated by employing L4–type ligands in the catalytic system.

4.3.3.2 Carbonylation vs*. hydrogenation*

In general, more carbonylation products (MPC, DPU) are formed relative to hydrogenation products ($PhNH_2$, DPU) when equipping the ligand with *ortho*–methoxy groups or when using ligands with a smaller bite angle.

The effect of the *ortho*–methoxy substitution on the product distribution can be rationalized with the understanding of this part of the mechanism as shown in Scheme 4.8. First, the imido nitrogen can be protonated by a CH_3OH molecule that is approaching the Pd–centre *via* the sterically not so demanding equatorial positions (see also Figure 4.19), thus forming **C12**. As this species does not have any open sites in the equatorial positions, a second CH_3OH molecule must approach the Pd–centre *via* its axial positions, resulting in the formation of aniline and the $P_2Pd^{II}(OCH_3)_2$ complex **C14**. The *o*–MeO groups will hamper this second protonation step as they shield the axial positions of Pd.[40, 67, 68] Hence, less $PhNH_2$ is formed. MPC is formed instead by an associative displacement of the CH_3O^- anion in **C12** by a smaller and neutral CO molecule, followed by

nucleophilic attack of nearby CH_3O^- on coordinated CO (giving **C13**) and reductive elimination to yield MPC and P_2Pd^0 (**C1**).

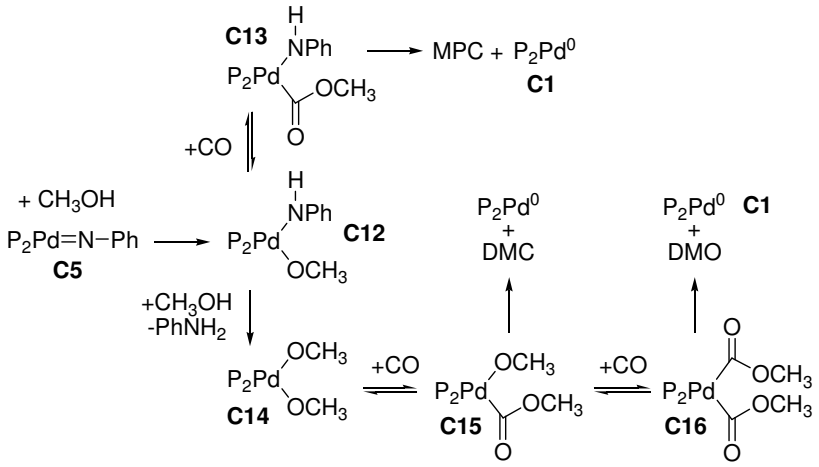

Scheme 4.8. Mechanistic scheme showing the related production of MPC and $PhNH_2$ (+DMC/DMO)

The effect of the larger ligand bite–angle giving a lower amount of carbonylation product relative to the hydrogenation product could be the consequence of a relatively better accessibility at P_2Pd^{II} by a charge–polarized methanol ($CH_3O^-\cdots H^+$) molecule at the fifth and sixth coordination site, relative to a neutral CO molecule, which would lead to a simultaneous coordination of an anionic CH_3O^- and protonation at PhN^{2-} to give **C14**, rather than **C13**.

An electronic effect may play an additional role in the relative weight of **C12→C13** (carbonylation) *vs*. **C12→C14** (hydrogenation). The difference in orbital overlap (between Pd and the P–donor atoms) caused by the L3 *vs*. L4 ligands can render the palladium centre in L4–complexes more electrophilic than in L3–complexes and therefore more susceptible by attack by methanol, relative to CO.

It is important to note that when methanol is replaced by H_2O (formed *in situ* during $PhNO_2$ de–oxygenation with CH_3OH) in the above processes, both pathways shown in Scheme 4.8 will lead to $PhNH_2$ and CO_2 as the carbonylation product instead of MPC or DMC/DMO. It was shown in Chapter 3 that this

readily occurs when using L3–ligands but much less so with L4–ligands,[39] which is consistent with the fact that catalysts equipped with the L4 ligand also produce relative less MPC/DPU.

Summarizing, catalysts with L3–ligands follow mostly (and with the oMeO–functionality almost only) the reaction sequence **C5→C12⇆C13→C1** (with CH_3OH to give MPC, *or* with H_2O to give $PhNH_2$ and CO_2), while catalysts supported with L4–ligands react for a larger portion *via* the sequence **C5→C12→C14⇆C15(⇆C16)→C1**.

4.3.4. Effects of the acidity

Interestingly, the effect of making the reaction medium more acidic is radically different for the two catalytic systems based on Pd^{II}(L4X) or Pd^{II}(o–MeO–L3X). In the reaction catalyzed with Pd^{II}(L4X), an increase in the acidity results in suppression of the coupling reaction in favor of the hydrogenation and carbonylation reactions. This is in agreement with the hypothesis that methanol and nitrobenzene compete for reaction with the imido intermediate; making the reaction more acidic facilitates the protonation of P_2Pd^{II}=NPh and thus favors the hydrogenation *and* carbonylation reactions. That the hydrogenation is promoted more than the carbonylation reaction can then be ascribed to the facilitation of the second protonation (i.e., reaction of CH_3OH with **C12** in Scheme 4.8).

On the other hand, the selectivity of the catalytic system based on Pd^{II}(o–MeO–L3X) is far less affected by the addition of acid. This observation is easily understood when realizing that with this specific catalyst the imido–intermediate is *already* predominantly involved in the carbonylation reaction following the sequence **C5→C12⇆C13→C1** route shown in Scheme 4.8. That is, the oMeO–moieties of this ligand shield the palladium centre in the catalyst, thus hampering the second protonation by methanol (from **C12** to **C14**).

4.4. Summary and conclusions

Nitrobenzene reduction in a CO/CH_3OH environment is catalyzed by Pd–diphosphane complexes. The fully deoxygenated nitrobenzene 'PhN' moiety can end up in carbonylation products, hydrogenation products and coupling products. It was shown that the selectivity for these three reactions can be altered by

adjusting the steric and electronic properties of the ligand in the catalyst, by changing the concentration of CO or $PhNO_2$, and by varying the acidity of the reaction medium. These findings could be rationalized by a relatively simple mechanistic scheme, that is centered around the palladium–imido complex 'P_2Pd^{II}=NPh' as the central product-releasing intermediate (see also Chapter 3).

As an alternative product-releasing intermediate for the carbonylation products MPC and DPU, the palladacycle '$L_2PdC(O)N(Ph)OC(O)$' (see Figure 4.2a) was considered, which is commonly proposed as product-releasing species when L_2 is the N–donor ligand 1,10–phenanthroline. It was concluded from NMR studies, GLC(–MS), and ESI–MS analysis, that 5–membered 'L3X–palladacycle' (**II**) – obtained by a ligand exchange reaction of 'phen–palladacycle' (**I**) with diphosphane ligand L3X– readily decomposes under mild conditions *via* a reversible decarbonylation reaction to give L3X–palladacycles (**III**) and/or (**IV**). This clearly suggests that the barrier for decarbo**n**ylation of palladacycle (**II**) must be significantly lower than that of decarbo**x**ylation of this species. The low stability of a diphosphane–palladacycle relative to a phen–palladacycle is mainly attributed to increased steric constraints imposed on the palladacycle by the diphosphane ligands. This is supported by DFT calculations.

Decomposition of palladacycle (**III**) by loss of CO_2 would give the thus far elusively palladium–imido species $(L3X)Pd^{II}$=NPh, which in the presence of excess of L3X under the mild ligand-exchange conditions and in the absence of CO rapidly is converted to $[Pd^0(L3X)_2]$ and a manifold of aromatic compounds. Aniline and nitrosobenzene account for only about 10% of the aromatic compounds, while mere traces of phenyl isocyanate were observed.

Evidence for a '(L3X)Pd=NPh' type of intermediate under real carbonylation conditions was obtained from *in situ* trapping experiments with cyclohexene. Additional proof for the existence of a P_2Pd–imido species and its reactivity comes from the synthesis of the model complex $(bpap)Pd^{II}$=NMes, as observed by ^{31}P–NMR and ESI–MS. This $(bpap)Pd^{II}$=NMes complex was shown to react with CO and methanol to give methyl mesityl carbamate, already under mild conditions.

Based on the presented organometallic data, it is proposed that under real carbonylation conditions (relatively high CO pressure and elevated temperatures), the existing palladacyclic complexes (**C3**, **C4**, **C6**, and **C7** in Scheme 4.7) are engaged in reversible carbonylation/decarbonylation reactions. Irreversible product release from this set of –presumably equilibrated– palladacycles can occur by low–barrier loss of CO_2 from intermediate **C4** to give the highly reactive P_2Pd^{II}=NPh intermediate (**C5**). Such a P_2Pd^{II}=NPh species is not only able to release reduction products like aniline (by protonation) and Azo(xy) (by coupling with nitrosobenzene or nitrobenzene), but also to release the carbonylation products MPC and DPU (by reaction with CO and methanol or aniline, respectively).

The combined catalytic and organometallic data thus all point strongly to a P_2Pd^{II}=NPh complex as the *sole most probable product releasing* intermediate species in the Pd/diphosphane catalyzed reduction reactions of nitrobenzene in a methanol/CO environment.

4.5. Experimental section

4.5.1. General remarks

All ligands were generously provided by Shell Global Solutions Amsterdam b.v., where they were synthesized according to literature procedures.[51, 56, 69-77] All other solids were purchased from Acros organics and used as received. Methanol, nitrobenzene and aniline were all of analytical reagent purity, and were distilled under an argon atmosphere over the appropriate drying agent.[78] After the distillation, these liquids were saturated with argon. It was ensured that no water was present using an analytical reaction with trimethylorthoformate according to a modified literature procedure[79] (see below and also SI). Carbon monoxide (> 99% pure)[80] was purchased from Linde gas Benelux B.V. and used as received.

^{1}H–, ^{31}P{^{1}H}–, and ^{13}C–NMR spectra were recorded on a Bruker DPX300 (300 MHz) or a Bruker DMX400 (400 MHz) machine. Chemical shifts are recorded in δ (parts per million) relative to the solvent peak (^{1}H– and ^{13}C–NMR) or relative to phosphoric acid as external standard (^{31}P{^{1}H}–NMR). IR–spectra were recorded with 4 cm^{-1} resolution on a Perkin Elmer Paragon 1000 FT–IR fitted with a Golden Gate Diamond ATR. Elemental analyses were performed using a Perking Elmer 2400 Series II CHNS/O analyzer. A Finnigan Aqua Mass Spectrometer (MS) with electro spray ionization (ESI) was used to record mass spectra. Sample introduction was achieved through a Dionex ASI–100 automated sample injector with the eluent CH_3CN flowing at 0.2 ml/min. The voltage of the capillary and the voltage for the aquamax were set at 3 kV and 20 V respectively. High pressure catalysis experiments were conducted in stainless steel autoclaves (100 ml) equipped with two inlet/outlet valves, a burst disc, a pressure sensor, and a thermocouple. The autoclaves were heated by a HEL© polyBLOCK electrical heating system. Temperatures and pressures where measured with probes connected to a computer interface making it possible to record these parameters throughout the course of the reaction. GLC–MS measurements were performed on a Hewlett Packard series 2 type 5890 gas chromatograph equipped with a Hewlett Packard 5971 mass

selective detector. Details of the catalytic experiments and analysis have been described in Chapter 3.[39]

4.5.2. General procedure DFT studies

Calculations were done with the SPARTAN '04 package (Wavefunction, Inc; www.wavefun.com), using density functional theory (DFT)[81, 82] with the Becke and Perdew (BP) functional.[83, 84] Geometry optimizations were carried out using Pople's 6–31G* (d,p) for H, C, O, and P atoms[85] and the LANL2DZ effective core potential for palladium.[86-88] All of the geometrical parameters were fully optimized, and all of the structures located on the PESs were characterized as minima. No constraints to bonds, angles, or dihedral angles were applied in the calculations, and all atoms were free to be optimized.

4.5.3. Starting geometries for DFT studies

Initial atomic coordinates were extracted from $Pd(L3)Cl_2$ (CSD refcode DPPPDC)[89] and $Pd(L4)Cl_2$ (CSD refcode RINZOD).[90] The chloride anions were manually deleted and the rest of the molecule was 'frozen' using the 'freeze centre' option in Spartan. From these geometries, the diphosphane ligands were adjusted to L3X and oMeOL3X (starting from 'Pd(L3)'), and pMeOL4 and L4X (starting from 'Pd(L4)'), and a geometry optimization was performed using molecular mechanics (MMFF), while the 'frozen atoms' remained frozen. All atoms in these 'P_2Pd' complexes were then 'frozen', and used to generate the $P_2Pd(CO)_2$, P_2Pd–palladacycle, and P_2Pd=NPh complexes reported in this study. For the $P_2Pd(CO)_2$ complexes, two CO ligands were added to Pd in the appropriate 'P_2Pd' complex, the PPPd–PdCC angle was fixed to 90°, and a geometry optimization was performed using molecular mechanics (MMFF). All constraints were then released, and the DFT geometry optimization was started as described above. For the P_2Pd–palladacycle complexes, a planar 'C(O)N(Ph)OC(O)' fragment was added to Pd, the PPPd – PdCC angle was fixed to 0°, and a geometry optimization was performed using molecular mechanics (MMFF). All constraints were then released, and the DFT geometry optimization was started as described above. For the P_2Pd=NPh complexes, a 'NPh' ligand was added to Pd, the Pd–N–C angle was set to 180°, the P–Pd–N angles were set so that the imido–N was positioned in the plane of coordination and exactly in between the two P–atoms. A geometry optimization was then performed using molecular mechanics (MMFF). All constraints were then released, and the DFT geometry optimization was started as described above.

4.5.4. NMR kinetic measurements

9.00 mg (20 μmol) of 'phen–palladacycle'[16] (see Figure 4.2a) was weighed into an NMR tube and put under argon. In another tube, the appropriate amount of phosphane ligand was dissolved in 1 ml (d^5–)nitrobenzene under an argon atmosphere. Of this solution, 0.8 ml was added to the 'phen–palladacycle' complex using a 1 ml syringe, which was dry and flushed with argon. The thus obtained yellow suspention (20 mM 'phen–palladacycle') was thoroughly mixed using a vortex mixer and measured. After the first measurements, the reaction mixture was carefully heated to about 60 ºC, resulting in a clear yellow–orange solution. This solutions were monitored with ^1H– and $^{31}P\{^1H\}$–NMR spectroscopy, over a period of fourteen hours. For the proton measurements, the number of free inductive decays (FIDs) was 16 and for the phosphorus NMR spectra the number of FIDs was 40. The same procedure was applied for the experiment under a CO atmosphere, but nitrobenzene was first saturated with CO gas, the NMR–tube was put under a CO atmosphere and the 1 ml syringe was flushed with CO.

4.5.5. Synthesis of 2,4,6–trimethylphenyl azide (N_3Mes)

N_3Mes was obtained in 86% yield (9.58 g) as clear colorless liquid from 2,4,6–trimethylaniline following a literature procedure.[91, 92] GLC–MS: t_R = 16.96 min, *m/z* found (calc): 161 (161.10)

$[N_3Mes]^+$, 133 (133.09) $[NMes]^+$, 119 (119.09) $[Mes]^+$, 104 (104.06) $[Mes–CH_3]^+$. ^{1}H–NMR (300 MHz, $CDCl_3$, 25 °C) δ = 2.45 (s, 3H, *p*–C*H*$_3$), 2.52 (s, 6H, *o*–C*H*$_3$), 6.99 (s, 2H, *m*–*H*) ppm; ^{13}C–NMR (75 MHz, $CDCl_3$, 25 °C) δ = 17.91 (s, *o*–*C*H$_3$), 20.59 (s, *p*–*C*H$_3$), 129.45 (s, N_3CC(CH3)*C*H) 131.72 (s, N_3C*C*(CH3), 134.36 (s, N_3CC(CH3)CH*C*(CH3)), 135.19 (s, N_3*C*) ppm. IR (neat, cm^{-1}): 2919 (weak, CH), 2114 (very strong, N_3), 1477 (strong, Ph), 1278 (strong, N_3 (organic)), 852 (strong, Ph C=C).

4.5.6. Synthesis of Pd(bpap)(dba)

In 15 ml toluene were successively dissolved 112.2 mg (0.12 mmol) $Pd_2(dba)_3$ (dba = dibenzylideneacetone) and 118.6 mg (0.25 mmol) of a *rac* (*αα*/*ββ*) and *meso* (*α*/*β*) diastereoisomeric mixture of 1,3–bis(1,3,5,7–tetramethyl–4,6,8–trioxa–2–phosphaneamantane)propane (bpap). The resulting dark red solution was stirred for one hour, while shielding the reaction vessel from light with tin foil. After the solution turned green, it was filtered over a 0.45 µm micro–filter. Solvent was removed *in vacuo* from the yellow–gold colored filtrate. The residue was dissolved in 1 ml of dichloromethane followed by the addition of several milliliters of *n*–hexane. Within minutes a precipitate was obtained. The solid was collected by filtration dried *in vacuo*, and analyzed as Pd(bpap)(dba) · toluene (120 mg, 54%). Elemental analysis calcd. for $C_{40}H_{52}O_7P_2Pd$ · Toluene (Mw = 905.34): C, 62.35; H, 6.68%. Found: C, 62.44; H, 6.67%. MS (ESI) found (calc): *m/z* 812.85 (812.22) $[Pd(bpap)(dba)]^+$. ^{1}H–NMR (300 MHz, $CDCl_3$, 25 °C) δ = 1.00–2.50 (m, 38H, bpap), 7.09 (d, 2H, –C(=O)C*H*=CH–Ph), 7.34 (d, 4H, *o*–*H*), 7.62 (m, 6H, *m*/*p*–*H*), 7.75 (d, 2H, –C(=O)CH=C*H* –Ph) ppm; ^{31}P{^{1}H}–NMR (121 MHz, $CDCl_3$, 25 °C) δ = 4.06 (s, *meso*), –0.63 (s, *rac*) ppm. IR (neat, cm^{-1}): 2978 (weak, CH_2), 1574 (medium, cage), 1436 (strong, cage), 1286 (string, C–O), 1232 (strong, C–O), 1031 (stong, C–O–C), 750 (very strong, P–C).

4.5.7. *In situ* synthesis of (bpap)Pd=NMes

3.89 mg (4.3 μmol) of Pd(bpap)(dba)·toluene was weighed into an NMR tube and put under argon. The complex was dissolved in 0.3 ml dry and degassed d^8–toluene, which was added with a dry and argon flushed 1 ml syringe. In a similar fashion, 0.3 ml N_3Mes was added, which was saturated with argon prior to use. The resulting clear solution was heated to 50 °C in about 45 minutes, where after the solution was heated to 100 °C, also in about 45 minutes. The reaction mixture was then allowed to cool to laboratory temperature. The whole process was monitored with ^{1}H– and ^{31}P{^{1}H}–NMR spectroscopy, and after cooling the reaction mixture was analyzed with ESI–MS.

References

[1] www.gem-chem.net/capacity.html, **November 2011**

[2] A. J. Ryan, J. L. Stanford, *in: G. Allen, J.C. Bevington (eds.), Comprehensive Polymer Science, Vol. 5*, Pergamon, New York, **1989**.

[3] K. Weisermel, H. J. Arpe, *Industrielle Organische Chemie*, VCH Verslagsgesellschaft GmbH, Weinheim, Germany, **1988**.

[4] H. Ulrich, *Ullmann's Encyclopedia of Industrial Chemistry, Vol. A14*, VCH publishers, New York, **1989**.

[5] *Registry of Toxic Effects of Chemical Substances (RTECS, online database)*, United States Department of Health and Human Services (National Toxicology Information, National Library of Medicine), Bethesda, MD, **1993**.

[6] R.C. Weast (Ed.), *Handbook of Chemistry and Physics*, D-110, 58 ed., CRC Press Inc., Cleveland, **1977-1978**.

[7] F. Paul, *Coord. Chem. Rev.* **2000**, *203*, 269.

[8] F. Ragaini, *Dalton Trans.* **2009**, 6251.

[9] E. Drent, P. W. N. M. van Leeuwen, EU 0086281A1, **1982**.

[10] E. Drent, EU 224292, **1987**.

[11] E. Drent, EU 0231045A2, **1987**.

[12] E. Drent, *Pure Appl. Chem.* **1990**, *62*, 661.
[13] A. Bontempi, E. Alessio, G. Chanos, G. Mestroni, *J. Mol. Catal.* **1987**, *42*, 67.
[14] S. Cenini, F. Ragaini, M. Pizzotti, F. Porta, G. Mestroni, E. Alessio, *J. Mol. Catal.* **1991**, *64*, 179.
[15] R. Santi, A. M. Romano, F. Panella, G. Mestroni, A. Sessanti, A. S. o Santi, *J. Mol. Catal. A-Chem.* **1999**, *144*, 41.
[16] P. Leconte, F. Metz, A. Mortreux, J. A. Osborn, F. Paul, F. Petit, A. Pillot, *J. Chem. Soc.-Chem. Commun.* **1990**, 1616.
[17] P. Wehman, V. E. Kaasjager, W. G. J. de Lange, F. Hartl, P. C. J. Kamer, P. W. N. M. van Leeuwen, J. Fraanje, K. Goubitz, *Organometallics* **1995**, *14*, 3751.
[18] P. Wehman, G. C. Dol, E. R. Moorman, P. C. J. Kamer, P. W. N. M. van Leeuwen, J. Fraanje, K. Goubitz, *Organometallics* **1994**, *13*, 4856.
[19] P. Wehman, PhD thesis, University of Amsterdam (UvA) **1995**.
[20] P. Wehman, L. Borst, P. C. J. Kamer, P. W. N. M. van Leeuwen, *J. Mol. Catal. A-Chem.* **1996**, *112*, 23.
[21] F. Ragaini, C. Cognolato, M. Gasperini, S. Cenini, *Angew. Chem.* **2003**, *42*, 2886.
[22] F. Ragaini, M. Gasperini, S. Cenini, *Adv. Synth. Catal.* **2004**, *346*, 63.
[23] E. Drent, P. E. Prillwitz, EU ZA8609251 (A), **1985**.
[24] J. H. Grate, D. R. Hamm, D. H. Valentine, US 4.603.216, **1986**.
[25] P. Wehman, R. E. Rulke, V. E. Kaasjager, P. C. J. Kamer, H. Kooijman, A. L. Spek, C. J. Elsevier, K. Vrieze, P. W. N. M. van Leeuwen, *J. Chem. Soc.-Chem. Commun.* **1995**, 331.
[26] P. Wehman, H. M. A. van Donge, A. Hagos, P. C. J. Kamer, P. W. N. M. van Leeuwen, *J. Organomet. Chem.* **1997**, *535*, 183.
[27] P. Wehman, L. Borst, P. C. J. Kamer, P. W. N. M. van Leeuwen, *Chem. Ber.-Recl.* **1997**, *130*, 13.
[28] N. Masciocchi, F. Ragaini, S. Cenini, A. Sironi, *Organometallics* **1998**, *17*, 1052.
[29] A. S. o Santi, B. Milani, E. Zangrando, G. Mestroni, *Eur. J. Inorg. Chem.* **2000**, 2351.
[30] K. Nomura, *J. Mol. Catal. A.* **1998**, *130*, 1.
[31] J. E. Yanez, A. B. Rivas, J. Alvarez, M. C. Ortega, A. J. Pardey, C. Longo, R. P. Feazell, *J. Coord. Chem.* **2006**, *59*, 1719.
[32] F. J. Weigert, *J. Org. Chem.* **1973**, *38*, 1316.
[33] T. Kajimoto, J. Tsuji, *Bul. Chem. Soc. Jpn.* **1969**, *42*, 827.
[34] Smolinsk.G, B. I. Feuer, *J. Org. Chem.* **1966**, *31*, 3882.
[35] M. Akazome, T. Kondo, Y. Watanabe, *J. Org. Chem.* **1994**, *59*, 3375.
[36] R. Waterman, G. L. Hillhouse, *J. Am. Chem. Soc.* **2008**, *130*, 12628.
[37] R. Waterman, G. L. Hillhouse, *J. Am. Chem. Soc.* **2003**, *125*, 13350.
[38] D. J. Mindiola, G. L. Hillhouse, *J. Am. Chem. Soc.* **2001**, *123*, 4623.
[39] T. J. Mooibroek, L. Schoon, E. Bouwman, E. Drent, *Chem. Eur. J.* **2011**, DOI: 10.1002/chem.201100923.
[40] T. J. Mooibroek, E. Bouwman, M. Lutz, A. L. Spek, E. Drent, *Eur. J. Inorg. Chem.* **2010**, *2*, 298.
[41] Note that DPU can be formed by the reaction of nitrobenzene, CO and (*in situ* generated) aniline, but also by the transesterification of MPC with aniline. In both cases, aniline is formed first and DPU is thus derived from aniline.
[42] T. J. Mooibroek, E. Bouwman, E. Drent, *Organometallics* **2011**, submitted.
[43] When using some ligands with an ethylene backbone (not shown in the table), the conversion was very low and a significant amount of plating (Pd^0) was observed. This was the case for both pre synthesized and *in situ* prepared catalyst precursors, indicating that $P_2Pd(OAc)_2$ complexes with these ligands are not stable under typical reaction conditions. An additional difficulty with such ligands is that the anticipated $P_2Pd(OAc)_2$ catalyst precursor is not the kinetic product of the complex forming reaction. NMR studies performed with 1,2-bis(diphenylphosphane)ethane (L2) as the P_2 ligand indeed showed that the catalytically inactive $[(L2)_2Pd](OAc)_2$ is the kinetic product of complex forming

in methanol (see Chapter 2 and references 40 and 68). For these reasons, the results of these experiments will not be discussed.

[44] P. Dierkes, P. W. N. M. van Leeuwen, *J. Chem. Soc. Dalton Trans.* **1999**, 1519.

[45] T. Hayashi, M. Konishi, Y. Kobori, M. Kumada, T. Higuchi, K. Hirotsu, *J. Am. Chem. Soc.* **1984**, *106*, 158.

[46] S. Ross, The Proton: applications to organic chemistry in *Organic Chemistry; a series of monographs, Vol. 46* (Ed.: H. H. Wasserman), Academic Press Inc., London, **1985**.

[47] A. S. o Santi, B. Milani, G. Mestroni, E. Zangrando, L. Randaccio, *J. Organomet. Chem.* **1997**, *546*, 89.

[48] After 180 minutes, the solution contained 17% of 'phen-palladacycle' and 83% phen (^{1}H-NMR), meaning that only 83% of the initially added palladium can end up as L3X-complex. The percentage of a specific L3X-Pd complex (relative to palladium) can thus be calculated by: $\int_{\text{L3X-complex}} / \Sigma_{\int \text{ all L3X-complexes}} * 83\%$. Thus, the species detected with ^{31}P{^{1}H}-NMR that were assigned to Pd-containing species (see also Figure A.III.2 in Appendix III) are (δ ($\int$; assignment; percentage based on Pd)): 1.0 (1.00; $Pd^0(L3X)_2$; 33%); 5.0 (0.06; 'L3X-palladacycle'; 4%); 13 - 20 (0.33; unknown Pd complexes; 22%); 24/-7 (0.32; de*carbonylated* 'L3X-palladacycle'; 21%); 35 (0.05; unknown Pd complex; 3%); $\Sigma\int$ = 1.76. The solution also contained L3X (-25 ppm, $\int$ = 0.33) and 'L3X=O' (26/-24 ppm, $\int$ = 0.30), which is ((0.33+0.30)/1.76*100% =) 26% of the initially added L3X. Hence, 74% of L3X is thus bound to palladium; this is indeed roughly one equivalent with respect to the 83% Pd-complex, computed based on ^{1}H-NMR.

[49] $\int_{0.5 \text{ ppm}}$ = 100 ($Pd^0(L3X)_2$ = 4P); $\int_{14.3+(-26.2) \text{ ppm}}$ = 2.2 ('L3X=NPh', 2P). Hence: 2.2/(100/2+2.2)*100% = 4.2%, and 4.2% of 10 μmol (the amount of phen-palladacycle present) is ~0.4 μmol.

[50] The estimated cone-angle in of dpap is 173° (V. Gee *et al.*, *Chem. Comm.*, **1999**, p901); compare to 155° for $((t\text{-Bu})_2P)_2(CH_2)_3$ in its $PtCl_2$ complex (M. Harada *et al.*, *Bull. Chem. Soc. Jpn.*, **1979**, 52, p390).

[51] V. Gee, A. G. Orpen, H. Phetmung, P. G. Pringle, R. I. Pugh, *Chem. Commun.* **1999**, 901.

[52] K. C. Gross, P. G. Seybold, C. M. Hadad, *Int. J. Quant. Chem.* **2002**, *90*, 445.

[53] A. E. Reed, R. B. Weinstock, F. Weinhold, *J. Chem. Phys.* **1985**, *83*, 735.

[54] The natural population analysis provides the most reliable indictor of charge and basicity, and is relatively basis-set independent (see reference 52 and K. B. Wiberg, P. R. Rablen, *J. Comp. Chem.* **1993**, *14*, 1504).

[55] M. J. McGlinch, F. G. A. Stone, *Chem. Comm.* **1970**, 1265.

[56] J. H. Downing, J. Floure, K. Heslop, M. F. Haddow, J. Hopewell, M. Lusi, H. Phetmung, A. G. Orpen, P. G. Pringle, R. I. Pugh, D. Zambrano-Williams, *Organometallics* **2008**, *27*, 3216.

[57] The option was considered that an un-symmetric complex was formed, that may give rise to a double doublet (one around 28 ppm and one around -15 ppm) in the ^{31}P{^{1}H}-NMR spectrum. This was excluded as follows. The resonances at -15.3 and -15.8 would have a coupling constant of 0.5 ppm. No such presumed coupling is observed between the resonance around 27.6 ppm and one of the smaller peaks around 27.9 or 28.0 ppm. Also, both resonances around 27.9 and 28.0 ppm are considerably smaller ($\int$ = 0.14 and 0.34 respectively, relative to 1.00 for -15.3 ppm) than the resonance around -15.82 ppm ($\int$ = 0.51).

[58] S. Brase, C. Gil, K. Knepper, V. Zimmermann, *Angew. Chem.* **2005**, *44*, 5188.

[59] The other peaks were of mesitylene azide (t_R = 16.8 minunes (60%), *m/z* = 161 $[M]^+$; 133 $[M\text{-}N_2]^+$) and azo mesitylene (t_R = 27.8 minunes (20%), *m/z* = 266 $[M]^+$).

[60] J. P. Collman, M. Kubota, J. W. Hosking, *J. Am. Chem. Soc.* **1967**, *89*, 4809.

[61] E. Drent, P. H. M. Budzelaar, *Chem. Rev.* **1996**, *96*, 663.

[62] P. W. N. M. van Leeuwen, P. C. J. Kamer, J. N. H. Reek, P. Dierkes, *Chem. Rev.* **2000**, *100*, 2741.

[63] R. J. van Haaren, K. Goubitz, J. Fraanje, G. P. F. van Strijkdonk, H. Oevering, B. Coussens, J. N. H. Reek, P. C. J. Kamer, P. W. N. M. van Leeuwen, *Inorg. Chem.* **2001**, *40*, 3363.
[64] E. Zuidema, P. W. N. M. van Leeuwen, C. Bo, *Organometallics* **2005**, *24*, 3703.
[65] M. N. Birkholz, Z. Freixa, P. W. N. M. van Leeuwen, *Chem. Soc. Rev.* **2009**, *38*, 1099.
[66] B. Marciniec, E. Mackowska, *J. Mol. Cat.* **1989**, *51*, 41.
[67] I. M. Angulo, E. Bouwman, M. Lutz, W. P. Mul, A. L. Spek, *Inorg. Chem.* **2001**, *40*, 2073.
[68] A. Marson, A. B. van Oort, W. P. Mul, *Eur. J. Inorg. Chem.* **2002**, *11*, 3028.
[69] F. Bickelhaupt, US 4874897, **1989**.
[70] W. Eilenberg, EU 364046, **1991**.
[71] J. A. van Doorn, US 4994592, **1991**.
[72] R. van Ginkel, US 6548708, **2003**.
[73] E. Drent, US 5091587, **1992**.
[74] C. F. Hobbs, US 4120901, **1987**.
[75] P. W. Clark, B. J. Mulraney, *J. Organomet. Chem.* **1981**, *217*, 51.
[76] J. M. Brown, B. A. Murrer, *Tetrahedron Lett.* **1980**, *21*, 581.
[77] R. L. Wife, A. B. van Oort, J. A. van Doorn, P. W. N. M. van Leeuwen, *Synthesis* **1983**, *1*, 71.
[78] W. L. F. Armarego, C. L. L. Chai, *Purification of laboratory chemicals*, 5th ed., Elsevier, Amsterdam, **2003**.
[79] J. Chen, J. S. Fritz, *Anal. Chem.* **1991**, *63*, 2016.
[80] customer.linde.com/FIRSTspiritWeb/linde/LGNL/media/datasheets/NL-PIB-0024.pdf, **November 2011**
[81] W. Koch, M. C. Holthausen, *A Chemist's Guide to Density Functional Theory*, 2nd ed., Wiley-VCH, Weinheim, **2000**.
[82] K. Eichkorn, O. Treutler, H. Ohm, M. Haser, R. Ahlrichs, *Chem. Phys. Lett.* **1995**, *240*, 283.
[83] A. D. Becke, *Phys. Rev. A* **1988**, *38*, 3098.
[84] J. P. Perdew, *Phys. Rev. B* **1986**, *33*, 8822.
[85] W. J. Hehre, L. Radom, P. R. van Schleyer, J. A. Pople, *Ab Initio Molecular Orbital Theory*, Wiley, New York, **1986**.
[86] P. J. Hay, W. R. Wadt, *J. Chem. Phys.* **1985**, *82*, 270.
[87] P. J. Hay, W. R. Wadt, *J. Chem. Phys.* **1985**, *82*, 299.
[88] W. R. Wadt, P. J. Hay, *J. Chem. Phys.* **1985**, *82*, 284.
[89] W. L. Steffen, G. J. Palenik, *Inorg. Chem.* **1976**, *15*, 2432.
[90] V. D. Makhaev, Z. M. Dzhabieva, S. V. Konovalikhin, O. A. Dyachenko, G. P. Belov, *Russ. J. Coord. Chem. (Koord. Khim.)* **1996**, *22*, 598.
[91] S. W. Kwok, J. R. Fotsing, R. J. Fraser, V. O. Rodionov, V. V. Fokin, *Org. Lett.*, *12*, 4217.
[92] R. E. Conrow, W. D. Dean, *Org. Proc. Res. Dev.* **2008**, *12*, 1285.

Chapter 5

Mechanistic study of the palladium-diphosphane catalyzed oxidative carbonylation of methanol, using nitrobenzene as oxidant.

Abstract: The reactivity of palladium complexes supported by bidentate diaryl phosphane ligands has been studied in the oxidative carbonylation of methanol to dimethyl carbonate/oxalate (DMC/DMO) using $PhNO_2$ as terminal oxidant. Different ligands were employed with variation in backbone length and aryl ring substituent, and the acidity, CO pressure or H_2 partial pressures were varied. Two key intermediate stages exist in the catalytic cycle that may each evolve one equivalent of DMC/DMO relative to one $PhNO_2$ reduced.

At stage 'one', starting from P_2Pd^0, oxidative carbonylation of CH_3OH is coupled with $PhNO_2$ reduction to produce the first DMC/DMO molecule and a 'P_2Pd=NPh' species. Formation of DMC/DMO at this stage is avoided when only CO acts as reductant, or when $PhNO_2$ reduction is coupled with CH_3OH oxidative dehydrogenation to CO (or methyl formate). At stage 'two', the P_2Pd=NPh species may react with methanol to form the second DMC/DMO molecule with the co-production of aniline. This pathway is avoided when the intermediate 'P_2Pd=NPh' species reacts with $PhNO_2$ and CO to azoxybenzene and CO_2, or when it is carbonylated to methyl phenylcarbamate. All three processes are catalytic as they re-form the original P_2Pd^0 species of stage 'one'.

The selectivity for DMC relative to DMO is thought to be determined in a $[P_2PdC(O)OCH_3(R)]$–type species; the DMO/DMC ratio can be increased by increasing the CO pressure, addition of an acid, or by using a ligand with a relatively large bite-angle.

Based on the collected results, it is concluded that an ideal catalyst for oxidative carbonylation would have a relatively acidic palladium centre, be sterically undemanding in the axial positions, but sterically demanding in the equatorial positions of palladium. The palladium complex of bis(diphenylphosphanyl)-ferrocene meets these criteria and was found to use nitrobenzene as oxidant for the oxidative carbonylation of methanol most efficiently of the series studied, i.e with about 50% of the theoretical maximum efficiency with a 2:1 ratio between DMC/DMO and reduced nitrobenzene.

5.1. Introduction

One of the challenges in current day catalysis is to replace wasteful and dangerous industrial processes by more environmentally friendly and safer ones. An example of such a challenge is to replace the highly toxic and corrosive phosgene,[1, 2] which is often used as carbonylating agent. For example, in the synthesis of aromatic isocyanates[3, 4] such as TDI and MDI,[5, 6] phosgene is employed on the megaton scale[7] to carbonylate a reduced nitroaromatic compound (Scheme 5.1).

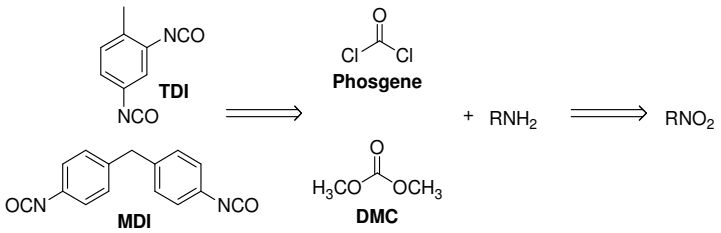

Scheme 5.1. Two industrially important aromatic isocyanated (MDI, TDI) and two carbonylating reagents (phosgene, DMC)

Dimethyl carbonate (DMC),[8-12] and to a lesser extend dimethyl oxalate (DMO),[13] have been proposed to replace phosgene as carbonylating agent (Scheme 5.1), which by transesterification with an aromatic amine will liberate methanol to form a carbamate, and which in turn can be pyrolized to the isocyanate (e.g. TDI or MDI). Such (aliphatic but also aromatic) carbonates and oxalates can be prepared by a palladium-catalyzed oxidative carbonylation of the alcohol (e.g. methanol to DMC and DMO).[14-31] The terminal oxidant usually is O_2, but a metal co-catalyst such as Cu^{2+}/Cu^{+}[24, 26] or Pb^{4+}/Pb^{2+}[25] is often necessary to reoxidize palladium, which is difficult to oxidize with molecular oxygen. Notably, alkyl nitrites (RON=O) have been used to replace O_2 as the oxidant in the synthesis of DMC.[27]

Working with strong oxidants such as O_2 and RON=O is not too problematic when the palladium catalyst is stabilized by N- or O-donor ligands, but nitrogen and oxygen are generally poor ligands for palladium, since they cannot be involved in π back-bonding. P-donor ligands on the other hand are very good ligands for palladium for that very reason, but easily react with strong oxidants

such as O_2 and RON=O to form phosphane oxides leading to catalyst degradation. It is therefore not surprising that reports of the carbonate and oxalate synthesis employing P-donor ligands are mainly stoichiometric on palladium.[14, 15, 20, 22, 23] For this reaction to be catalytic in palladium, milder oxidants have been considered such as 1,4-benzoquinone[24-26, 28, 32] and $NaNO_2/NaNO_3$,[32] but the co-products that are then obtained stoichiometrically on the carbonate/oxalate, cannot easily be utilized on a large scale.

Notably, for the oxidative carbonylation of phenols to diphenyl carbonate (DPC), it has been proposed to use nitrobenzene as the oxidant. Demonstrated yields, however, were less than stoichiometric on palladium.[33] To the best of my knowledge, nitrobenzene has never before been used or proposed as oxidant for the preparation of DMC or DMO. What is more, nitrobenzene may be reduced to aniline by the hydrogen atoms liberated by DMC/DMO formation, thus establishing a catalytic coupling between methanol oxidation and nitrobenzene hydrogenation chemistry. This potentially unlocks a novel procedure to prepare the reactants aniline and DMC, which can be used to make aromatic isocyanates via methyl phenyl carbamate (Scheme 5.2). Furthermore, the product DMO is an industrially interesting intermediate for the sustainable production of mono ethylene glycol (MEG), solely from synthesis gas as feedstock, which can be produced from practically any carbon source, including coal, gas, bio waste or even CO_2.

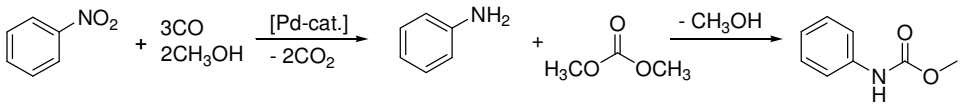

Scheme 5.2. A novel synthetic route to prepare aromatic isocyanates (in the carbamate form) from dimethyl carbonate and aniline, formed by the oxidative carbonylation of methanol using nitrobenzene as the terminal oxidant.

The reductive carbonylation of nitrobenzene in methanol forming methyl phenyl carbamate is a reported alternative for the industrial preparation of aromatic isocyanates such as TDI and MDI, which have been studied using palladium-diphosphane catalytic systems as described in Chapters 3 and 4. In these studies it was found that for some diphosphane-supported palladium catalysts, apart from

the desired nitrobenzene carbonylation product large amounts of DMC, DMO and aniline were formed. The observation of the methanol oxidation products along with nitrobenzene reduction products provided an important hint towards mechanistic details in the carbonylation of nitrobenzene in alcoholic media. It became clear that in the Pd/diphosphane/CH_3OH catalytic system nitrobenzene reduction is catalytically coupled with methanol oxidation (Chapter 3), and in Chapter 4 the focus has been on the mechanism of formation of the nitrobenzene reduction products.

The focus of the present Chapter is on the genesis of methanol oxidation products, in particular the useful oxidative carbonylation products DMC and DMO, and how the production and selectivity for these products depends on the structure of the catalyst and on reaction conditions.

5.2. Results

5.2.1. General considerations

In the catalytic reactions for the oxidation of methanol / the reduction of nitrobenzene the catalyst was formed *in situ* from $Pd(OAc)_2$ and a bidentate phosphane ligand (1:1.5). Complex formation is instantaneous in methanol with the ligands used in this study (see Chapter 2), and identical results were obtained when the activity of selected pre-formed complexes was tested. It was ensured that methanol and nitrobenzene were anhydrous by thoroughly drying these liquids (see experimental of Chapter 3 for details). In the initial screening studies a large variety of diarylphosphane ligands have been used, with variations in the substituents on the phenyl rings as well as in the length and flexibility of the backbone spacer.

In the carbonylation of nitrobenzene with diphosphane-palladium catalyst systems, both methanol oxidative carbonylation products DMC and DMO, as well as methanol oxidation products methyl formate (MF) and carbon monoxide (CO) are formed (Scheme 5.3). It is noteworthy that another possible methanol oxidation product, i.e. formaldehyde (or its expected derivative dimethoxymethane (DMM)) was *not* observed. The formation of gaseous CO originating from methanol was confirmed from an independent nitrobenzene

carbonylation experiment involving the use of ^{13}C-isotope enriched methanol as substrate, conducted under low CO pressure. It proved possible to experimentally establish the generation of gaseous ^{13}CO, in an estimated amount that closed the overall hydrogen mass balance between oxidation and reduction products (see Chapter 3).

The 'PhN-containing' reduction products of nitrobenzene are methyl phenyl carbamate (MPC), *N*,*N*'diphenyl urea (DPU), aniline, azobenzene (Azo) and azoxybenzene (Azoxy). Other reduction products of nitrobenzene are CO_2 and H_2O, both containing one oxygen atom from $PhNO_2$. H_2O, aniline and DPU, are derived from methanol oxidation, as the (OH, NH) hydrogen atoms in these molecules originate from methanol (see also Chapter 3).

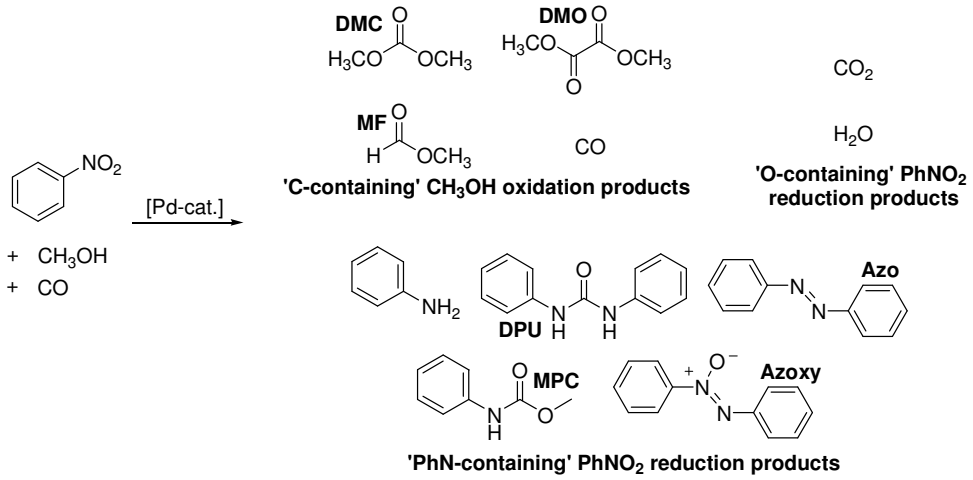

Scheme 5.3. Overview of the different products that are formed in the palladium-catalyzed reaction of nitrobenzene with CO in methanol.

The selectivity of the catalysts for the various products is highly dependent on the ligand structure. The trends in reactivity and selectivity will be discussed using the ligands shown in Figure 5.1. These ligands have either a propylene (L3), butylene (L4), or Ferrocene (L5Fc) backbone, which in some cases is made more rigid by substitution (indicated by 'X'). The aryl rings of the ligands can be functionalized with methoxy moieties in the *ortho* or *para* position (oMeO- or pMeO-) to allow discrimination of steric from electronic effects.

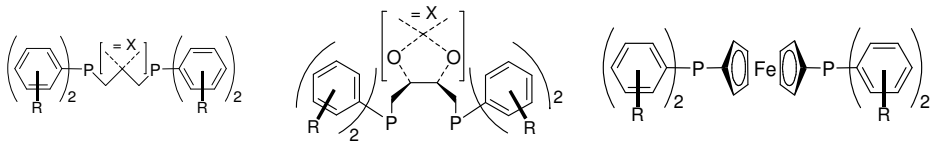

L3	(R=H)	**L4**	(R=H)	**L5Fc**	(R=H)
L3X	(R=H)	**L4X**	(R=H)	**oMeO–L5Fc**	(R=*o*–MeO)
oMeO–L3	(R=*o*–MeO)	**oMeO–L4X**	(R=*o*–MeO)		
oMeO–L3X	(R=*o*–MeO)	**pMeO–L4**	(R=*p*–MeO)		
pMeO–L3	(R=*p*–MeO)				

Figure 5.1. Overview of the ligands used in this study.

5.2.2. Ligand effects in the oxidation of methanol

5.2.2.1 Dehydrogenation to CO and MF vs. carbonylation to DMC and DMO

The quantities (in mmol) of the C-containing oxidation products of methanol and H-containing nitrobenzene reduction products formed in nitrobenzene carbonylation experiments with a selected number of diphosphane-supported palladium catalysts, as analyzed with GC, are given in Table 5.1.

Table 5.1. Results of the reactions of nitrobenzene with CO in methanol, catalyzed by a variety of *in situ* formed Pd^{II}(ligand) complexes.[a]

			'C-containing' oxidation products			'H-containing' Reduction products			
Entry	**Ligand**	**$PhNO_2$**	**MF**	**DMC**	**DMO**	**H_2O**	**$PhNH_2$**	**DPU**	**E_{OC}[b]**
1	**L3**	8.1	0.1	3.6	3.3	3.0	5.1	1.7	45
2	**L3X**	8.1	0.2	4.2	3.1	3.4	8.3	0.8	45
3	**oMeO-L3**	11.5	0.6	0.6	0.5	n.d.	4.1	0.9	10
4	**oMeO-L3X**	0.6	1.1	0.4	0.4	0.7	5.7	3.1	5
5	**pMeO-L3**	11.3	0.1	2.2	2.1	n.d.	3.9	1.9	30
6	**L4**	9.8	0.3	2.4	5.6	3.9	5.4	0.8	55
7	**L4X**	11.8	0.2	2.3	5.9	10.0	1.9	0.5	65
8	**oMeO-L4X**	2.4	0.6	2.1	7.3	8.7	10.5	1.9	40
9	**pMeO-L4**	14.7	0.2	1.7	3.7	n.d.	5.9	0.0	60
10	**L5Fc**	7.2	0.4	4.3	13.7	n.d.	7.2	0.2	105
11	**oMeO-L5Fc**	0.0	1.8	2.5	8.0	n.d.	11.2	2.6	45

[a] Reactions were heated for four hours at 110 ºC in 25.0 ml dry and degassed methanol under 50 bar CO pressure. The catalyst was always generated *in situ* from 0.05 mmol $Pd(OAc)_2$. Mole ratio's are: $Pd(OAc)_2$: Ligand : nitrobenzene = 1 : 1.5 : 488. Quantities are reported in mmol and 'n.d.' stands for 'not determined'. [b] E_{OC} = estimated efficiency of methanol oxidative carbonylation based on nitrobenzene conversion: E_{OC} = (DMC + DMO) / ($PhNO_2$ converted).

The data reported in this table have been used to generate the bar-diagrams shown in this chapter. A full analysis of the reaction mixtures was always performed, however, and the data of the other reaction products are available in Table AIV.1 in Appendix IV. The mechanism of formation of all phenyl-containing reduction products of nitrobenzene has already been discussed in detail in Chapter 4.

DMC, DMO, and MF can be easily quantified using GLC analysis, but the amount of CO produced in typical catalytic carbonylation experiments could not be determined using this latter technique, and has been deduced from the hydrogen mass balance. That is, the amount of hydrogen atoms produced (2DMC+2DMO+4MF) should equal the amount of hydrogen atoms consumed ($2PhNH_2$+2DPU+$2H_2O$) for a catalytic system that does not dehydrogenate methanol to CO. From any significant violation of this balance, it follows that CO must have been produced by the complete dehydrogenation of methanol. The fraction of nitrobenzene that is deoxygenated by the hydrogen atoms that are liberated from this complete methanol dehydrogenation to CO (relative to the total amount of $PhNO_2$ reduced), can be derived directly from any significant violation of the hydrogen mass balance.[34] It appears that this fraction (shown within brackets in Figure 5.2) depends significantly on the structure of the catalyst (Figure 5.2).

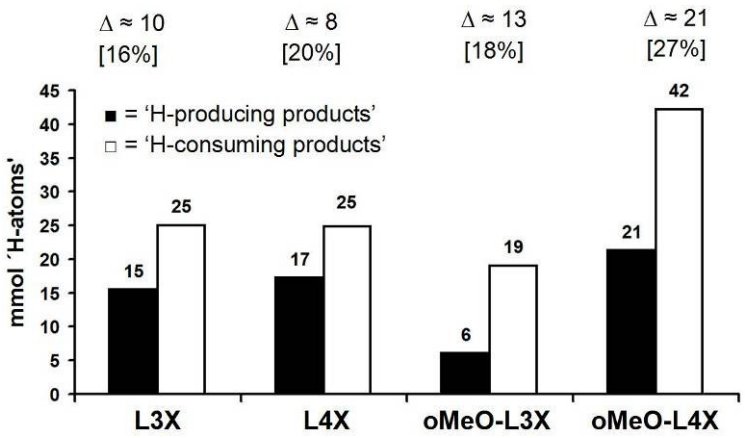

Figure 5.2. The hydrogen mass-balance for selected ligands, showing the amount of hydrogen atoms produced (2DMC+2DMO+4MF; ■) and consumed ($2PhNH_2$+2DPU+$2H_2O$; □). For each ligand, the offset of the H-mass balance (Δ) is given; the percentage of $PhNO_2$ that was fully deoxygenated (to a 'PhN-fragment') using the H-atoms that must originate from the dehydrogenation of methanol to CO is given in brackets.[34]

For the catalyst with the unsubstituted ligands L3X and L4X, about 16–20% of the nitrobenzene is deoxygenated by the hydrogen atoms must have been produced by full dehydrogenation of methanol to CO. This increased significantly (15–35%)[35] to approximately 18–27% when the aryl rings of the ligand in these catalysts were fitted with methoxy groups in the *ortho* position (oMeO-L3X and oMeO-L4X). Likewise, the 16–18% for the catalysts comprising a C_3 backbone ((oMeO)L3X) is significantly (25–59%)[35] increased to 20–27% when the backbone is longer (oMeO(L4X)).

5.2.2.2 Oxidative carbonylation of methanol to DMC and DMO

A comparison of the amount of DMO/DMC produced by the various catalysts supported by the ligands L3, L4X and L5Fc with the available *ortho*-methoxy and *para*-methoxy analogues is shown in Scheme 5.3. The amount of DMC and DMO produced is highest when employing the unsubstituted ligands L3, L4X, and L5Fc (left). When the oMeO-analogues of these ligands were employed, the production of DMC and DMO is significantly suppressed (middle). Note that twice as much nitrobenzene was converted when using oMeO-L4X (90%) *versus* L4X (52%) as supporting ligand. The suppression of DMC and DMO production was considerably less pronounced when employing ligands with *para*-methoxyphenyl rings (right), indicating that the effect must be predominantly steric in nature.

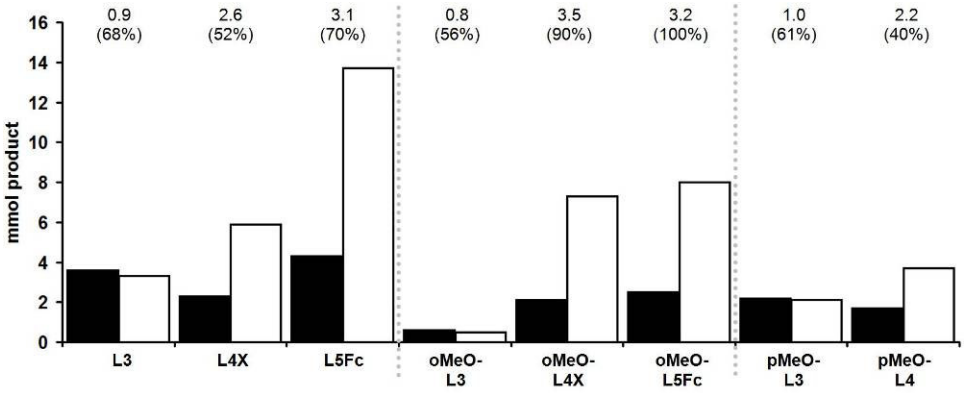

Figure 5.3. The influence of selected ligands on the selectivity and productivity of the catalysts for DMC (■) and DMO (□). The DMO over DMC ratio is given on top; the conversion of nitrobenzene is given in parentheses.

The selectivity for either DMC or DMO appeared to vary significantly as a function of the bite-angle (β) of the ligand used, as indicated by the increasing DMO/DMC ratio from ~0.75 to about 2.5 – 3.1 when using the ligands L3X ($\beta \approx$ 90º) and L4X/L5Fc ($\beta \approx$ 96º), respectively. The DMO/DMC ratio does not significantly change when the supporting ligand in the catalyst is functionalized with electron-donating methoxy groups in either the *ortho* or *para* position.

5.2.3. The effects of reactants and additives in the oxidation of methanol

5.2.3.1 Effect of the acidity of the reaction medium

To investigate the effect of acidity on the product formation, a series of experiments was conducted wherein 5 equivalents (on Pd) of 2,4,6-trimethylbenzoic acid (TMBA) or 10 equivalents of Proton-sponge (1,8-bis(dimethylamino)-naphthalene, DMAN) were added. The catalyst of choice for these experiments is Pd^{II}(L3), as this catalyst proved to be relatively active for the formation of methanol carbonylation products (DMC+DMO ≈ 7 mmol), but rather non-preferential with respect to DMO/DMC ratio (≈ 1). For comparison, the oMeO-functionalized catalyst Pd^{II}(oMeO-L3X) was used. The results are shown in Figure 5.4.

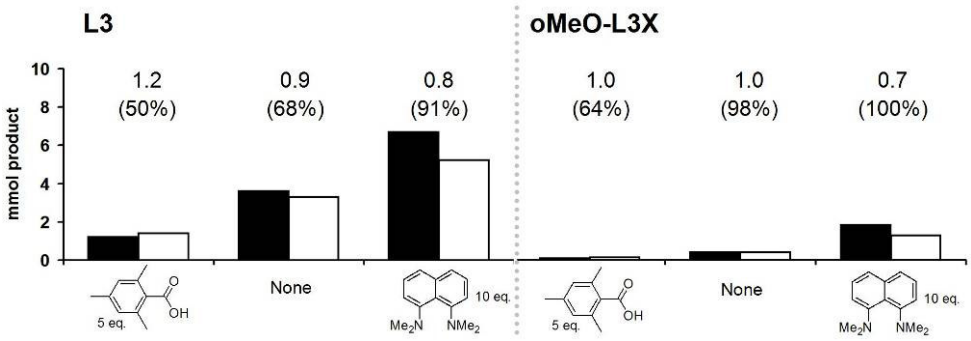

Figure 5.4. The selectivity and productivity for DMC (■) and DMO (□) as a function of the acidity (adding acid or base) for catalysts with the ligand L3 (a) and oMeO-L3X (b). The DMO over DMC ratio is shown on top; the conversion of nitrobenzene is given in parentheses.

Upon addition of 5 equivalents (on Pd) of TMBA to the catalytic system comprising L3, the DMC and DMO production decreased from 6.9 to 2.6 mmol and the conversion of nitrobenzene also decreased (from 68 to 50%). For the

system Pd^{II}(oMeO-L3X) the effect was similar, although less pronounced due to the rather low oxidative carbonylation activity. When adding 10 equivalents (on Pd) of the base DMAN, the opposite occurred: the DMC and DMO production increased from 6.9 to 11.9 mmol and the nitrobenzene conversion increased from 68 to 91% for the catalytic system based on L3. Again, a similar but less pronounced effect was observed for Pd^{II}(oMeO-L3X). The DMO/DMC ratio decreased from about 1.2 to about 0.8 when going from the acidic to the basic system.

5.2.3.2 Effect of the concentration of CO and H_2

The CO pressure was varied in a series of catalytic runs using the complexes Pd^{II}(L3) and Pd^{II}(L4). The results of these experiments are shown in Figure 5.5. When increasing the CO pressure from 25 to 50 to 100 bar, the DMO/DMC ratio increased from 0.3 to 0.9 to 2.0 when using Pd^{II}(L3) and from 1.2 to 2.5 to 5.0 when using Pd^{II}(L4). The conversion of nitrobenzene roughly doubled for both catalyst systems with increasing CO pressures (see also Table AIV.1 in Appendix IV).

When applying higher CO pressures the total amount of DMC + DMO produced significantly increased when using L4 (5.7 vs 9.6 mmol at 25 and 100 bar CO), in line with the increased nitrobenzene conversion. For L3 the effect of increasing pressure on the amount of DMC+DMO produced is less significant; 6.2 vs 7.4 mmol at 25 and 100 bar CO, whereas the nitrobenzene conversion is nearly doubled.

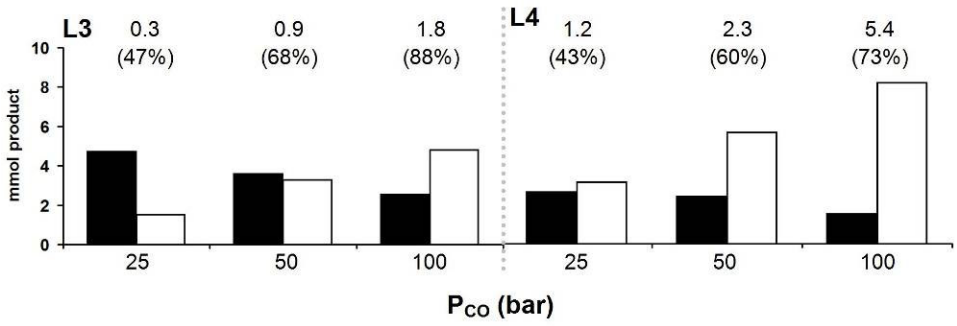

Figure 5.5. The selectivity and productivity of the catalysts Pd^{II}(L3) and Pd^{II}(L4) for DMC (■) and DMO (□) as a function of CO pressure. The DMO over DMC ratio is given on top; the conversion of nitrobenzene is given in parentheses.

Several catalytic runs were performed under an atmosphere of H_2 and CO (15/35 bar). As expected the presence of hydrogen resulted in most cases in an increase in aniline formation. In particular, the catalyst supported with the ligand oMeO-L3X led to a high yield of aniline (22.6 mmol, 90% selectivity; see also Appendix IV, Table AIV.1).

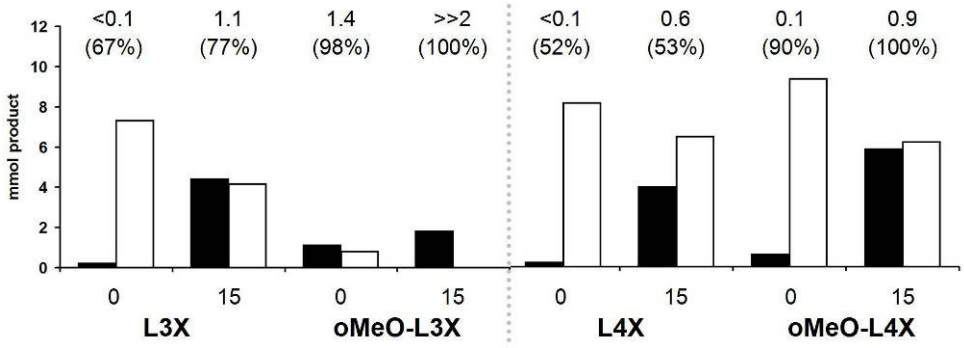

Figure 5.6. The selectivity and productivity for MF (■) and DMC+DMO (□) as a function of the partial pressure of H_2 (total = 50 bar) for catalysts comprising a ligand with a propylene backbone (left) or a butylene backbone (right). The MF over (DMC+DMO) ratio is given on top; the nitrobenzene conversion is given in parentheses.

Whereas in the absence of H_2 all catalysts produce relatively small amounts of MF (0.2 – 1.1 mmol), under an atmosphere containing 15 bar H_2 significantly more MF is produced (1.8 – 5.9 mmol) at the expense of DMC and DMO production, as reflected by the higher MF/(DMC+DMO) ratios (Figure 5.6). The conversion of nitrobenzene is only slightly affected in all cases.

5.3. Discussion

5.3.1. Overall mechanism with P_2Pd catalysts

During the studies into the reductive carbonylation of nitrobenzene in methanol, it was found that besides CO, methanol also acts as the reductant for nitrobenzene to eventually give a palladium-imido complex as the central 'PhN' product releasing species (see Chapters 3 and 4). This deoxygenation process involves oxidation of Pd^0 to Pd^{II}, and can be described by the half–reactions given in Equations 1a–c. The equations marked with an asterisk are similar to the unmarked equations, but with a slightly different stoichiometry, forming a different (but related) product (DMO *vs*. DMC; MF *vs*. CO; MPC *vs*. DPU; Azo *vs*. Azoxy).

$P_2Pd^0 + PhNO_2 + 2\ CO \rightarrow P_2Pd^{II}{=}NPh + 2\ CO_2$ (1a)

$P_2Pd^0 + PhNO_2 + 2\ CO + 2\ CH_3OH \rightarrow P_2Pd^{II}{=}NPh + H_2O + CO_2 + DMC$ (1b)

$P_2Pd^0 + PhNO_2 + 3\ CO + 2\ CH_3OH \rightarrow P_2Pd^{II}{=}NPh + H_2O + CO_2 + DMO$ (1b)*

$P_2Pd^0 + PhNO_2 + CH_3OH \rightarrow P_2Pd^{II}{=}NPh + CO + 2\ H_2O$ (1c)

$P_2Pd^0 + PhNO_2 + 2\ CH_3OH \rightarrow P_2Pd^{II}{=}NPh + MF + 2\ H_2O$ (1c)*

The reduction of Pd^{II}=NPh to Pd^0 and the various 'PhN' containing products as described by Equations 2a-c makes the processes catalytic.

$P_2Pd^{II}{=}NPh + CO + CH_3OH \rightarrow P_2Pd^0 + MPC$ (2a)

$P_2Pd^{II}{=}NPh + CO + PhNH_2 \rightarrow P_2Pd^0 + DPU$ (2a)*

$P_2Pd^{II}{=}NPh + CO + 2\ CH_3OH \rightarrow P_2Pd^0 + PhNH_2 + DMC$ (2b)

$P_2Pd^{II}{=}NPh + 2CO + 2\ CH_3OH \rightarrow P_2Pd^0 + PhNH_2 + DMO$ (2b)*

$P_2Pd^{II}{=}NPh + CO + PhNO_2 \rightarrow P_2Pd^0 + Azoxy + CO_2$ (2c)

$P_2Pd^{II}{=}NPh + 2CO + PhNO_2 \rightarrow P_2Pd^0 + Azo + 2\ CO_2$ (2c)*

$P_2Pd^{II}{=}NPh + CO + PhNO_2 + 2\ CH_3OH \rightarrow P_2Pd^0 + Azoxy + H_2O + DMC$ (2d)

$P_2Pd^{II}{=}NPh + 2CO + PhNO_2 + 2\ CH_3OH \rightarrow P_2Pd^0 + Azoxy + H_2O + CO_2 + DMO$ (2d)*

A combination of the half–reactions that oxidize Pd^0 to Pd^{II} (Eqs. 1) with the half–reactions that reduce Pd^{II} to Pd^0 (Eqs. 2), leads to the overall possible stoichiometries as described in Chapter 3. Such a combination allows for the construction of a relatively simple and unifying catalytic scheme, rationalizing the formation of *all* methanol oxidation products and *all* nitrobenzene reduction products, as is summarized in Scheme 5.4.

In this scheme, nitrobenzene is always the substrate. However, nitrosobenzene (PhNO) may be intermediately produced and enter the reaction described by Equation 1a. Traces of nitrosobenzene were indeed frequently observed after a catalytic experiment. It is unlikely that nitrosobenzene is deoxygenated by methanol via Equations 1b-c, as it is well-documented that the first de-oxygenation (with CO) of nitrobenzene (to nitrosobenzene) is considerably slower and energetically less favorable compared to nitrosobenzene de-oxygenation with CO.[36, 37]

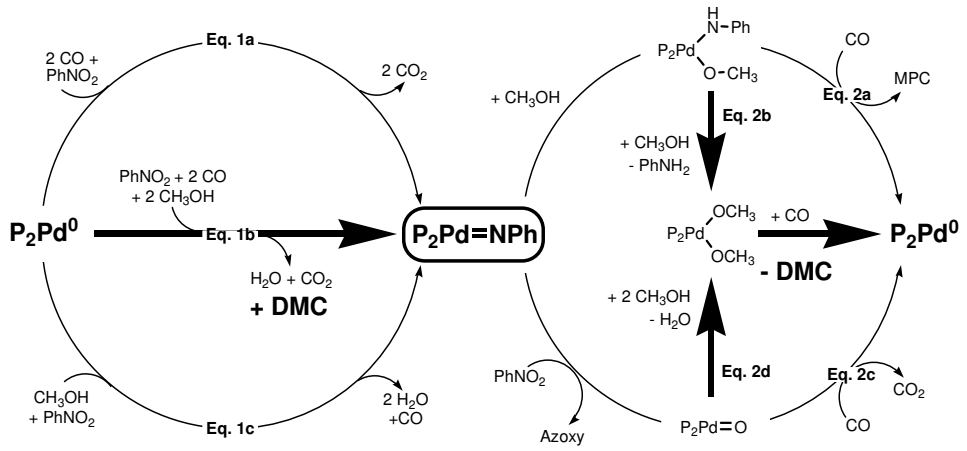

Scheme 5.4. Proposed reaction scheme for the overall catalytic processes.

5.3.2. Two pathways to oxidative carbonylation products DMC and DMO

From Scheme 5.4 it is clear that the methanol oxidative carbonylation products DMC and DMO can be produced at two stages: the first stage starts at a P_2Pd^0 species with oxidation of methanol and concomitant reduction of nitrobenzene according to Equation 1b to produce a 'P_2Pd=NPh' species and one equivalent of DMC/DMO on nitrobenzene. In the second stage DMC/DMO is produced from a reaction of P_2Pd=NPh with either CO/CH_3OH (giving one equivalent of aniline coproduced per mol of DMC/DMO (Eq. 2b)), or with $PhNO_2/2CH_3OH$ (giving one Azoxy, a water, and a DMC/DMO (Eq. 2d)) while the initial P_2Pd^0 species is regenerated. The sum of Equations 1b and 2b or 2d results in the overall stoichiometries given in Equations 3a and 3b respectively.

$PhNO_2 + 3\ CO + 4\ CH_3OH \rightarrow 2\ DMC + PhNH_2 + H_2O + CO_2$ (3a)
$PhNO_2 + 5\ CO + 4\ CH_3OH \rightarrow 2\ DMO + PhNH_2 + H_2O + CO_2$ (3a)*
$2\ PhNO_2 + 3\ CO + 4\ CH_3OH \rightarrow 2\ DMC + Azoxy + 2\ H_2O + CO_2$ (3b)
$2\ PhNO_2 + 5\ CO + 4\ CH_3OH \rightarrow 2\ DMO + Azoxy + 2\ H_2O + CO_2$ (3b)*

The efficiency of oxidative carbonylation (E_{OC}) is defined here as the ratio of mole of DMC+DMO produced per mole of nitrobenzene converted (i.e. the sum of products containing nitrobenzene 'PhN' fragments

[MPC+$PhNH_2$+2Azo(xy)+2DPU] × 100%). The maximum value for E_{OC} is 200%; i.e. when the sequence of reactions 1b and 2b are exclusively proceeding. Lower efficiencies indicate that the other reactions along the periphery of the cycles in Scheme 4 (Eqs. 1a,c and 2a,c) are also operative. One should note that the amounts of aniline and DMC/DMO produced are not necessarily linked only via Equations 3. Aniline can also be formed as a consecutive product (e.g. by replacing methanol with H_2O in Eq. 2a) from water that is produced via Equations 1b or 1c.

The E_{OC} for catalytic systems based on ligands comprising unsubstituted aryl rings and a C_3 backbone is about 45% (Table 5.1). For catalytic systems based on similar ligands with a larger size backbone (i.e. a larger bite-angle), the E_{OC} is larger; 65% for L*4*X and even 105% for L5Fc. This means that with some catalysts nitrobenzene can be more efficiently used as an oxidant than for other catalysts in the Pd-catalyzed synthesis of DMC/DMO.

To unlock potentially even more efficient or selective catalytic systems, it will be necessary to comprehend the effects of structural catalyst parameters on catalysis and thereby gain insight in the mechanistic details underlying the reactions summarized in Scheme 5.4. The current understanding of the molecular details of nitrobenzene de-oxygenation, together with the formation of MPC and Azoxy has been discussed in some detail in Chapters 3 and 4. Further details, especially concerning the evolution of Azoxy, are discussed in more detail in the next chapter (Chapter 6). The complexity of the parallel reactions shown in Scheme 5.4, which together make up the overall efficiency with which nitrobenzene can act as the oxidant in methanol carbonylation, makes it impossible at this stage to present a fully detailed molecular picture of the catalytic consequences of structural catalyst variations. Instead, the focus here will be on some of the most outspoken catalytic observations attempting to rationalize these.

5.3.3. Effects of catalyst structure

5.3.3.1 Effect of p-MeO- and o-MeO-substituents

A most prominent effect on DMC/DMO yield is observed with the introduction of o-MeO substituents in L3 type ligands (Table 5.1). Formation of DMC/DMO is

strongly inhibited by almost an order of magnitude compared to applying the unsubstituted ligands. Irrespective of the stage in which DMC/DMO is produced (Scheme 5.4; via 1b or 2b), a serious inhibition of methanol carbonylation takes place. The significantly weaker effects observed with p-MeO substitution suggests that steric rather than electronic effects play a dominant role with o-MeO substitution.

The first stage DMC/DMO formation (Eq. 1b) is in competition with reduction of nitrobenzene using CO only (Eq. 1a) and oxidative dehydrogenation of methanol (producing CO or MF, Eq. 1c). The first product-determining step is de reaction of the zero-valent palladium centre in **C0** giving oxidative coupling of CO and nitrobenzene or oxidative addition of methanol as shown in Scheme 5.5.

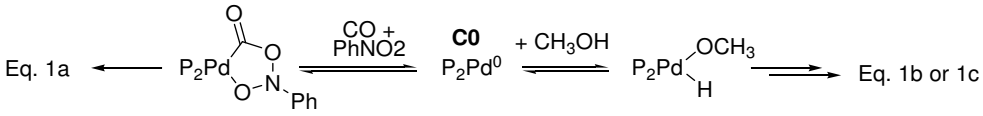

Scheme 5.5. Discriminating steps in stage 1: oxidative coupling of nitrobenzene and CO (Eq 1a) or oxidative addition of methanol (Eq 1b, 1c) at complex C0.

It was shown in Chapters 3 and 4 that oxidative coupling of CO with nitrobenzene is promoted with the use of more electron-donating ligands, resulting in higher electron density at the Pd center, which thus partly explains the lower amount of DMC/DMO produced with the catalytic systems containing ortho- or para-methoxy-substituted ligands. Discrimination of the oxidative *carbonylation* of methanol forming DMC or DMO (Eq. 1b) over the oxidative *dehydrogenation* to form CO or MF (Eq. 1c) most likely occurs *after* the first deoxygenation of nitrobenzene by methanol (Chapter 3) by the two different fates of the methoxide complex $[P_2Pd(OCH_3)(ONPh)]^+$ **C1** (Scheme 5.6) (Chapters 3 and 4).

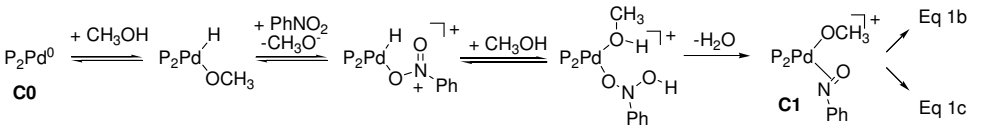

Scheme 5.6. First reaction intermediates in the deoxygenation of nitrobenzene that are common for Eq. 1b and 1c.

Associative displacement of the nitrosobenzene ligand in **C1** by CO (forming **C1b**) or methoxide (forming **C1a**) (Scheme 5.7) will be hampered by the presence of o-methoxy groups protecting the axial coordination sites of palladium, thus making the conversion to DMC/DMO precursors less likely.

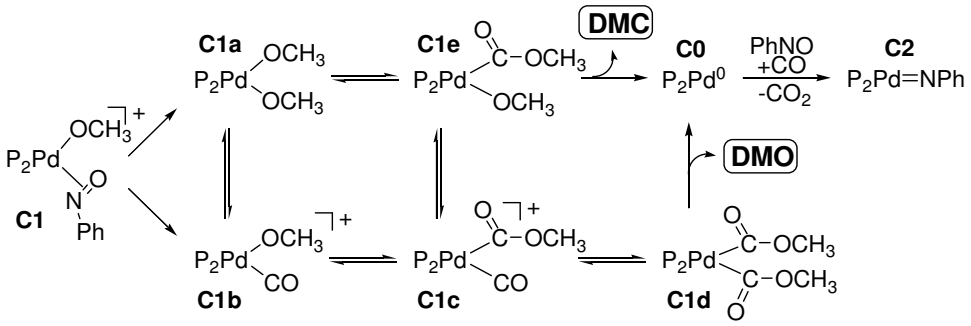

Scheme 5.7. Proposed intermediates for DMC or DMO production in in the first stage following Eq. 1b.

On the other hand, without a rapid displacement from the palladium coordination sites, nitrosobenzene becomes more likely involved in H-atom transfer at Pd from methoxide to nitrosobenzene (Scheme 5.8), thus ultimately leading to oxidative dehydrogenation of methanol to CO/MF and 'P_2Pd=NPh' without the production of DMC/DMO. As shown in section 5.2.2.1, the use of catalytic systems with oMeO-substituted ligands indeed results in slightly higher selectivity for MF (and CO, as derived from the hydrogen mass ballance). An increase in the relative importance of the methanol oxidative dehydrogenation pathway with oMeO-containing ligands has been noted previously from a detailed quantitative product analysis, as described in Chapter 4. It is interesting to note that formaldehyde or its derivative dimethoxy methane (DMM) was never observed amongst the reaction products, indicating a rapid hydrogen transfer at Pd between formaldehyde and nitrosobenzene at this stage.

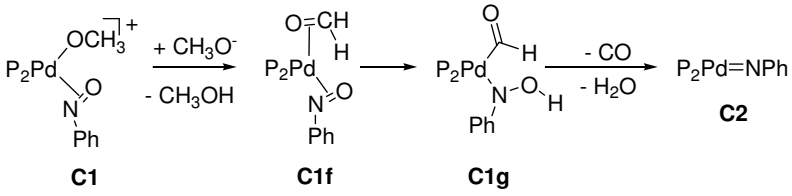

Scheme 5.8. Proposed intermediates for methanol dehydrogenation following Eq. 1c.

In Chapter 3 some arguments have been developed for the competition in DMC/DMO forming stage 2 with the reactions following Equations 2a and 2b (Scheme 5.4). In this stage the presence of the axially protective o-methoxy substituents prevents ready protonation and associative displacement of the phenylazanide ($PhNH^-$) ligand in $[P_2Pd(OCH_3)(NHPh)]$ **C2a** by methanol to generate aniline and $[P_2Pd(OCH_3)_2]$ **C2b**, a precursor species for DMC/DMO formation (Scheme 5.9). Instead, displacement of the methoxide anion in **C2a** by coordination of the smaller neutral CO can occur, thus leading to carbonylation of **C2a** and ultimately to the formation of MPC. This thus rationalizes the concomitant increase in MPC formation (Eq. 2a) with a decrease in DMC/DMO formation (Eq. 2b), as is schematically illustrated in Scheme 5.9. That a decrease in Azoxy is not observed with increasing amounts of DMC/DMO, is because the formation of Azoxy can, contrary to MPC genesis, be coupled with DMC/DMO production in the second stage (Eq. 3b) via the protonation of an intermediate $P_2Pd{=}O$ species to dimethoxide species **C1a** (Scheme 5.9, see also Chapter 3).

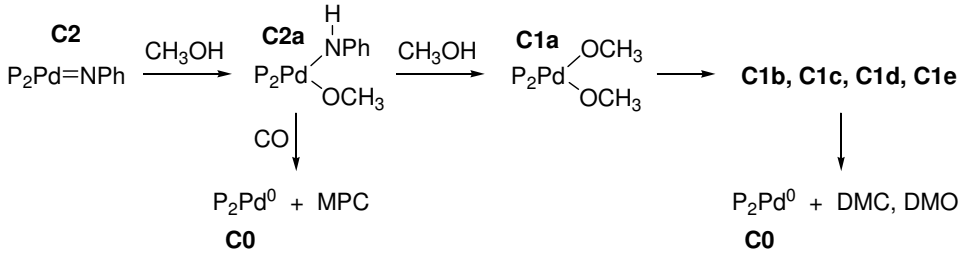

Scheme 5.9. Proposed mechanism for the formation of the 'second' equivalent of DMC and DMO (and aniline) in competition with MPC production.

Although less pronounced, also with the larger bite angle ligands, L4X and L5Fc o-MeO substituents are expected to play a similar role in reducing the efficiency of nitrobenzene as the oxidant in oxidative carbonylation of methanol. In addition, a significant decrease in the formation of Azoxy is observed with these ligands, when either p-methoxy or o-methoxy substituents are present in L4(X) ligands or L5Fc (Table AIV.1 in Appendix IV). Apparently the attack of $P_2Pd{=}NPh$ intermediates by nitrobenzene become less likely in comparison with protonation by methanol (eventually leading to relatively more aniline and DMC/DMO, or MPC) for a more basic $P_2Pd{=}NPh$ centre (further details are given and discussed in Chapter 6).

5.3.3.2 Effect of the ligand bite-angle

The catalysts based on ligands with larger bite angles, such as L4, L4X, and L5Fc, systematically produce significantly larger amounts of the methanol oxidative carbonylation products DMC and DMO, than the systems with the propylene-bridged ligands (Table 5.1). The most remarkable catalytic observation, however, is that the DMO/DMC ratio increases significantly with increasing bite angle of the ligand. A higher efficiency of nitrobenzene as the oxidant for oxidative carbonylation of methanol could in principle occur at both DMC/DMO generating stages 1 and 2.

In stage 1, restricted coordination space at equatorial positions around Pd, such as in L4(X) and L5Fc, could favor oxidative addition of methanol at Pd^0, ultimately leading to reactions following Equations 1b and 1c, over the space-demanding oxidative coupling of CO and nitrobenzene (Eq. 1a; Scheme 5.5). This hypothesis is in correspondence with the increased contribution of CH_3OH as (co-)reductant of nitrobenzene (both Eqs. 1b and 1c), as suggested from quantitative product simulations, comparing ligands L3X and L4X (see also Chapter 3). This may thus at least partly account for an increase in the formation of DMC/DMO with the ligand L4X.

In stage 2, one might expect that coordination of the bulky phenylazanide ligand in the Pd^{II} complex **C2a** (Scheme 5.9) is less favourable at the restricted coordination space in L4(X) and L5Fc relative to L3(X) ligands. Therefore, coordination of a smaller CO or methoxide ligand, becomes more likely, thus producing a DMC/DMO precursor complex (**C2b** or **C1b**) rather than the MPC precursor complex. This argument may thus rationalize a lower production of MPC with concomitantly higher DMC/DMO formation as observed with L4(X) and L5Fc catalysts.

The same concept of restriction in equatorial coordination space with larger bite angle ligands can also rationalize an increase in the DMO/DMC ratio observed with larger bite angle ligands as depicted in Scheme 5.7. Thus, CO displacement of methoxide from the first coordination sphere of Pd in **C1a** can occur, resulting in Pd carbonyl complexes such as **C1b** and/or **C1c** (Scheme 5.7). It is thought that a restricted first coordination space at Pd, such as in the L4 and L5 type ligands, will relatively favor coordination of the small neutral CO molecules over the

larger sized methoxide anion. The latter can be suitably accommodated by solvation and hydrogen bonding with methanol solvent molecules in close proximity of the Pd centre.

The competition between the formation of **C1c** and **C1e** (Scheme 5.7) follows the same steric rules. Thus, the small CO molecule will be more advantageous for coordination than methanol in the acyl complex **C1c** when the coordination space is more restricted, thus shifting the equilibrium towards the di-carbomethoxy complex **C1d**. This restricted space argument thus also rationalizes the increase in DMO/DMC ratios (up to ~3, for L5Fc) when large bite-angle ligands are applied instead of ligands with a smaller bite angle (e.g. a ratio of ~1 with L3).

5.3.4. Effects of reaction conditions

Addition of H_2 during oxidative carbonylation of methanol results in the formation of more methyl formate at the expense of DMC/DMO. This can be rationalised by the existence of the intermediate $[PdC(O)OCH_3]^+$–type species for DMC/DMO formation, such as **C1c** and **C1e** (see Scheme 5.7). Such species are also prone to undergo hydrogenolysis by a reaction with dihydrogen, thus forming MF at the expense of DMC and DMO.

The decreased DMO/DMC ratio upon addition of a base (and the reverse effect when adding an acid) can also be rationalized by the process summarized in Scheme 5.7; a higher methoxide concentration will favour rapid coordination of the methoxide anion to form **C1e**, as a result forming more DMC.

Likewise, the observed effect of increasing CO pressure giving a higher DMO/DMC ratio can be easily rationalised. A higher CO concentration makes the competition of CO for the coordination site in the **C1c⇆C1e** equilibrium, relative to that of methoxide, more successful, producing more of complex **C1e** and as a result giving a higher DMO/DMC ratio.

5.4. Summary and conclusions

The catalytic reactivity of palladium complexes supported by bidentate diarylphosphane ligands has been studied in the oxidative carbonylation of methanol to dimethyl carbonate (DMC) and dimethyl oxalate (DMO) using nitrobenzene as terminal oxidant.

Insight into the molecular mechanism of the methanol oxidative carbonylation process has been obtained from catalytic experiments employing a variety of bis-diarylphosphane ligands with variations in the substituents on the phenyl rings as well as in the length of the backbone spacer, and on experiments in which the acidity or the CO pressure were varied, or in which an additional H_2 partial pressure was applied.

It was found that two key intermediate stages exist at which the methanol oxidative carbonylation process can be identified. These stages were shown to be helpful in rationalizing the observed influence that the catalyst structure and reaction conditions can have on the oxidative carbonylation process.

Based on the mechanistic insights, it is concluded that an ideal P_2Pd catalyst for the oxidative carbonylation of methanol with nitrobenzene as the oxidant, would need a relatively acidic palladium centre, be sterically open in the axial coordination positions, but have restricted coordination space at the equatorial coordination positions of palladium. The palladium complex of the ligand bis(diphenylphosphanyl)-ferrocene (L5Fc) meets these criteria and was found to use nitrobenzene as oxidant for the oxidative carbonylation of methanol most efficiently, with an E_{OC} of 105% of the 200% theoretical maximum efficiency possible. Based on these initial results and the mechanistic information generated by the present work, even more active and/or selective catalytic systems may reasonably be anticipated for the oxidative carbonylation of methanol using nitrobenzene as oxidant.

5.5. Experimental section

5.5.1. General remarks

All ligands were generously provided by Shell Global Solutions Amsterdam b.v., where they were synthesized according to literature procedures.[38-46] All other solids were purchased from Acros organics and used as received. Methanol, nitrobenzene and aniline were all of analytical reagent purity, and were distilled under an argon atmosphere over the appropriate drying agent.[47] After distillation these liquids were stored under argon. It was ensured that no water was present using an analytical reaction with trimethyl orthoformate according to a literature procedure.[48] Carbon monoxide (> 99% pure)[49] was purchased from Linde gas benelux B.V. and used as received.

^{1}H–, and ^{13}C–NMR spectra were recorded on a Bruker DPX300 (300 MHz) or a Bruker DMX400 (400 MHz) machine. High pressure experiments were conducted in stainless steel autoclaves (100 ml) equipped with two inlet/outlet valves, a burst disc, a pressure sensor, and a thermocouple. The

autoclaves were heated by a HEL polyBLOCK electrical heating system. Temperatures and pressures where measured with probes connected to a computer interface making it possible to record these parameters throughout the course of the reaction.

5.5.2. Catalytic / high pressure reactions

In a typical catalytic experiment, 0.05 mmol $Pd(OAc)_2$ and 0.075 mmol ligand (and if relevant another additive) were weighed and transferred into an autoclave, together with a magnetic stirring rod. The autoclave was tightly closed and subsequently filled with argon using a Schlenk-system that was connected to the one of the valves of the autoclave. Through the other valve was added 2.50 ml (24.4 mmol) dried and degassed nitrobenzene, under a continuous flow of argon. In a similar fashion, 25.0 ml dried and degassed methanol was then added. This reaction mixture was allows to stir at 500 rpm for about 15 minutes to ensure that complex formation was complete.[50] The autoclave was then inserted into the heating block and put under 50 bar carbon monoxide gas. The reaction mixture was heated to 110 ºC (within 30 minutes) under stirring at 500 rpm. After standing for four hours at this temperature, the autoclave was cooled to room temperature in about one hour. The autoclave was then slowly vented to atmospheric pressure and the reaction mixture was analyzed as described in Chapter 3. To ensure reproducibility, some catalytic reactions were performed in quadruplet, and the relative standard deviation was always less than 5% for all products.

References

[1] *Registry of Toxic Effects of Chemical Substances (RTECS, online database)*, United States Department of Health and Human Services (National Toxicology Information, National Library of Medicine), Bethesda, MD, **1993**.

[2] R.C. Weast (Ed.), *Handbook of Chemistry and Physics*, D-110, 58 ed., CRC Press Inc., Cleveland, **1977-1978**.

[3] R. H. Richter, R. D. Priester, *in: J.L. Kroschmitz, M. Howe-Grand (Eds.), Kirk-Othmer Encyclopedia of Chemical Technology, Vol. 14*, Wiley, New York, **1995**.

[4] H. Ulrich, *Ullmann's Encyclopedia of Industrial Chemistry, Vol. A14*, VCH publishers, New York, **1989**.

[5] A. J. Ryan, J. L. Stanford, *in: G. Allen, J.C. Bevington (eds.), Comprehensive Polymer Science, Vol. 5*, Pergamon, New York, **1989**.

[6] K. Weisermel, H. J. Arpe, *Industrielle Organische Chemie*, VCH Verslagsgesellschaft GmbH, Weinheim, Germany, **1988**.

[7] www.gem-chem.net/capacity.html, **November 2011**

[8] Y. Ono, *Pure & Appl. Chem.* **1996**, *68*, 367.

[9] Y. Ono, *Appl. Catal. A.* **1997**, *155*, 133.

[10] Y. Ono, *Catalysis Today* **1997**, *35*, 15.

[11] F. Rivetti, *CR Acad. Sci. II C* **2000**, *3*, 497.

[12] P. Tundo, M. Selva, *Acc. Chem. Res.* **2002**, *35*, 706.

[13] J. L. Gong, X. B. Ma, S. P. Wang, *Appl. Cat. A* **2007**, *316*, 1.

[14] R. Bertani, G. Cavinato, L. Toniolo, G. Vasapollo, *J. Mol. Catal.* **1993**, *84*, 165.

[15] T. W. Dekleva, D. Forster, *Adv. Catal.* **1986**, *34*, 81.

[16] D. Delledonne, F. Rivetti, U. Romano, *J. Organomet. Chem.* **1995**, *488*, C15.

[17] P. Giannoccaro, *J. Organomet. Chem.* **1994**, *470*, 249.

[18] W. B. Kim, U. A. Joshi, J. S. Lee, *Ind. Eng. Chem. Res.* **2004**, *43*, 1897.

[19] J. Muzart, *Tetrahedron* **2005**, *61*, 9423.

[20] F. Rivetti, U. Romano, *J. Organomet. Chem.* **1978**, *154*, 323.

[21] D. M. Fenton, Steinwan.Pj, *J. Org. Chem.* **1974**, *39*, 701.

[22] F. Rivetti, U. Romano, *J. Orgmet. Chem.* **1979**, *174*, 221.

[23] F. Rivetti, U. Romano, *Chim. Ind. (Milan)* **1980**, *62*, 7.

[24] M. Goyal, R. Nagahata, J. Sugiyama, M. Asai, M. Ueda, K. Takeuchi, *Catal. Lett.* **1998**, *54*, 29.
[25] M. Takagi, H. Miyagi, T. Yoneyama, Y. Ohgomori, *J. Mol. Cat. A. Chem.* **1998**, *129*, L1.
[26] M. Goyal, R. Nagahata, J. Sugiyama, M. Asai, M. Ueda, K. Takeuchi, *J. Mol. Cat. A. Chem.* **1999**, *137*, 147.
[27] S. Uchiumi, K. Ataka, T. Matsuzaki, *J. Orgmet. Chem.* **1999**, *576*, 279.
[28] S. P. Current, *J. Org. Chem.* **1983**, *48*, 1779.
[29] D. Delledonne, F. Rivetti, U. Romano, *Appl. Catal. A.* **2001**, *221*, 241.
[30] H. Ishii, M. Goyal, M. Ueda, K. Takeuchi, M. Asai, *Appl. Cat. A.* **2000**, *201*, 101.
[31] H. Yasuda, K. Watarai, J. C. Choi, T. Sakakura, **2005**, *236*, 149.
[32] E. Amadio, G. Cavinato, A. Dolmella, L. Toniolo, *Inorg. Chem.* **2010**, *49*, 3721.
[33] Moiseev, II, M. N. Vargaftik, T. V. Chernysheva, T. A. Stromnova, A. E. Gekhman, G. A. Tsirkov, A. M. Makhlina, *J. Mol. Catal. A-Chem.* **1996**, *108*, 77.
[34] The relative amount of 'CH_3OH-only de-oxygenation' is given by the total amount of nitrobenzene that is fully reduced (to a 'PhN' fragment) by this route, divided by the total amount of nitrobenzene molecules that are fully reduced (to a 'PhN' fragment) times 100%. The amount of complete $PhNO_2$ de-oxygenation by methanol as reductant can be derived from the hydrogen mass balance as follows. The hydrogen mass balance is given by ($2PhNH_2$ + 2DPU + $2H_2O$) - (2DMC + 2DMO + 4MF), which will give the amount of CO produced when multiplied by 0.25 (the production of one CO liberates 4 hydrogen atoms). As MF is also a form of CO and because the production of one CO can fully strip one $PhNO_2$ of its oxygen atoms (to form 2 H_2O), the amount of $PhNO_2$ that has been reduced completely via the 'methanol-only' pathway simple equals the amount of MF + CO produced. The amount of fully de-oxygenated $PhNO_2$ is given by the amounts of 'PhN-containing' nitrobenzene reduction products according to: $PhNH_2$ + MPC + 2(DPU + Azo) + 1.5Azoxy. Hence, the relative amount of 'CH_3OH-only de-oxygentaion' can be computed by: {MF + 0.25[($2PhNH_2$ + 2DPU + $2H_2O$) - (2DMC + 2DMO + 4MF)]} / [$PhNH_2$ + MPC + 2(DPU + Azo) + 1.5Azoxy] x 100%.
[35] For L3X vs. oMeOL3X = (18-16)/16x100% = 13%; for L4X vs. oMeOL4X = (27-20)/20x100% = 35%; for L3X vs. L4X = (20-16)/16x100% = 25%; for oMeOL3X vs. oMeOL4X = (27-17)/17x100% = 59%.
[36] H. Lund, in *Organic Electrochemistry. An Introduction and a Guide*, 3 ed. (Eds.: H. Lund, M. M. Lund, Baizer), Marcel Dekker, New York, **1991**, p. 411.
[37] T. J. Mooibroek, E. Bouwman, E. Drent, *Organometallics* **2011**, submitted.
[38] F. Bickelhaupt, US 4874897, **1989**.
[39] W. Eilenberg, EU 364046, **1991**.
[40] J. A. van Doorn, US 4994592, **1991**.
[41] R. van Ginkel, US 6548708, **2003**.
[42] E. Drent, US 5091587, **1992**.
[43] C. F. Hobbs, US 4120901, **1987**.
[44] P. W. Clark, B. J. Mulraney, *J. Organomet. Chem.* **1981**, *217*, 51.
[45] J. M. Brown, B. A. Murrer, *Tetrahedron Lett.* **1980**, *21*, 581.
[46] R. L. Wife, A. B. van Oort, J. A. van Doorn, P. W. N. M. van Leeuwen, *Synthesis* **1983**, *1*, 71.
[47] W. L. F. Armarego, C. L. L. Chai, *Purification of laboratory chemicals*, 5th ed., Elsevier, Amsterdam, **2003**.
[48] J. Chen, J. S. Fritz, *Anal. Chem.* **1991**, *63*, 2016.
[49] customer.linde.com/FIRSTspiritWeb/linde/LGNL/media/datasheets/NL-PIB-0024.pdf, **November 2011**
[50] T. J. Mooibroek, E. Bouwman, M. Lutz, A. L. Spek, E. Drent, *Eur. J. Inorg. Chem.* **2010**, *2*, 298.

Chapter 6

Mechanistic study of the L_2Pd catalyzed reduction of nitrobenzene with CO in methanol; a comparative study between diphosphane and 1,10-phenanthroline ligated complexes.

Abstract: The reactivity of Pd^{II} compounds supported by 1,10-phenanthroline ('phen') or the bidentate diaryl phospane 'L4X' has been studied in the reaction of nitrobenzene with CO in methanol. Both are ~70% selective for the 'NPh-containing' coupling products azo(xy)benzene (azo(xy)), but also produce carbonylation products (methylphenyl carbamate (MPC), N,N-diphenylurea (DPU)) and hydrogenation products (aniline and DPU (derived form aniline)). Only the Pd^{II}(L4X) system concurrently produced *significant* amounts of methanol oxidation products (dimethyl carbonate (DMC), dimethyl oxalate (DMO), water). These findings could be rationalized by the mechanism developed for Pd/diphosphane catalysts, that is centred around a palladium-imido complex (Pd=NPh) being the terminal product of nitrobenzene de-oxygenation, and the *sole product releasing* species for *all* 'NPh-containing' products.

The palladacycle **C7** (PdC(O)N(Ph)OC(O)) was considered as an alternative carbonylation product releasing species, but the ESI-MS spectrum of 'phen–**C7**', a ligand exchange experiment of 'phen–**C7**' with L4X, and a DFT study of nitrobenzene deoxygenation to (ligand)Pd=NPh all suggest that this is not the case; the barrier for **C7** decarbo**n**ylation (–CO) is lower than decarbo**x**ylation ($-CO_2$). Instead, **C7** is part of several CO-equillibrated palladacycles that merely act as temporary 'NPh-reservoir'. As suggested by the catalytic data and other literature reports however, under *acidic* conditions the decarbo**x**ylation *barrier* is lowered; for 'phen–**C7**' to the point where CO_2 extrusion is favored relative to decarbo**n**ylation, but for 'L4X–**C7**' the decarbo**n**ylation barrier is still lowest due to the destabilizing effect that this bulkier ligand has on such palladacycles.

It is thus concluded that the Pd=NPh complex is the prime 'NPh' product releasing intermediate and *only* under acidic condition **C7** *may* –depending on the ligand– *become* carbonylation product releasing.

6.1. Introduction

Studies in homogeneous catalysis are often motivated by financial and/or ecological incentives. One process in which both motivators are in play is the synthesis of the aromatic isocyanates[1, 2] such as the polymer precursors MDI and TDI[3, 4] (Figure 6.1). Both molecules are produced on the megaton scale per annum, using nitrobenzene as feedstock and employing the highly toxic[5, 6] and corrosive[2] phosgene as carbonylating reagent.

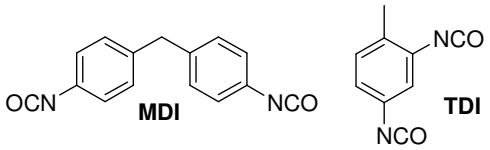

Figure 6.1. Two industrially produced aromatic isocyanates.

Phosgene can in principal be replaced by the less toxic carbon monoxide as deoxygenating and carbonylating reagent, which in known to proceed in the presence of a transition metal catalyst.[7] When this reaction is conducted in a protic medium such as an alcohol or an amine, a carbamate or urea is obtained (Scheme 6.1a) which can by pyrolized to the isocyanate with the recovery of the alcohol/amine (Scheme 6.1b).

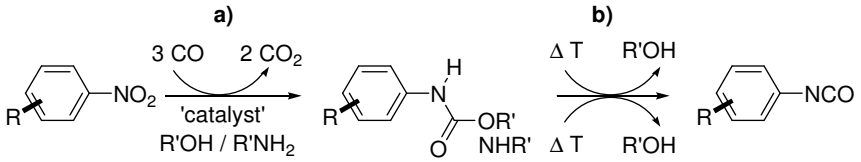

Scheme 6.1. Alternative route to make aromatic isocyanates by a carbonylation (a), followed by a pyrolisis (b).

It was disclosed already in the advent of the 1980s working in methanol as the solvent, that reasonably active (~500 turn over numbers) palladium–based catalysts were obtained if the Pd–centre was stabilized by bidentate N–, or P–ligands.[8] The ligand 1,10–phenanthroline (phen) proved most active (in the presence of an acid co–catalyst), which resulted in the focus of the scientific community on this Pd/phen/H^+/CH_3OH catalytic system.[12–23] Despite the fact that a very active catalytic system has been reported (~10^5 turn over numbers),[9] a clear–cut mechanism for this reaction involving common intermediates has yet to emerge. In general however, most proposals start from an *in situ* formed zero–valent palladium species, which is oxidized by nitrobenzene and CO to a

palladacyclic compound such as the one shown in Scheme 6.2a. Methylphenylcarbamate (MPC) can then be formed by a reaction with methanol.

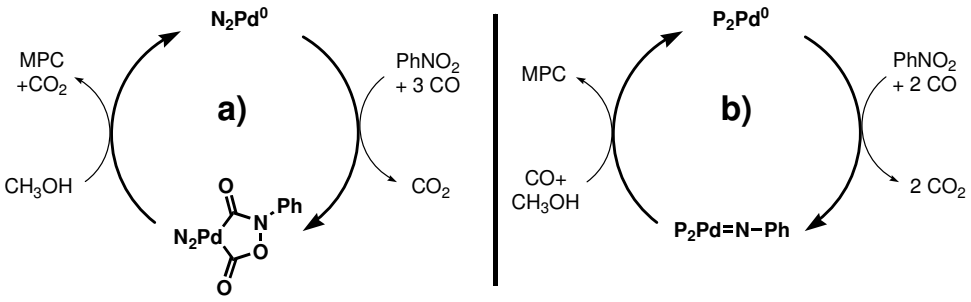

Scheme 6.2. Two simplified mechanistic proposals for the reductive carbonylation of nitrobenzene, catalyzed by a L_2Pd–catalyst wherein: a) L_2 is the N_2–donor ligand 1,10–phenanthroline; b) L_2 is a P_2–donor ligand such as bidentate diarylphosphanes.

Chapters 3–5 reported on mechanistic studies of this carbonylation reaction in methanol, using bidentate diarylphospane ligands and palladium.[10, 11] During these studies, a detailed mechanistic scheme was unravelled, wherein a palladium imido complex ('Pd=NPh') is the central key–intermediate species, rationalizing the formation of all observed products.[10, 11] A simplified version of this mechanism to rationalize the formation of MPC is shown in Scheme 6.2b. It was found that the postulation of a palladacyclic intermediate such as the one shown in Scheme 6.2a is, as *product releasing* species, both unlikely and explanatorily redundant in the $Pd/P_2/CH_3OH$ catalytic system (see Chapters 3 and 4).[11]

During the studies described in the preceding chapters, it was unexpectedly found that the product distribution of the aryl–containing nitrobenzene reduction products is very similar when employing the N–donor ligand phen Figure 6.2, left) or the P–donor ligand L4X (Figure 6.2, right). Fascinated by this finding, it was investigated in what way proposed reaction mechanism (for phosphane stabalized Pd complexes) as outlined in Chapters 3–5 might be (a)similar for phen stabalized Pd complexes.

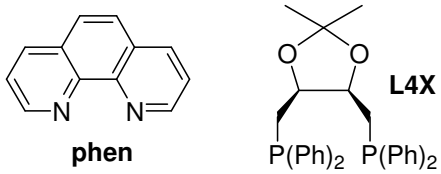

Figure 6.2. The N–donor ligand (phen) and the P–donor ligand (L4X) used in this study.

6.2. Results

6.2.1. General considerations

In all catalytic reactions, the catalyst precursor was formed *in situ* from 0.05 mmol $Pd(OAc)_2$ and a certain amount of ligand, as testing the catalytic activity of pre–formed complex gave identical results. By thoroughly drying of the reagents (see experimental), it was ensured that the reaction conditions were strictly anhydrous (<100 ppm H_2O).

The products that were observed in the catalytic reactions are shown in Scheme 6.3. Full analytical details for these products are given in Table AV.1 in Appendix V for all catalytic reactions. The aryl containing reduction products of nitrobenzene can be divided in the carbonylation products ('NCO') methylphenylcarbamate (MPC), and *N*,*N*'diphenylurea (DPU), the coupling products ('N=N') azobenzene (Azo) and azoxybenzene (Azoxy), and the hydrogenation products ('NH') aniline ($PhNH_2$) and also DPU (derived from aniline).[12]

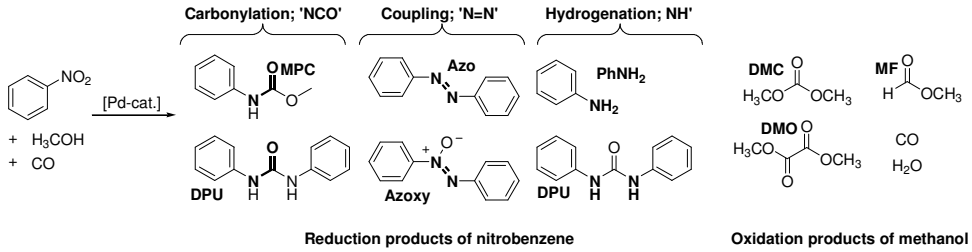

Scheme 6.3. Overview of the different products that are formed in the palladium–catalyzed reaction of nitrobenzene with CO in methanol.

Azo and azoxy are frequently reported side–products, as are aniline and DPU.[7] Azo and azoxy are derived from nitrobenzene only, but for the formation of aniline and DPU, H-atoms are required. Their formation is therefore commonly attributed to the presence of water, either in the reagents or formed *in situ*, e.g. *via* acid–catalyzed etherification of methanol. However, it was shown in Chapter 3 that these H-atoms can also originate from methanol oxidation, resulting in the oxidative carbonylation products dimethyl carbonate (DMC) and dimethyl oxalate (DMO), and in the oxidative dehydrogenation products methyl formate (MF) and

carbon monoxide. The H-atoms are then transferred to water, and aniline (and thus also DPU; see Chapter 3 for details).

It is noteworthy that neither dimethyl ether (DME) nor dimethoxy methane (DMM, commonly observed in palladium catalyzed carbonylation experiments under reducing or redox neutral conditions involving methanol as substrate)[13] has been observed as a reaction product. This indeed excludes methanol self–etherification or etherification with any possibly formed (uncoordinated) formaldehyde under reaction conditions as a source of water and/or protons for aniline and DPU.

As it is known that at reaction temperatures (110–130 ºC) DPU reacts with methanol to MPC and aniline,[10] it is best to view DPU and MPC *together* as carbonylation products, and aniline and DPU *together* as hydrogenation products. Although the coupling products Azo and Azoxy were almost always detected, Azoxy is always the major product and Azo the minor product (< 2% selectivity).

6.2.2. Catalytic experiments

6.2.2.1 Reactivity without additives or co–catalysts

Using GLC analysis of the reaction mixtures, all products could be quantified with calibration lines made from authentic samples. The accuracy of the quantitative analysis of the phenyl–containing products is excellent as confirmed by the sum of the aryl rings (column $\Sigma_{\varnothing}$ in Table 6.1).

When employing Pd^{II}(phen), and operating at 110 ºC (entry 1), only 17% conversion was achieved, whereas operating at 130 ºC (entry 2), 56% nitrobenzene was converted. This reactivity at 130 ºC is similar as for the Pd^{II}(L4X) catalytic system at 110 ºC (52% conversion, entry 3).

Both catalytic systems are roughly equally selective for the reductive coupling product Azoxy (~70%); Pd^{II}(phen) is more selective towards carbonylation (20%) while Pd^{II}(L4X) is more selective towards hydrogenation (20%). Notably, using Pd^{II}(L4X), large quantities of oxidation products of methanol were co-produced (DMC, DMO, MF, and H_2O), whereas these products are hardly formed when using Pd^{II}(phen).

Table 6.1. Reactions of nitrobenzene with CO in methanol, using $Pd^{II}(phen)(OAc)_2$ or $Pd^{II}(L4X)(OAc)_2$ as catalyst precursor.[a]

		Temp.	Conv.		Selectivity (%)			mmol		
Entry	Ligand	(ºC)	(%).[b]	$\Sigma_{ø}$	NCO[c]	N=N[d]	NH[e]	MF	H_2O	DMC/O
1	**phen**	110	17	24.7	23	71	6	0.0	0.0	0.0
2	**phen**	130	56	24.3	22	71	7	0.2	0.3	0.5
3	**L4X**	110	52	24.4	8	73	19	0.2	10.1	8.2

[a] Reactions were heated for four hours at the indicated temperature in 25.0 ml dry and degassed methanol under 50 bar CO. The catalyst was always generated *in situ* from 0.05 mmol $Pd(OAc)_2$. Mole ratio's are: $Pd(OAc)_2$: Ligand : nitrobenzene = 1 : 1.5 : 488. All reactions were performed in quadruplet and the relative standard deviation of all analytes was < 5% in all cases. [b] Conversion = $(\Sigma_{aryl\ converted})/24.4 \times 100\%$. [c] Selectivity towards carbonylation products = (MPC + DPU) / $\Sigma_{aryl\ converted} \times 100\%$. [d] Selectivity towards coupling products = $(2 \times Azo + 2 \times Azoxy) / \Sigma_{aryl\ converted} \times 100\%$. [e] Selectivity towards hydrogenation products = $(PhNH_2 + DPU) / \Sigma_{aryl\ converted} \times 100\%$.

6.2.2.2 The effects of the initial nitrobenzene concentration

Intrigued by the similar selectivity for reductive coupling products (mainly Azoxy) of $Pd^{II}(phen)$ and $Pd^{II}(L4X)$ catalyst systems, it was investigated if the selectivity for these coupling products can also be manipulated in the same way. As it was suspected that the coupling products stem form a disproportionation or 'metathesis' of a palladium–imido complex ("Pd=NPh") and nitrobenzene,[10] and because it is known that the selectivity towards coupling products depends on the concentration of nitrobenzene when using $Pd^{II}(L4X)$,[11] the initial concentration of the nitrobenzene was varied in the $Pd^{II}(phen)$ catalytic system. As is shown in Figure 6.3 (derived from data in Table S1), the relative ratio of carbonylation (NCO) and hydrogenation (NH) products over coupling (N=N) products decreases significantly with increasing nitrobenzene concentrations. This suggests that the formation of Azo(xy) coupling products from nitrobenzene involves a directly competing step with its carbonylation and hydrogenation, but with higher order kinetics in nitrobenzene.

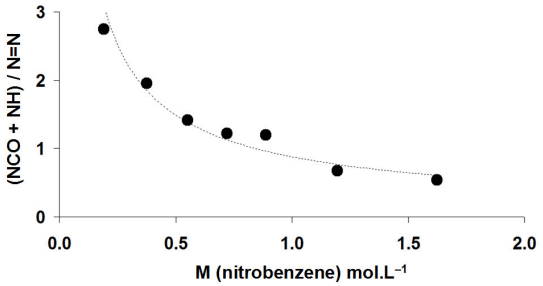

Figure 6.3. Plot of the ratio of (carbonylation (NCO) and hydrogenation (NH) products) relative to the amount of coupling products (N=N) as a function of the initial concentration of nitrobenzene in $mol.L^{-1}$, when using $Pd^{II}(phen)$ as catalyst precursor. The line is added as an aid for the eye.

6.2.2.3 The effects of the added acid

The selectivity towards coupling products in the Pd^{II}(L4X) catalytic system is sensitive to (sub)stoichiometric amounts of acid.[10] It is known that stoichiometric amounts of acid influence the selectivity for the Pd^{II}(phen) catalytic system.[14-16] Thus, some experiments were conducted wherein *sub*-stoichiometric amounts (on Pd) of *para*–toluenesulfonic acid (HOTs) were added, using the standard experimental conditions (i.e., 110 ºC for Pd^{II}(L4X) and 130 ºC for Pd^{II}(phen)).

As shown in Figure 6.4a for the Pd^{II}(L4X) catalytic system, the conversion increases when adding more HOTs, whereas for the Pd^{II}(phen) catalytic system (Figure 6.4b), the conversion remains constant. Interestingly, in both systems the coupling reaction is significantly suppressed already when adding *sub*-stoichiometric amounts of HOTs. The *selectivity* becomes however, drastically different for the two catalysts: when using Pd^{II}(L4X) as catalyst precursor, both the hydrogenation and carbonylation reactions become more important, whereas the carbonylation reaction becomes highly dominant when employing Pd^{II}(phen). This indicates that the influence of acid operates through a different reaction mechanism for both systems.

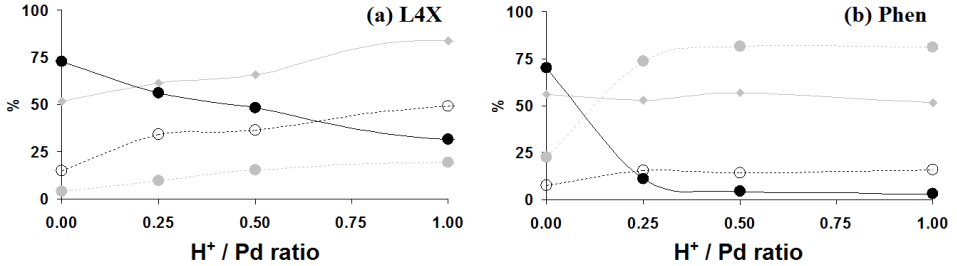

Figure 6.4. Plot of the conversion (♦) and selectivity towards coupling products (●, Azo(xy)), hydrogenation products (○, DPU+$PhNH_2$), and carbonylation products (●, MPC+DPU) as a function of the amount of *p*–toluenesulphonic acid added (relative to Pd), when using the ligands L4X @ 110 ºC (a) and phen @ 130 ºC (b). The lines are added as a guide for the eye.

To investigate if this effect may be related to the anion of the acid, rather than the acidity itself, some reactions were performed, adding half an equivalent of 1,3,5–trimethylbonzoic acid (TMBA, pK_a = 3.43),[17] HOTs (pK_a = –2.7),[17] or the dibasic phenylphosphonic acid (PPA, pK_{a1} = 1.85).[17] For the Pd^{II}(L4X) catalytic system (Figure 6.5a), the conversion increases in the order TMBA < HOTs < PPA, and the coupling is always suppressed mainly in favor of the hydrogenation.

For the Pd^{II}(phen) catalytic system, the conversion also increases in the order TMBA < HOTs < PPA, and the coupling reaction is also suppressed, but now very predominantly in favor of the carbonylation reaction.

That the effect with TMBA is less pronounced in the Pd^{II}(phen) system can be due to the relatively low acidity of this acid (compared to HOTs and PPA) or because TMBA can be partly esterificated with methanol at 130 ºC, as it has been reported that adding more of this acid also results in higher selectivity towards carbonylation products when using Pd^{II}(phen).[15]

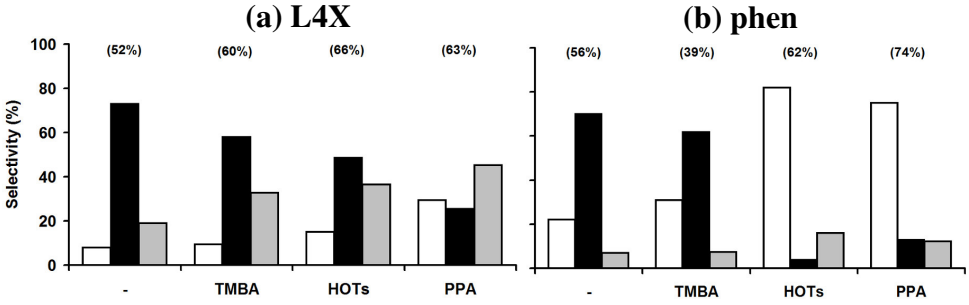

Figure 6.5. The selectivity when using Pd^{II}(L4X) @ 110 ºC (a) or Pd^{II}(phen) @ 130 ºC (b), and adding 0.5 equivalent (on Pd) of the indicated acid. Carbonylation products = □ (MPC+DPU), coupling products = ■ (Azo+Azoxy) and hydrogenation products = ■ ($PhNH_2$+DPU). The conversion based on nitrobenzene (within parentheses) is also given. All experiments were performed (using the same conditions as reported in Table 6.1) in triplo and the relative standard deviation of all analytes was always < 5%.

To further investigate if the effect of adding HOTs to the Pd^{II}(phen) system is really due to the proton concentration, it was attempted to buffer this strong acid by adding a weak base in the form of extra phen ligand. Shown in Figure 6.6a and b are the control experiments wherein the Pd:phen:HOTs molar ratio is 1:1.5:0 (Figure 6.6a) or 1:1.5:0.5 (Figure 6.6b), showing a ~7-fold decrease in coupling products on addition of acid. When using 5 equivalents of phen on Pd (Figure 6.6c), and adding 0.5 equivalents of HOTs (Figure 6.6d) led to ~5-fold decrease in coupling products. Adding more HOTs (Figure 6.6e), gives a gain in carbonylation selectivity to about 90 %, while a ~12 fold decrease in coupling products results compared to the experiment without adding HOTs (Figure 6.6c).

Note that in all three experiments using 5 equivalents of phen ligand (Figure 6.6c–e) the conversion increased (roughly from 50 to 90%). This can be ascribed to the stabilizing effect that extra phen ligand can have on zero valent palladium reaction intermediates.[16]

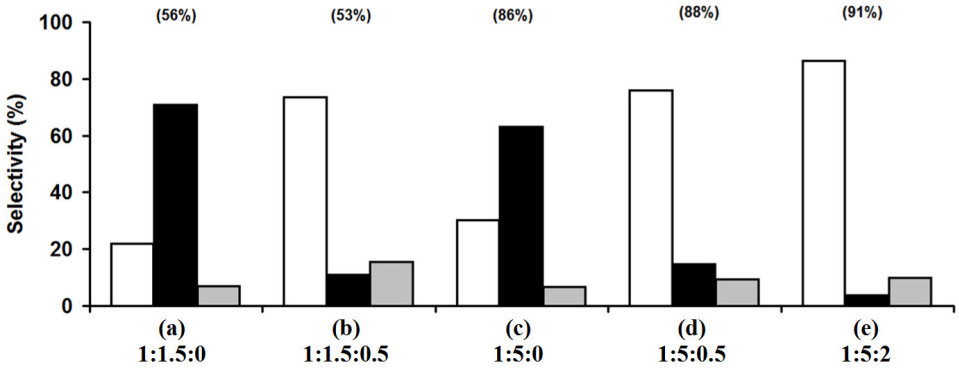

Figure 6.6. The selectivity when using a $Pd(OAc)_2$:phen:HOTs ratio of: (a) 1:1.5:0; (b) 1:1.5:0.5; (c) 1:5:0; (d) 1:5:0.5; (e) 1:5:2. Carbonylation products = □ (MPC+DPU), coupling products = ■ (Azo+Azoxy) and hydrogenation products = ■, ($PhNH_2$+DPU). The conversion based on nitrobenzene (within parentheses) is also given. All experiments were performed (using the same conditions as reported in Table 6.1) in triplo and the relative standard deviation of all analytes was always < 5%.

It thus appears for both catalytic systems, that when working under (mildly) acidic conditions, the coupling reaction is suppressed in favour of either the carbonylation product (Pd^{II}(phen)) or of both carbonylation and hydrogenation products (Pd^{II}(L4X)). For the Pd^{II}(phen) system, HOTs could be buffered by adding a weak base in the form of extra phen ligand.

6.2.2.4 Nitrosobenzene as intermediate for Azo or Azoxy?

It has been suggested that in the Pd^{II}(phen) catalytic system, nitrobenzene becomes first reduced to 'free' nitrosobenzene and then reacts further to form mainly Azoxy (and some Azo).[18, 19] It was investigated if elevated amounts of Azo and Azoxy could be detected when adding 2.5 mmol nitrosobenzene during a catalytic run (see experimental for details). As can be seen in Figure 6.7 however, when employing either Pd^{II}(L4X) or Pd^{II}(phen), both the conversion and selectivity are nearly identical to a 'normal' catalytic experiment. No significant increase in the selectivity for Azo (max. 1.5%) and Azoxy could be observed. Interestingly, no nitrosobenzene could be detected after the catalytic run, while a

significant amount of nitrobenzene was still present. This shows, that, consistent with the observation of only traces of nitrosobenzene in ordinary catalytic experiments, whereas nitrosobenzene is more prone to reductive carbonylation reactions[20] than is nitrobenzene, still a very similar product composition is obtained, and that nitrosobenzene must thus not be considered as prime intermediate towards Azo or Azoxy.

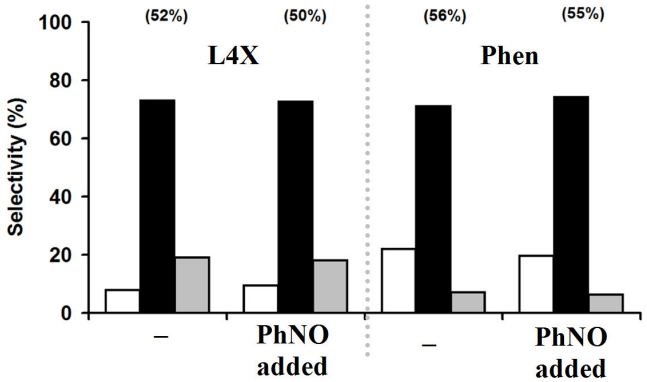

Figure 6.7. The selectivity when using Pd^{II}(L4X) @ 110 ºC (left) or Pd^{II}(phen) @ 130 ºC (right), with or without adding 2.5 mmol nitrosobenzene during a catalytic run. Carbonylation products = □ (MPC+DPU), coupling products = ■ (Azo+Azoxy) and hydrogenation products = ■ ($PhNH_2$+DPU). The conversion based on nitrobenzene(+nitrosobenzene) is given within parentheses. Conversion is based on ($\Sigma_{aryl\ converted}$)/(24.4+mmol PhNO added) × 100%. Reaction conditions were as reported in Table 6.1.

6.2.2.5 Azo or Azoxy as intermediate for MPC, DPU or aniline?

Azo or Azoxy, might be themselves intermediately produced and could react further to MPC, DPU and/or aniline, as is suggested when working with the Pd/phen/H^+ system at 155 ºC.[21] As shown in Table 6.2 however, when adding 2.5 mmol Azo (entry 2) or Azoxy (entry 3) to the Pd^{II}(phen) catalytic system, the same amount (plus the amount formed, entry 1) could be detected after the catalytic run, even when using 1 equivalent of HOTs and 2.5 mmol Azoxy (entry 4). This means that Azo and Azoxy are stable reaction products and cannot be intermediates towards MPC, DPU or aniline employing the standard reaction conditions of 130 ºC and 50 bar CO.

Table 6.2. Catalytic reaction employing $Pd^{II}(phen)(OAc)_2$ and using 4.9 mmol $PhNO_2$ and the indicated additives.[a]

			mmol analyte					
Entry	**Additive (mmol)**	**$\Sigma_{\varnothing}$**	**$PhNO_2$**	**$PhNH_2$**	**MPC**	**DPU[b]**	**Azo**	**Azoxy**
1	–	4.8	0.1	0.5	1.6	–	0.2	1.1
2	2.5 Azo	10.0	0.8	0.4	1.5	–	2.7	1.0
3	2.5 Azoxy	10.1	1.4	0.3	0.5	–	0.3	3.6
4	2.5 Azoxy + 0.025 HOTs	10.1	0.3	0.4	1.3	–	0.5	3.6

[a] Reactions were heated for four hours at 130 ºC in 25.0 ml dry and degassed methanol under 50 bar CO pressure. The catalyst was always generated *in situ* from 0.05 mmol $Pd(OAc)_2$. Mole ratio's are: $Pd(OAc)_2$: phen : nitrobenzene = 1 : 1.5 : 98. [b] not detected as the reaction mixture was a clear solution.

6.2.3. Synthesis and characterisation of possible palladium intermediates

6.2.3.1 (Attempted) synthesis of a palladacyclic complex and DFT calculations

Most mechanistic proposals for the Pd/phen catalytic system are centered around palladayclic intermediates, in particular the one shown in Scheme 6.2a.[7, 21-23] This five-membered palladacyclic complex is thermally stable to about 170 ºC,[23] but upon addition of an acid and heating to 90 °C in ethanol this complex smoothly decomposes to yield ethylphenylcarbamate (80%).[23] This complex was therefore also considered as a possible (MPC, DPU) product releasing intermediate for the L4X-palladium catalytic system.

The palladacycle with phen as the supporting ligand could easily be obtained (see experimental for details) according to a literature procedure.[23] When applying the same procedure and using L4X as the ligand however, the anticipated 'L4X-palladacycle' could not be obtained, nor was an asymmetric complex observed in the resulting reaction mixture, such as previously detected in ($^{31}P\{^{1}H\}NMR$) measurements for other phosphane-palladium catalysts.[11] One possible explanation for the apparent lack of 'L4X-palladacycle' formation, is that the steric constraints in the equatorial position of such five–membered ring species lead to its de-stabilisation. Especially since the steric constraints in such complexes is influenced by the ligand bite angle (β), which is much smaller for the ligand phen (~78º), than for bidentate diaryl phosphane ligands with a butylene backbone (96º). Indeed, when the above experiment was conducted with the sterically less demanding 'L3X' (i.e. 1,3–bis(diphenylphosphino)–

2,2'dimethylpropane), the asymmetric complex, be it initially clearly formed, is gradually disappearing over time (during the workup). DFT calculations of the palladacycle with L3X,[10] but also with L4X and L4 (a simplified version of L4X) as the supporting ligand (see section AV.1. of Appendix V for details), indeed suggest that phosphane ligands can significantly (ca. 15 kcal.mol^{-1}) destabilize the palladacycle relative to the phen-analogue.

6.2.3.2 Ligand exchange experiment of 'phen-palladacycle' with L4X

An alternative strategy was envisaged to obtain a 'di-phosphane–palladacycle' by ligand exchange reaction between 'phen–palladacycle' and a phosphane ligand, such as shown successful for the L3X-palladium system.[11] When this ligand exchange experiment was repeated with L4X as the ligand (see experimental for details), the anticipated asymmetric palladacyclic species could not be detected however, but the final product of the palladacycle decomposition process, namely [$Pd^0(L4X)_2$], as well as 'free' phen ligand clearly evolved (see section AV.2 of Appendix V for details). This suggests that (like with L3X) a ligand exchange indeed took place, but that the decomposition of the resulting strained 5-ring is expedited so much as to prevent significant build-up of intermediate concentrations, probably due to the even larger bite angle of L4X (96º) compared to L3X (90º).[24]

6.2.3.3 ESI-MS analysis of 'phen-palladacycle'

The decomposition *pathway* of 'L3X-palladacycle' (and probably also of 'L4X-palladacycle') was shown to proceed likely first *via* a *reversible* decarbo**n**ylation (–CO), and followed by an *irreversible* decarbo**x**ylation (–CO_2) to give a reactive palladium-imido ('Pd^{II}=NPh') complex from which organic 'PhN' containing products ultimately evolve.[10, 11] This means that, at least under the mild ligand-exchange conditions, the barrier for decarbo**n**ylation of 'L3X-palladacycle' must be lower than that of the decarbo**x**ylation (in which case the palladacycle would have been an *isocyanate releasing* species). A prime source of evidence for this reaction sequence was the defragmentation pattern of 'L3X–palladacycle' as obtained from an electron spray ionization mass spectrum (ESI–MS) taken directly after the ligand exchange took place. As the 'phen–palladaclycle' could be synthesized *and* isolated as a thermodynamically stable compound (see

experimental for details),[23] its defragmentation with ESI–MS was studied in order to see whether the 'phen–palladacycle' would decompose in a similar manner as the 'L3X–palladacycle'.

Due to the poor solubility of 'phen–palladaycle' in various common solvents, a saturated solution of 'phen–palladacycle' in nitrobenzene was introduced *directly* into the ESI–source (instead of using an injector with an eluent). However, when using the same ionization conditions that were successful for measuring the defragmentation of 'L3X–paladacycle' (i.e., 3 kV and 300 °C), no clear mass spectrum could be obtained. Only when the ionization temperature was elevated to 450 °C could a proper mass spectrum be recorded; this is in line with the DFT–calculations, which suggested that the palladacycle is more stable when the supporting ligand is phen, relative to a diphosphane ligand such as L3X[10] or L4X (*vide supra*). The mass spectrum of this experiment is shown in Figure 6.8a and a simulation of the most prominent peaks is given in Figure 6.8b.

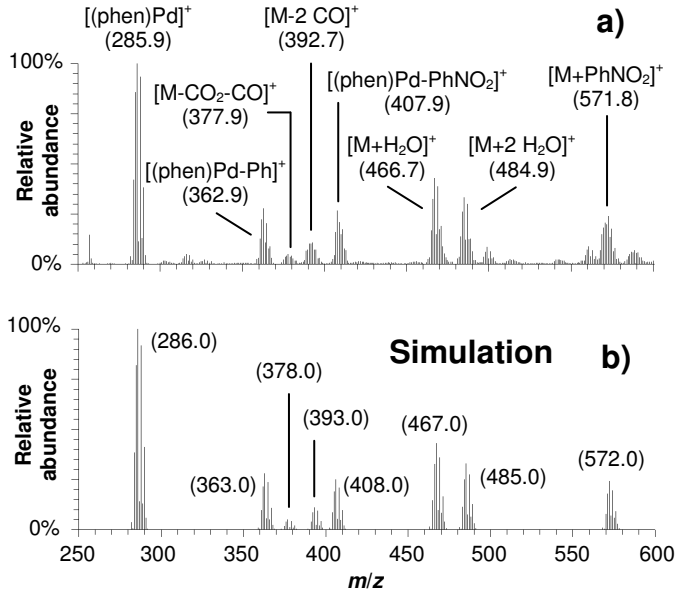

Figure 6.8. (a) ESI mass spectrum of a saturated solution of 'phen–palladacycle' (M) in nitrobenzene; (b) simulation of the most prominent MS peaks.

The highest significant mass around m/z = 571.8 is consistent with a nitrobenzene solvent adduct of 'phen–palladacycle' (exact mass is 572.0; recall that the solid state structure of 'phen–paladacycle' also contains a nitrobenzene molecule in its

lattice). The mass and isotope distributions of the two features found around *m/z* = 466.7 and 484.9 are in perfect agreement with $[M + H_2O]^+$ and $[M + 2\ H_2O]^+$ respectively, as is also explicitly shown in Figure 6.9. The H_2O in these adducts probably derives from trace amounts of water in the solvent nitrobenzene.

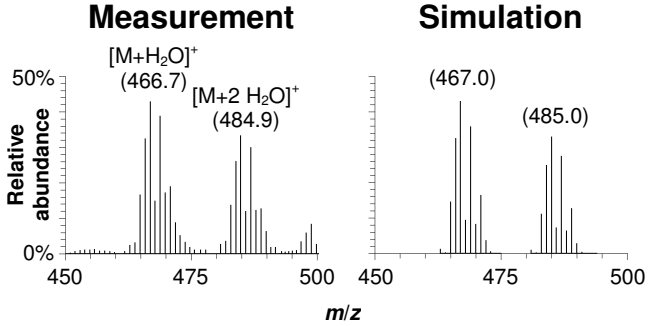

Figure 6.9. Zoom–in and assignment of the ESI mass spectrum of 'phen–palladacycle' ('M', see Figure 6.8) together with a simulation of the mass and isotope distribution.

Although the structure of 'phen–palladacycle' is well-documented,[22, 23] and the purity of the batch used was verified by elemental analysis, IR–, and ^1H–^1H–COSY–NMR spectroscopy (see experimental and Appendix V, Figure AV.3), the $[M]^+$ peak (exact mass is 449.0) was not observed. Also, the mono–decarbo**n**ylated fragment ($[M–CO]^+$, exact mass of 421.0) was not observed, while the mass of the di–decarbo**n**ylated fragment $[M–2CO]^+$ (i.e. a nitrosobenzene complex) is present around *m/z* = 392.7 (exact mass 393.0). Surprisingly, the feature around *m/z* = 407.9 cannot be ascribed to the anticipated palladium bound phenylisocyanate (i.e. $[M–CO_2]^+$), as the exact mass of this species (405.0) differs three units. Instead, it is tentatively assigned to a $[(phen)Pd–C_6H_4NO_2]^+$ complex as follows. The most abundant mass observed is that of $[(phen)Pd]^+$ around *m/z* 285.9 (exact mass 286.0), and a phenyl–adduct of this species seems also to be present (i.e., *m/z* = 362.9; $[(phen)Pd–Ph]^+$, exact mass 363.0). As the experiment was performed in a nitrobenzene solvent matrix, the mass around 407.9 can thus best be assigned to a nitrophenyl–adduct of $[(phen)Pd]^+$, i.e.: $[(phen)Pd–C_6H_4NO_2]^+$ (exact mass is 408.0). Interestingly, the mass of the very small peak around *m/z* = 377.9 is in agreement with a $(phen)Pd^{II}$=NPh complex (i.e., $[M–CO_2–CO]^+$, exact mass 378.0).

As the ESI mass spectrum is very likely to reflect the thermal decomposition of 'phen-palladacycle', the defragmentation pattern surprisingly suggests that 'phen–palladacycle' may decompose (like 'L3X–palladacycle') predominantly *via* an initial decarbo**n**ylation (–CO) instead of a direct decarbo**x**ylation ($-CO_2$) , to palladium bound phenylisocyanate). After the first decarbo**n**ylation a second may follow, or CO_2 can be extruded to form the imido intermediate '(phen)Pd^{II}=NPh', which may decompose further to $[(phen)Pd]^+$ (thus giving rise to the observed adducts thereof).

6.2.3.4 In situ trapping of a Pd–imido complex in the Pd^{II}(phen) system

It was demonstrated elsewhere in Chapters 3 and 4,[10] that a palladium imido complex 'Pd^{II}=NPh' is by far the most likely species to be considered as prime intermediate in Pd/diphosphane catalyzed reductive carbonylation of nitrobenzene. One piece of additional evidence for the possible intermediacy of 'Pd^{II}=NPh' under reaction conditions when employing diphenyl phosphane ligands such as L4X, comes from nitrobenzene carbonylation experiments in which cyclohexene[25] was added to trap the nitrene ligand ('NPh') in these species; a reaction analogous to trapping of carbenes by alkenes.[26-29] Convincing mass spectroscopic evidence was thus obtained for the formation of a three membered cyclic amine *via* a reaction as depicted in Scheme 6.4:

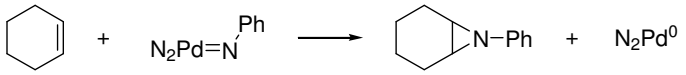

Scheme 6.4. Trapping reaction of an imido complex with cyclohexene.

As the above ESI–MS experiment suggests that '(phen)Pd^{II}=NPh' may be formed from 'phen–palladacycle', it seems likely that such an imido complex may be an intermediate in Pd/phen catalytic system as well. The trapping experiment was therefore repeated with Pd^{II}(phen) as the catalyst precursor (at 130 °C, see experimental for details), indeed revealing the presence of the same trapping product (GLC–MS analysis). This thus lends credibility to the presence of a palladium–imido complex ('Pd^{II}=NPh') under actual catalytic carbonylation conditions.

6.2.4. DFT study of nitrobenzene de-oxygenation with CO

The above data suggests that the palladacyclic species shown in Scheme 6.2a may decompose to an imido intermediate when the supporting ligand is either phen or a phosphane ligand such as L3X or L4X. To relate these data to the actual catalytic process under carbonylation conditions, the possible deoxygenation pathways of nitrobenzene to the palladayclic and/or palladium-imido complex were studied using DFT calculations. Because of computational limitations, no attempts were undertaken to estimate the reaction barrier from one complex to another. Instead, the approach here was to estimate the Gibbs free energies for the relevant complexes (see Scheme 6.5), *via* the methodology explained and validated in sections AV.3. and AV.4. of Appendix V. In essence, the enthalpy differences were estimated using DFT calculations and the changes in entropy were estimated at the relevant reaction temperature from literature data (standard molar entropy (S°) in $J.mol^{-1}.K^{-1}$). Hence, the data shown in Scheme 6.5 are the estimated Gibbs free energies at 110 °C for complexes containing L4X, and at 130 °C for complexes containing phen as the supporting ligand.

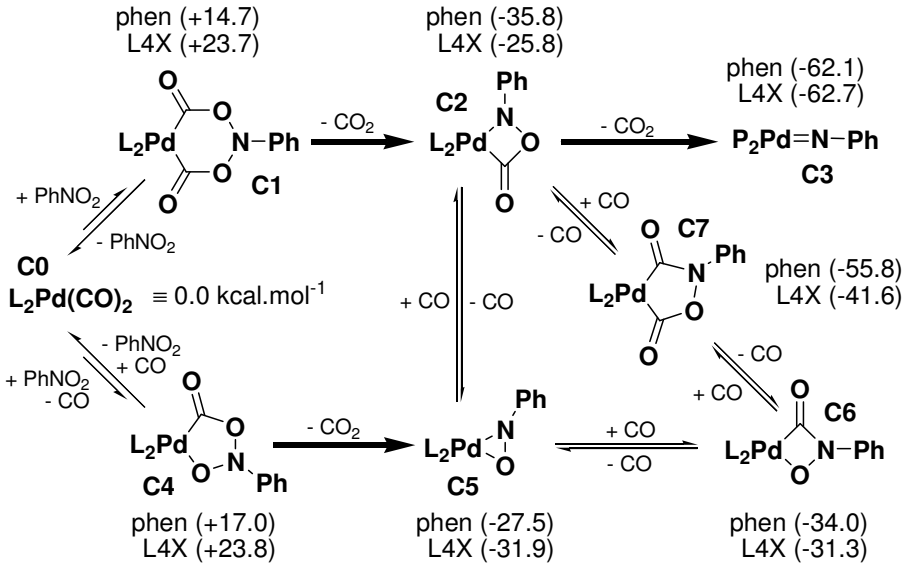

Scheme 6.5. L_2Pd-catalyzed nitrobenzene de-oxygenation process with CO, as computed with DFT calculations (see sections AV.3. and AV,4, of Appendix V for details) for L_2 is phen (@ 130 °C) or L4X (@ 110 °C. Data is given in $kcal.mol^{-1}$ relative to complex **C0**.

The starting compound for the nitrobenzene reduction process is most likely the zero-valent complex $L_2Pd(CO)_2$ (**C0**), which is therefore defined as 0.0 kcal.mol^{-1}. The oxidative coupling of **C0** with nitrobenzene can proceed either *via* **C1** or **C4.** No preference can be given as **C1** and **C4** are similar in energy for both phen and L4X. Also, the *irreversible* CO_2 extrusions **C1→C2** and **C4→C5** are both roughly equally highly exothermic (ca. –50 kcal.mol^{-1}), thereby completing the first deoxygenation step of nitrobenzene.

Complexes **C2** and **C5** differ merely ca. 8 kcal.mol^{-1}; both may thus very well interconvert into each other *via* a reversible carbonylation/decarbonylation process. Likewise, the equilibrium reactions **C2⇆C7**, **C5⇆C6**, and **C6⇆C7** are all likely to be reversible carbonylation/decarbonylation reactions, meaning that **C2**, **C5**, **C6** and **C7** are probably all interconvertable into one another. Note that the palladacycle **C7** in the most stable complex of these (presumably) CO equilibrated species, both when phen and when L4X is the supporting ligand. Note also that the oxidative coupling of nitrosobenzene with CO (i.e. **C5⇆C2** and **C5⇆C6**) is exothermic by ca. –8 kcal.mol^{-1} whereas the oxidative coupling of nitrobenzene with CO is endothermic (i.e., **C0⇆C1** and **C0⇆C4**) by ca. +20 kcal.mol^{-1}; this is in line with the finding (section 3.2.2.4) and literature data[20] that nitrosobenzene is more easily reduced than nitrobenzene.

The second de-oxygenation of nitrobenzene can only occur by the *irreversible* CO_2 extrusion from **C2** to the imido complex **C3**, which is also the most thermodynamically stable complex (ca. –62 kcal.mol^{-1}). Finally, it is worth noting that all the palladacycles that are formally Pd^{II} species and sterically crowded in the equatorial positions of Pd (i.e., **C1**, **C2**, **C4**, and **C7**) are all destabilized by ca. 10 kcal.mol^{-1} by the bulkier L4X ligand relative to phen. The formally zero-valent palladium-nitrosobenzene complex **C5** is more stable when L4X is the supporting ligand due to the increased acidity of palladium as induced by the increaded π-backbonding from Pd to P.

These data thus strongly suggest that the main de-oxygenation pathway is **C0⇆C1→C2→C3**, and that complexes **C5**, **C6**, and **C7** can be seen as carbo**n**ylatio/decarbo**n**ylation equilibrated equivalents of **C2**.

6.3. Discussion

6.3.1. Overall mechanism with P_2Pd catalysts: a network centered around a P_2Pd^{II}=NPh complex

During the studies into the reductive carbonylation of nitrobenzene in methanol, as described in Chapters 3–5, it was discovered that besides CO, methanol acts as the (co-)reductant for nitrobenzene to eventually give a palladium-imido complex as the central 'PhN' product releasing species.[10, 11] This deoxygenation process involves oxidation of Pd^0 to Pd^{II}, and can be described by the half–reactions given in Equations 1a–c.

$P_2Pd^0 + PhNO_2 + 2\ CO \rightarrow P_2Pd^{II}{=}NPh + 2\ CO_2$ (1a)
$P_2Pd^0 + PhNO_2 + 2\ CO + 2\ CH_3OH \rightarrow P_2Pd^{II}{=}NPh + H_2O + CO_2 + DMC$ (1b)
$[P_2Pd^0 + PhNO_2 + 3\ CO + 2\ CH_3OH \rightarrow P_2Pd^{II}{=}NPh + H_2O + CO_2 + DMC$ (1b)*]
$P_2Pd^0 + PhNO_2 + CH_3OH \rightarrow P_2Pd^{II}{=}NPh + CO + 2\ H_2O$ (1c)
$[P_2Pd^0 + PhNO_2 + 2\ CH_3OH \rightarrow P_2Pd^{II}{=}NPh + MF + 2\ H_2O$ (1c)*]

The reduction of Pd^{II}=NPh to Pd^0 and the various 'PhN' containing products as described by Equations 2a-c makes the process catalytic.

$P_2Pd^{II}{=}NPh + CO + CH_3OH \rightarrow P_2Pd^0 + MPC$ (2a)
$[P_2Pd^{II}{=}NPh + CO + PhNH_2 \rightarrow P_2Pd^0 + DPU$ (2a)*]
$P_2Pd^{II}{=}NPh + CO + 2\ CH_3OH \rightarrow P_2Pd^0 + PhNH_2 + DMC$ (2b)
$[P_2Pd^{II}{=}NPh + 2CO + 2\ CH_3OH \rightarrow P_2Pd^0 + PhNH_2 + DMO$ (2b)*]
$P_2Pd^{II}{=}NPh + CO + PhNO_2 \rightarrow P_2Pd^0 + Azoxy + CO_2$ (2c)
$[P_2Pd^{II}{=}NPh + 2CO + PhNO_2 \rightarrow P_2Pd^0 + Azo + 2\ CO_2$ (2c)*]

A combination of the half–reactions that oxidize Pd^0 to Pd^{II} (eq. 1) with the half–reactions that reduce Pd^{II} to Pd^0 (eq. 2), naturally leads to the overall possible stoichiometries as described in detail in Chapter 3.[10] Such a combination allows for the construction of a relatively simple and unifying catalytic scheme, rationalizing the formation of *all* methanol oxidation products and *all* nitrobenzene reduction products (Scheme 6.6).

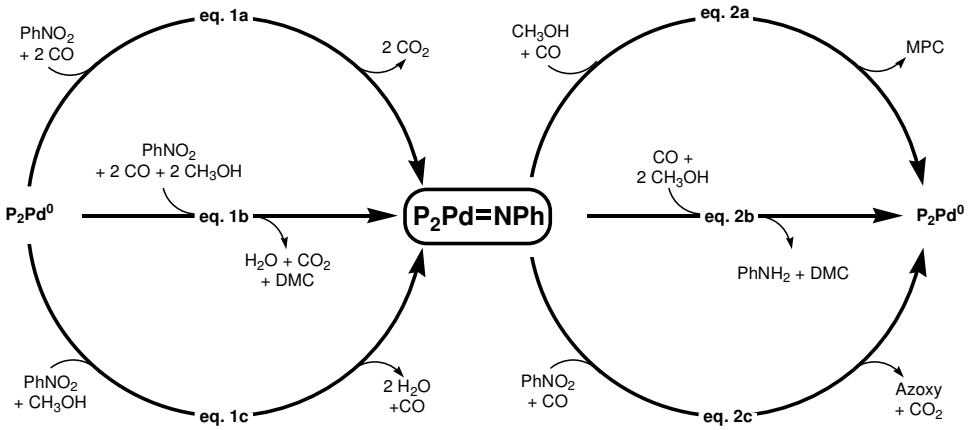

Scheme 6.6. Proposed reaction scheme for the overall catalytic processes.

6.3.2. Molecular mechanism of nitrobenzene deoxygenation

The current understanding of the molecular basis underlying the de-oxygenation stoichiometries given by Equations 1a-c for phosphanes as the supporting ligand (L_2) is shown in Scheme 6.7.[11]

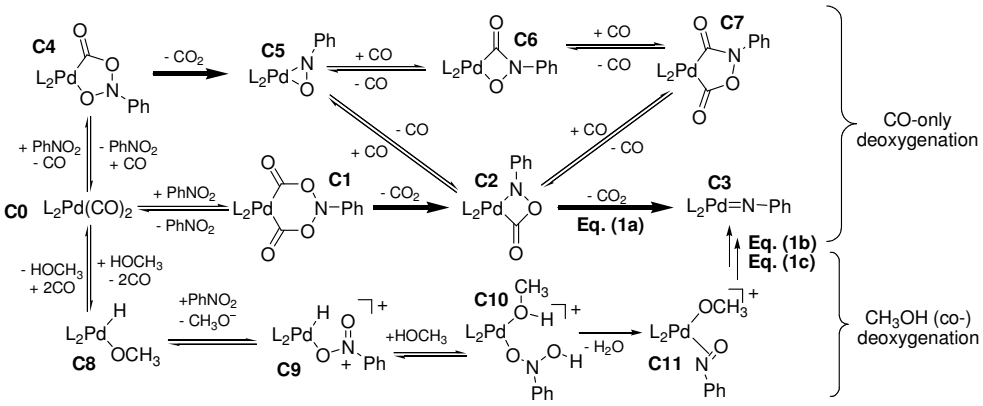

Scheme 6.7. Working hypothesis for the formation the palladacyclic intermediate (top) and the Pd–imido intermediate (centre and bottom), in the deoxygenation of nitrobenzene.

As also supported by the DFT calculations reported in this chapter, the most likely CO-only deoxygenation route commences with an oxidative coupling of nitrobenzene and CO in $L_2Pd^0(CO)_2$ (**C0**) to form **C1**, followed by a series of *irreversible* decarbo**x**ylation steps (i.e., **C1→C2→C3**, centre in Scheme 6.7). The final product **C3**, i.e., the Pd-imido complex, is then the *sole* 'PhN'-containing product releasing species (i.e., producing MPC, DPU, $PhNH_2$, and Axo(xy), *vide infra*).[10, 11] The carbo**n**ylation/decarbo**n**ylation equilibrated species **C5**, **C6**, and **C7** (top in Scheme 6.7) all act merely as temporary reservoir of the 'PhN' fragment, and none are likely to be a product releasing species. Not even the palladacycle **C7** should be considered as such, as it was found that the barrier for decarbo**x**ylation (CO_2 loss) is higher than the barrier for decarbo**n**ylation (CO loss) of **C7**, at least when using bidentate diaryl phosphane ligands (see Chapter 4).[11] The methanol de-oxygenation routes are thought to commence by oxidative addition of methanol on 'L_2Pd^0' (bottom in Scheme 6.7) to **C8** and most likely proceed *via* (**C8⇆C9⇆C10→C11**) palladium hydride chemistry to eventually form the same palladium-imido intermediate **C3**, as is discussed in more detail elsewhere.[11]

Clearly, the fraction of nitrobenzene that is de-oxygenated with CO-only or (also) with methanol *must* depend on the characteristics of the catalyst employed, as predetermined by the properties of the supporting ligand. Indeed, when employing L4X in the catalyst, the CO-only de-oxygenation route contributes merely 9%, whereas this is 72% when this ligand is functionalized with electron-donating methoxy groups.[10] Likewise, when using the even more basic phen as the supporting ligand, the CO-only de-oxygenation pathway contributes 97%,[30] meaning that the oxidation of methanol is almost completely suppressed. This relationship between the basicity of the Pd-centre (induced by that of the ligand) and the fraction of CO-only de-oxygenation may come as no surprise: it is indeed well-known that when palladium is made more basic, it binds stronger to carbon monoxide by increased electron backdonation of the filled dπ orbitals of Pd into the empty π^* orbitals of CO.[31] Hence, the dissociation of CO from **C0** to open the pathway towards **C8** will be hampered, thus effectively blocking methanol oxidation while facilitating the CO-only de-oxygenation.

Based on the ESI-MS spectrum of the 'phen-palladacycle' (i.e. 'phen-**C7**'), the trapping experiment with cyclohexene, the ligand exchange experiment, the

dependency of the Azo(xy) selectivity on the nitrobenzene concentration, and the DFT results, it is propose here that the molecular mechanism of the CO-only deoxygenation shown in Scheme 6.7 is a general one and is also valid for the Pd/phen catalytic system. That is, it is proposed that 'phen-**C7**' –commonly thought to be the product releasing species– in *not* a (main) product releasing species under normal (acid-free) catalytic carbonylation conditions. Instead, 'phen-**C7**' merely is part of the several CO-equilibrated species (**C2**, **C5**, and **C6**) that together act as temporary 'PhN' reservoir.

This insight, together with the DFT studies also explains why 'phen-**C7**' can be obtained under mild carbonylation conditions (60 °C, ethanol);[23] **C7** is the thermodynamically most stable of the CO-equilibrated species and is therefore thought to be the resting state of the catalyst. At elevated temperatures, 'phen-**C7**' *may* be decarbo**x**ylated to phenylisocyanate (and thus MPC and DPU), but judging from the product distribution of the reaction under 'normal' conditions, this cannot be the (dominant) pathway; merely 20% MPC but 70% Azoxy are produced. This must mean that, in line with the results reported above, that the reaction barrier for 'phen-**C7**' decarbo**x**ylation (to 'PhNCO') is higher than that of 'phen-**C7**' decarbo**n**ylation (to **C2** and/or **C6**). Irreversible decarbo**x**ylation of **C2→C3** then removes the catalyst from the CO-equillibrated 'PhN' reservoir.

The different temperature required when phen (130 °C) or L4X (110 °C) is used as the supporting ligands may be ascribed to the destabilizing effect that the bulkier L4X has on palladacycles such as **C7** (as indicated by DFT); both the decarbo**n**ylation barriers (of e.g. **C7⇆C2**), as well as the barrier for decarbo**x**ylation of **C2→C3** will be lowered, thus allowing the 'PhN' fragment to escape the temporary reservoir more easily and thus also allowing the application of milder temperatures.

6.3.3. Molecular mechanism of reaction of the Pd^{II}=NPh intermediate

As is shown in Scheme 6.8,[10, 11] once the imido intermediate **C3** has been formed, it can undergo a disproportionation reaction with nitrobenzene and CO to produce and azoxybenzene and CO_2 as stable end products. It has been proposed that Azoxy stems from a reaction between 'free' nitrosobenzene and a nitrene ('PhN'),[15, 18] or a supposed condensation reaction of nitrobenzene with aniline.[19]

It was shown however, that adding extra nitrosobenzene during a catalytic run did not result in more Azoxy. It was also observed that nitrosobenzene is more easily reduced than nitrobenzene, which is corroborated by the DFT–studies reported in this chapter, and finds support in literature as well.[18, 32, 33] Besides, it is known that Azoxy cannot be formed by a condensation reaction of aniline and nitrobenzene during catalysis, as a carbonylation experiment with deuterated nitrobenzene and undeuterated aniline gave only fully deuterated Azoxy when working with the Pd/phen catalytic system.[34] As an alternative to the disproportionation, the imido intermediate **C3** can also be protonated by methanol to produce $PhNH_2$ (bottom right) and/or MPC (top right); all three reactions result in a zero-valent palladium species that can re-enter the catalytic cycle and thus make the overall processes catalytic (see also Scheme 6.6).

Because one N=O bond in nitrobenzene is formally fully polarized, nitrobenzene is thought to associate strongest to the (also very polarized) Pd=N bond in **C3** (relative to charge-neutral methanol). As a result, the disproportionation reaction dominates, resulting in the observed selectivity towards Azoxy (70%) for both catalyst systems.

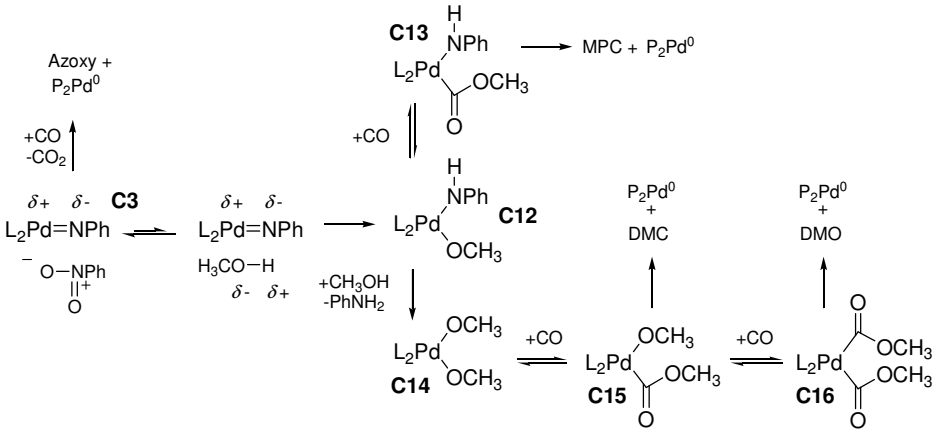

Scheme 6.8. Working hypothesis for the molecular mechanism of L_2Pd^{II}=NPh (**C3**) reduction to 'L_2Pd^0' and the various aryl-containing nitrobenzene reduction products.

The protonation of **C3** by methanol will give **C12** which may undergo a carbonylation to **C13** *via* an associative displacement of CH_3O^- by the smaller and charge neutral CO, followed by nucleophilic attack of nearby CH_3O^- on

coordinated CO and finally a reductive elimination to produce MPC. Such a mechanism to produce MPC is very similar to the one recently proposed by Ragaini and co-workers involving first full reduction of nitrobenzene to aniline and a phenPd($C(O)OCH_3$)$_2$ species, which is supposed to react with aniline to give the isocyanate.[19, 35] Yet the mechanism proposed in this chapter differs significantly in that it is the precursor for aniline formation –i.e. the palladium imido intermediate– that is methoxycarbonylated to MPC. Any Pd-imido that escapes methoxy carbonylation may convert to azoxy (by a reaction with nitrobenzene) or aniline by protonation by methanol and subsequent DMC/O formation. Thus, as an alternative to MPC formation, **C12** may be protonated to **C14** while liberating aniline. **C14** will then be carbonylated once or twice *via* associative displacement/nucleophilic attack to give **C15** and **C16**, from which reductive elimination will produce DMC and DMO respectively.

As it appears from the data in this chapter, the carbonylation of **C12** is favoured when phen is the supporting ligand (20% MPC), whereas the protonation of **C12** is favored in case of L4X (20% $PhNH_2$). This effect can be understood by the difference in basicity of both ligands; the more basic phen will destabilize the Pd–OCH_3 bond in **C12** more, thus facilitating the associative displacement by CO leading to MPC (*via* **C13**).

What all the above means, is that the mechanistic understanding of nitrobenzene reductive carbonylation in a CO/CH_3OH environment with diphosphane stabilized palladium complexes (as developed in this thesis), translates directly to the mechanism of this reaction when phen is the supporting ligand. Here too the network of catalytic cycles centered around a palladium-imido intermediate (Scheme 6.6) can rationalize the formation of *all* the products observed, and –moreover– can relate the catalyst performance to its characteristics as imposed by the supporting ligand (Scheme 6.7 and Scheme 6.8), whether this is a N- or P-donor.

6.3.4. Effect of added acid

With the understanding of the mechanism unfolded above, it can also be easily rationalized why adding sub-stoichiometric amounts (on Pd) of acid has such a dramatically different effect on the selectivity of the Pd^{II}(phen) (> MPC) and the

Pd^{II}(L4X) (>$PhNH_2$) catalytic systems. As explained above, under 'normal' conditions, the palladacycle **C7** (with either phen or L4X) is *not* a (main) product releasing species due to the too high barrier for decarbo**x**ylation relative to decarbo**n**ylation. When an acid as co-catalyst is added however, the decarbo**x**ylation *barrier* is dramatically lowered, presumably by protonation at N of the palladacycle; in the case of 'phen-**C7**' apparently to the point where CO_2 extrusion is favored relative to decarbo**n**ylation. As a result, now 'phen-**C7**' *becomes the main product releasing species*, selectively producing MPC. The imido-intermediate 'phen-**C3**' will then only scarcely be formed, hence explaining the strongly decreased azoxybenzene selectivity (from 71 to ~15%). This is in line with the findings of Osborn and co-workers, whom reported that 'phen-**C7**' is thermally very stable, but in the presence of an acid (catalyst) smoothly decomposes to ethyl phenyl carbamate when heated in ethanol at merely 90 °C.[23]

For the Pd^{II}(L4X) system however, although the barrier for 'L4X-**C7**' decarbo**x**ylation is most probably also lowered when adding acid, the barrier for 'phen-**C7**' decarbo**n**ylation is still lowest. This is most likely due to the fact that, as corroborated by DFT, 'L4X-**C7**' is less stable than 'phen-**C7**' which surely must have a similar effect of the 'L4X-**C7**' decarbo**n**ylation reaction *barrier*. As a consequence, 'L4X-**C3**' will still be formed predominantly, and thus remains the (main) product releasing species. The suppressing effect on azoxybenzene production in favor of the carbonylation *and* hydrogenation (see Figure 6.4), can be rationalized by an acid-assisted protonation of **C3** to **C12**, thereby hampering the disproportionation. Note that the suppressing effect on Azoxy production is less than that observed for the Pd/phen/H^+ system, because the 'Pd=NPh' species is hardly formed in this phen/H^+-system in the first place. That in the Pd/L4X/H^+ system the hydrogenation is promoted somewhat more that the carbonylation can easily be understood; protonation of the [$PhNH^-$] ligand in **C12** to aniline will be facilitated by the acid, in expense of the associative replacement of the [CH_3O^-] ligand in **C12** by CO. It is important to note that in line with this mechanism, when adding an acid to the Pd^{II}(phen) system, the amount of DMC+DMO produced declines (from 0.5 to 0.2 mmol being very small), whereas the amount of DMC+DMO is increased (from 8.2 to ~13 mmol) when employing Pd^{II}(L4X) (see Table S1 for details).

6.4. Conclusions

The palladium-imido species L2Pd=NPh (**C3**) and the palladacycle L2PdC(O)N(Ph)OC(O) (**C7**) were considered as possible carbonylation product-releasing species for both phen and L4X. The results of catalytic experiments, supported by spectroscopic (ESI-MS and NMR) evidence and a DFT study suggest that the palladacyclic compound **C7** is not the major product-releasing intermediate in reactions performed in the absence of acid. The unified mechanistic proposal for the carbonylation of nitrobenzene in methanol, catalyzed by the palladium-phenanthroline system is illustrated in Scheme 6.9. In the absence of acid the proposed mechanism for Pd/diphosphane catalysts (Scheme 6.6)[10, 11] *applies directly* to the Pd/phen catalytic system: the Pd-imido complex **C3** is the central 'PhN-containing' (Azoxy, MPC, $PhNH_2$) product releasing species, producing mainly the coupling product Azoxy. On the other hand, in the presence of acid the palladacyclic complex **C7** *becomes* the major product-releasing species, resulting in the selective formation of the nitrobenzene carbonylation product MPC.

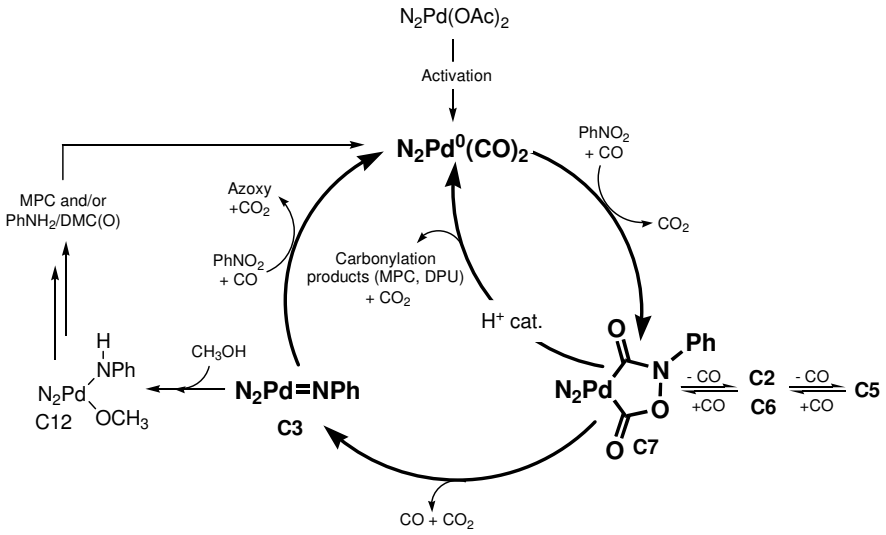

Scheme 6.9. Working hypothesis for the overall catalytic processes in the palladium catalyzed reduction reactions of nitrobenzene when 1,10–phenanthroline (N_2) is the supporting ligand.

6.5. Experimental section

6.5.1. General remarks

All solids were purchased from Acros organics and used as received. Methanol, nitrobenzene and aniline were all of analytical reagent purity, and were distilled under an argon atmosphere over the appropriate drying agent.[36] After the distillation, these liquids were saturated with argon. It was ensured that no water was present using an analytical reaction with trimethylorthoformate according to a literature procedure.[37] Carbon monoxide (> 99% pure)[38] was purchased from Linde gas benelux B.V. and used as received.

^{1}H–, and ^{13}C–NMR spectra were recorded on a Bruker DPX300 (300 MHz) or a Bruker DMX400 (400 MHz) machine. A Finnigan Aqua Mass Spectrometer (MS) with electro spray ionization (ESI) was used to record mass spectra. Samples were directly introduced into ESI–source that was heated at 450 °C. The voltage of the capillary and the voltage for the aquamax were set at 3 kV and 50 V respectively. High pressure experiments were conducted in stainless steel autoclaves (100 ml) equipped with two inlet/outlet valves, a burst disc, a pressure sensor, and a thermocouple. The autoclaves were heated by a Hell© polyBLOCK electrical heating system. Temperatures and pressures where measured with probes connected to a computer interface making it possible to record these parameters throughout the course of the reaction.

6.5.2. Catalytic / high pressure reactions

In a typical catalytic experiment, 0.05 mmol $Pd(OAc)_2$ and 0.075 mmol ligand (and if relevant another additive) were weighed and transferred into an autoclave, together with a magnetic stirring rod. The autoclave was tightly closed and subsequently filled with argon using a Schlenk–system that was connected to the one of the valves of the autoclave. Through the other valve was added 2.50 ml (24.4 mmol) dried and degassed nitrobenzene, under a continuous flow of argon. In a similar fashion, 25.0 ml dried and degassed methanol was then added. This reaction mixture was allows to stir at 500 rpm for about 15 minutes to ensure that complex formation was complete.[39] The autoclave was then inserted into the heating block and put under 50 bar carbon monoxide gas. The reaction mixture was heated to 110 or 130 ºC (within 30 minutes) under stirring at 500 rpm. After standing for four hours at a certain temperature, the autoclave was cooled to room temperature in about one hour. The autoclave was then slowly vented to atmospheric pressure and the reaction mixture was analyzed as described in Chapter 3.[10] To ensure reproducibility, some standard catalytic reactions were performed in quadruplet, and the relative standard deviation was always less than 5% for each analyte.

6.5.3. Adding a reactant during a catalytic run

In experiments wherein a compound was added during a catalytic run, the experiment was first started as a normal high pressure experiment (see above). A stainless steel hollow pipe (10 ml), sealed with two valves on each side was then put under an argon atmosphere, and nitrosobenzene (2.5 mmol in 5 ml methanol) or cyclohexene (2.5 mmol, 0.25 ml) were transferred into the hollow pipe using standard Schlenk techniques. The bottom valve of the hollow pipe was then mounted on one of the valves of the autoclave, connected to the CO supply, and pressurized to about five bar above the pressure inside the autoclave. At about one hour reaction time, nitrosobenzene or cyclohexene was added to the reaction mixture by opening the two valves in between the autoclave and the hollow pipe. The reaction was then allowed to run for the remaining reaction time, and treated as any other catalytic experiment.

6.5.4. NMR experiment

4.50 mg (10 μmol) of 'phen–**C7**'[23] was weighed into an NMR tube and put under argon. In another tube, 8.96 mg (18 μmol) of L4X was dissolved in 0.6 ml d^5–nitrobenzene under an argon atmosphere. Of this solution, 0.5 ml (15 μmol of L4X) was added to the 'phen–**C7**' complex using a 1 ml syringe, which was dry and flushed with argon. The thus obtained mixture (30 mM L4X, 20 mM 'phen–**C7**') was thoroughly mixed using a vortex mixer and measured with $^{31}P\{^1H\}$–NMR spectroscopy. After the first measurements, the yellow suspension was carefully heated to about 50 ºC, resulting in a clear yellow–orange solution which was again measured. While maintaining the temperature within the NMR spectrometer at 50 ± 2 ºC,[39] proton and phosphorus spectra were recorded with 15 minute intervals for several hours. The number of free inductive decays (FIDs) for the phosphorus and proton NMR spectra was 40 and 16 respectively.

6.5.5. DFT studies

Calculations were done with the SPARTAN '04 package (Wavefunction, Inc; www.wavefun.com), using density functional theory (DFT)[40, 41] with the Becke and Perdew (BP) functional.[42, 43] Geometry optimizations were carried out using Pople's 6–31G* (d,p) for H, C, O, and P atoms[44] and the LANL2DZ effective core potential for palladium.[45-47] All of the geometrical parameters were fully optimized, and all of the structures located on the PESs were characterized as minima. No constraints to bonds, angles, or dihedral angles were applied in the calculations, and all atoms were free to be optimized.

6.5.6. Synthesis of 'phen–palladacycle' / 'phen-C7'

'phen–palladacycle' (i.e., 'phen-**C7**') was synthesized according to a literature procedure,[23] and the product was isolated as a bright yellow powder in 83% yield. ^1H–NMR (300 MHz, d_5–$PhNO_2$)): δ 10.2 (d, 4.8 Hz, 1H, *o*–phen^1), 10.1 (d, 4.8 Hz, 1H, *o*–phen^2), 8.7 (t, 6.9 Hz, 2H, *p*–phen^{1+2}), 8.2 (m, 3H, *m*–phen^1 + *o*–Ph), 8.1 (s, 2H, phen), 8.0 (dd, 8.1 Hz, 1H, *m*–phen^2), 7.6 (dd, 7.8 Hz, 2H, *m*–Ph), 7.3 (t, 7.2 Hz, 1H, *p*–Ph) ppm (see Figure AV.3 for ^1H–^1H–COSY spectrum); Main IR absorptions: 1691 (OC=O), 1622 (NC=O), 1587 (N–O), 1428 (OC–O), 1253 (OC–N), 1045, 950, 850, 722 (C=C and C=N) cm^{-1}; Elemental analysis for 'phen–palladacycle', $C_{20}H_{13}N_3O_3Pd$ (449.0) • 0.2 Pd: calcd. C 50.64, H 2.76, N 8.86; found C 50.47, H 2.72, N 8.97. ESI Mass Spectroscopy, *m/z* found (calcd): $[M+H_2O]^+$ = 466.7 (467.0); $[M+2H_2O]^+$ = 484.9 (485.0); see also Figure 6.8 and Figure 6.9.

References

[1] R. H. Richter, R. D. Priester, *in: J.L. Kroschmitz, M. Howe-Grand (Eds.), Kirk-Othmer Encyclopedia of Chemical Technology, Vol. 14*, Wiley, New York, **1995**.

[2] H. Ulrich, *Ullmann's Encyclopedia of Industrial Chemistry, Vol. A14*, VCH publishers, New York, **1989**.

[3] A. J. Ryan, J. L. Stanford, *in: G. Allen, J.C. Bevington (eds.), Comprehensive Polymer Science, Vol. 5*, Pergamon, New York, **1989**.

[4] K. Weisermel, H. J. Arpe, *Industrielle Organische Chemie*, VCH Verslagsgesellschaft GmbH, Weinheim, Germany, **1988**.

[5] *Registry of Toxic Effects of Chemical Substances (RTECS, online database)*, United States Department of Health and Human Services (National Toxicology Information, National Library of Medicine), Bethesda, MD, **1993**.

[6] R.C. Weast (Ed.), *Handbook of Chemistry and Physics*, D-110, 58 ed., CRC Press Inc., Cleveland, **1977-1978**.

[7] F. Paul, *Coord. Chem. Rev.* **2000**, *203*, 269.

[8] E. Drent, P. W. N. M. van Leeuwen, EU 0086281A1, **1982**.

[9] F. Ragaini, C. Cognolato, M. Gasperini, S. Cenini, *Angew. Chem.* **2003**, *42*, 2886.

[10] T. J. Mooibroek, L. Schoon, E. Bouwman, E. Drent, *Chem. Eur. J.* **2011**, DOI: 10.1002/chem.201100923.
[11] T. J. Mooibroek, W. Smit, E. Bouwman, E. Drent, **2011**, to be submitted.
[12] Note that DPU can be formed by the reaction of nitrobenzene, CO and (*in situ* generated) aniline, but also by the transesterification of MPC with aniline. In both cases, aniline is formed first and DPU is thus derived from aniline.
[13] R. I. Pugh, E. Drent, *Adv. Synth. Catal.* **2002**, *344*, 837.
[14] E. Drent, P. W. N. M. van Leeuwen, EU 86281, **1981**.
[15] P. Wehman, L. Borst, P. C. J. Kamer, P. W. N. M. van Leeuwen, *J. Mol. Catal. A-Chem.* **1996**, *112*, 23.
[16] F. Ragaini, M. Gasperini, S. Cenini, *Adv. Synth. Catal.* **2004**, *346*, 63.
[17] S. Ross, The Proton: applications to organic chemistry in *Organic Chemistry; a series of monographs, Vol. 46* (Ed.: H. H. Wasserman), Academic Press Inc., London, **1985**.
[18] P. Wehman, L. Borst, P. C. J. Kamer, P. W. N. M. van Leeuwen, *Chem. Ber.-Recl.* **1997**, *130*, 13.
[19] F. Ragaini, *Dalton Trans.* **2009**, 6251.
[20] H. Lund, in *Organic Electrochemistry. An Introduction and a Guide*, 3 ed. (Eds.: H. Lund, M. M. Lund, Baizer), Marcel Dekker, New York, **1991**, p. 411.
[21] A. S. o Santi, B. Milani, E. Zangrando, G. Mestroni, *Eur. J. Inorg. Chem.* **2000**, 2351.
[22] A. S. o Santi, B. Milani, G. Mestroni, E. Zangrando, L. Randaccio, *J. Organomet. Chem.* **1997**, *546*, 89.
[23] P. Leconte, F. Metz, A. Mortreux, J. A. Osborn, F. Paul, F. Petit, A. Pillot, *J. Chem. Soc.-Chem. Commun.* **1990**, 1616.
[24] T. Hayashi, M. Konishi, Y. Kobori, M. Kumada, T. Higuchi, K. Hirotsu, *J. Am. Chem. Soc.* **1984**, *106*, 158.
[25] Cyclohexene was chosen because it is easy to handle and because it is known that a P_2Ni=NR complex can react stoichiometrically with double bonds (see reference 29).
[26] S. U. Tumer, J. W. Herndon, L. A. McMullen, *J. Am. Chem. Soc.* **1992**, *114*, 8394.
[27] S. Lopez, E. Herrero-Gomez, P. Perez-Galan, C. Nieto-Oberhuber, A. M. Echavarren, *J. Am. Chem. Soc.* **2006**, *45*, 6029.
[28] W. V. Doering, A. K. Hoffmann, *J. Am. Chem. Soc.* **1954**, *76*, 6162.
[29] R. Waterman, G. L. Hillhouse, *J. Am. Chem. Soc.* **2003**, *125*, 13350.
[30] When performing an analysis for the simulation of the products distribution as described in Chapter 3 (and in more detail in the supporting information for that chapter in Appendix II), and using the reaction stoichiometries described therein, the following results (NB: the equation numbers refer to those in Chapter 3 and Appendix II): For Pd^{2+}(Phen), added water is hardly (net) consumed, meaning that the contribution of eq. 10/11*, 13/14*, and 16/17* should be kept as low as possible relative to eq. 11, eq. 14, and eq. 17 (together accounting for the aniline produced). Thus, various fraction (of eq. X vs eq. X*) were considered and an excellent fit was obtained when the water 'consuming' reactions (eq. X*) contribute for 35.0%. The (aryl) product distribution is: MPC (34.5%); $PhNH_2$ (11.5%); Azoxy (54.0%), with $PhNH_2$/MPC = 0.33, and Azoxy/MPC = 1.57. 0.28 mmol nitrobenzene was reduced with methanol alone, so: CH_3OH reduction: (0.28 x 0.345 x eq. 16) + (0.28 x 0.115 x 0.65 x eq. 17) + (0.28 x 0.115 x 0.35 x eq. 16/17*) + (0.28 x 0.540 x eq. 18) = 0.10 MPC + 0.03 $PhNH_2$ + 0.15 Azoxy + 0.55 H_2O + 0.02 DMC. As next calibration point, we can take MPC; there is still 3.00 - 0.10 = 2.90 mmol unaccounted for. This must have been produced via CO-only reduction and/or via the co-reduction of CO and the acidic protons of CH_3OH molecules. Thus, there must be an optimal fraction of CO-only reduction, so that the simulation approaches perfection (and the aryl product distribution is respected). Several options were considered, and a fraction of 1.00 CO reduction was found to fit best, meaning that 2.90 mmol nitrobenzene was reduced with CO alone, and none by $CO/2CH_3OH$. Thus: CO only reduction: (2.90 x 1.00 x eq. 10) + (2.90 x 0.33 x 0.650 x eq. 11) + (2.90 x 0.33 x 0.350 x eq. 10/11*) + (2.90 x

1.57 x eq. 12) = 2.90 MPC + 0.95 $PhNH_2$ + 4.55 Azoxy + 0.62 DMC + (-0.33) H_2O. Adding all three reduction pathways leads to an excellent simulation of sim. (exp.) = 3.0 (3.0) MPC; 1.0 (1.0) $PhNH_2$; 4.7 (4.7) Azoxy; 0.6 (0.5) DMC; 0.2 (0.3) H_2O. This means that the respective contributions of CO-only / CO+2CH_3OH / CH_3OH -only = 97% / 0% / 3%.

[31] R. H. Crabtree, The organometallic chemistry of the transition metals, 4th ed., Wiley-Interscience, New Jersey (USA), **2005**, pp. 87.

[32] F. Ragaini, S. Cenini, A. Fumagalli, C. Crotti, *J. Organomet. Chem.* **1992**, *428*, 401.

[33] P. Zuman, Z. Fijalek, D. Dumanovic, D. Suznjevic, *Electroanal.* **1992**, *4*, 783.

[34] M. Gasperini, F. Ragaini, C. Remondini, A. Caselli, S. Cenini, *J. Organomet. Chem.* **2005**, *690*, 4517.

[35] F. Ragaini, M. Gasperini, S. Cenini, L. Arnera, A. Caselli, P. Macchi, N. Casati, *Chem. Eur. J.* **2009**, *15*, 8064.

[36] W. L. F. Armarego, C. L. L. Chai, *Purification of laboratory chemicals*, 5th ed., Elsevier, Amsterdam, **2003**.

[37] J. Chen, J. S. Fritz, *Anal. Chem.* **1991**, *63*, 2016.

[38] customer.linde.com/FIRSTspiritWeb/linde/LGNL/media/datasheets/NL-PIB-0024.pdf, **November 2011**

[39] T. J. Mooibroek, E. Bouwman, M. Lutz, A. L. Spek, E. Drent, *Eur. J. Inorg. Chem.* **2010**, *2*, 298.

[40] W. Koch, M. C. Holthausen, *A Chemist's Guide to Density Functional Theory*, 2nd ed., Wiley-VCH, Weinheim, **2000**.

[41] K. Eichkorn, O. Treutler, H. Ohm, M. Haser, R. Ahlrichs, *Chem. Phys. Lett.* **1995**, *240*, 283.

[42] A. D. Becke, *Phys. Rev. A* **1988**, *38*, 3098.

[43] J. P. Perdew, *Phys. Rev. B* **1986**, *33*, 8822.

[44] W. J. Hehre, L. Radom, P. R. van Schleyer, J. A. Pople, *Ab Initio Molecular Orbital Theory*, Wiley, New York, **1986**.

[45] P. J. Hay, W. R. Wadt, *J. Chem. Phys.* **1985**, *82*, 270.

[46] P. J. Hay, W. R. Wadt, *J. Chem. Phys.* **1985**, *82*, 299.

[47] W. R. Wadt, P. J. Hay, *J. Chem. Phys.* **1985**, *82*, 284.

Chapter 7

The use of nucleophiles other than methanol in reductive carbonylation of nitrobenzene.

Abstract: The nucleophiles *p*-cresol, *i*-propanol, 2,2,2-trifluoroethanol (TFE), and aniline were used instead of methanol in the palladium-catalyzed reductive carbonylation of nitrobenzene to an aromatic carbamate or urea.
It was found that when employing *p*-cresol (2 M in toluene) under strictly anhydrous conditions, significant amounts of the H-containing nitrobenzene reduction products $PhNH_2$ and *N,N*'-diphenylurea (DPU) were formed when using either $(L3)Pd(OAc)_2$ or $[Pd(phen)_2](OTs)_2$ as catalyst precursor (L3 = 1,3-bis(diphenylphosphino)-propane; phen = 1,10-phenanthroline). Based on a careful weight, ^{1}H-NMR and GLC-MS analysis of fractions obtained after a column chromatographic separation of a reaction mixture, and based on an HPLC-UV/MS analysis of a similar reaction mixture, it is concluded that *p*-cresol can be oxidatively dehydrogenated to hereto unidentified compounds, probably oligomers/polymers. It was found that *i*-propanol is an effective H-donor via oxidative dehydrogenation (>acetone produced) when using $(oMeOL3X)Pd(OAc)_2$, but reacts mainly via the oxidative carbonylation when using $(L3X)Pd(OAc)_2$ (>carbonate and oxalate produced) ([oMeO]L3X = 1,3-bis(di[-*o*-methoxy]phenylphosphino)2,2-dimethylpropane). With the catalytic system $(L3X)Pd(OAc)_2$ in TFE, an unprecedented 95% selectivity for the carbamate is obtained at a 90% nitrobenzene conversion. Moreover, the carbamate was found to pyrolize readily to form phenylisocyanate. Applying aniline as the nucleophilic reagent and using $(L3X)Pd(OAc)_2$ as catalyst precursor, 3-methylnitrobenzene was quantitatively converted to 3-methylaniline with the co-production of the carbonylation products DPU (90%) and *N,N*'-diphenyloxalamide (DPO, 10%) when working below the transesterification temperature (70–80 °C). Based on these data, the molecular mechanistic details of this reaction were proposed to be very similar to those of the nitrobenzene carbonylation and methanol oxidation processes in the Pd/diphosphane/CH_3OH system.
It is concluded that *p*-cresol and *i*-propanol are inappropriate substitutes for methanol. Aniline may be a promising alternative, but TFE is the most promising (and practically viable) nucleophilic reagent in Pd/diphosphane catalyzed nitrobenzene carbonylation reactions.

7.1. Introduction

One of the most important observations when studying the reductive carbonylation of nitrobenzene in methanol as described in the preceding chapters, is that methanol acts as a reductant for nitrobenzene, effectively acting as a transfer hydrogenation reagent. This coupling between nitrobenzene reduction chemistry and methanol oxidation chemistry provided a unique opportunity to study the mechanism of the complicated reactions that underlie the genesis of molecules of industrial potential such as methyl phenyl carbamate, (MPC), N,N'-diphenyl urea (DPU), dimethyl carbonate (DMC), and dimethyl oxalate (DMO).

From a more practical point of view, however, this coupling makes the Pd/phosphane/CH_3OH system impractically complicated; in order to be able to utilize the molecules produced a not-so-straightforward separation of these compound from the complex reaction mixtures is required. Thus, for any real application in the synthesis of aromatic isocyanates to result from the research described in the preceding chapters, it is evidently necessary to produce MPC (or a nitrobenzene carbonylation product in general) more selectively. Although the fine-tuning of the catalyst may realize this to some extend, one could also try to apply a different nucleophile than methanol. Besides possibly preventing the formation of methanol oxidation products, applying another nucleophile can have an additional advantage; methyl phenyl carbamate is quite stable and not easily pyrolized to methanol and phenyl isocyanate, whereas carbamates (or ureas) of other (more bulky, less nucleophilic) nucleophiles may be pyrolized more readily.

Thus, some preliminary investigations were made to substitute methanol for another nucleophile such as *p*-cresol, *i*-propanol, 2,2,2-trifluoroethanol (TFE), and aniline. These nucleophiles were selected based on their larger size (relative to methanol) to hopefully prevent formation of the carbonate and/or oxalate; *p*-cresol and TFE were also selected on their decreased nucleophilicity, in order to obtain a carbamate that is more readily pyrolized. Aniline was chosen because the oxidative carbonylation of aniline and the reductive carbonylation of nitrobenzene will both give the same product DPU.

7.2. Results and discussion

7.2.1. Reactions with *p*-cresol

7.2.1.1 General considerations

To ensure that *p*-cresol was dry, the solid was stored for a week in a vacuum desiccator with P_2O_5 as the drying reagent. To allow easier handling of the solid cresol, a 2 M stock solution of *p*-cresol was prepared in toluene. It was checked that this stock solution was dry by using a reaction with trimethyl orthoformate (tmof) (see experimental of Chapter 3 for details). Quantitative analysis of reaction products, nitrobenzene, and *p*-cresol were all performed using calibration lines made from authentic samples and using GLC-FID (see experimental section of Chapter 3 for details). It is worth noting that the anticipated carbamate could not be detected using this technique, as it pyrolized quantitatively within the GLC injection port. Thus, the amount of phenylisocyanate was measured instead. The experimental procedure for performing the catalytic reactions has been described in Chapter 3; 25 ml of the 2 M stock solution of *p*-cresol was used instead of 25 ml methanol (amounting to 50 mmol *p*-cresol).

Initial screening studies using a large variety of reaction conditions and additives, were undertaken using pre-synthesized (L3)$Pd(OAc)_2$ and $[Pd(phen)_2](OTs)_2$ (L3 = 1,3-bis(diphenylphosphanyl)propane; phen = 1,10-phenanthroline; see also Chapter 3 and Chapter 6). Using these two catalyst precursor complexes, a conversion of 100% could be reached within 10 hours under more or less optimized conditions (see Table 7.1). The aryl mass balance of the phenyl rings that must have originated from nitrobenzene appeared to be correct; the apparently missing 0.4 mmol (2% of 24.4) in both reactions is within the experimental error of ~5%.

Table 7.1. Reactions of nitrobenzene with CO in 2 M *p*-cresol (in toluene), using (L3)$Pd(OAc)_2$ or $[Pd(phen)_2](OTs)_2$ as catalyst precursor.

Complex	Analytes (mmol)					
	p-cresol	$PhNO_2$	PhNCO	$PhNH_2$	DPU	Azoxy
(L3)$Pd(OAc)_2$[a]	42.3	0.0	1.0	2.0	10.5	0.0
$[Pd(phen)_2](OTs)_2$[b]	41.8	0.0	14.1	0.7	3.9	0.7

[a] 0.05 mmol Pd-complex, 0.25 mmol ligand, 110˚C, 75 bar CO, 0.05 HOTs, 10 h, 24.4 mmol $PhNO_2$. [b] 0.1 mmol Pd-complex, 5.0 mmol ligand, 150˚C, 50 bar CO, 10 hrs, 24.4 mmol $PhNO_2$.

7.2.1.2 An uneven H-mass balance and 'missing' p-cresol

When (L3)Pd(OAc)$_2$ is used as catalyst precursor, aniline and DPU are formed almost exclusively (see Table 7.1). In the experiment with the [Pd(phen)$_2$](OTs)$_2$ complex, a large amount of DPU and some PhNH$_2$ are formed, but also a large amount of phenylisocyanate is detected. Since the presence of water was excluded by working under strictly anhydrous reaction conditions, hydrogen atoms from H$_2$O cannot account for the hydrogen atoms that are obviously present in PhNH$_2$ and DPU. It must therefore be concluded that *p*-cresol can somehow act as a hydrogen donor. Neither di-*p*-cresyl carbonate nor di-*p*-cresyl oxalate could be detected, thus excluding the oxidative carbonylation of *p*-cresol as the source of H-atoms. The only viable alternative is then the oxidative dehydrogenation of *p*-cresol (in analogy to the dehydrogenation of methanol described in Chapters 3 and 6) or another oxidation reaction, leading to compounds such as quinones or poly-phenols (see Scheme 7.1). The *p*-cresol may thus end up in (with GLC undetected) heavy ends such as oligomers or polymers, with the liberation of H-atoms by an overall 'oxidative polymerization'.[1-3]

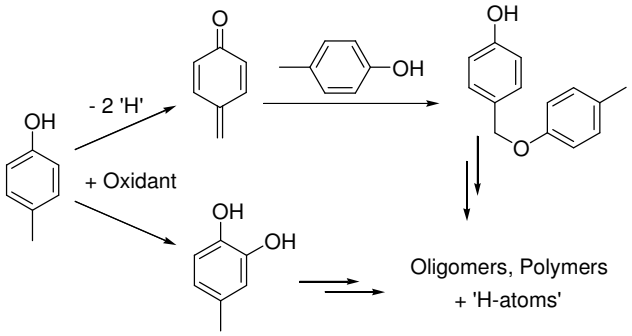

Scheme 7.1. Possible routes for the 'oxidative polymerization' of *p*-cresol

Irrespective of the exact mechanism for H-donation from *p*-cresol to nitrobenzene, the mere observation that products such as aniline and DPU are formed must mean that the amount of *p*-cresol detected should be less than the amount initially present (50 mmol). Indeed, when looking at the amount of *p*-cresol that is detected after these experiments, about 8 mmol appears to be 'missing'.

7.2.1.3 Weight, ^{1}H-NMR, GLC-MS, and HPLC-UV/MS analysis of reaction mixtures

In an attempt to obtain further evidence for the supposed dehydrogenation reaction of *p*-cresol to GLC-undetected reaction products, the reaction mixture of the reaction performed with $[Pd(phen)_2](OTs)_2$ was subjected to further analysis. Thus, after filtration of DPU (insoluble in toluene), the reaction mixture was concentrated, weighed, and separated into five fractions using silica column chromatography (see experimental). The five (combined) fractions were analyzed by ^{1}H-NMR and GLC-MS, and their weight was determined. The exercise of deriving quantitative data from these analyses is presented in Section AVI.1 of Appendix VI. From this analysis it is clear that about 8.5 mmol of aryl-containing products have been formed. These aryl rings must have originated from *p*-cresol, as the aryl mass balance of nitrobenzene derived products is even. Indeed, 8.2 mmol too few *p*-cresol was quantified with GLC (41.8 from the 50 mmol used, see Table 7.1). Also, in this experiment 4.6 mmol $PhNH_2$/DPU was detected, which roughly fits with a scenario wherein one *p*-cresol is dehydrogenated to deliver (net) one H-atom, thus requiring two mmol *p*-cresol for every mmol of $PhNH_2$ or DPU. Additional evidence for the genesis of *p*-cresol dehydrogenation products comes form an HPLC-UV/MS analysis (see section AVI.2 of Appendix VI for details) of the liquid phase of a similar catalytic experiment (standard conditions for $[Pd(phen)_2](OTs)_2$, additive 0.5 mmol KI). This analysis also clearly reveals the presence of several aryl-containing products other than those that can be anticipated from nitrobenzene reduction reactions ($PhNH_2$, *p*-cresyl-phenylcarbamate, DPU, Azo, Azoxy).

GLC-MS analysis of the five fractions obtained from column, and the MS spectra recorded for the with HPLC-UV unidentified products both afforded mass spectra that fit possible dehydrogenation / oxidation products of *p*-cresol such as quinone and polyol-like compounds. However, these possibly matching structures are highly speculative and most likely originate from unidentified higher molecular weight compounds, hopefully to be positively identified in future investigations.

In conclusion, the combined results from the catalytic experiments, column separation (with ^{1}H-NMR / GC-MS analysis) and the HPLC-UV/MS analysis, make it clear that reaction products have evolved that cannot originate from nitrobenzene; instead these products most likely originate from *p*-cresol via

oxidative dehydrogenation processes. This process (or processes) may function as H-source to account for the H-atoms found in aniline and DPU. Clearly, many of the details are unknown and should be clarified in future research. Especially the supposed oxidation products that evolve should be characterized. Nevertheless, for present purposes it may be noted that *p*-cresol apparently is not the ideal nucleophile to be employed for the reductive carbonylation of nitrobenzene, as it seems to participate in a reductive oligomerization reaction.

7.2.2. Reactions with *i*-propanol and 2,2,2-trifluoroethanol

7.2.2.1 General considerations

As other alternatives to methanol, *i*-propanol and 2,2,2-trifluoroethanol (TFE) were considered, using (oMeOL3X)Pd(OAc)$_2$ and (L3X)Pd(OAc)$_2$ as the catalyst precursors (see Chapters 2 – 4 for the structure of these diphosphane ligands). In the initial screening studies, *i*-propanol and TFE were not dried prior to use, but a freshly opened bottle of the solvent was saturated with, and stored under argon. Apart from this, the reactions were performed in the same manner and with the same quantities (of substrate/solvent/catalyst/ligand) as those conducted in methanol (see Chapter 3 for details). Calibration lines were not prepared from authentic samples in these matrices, and the GLC-FID chromatographs were thus evaluated in a qualitative way. In some cases, the amount of product was estimated using the calibration line for that analyte in methanol. Despite these inaccuracies, the data obtained from these experiments can yield some important insights / results, as discussed below.

7.2.2.2 i-Propanol as efficient transfer hydrogenation reagent

When using *i*-propanol as solvent and (oMeOL3X)Pd(OAc)$_2$ as catalyst precursor complex, nitrobenzene is converted almost exclusively to aniline (about 75%, at about 50% conversion). Clearly, this amount of aniline is unlikely to be formed from water in *i*-propanol, as this solvent contains less than 1.4 mmol water per 25 ml according to the manufacturer. Thus, *i*-propanol must act very efficiently as transfer hydrogenation reagent. Di-*i*-propyl carbonate or oxalate were not detected, thus excluding the oxidative carbonylation of *i*-propanol as H-source. Instead, a large quantity of acetone was found, the end product of *i*-propanol dehydrogenation (see also Chapter 3). When, employing (L3X)Pd(OAc)$_2$ in this solvent, again significant amounts of aniline and DPU were detected, alongside

some *i*-propyl phenyl carbamate. Once more, acetone was detected (albeit in smaller amounts than with the oMeO-L3X based catalyst), but now also di-*i*-propyl carbonate and oxalate were clearly present.

The above means that, in line with our findings for methanol (see Chapter 5), the transfer hydrogenation reaction proceeds for a large portion by an oxidative dehydrogenation mechanism for the (oMeOL3X)Pd(OAc)$_2$ catalyst. However, when using (L3X)Pd(OAc)$_2$ as the catalyst precursor, the hydrogen atoms are mainly delivered via an oxidative carbonylation mechanism. More importantly, these data clearly exclude *i*-propanol as a viable solvent and nucleophilic reagent in Pd/diphosphane catalyzed reductive carbonylation of nitrobenzene.

7.2.2.3 TFE as promising nucleophilic reagent and solvent

When using 2,2,2-trifluoroethanol (TFE) as nucleophilic reagent/solvent and (oMeOL3X)Pd(OAc)$_2$ as the catalyst precursor, nitrobenzene is hardly converted and merely an estimated 5% yield (1 mmol) of aniline was found after the reaction. As oxidative carbonylation or dehydrogenation products of CF_3CH_2OH were not found, is seems likely that only the small amount of water (< 1.4 mmol / 25 ml) has acted as the H-source. This must mean that TFE, in contrast with *i*-propanol, appears not a good transfer hydrogenation reagent.

Surprisingly, when applying (L3X)Pd(OAc)$_2$ as catalyst precursor complex, approximately 50% of the nitrobenzene is converted within the standard four hours reaction time. Even more surprisingly, the sole products that were identified with GLC were trifluoroethyl phenyl carbamate and its pyrolysis product phenylisocyanate (both estimated at ~25% yield). This means that with this weak nucleophilic reagent as solvent the corresponding carbamate seems to be formed with an unprecedented 100% selectivity using the catalyst based on L3X. When extending the reaction time to 10 hours, nearly all nitrobenzene was converted (~90%) to trifluoroethyl phenyl carbamate. Only small amounts of aniline (~2% yield mmol) and DPU (~3% yield) were observed after this experiment, but these may arise from the small amount of water present. The selectivity towards the desired carbamate in this reaction is thus about 95%.

What also stands out from these preliminary results is that *neither carbonate nor oxalate* was observed; products that are readily formed from methanol oxidative

carbonylation when using the L3X-based catalyst (see Chapter 5). However, at this stage it cannot be excluded that any bis(trifluoroethyl) carbonate is formed in an oxidative carbonylation of TFE (i.e. $OC(OCH_3CF_3)_2$). This carbonate contains an activated carbonyl with a good leaving group. In fact, $OC(OCH_3CF_3)_2$ has been proposed to replace phosgene as carbonylation reagent in the preparation of aromatic isocyanates by reaction with an aromatic amine at merely 60 °C (using a Lewis acidic catalyst).[4]

From the above, it seems reasonable to propose that the use of TFE as a solvent and reagent effectively prevents the oxidative dehydrogenation reaction – presumably by inhibiting beta-H abstraction from the strongly electron withdrawing alkoxide moiety– whereas oxidative carbonylation (if it occurs) produces aniline and the carbonate (or oxalate) in equimolar amounts (Eq. 1). If formed, these products will rapidly react to the desired carbamate and TFE (Eq. 2). As a result, only trifluoroethyl phenyl carbamate (and its pyrolysis product phenylisocyanate) is observed (Eq. 3).

$PhNO_2 + 3\ CO + 2\ CF_3CH_2OH \rightarrow PhNH_2 + 2\ CO_2 + OC(OCH_2CF_3)_2$ Eq. 1

$PhNH_2 + OC(OCH_2CF_3)_2 \rightarrow PhNH(CO)OCH_2CF_3 + CF_3CH_2OH$ Eq. 2 +

$PhNO_2 + 3\ CO + CF_3CH_2OH \rightarrow PhNH(CO)OCH_2CF_3 + 2\ CO_2$ Eq. 3

Clearly the above results are merely only rough indications and not yet fully proven or well understood. Notwithstanding this, it is however clear that TFE is a highly promising nucleophilic reagent in the Pd/diphosphane catalyzed nitro arene carbonylation reaction, that requires further investigation. Moreover, the facile pyrolisis of the produced carbamate can make it an attractive platform to produce isocyanates, while recycling TFE.

7.2.3. Reactions with aniline

7.2.3.1 General considerations

In the previous sections, some results are described of the use of other alcohols as nucleophiles in the carbonylation of nitrobenzene. In this section another alternative is considered: to use aniline as the nucleophile and solvent. The first reason to use this nucleophilic reagent is because it was anticipated that the oxidative dehydrogenation reaction does not occur with aniline. Secondly, it can –

based on the mechanistic knowledge obtained from working in a methanolic environment (Chapters 3–6)– reasonably be expected that only Azo and Azoxy will be formed as side-products. That is, when aniline replaces methanol in the oxidative carbonylation reactions (either during nitrobenzene de-oxygenation to an imido complex or thereafter, see Chapter 5) DPU (or diphenyl oxalamide, DPO) will be the likely reaction product. The product of nitrobenzene carbonylation will also be DPU. Any possibly formed aniline is not a waste product in this system, as it will be re-used in the oxidative carbonylation of aniline to DPU. This thus means that, when aniline is used as the nucleophilic solvent, the only side-products that can reasonably be anticipated are the reductive coupling products Azo and Azoxy; *all other reactions lead directly to DPU*.

In this section some initial studies are described of nitrobenzene / aniline carbonylation reactions performed in aniline as the solvent, and aimed at applying the mechanistic insights gained by studying the carbonylation of nitrobenzene in methanol (Chapters 3 – 6). In these studies, care was taken to prepare strictly water-free nitrobenzene and aniline, by distilling these liquids from P_2O_5 under an argon atmosphere, and storing them under argon. The amounts of substrate/solvent/Pd/ligand, and the procedure for the catalytic reactions and quantitative analysis are identical to those described in the experimental section of Chapter 3 for the reaction performed in methanol.

7.2.3.2 Literature data; three stoichiometries?

It must be noted beforehand that the oxidative carbonylation of aniline to DPU has been studied for years. Very often, molecular oxygen is used as the terminal oxidant,[5-11] but milder oxidants such as SeO_2 have also been proposed.[12] The link between aniline oxidative carbonylation and nitrobenzene reductive carbonylation has also been known for decades; effectively nitrobenzene is used as the terminal oxidant,[13-19] in analogy to the oxidative carbonylation of methanol (see Chapter 5). The oxidative carbonylation of aniline typically is performed with a homogeneous catalyst; proposed systems include Se-based catalysts,[17] but notably also Pd/phen[16] and Pd/phosphane[14, 15] based systems have been applied. The selectivity is generally very high (~100%) and nitrobenzene is typically fully converted within several hours reaction time at relatively mild reaction conditions (90–120 °C).

Mechanistically, this reaction may bear very strong resemblance to our Pd/diphosphane/CH_3OH systems (see Chapters 3 – 6). It is for example frequently proposed that an imido complex is an important intermediate in this reaction.[13-15, 18] It has also been speculatively proposed that there are two reaction stoichiometries for the reduction of nitrobenzene in aniline; one is which CO is the only reductant, and one in which the H-atoms from aniline act as the only reductant, as is shown by Equations 4 and 5 respectively:[13]

$$PhNO_2 + PhNH_2 + 3\ CO \rightarrow PhNHC(O)NHPh + 2\ CO_2 \qquad \text{Eq. 4}$$

$$PhNO_2 + 5PhNH_2 + 3\ CO \rightarrow 3\ PhNHC(O)NHPh + 2\ H_2O \qquad \text{Eq. 5}$$

It must be noted that these two stoichiometries bear strong resemblance to respectively the CO-only and the CH_3OH-only nitrobenzene de-oxygenation routes described in Chapters 3 and 4. As also explained in these chapters however, it is unlikely that both extremes are operative without the intermediate option also playing a role, i.e., the stoichiometry described by Equation 6:

$$PhNO_2 + 3PhNH_2 + 3\ CO \rightarrow 2\ PhNHC(O)NHPh + CO_2 + H_2O \qquad \text{Eq. 6}$$

These similarities notwithstanding, it is important to note that the stoichiometries given by Equations 5 and 6 are speculative and not at all proven. For example, in the paper in which Equation 5 is proposed,[13] water was not analyzed. The evidence for the stoichiometry given by Eq. 5, is that mixed ureas are observed when using a substituted (or deuterated) nitrobenzene.[13, 19] It is important to note, however, that these catalytic reactions were performed at 90[19] and 120 °C.[13] It may be expected that at these temperatures, a transamidation reaction occurs between the urea and the aniline present, thus accounting for the asymmetric ureas observed.

7.2.3.3 Catalytic experiments; one stoichiometry only

One obvious way to elucidate the correct stoichiometry is to measure the amount of water produced in a reaction. However, it is not straightforward to measure water in aniline; our methodology developed to quantify water in methanol required a slightly acidic environment (using tmof, see experimental section of Chapter 3). Another way to shed light on the above stoichiometries, however, is to quantify the amount of DPU formed relative to the amount of nitrobenzene

converted; when only Equation 4 operates the amount of DPU formed cannot exceed the amount of nitrobenzene converted. When more than two equivalents of DPU are formed relative to the amount of nitrobenzene converted, Equation 5 must be –at least partially– operative.

During the initial screening studies (see Chapter 4 for the ligands used), it appeared that nearly all the Pd/diphosphane catalysts tested were highly active in this reaction, reaching (near) full conversion typically within several (1–4) hours reaction time. The amount of DPU formed was always 1:1 stoichiometric based on the amount of nitrobenzene converted; apparently, the reaction stoichiometry when working at 110 °C with this Pd/diphosphane/$PhNH_2$ system can best be described by Equation 4.

7.2.3.4 Carbonylation reaction of 3-methylnitrobenzene in aniline below the transamidation temperature to gain mechanistic insights

Although it thus seems that only the stoichiometry given by Equation 4 is actually operating in the Pd/diphosphane/$PhNH_2$ system, the molecular mechanism for the formation of DPU is still to well understood. In an attempt to acquire this mechanistic knowledge, 3-methylnitrobenzene was used as the substrate and the reaction was carried out below the transamidation temperature.

For this experiment, (L3X)$Pd(OAc)_2$ was chosen as catalyst precursor complex (see Chapter 2 for the structure of L3X) because it was found that nitrobenzene could be fully converted within three hours when applying a CO pressure of 50 bar and working at a reaction temperature of 60 °C. Conveniently, transamidation does not occur at this temperature; only at about 70–80 °C was a significant (3–7%) conversion observed when 6 mmol DPU was heated in 25 ml 3-methylaniline under 50 bar CO for two hours. This means that any 3-methylaniline detected after a carbonylation experiment at 60 °C with 3-methynitrobenzene as substrate in aniline, cannot be due to a transamidation of possibly formed *N,N'*-di(3-methylphenyl)urea (DMPU) or 3-methylphenyl phenylurea (MPPU) with aniline.

After the catalytic carbonylation experiment with (L3X)$Pd(OAc)_2$ at 60 °C, using 3-methylnitrobenzene as the substrate and unsubstituted aniline as the nucleophilic reagent and solvent, a quantitative conversion of 3-

methylnitrobenzene was observed, and GLC-FID analysis revealed the presence of 3-methylaniline (24.4 mmol) as the only product in the liquid phase. ^{1}H- and ^{13}C-NMR analysis of the solid revealed that symmetric DPU was produced with 90% selectivity, with the remaining 10% being the corresponding diphenyl oxalamide (DPO, verified by ESI-MS). Notably, the combined amount of DPU and DPO formed amounts to about 24 mmol, meaning that a similar reduction stoichiometry as shown in Equation 4 is the only stoichiometry operating in this system, also at 60 °C.

The absence of the asymmetric urea MPPU and symmetric urea DMPU, together with the stoichiometric formation of 3-methylaniline must mean that the N-aryl groups derived from 3-methylnitrobenzene, at some stage have been exchanged by those derived from aniline *via* a mechanism other than a transamidation of initially formed MPPU and/or DMPU with solvent aniline. The nitro arene must undoubtedly interact with the catalyst in order to be de-oxygenated and form the corresponding palladium-imido intermediate; it is thought that the exchange of aryl rings takes place at this intermediate. Such a process can be rationalized by the hypothesis shown in Scheme 7.2.

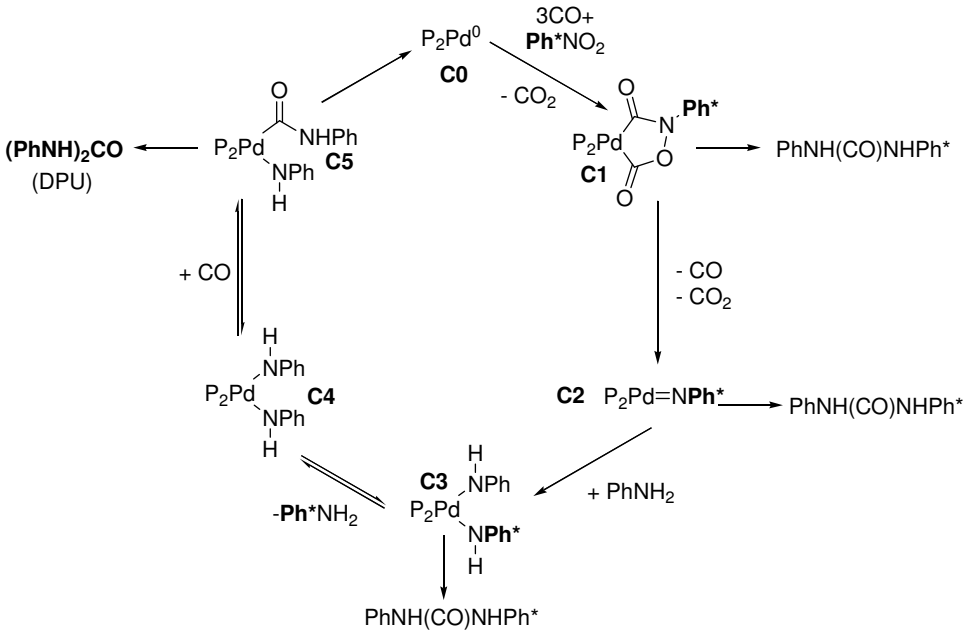

Scheme 7.2. Working hypothesis for the formation of DPU in the Pd/diphosphane catalyzed reduction of 3-methylnitrobenzene (Ph*NO_2) in aniline.

The proposal shown in this scheme represents a nearly identical mechanistic picture as was developed for nitrobenzene CO-only reduction chemistry (see Chapter 3) coupled with nitrobenzene carbonylation chemistry (Chapter 4) and methanol carbonylation chemistry (see Chapters 3 and 5). The only difference is that methanol is replaced by aniline.

It is thus thought that 3-methylnitrobenzene (Ph^*NO_2 in Scheme 7.2) is first stripped of oxygen using only CO (eventually amounting to the stoichiometry given by Eq. 4) to form the imido-intermediate (**C2**)[13-15, 18] via the palladacycle **C1** (and related CO-equilibrated palladacycles, see Chapter 4). As was shown in Chapter 4, **C1** can indeed be formed under mild (90 °C) carbonylation conditions in ethanol, but it is instable and decomposes by a decarbonylation (to **C2**) instead of a decarboxylation (to give carbonylation products). As the unsymmetrical urea was not observed in the present experiment, it seems that also in aniline, palladacycle **C1** is not a product-releasing species. Once the imido intermediate (**C2**) is formed, there must be a competition between CO and aniline for the reaction with this same species; apparently, reaction with CO does not occur, as this would have lead to the unsymmetrical urea. Instead, a net protonation will give **C3**, for which there will be a competition between CO insertion and – importantly– a ligand exchange with the abundantly present solvent aniline to liberate 3-methylaniline (**C3⇆C4**). Clearly this ligand exchange reaction must be faster than the CO insertion, as otherwise the unsymmetrical urea would have been formed. This process then explains why only DPU (and some DPO) was observed. Starting from **C4**, DPU is formed by a CO insertion (**C4⇆C5**) followed by a reductive elimination (**C5→C0**) to return palladium in the catalytic cycle. The oxalamide (DPO) is formed by two CO insertions into **C4**, followed by reductive elimination. Both reactions are analogous to the evolution of DMC and DMO when methanol is the nucleophile (see Chapter 5).

In conclusion, the mechanistic insights gained by studying the reductive carbonylation of nitrobenzene in methanol, apply directly to nitrobenzene carbonylation chemistry in aniline; both reactions likely proceed via very similar chemistry.

7.3. Summary and conclusions

Studies were undertaken to replace methanol by *p*-cresol, *i*-propanol, TFE and aniline as the nucleophile in the palladium-catalyzed reductive carbonylation of nitrobenzene to form an aromatic carbamate or urea. When employing *p*-cresol, the significant formation of H-containing nitrobenzene reduction products ($PhNH_2$, DPU), implies that *p*-cresol is oxidatively dehydrogenated. This conclusion was corroborated by a careful weight, ^{1}H-NMR and GLC-MS analysis of fractions obtained after a column chromatographic separation of a reaction mixture, and by an HPLC-UV/MS analysis of a similar reaction mixture.

It was found that *i*-propanol acts very efficiently as transfer hydrogenation reagent in the hydrogenation of nitrobenzene to aniline when employing the catalytic system based on (oMeOL3X)$Pd(OAc)_2$. When using (L3X)$Pd(OAc)_2$, *i*-propanol is carbonylated to di-isopropyl carbonate and oxalate.

When employing TFE as the reagent and solvent and using (L3X)$Pd(OAc)_2$ as catalyst precursor, an unprecedented 95% selectivity towards the desired carbamate was observed at a nitrobenzene conversion of about 90%. Moreover, the resulting carbamate is readily pyrolized, as evident from the large amounts of phenylisocyanate detected with GLC-FID.

Applying aniline as the nucleophilic reagent and applying a range of diphosphane ligands typically gave a full conversion of nitrobenzene with excellent selectivities for DPU. Notably, using (L3X)$Pd(OAc)_2$ as catalyst precursor, it was found that 3-methylnitrobenzene can fully be converted to the carbonylation products DPU (90%) and DPO (10%) even when working below the transamidation temperature (70–80 °C). From these data, together with the quantitative formation of 3-methylaniline and the absence of the unsymmetrical urea or *N,N*'di(3-methylphenyl)urea, it was concluded that the N-aryl groups derived from 3-methylnitrobenzene are exchanged with those derived from aniline at the intermediate palladium-imido catalytic stage of the Pd-catalyst. The molecular mechanistic details of this process, the nitroarene de-oxygenation, and the formation of DPU and DPO were proposed to be similar to those of the nitrobenzene carbonylation and methanol oxidation processes in the Pd/diphosphane/CH_3OH system (see Chapters 3 to 5).

Based on these results, it is concluded that *p*-cresol and *i*-propanol are inappropriate substitutes for methanol. Aniline may be a promising alternative, but the difficulties to pyrolize DPU (relative to carbamates with a good leaving group) may render this alternative unpractical. TFE on the other hand is a promising (weakly) nucleophilic reagent to perform Pd/diphosphane catalyzed nitrobenzene carbonylation reactions, producing the corresponding carbamate in high selectivity. Facile pyrolysis of trifluoroethyl phenyl carbamate makes this an attractive platform for isocyanate synthesis while recovering TFE.

7.4. Experimental

Catalytic experiments, GLC-FID analysis of reaction mixtures (using a polar and an apolar column) and other standard analyses were performed using the equipment and settings described in the experimental section of Chapter 3. HPLC was carried out using a normal phase Prevail Silica 3 μ column (length 150 mm, 4.6 mm internal diameter) with eluents *n*-hexane and *i*-propanol (1%) (20 μL injection 1 mg/mL sample, 1 mL/min). The HPLC was coupled to a Mass Spectrometer and a UV detector. UV detection was carried out at 200 nm using a Dionex Ultimate 3000 Photodiode Array Detector. Mass spectrometry was carried out using a Finnigan Aqa Mass Spectrometer equipped with an electrospray ionization (ESI) source. Sample solutions (10 µL of a 1 mg/mL solution) were introduced in the ESI source by using a Dionex ASI-100 automated sampler injector and an eluent running at 0.2 mL/min. The probe temperature was 350 °C, ionization voltage 3 kV and aqa source voltage 20 V.

Prior to column separation, the reaction mixture was filtered over a Düren 640d filtration paper to remove (and quantify) the DPU precipitate. The filtrate was run over a silica column (95:5 petroleum ether: ethyl acetate). Four 200 mL fractions ('1st fraction'), two 200 mL fractions ('2nd fraction') and eleven 50 mL fractions ('3rd fraction') were collected after which the eluent was modified to 95:5 dichloromethane:methanol. Three 100 mL fractions ('4th fraction') were collected, followed by five 50 mL fractions ('5th fraction'). The column was darkly colored at the end of the run. The combined fractions were concentrated by evaporation of the solvent, after which their weight was determined and they were analyzed by ^{1}H-NMR and GLC-MS analysis.

References

[1] S. Kobayashi, H. Higashimura, *Prog. Polym. Sci.* **2003**, *28*, 1015.
[2] J. S. Dordick, M. A. Marletta, A. M. Klibanov, *Biotechnol. Bioeng.* **1987**, *30*, 31.
[3] A. S. Hay, H. S. Blanchard, G. F. Endres, J. W. Eustance, *J. Am. Chem. Soc.* **1959**, *81*, 6335.
[4] A. Corma Canós, R. Juarez Marin, H. Garcia Gomez, EU 2316822, **2011**.
[5] S. P. Gupte, R. V. Chaudhari, *J. Catal.* **1988**, *114*, 246.
[6] V. Macho, M. Harustiak, *J. Mol. Cat.* **1994**, *91*, L155.
[7] K. V. Prasad, R. V. Chaudhari, *J. Catal.* **1994**, *145*, 204.
[8] S. A. R. Mulla, C. V. Rode, A. A. Kelkar, S. P. Gupte, *J. Mol. Catal. A-Chem.* **1997**, *122*, 103.
[9] H. S. Kim, Y. J. Kim, H. Lee, S. D. Lee, C. S. Chin, *J. Catal.* **1999**, *184*, 526.
[10] F. Shi, Y. Q. Deng, *J. Catal.* **2002**, *211*, 548.

[11] B. Chen, S. S. C. Chuang, *J. Mol. Catal. A-Chem.* **2003**, *195*, 37.
[12] H. S. Kim, Y. J. Kim, H. Lee, K. Y. Park, C. Lee, C. S. Chin, *Angew. Chem.* **2002**, *41*, 4300.
[13] S. M. Lee, N. S. Cho, K. D. Kim, J. S. Oh, C. W. Lee, J. S. Lee, *J. Mol. Cat.* **1992**, *73*, 43.
[14] C. W. Lee, J. S. Lee, S. M. Lee, K. D. Kim, N. S. Cho, J. S. Oh, *J. Mol. Cat.* **1993**, *81*, 17.
[15] C. W. Lee, S. M. Lee, J. S. Oh, J. S. Lee, *Catal. Lett.* **1993**, *19*, 217.
[16] M. Gasperini, F. Ragaini, C. Remondini, A. Caselli, S. Cenini, *J. Organomet. Chem.* **2005**, *690*, 4517.
[17] X. F. Wang, P. Li, X. H. Yuan, S. W. Lu, *J. Mol. Catal. A-Chem.* **2006**, *253*, 261.
[18] A. M. Tafesh, J. Weiguny, *Chem. Rev.* **1996**, *96*, 2035.
[19] H. A. Dieck, R. M. Laine, R. F. Heck, *J. Org. Chem.* **1975**, *40*, 2819.

Chapter 8

Summary, conclusions, and outlook

8.1. Summary

8.1.1. General Introduction; alternative routes to TDI and MDI (Ch 1)

In Chapter 1 a summary is given of conventional and alternative strategies for the large-scale production of aromatic isocyanates such as toluene di-isocyanate (TDI) and methylene diphenylisocyanate (MDI). In the current production of TDI and MDI, phosgene is used to carbonylate an aromatic amine. Not only is phosgene extremely toxic, this process co-produces stoichiometric amounts of the corrosive hydrochloric acid; this can lead to reactor degradation and the formation of difficult to remove chlorinated side products. Despite these drawbacks, this 'phosgene route' remains the most (cost) efficient synthetic procedure and is thus still applied on the megaton scale today. Several alternative strategies for this process have been proposed over the years, and the most viable alternatives use CO as reduction and carbonylation reagent in the transition metal catalyzed reductive carbonylation of a nitro aromatic compound. In the reported studies, nitrobenzene ($PhNO_2$) is typically used as a model substrate, and the use of palladium proved to result in the most effective catalytic systems. The catalytic carbonylation of nitrobenzene is generally performed in methanol as the solvent, using homogeneous palladium complexes supported by bidentate N- or P-donor ligands. In a methanol environment, methyl phenyl carbamate (MPC) is formed (instead of phenylisocyanate) which can –in principle– be pyrolized to phenylisocyanate with the recovery of methanol.

In particular, the use of the N-donor ligand 1,10-phenanthroline (phen) with an acid co-catalyst resulted in relatively active and selective catalytic systems. As a result of these initial findings, the academic community has focussed on studying the Pd/phen/CH_3OH/H^+ –and related– catalytic systems, and catalyst turnover numbers (mol/mol) as large as ~10^5 have been reported. These studies notwithstanding, a clear and generally agreed upon mechanistic picture has yet to emerge for this reaction. Many proposals have been put forward over the years, most of which involve palladacyclic intermediates, but the apparent lack of empirical data for these proposals has hampered their firm establishment. Yet a prime paradigm in the field of homogeneous catalysis is that in order for commercially applicable catalysts to be developed, intimate knowledge of the underlying molecular mechanism of a certain reaction is essential.

A prime aim of the research described in this thesis is therefore to gain understanding into the molecular mechanism of the palladium-mediated reductive carbonylation of nitrobenzene in methanol. For these studies, diphosphane ligands were chosen as the supporting ligand for palladium; not only has the Pd/phosphane/CH_3OH system been scarcely studied, but phosphane ligands are also known to be better ligands, in particular for zero valent palladium, than N-donor ligands such as phen. In addition, their steric and electronic properties can be more easily fine-tuned than aromatic N-donor ligands. It is believed that the molecular relation between the stereo-electronic properties of the catalyst complexes and their respective catalytic performances will lead to a better mechanistic understanding necessary for the development of active and selective catalysts for a sustainable, phosgene-free, synthesis of aromatic isocyanates.

8.1.2. Catalyst precursor complex formation and structure (Ch 2)

Many of the catalytic reactions that are reported in this thesis have been carried out with catalyst precursors of the type [Pd(ligand)$(anion)_2$], wherein the supporting ligand is a bidentate diarylphosphane ligand. Such catalyst precursors are commonly synthesized *in situ,* prior to the catalytic experiment. However, for a proper interpretation of the data that arise from such catalytic experiments, it is pivotal to know whether or not the anticipated complex actually is formed. Also, intimate structural knowledge is required to link catalyst performances to their structures.

In Chapter 2 the synthetic pathways towards [Pd(ligand)$(anion)_2$] and [Pd$(ligand)_2$]$(anion)_2$ complexes is described; eighteen different ligands have been used in combination with strongly (acetate, OAc^-) or weakly (tosylate, OTs^-) coordinating anions. Of some representative complexes the solid state structure has been determined with X-ray crystallography. It is shown that the solid state structures are fully retained in solution, and that the axial positions of palladium are sterically shielded when the ligand in the complex is functionalized with oMeO substituents. The formation of [Pd(ligand)$(anion)_2$]-type complexes was studied in detail using ^{1}H- and ^{31}P-NMR spectroscopy. Depending on the ligand structure this complex is formed instantaneously, or *via* a polynuclear intermediate or it is not formed at all. It was also found that the coordinating

ability of the anions can alter the kinetic and/or the thermodynamic product formed.

Which complex is formed in solution is demonstrated to depend on the length and rigidity of the ligand backbone, and on the steric bulk at the ortho position of the phenyl rings on phosphorus. Notably, when the steric bulk at the ortho position of the phenyl rings on phosphorus is enlarged, complex formation is retarded and in some cases prevented altogether. This retarding effect can be overcome completely by making the backbone spacer of the ligand more rigid, which always results in instantaneous formation of the desired [Pd(ligand)(anion)$_2$] complex in methanol.

8.1.3. An unexpectedly complex network of catalytic reactions, centred around a Pd-imido intermediate (Ch 3)

In Chapter 3, the catalytic reactivity is described of palladium compounds of bidentate diarylphosphane ligands in the reaction of nitrobenzene with CO in methanol. The four ligands that were used in this study were selected partially based on the rigidity of their backbone, thus ensuring instantaneous complex formation (see Chapter 2).

Careful analysis of the reaction mixtures revealed that besides the frequently reported reduction products of nitrobenzene (MPC, *N,N'*diphenyl urea (DPU), aniline ($PhNH_2$), azobenzene (Azo) and azoxybenzene (Azoxy)), large quantities of oxidation products of methanol were co-produced as well (dimethyl carbonate (DMC), dimethyl oxalate (DMO), methyl formate (MF), H_2O, and CO). From a detailed *quantitative analysis* of the various observed reaction products, it can be concluded that several catalytic processes must operate simultaneously, coupled *via* shared catalytic intermediates. Based on simulations of observed product compositions in terms of theoretically derived stoichiometries, it was possible to determine relative weight and catalytic connectivity of the several catalytic processes occurring. It is proposed that the catalytic cycles form a complex reaction network that is centred around a palladium-imido intermediate ('P_2Pd^{II}=NPh'), as is schematically shown in Scheme 8.1.

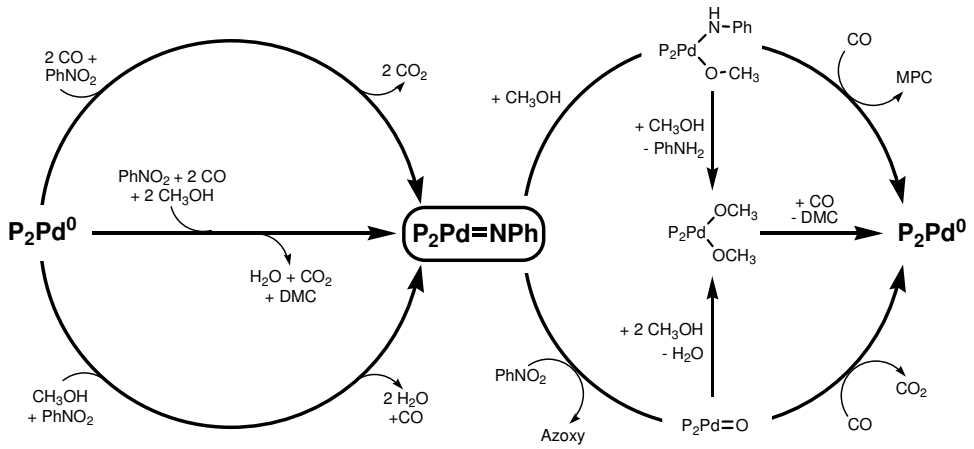

Scheme 8.1. Overall mechanistic proposal, centered around a palladium-imido intermediate, for the catalytic coupling between nitrobenzene reduction and methanol oxidation chemistry when working with the Pd/phosphane/CH_3OH catalytic system.

Starting from an *in situ* formed P_2Pd^0 compound, oxidation to a palladium-imido compound 'P_2Pd^{II}=NPh', can be achieved by *de-oxygenation* of nitrobenzene via three different pathways (Scheme 8.1, left): with two molecules of CO (top left), with two molecules of CO and the acidic protons of two methanol molecules (centre left), or with all four hydrogen atoms of one methanol molecule (bottom left).

Formation of the imido intermediate can be followed by a protonation to form $P_2Pd^{II}(OCH_3)NHPh$ (top right) or a "disproportionation" to form Azo(xy) and 'P_2Pd=O' (bottom right). Both intermediates can be carbonylated to form respectively, MPC (top right) or CO_2 (bottom right) and re-form the initial P_2Pd^0 species to make these reactions catalytic. Alternatively, both intermediates can be protonated to form $P_2Pd^{II}(OCH_3)_2$ and aniline (top right) or water (bottom right). Carbonylation of this $P_2Pd^{II}(OCH_3)_2$ complex will produce DMC/DMO and regenerate P_2Pd^0 (centre right), allowing these reactions to proceed catalytically as well.

It is thus proposed that the Pd-imido species is the central key-intermediate species that links together all reduction products of nitrobenzene and all oxidation products of methanol in one unified mechanistic scheme. It has been shown that the relative occurrence of the various catalytic processes is dependent on the stereo-electronic characteristics of the catalyst, as imposed by those of the ligand.

8.1.4. A palladium-imido complex as the central product-releasing species (Ch 4)

In a mechanistic study described in Chapter 4, a variety of *in situ* formed palladium complexes of bidentate diarylphosphane ligands has been applied as catalyst precursors in the carbonylation of nitrobenzene. Variation in the length and rigidity of the backbone spacer of the chelating ligands, some carrying a methoxy-substituent on the aryl rings, was aimed to differentiate between electronic and steric effects of the catalysts' ligand on the quantitative product distribution. Additional mechanistic information has been gathered from studying the effects of reaction conditions on the product composition.

It was found that more carbonylation products (MPC and DPU) are formed relative to hydrogenation products ($PhNH_2$ and DPU) when using a ligand with smaller bite–angle (C_3–backbone) or when using a ligand with *ortho*–methoxy groups. Up to 73% of coupling products (azo(xy)benzene) was obtained when using a ligand with a larger bite–angle (C_4–backbone). Based on these observations and the dependencies of the product formation on reactant concentrations ($PhNO_2$, CO) it is proposed that, in line with the mechanistic proposal outlined in Chapter 3, formation of all aryl-containing products must compete for the same palladium–imido (P_2Pd^{II}=NPh) intermediate.

A palladacycle that is generally proposed to be the product-releasing intermediate in the Pd/phen/CH_3OH(/H^+) catalytic system (**I** in Scheme 8.2) was also considered as a possible intermediate in the Pd/phosphane/CH_3OH system (**II** in Scheme 8.2). However, as summarized in Scheme 8.2, ligand exchange reactions of the stable phen-palladacycle **I** with diphosphane ligands (studied with $^{31}P\{^1H\}$–NMR and ESI-MS) show that the formed 5–membered diphosphane-palladacycle **II** readily decomposes under mild conditions by loss of CO rather than CO_2. This eventually leads to the formation of the P_2Pd^{II}=NPh intermediate (**V**) instead of expected carbonylation products (isocyanates or MPC) after a decarboxylation of palladacycle **II**. The latter process apparently has a higher activation barrier.

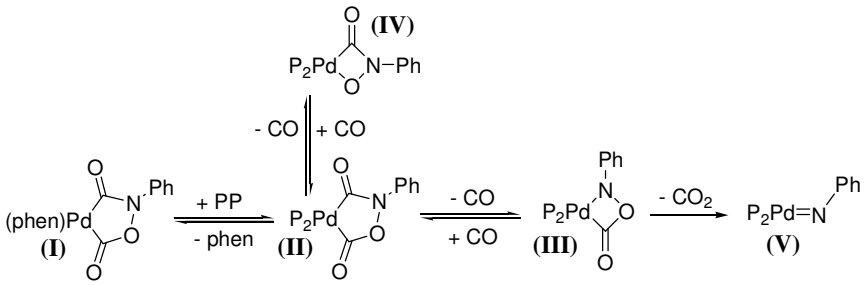

Scheme 8.2. Proposed reaction sequence of the ligand exchange between palladacycle **I** and a diphosphane ligand, followed by decomposition of **II** to the imido complex **V** by initial loss of CO.

DFT calculations indicate that compound **II** indeed has a lower stability than **I**, and apparently therefore readily decomposes (by decarbonylation). The observed decrease in the rate of decomposition of the palladacycle **II** in an atmosphere of CO suggests that decarbonylation of this species proceeds by a *reversible,* low barrier carbonylation/de-carbonylation sequential process. Under certain ligand exchange conditions, additional $^{31}P\{^{1}H\}$–NMR resonances are indeed observed that can be most probably assigned to palladacycle **III**, presumably obtained via decarbonylation of palladacycle **II**. By conjecture, it is proposed that all palladacycles, **II** and **III** and **IV**, shown in Scheme 8.2 are reversibly and mutually connected by carbonylation/decarbonylation cycles. Irreversible escape from these mutually equilibrated palladacycles can only take place via decarboxylation (–CO_2) of intermediate **III** to give a palladium-imido species **V**. However, until now, the direct spectroscopic characterisation of V has remained elusive due to a rapid further decomposition under the aprotic, pressure-less conditions used in the ligand exchange model experiments, giving only a well-identified reduced Pd^{0}(diphosphane)$_2$ complex together with mainly unidentified organic products containing the 'NPh' fragment.

Proof for the possible *existence and reactivity* of a P_2Pd^{II}=NPh type species comes from a combined $^{31}P\{^{1}H\}$NMR and ESI–MS analysis of a reaction between a P_2Pd^{0} compound, containing a very bulky diphosphane ligand (1,3-bis(1,3,5,7-tetramethyl-4,6,8-trisoxa-2-phospaadamantyl)propane), and mesityl azide forming what appears to be likely a P_2Pd-imido complex (sterically) protected against rapid thermal decomposition. This complex was indeed shown to react with CO and methanol to give methyl mesityl carbamate, even under ambient mild conditions.

Under actual high CO pressure catalytic nitrobenzene carbonylation conditions in methanol as solvent, it is thought that subsequent reactions of palladium-imide **V** gives respectively, i) MPC and DPU (by methoxy- and amino-carbonylation), ii) azoxybenzene and azobenzene (by 'disproportionation' with respectively nitrobenzene and nitrosobenzene) and iii) $PhNH_2$ (by protonation by methanol) and linked formation of DMC/DMO by methanol carbonylation.

The combined catalytic and organometallic data thus all point strongly to a P_2Pd^{II}=NPh complex as *a most probable ultimately product-releasing* intermediate species under nitrobenzene carbonylation conditions.

8.1.5. Oxidative carbonylation of methanol (Ch 5)

It was disclosed in Chapter 3 that in the Pd/diphosphane/CH_3OH system, nitrobenzene reduction chemistry is catalytically coupled with methanol oxidation chemistry. The molecular aspects of these coupled reactions were studied in more detail from the perspective of nitrobenzene reduction chemistry in Chapter 4. In Chapter 5 a similar study is reported, but then from the perspective of methanol oxidation chemistry. The system is viewed from the perspective of the formation of the industrially important oxidative methanol carbonylation products DMC and DMO, for which nitrobenzene clearly functions as the terminal oxidant. It was found that the overall mechanistic insights gained by studying the reductive carbonylation of nitrobenzene (Chapters 3 and 4) apply directly to the overall mechanism for the oxidative carbonylation of methanol. In fact, the overall mechanistic scheme as shown in Scheme 8.1 reveals directly how the catalytic cycle for formation of DMC and DMO is coupled with nitrobenzene reduction chemistry. Two key intermediate stages exist in the catalytic cycle that may each evolve one equivalent of DMC/DMO relative to one $PhNO_2$ reduced.

At stage 'one', starting from P_2Pd^0, oxidative carbonylation of CH_3OH is coupled with $PhNO_2$ reduction to produce the first DMC/DMO molecule and a 'P_2Pd=NPh' species (centre left in Scheme 8.1). Formation of DMC/DMO at this stage is avoided when only CO acts as reductant (top left in Scheme 8.1), or when $PhNO_2$ reduction is coupled with CH_3OH oxidative dehydrogenation to CO (or methyl formate, bottom left in Scheme 8.1).

At stage 'two', (right in Scheme 8.1) the P_2Pd^{II}=NPh species may react in two related manners to eventually produce aniline (top right in Scheme 8.1) or Azoxy (bottom right in Scheme 8.1) respectively, and the second equivalent of DMC/DMO via a common $P_2Pd^{II}(OCH_3)_2$ complex (centre right in Scheme 8.1). The $PhNH_2$/DMC/O pathway (top right in Scheme 8.1) proceeds first *via* a $P_2Pd^{II}(OCH_3)NHPh$ complex; production of DMC/O is avoided when this complex is carbonylated to MPC. The Azoxy/H_2O/DMC/O pathway (bottom right in Scheme 8.1) proceeds first *via* a P_2Pd^{II}=O complex; the production of DMC/O is avoided when this complex is carbonylated to CO_2. All these processes are catalytic as they re-form the original P_2Pd^0 species of stage 'one'.

The selectivity for DMC relative to DMO is thought to be determined in a $[P_2PdC(O)OCH_3(R)]$–type species; the DMO/DMC ratio can be increased by increasing the CO pressure, addition of an acid, or by using a ligand with a relatively large bite-angle.

Based on the collected results, it is concluded that an ideal catalyst for oxidative carbonylation would have a relatively acidic palladium centre, be sterically undemanding in the axial positions, but sterically demanding in the equatorial positions of palladium. The palladium complex of bis(diphenylphosphanyl)-ferrocene meets these criteria and was found to use nitrobenzene as oxidant for the oxidative carbonylation of methanol most efficiently of the series studied, i.e with about 50% of the theoretical maximum efficiency with a 2:1 ratio between DMC/DMO and reduced nitrobenzene.

8.1.6. A comparative study of diphosphane and phen palladium complexes (Ch 6)

Chapter 6 reports on a comparative study of the reactivity of palladium complexes supported by phen or diphosphane ligands in the reduction of nitrobenzene, as it was found that the reactivity of palladium catalytic systems supported by phen or the bidentate diarylphospane ligand 'L4X' is remarkably similar. Both are about 70% selective for the 'PhN-containing' coupling products Azo(xy), but also produce carbonylation products (MPC and DPU) and hydrogenation products ($PhNH_2$ and DPU). In contrast, only the Pd/L4X system concurrently produces significant amounts of methanol oxidation products (DMC, DMO, MF, CO and

H_2O). For both the Pd/phen/CH_3OH and the Pd/L4X/CH_3OH catalyst systems, it was found that Azoxy cannot result from a condensation reaction between aniline and nitrobenzene, nor does Azoxy evolve from 'free' nitrosobenzene. Instead, it is highly plausible that Azoxy is formed by the disproportionation of nitrobenzene with a L_2Pd=NPh intermediate, as the selectivity for Azoxy depends on the nitrobenzene concentration. The possible presence of such an imido-intermediate during carbonylation experiments is corroborated by the trapping of the 'NPh' fragment in this compound by cyclohexene, resulting in the formation of the corresponding azaridine.

The palladium-imido complex L_2Pd=NPh and the 5-membered palladacycle **I/II** (see Scheme 8.2) were both considered as possible *carbonylation* product-releasing species when employing phen and L4X as the supporting ligand. However, the ESI-MS spectrum of 'phen–palladacycle', together with a ligand exchange experiment of 'phen–palladacycle' with L4X and a theoretical (DFT) study of nitrobenzene deoxygenation to L_2Pd=NPh all suggest that this 5-membered palladacycle is *not* the major carbonylation product-releasing intermediate; the barrier for decarbonylation (–CO) is lower than that of decarboxylation (–CO_2).

As a result, the palladacycle is one of several CO-equillibrated palladacycles that merely act as temporary 'PhN-reservoir', as was already disclosed for the diphosphane systems in Chapter 4. Under acidic conditions, however, the decarboxylation barrier (–CO_2) is lowered; for 'phen–palladacycle' to the point where CO_2 extrusion is favored relative to loss of CO (in line with the observations of Osborn and co-workers),[1] but for 'L4X–palladacycle' the decarbonylation (–CO) barrier is still lowest due to the destabilizing effect that this bulkier ligand apparently has on such palladacycles.

As is also illustrated in Scheme 8.3, it is concluded that i) with catalysts supported by a phen ligand de-oxygenation of nitrobenzene, in contrast with catalysts supported by the diphosphane L4X, occurs almost exclusively by CO, ii) in the absence of acid the L_2Pd=NPh complex is the dominant 'PhN' product releasing intermediate, both for diphosphane and phen based catalysts and iii) *only* under acidic conditions, 5-membered palladacycle **I** may –for the ligand phenanthroline– become the major carbonylation product-releasing intermediate.

Already substoichiometric amounts (on Pd) of acids as co-catalysts lead to a lowering of the barrier for decarboxylation, presumably initiated by protonation of the palladacycle's nitrogen atom.

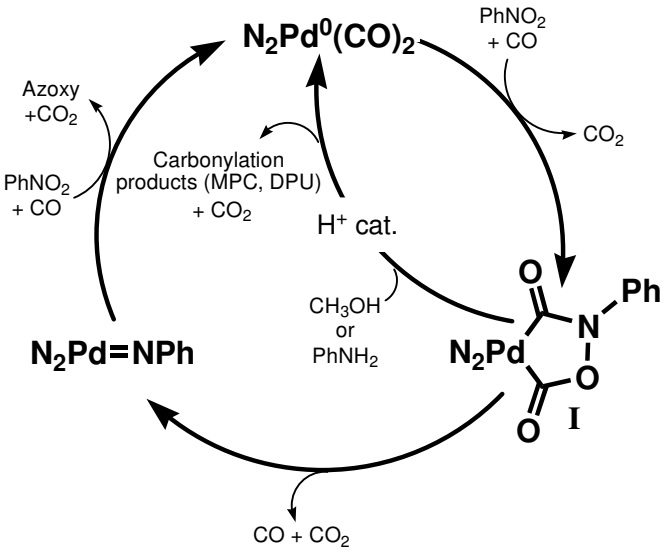

Scheme 8.3. Proposed mechanism for the nitrobenzene reduction chemistry in the Pd/phen/CH_3OH(/H^+) system. N_2 = phen.

It is noteworthy that the mechanistic proposal shown in Scheme 8.3 bears strong resemblance to –but is crucially distinct from– a recent proposal by Ragaini and co-workers.[2, 3] This proposal involves first full reduction of nitrobenzene to aniline and a (phen)Pd($C(O)OCH_3$)$_2$ species (via an unknown and un-elaborated-on pathway), which is supposed to react with aniline to give MPC. The mechanistic proposal outlined in this chapter is distinctly different in that the precursors for aniline formation itself (i.e., the palladium-imido intermediate or the palladacycle **I**), are direct antecedents for MPC genesis; however, under acid-free conditions the imido-complex, generated from (**I**) via de-carbonylation and subsequent de-carboxylation, reacts predominantly with nitrobenzene to give azoxybenzene as the main product while under slightly acidic conditions palladacycle **I** decomposes by decarboxylation to form MPC in good selectivity.

The complex (phen)Pd($C(O)OCH_3$)$_2$ is then better viewed as precursor to DMC/DMO via the (aniline liberating) double protonation of the imido

intermediate. DMC and DMO were indeed found in small amounts when working under acid-free conditions, but were (in line with the data reported by Ragaini) absent when working under acidic condition; this strongly suggests that such a (phen)Pd(C(O)OCH_3)$_2$ complex is not at all formed under acidic conditions.

8.1.7. Using other nucleophiles than methanol (Ch 7)

As was outlined in Chapters 3–5, the coupling between nitrobenzene reduction chemistry and methanol oxidation chemistry in the Pd/diphosphane/CH_3OH system provided a unique and clear hint towards mechanistic details of nitrobenzene carbonylation reactions. From a more practical point of view, however, this coupling of several catalytic reactions makes the Pd/diphosphane/CH_3OH system impractically complicated when aiming only for nitrobenzene carbonylation products. For any real application in the synthesis of aromatic isocyanates to result from the research described in this thesis, it is necessary to produce carbonylation products (e.g. a carbamate or urea) more selectively.

In Chapter 7 some preliminary studies are reported that were directed at replacing methanol by respectively *p*-cresol, *i*-propanol, 2,2,2-trifluoroethanol (TFE), and aniline with the aim of preventing the oxidation reactions of the respective nucleophilic reagent. These nucleophiles were selected based on their larger size (relative to methanol) to hopefully prevent formation of the carbonate and/or oxalate; *p*-cresol and TFE were also selected for their lower nucleophilicity, in order to obtain a carbamate that is more readily pyrolized. Furthermore, the oxidative carbonylation of aniline and the reductive carbonylation of nitrobenzene are anticipated to both give the same product, namely DPU.

When employing *p*-cresol under strictly anhydrous conditions, again significant amounts of the H-containing nitrobenzene reduction products $PhNH_2$ and DPU were formed when using typical diphosphane palladium-based catalyst systems, such as either those formed from (L3)Pd$(OAc)_2$ or to a lesser extent from [Pd$(phen)_2$]$(OTs)_2$ as catalyst precursor. Qualitative analysis of obtained reaction mixtures by ^{1}H-NMR and GLC-MS, HPLC-UV/MS and of several fractions obtained after a column chromatographic separation of reaction mixtures were undertaken. From these experiments, it is concluded that *p*-cresol can, contrary to

expectations, be involved in oxidative dehydrogenation reactions to give mainly unidentified products. Mass analysis indicates formation of probably oligomeric cresylene oxides.

When using (oMeOL3X)Pd(OAc)$_2$ as catalyst precursor, and *i*-propanol was used as the nucleophilic reagent and solvent in the carbonylation of nitrobenzene, it was found that this alcohol is a most effective H-donor via oxidative dehydrogenation of *i*-propanol, thus producing mainly acetone and aniline stoichiometrically. On the other hand, while using (L3X)Pd(OAc)$_2$ as catalyst precursor oxidative carbonylation of *i*-propanol as a significant hydrogen producing process also occurs.

When using 2,2,2-trifluoroethanol (TFE) as a weakly nucleophilic reagent, an unprecedented 95% selectivity for carbamate is observed at 90% nitrobenzene conversion with (L3X)Pd(OAc)$_2$ as catalyst precursor. Moreover, the trifluoroethyl phenyl carbamate was found to readily pyrolyze to phenylisocyanate at relatively low temperatures of 200-250 °C.

Applying aniline as the nucleophilic reagent and applying a range of diphosphane ligands typically gave a full conversion of nitrobenzene with excellent selectivities for DPU. Notably, using (L3X)Pd(OAc)$_2$ as catalyst precursor, it was found that 3-methylnitrobenzene is fully converted to 3-methylaniline, with the formation of the carbonylation products DPU (90%) and DPO (10%) even when working below the transamidation temperature of 70-80 °C. From these data, together with the quantitative formation of 3-methylaniline and the absence of the unsymmetrical urea or *N,N*'-di(3-methylphenyl)urea, is was proposed that the N-aryl groups from 3-methylnitrobenzene are transferred into 3-methylaniline via an imido N-aryl ligand exchange mechanism with aniline involving the Pd-catalyst. The molecular mechanistic details of this process, the nitroarene de-oxygenation, and the formation of DPU and DPO were proposed to be very similar to those of the nitrobenzene carbonylation and methanol oxidation processes in the Pd/diphosphane/CH_3OH system (see Chapters 3 – 5).

Based on the above findings, it is concluded that *p*-cresol and *i*-propanol are inappropriate substitutes for methanol. Aniline may be a promising alternative, but the difficulties to pyrolize DPU (relative to carbamates with a good leaving

group) may render this alternative unpractical. TFE on the other hand is a promising (weakly) nucleophilic reagent to perform Pd/diphosphane catalyzed nitrobenzene carbonylation reactions, producing the corresponding carbamate in high selectivity. Facile pyrolysis of the TFE carbamate makes this an attractive platform for isocyanate synthesis, while recovering TFE.

8.2. Conclusions and outlook; one step at a time

8.2.1. General conclusions

The incentive of the work described in this thesis is the development of catalytic systems that allow phosgene to be replaced by CO in an industrial process to aromatic isocyanates such as MDI and TDI. The first step towards this goal, and the prime aim of this thesis, has been to gain intimate knowledge of the molecular mechanisms of catalytic systems in the reductive carbonylation of nitroaromatic compounds. It was expected that in the long term such molecular understanding will be an important factor for the successful development of sustainable alternative MDI or TDI synthetic pathways.

To make this first step, many different *in situ* formed diphosphane-palladium complexes of the type [Pd(ligand)(anion)$_2$] were used as catalyst precursors to study the chemistry of nitrobenzene reduction with CO in methanol. With the help of these catalytic experiments and various organometallic and DFT studies, a general mechanistic picture has emerged for this reaction in which nitrobenzene reduction chemistry is catalytically coupled with methanol oxidation chemistry by a palladium-imido intermediate. With the detailed mechanistic understanding of these processes developed in this thesis, most effects that various ligands and reaction conditions have on the course of these reactions could be rationalized.

Applying methanol as the solvent thus provided a unique opportunity to unravel a detailed molecular mechanism not only for nitrobenzene reduction chemistry, but also for methanol oxidation chemistry (Chapters 3 and 4). Moreover, the understanding of these mechanisms translates directly to closely-related catalytic systems that are hereto mainly studied in isolation of one another. Indeed, it was shown that the overall mechanistic picture can be of help to illuminate the mechanism of the oxidative carbonylation of methanol (Chapter 5), the

Pd/phen/CH_3OH(/H^+) catalyzed reductive carbonylation of nitrobenzene (Chapter 6), and the Pd-catalyzed synthesis of DPU from nitrobenzene in aniline (Chapter 7).

It is therefore concluded that the studies reported in the first chapters of this thesis unveiled a *generally applicable* mechanism for Pd-mediated nitroarene reduction chemistry, (aliphatic) alcohol oxidation chemistry, and (supposed) aniline oxidation chemistry. With this mechanistic picture, the first step has been made towards the development of optimally performing catalytic systems in alternative MDI and TDI synthetic strategies.

8.2.2. Outlook

8.2.2.1 Proposed improvements in the synthetic strategy towards TDI

In nearly all catalytic experiments described in this thesis, nitrobenzene was used as the model substrate, whereas dinitrotoluene is actually used to prepare TDI. Nevertheless, the mechanistic knowledge collected in this thesis may be used in the actual design and synthesis of more efficient catalytic systems to eventually make TDI. An obvious option is to further fine-tune the ligand in the catalyst. In this respect, bulky bidentate alkylphosphanes with a rigid backbone spacer could be studied in methanol at low temperatures (60 °C) and high CO pressure (100 bar), for several reasons: i) methanol oxidation chemistry could be blocked by applying a more basic catalyst (alkyl *vs*. aryl) and by applying a higher CO pressure; ii) the palladacycle **I** (see Scheme 8.2) is formed at merely 60 °C (in ethanol), meaning that the nitrobenzene CO-only de-oxygenation route is already operative at this temperature but is trapped in this stable palladacycle instead of decomposing to the product-releasing imido complex; iii) moreover, palladacycles such as **I** were shown to be destabilized by bulky diphosphane ligands, thus possibly allowing the application of a very mild reaction temperature, provided that the ligand is bulky enough (e.g. *t*-Bu *vs*. phenyl, >β); iv) the rigid backbone is necessary to prevent ligand dissociation, as uncoordinated alkylphosphanes will easily be oxidized by the nitroarene.

Another way towards more ideal catalytic systems is to replace the easily oxidized methanol by another nucleophilic reagent. The requirements of such a nucleophile are threefold: i) it should resist oxidation by nitrobenzene; ii) the resulting

carbamate or urea should pyrolize easily; iii) the resulting carbamate or urea should preferably crystallize from the solution to allow easy separation of the product from the homogeneous catalyst. Thus, another clear indication for further research is the systematic exploration of applying various alcohols and amines. Although *p*-cresol was discarded as a viable alternative, other phenols may be less prone to oxidation. For example pentafluorophenol cannot be oxidized to quinone-like species that are likely to be intermediately produced when using *p*-cresol as nucleophile. Also, 4-hydroxy benzoic acid may be an attractive phenol; the acidic group may act as co-catalyst, and cannot be further oxidized. As for aliphatic alcohols, only TFE seems to be a viable alterative, as other alcohols will likely also participate in oxidative carbonylation and/or dehydrogenation reactions. However, trifluoroethyl phenylcarbamate is soluble in TFE; it may thus be worthwhile to test the performance of TFE in an aprotic and relatively apolar medium such as toluene. The resulting carbamate surely is readily pyrolized and perhaps also precipitates from the apolar medium; in such a case TFE appears to be an ideal nucleophile for an alternative TDI synthesis. Using aniline as the nucleophilic reagent also gave promising results; reaching a full conversion at merely 60 °C with over 90% selectivity towards DPU, which crystallizes from aniline. However, the pyrolisis of such ureas is generally more difficult than the pyrolisis of carbamates. More importantly, it was disclosed that the N-aryl group of the nitroarene is actually converted to the amine, meaning that dinitrotoluene may well be converted to its corresponding amine with the co-production of DPU (instead of the desired di-urea). Unless this exchange of N-aryl groups can be avoided, using an aromatic amine as the nucleophile in this system is not a viable option.

8.2.2.2 Proposed improvements in the synthetic strategy towards MDI

For an alternative synthetic route towards MDI, there are two distinct strategies available, owing to the condensation reaction of two aniline molecules with formaldehyde to methylenedianiline (MDA) that is required to link two aromatic rings together. Note that nitrobenzene cannot be coupled directly to a dinitro compound due to the deactivating effect of the nitro group on the *para*-position of the aryl ring in nitrobenzene. The first strategy can be to use nitrobenzene directly as the feedstock, and carbonylate it to the corresponding carbamate or urea. The carbamate or urea may then be coupled by a condensation reaction with

formaldehyde to form the di-carbamate or di-urea; both will liberate MDI upon pyrolisis while recovering the alcohol or amine applied. In this first strategy, the proposed improvements for nitro-arene reduction chemistry made above for an alternative TDI synthesis apply directly. Additionally, instead of aniline, (tri- or penta-)fluoroaniline could be applied as nucleophile, as the resulting urea will pyrolize much easier. Questionable will be whether the nucleophilicity will remain sufficient for fluoro analogous substrates to efficiently form corresponding ureas. In addition, it is questionable whether the coupling reaction of the resulting carbamates or ureas with formaldehyde will proceed in similar yield and selectivity as the currently applied coupling of aniline to MDA. Serious obstacles that may be anticipated include the deactivation of the para-position in the carbamate or urea (relative to aniline), the possible coupling of the alcoholic group (instead of the isocyanate group), and the likely oligomerization and/or polymerization during the coupling reaction (especially when using DPU). Owing to these anticipated difficulties, it seems unlikely that nitrobenzene carbonylation is an alternative strategy in a *commercially viable* synthetic route to MDI.

Instead, the second –and probably more practical– strategy would leave the coupling reaction of aniline to MDA unperturbed and instead use MDA as its feedstock. A urea or a carbamate can then be used as an alternative to phosgene as the carbonylation reagent via transamidation reactions. In this respect, the efficient and selective catalytic synthesis of DPU (which crystallized quantitatively from aniline) may prove important. When using DPU as carbonylation reagent (synthesized via Eq. 1), MDA as feedstock (synthesized via Eq. 2), and an aromatic alcohol as the solvent (and reactant), the reaction sequence given by Equations 3 to 5 may operate, thus leading to the overall stoichiometry given by Equation 6.

$PhNO_2 + PhNH_2 + 3\ CO$	$\rightarrow DPU + 2\ CO_2$	Eq. 1
$2\ PhNH_2 + H_2C{=}O$	$\rightarrow CH_2(PhNH_2)_2 + H_2O$	Eq. 2
$CH_2(PhNH_2)_2 + 2\ DPU$	$\leftrightarrows CH_2(PhNH(CO)NHPh)_2 + 2\ PhNH_2$	Eq. 3
$CH_2(PhNH(CO)NHPh)_2 + 2\ ROH$	$\leftrightarrows CH_2(PhNH(CO)OR)_2 + 2\ PhNH_2$	Eq. 4
$CH_2(PhNH(CO)OR)_2$	$\leftrightarrows CH_2(PhNCO)_2 + 2\ ROH$	Eq. 5
		+
$2\ PhNO_2 + H_2C{=}O + 6\ CO$	$\rightarrow CH_2(PhNCO)_2 + 4\ CO_2 + H_2O$	Eq. 6

Some preliminary model studies have already been conducted to tentatively assess the viability of this proposal. As a model to the transamidation reaction described by Equation 3, DPU was reacted with 4-ethylaniline by means of a reactive distillation (in 4-ethylaniline) to remove aniline; a full conversion to the symmetrical *N,N'*-di(4-ethylphenyl)urea was observed within 45 minutes reaction time. Likewise, as a model to reaction for the transamidation reaction described by Equation 4, a reactive distillation of DPU in 3,5-dimethylphenol resulted in an 80% conversion to 3,5-dimethylphenyl phenylcarbamate within about 90 minutes. Clearly, more research is required to further test the viability of this novel alternative synthetic pathway to MDI, but the above results are hopeful.

Even though an alternative, industrially applicable process to TDI or MDI has not been developed, the research described in this thesis has made an important first step by generating knowledge that can help to develop such systems. Indeed, the mechanism of nitro arene reduction chemistry is now well-understood for [Pd(ligand)(anion)$_2$]–type catalytic systems, thus opening the way to the rational design of more active and selective catalysts for the carbonylation of nitro-aromatic compounds. Moreover, the crucial importance of the nucleophilic reagent applied also unlocks a wide range of novel ventures that can lead to alternative synthetic pathways to industrially important di-isocyanates such as TDI or MDI. The first step has thus been made, and the author eagerly anticipates the new steps that will undoubtedly follow, as it is still a realistic hope that catalytic nitro arene reductive carbonylation chemistry will one day replace the dangerous and wasteful 'phosgene-routes'.

References

[1] P. Leconte, F. Metz, A. Mortreux, J. A. Osborn, F. Paul, F. Petit, A. Pillot, *J. Chem. Soc.-Chem. Commun.* **1990**, 1616.
[2] F. Ragaini, M. Gasperini, S. Cenini, L. Arnera, A. Caselli, P. Macchi, N. Casati, *Chem. Eur. J.* **2009**, *15*, 8064.
[3] F. Ragaini, *Dalton Trans.* **2009**, 6251.

Appendix I

Supporting Information of Chapter 2

-^{1}H, ^{31}P{^{1}H}-NMR, MS and EA, data and yields of ligands and complexes-

Appendix I

Ligand / Complex		1H Solvent	*o*-Ph-*H*	*m*-Ph-*H* / MeOC=C-*H*	*p*-Ph-*H*	*m*-Ph-*H*	*o*-Ph-*H*	OC*H*3 / OC*H*2CH3
oMeOtpp		CDCl3		6.90(d,3H)	7.32(t,3H)	6.70(t,3H)	6.83(d,3H)	3.74(s,9H)
oEtOtpp		CDCl3		6.84(m,9H)	7.29(t,3H)	6.84(m,9H)	6.84(m,9H)	3.98(q,6H)
C2 - bridged								
L1		CDCl3	7.32(m,20H)	7.32(m,20H)	7.32(m,20H)			
[Pd(L1)(OAc)2]		MeOD	7.45(t,8H)	7.80(q,8H)	7.52(m,4H)			
[Pd(L1)(OTs)2]		Acetone	7.63(m,8H)	7.95(q,8H)	7.76(m,4H)			
[Pd(L1)2][OTs]2		CDCl3	7.26(m,20H)	7.46(m,20H)	7.26(m,20H)			
L2		CDCl3		7.05(d,4H)	7.30(t,4H)	6.86(m,8H)	6.86(m,8H)	3.73(s,12H)
[Pd(L2)(OAc)2]		CDCl3		7.04(t,4H)	7.50(t,4H)	6.92(q,4H)	8.04(q,4H)	3.72(s,12H)
[Pd(L2)(OTs)2]		Acetone		7.24(t,4H)	7.65(m,8H)	7.09(m,8H)	7.65(m,8H)	3.80(s,12H)
[Pd(L2)2][OAc]2	{ax}	CDCl3		7.11(d,4H)	7.80(t,4H)	7.54(m,4H)	8.14(br,4H)	3.68(2,12H)
	{eq}			6.88(d,4H)	6.46(t,4H)	7.35(m,4H)	5.88(br,4H)	3.59(s,12H)
[Pd(L2)2][OTs]2	{ax}	CDCl3		6.97(d,4H)	7.81(t,4H)	7.50(t,4H)	8.08(br,4H)	3.67(s,12H)
	{eq}			6.82(d,4H)	6.56(t,4H)	7.26(t,4H)	5.84(br,4H)	3.52(s,12H)
L3		CDCl3		7.17(s,4H)	7.23(t,4H)	6.76(d,4H)	6.83(t,4H)	3.89(m,8H)
[Pd(L3)(OAc)2]		CDCl3		6.90(q,4H)	7.00(t,4H)	7.47(t,4H)	8.01(q,4H)	4.00(m,8H)
C4 - bridged								
L14		CDCl3	7.31(m,12H)	7.31(m,12H)	7.39(t,8H)			
[Pd(L14)(OAc)2]		MeOD	7.63(q,8H)	7.34(t,8H)	7.47(t,4H)			
[Pd(L14)(OTs)2]		CDCl3	7.40(m,8H)	7.54(t,8H)	7.70(t,8H)			
L15		CDCl3		7.09(t,4H)	7.30(t,4H)	6.86(m,8H)	6.86(m,8H)	3.75(s,12H)
L16		CDCl3		7.24(m,8H)	7.24(m,8H)	6.87(t,4H)	6.79(dd,4H)	3.94(m,8H)
L17		CDCl3	7.30(dd,8H)	6.85(d,8H)				3.80(s,12H)
[Pd(L17)(OAc)2]		CDCl3	7.64(t,8H)	6.97(d,8H)				3.89(s,12H)
L18		CDCl3	7.31(m,12H)	7.41(m,8H)	7.31(m,12H)			
[Pd(L18)(OAc)2]		CDCl3	7.75(dq,8H)	7.46(m,8H)	7.55(t,4H)			
L19		CDCl3		7.24(m,8H)	7.24(m,8H)	6.85(m,8H)	6.85(m,8H)	3.70(d,12H)
[Pd(L19)(OAc)2]	{+,+}	CDCl3		7.04(d,4H)	7.74(t,4H)	7.74(t,4H)	9.78(br,4H)	4.06(s,12H)
	{+,-}	6.72(m,8H)	6.72(m,8H)	6.99(m,4H)	7.43(br,4H)	3.74(s,12H)		2.67(q,4H)

Ligand / Complex		1H Solvent	*o*-Ph-*H*	*m*-Ph-*H* / MeOC=C-*H*	*p*-Ph-*H*	*m*-Ph-*H*	*o*-Ph-*H*	OC*H*3 / OC*H*2CH3	OCH2C*H*3	PC*H*2
C3 - bridged										
L4		CDCl3	7.35(m,8H)	7.29(m,12H)	7.29(m,12H)					2.19(t,4H)
[Pd(L4)(OAc)2]		CDCl3	7.34(m,12H)	7.72(m,8H)	7.34(m,12H)					2.51(m,4H)
[Pd(L4)(OTs)2]		CDCl3	7.67(q,8H)	7.26(t,8H)	7.41(m,8H)					2.83(m,4H)
[Pd(L4)2][OAc]2		CDCl3	7.04(m,8H)	7.31(m,8H)	7.11(m,4H)					2.22(m,4H)
L5		CDCl3	7.28(m,12H)	7.42(m,8H)	7.28(m,12H)					2.33(d,4H)
[Pd(L5)(OAc)2]		CDCl3	7.90(m,8H)	7.44(m,12H)	7.44(m,12H)					2.29(d,4H)
[Pd(L5)(OTs)2]		MeOD	7.58(br,8H)	7.29(m,16H)	7.29(m,16H)					2.59(br,4H)
[Pd(L5)2][OTs]2		MeOD	7.60(br,16H)	7.26(m,28H)	7.26(m,28H)					2.62(br,8H)
L6		CDCl3		7.11(m,12H)	7.11(m,12H)	7.20(q,4H)	7.11(m,12H)	2.37(s,12H)		2.11(t,4H)
[Pd(L6)(OAc)2]		CDCl3			7.24(m,8H)	7.40(t,4H)	8.19(br,4H)	2.48(s,12H)		2.52(m,4H)
L7		CDCl3		7.07(t,4H)	7.28(t,4H)	6.85(m,8H)	6.85(m,8H)	3.72(s,12H)		2.22(t,4H)
[Pd(L7)(OAc)2]		CDCl3		6.94(d,4H)	7.50(t,4H)	7.08(br,4H)	8.25(br,4H)	3.76(s,12H)		2.44(m,4H)
[Pd(L7)2][OAc]2	{ax}	MeOD		7.05(m,8H)	7.46(t,4H)	7.74(t,4H)	8.59(br,4H)	4.23(s,12H)		2.90(m,4H)
	{eq}			7.05(m,8H)	7.30(t,4H)	6.61(t,4H)	5.91(br,4H)	3.42(s,12H)		2.38(m,4H)
[Pd(L7)2][OTs]2	{ax}	CDCl3		6.99(d,4H)	7.64(t,4H)	7.73(t,4H)	8.51(br,4H)	4.33(s,12H)		2.85(m,4H)
	{eq}			6.83(d,4H)	7.20(m,8H)	6.47(t,4H)	5.82(br,4H)	3.38(s,12H)		2.25(m,4H)
L8		CDCl3		7.16(t,4H)	7.23(t,4H)	6.76(dd,4H)	6.84(t,4H)	3.91(q,8H)	1.20(t,12H)	2.29(t,4H)
[Pd(L8)(OAc)2]		CDCl3		7.87(d,4H)	6.98(br,4H)	7.46(t,4H)	8.25(br,4H)	3.98(m,8H)	0.89(t,12H)	2.49(br,4H)
L9		CDCl3	7.28(t,8H)	6.83(d,8H)				3.79(s,12H)		2.10(t,4H)
[Pd(L9)(OAc)2]		CDCl3	7.63(q,8H)	6.89(d,8H)				3.82(s,12H)		2.38(m,4H)
L10		CDCl3		7.18(t,4H)	7.26(t,4H)	6.75(dd,4H)	6.86(t,4H)	3.71(s,12H)		2.28(d,4H)
[Pd(L10)(OAc)2]		CDCl3		6.92(d,4H)	7.07(m,4H)	7.51(t,4H)	8.15(br,4H)	3.86(s,12H)		2.58(d,4H)
[Pd(L10)(OTs)2]		Acetone		7.08(m,8H)	7.27(m,4H)	7.68(t,4H)	7.75(m,4H)	4.09(s,12H)		2.87(d,4H)
[Pd(L10)2][OAc]2	{ax}	MeOD		7.11(d,4H)	7.30(m,8H)	7.64(t,4H)	8.36(br,4H)	4.26(s,12H)		2.78(d,4H)
	{eq}			6.92(d,4H)	7.30(m,8H)	6.70(t,4H)	6.48(br,4H)	3.41(s,12H)		2.44(d,4H)
[Pd(L10)2][OTs]2	{ax}	CDCl3		7.07(d,4H)	7.56(m,8H)	7.56(m,8H)	8.29(br,4H)	4.38(s,12H)		2.70(d,4H)
	{eq}			6.68(d,4H)	7.16(m,8H)	6.53(t,4H)	6.34(br,4H)	3.38(s,12H)		2.30(d,4H)
L11		CDCl3		7.21(m,8H)	7.21(m,8H)	6.76(dd,4H)	6.84(t,4H)	3.67(s,12H)		2.25(d,4H)
[Pd(L10)(OAc)2]		CDCl3		6.93(d,4H)	7.08(t,4H)	7.51(t,4H)	8.23(br,4H)	3.84(s,12H)		2.58(d,5H)
[Pd(L10)2][OAc]2	{ax}	MeOD		7.11(d,4H)	7.28(m,8H)	7.63(t,4H)	8.36(br,4H)	4.23(s,12H)		2.56(br,8H)
	{eq}			6.93(d,4H)	7.28(m,8H)	6.71(t,4H)	6.54(br,4H)	3.39(s,12H)		
L12		CDCl3		7.26(t,4H)	7.19(t,4H)	6.70(dd,4H)	6.82(t,4H)	3.88(s,8H)	1.18(t,12H)	2.32(d,4H)
[Pd(L12)(OAc)2]		Acetone		7.00(m,8H)	7.00(m,8H)	7.51(t,4H)	8.28(br,4H)	4.09(m,8H)	1.08(m,16H)	2.77(d,4H)
L13		CDCl3		7.23(m,8H)	7.23(m,8H)	6.81(m,8H)	6.81(m,8H)	3.70(d,12H)		3.88(s,4H)
[Pd(L13)(OAc)2]		CDCl3		6.94(d,4H)	7.08(br,4H)	7.52(br,4H)	8.50(br,4H)	3.88(s,12H)		2.68(s,4H)
[Pd(L13)(OTs)2]		Acetone		7.29(m,4H)	7.14(t,4H)	7.73(t,4H)	7.86(br,4H)	4.03(s,12H)		2.94(d,4H)
[Pd(L13)2][OAc]2	{ax}	MeOD		7.14(d,4H)	7.34(t,4H)	6.78(t,4H)	8.35(br,4H)	4.30(s,12H)		2.88(d,4H)
	{eq}			6.97(d,4H)	7.29(t,4H)	6.72(t,4H)	6.48(br,4H)	3.42(s,12H)		2.56(m,12H)
[Pd(L13)2][OTs]2	{ax}	CDCl3		7.20(m,12H)	7.60(m,8H)	7.60(m,8H)	8.28(br,4H)	4.44(s,12H)		2.73(d,4H)
	{eq}			6.74(d,4H)	7.17(m,20H)	6.54(t,4H)	6.34(br,4H)	3.40(s,12H)		2.44(m,18H)

OCH2CH3	PCH2	PCH2CH2 / PCH2CH	CHOCCH3	OCCH2CH2CH2	OC(O)CH3	o-OTs-H	m-OTs-H	p-OTs-CH3
1.12(t,9H)								
	2.09(t,4H)							
	2.50(m,4H)				1.49(s,6H)			
	3.08(m,4H)					7.51(d,4H)	7.11(d,4H)	2.32(s,6H)
	3.16(m,8H)					8.08(d,4H)	7.46(m,20H)	2.39(s,6H)
	2.18(t,4H)							
	2.63(d,4H)				1.36(s,6H)			
	3.05(m,4H)					7.50(d,4H)	7.09(m,8H)	2.29(s,6H)
	3.20(m,8H)				2.02(s,6H)			
	3.03(m,8H)					7.89(d,4H)	7.12(d,4H)	2.33(s,6H)
1.15(m,12H)	2.25(s,4H)							
1.10(m,12H)	2.84(m,4H)				1.42(br,6H)			
	2.01(m,4H)	1.54(m,4H)						
	2.44(br,4H)	1.93(m,4H)		1.32(br,6H)				
	2.58(br,4H)	2.15(m,4H)				7.40(m,8H)	6.93(d,4H)	2.31(s,6H)
	2.06(m,4H)	1.59(m,4H)						
1.21(t,12H)	2.12(m,4H)	1.59(m,4H)						
	1.93(m,4H)	1.50(m,4H)						
	2.30(br,4H)	2.00(m,4H)			1.40(s,6H)			
	2.35(m,4H)	3.91(m,2H)	1.34(s,6H)					
	2.71(dt,4H)	4.03(m,2H)	1.20(s,6H)		1.34(br,6H)			
	2.45(m,4H)	4.00(q,2H)	1.32(s,6H)					
	3.15(t,4H)	3.37(br,4H)	1.06(s,12H)		1.17(s,12H)			

PCH2	PCH2CH2 / PCH2CH	CCH3 / CCH2	CCH2CH3	OCCH2	OCCH2CH2	OCCH2CH2CH2	OC(O)CH3	o-OTs-H	m-OTs-H	p-OTs-CH3
2.19(t,4H)	1.60(m,2H)									
2.51(m,4H)	2.15(m,2H)						1.34(s,6H)			
2.83(m,4H)	2.25(m,2H)							7.41(m,8H)	6.86(d,4H)	2.31(s,6H)
2.22(m,4H)	1.43(m,2H)						2.14(s,6H)			
2.33(d,4H)	1.03(s,6H)									
2.29(d,4H)		0.91(s,6H)					1.44(s,6H)			
2.59(br,4H)		0.26(s,6H)						7.88(d,4H)	7.29(m,16H)	2.38(s,6H)
2.62(br,8H)		0.26(s,12H)						8.00(d,4H)	7.26(m,28H)	2.38(s,6H)
2.11(t,4H)	1.61(m,2H)									
2.52(m,4H)	2.00(m,2H)									
2.22(t,4H)	1.65(m,2H)									
2.44(m,4H)	1.95(m,2H)						1.26(br,6H)			
2.90(m,4H)	1.63(m,4H)						1.87(s,6H)			
2.38(m,4H)										
2.85(m,4H)	1.52(br,4H)							7.96(d,4H)	7.20(m,8H)	2.36(s,6H)
2.25(m,4H)										
2.29(t,4H)	1.65(m,2H)									
2.49(br,4H)	1.94(m,2H)						1.21(br,6H)			
2.10(t,4H)	1.54(m,2H)									
2.38(m,4H)	2.01(m,2H)						1.33(s,6H)			
2.28(d,4H)		1.12(s,6H)								
2.58(d,4H)		0.66(s,6H)					1.20(s,6H)			
2.87(d,4H)		0.97(s,6H)						7.45(d,4H)	7.08(m,8H)	2.32(s,6H)
2.78(d,4H)		0.22(s,12H)					1.88(s,6H)			
2.44(d,4H)										
2.70(d,4H)		0.12(s,12H)						7.95(d,4H)	7.16(m,8H)	2.36(s,6H)
2.30(d,4H)										
2.25(d,4H)		1.59(q,4H)	0.66(t,6H)							
2.58(d,5H)		0.92(m,4H)	0.55(t,6H)				1.26(s,6H)			
2.56(br,8H)		0.36(m,20H)	0.36(m,20H)				1.88(s,6H)			
2.32(d,4H)		1.58(q,4H)	0.62(t,6H)							
2.77(d,4H)		1.08(m,16H)	0.59(t,6H)				1.17(br,6H)			
3.88(s,4H)		2.45(d,4H)		1.77(br,4H)	1.47(br,4H)	1.37(br,2H)				
2.68(s,4H)		3.09(s,4H)		1.57(m,4H)	1.37(m,6H)	1.37(m,6H)	1.21(s,6H)			
2.94(d,4H)		3.36(s,4H)		1.65(m,4H)	1.37(m,6H)	1.37(m,6H)		7.40(d,4H)	7.06(d,4H)	2.31(s,6H)
2.88(d,4H)		2.56(m,12H)		1.37(m,8H)	1.23(m,12H)	1.23(m,12H)	1.88(s,6H)			
2.56(m,12H)										
2.73(d,4H)		2.44(m,18H)		1.42(br,8H)	1.23(dr,12H)	1.23(br,12H)		8.00(d,4H)	7.17(m,20H)	2.44(m,18H)
2.44(m,18H)										

Code	X	R
L1	H	
L2	*o*-MeO	
L3	*o*-EtO	
L4	H	H
L5	H	CH_3
L6	*o*-Me	H
L7	*o*-MeO	H
L8	*o*-EtO	H
L9	*p*-MeO	H
L10	*o*-MeO	CH_2
L11	*o*-MeO	CH_2CH_3
L12	*o*-EtO	CH_2CH_3
L13	*o*-MeO	R*
L14	H	H
L15	*o*-MeO	H
L16	*o*-EtO	H
L17	*p*-MeO	H
L18	H	R**
L19	*o*-MeO	R**

Appendix I

Ligand / Complex	31P	MS found (calc.)	EA found (calculated) % C	% H	% S	Isolated yield (%)
oMeOtpp	-38.94	353.12 (352.12)	70.79 (71.58)	5.71 (6.01)		78
oEtOtpp	-34.34	395.36 (394.17)	72.31 (73.08)	6.60 (6.90)		41
C2 - bridged						
L1	-11.70		Commercial			
[Pd(L1)(OAc)2]	63.66	562.66 (563.05)	53.58 (53.79)	4.65 (4.62)		97
[Pd(L1)(OTs)2]	74.26	647.70 (675.05)	54.24 (54.24)	5.00 (5.08)	5.91 (5.88)	89
[Pd(L1)2][OTs]2	56.74		Detected *in situ*			
L2	-30.70	518.93 (518.52)	67.83 (69.49)	6.24 (6.22)		
[Pd(L2)(OAc)2]	60.91		Detected *in situ*			
[Pd(L2)(OTs)2]	57.50	794.77 (796.13)	51.67 (51.60)	4.64 (4.75)	2.82 (2.97)	68
[Pd(L2)2][OAc]2	55.83	571.72 (571.73)	52.35 (52.63)	5.93 (5.70)		73
[Pd(L2)2][OTs]2	55.95	1312.79 (1313.27)	56.04 (55.93)	5.88 (5.70)	3.80 (3.63)	30
L3	-26.51	575.00 (574.63	70.00 (71.07)	7.42 (7.02)		
[Pd(L3)(OAc)2]	60.83		Detected *in situ*			
C3 - bridged						
L4	-16.90		Commercial			
[Pd(L4)(OAc)2]	9.74	576.65 (577.91)	56.64 (56.16)	5.33 (5.35)		93
[Pd(L4)(OTs)2]	15.88	688.71 (689.07)	55.73 (55.63)	4.79 (4.86)	5.51 (5.15)	78
[Pd(L4)2][OAc]2	4.30		Detected *in situ*			
L5	-24.00	440.68 (414.18)	78.40 (79.07)	7.12 (6.86)		87
[Pd(L5)(OAc)2]	16.35	604.77 (605.10)	58.66 (58.62)	5.57 (5.65)		96
[Pd(L5)(OTs)2]	6.72	688.71 (689.07)	55.37 (55.29)	5.19 (5.30)	4.69 (4.52)	83
[Pd(L5)2][OTs]2	5.63	1156.91 (1157.28)	63.73 (63.83)	6.24 (6.00)	4.62 (4.33)	92
L6	-38.61	468.90 (468.00)	77.72 (79.46)	7.37 (7.31)		
[Pd(L6)(OAc)2]	14.39		Detected *in situ*			
L7	-36.90	533.67 (532.19)	69.88 (69.92)	6.29 (6.44)		
[Pd(L7)(OAc)2]	14.50	698.62 (698.01)	54.18 (54.35)	6.21 (6.08)		87
[Pd(L7)2][OAc]2	5.56	584.83 (585.15)	55.91 (55.96)	6.58 (6.43)		94
[Pd(L7)2][OTs]2	4.81	1340.53 (1341.30)	59.48 (59.72)	5.87 (5.52)	3.96 (4.10)	72
L8	-32.20	588.92 (588.65)	70.05 (71.41)	7.47 (7.19)		
[Pd(L8)(OAc)2]	16.79		Detected *in situ*			
L9	-20.57	532.86 (532.19)	68.74 (69.92)	6.61 (6.44)		
[Pd(L9)(OAc)2]	8.00		Detected *in situ*			
L10	-45.70		70.67 (70.70)	6.69 (6.83)		
[Pd(L10)(OAc)2]	20.84	724.77 (726.06)	54.39 (54.51)	5.96 (6.01)		96
[Pd(L10)(OTs)2]	26.24		Detected *in situ*			
[Pd(L10)2][OAc]2	10.88	613.43 (613.18)	56.97 (57.28)	6.90 (6.44)		97
[Pd(L10)2][OTs]2	10.10	1396.47 (1397.36)	58.40 (58.87)	5.99 (5.79)	3.51 (3.92)	89
L11	-46.50	588.92 (588.26)	73.64 (74.41)	7.43 (7.19)		
[Pd(L10)(OAc)2]	19.43		Detected *in situ*			
[Pd(L10)2][OAc]2	10.30		Detected *in situ*			
L12	-41.86	644.98 (644.76)	71.01 (72.65)	7.91 (7.82)		
[Pd(L12)(OAc)2]	19.17		Detected *in situ*			
L13	-47.90	672.28 (673.01)	69.10 (69.29	6.54 (6.73)		
[Pd(L13)(OAc)2]	18.05	836.82 (838.19)	57.00 (57.56)	6.16 (5.84)		94
[Pd(L13)(OTs)2]	25.67		Detected *in situ*			
[Pd(L13)2][OAc]2	8.82	725.15 (725.23)	62.00 (62.03)	6.46 (6.45)		70
[Pd(L13)2][OTs]2	8.03	726.50 (725.94)	60.84 (60.84)	5.90 (5.90)	3.02 (3.50)	63
C4 - bridged						
L14	-15.63		Commercial			
[Pd(L14)(OAc)2]	28.56	590.73 (591.08)	51.88 (51.69)	4.93 (4.79)		96
[Pd(L14)(OTs)2]	32.80	702.62 (703.08)	54.22 (54.08)	5.00 (5.13)	5.13 (5.02)	92
L15	-35.93	546.89 (546.57)	70.51 (70.32)	6.68 (6.64)		77
L16	-31.03	603.11 (602.27)	71.06 (71.71)	7.19 (7.36)		17
L17	-19.25		Commercial			
[Pd(L17)(OAc)2]			Detected *in situ*			
L18	-22.90	498.63 (498.19)	74.36 (74.69)	6.75 (6.47)		
[Pd(L18)(OAc)2]	14.59		Detected *in situ*			
L19	-39.80	618.23 (618.85)	67.52 (67.95)	6.39 (6.52)		
[Pd(L19)(OAc)2]	19.21		Detected *in situ*			

Appendix II

Supporting Information of Chapter 3

-Full analytical details of catalytic reactions-
-Mass spectroscopic analysis of the gas phase of reaction mixtures-
-Verification that reaction mixtures are anhydrous-
-Verifying that water can be analyzed quantitatively in a reaction mixture-
-Testing the catalyst sensitivity for water-
-Determination of the overall possible reaction stoichiometries and simulation of experiments-

Table AII.1. Overview of the results of catalytic reactions performed in 25 ml dry and degassed methanol. This data was used in the paper in places indicated in the table. Quantities are reported in mmol.[a]

Entry	Catalyst	$PhNO_2$	Additives	P_{CO}	MF	DMM	DMC	DMO	$PhNH_2$	MBA	$PhNO_2$	MPC	Azo	Azoxy	DPU
1	L3X	24.4	-	50	0.2	-	4.2	3.1	8.3	-	8.1	5.3	0.1	0.4	0.8
2	``	24.4	18.3 tmof[b]	50	3.6	-	4.1	3.3	8.6	-	8.4	5.2	0.1	0.3	0.6
3	``	24.4	12 H_2O; 36.6 tmof[b]	50	7.6	-	1.5	2.0	11.1	-	8.3	4.0	0.1	0.3	0.0
4	oMeO-L3X	24.4	-	50	1.1	-	0.4	0.4	5.7	0.1	0.6	11.6	0.1	0.1	3.1
5	``	24.4	18.3 tmof[b]	50	1.8	-	0.5	0.4	5.9	-	0.3	11.4	0.1	0.1	3.3
6	``	24.4	12 H_2O; 36.6 tmof[b]	50	3.0	-	0.1	0.1	11.1	-	0.1	6.4	0.1	0.5	2.9
7	None	-	10 $(H_2CO)_n$	50	trace	3.7	n.d.	n.d.	n.d.	n.d.	n.d.	n.d.	n.d.	n.d.	n.d.
8	oMeO-L3X	24.4	10 $(H_2CO)_n$	50	7.8	trace	0.1	0.1	5.5	trace	9.2	1.6	0.1	0.4	n.d.
9	``	4.9	10 $(H_2CO)_n$; 10 $PhNH_2$	5	3.0	-	0.0	0.0	6.8[c]	1.6	3.6	0.0	0.0	0.0	n.d.
10	``	24.4	4 % (v/v) $^{13}CH_3OH$	5	1.3	-	0.0	0.0	1.8	0.1	22.1	0.2	0.1	0.3	-
11	``	24.4	18.3 tmof[b]	5	3.4	-	0.0	0.0	0.0	0.0	22.0	0.2	0.1	0.2	
12	``	24.4	4 % (v/v) $^{13}CH_3OH$	0	1.7	-	0.0	0.0	0.2	0.6	23.2	0.0	0.1	0.0	-
13	L4X	24.4	-	50	0.2	-	2.3	5.9	1.9	-	11.8	0.5	0.1	4.5	0.5
14	``	24.4	18.3 tmof[b]	50	10.2	-	2.2	5.4	1.7	-	12.8	0.5	0.1	4.2	0.3
15	``	24.4	12 H_2O; 36.6 tmof[b]	50	22.5	-	2.0	5.8	1.9	-	12.4	0.5	0.1	4.3	0.4
16	oMeO-L4X	24.4	-	50	0.6	-	2.1	7.3	10.5	0.1	2.4	5.6	0.5	0.6	1.9
17	``	24.4	18.3 tmof[b]	50	9.3	-	2.1	7.1	10.4	-	2.6	5.7	0.4	0.7	2.1
18	``	24.4	12 H_2O; 36.6 tmof[b]	50	19.4	-	1.9	7.7	11.6	-	3.1	4.9	0.1	0.5	1.7

[a] The catalyst was always generated *in situ* from 0.05 mmol $Pd(OAc)_2$. Mole ratio's are: $Pd(OAc)_2$: Ligand : nitrobenzene : methanol = 1 : 1.5 : 488 : 12350. The experiments in entries 1, 4, 12 and 15 were performed in quadruplicate to ensure that the reactions were reproducible (error < 5%). The standard deviations are not given for the sake of clarity, but are < 5% in all cases. [b] 2 or 4 ml of a 0.55 M HOTs solution in trimethylorthoformate (tmof) was added after the catalytic reaction. See experimental for more details. [c] Some coupling product of aniline with formaldehyde was present as well, rationalizing the 'missing' aryl rings. 'n.d.' stands for 'not determined'.

AII.1. Mass spectroscopic analysis of the gas phase of reaction mixtures.

AII.1.1. Using a $Ni(SO_4)$ column to prevent interference from methanol

Without using a $Ni(SO_4)$ column in between the autoclave and the mass spectrometer, the relative abundance (when using 5 bar CO) of the peak around m/z = 29 (versus 28) was determined to be 3.81 ± 0.04% (see Figure AII.1a). This is clearly not ^{13}CO, as the natural abundance of this isotope should be 1.11 ± 0.08% (see Table AII.2). The peak interfering at m/z = 29 is ascribed to $[COH]^+$, e.g. of protonated CO. The proton source is methanol, as peaks were observed with a mass of 31 (OCH_3^+), and 15 (CH_3^+), as is indicated in Figure AII.1a. To solve this problem, a column was made consisting out of thoroughly dried $Ni(SO_4)$. This column was then mounted between the autoclave and the mass spectrometer. In this way, methanol could be removed from the gas that flows from the autoclave into the spectrometer. As can be seen in Figures AII.1b, no peaks could be detected with an m/z ratio of 31 (OCH_3^+) or 15 (CH_3^+). Furthermore, 1.27 ± 0.03% m/z = 29 was now detected; for pure CO (so without methanol present in the autoclave) this is 1.24 ± 0.02%. It can therefore be concluded that the $Ni(SO_4)$ column is an efficient methanol scavenger, and that the fraction of ^{13}CO in the gas phase can accurately be determined with this method.

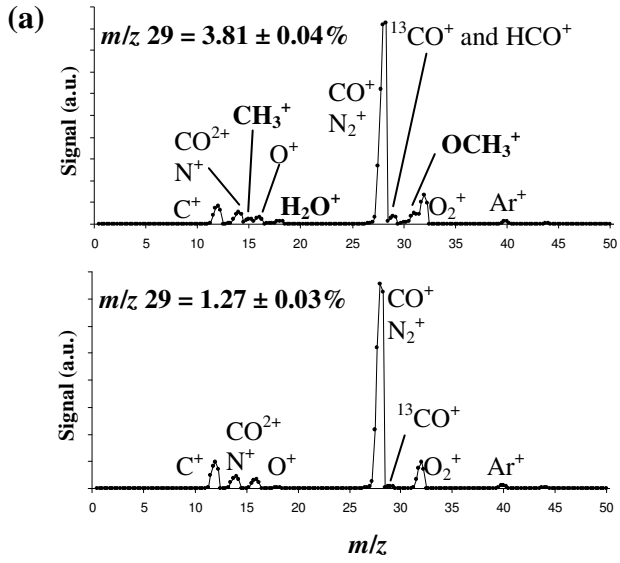

Figure AII.1 Mass spectroscopic analyses of the gas phase of an autoclave filled with 25 ml methanol and 5 bar CO. The gas was measured without (a) and with (b) a $Ni(SO_4)$ column between the autoclave and the mass spectrometer.

AII.1.2. Verifying the dehydrogenation of methanol

To verify if methanol can be fully dehydrogenated to CO, the gas phase was analyzed of a catalytic reaction that was conducted in 4% (v/v) $^{13}CH_3OH$ and using 5 bar CO.[1] The ligand used in this experiment is oMeOL3X because the hydrogen mass-balance is significantly upset when using this

[1] Assume we use 5 bar CO (~15 mmol) and 25 ml methanol (4 % (v/v) $^{13}CH_3OH$). If 1 mmol of methanol is fully dehydrogenated, the relative abundance of *m/z* = 29 (*versus* 28) should then be 1.35 %. That is an increase of 22% (compared to 1.11 ± 0.08 % calculated for pure CO). Note that less CO (5 bar) was used as usual (50 bar) because this allowed us to use less $^{13}CH_3OH$, and because the carbonylation reactions will then be less relatively suppressed.

ligand. Important data of this experiment and theoretical isotope distributions are shown in Table AII.2. The natural abundance of the mass 29 (relative to the mass 28) should be 1.11 ± 0.08 % in pure CO (entry 1).[2]

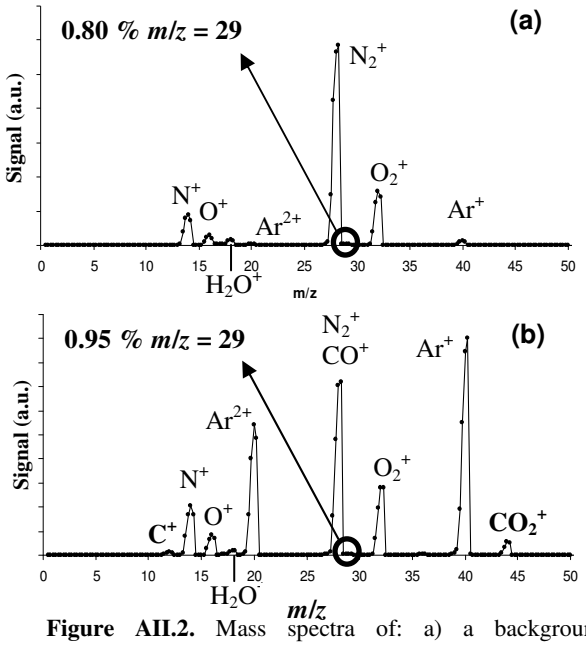

Figure AII.2. Mass spectra of: a) a background measurement; b) the gas phase after a catalytic reaction using 25 ml methanol (4% v/v $^{13}CH_3OH$), 24.4 mmol nitrobenzene, 0 bar CO, 0.05 mmol $Pd(OAc)_2$ and 0.075 mmol oMeO-L3X. The reaction was heated for four hours at 110 ºC.

Table AII.2. List of isotope distributions of m/z = 29 (versus 28) for: pure CO calculated (entry 1); pure CO as measured (entry 2); background the gas phase after a catalytic reaction.[a]

Entry	Description	m/z = 29 (%) (versus 28)	σ (%) (n=5)
1	Theoretical (pure CO)[b]	1.11	0.08
2	Measured (pure CO)	1.24	0.02
3	Background (pure CO in AC)[c]	1.27	0.03
4	After the reaction	1.46	0.02

[a] Using 25 ml methanol (4% v/v $^{13}CH_3OH$), 24.4 mmol nitrobenzene, 5 bar CO, 0.05 mmol $Pd(OAc)_2$ and 0.075 mmol oMeO-L3X. The reaction was heated for four hours at 110 ºC. [b] This value was calculated from the isotope distributions of carbon and oxygen, available in the handbook of chemistry and physics (88th edition). [c] 50 bar CO in an autoclave containing 25 ml methanol.

[2] This value was calculated from the isotope distributions of carbon and oxygen, available in the handbook of chemistry and physics (88th edition)

Using the experimental setup as shown in Figure 3.5 in the experimental section, the abundance of mass 29 (relative to the mass 28) was determined to be 1.24 ± 0.02% (n=5) in pure CO (entry 3). When repeating this experiment using an autoclave charged with 5 bar CO and also 25 ml methanol, the relative abundance was 1.27 ± 0.3% (n=5) (see section 1.1) If methanol is fully dehydrogenated to CO, the relative abundance of m/z = 29 should be increased after the reaction. Indeed, as is shown in entry 4, 1.46 ± 0.02% (n=5) of m/z = 29 could be detected after four hours reaction time; a significant increase of 15 %.[3]
To further verify that methanol is indeed fully dehydrogenated to CO, the experiment was repeated under an argon atmosphere (so in the absence of CO). After four hours reaction time, the gas phase of this experiment was analyzed using mass spectroscopic analysis. In Figure AII.2, the mass spectra are shown of the background signal (a) and of the gas phase of the reaction mixture (b).

As can be seen in Figure AII.2a, the main constituents of the background signal are dinitrogen (28 and 14), dioxygen (32 and 16), and a small amount of argon (40 and 20) and water (18). Note that there is no CO_2^+ (44), nor a C^+ (12) peak present. Note also that the fraction of m/z = 29 (versus 28) for N_2 (0.80%)[4] is within the error of the theoretical value (0.73 ± 0.08%).[5] In the mass spectrum of the gas phase (Figure AII.2b) it can be seen that the main constituents are argon (40 and 20), dioxygen (32 and 16), and dinitrogen (28 and 14). Note however, that the fraction of m/z = 29 (versus 28+29) is now 0.95% instead of 0.80%; an increase of 19%. It is thus likely that some CO is present as well (m/z = 29 = 1.11 ± 0.08% (theoretical) and 1.24 ± 0.02% (measured), see Table AII.2). What is more; a CO_2^+ peak (44) is observed, together with a C^+ peak (12). Since the only possible source of CO (and thus CO_2) is methanol, this verifies that methanol must have been fully dehydrogenated to CO. In addition, the liquid phase of this experiment contained 0.2 mmol aniline and 0.6 mmol MBA (see Table AII.1 entry 11); both can be seen as hydrogenation products of nitrobenzene. Also, 1.7 mmol MF could be detected, which can be seen as the entrapment of formaldehyde by methanol.

AII.2. Verifying that the reaction mixtures are anhydrous

First, it was tested if the reaction of ~20 mmol water with an equimolar amount of trimethylorthoformate (tmof) in 25 ml (dried) methanol is quantitative when heating such a mixture to 100 ºC within about 30 minutes (then cooled again). As can be seen in entry 1 of Table AII.3, the reaction was nearly quantitative, as 17.8 mmol MF could be detected. When the experiment was repeated using ~10 mmol water, 10.5 mmol MF could be detected, suggesting that an excess of tmof is necessary for the reaction to be quantitative. Using this methodology, it was furthermore tested how much water is present in undried methanol. As shown in entry 3, 2.0 mmol

Table AII.3. Reactions performed to test if tmof could be used to determine the water contents in methanol mixtures.[a]

Entry	Additive	MF
1	20 tmof / 20 H_2O	17.8
2	20 tmof / 10 H_2O	10.5
3[b]	10 tmof	2.0
4	24.4 $PhNO_2$ / 10 tmof	0.1

[a]The solvent is 25 ml of dry methanol unless stated otherwise. The reaction mixture was heated at 100 ºC for 30 minutes. Quantities reported in mmol. [b]

[3] See Table S1 for the analysis of the liquid phase.
[4] No standard deviation is available, since this is a single measurement. This was necessary because without an over-pressure inside the autoclave, it is impossible to reach a steady flow (and thus a reproducible mass spectrum).
[5] This value was calculated from the isotope distributions of nitrogen, available in the handbook of chemistry and physics (88th edition).

MF could be detected, meaning that undired methanol contains about 0.14 % (v/v) water (2 mmol / 25 ml). Next, it was ensured that the drying of methanol and nitrobenzene was efficient enough. As can be seen in entry 4, when 10 mmol tmof was added to a mixture of 25 ml methanol and 2.5 ml (24.4 mmol) nitrobenzene, only 0.1 mmol MF could be detected, which is roughly the amount of MF also present in tmof itself.

AII.3. Verifying that water can be analyzed quantitatively in a reaction mixture

To verify that water could be quantitatively analyzed in a reaction mixture that is rendered basic by aniline / DPU, some experiments were conducted as listed in Table AII.4. I all three experiments, a mixture of 12 mmol water, 24.4 mmol (2.5 ml) nitrobenzene, 5 mmol DPU and an amount of aniline were heated for four hours at 110 ºC in 25 ml methanol under 50 bar CO. The reaction mixture was cooled, vented, and 2 ml of a 0.55 M HOTs solution in tmof was added. The autoclave was then pressurized with 50 bar N_2, and heated to 70 ºC for 2 hours where after the reaction mixture was analyzed. As can be seen in entry 1 of the table, when adding 15 mmol aniline the reaction medium is apparently too basic to allow a full conversion of water to MF (8.5 mmol found). When the medium is less basic, (e.g., 10 or 5 mmol aniline, entries 2 and 3 respectively), water is quantitatively converted to MF (roughly 12 mmol found). It can therefore be concluded that if the reaction medium is acidic enough, water can be quantitatively converted with tmof to MF.

Table AII.4. Reaction of 12 mmol water with tmof / HOTs in a methanol / nitrobenzene / DPU / matrix and different amounts of aniline.[a]

Entry	$PhNH_2$ added	MF[b]	$PhNO_2$	$PhNH_2$[c]	MPC	DPU
1	15	8.5	24.7	12.1	2.4	2.5
2	10	11.9	24.6	8.7	2.3	2.6
3	5	12.4	24.8	3.3	2.6	2.1

[a] First a mixture of ~12 mmol water, 24.4 mmol (2.5 ml) nitrobenzene, 5 mmol DPU and the indicated amount of aniline were heated for four hours at 110 ºC in 25 ml methanol under 50 bar CO. The reaction mixture was cooled, vented, and 2 ml of a 0.55 M HOTs solution in tmof was added. The autoclave was then pressurized with 50 bar N_2, and heated to 70 ºC for 2 hours where after the reaction mixture was analyzed. Quantities reported are in mmol. [b] The amount shown is the amount detected minus the amount present in the HOTs solution in tmof (0.6 mmol/ml). [c] The analysis of aniline is disturbed by the HOTs/tmof mixture and in all several mmol aniline seems to be missing.

Note that the amount of DPU added (5 mmol) could fully be accounted for, partly as DPU and partly as MPC. Note also that (just as in Table S1) the analysis of aniline is disturbed which can be due to the formation of a salt with HOTs or due to matrix effects of the HOTs/tmof mixture.

AII.4. Testing the catalyst sensitivity for water

For each ligand, three experiments were conducted. First, a 'normal' catalytic experiment was performed and the amount of methyl formate (MF) was determined. Then, the reaction was repeated, but this time, 2 ml of a 0.55 M HOTs solution in trimethylorthoformate (tmof, ~18.3 mmol) was added after the catalytic run, whereafter the reaction mixture was heated to 70 ºC for two hours, cooled to laboratory temperature and analyzed for MF. Subtraction of the amounts of methyl formate found in these two experiments gives the amount of water that was present after a catalytic run. The reaction was repeated for the third time, but 12 mmol water was added prior to the catalytic run. After the catalytic run, 4 ml of a 0.55 M HOTs solution in tmof (~36.6 mmol) was added, whereafter the reaction mixture was heated to 70 ºC for two hours, cooled to laboratory temperature and analyzed for MF. The amount of MF analyzed in this experiment minus the amount of MF

normally present after a catalytic run will then give the amount of water still present in the reaction mixture, thus indicating how sensitive a given catalyst is for water. See also Table AII.1.

AII.5. Determination of the overall possible reaction stoichiometries and simulation of experiments

In order for the reactions to be catalytic, one must start and end in the same species, which in this case it taken to be Pd^0 (see also Scheme AII.1, *vide infra*).

Starting with the oxidation of Pd^0, one can write down three starting stoichiometries, one using only CO as reductant (eq. 5a), one with CO and two acidic H-atoms of CH_3OH as reductant (eq. 5b), and one with all protons of CH_3OH as reductant (eq. 5c). Note that (for simplification) equations 5b and 5e are left out, that DMC can be read as DMO, and that MPC can be read as DPU. Thus, the half-reactions that oxidize Pd^0 are:

$Pd^0 + PhNO_2 + 2\ CO$	→	$Pd^{II}{=}NPh + 2\ CO_2$	(5a)
$Pd^0 + PhNO_2 + 2\ CO + 2\ CH_3OH$	→	$Pd^{II}{=}NPh + CO_2 + H_2O + DMC$	(5b)
$Pd^0 + PhNO_2 + CH_3OH$	→	$Pd^{II}{=}NPh + CO + 2\ H_2O$	(5c)

Starting form the imido-species, there are four pathways to re-form Pd^0, producing MPC(/DPU/'PhNCO') (eq. 9), aniline and DMC (eq. 6 and 7a), Azoxy and DMC (eq. 8a, 8c and 7a), or Azoxy and CO_2 (eq. 8a and 8b). Thus, the half-reactions that reduce Pd^{II}=NPh are:

$Pd^{II}{=}NPh + CO + CH_3OH$	→	$Pd^0 + MPC$	(9)
$Pd^{II}{=}NPh + 2\ CH_3OH + CO$	→	$Pd^0 + PhNH_2 + DMC$	(6+7a)
$Pd^{II}{=}NPh + PhNO_2 + 2\ CH_3OH + CO$	→	$Pd^0 + PhN(O)NPh + H_2O + DMC$	(8a+8b+7a)
$Pd^{II}{=}NPh + PhNO_2 + CO$	→	$Pd^0 + PhN(O)NPh + CO_2$	(8a+8c)

By systematically combining the half-reactions that oxidize Pd^0 to Pd^{II}=NPh with the half-reactions that reduce Pd^{II}=NPh to Pd^0, the overall possible stoichiometries can be deduced. These will set the limits of the reactions possible. However, whenever a stoichiometry is logically possible, but is not necessary to simulate the results, this stoichiometry can be left out. Many combinations were tested, and it was found that the stoichiometries that combine equations (8a+8b+7a) with the three reduction pathways (5a-c) were redundant. Thus, the overall stoichiometries are 10 – 18, as given in Table AII.5 and schematically presented in Scheme AII.1.

As a water molecule may replace a methanol molecule in the reactions 10 – 18, a similar set of stoichiometries should be considered wherein one CH_3OH is replaced by one H_2O (as indicated by '*'). For the reaction that normally give MPC (eq. 10, 13, and 16) and the reactions that normally give aniline and DMC (eq. 11, 14, and 17), this will amount to the exact same stoichiometry, thus giving stoichiometries 10/11*, 13/14*, and 16/17* (Table AII.5). Mechanistically, for these stoichiometries water must be consumed after the imido intermediate is formed (Scheme AII.1). In the reactions normally producing Azoxy (eq. 12, 15, and 18), no new reaction stoichiometries are obtained. That is, there is no methanol to replace in equation 12; replacing a methanol with water in equation 15 leads to equation 12; and if water was to replace methanol in equation 18 this would lead to H_2 and O_2 production, which is clearly highly endothermic (i.e. $2\ PhNO_2 + 3\ H_2O$ → Azoxy $+ 3\ H_2 + 3\ O_2 = +163.0$ kcal.mol^{-1}).

Table AII.5. The possible reaction stoichiometries derived from the half-reactions 5-9. (see also Scheme S1).

Equation	Combination	Reaction stoichiometry	ΔH_f^o [a]	Comment
10	5a+9	$PhNO_2 + 3\ CO \rightarrow$ 'PhNCO'[b] $+ 2\ CO_2$	-139.3	Reduction with CO only
11	5a+6+7a	$PhNO_2 + 2\ CH_3OH + 3\ CO \rightarrow$ $PhNH_2 + 2\ CO_2$ + DMC	-137.4	
12	5a+8c	$2\ PhNO_2 + 3\ CO \rightarrow$ Azoxy $+ 3\ CO_2$	-176.5	
13	5c+9	$PhNO_2 + 3\ CH_3OH + 3\ CO \rightarrow$ 'PhNCO'[b] $+ CO_2 + H_2O$ + DMC	-118.9	Reduction with CO and acidic H from CH_3OH
14	5c+6+7a	$PhNO_2 + 4\ CH_3OH + 3\ CO \rightarrow$ $PhNH_2 + CO_2 + H_2O$ + 2 DMC	-117.0	
15	5c+8a+8b+7a	$2\ PhNO_2 + 2\ CH_3OH + 3\ CO \rightarrow$ Azoxy $+ H_2O + 2\ CO_2$ + DMC	-156.1	
16	5d+9	$PhNO_2 + CH_3OH \rightarrow$ 'PhNCO'[b] $+ 2\ H_2O$	-97.0	Reduction with all H from CH_3OH
17	5d+6+7a	$PhNO_2 + 3\ CH_3OH \rightarrow$ $PhNH_2 + 2\ H_2O$ + DMC	-95.1	
18	5d+8a+8b+7a	$2\ PhNO_2 + CH_3OH \rightarrow$ Azoxy $+ 2\ H_2O + CO_2$	-134.2	
10/11*	5a+9(H_2O)	$PhNO_2 + H_2O + 3\ CO \rightarrow$ $PhNH_2 + 3\ CO_2$	-157.8	Water consumption after formation of imido complex
13/14*	5c+9(H_2O)	$PhNO_2 + 2\ CH_3OH + 3\ CO \rightarrow$ $PhNH_2 + 2\ CO_2$ + DMC	-137.4	
16/17*	5d+9(H_2O)	$PhNO_2 + CH_3OH \rightarrow$ $PhNH_2 + H_2O + CO_2$	-115.6	

[a] Derived from literature values and given in kcal.mol^{-1}: H_2 (0, reference);[1] CO (-26.4);[1-3] CO_2 (-94.0);[1, 4-6] H_2O (-68.3);[1, 4] CH_3OH (-70.1);[1] DMC (-145.5);[7] $PhNO_2$ (+15.9);[8] $PhNH_2$ (-7.4);[9, 10] 'PhNCO' (-14.6);[11] cis-Azoxy (+58.2).[12] Similar values are obtained when DMC is replaced by DMO (-180.9),[13, 14] when Azoxy is replaced by cis-Azo (+85.5)[15] or trans-Azo (+76.5),[15, 16] or when 'PhNCO' is replaced by DPU (-27.9).[17] Thermodynamic data for MPC could not be found. [b] In this table 'PhNCO' is used instead of 'MPC' (as in the article text and the rest of the ESI), because thermodynamic data for MPC could not be found. Hence, equations 10, 13, and 16 from this table 'miss' a CH_3OH molecule as reactant.

Stoichiometries 10 – 18 can also be derived in a family tree-type fashion (Scheme AII.1), starting from Pd^0 and following the possible reaction pathways along the branches of the tree until Pd^0 is re-formed. This makes clear intuitively how the various processes and stoichiometries are related to one another.

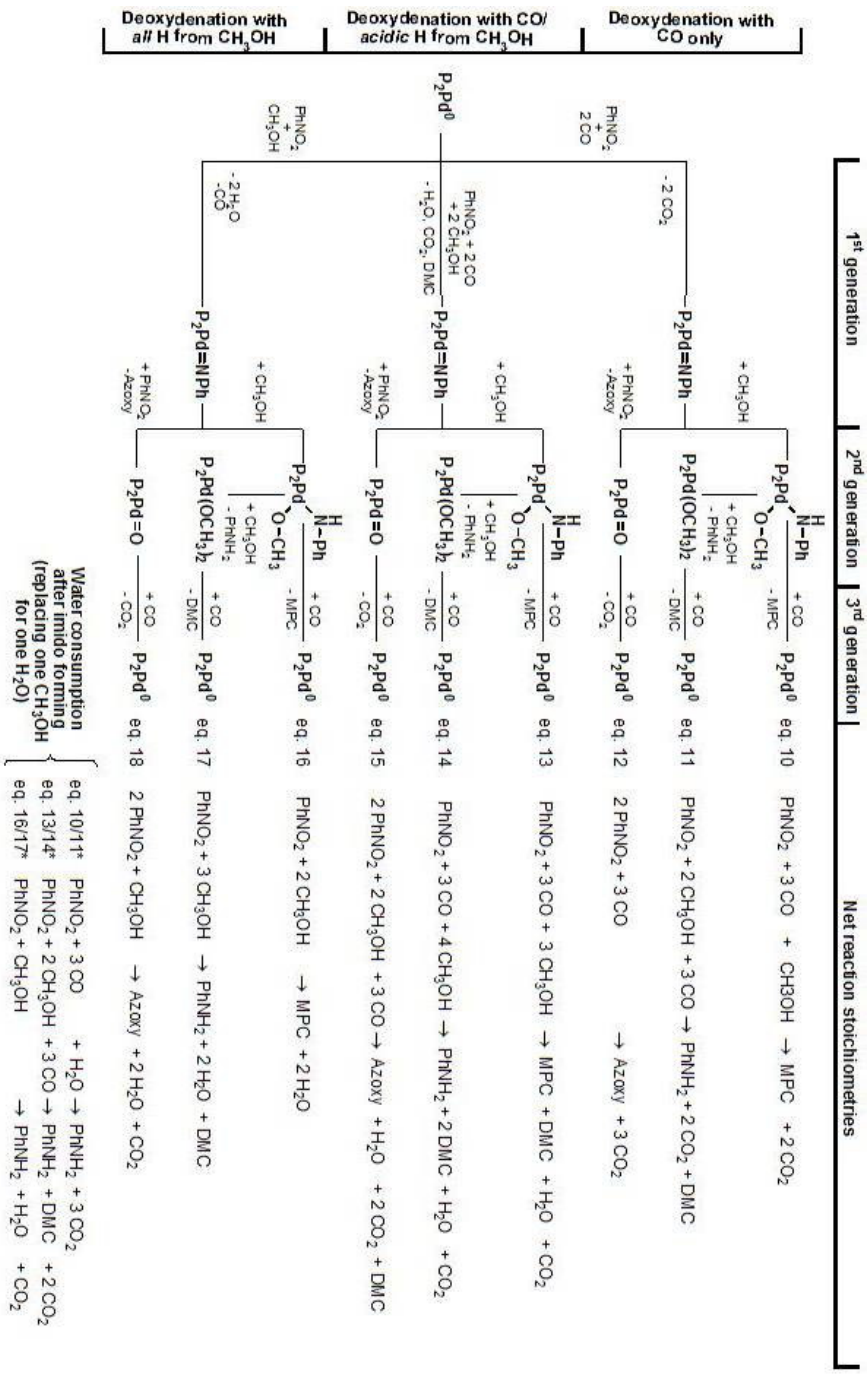

Scheme AII.1. Family tree type scheme of the possible reaction stoichiometries as prescribed by the mechanistic working hypothesis (Scheme 3.8). The calculated heat of formation, derived from literature values, is given within parentheses. See also Table AII.5.

The observed product distributions can now be simulated using the reactions shown in Table AII.5 and Scheme AII.1. Note that DPU should be counted both as 'MPC' and as aniline, MPC should be read as MPC + DPU, and that DMC and DMO are essentially the same product, as are azoxybenzene and azobenzene. The raw data derived from Table AII.1 is then shown in Table AII.6. Note that the violation of the hydrogen mass balance is also given (ΔH). When it is realized that these H-atoms originate from a full methanol dehydrogenation to CO, that MF is also a from of CO, and that four H-atoms can fully de-oxygenate nitrobenzene (bottom branch in Scheme AII.1) then it should be clear that 'MF+(ΔH/4)' represents the amount of nitrobenzene reduced with methanol alone (bottom branch in Scheme AII.1). Thus, this number can be seen as calibration point for all simulations. Another calibration point is the measured product distribution of MPC:$PhNH_2$:Azo(xy), which must be the same for all 2nd / 3rd generations in Scheme AII.1. That is, because the imido complex is always the final stage of the reduction process (first generation in Scheme AII.1), the selectivity in all three branches of the family tree should be identical.

Table AII.6. Experimental data used to simulate the observed product distributions.

Complex	MPC	$PhNH_2$	Azo(xy)	DMC/O	H_2O	MF	ΔH	MF+(ΔH/4)
Pd^{II}(L3X)	6.1	9.1	0.5	7.3	3.4	0.2	10	2.7
Pd^{II}(oMeO-L3X)	14.7	8.8	0.2	0.8	0.7	1.1	13	4.5
Pd^{II}(L4X)	1.0	2.4	4.6	8.2	10.0	0.2	8	2.2
Pd^{II}(oMeO-L4X)	7.5	12.4	1.1	9.4	8.7	0.6	21	5.9

For **Pd^{II}(L3X)**,it was shown that water can be consumed, meaning that eq. 10/11*, 13/14*, and 16/17* may play an important role. The (aryl) product distribution is: MPC (38.9%); $PhNH_2$ (58.0%); Azoxy (3.2%), with $PhNH_2$/MPC = 1.492, and Azoxy/MPC = 0.082. 2.7 mmol nitrobenzene was reduced with methanol alone, so:

CH_3OH red.: 2.7 x 0.389 = 1.05 x eq. 16 = 1.05 MPC + 2.10 H_2O
2.7 x 0.580 = 1.57 x eq. 16/17* = 1.57 $PhNH_2$ + 1.57 H_2O
2.7 x 0.032 = 0.09 x eq. 18 = 0.09 Azoxy + 0.18 H_2O +
1.05 MPC + 1.57 $PhNH_2$ + 0.09 Azoxy + 3.85 H_2O

As next calibration point, MPC can be taken; there is still 6.1 – 1.05 = 5.05 mmol unaccounted for. This must have been produced via CO reduction (top branch in Scheme AII.1) and via the co-reduction of CO and the acidic protons of CH_3OH molecules (centre branch in Scheme eq. 10). Thus, there must be an optimal fraction of CO reduction, so that the simulation approaches perfection (and the aryl product distribution is respected). Several options were considered, and a fraction of 0.448 CO reduction was found to fit best. Thus, 5.05 x 0.448 = 2.26 mmol nitrobenzene was reduced with CO alone, and 5.05 – 2.26 = 2.79 mmol by CO/2CH_3OH. Thus:

CO only red.: 2.26 x 1.000 = 2.26 x eq. 10 = 2.26 MPC
2.26 x 1.492 = 3.37 x eq. 10/11* = 3.37 $PhNH_2$ + (– 3.37) H_2O
2.26 x 0.082 = 0.19 x eq. 12 = 0.19 Azoxy +
2.26 MPC + 3.37 $PhNH_2$ + 0.19 Azoxy + (–3.37)H_2O

CO/2CH_3OH red.: 2.79 x 1.000 = 2.79 x eq. 13 = 2.79 MPC + 2.79 DMC + 2.79 H_2O
2.79 x 1.492 = 4.16 x eq. 13/14* = 4.16 $PhNH_2$ + 4.16 DMC
2.79 x 0.082 = 0.23 x eq. 15 = 0.23 Azoxy + 0.23 DMC + 0.23 H_2O +
2.79 MPC + 4.16 $PhNH_2$ + 0.23 Azoxy + 7.18 DMC + 3.02 H_2O

Thus, adding all three reduction pathways leads to an excellent simulation of sim. (exp.) =
6.1 (6.1) MPC; 9.1 (9.1) $PhNH_2$; 0.5 (0.5) Azoxy; 7.2 (7.3) DMC; 3.5 (3.4) H_2O

For **Pd^{II}(oMeOL3X)**, it was shown that water can be consumed, meaning that eq. 10/11*, 13/14*, and 16/17* may play an important role. The (aryl) product distribution is: MPC (62.0%); $PhNH_2$ (37.1%); Azoxy (0.8%), with $PhNH_2$/MPC = 0.599, and Azoxy/MPC = 0.014. 4.35 mmol nitrobenzene was reduced with methanol alone, so:

CH_3OH red.: 4.35 x 0.620 = 2.70 x eq. 16 = 2.70 MPC + 5.40 H_2O
4.35 x 0.371 = 1.61 x eq. 16/17* = 1.61 $PhNH_2$ + 1.61 H_2O
(NB: note that eq. 17 definitely cannot be used as this would lead to too much DMC)
4.35 x 0.008 = 0.03 x eq. 18 = 0.03 Azoxy + 0.06 H_2O +
2.70 MPC + 1.61 $PhNH_2$ + 0.03 Azoxy 7.07 H_2O

As next calibration point, MPC can be taken; there is still 14.7 – 2.70 = 12.0 mmol unaccounted for. This must have been produced via CO reduction (top branch in Scheme AII.1) and via the co-reduction of CO and the acidic protons of CH_3OH molecules (centre branch in Scheme AII.1). Thus, there must be an optimal fraction of CO reduction, so that the simulation approaches perfection (and the aryl product distribution is respected). Several options were considered, and a fraction of 0.959 CO reduction was found to fit best. Thus, 12.0 x 0.959 = 11.51 mmol nitrobenzene was reduced with CO alone, and 12.0 – 11.51 = 0.49 mmol by CO/2CH_3OH. Thus:

CO only red.: 11.51 x 1.000 = 11.51 x eq. 10 = 11.51 MPC
11.51 x 0.599 = 6.89 x eq. 10/11* = 6.89 $PhNH_2$ + (– 6.89) H_2O
11.51 x 0.014 = 0.16 x eq. 12 = 0.16 Azoxy +
11.51 MPC + 6.89 $PhNH_2$ + 0.16 Azoxy + (– 6.89) H_2O

CO/2CH_3OH red.: 0.49 x 1.000 = 0.49 x eq. 13 = 0.49 MPC + 0.49 DMC + 0.49 H_2O
0.49 x 0.599 = 0.29 x eq. 13/14* = 0.29 $PhNH_2$ + 0.29 DMC
0.49 x 0.014 = 0.01 x eq. 15 = 0.01 Azoxy + 0.01 DMC + 0.01 H_2O +
0.49 MPC + 0.29 $PhNH_2$ + 0.01 Azoxy + 0.79 DMC + 0.50 H_2O

Thus, adding all three reduction pathways leads to an excellent simulation of sim. (exp.) =
14.7 (14.7) MPC; 8.8 (8.8) $PhNH_2$; 0.2 (0.2) Azoxy; 0.8 (0.8) DMC; 0.7 (0.7) H_2O

For **Pd^{II}(L4X)**, it was shown that added water is not (net) consumed, meaning that the contribution of eq. 10/11*, 13/14*, and 16/17* should be kept as low as possible relative to eq. 11, eq. 14, and eq. 17 (together accounting for the aniline produced). Thus, various fraction (of eq. X vs eq. X*) were considered and an excellent fit was obtained when the water 'consuming' reactions (eq. X*) contribute for 24.0%. The (aryl) product distribution is: MPC (11.1%); $PhNH_2$ (37.8%); Azoxy (51.1%), with $PhNH_2$/MPC = 3.4, and Azoxy/MPC = 4.6. 2.20 mmol nitrobenzene was reduced with methanol alone, so:

CH_3OH red.: 2.20 x 0.111 = 0.24 x eq. 16 = 0.24 MPC + 0.48 H_2O
2.20 x 0.378 x 0.760 = 0.63 x eq. 17 = 0.63 $PhNH_2$ + 1.26 H_2O + 0.63 DMC
2.20 x 0.378 x 0.240 = 0.20 x eq. 16/17* = 0.20 $PhNH_2$ + 0.20 H_2O
2.20 x 0.511 = 1.12 x eq. 18 = 1.12 Azoxy + 2.24 H_2O +
0.24 MPC + 0.83 $PhNH_2$ + 1.12 Azoxy + 4.18 H_2O + 0.63 DMC

As next calibration point, MPC can be taken; there is still 1.00 – 0.24 = 0.76 mmol unaccounted for. This must have been produced via CO reduction (top branch in Scheme S1) and via the co-reduction of CO and the acidic protons of CH_3OH molecules (centre branch in Scheme AII.1). Thus, there must be an optimal fraction of CO reduction, so that the simulation approaches perfection (and the aryl product distribution is respected). Several options were considered, and a fraction of 0.12 CO reduction was found to fit best. Thus, 0.76 x 0.12 = 0.09 mmol nitrobenzene was reduced with CO alone, and 0.76 – 0.09 = 0.67 mmol by CO/2CH_3OH. Thus:

CO only red.:
0.09 x 1.00 = 0.09 x eq. 10 = 0.09 MPC
0.09 x 3.40 x 0.760 = 0.23 x eq. 11 = 0.23 $PhNH_2$ + 0.23 DMC
0.09 x 3.40 x 0.240 = 0.07 x eq. 10/11* = 0.07 $PhNH_2$ + (–0.07) H_2O
0.09 x 4.60 = 0.41 x eq. 12 = 0.42 Azoxy +
0.09 MPC + 0.30 $PhNH_2$ + 0.42 Azoxy + 0.23 DMC + (–0.07) H_2O

$CO/2CH_3OH$ red.:
0.66 x 1.00 = 0.66 x eq 13 = 0.66 MPC + 0.66 DMC + 0.66 H_2O
0.66 x 3.40 x 0.760 = 1.71 x eq 14 = 1.72 $PhNH_2$ + 3.44 DMC + 1.72 H_2O
0.66 x 3.40 x 0.240 = 0.54 x eq 13/14* = 0.54 $PhNH_2$ + 0.54 DMC
0.66 x 4.60 = 3.04 x eq 15 = 3.06 Azoxy + 3.06 DMC + 3.06 H_2O+
0.66 MPC + 2.26 $PhNH_2$ + 3.06 Azoxy + 7.70 DMC + 5.44 H_2O

Thus, adding all three reduction pathways leads to an excellent simulation of sim. (exp.) = 1.0 (1.0) MPC; 3.4 (3.4) $PhNH_2$; 4.6 (4.6) Azoxy; 8.6 (8.2) DMC; 9.6 (10.0) H_2O

For **Pd^{II}(oMeOL4X)**, it was shown that only about 2 mmol of added water is (net) consumed, meaning that the contribution of eq. 10/11*, 13/14*, and 16/17* should be considered, but also must be kept as low as possible relative to eq. 11, eq. 14, and eq. 17 (together accounting for the aniline produced). Thus, various fraction (of eq. X vs eq. X*) were considered and an excellent fit was obtained when the water 'consuming' reactions (eq. X*) contribute for 24.2%. The (aryl) product distribution is: MPC (35.7%); $PhNH_2$ (59.1%); Azoxy (5.2%), with $PhNH_2$/MPC = 1.653, and Azoxy/MPC = 0.147. 5.85 mmol nitrobenzene was reduced with methanol alone, so:

CH_3OH red.:
5.85 x 0.357 = 2.09 x eq. 16 = 2.09 MPC + 4.18 H_2O
5.85 x 0.591 x 0.758 = 2.62 x eq. 17 = 2.62 $PhNH_2$ + 5.24 H_2O + 2.62 DMC
5.85 x 0.591 x 0.242 = 0.80 x eq. 16/17* = 0.80 $PhNH_2$ + 0.80 H_2O
5.85 x 0.052 = 0.30 x eq. 101 = 0.30 Azoxy + 0.60 H_2O +
2.09 MPC + 3.42 $PhNH_2$ + 0.30 Azoxy + 10.82 H_2O + 2.62 DMC

As next calibration point, MPC can be taken; there is still 7.5 – 2.09 = 5.41 mmol unaccounted for. This must have been produced via CO reduction (top branch in Scheme AII.1) and via the co-reduction of CO and the acidic protons of CH_3OH molecules (centre branch in Scheme AII.1). Thus, there must be an optimal fraction of CO reduction, so that the simulation approaches perfection (and the aryl product distribution is respected). Several options were considered, and a fraction of 1.000 CO reduction was found to fit best. This means that all 5.41 mmol nitrobenzene was reduced with CO alone, and none by $CO/2CH_3OH$. Thus:

CO only red.:
5.41 x 1.000 = 5.41 x eq. 10 = 5.41 MPC
5.41 x 1.653 x 0.758 = 6.78 x eq. 11 = 6.78 $PhNH_2$ + 6.78 DMC
5.41 x 1.653 x 0.242 = 2.16 x eq. 10/11* = 2.16 $PhNH_2$ + (–2.16) H_2O
(NB: this corresponds well with the observed 2 mmol water consumed)
5.41 x 0.147 = 0.80 x eq. 12 = 0.80 Azoxy +
5.41 MPC + 8.94 $PhNH_2$ + 0.80 Azoxy + 6.78 DMC + (–2.16) H_2O

Thus, adding all three reduction pathways leads to an excellent simulation of sim. (exp.) = 7.5 (7.5) MPC; 12.4 (12.4) $PhNH_2$; 1.1 (1.1) Azoxy; 9.4 (9.4) DMC; 8.7 (8.7) H_2O

It is thus possible to reasonably simulate the experimental data to (near) perfection, as is schematically shown in Table AII.7. Also based on these simulations, the respective contributions of the three different reduction routes can be estimated, as is shown in Table AII.8.

Table AII.7. Experimental data used to simulate the observed product distributions.

Ligand	Data	MPC	$PhNH_2$	Azo(xy)	DMC/O	H_2O
L3X	Exp.	6.1	9.1	0.5	7.3	3.4
	Sim.	6.1	9.1	0.5	7.2	3.5
oMeO-L3X	Exp.	14.7	8.8	0.2	0.8	0.7
	Sim.	14.7	8.8	0.2	0.8	0.7
L4X	Exp.	1.0	2.4	4.6	8.2	10.0
	Sim.	1.0	2.4	4.6	8.6	9.6
oMeO-L4X	Exp.	7.5	12.4	1.1	9.4	8.7
	Sim.	7.5	12.4	1.1	9.4	8.7

Table AII.8. Experimental and simulated data of the observed product distributions.

	Reductant		
Ligand	CO	$CO/2CH_3OH$	CH_3OH
L3X	37%	46%	17%
oMeO-L3X	78%	3%	18%
L4X	9%	66%	24%
oMeO-L4X	72%	0%	28%

References:

[1] R. D. Lide (Ed.), *Handbook of Chemistry and Physics*, 88th ed., CRC Press Inc., Cleveland, **2007-2008**.

[2] D. D. Wagman, J. E. Kilpatrick, W. J. Taylor, K. S. Pitzer, F. D. Rossini, *J. Res. Nat. Bur. Stand. (U.S.)* **1945**, *34*, 143.

[3] B. J. McBride, S. Heimel, J. G. Ehlers, S. Gordon, *NASA-SP-3001* **1963**, 165.

[4] B. Ruscic, R. E. Pinzon, M. L. Morton, G. von Laszevski, S. J. Bittner, S. G. Nijsure, K. A. Amin, M. Minkoff, A. F. Wagner, *J. Phys. Chem. A* **2004**, *108*, 9979.

[5] B. J. McBride, S. Heimel, J. G. Ehlers, S. Gordon, *NASA-SP-3001* **1963**, 166.

[6] E. J. Prosen, R. S. Jessup, F. D. Rossini, *J. Res. Nat. Bur. Stand. (U.S.)* **1944**, *33*, 447.

[7] W. V. Steele, R. D. Chirico, S. E. Knipmeyer, A. Nguyen, N. K. Smith, *J. Chem. Eng. Data* **1997**, *42*, 1037.

[8] R. Shaw, *J. Phys. Chem.* **1971**, *75*, 4047.

[9] L. G. Cole, E. C. Gilbert, *J. Am. Chem. Soc.* **1951**, *73*, 5423.

[10] C. M. Anderson, E. C. Gilbert, *J. Am. Chem. Soc.* **1942**, *64*, 2369.

[11] W. V. Steele, R. D. Chirico, S. E. Knipmeyer, A. Nguyen, N. K. Smith, I. R. Tasker, *J. Chem. Eng. Data* **1996**, *41*, 1269.

[12] W. E. Acree, J. J. Kirchner, S. A. Tucker, G. Pilcher, M. Dasilva, *J. Chem. Thermodyn.* **1989**, *21*, 443.

[13] M. E. Anthoney, A. Finch, M. Stephens, *Thermochim. Acta* **1975**, *12*, 427.

[14] M. E. Anthoney, A. S. Carson, P. G. Laye, M. Yurekli, *J. Chem. Thermodyn.* **1976**, *8*, 1009.

[15] A. R. Dias, M. E. M. Dapiedade, J. A. M. Simoes, J. A. Simoni, C. Teixeira, H. P. Diogo, M. Y. Yang, G. Pilcher, *J. Chem. Thermodyn.* **1992**, *24*, 439.

[16] C. F. Davies, E. C. Gilbert, *J. Am. Chem. Soc.* **1941**, *63*, 1583.

[17] V. V. Simirsky, G. J. Kabo, M. L. Frenkel, *J. Chem. Thermodyn.* **1987**, *19*, 1121.

Appendix III

Supporting Information of Chapter 4

-Full analytical details of catalytic experiments-
-NMR spectra of ligand exchange experiments of 'phen–palladacycle' and L3X and bpap-
-Attempts to positively identify and quantify the 'PhN'–containing products-
-GLC–MS analysis of in situ synthesized methylmesitylene carbamate-

Entry	Used in	Catalyst	Comment	Quantities analyzed (mmol)										%			
				H_2O	MF	DMC	DMO	$PhNH_2$	$PhNO_2$	MPC	Azo	Azoxy	DPU	Conv.[a]	N–CO[b]	N=N[c]	N–H[d]
1	Tab. 1	L2	–	n.d.	0.1	1.4	0.8	2.5	20.8	0.9	0.0	0.2	0.0	15	24	11	66
2	"	oMeO–L2	–	n.d.	0.1	0.1	0.1	1.2	22.5	0.8	0.0	0.0	0.0	8	40	0	60
3	Tab. 1, Fig. 4	L3	–	3.0	0.1	3.6	3.3	5.1	8.1	5.9	0.1	0.4	1.7	67	49	6	44
4	Tab. 1	L3X	–	3.4	0.2	4.2	3.1	8.3	8.1	5.3	0.1	0.4	0.8	67	38	6	56
5	"	oMeO–L3	–	n.d.	0.6	0.6	0.5	4.1	11.5	6.6	0.1	0.1	0.9	53	58	3	39
6	Tab. 1, Fig. 8, 9	oMeO–L3X	–	0.7	1.1	0.4	0.4	5.7	0.6	11.6	0.1	0.1	3.1	98	62	2	37
7	Tab. 1	pMeO–L3	–	n.d.	0.1	2.2	2.1	3.9	11.3	5.2	0.0	0.1	1.9	54	55	1	45
8	Tab. 1, Fig. 4, 5	L4	–	3.9	0.3	2.4	5.6	5.4	9.8	3.0	0.2	2.1	0.8	60	26	32	42
9	Tab. 1, Fig. 6, 7, 9	L4X	–	10.0	0.2	2.3	5.9	1.9	11.8	0.5	0.1	4.5	0.5	52	8	73	19
10	Tab. 1	oMeO–L4	–	n.d.	0.3	0.1	1.7	2.2	20.2	2.2	0.0	0.2	0.0	17	46	8	46
11	"	oMeO–L4X	–	8.7	0.6	2.1	7.3	10.5	2.4	5.6	0.5	0.6	1.9	90	34	10	56
12	"	pMeO–L4	–	n.d.	0.2	1.7	3.7	5.9	14.7	2.6	0.0	0.3	0.0	40	29	7	65
13	Fig. 4	L3	25 bar CO	n.d.	n.d.	4.7	1.5	4.9	13.0	3.1	0.1	0.5	1.2	47	37	10	53
14	"	"	100 bar CO	n.d.	n.d.	2.6	4.8	5.2	2.8	7.8	0.1	0.2	4.0	88	55	3	43
15	"	L4	25 bar CO	n.d.	n.d.	2.6	3.1	2.7	14.0	1.2	0.1	1.5	0.0	29	18	45	38
16	"	"	100 bar CO	n.d.	n.d.	1.5	8.1	5.7	6.5	3.8	0.1	1.3	2.0	66	36	17	48
17	Fig. 5	L4	4.9 mmol $PhNO_2$	n.d.	n.d.	1.2	3.8	3.0	0.0	0.9	0.1	0.0	n.d.	MPC / (Azo + Azoxy) =			7.6
18	"	"	9.7 mmol $PhNO_2$	n.d.	n.d.	2.2	5.6	4.9	0.0	2.0	0.1	0.5	n.d.	MPC / (Azo + Azoxy) =			3.3
19	"	"	14.6 mmol $PhNO_2$	n.d.	n.d.	2.4	5.1	2.4	1.2	2.7	0.1	1.2	n.d.	MPC / (Azo + Azoxy) =			2.1
20	"	"	19.6 mmol $PhNO_2$	n.d.	n.d.	1.9	4.5	2.4	9.0	1.7	0.1	1.3	n.d.	MPC / (Azo + Azoxy) =			1.2
21	"	"	34.1 mmol $PhNO_2$	n.d.	n.d.	2.3	6.8	5.6	18.9	2.3	0.1	1.8	n.d.	MPC / (Azo + Azoxy) =			1.2
22	"	"	48.8 mmol $PhNO_2$	n.d.	n.d.	2.2	6.3	3.2	33.0	2.0	0.1	2.1	n.d.	MPC / (Azo + Azoxy) =			0.9
23	Fig. 6	L4X	0.25 eq. HOTs	n.d.	n.d.	2.3	10.3	4.2	9.4	1.2	0.2	3.3	0.0	61	9	56	34
24	Fig. 6, 10	"	0.5 eq. HOTs	n.d.	n.d.	3.2	13.4	6.3	8.4	2.6	0.3	3.9	0.0	66	15	48	36
25	Fig. 6, 7	"	1 eq. HOTs	n.d.	n.d.	2.4	13.8	8.1	4.0	3.2	0.4	2.2	0.0	84	19	32	49
26	Fig. 6	"	2 eq. HOTs	n.d.	n.d.	2.2	10.6	5.5	11.2	1.5	0.1	1.5	0.0	54	14	33	53
27	"	"	4 eq. HOTs	n.d.	n.d.	1.6	9.7	5.5	12.9	1.2	0.1	0.7	0.0	47	15	20	65
28	Fig. 7	"	2 eq. H–sponge	n.d.	n.d.	0.8	1.6	0.3	19.4	0.0	0.1	2.2	0.0	20	0	94	6
29	Fig. 10	"	0.5 eq. TMBA	n.d.	n.d.	2.4	10.9	4.5	9.8	1.3	0.2	3.8	0.0	60	9	58	33
30	Fig. 8	oMeO–L3X	0.25 eq. HOTs	n.d.	n.d.	0.3	0.3	4.9	4.0	9.2	0.1	0.1	2.4	19	61	2	38
31	Fig. 8, 10	"	0.5 eq. HOTs	n.d.	n.d.	0.2	0.2	4.0	9.3	6.8	0.1	0.1	1.6	61	59	1	39
32	Fig. 8, 9	"	1 eq. HOTs	n.d.	n.d.	0.2	0.1	5.0	12.3	4.6	0.0	0.1	1.6	49	48	2	51
33	Fig. 8	"	2 eq. HOTs	n.d.	n.d.	0.1	0.1	2.1	21.3	1.0	0.0	0.0	0.0	12	31	0	69
34	"	"	4 eq. HOTs	n.d.	n.d.	0.0	0.0	1.7	22.6	0.6	0.0	0.0	0.0	7	28	0	72
35	Fig. 9	"	2 eq. H–sponge	n.d.	n.d.	1.9	1.2	5.0	5.1	7.4	0.1	0.1	3.3	80	55	2	43
36	Fig. 10	"	0.5 eq. TMBA	n.d.	n.d.	0.7	0.5	4.0	3.1	11.0	0.1	0.1	3.3	72	64	2	34

AIII.1. Full analytical details.

[previous page:] **Table AIII.1.** Overview of the results of catalytic reactions performed in 25 ml dry and degassed methanol under 50 bar CO pressure. This data was used in the paper in places indicated in the table. The catalyst was always generated *in situ* from 0.05 mmol $Pd(OAc)_2$. Mole ratio's are: Pd(OAc)2 : Ligand : nitrobenzene : methanol = 1 : 1.5 : 488 : 12350. The experiments in entries 1 – 6 and 8 – 11 were performed in quadruplicate to ensure that the reactions were reproducible. The standard deviations are not given for the sake of clarity, but are < 5% in all cases. Quantities are reported in mmol. 'n.d.' stands for 'not determined'.

[Table Foot of previous page:] [a] Conversion = (24.4 – $PhNO_2$)/24.4 × 100%. bc] Selectivity towards carbonylation products = (MPC + DPU) / ($\Sigma_{\varnothing}$ – $PhNO_2$) × 100%. [c] Selectivity towards coupling products = (2×Azo + 2×Azoxy) / ($\Sigma_{\varnothing}$ – $PhNO_2$) × 100%. [d] Selectivity towards hydrogenation products = ($PhNH_2$ + DPU) / ($\Sigma_{\varnothing}$ – $PhNO_2$) × 100%.

Table AIII.2. Reactions performed to investigate if the reaction products are inert.[a]

Entry	Reactant 1 (mmol)	Reactant 2 (mmol)	Comment	Expected product(s) (mmol)
1	DPU (6)	MeOH	110 ºC in MeOH	MPC (3.2)
2	``	``	100 ºC in MeOH	MPC (1.5)
3	``	``	90 ºC in MeOH	MPC (1.6)
4	``	``	80 ºC in MeOH	MPC (0.4)
5	DPU (6)	DMC (12)	120 ºC in diglyme	MPC (0.0)
6	MPC (6)	MeOH	120 ºC in MeOH	DMC (0.0)
7	$PhNH_2$ (6)	DMC (12)	120 ºC in MeOH	MPC (0.0)
8	$PhNH_2$ (6)	DMO (12)	120 ºC in MeOH	$PhNH(CO)_2OMe$ (0.4)[b]
9	Azo (2.5)	50 bar CO	120 ºC in MeOH	PhNCO[c] (0.0)
10	Azo (2.5)	50 bar H_2	120 ºC in MeOH	$PhNH_2$ (0.0)
11	Azoxy (2.5)	50 bar CO	120 ºC in MeOH	Azo (0.0); PhNCO* (0.0)
12	Azoxy (2.5)	50 bar H_2	120 ºC in MeOH	Azo (0.0); $PhNH_2$ (0.0)

[a] The reaction mixture was heated for four hours at 110 ºC under an atmosphere of 50 bar CO, unless stated otherwise.[b] Detected with GLC–MS and the quantity was estimated using the calibration line of MPC. This product was occasionally detected in trace amounts after catalytic experiments wherein a large amount of DMO was produced. [c] Measured in the form of MPC and DPU.

AIII.2. NMR spectra of ligand exchange experiments of 'phen–palladacycle' and L3X and bpap.

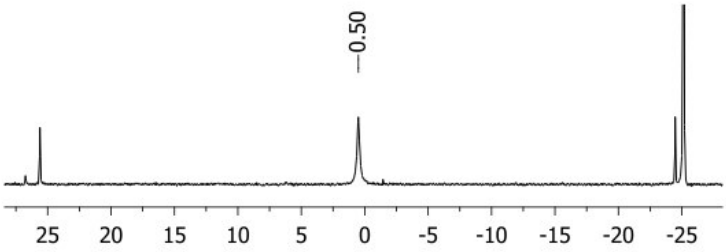

Figure AIII.1. ^{31}P–NMR spectrum of *in situ* synthesis of $Pd^0(L3X)_2$ from $Pd_2(dba)_3$ and 10 eq. L3X in nitrobenzene. This spectrum was taken after 12 hours reaction time.

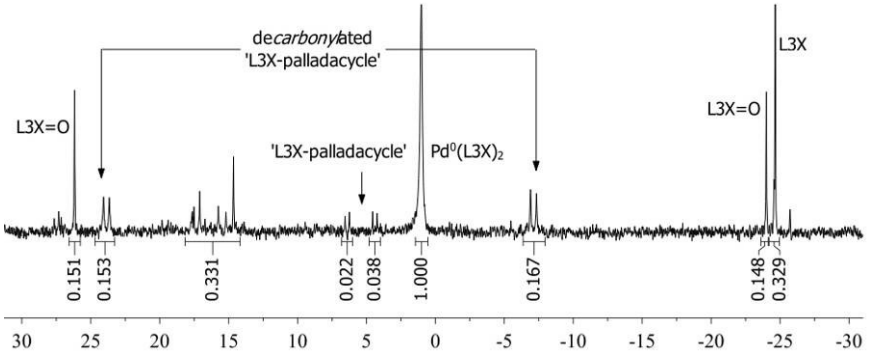

Figure AIII.2. $^{31}P\{^{1}H\}$–NMR spectrum for a solution containing 'phen–palladacycle' and 1 eq. of L3X in nitrobenzene after standing for 180 minutes at room temperature. This solution contained 17% of 'phen–palladacycle' and 83% phen (^{1}H–NMR), meaning that only 83% of the initially added palladium can end up as L3X–complex. The percentage of a specific L3X–Pd complex (relative to palladium) can thus be calculated by: $\int_{L3X-complex} / \Sigma_{\int\ all\ L3X-complexes} * 83\%$. Thus, the species detected with $^{31}P\{^{1}H\}$–NMR that were assigned to Pd–containing species are (δ ($\int$; assignment; percentage based on Pd)): 1.0 (1.00; $Pd^{0}(L3X)_2$; 33%); 5.0 (0.06; 'L3X–palladacycle'; 4%); 13 – 20 (0.33; unknown Pd complexes; 22%); 24/–7 (0.32; de*carbonylated* 'L3X–palladacycle'; 21%); 35 (0.05; unknown Pd complex; 3%); $\Sigma\int$ = 1.76. The solution also contained L3X (–25 ppm, $\int$ = 0.33) and 'L3X=O' (26/–24 ppm, $\int$ = 0.30), which is ((0.33+0.30)/1.76*100% =) 26% of the initially added L3X. Hence, 74% of L3X is thus bound to palladium; this is indeed roughly one equivalent with respect to the 83% Pd–complex, computed based on ^{1}H–NMR.

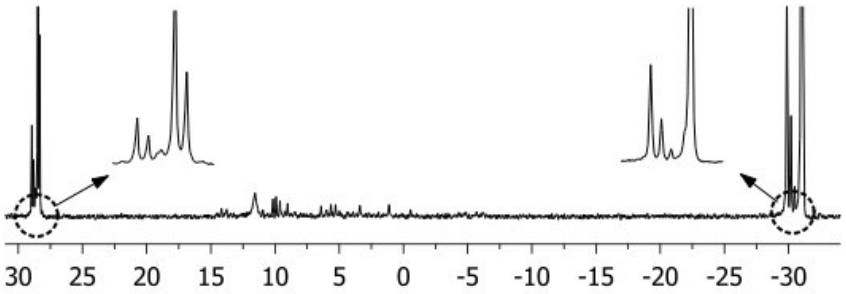

Figure AIII.3. $^{31}P\{^{1}H\}$–NMR spectrum of a solution containing 'phen–palladacycle' and 5 eq. of bpap in nitrobenzene, recorded at room temperature after heating four hours at 100 °C. The inset figures are enlargements of the indicated area. The resonances of the free ligand lie around –31.0 (*rac*) and –30.2 (*meso*) ppm. The resonances around 28 – 29 ppm must originate from ligand oxide (2 × 'PP=O' and 2 × 'O=PP=O') and/or 'bpap=NPh' / 'PhN=bpap=NPh'.

AIII.3. Attempts to positively identify and quantify the 'PhN'–containing products.

AIII.3.1. NMR analysis of ligand exchange experiments in CH_3NO_2 and CD_2Cl_2

With GLC(–MS) analysis after a ligand exchange experiment of phen–palladacycle with L3X in nitrobenzene, we were unable to quantitatively identify the fate of the initially present 'PhN' moiety in possibly anticipated products, PhNCO, azo(xy)benzene, $PhNH_2$ and nitrosobenzene. The aromatic region in the ^{1}H–NMR spectra of these experiments is obviously too crowed (due to the solvent $PhNO_2$ and the excess of $Pd^0(L3X)_2$ and/or L3X) to allow the positive identification of the 'PhN' containing product or products that *are* formed quantitatively with respect to the starting compound phen–palladacycle. In an attempt to circumvent this difficulty, two –instead of five– equivalents of L3X in nitro*methane* were added to phen–palladacycle, after which the yellow suspension was heated until a clear orange solution was obtained. Upon cooling however, a yellow precipitate was formed (probably $Pd^0(L3X)_2$) which could not be re–dissolved upon further heating. In the ^{1}H–NMR spectrum of this suspension, the resonances of uncoordinated phen are clearly present (see Figure S4), together with about 0.2 equivalent of a relatively isolated resonance that is (at least also) characteristic for aniline (~6.7 ppm). Besides the presence of some remaining ligand and ligand oxide (as indicated by ^{31}P{^{1}H}–NMR), various other aromatic species were clearly present, albeit the aromatic region between 7–9 ppm was still too crowded to allow a possible identification of these compounds (see Figure AIII.4).

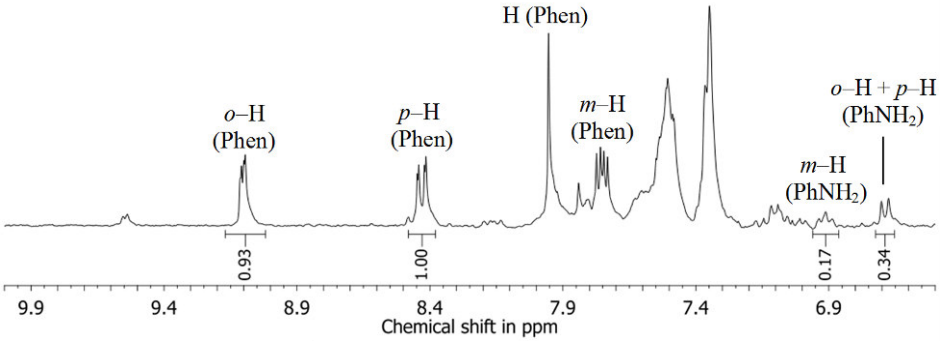

Figure AIII.4. Partially integrated ^{1}H–NMR spectrum of the yellow suspension obtained after the ligand exchange reaction of phen–palladacycle and two equivalents of L3X in nitromethane.

When two equivalents of L3X in CD_2Cl_2 were added to phen–palladacycle, a clear orange solution was obtained after allowing the yellow suspension to stand for several hours in an ultrasonic bath. This solution contained mostly $Pd^0(L3X)_2$ complex (^{31}P{^{1}H}–NMR), and the ^{1}H–NMR again clearly contained –besides $Pd^0(L3X)_2$– uncoordinated phen, presumably some aniline (6.7 ppm, ~0.2 equivalent on phen), and *various* other aromatic compound (see Figure AIII.5a). What is more, the ^{13}C–NMR spectrum of this clear solution also reveals an *abundance* of several aromatic compounds (besides phen and $Pd^0(L3X)_2$; see Figure AIII.5b).

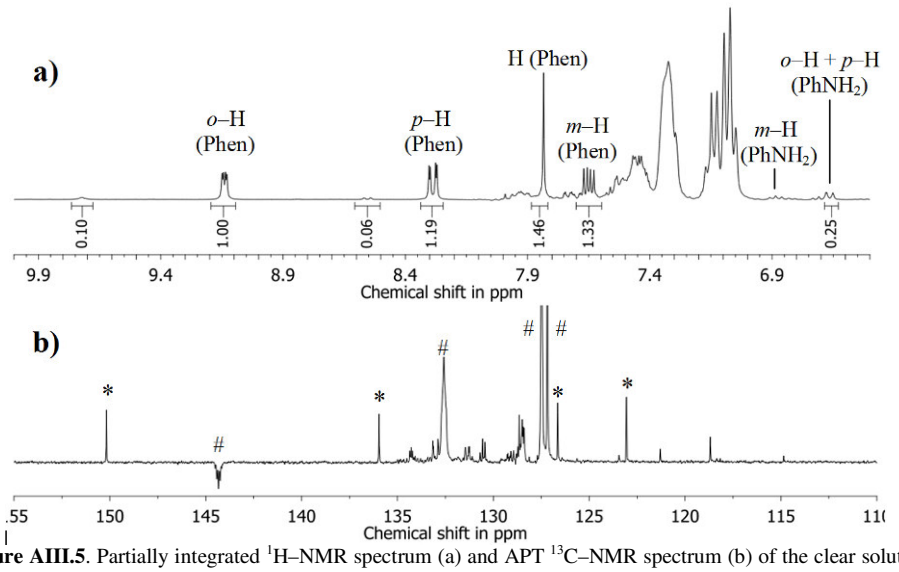

Figure AIII.5. Partially integrated ^{1}H–NMR spectrum (a) and APT ^{13}C–NMR spectrum (b) of the clear solution obtained after the ligand exchange reaction of phen–palladacycle and two equivalents of L3X in CD_2Cl_2. '*' = phen; '#' = $Pd^0(L3X)_2$.

AIII.3.2. NMR analysis of ligand exchange experiments with '(F_5–)L2' in $PhNO_2$, CH_3NO_2 and CD_2Cl_2

As the above experiments are again inconclusive, possibly due to the interference from the ^{1}H–NMR resonances of the aryl rings in L3X / $Pd^0(L3X)_2$, it was considered if the ligand L3X could be replaced by a similar ligand with pentafluorophenyl rings. 'F_5–L2' (1,2–*bis*(di–pentafluorophenyl–phosphino)–ethane) is commercially available and the ligand exchange experiment with two equivalents of its normal phenyl–analogue ('L2') gave essentially the same results as the experiment with L3X (i.e., formation of an asymmetric complex, followed by decomposition to $Pd^0(L2)_2$; see Figure AIII.6).

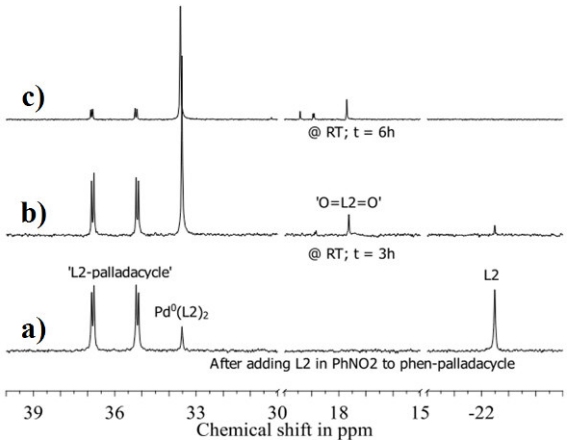

Figure AIII.6. ^{31}P–NMR spectra of a ligand exchange reaction of phen–palladacycle and two equivalents of L2 in nitrobenzene; a) after the addition of L2 in PhNO2 to phen–palladacycle; b) after standing for 3h; c) after standing for 6h.

Thus, a suspension of phen–palladacycle and two equivalents of F_5–L2 in nitrobenzene, was gently heated until a clear solution was obtained. The ^{1}H–NMR spectrum revealed only the phen–palladacycle (^{1}H–NMR, ~10 ppm) which started to precipitate during cooling. ^{31}P{^{1}H}–NMR revealed only pure F_5–L2 around –44.5 ppm.[46] The suspension was therefore heated at 80 °C and monitored with ^{31}P{^{1}H}– and ^{1}H–NMR (see Figure AIII.7).

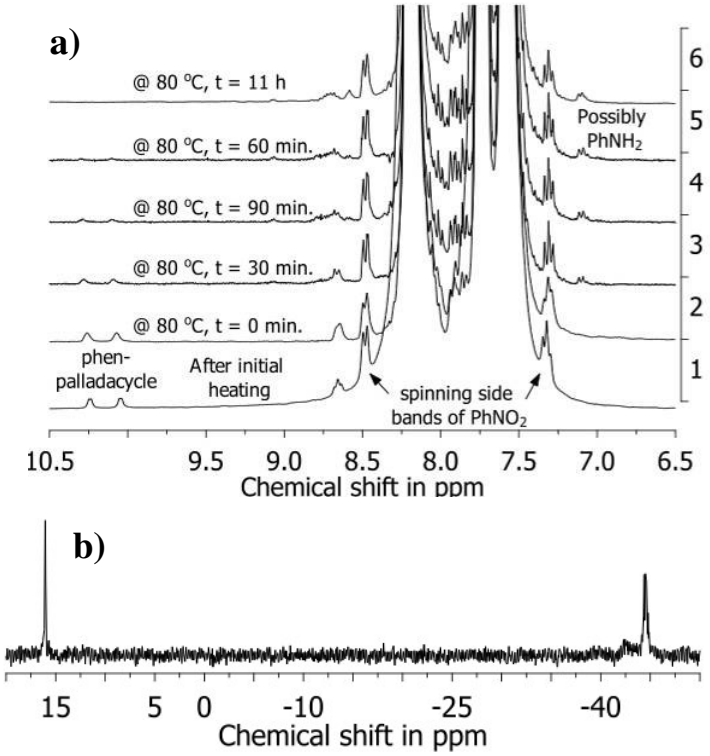

Figure AIII.7. a) ^{1}H–NMR spectra of a ligand exchange reaction of phen–palladacycle and two equivalents of F_5–L2 in nitrobenzene, measured at the indicated time and temperature; b) ^{31}P–NMR spectrum at ambient temperature of this experiment after heating for 11 hours at 80 °C.

After about 90 minutes, the phen–palladacycle had disappeared, and the aromatic region became more crowded. However, the characteristic ^{1}H–NMR resonance of uncoordinated phen (9.2 ppm) was not observed, nor did the ^{31}P{^{1}H}–NMR spectrum reveal the formation of a P_2Pd–complex (only ligand (–44.5 ppm) and some ligand oxide were detected (16.06 ppm)).[46] Thus, F_5–L2 does indeed *facilitate* the decomposition of phen–palladacycle (which is thermally stable in nitrobenzene at these temperatures), but the palladium centre probably ends up as a phen–complex (as no uncoordinated phen was observed).

Because the ^{1}H–NMR resonances of this presumed phen–complex and the resonances of the phen–palladacycle decomposition products are obscured by those of the solvent nitrobenzene, the experiment was repeated in CD_2Cl_2. However, no clear solution could be obtained, not even when allowing the suspension to stand in an ultrasonic bath for about 12 hours. The phen–palladacycle thus hardly dissolves in CD_2Cl_2 and the decomposition of the palladacycle is also much slower when using F_5–L2 (required heating at 80 °C for 5 hours in $PhNO_2$). Nevertheless, the ^{1}H–NMR

spectrum of this suspension did reveal the presence of several aromatic compounds that could now be clearly distinguished from one another. The ^{1}H–^{1}H–COSY spectrum is shown in Figure AIII.8, together with the assignment of most of the peaks.

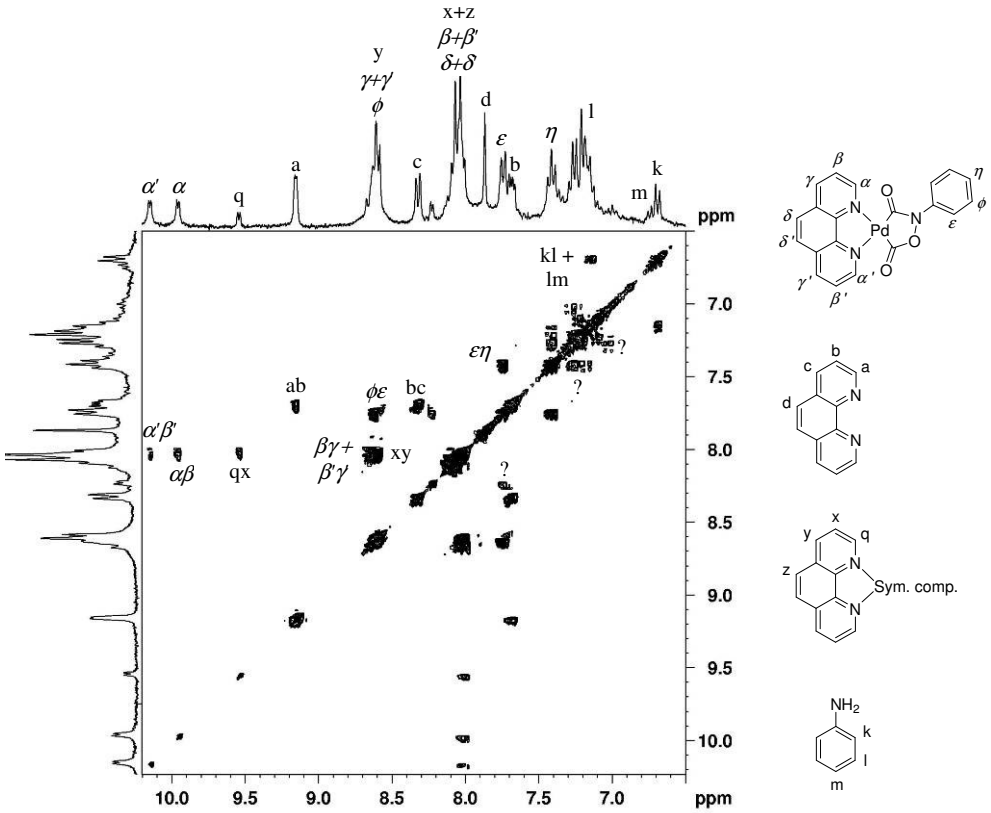

Figure AIII.8. ^{1}H–^{1}H–COSY NMR spectrum of a suspention of phen–palladacycle and F_5–L2 in CD_2Cl_2 after standing for 12 hours in an ultrasonic bath. The assignment of most peaks is also given.

The two doublets around 10 ppm originate from the ortho–protons of the phen ligand in phen–palladacycle (indicated by *α* / *α*' and defined as 'one' equivalent). The other resonances of phen in this complex are located around 8.6 and 8.0 ppm, and the resonances of the 'PhN' moiety of the phen–palladacycle are found at 8.0, 7.7, and 7.4 ppm. Also present is about 0.6 equivalents of uncoordinated phen ('a–d'; 9.1, 8.3, 7.8, and 7.6 ppm) and 0.2 equivalents of an unknown –symmetrical– phen–containing compound ('q–z'; 9.5, 8.6, and 8.0 ppm). The resonances around 6.7 ppm ('k' and 'm' witch couples with a resonance around 7.2 ppm) is assigned to about 0.5 equivalents of aniline, which probably result from the reaction of trace amounts of water with possibly formed PhNCO or 'Pd=NPh' complex. Because the meta–H triplet of PhNCO (around 7.3 ppm) was not observed, the presence of PhNCO itself was ruled out. What is more, the certain reaction product of PhNCO and $PhNH_2$ (which *is* present), namely *N,N*'diphenylurea (DPU) was also not observed (The para–H triplet of DPU lies at 6.9 ppm and its singlet NH resonance typically lies around 10 ppm). In addition to the resonances that could be assigned, there are –based on the integrals of isolated known resonances and the unsymetric form of some of the peaks– other aromatic compounds present as well (between 7 and 9 ppm, especially around 7.2 ppm). The total

amount of these unknown compounds is about six equivalent relative to the phen–palladacycle complex (as measured in this suspention; characteristically around 9.9 and 10.1 ppm), and these resonances are largely obscured by the aromatic resonances that could be assigned. This again suggest the formation, albeit in low amounts, of *several* aryl containing products which *must* originate from the phen–palladacycle (as the ligand nor the solvent contains aromatic H-atoms).

In a final attempt to obtain conclusive information about the possible decomposition product(s) containing the thusfar elusive 'PhN' group, the experiment was repeated in nitromethane. As both phen–palladacycle and the two equivalents of F_5–L2 are insoluble in CH_3NO_2, the suspension was heated to 80 °C and monitored with ^{1}H– and ^{31}P–NMR for about 20 hours, resulting in a clear yellow solution with a small amount of bright yellow crystals. After heating for about three hours, a multitude of aromatic compounds had evolved that remained unaltered during the rest of the 21 hour period (see Figure AIII.9).

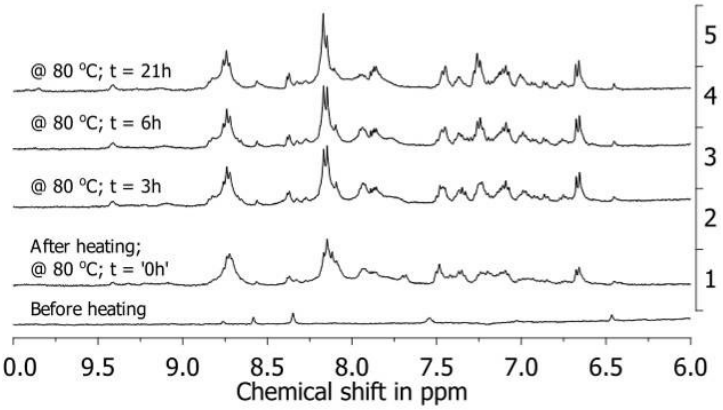

Figure AIII.9. ^{1}H–NMR spectra of a ligand exchange reaction of phen–palladacycle and two equivalents of F_5–L2 in nitromethane, measured at the indicated time and temperature.

The ^{31}P{^{1}H}–NMR spectrum at ambient temperatures after heating for 21 hours (see Figure AIII.10a) reveals mostly uncoordinated F_5–L2, some of its oxide, and trace amounts of several other phosphorus–containing compounds. The corresponding ^{1}H–NMR spectrum is shown in Figure AIII.10b.

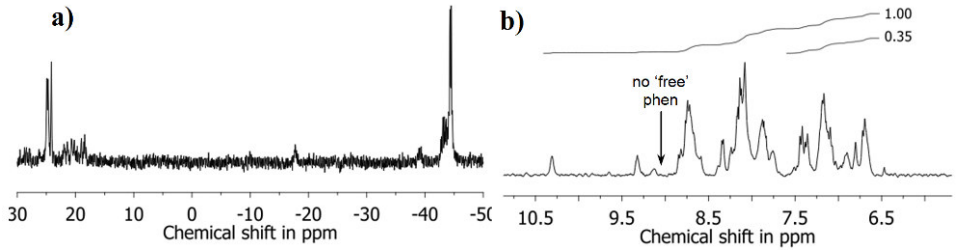

Figure AIII.10. ^{31}P–NMR spectrum (a) and ^{1}H–NMR spectrum with the integrals of the indicated regions (b) taken at ambient temperature after a ligand exchange reaction of phen–palladacycle and two equivalents of F_5–L2 in nitromethane (see also Figure AIII.10).

Note that *no* uncoordinated phen could be observed (ortho–H around 9.1 ppm), nor any other resonance that is characteristic for the ortho–protons of phen, suggesting that the crystals formed contain all of the phen ligand. More importantly, this means that the various aromatic compounds formed *must all* originate from the 'PhN' moiety that was initially present in the form of phen–palladacycle (i.e., there are no aromatic protons in the solvent nor in the F_5–L2 ligand). Although *some* –definitely not all– of the resonances between 6.5 and 7.5 may be ascribed to $PhNH_2$, PhNCO, or even DPU, it is important to note that this region represents merely $^1/_3$ of all aromatic resonances measured (10.5 to 6.5 ppm). This again points towards a phosphane–ligand assisted decomposition of the phen–palladacycle into *various* 'PhN' containing products, and not –as was initially expected– smoothly to a well–defined 'PhN' containing product such as PhNCO.

AIII.3.3. GLC–MS analysis of in situ synthesized methylmesitylene carbamate.

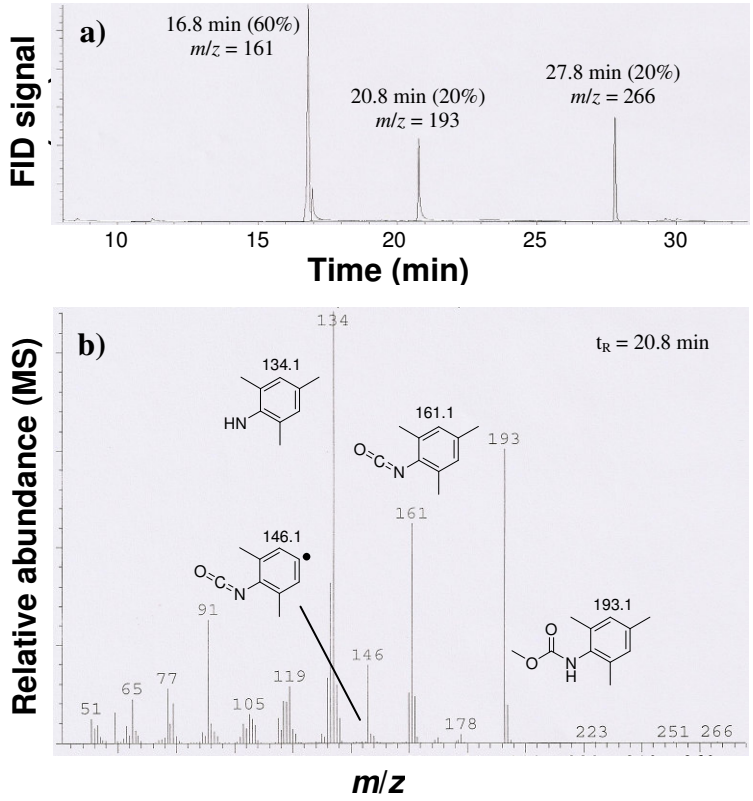

Figure AIII.11. a) GLC–MS chromatogram of a reaction mixture recorded after *in situ* synthesis of methylmesityl-ene carbamate b) mass spectrum of methylmesitylene carbamate (t_R = 20.8 minutes).

Appendix IV

Supporting Information of Chapter 5

-Full analytical details of catalytic experiments-

Table AIV.1. Overview of the results of catalytic reactions performed in 25 ml dry and degassed methanol under 50 bar CO pressure. This data was used in the paper in places indicated in the table. The catalyst was always generated *in situ* from 0.05 mmol $Pd(OAc)_2$. Mole ratio's are: $Pd(OAc)_2$: Ligand : nitrobenzene : methanol = 1 : 1.5 : 488 : 12350. The experiments in entries 1 – 6 and 8 – 11 were performed in quadruplicate to ensure that the reactions were reproducible. The standard deviations are not given for the sake of clarity, but are < 5% in all cases. Quantities are reported in mmol. 'n.d.' stands for 'not determined'.

Entry	Used for	Catalyst	Comment	H_2O	MF	DMC	DMO	$PhNH_2$	$PhNO_2$	MPC	Azo	Azoxy	DPU	E_{oc} (%)[a]
1	**Tab.1, Fig. 3, 4, 5**	L3	-	3.0	0.1	3.6	3.3	5.1	8.1	5.9	0.1	0.4	1.7	45
2	**Tab.1, Fig. 2, 6**	L3X	-	3.4	0.2	4.2	3.1	8.3	8.1	5.3	0.1	0.4	0.8	45
3	**Tab.1, Fig. 3**	oMeO-L3	-	n.d.	0.6	0.6	0.5	4.1	11.5	6.6	0.1	0.1	0.9	10
4	**Tab.1, Fig. 2, 4, 6**	oMeO-L3X	-	0.7	1.1	0.4	0.4	5.7	0.6	11.6	0.1	0.1	3.1	5
5	**Tab.1, Fig. 3**	pMeO-L3	-	n.d.	0.1	2.2	2.1	3.9	11.3	5.2	0.0	0.0	1.9	30
6	**Tab.1, Fig. 5**	L4	-	n.d.	0.3	2.4	5.6	5.4	9.8	3.0	0.2	2.1	0.8	55
7	**Tab.1, Fig. 2, 3, 6**	L4X	-	10.0	0.2	2.3	5.9	1.9	11.8	0.5	0.1	4.5	0.5	65
8	**Tab.1, Fig. 2, 3, 6**	oMeO-L4X	-	8.7	0.6	2.1	7.3	10.5	2.4	5.6	0.5	0.6	1.9	40
9	**Tab.1, Fig. 3**	pMeO-L4	-	0.1	0.2	1.7	3.7	5.9	14.7	2.6	0.0	0.3	0.0	60
10	**Tab.1**	L5Fc	-	n.d.	0.4	4.3	13.7	7.2	7.2	2.2	0.3	3.5	0.2	105
11	**Tab.1**	oMeOL5Fc	-	n.d.	1.8	2.5	8.0	11.2	0.0	7.6	0.1	0.1	2.6	45
12	**Fig. 4**	L3	+ 5 eq. TMBA	n.d.	n.d.	1.2	1.4	1.2	12.3	5.3	0.0	0.3	2.5	20
13	**Fig. 4**	``	+ 10 eq. H-sponge	n.d.	n.d.	6.7	5.2	5.7	2.2	6.0	0.1	0.7	4.4	55
14	**Fig. 5**	``	25 bar CO	n.d.	n.d.	4.7	1.5	4.9	13.0	3.1	0.1	0.5	1.2	45
15	**Fig. 5**	``	100 bar CO	n.d.	n.d.	2.6	4.8	5.2	2.8	7.8	0.1	0.2	4.0	35
16	**Fig. 5**	L4	25 bar CO	n.d.	n.d.	2.6	3.1	2.7	14.0	1.2	0.1	1.5	0.0	55
17	**Fig. 5**	``	100 bar CO	n.d.	n.d.	1.5	8.1	5.7	6.5	3.8	0.1	1.3	2.0	60
18	**Fig. 4**	oMeO-L3X	+ 5 eq. TMBA	n.d.	n.d.	0.1	0.1	1.6	8.8	9.8	0.1	0.3	1.7	0
19	**Fig. 4**	``	+ 10 eq. H-sponge	n.d.	n.d.	1.8	1.3	3.8	0.0	9.9	0.1	0.1	4.3	15
20	**Fig. 6**	L3X	15 bar H_2, 35 bar CO	n.d.	4.4	2.2	2.0	9.5	5.7	3.1	0.1	0.5	2.6	20
21	**Fig. 6**	oMeO-L3X	15 bar H_2, 35 bar CO	n.d.	1.8	0.0	0.0	22.6	0.0	0.4	0.3	0.0	0.4	0
22	**Fig. 6**	L4X	15 bar H_2, 35 bar CO	n.d.	4.0	1.8	4.7	3.7	11.5	0.5	0.1	3.4	0.2	55
23	**Fig. 6**	oMeO-L4X	15 bar H_2, 35 bar CO	n.d.	5.9	1.3	4.9	15.0	0.0	4.6	0.3	0.1	1.8	25

[a] E_{oc} = estimated efficiency of methanol oxidative carbonylation based on nitrobenzene reduction products = (DMC+DMO) / ($PhNO_2$ consumed) ≈ (DMC+DMO) / (MPC+$PhNH_2$+2(DPU+Azo(xy))) * 100%.

Appendix V

Supporting Information of Chapter 6

-Full analytical details of catalytic experiments-
-DFT calculations of 'palladacyclic' complexes-
-Ligand exchange experiment of 'phen-palladacycle' with L4X-
-Procedure to estimate Gibbs free energy differences and the validation of that procedure-
-^{1}H-^{1}H-COSY spectrum of 'phen-palladacycle'-

Table AV.1. Overview of the results of catalytic reactions performed in 25 ml dry and degassed methanol under 50 bar CO pressure and at 110 °C (L4X) or 130 °C (Phen). This data was used in the paper in places indicated in the table. The catalyst was always generated in situ from 0.05 mmol Pd(OAc)2. Typical mole ratio's are: Pd(OAc)2 : Ligand : nitrobenzene : methanol = 1 : 1.5 : 488 : 12350. Most experiments were performed in quadruplicate to ensure that the reactions were reproducible. The standard deviations are not given for the sake of clarity, but are < 5% in all cases. Quantities are reported in mmol. 'n.d.' stands for 'not determined'.used in the paper in places indicated in the table. Quantities are reported in mmol.

				Quantities analyzed (mmol)										%			
Entry	**Used in**	**Catalyst**	**Comment**	**H_2O**	**MF**	**DMC**	**DMO**	**$PhNH_2$**	**$PhNO_2$**	**MPC**	**Azo**	**Azoxy**	**DPU**	**Conv.[a]**	**NCO[b]**	**N=N[c]**	**NH[d]**
1	**Tab. 1, Fig. 6, 9**	L4X	–	10.1	0.2	2.3	5.9	1.9	11.8	0.5	0.1	4.5	0.5	52	8	73	19
2	**Tab. 1**	Phen	@ 110 °C	0.0	0.0	0.0	0.0	0.3	20.3	1.0	0.1	1.5	0.0	17	23	71	6
3	**Tab 1., Fig. 5, 6, 8, 9**	``	@ 130 °C	0.3	0.2	0.3	0.2	1.0	10.8	3.0	0.1	4.6	0.0	56	22	71	7
4	**Fig. 5**	``	4.9 mmol $PhNO_2$	n.d.	0.0	0.2	0.1	0.5	0.2	2.3	0.1	0.9	0.0	MPC / (Azo + Azoxy) =			2.7
5	``	``	9.7 mmol $PhNO_2$	n.d.	0.1	0.2	0.2	0.9	1.7	3.5	0.2	2.1	0.0	MPC / (Azo + Azoxy) =			2.0
6	``	``	14.6 mmol $PhNO_2$	n.d.	0.1	0.2	0.2	0.8	5.5	2.9	0.1	2.5	0.0	MPC / (Azo + Azoxy) =			1.4
7	``	``	19.5 mmol $PhNO_2$	n.d.	0.1	0.3	0.2	0.9	9.1	2.9	0.1	3.0	0.0	MPC / (Azo + Azoxy) =			1.2
8	``	``	34.1 mmol $PhNO_2$	n.d.	0.2	0.3	0.2	0.5	23.3	2.4	0.1	4.1	0.0	MPC / (Azo + Azoxy) =			0.7
9	``	``	48.7 mmol $PhNO_2$	n.d.	0.5	0.3	0.2	0.9	31.7	2.7	0.2	6.5	0.0	MPC / (Azo + Azoxy) =			0.5
10	**Fig. 6**	L4X	0.25 eq. HOTs	n.d.	n.d.	2.3	10.3	4.2	9.4	1.2	0.2	3.3	0.0	61	9	56	34
11	**Fig. 6, 7**	``	0.5 eq. HOTs	n.d.	n.d.	3.2	13.4	6.3	8.4	2.6	0.3	3.9	0.0	66	15	48	36
12	**Fig. 6**	``	1 eq. HOTs	n.d.	n.d.	2.4	13.8	8.1	4.0	3.2	0.4	2.2	0.0	84	19	32	49
13	**Fig. 7**	``	0.5 eq. TMBA	n.d.	n.d.	2.4	10.9	4.5	9.8	1.3	0.2	3.8	0.0	60	9	58	33
14	**Fig. 7**	``	0.5 eq. PPA	n.d.	n.d.	2.8	14.1	7.1	9.1	4.6	0.2	1.8	0.0	63	29	25	45
15	**Fig. 6**	Phen	0.25 eq. HOTs	n.d.	n.d.	0.2	0.1	2.0	11.5	9.5	0.1	0.6	0.0	74	11	16	53
16	**Fig. 6, 7, 8**	``	0.5 eq. HOTs	n.d.	n.d.	0.1	0.1	2.0	10.5	11.6	0.1	0.2	0.0	82	4	14	57
17	**Fig. 6**	``	1 eq. HOTs	n.d.	n.d.	0.1	0.1	2.1	11.8	10.6	0.0	0.2	0.0	81	3	16	52
18	**Fig. 7**	``	0.5 eq. TMBA	n.d.	n.d.	0.1	0.1	2.4	9.2	12.6	0.1	0.2	0.0	62	81	4	15
19	**Fig. 7**	``	0.5 eq. PPA	n.d.	n.d.	0.1	0.1	2.3	6.3	14.1	0.1	1.1	0.0	74	75	13	12
20	**Fig. 8**	5 eq. Phen	5 eq. Phen	n.d.	n.d.	0.1	0.1	1.5	3.5	6.8	0.4	6.7	0.0	86	30	63	7
21	``	``	0.5 eq. HOTS	n.d.	n.d.	0.1	0.1	2.0	2.9	15.9	0.2	1.3	0.0	88	76	15	9
22	``	``	2.0 eq. HOTs	n.d.	n.d.	0.0	0.1	2.1	2.1	18.8	0.1	0.3	0.0	91	86	4	10
23	**Fig. 9**	L4X	2.5 mmol PhNO	n.d.	n.d.	2.5	6.4	2.1	13.4	0.9	0.2	4.9	0.0	50	9	72	18
24	**Fig. 9**	Phen	2.5 mmol PhNO	n.d.	n.d.	0.2	0.3	0.9	12.0	2.9	0.2	5.2	0.0	55	20	74	6

[a] Conversion = $(24.4 - PhNO_2)/24.4 \times 100\%$. bc] Selectivity towards carbonylation products = (MPC + DPU) / $(\Sigma_{\varnothing} - PhNO_2) \times 100\%$. [c] Selectivity towards coupling products = $(2\times Azo + 2\times Azoxy) / (\Sigma_{\varnothing} - PhNO_2) \times 100\%$. [d] Selectivity towards hydrogenation products = $(PhNH_2 + DPU) / (\Sigma_{\varnothing} - PhNO_2) \times 100\%$.

AV.1. DFT calculations of 'paladacyclic' complexes.

The relative stabilities of a palladacyclic complex with the ligand Phen and two P–donor ligand with a butylene backbone (i.e., L4X and the simplified analogue L4) was investigated with DFT calculations. In Table AV.2, some geometric and energetic data are listed, and in Figure AV.1 perspective views are given of both calculated structures.

Table AV.2. Selected data of some (calculated) palladacyclic complexes of the type (ligand)PdC(O)N(Ph)OC(O).

Complex (→):	X–ray	DFT (BP / 6–31G*)		
Parameter (↓):	Phen	Phen	L4	L4X
L1 – Pd (Å)	2.128	2.203	2.416	2.412
L2 – Pd (Å)	2.130	2.203	2.420	2.440
L1 – Pd – L2 (º)	77.66	76.04	97.34	95.00
C1 – Pd – C2 (º)	82.02	82.00	80.79	80.84
LLPd/PdCC (º)	1.89	0.86	20.24	19.49
'ΔH' (kcal/mol)[a]	–	–75.4	–59.9	–60.2
'ΔH'$_{rel}$ (kcal/mol)[b]	–	0	+15.5	+15.2

[a] The enthalpy of formation was calculated from: Pd(Ligand)$(CO)_2$ + $PhNO_2$ + CO → Complex + CO_2. [b] Relative to 'phen–palladacycle'

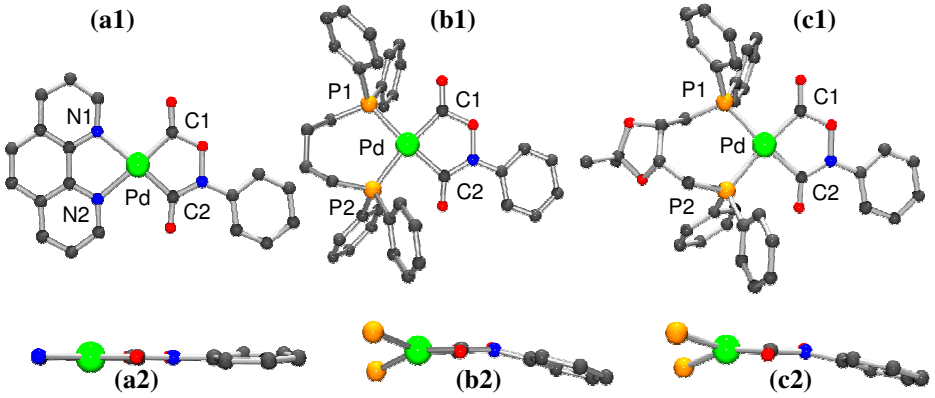

Figure AV.1. Perspective views of the calculated palladacyclic complexes with the ligands Phen (a1) L4 (b1) and L4X (c1). A side view for these complexes is shown in a2, b2 and c2 respectively, wherein only the donor–atoms of the ligands are shown for clarity. Color code: Pd (green), P (orange), N (bleu), O (red), C (grey), H are omitted for clarity.

As can be seen in Table AV.2, the structural characteristics of the DFT optimized structure of the Phen – palladacycle (see also Figure AV.1a) are nearly identical to those of the crystal structure of (Phen)PdC(O)ON(Ph)C(O) · $PhNO_2$, thus 'validating' the computational method used.[1] The minor variations might be due to crystal packing forces and/or the nitrobenzene molecule that occupies the lattice of the crystal structure.

Interestingly, for the palladacycles comprising L4 (Figure AV.1b) or L4X (Figure AV.1c), the dihedral angle between the P–Pd–P and C–Pd–C planes is about 20º larger than that of the Phen analogue, and both palladacycles are also about +15 kcal.mol^{-1} less stable than their Phen analogue. This strongly suggests that the palladacycle can indeed be destabilized when the ligand in the complex imposes more steric constraint in the equatorial positions (i.e., has a larger bite angle). This

also suggests that if such a palladacycle is formed wherein the ligand is a diarylphosphane ligand comprising a butylene backbone (such as L4 or L4X) decomposition may occur more easily, whereas when employing Phen this complex will be more stable.

AV.2. 'Ligand exchange' experiment of 'phen-palladacycle' with L4X

To investigate experimentally whether L4X could perhaps destabilize 'phen–palladacyle', it was attempted to perform a ligand exchange reaction, monitored by $^{31}P\{^{1}H\}$– and ^{1}H–NMR spectroscopy; such a reaction with a similar phosphane ligand containing a propane–backbone (i.e., 'L3X'; 1,3–bis(diphenylphosphino)–2,2'dimethylpropane) indeed resulted in the anticipated ligand exchange reaction, followed by decomposition of the 'L3X–palladacyle' into the bis–chelate complex $Pd^{0}(L3X)_2$ (see Chapter 4).

Thus, 1.25 eq. of L4X was dissolved in deuterated nitrobenzene and then added to 1 eq. of the Phen–palladacycle (see experimental for details). The yellow suspension (Phen–palladacycle is poorly soluble in $PhNO_2$ at 20 – 25 ºC) was measured with $^{31}P\{^{1}H\}$–NMR (Figure AV.2a1), revealing mainly pure ligand L4X (–23.2 ppm), but also a small resonance around –0.3 ppm. This resonance cannot be a divalent palladium complexes, as $Pd(L4X)(OAc)_2$ is characterized by a sharp singlet around 15 ppm, and cationic bischelate complexes with similar diarylphosphane ligands exhibit a broad resonance around 5 – 10 ppm (see Chapter 2 and 4 for details). As the $^{31}P\{^{1}H\}$–NMR resonance of $Pd^{0}(L4X)_2$ lies at –0.3 ppm in acetone (see Chapter 2), and a bis–chelate was also eventually obtained when employing the similar L3X as ligand, (see Chapter 4) the observed resonance around –0.3 ppm can be assigned to $Pd^{0}(L4X)_2$. In the ^{1}H–NMR spectrum of this suspension (Figure AV.2a2), a resonance is observed that is characteristic for the Phen–palladacycle (9.8 ppm), but there is also a resonance around 9.1 ppm, which is characteristic for uncoordinated Phen ligand. This suggests that most of the Phen–palladacycle complex that is dissolved is decomposed.

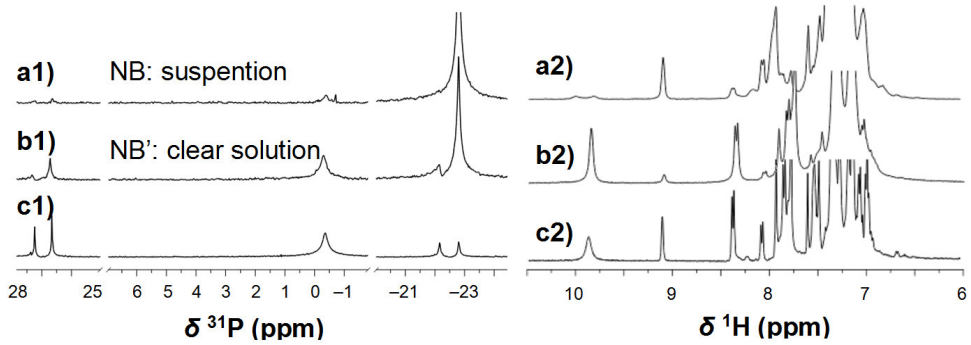

Figure AV.2. $^{31}P\{^{1}H\}$–NMR (a1–c1) and ^{1}H–NMR (a2–c2) spectra for a solution containing a Phen–palladacycle and 1 eq. of L4X in nitrobzene before heating (a), after heating shortly at 50 ºC (b), and after heating for two hours at 50 ºC (c).

After heating carefully to 50 ºC, a clear solution was obtained (Phen–palladacycle can be recrystallized from hot $PhNO_2$),[1] which was again measured with $^{31}P\{^{1}H\}$–NMR. As can be seen in Figure S2b2, the resonance around –0.3 ppm ($Pd^{0}(L4X)_2$) has become larger and some of the mono–oxide of the ligand was formed (26.6, –22.2 ppm). From the ^{1}H–NMR spectrum of this clear solution (Figure AV.2b2), it merely *appears* as if more Phen–palladacycle (9.8 ppm) and less uncoordinated Phen (9.1 ppm) are present, because all the Phen–palladacycle is now dissolved.

When the reaction mixture was heated for an additional two hours at 50 ºC, the $^{31}P\{^{1}H\}$–NMR spectrum (Figure AV.2c1) reveals that the $Pd^{0}(L4X)_2$ complex (–0.3 ppm) is now the main species, and more ligand oxide was formed (27.3 ppm (di–oxide); 26.6 and –22.2 ppm (mono–oxide)). Concurrently, the ^{1}H–NMR spectrum of this solution reveals that more free Phen ligand (9.1 ppm) is present in expense of the Phen–palladacycle (9.8 ppm).
Note also that the aromatic region (6 – 8 ppm) becomes more crowded throughout the series shown (Figure AV.2a2–c2), suggesting the appearance of aryl–containing molecules. Naturally, these resonances originate from $Pd^{0}(L4X)_2$, ligand–oxide, but also form decomposition products from the 'NPh' fragment of the 'phen–palladacycle'. We have obtained no clear indication however, of the final fate of the organic 'NPh' fragment. In particular, the formation of well–defined reaction products, such as the organic products phenylisocyanate or Azoxy, could not firmly be established. Clearly, these studies need to be repeated under more representative catalytic conditions, and also with more ligands other than L4X; a further experimental study aimed to unravel the exact fate of the 'NPh' fragment is presently underway in our laboratory.
As the Phen–palladacycle is perfectly stable under these conditions,[2] the above data strongly suggest that Phen can be expelled from the coordination sphere of Phen–palladacycle by L4X, followed by a rapid reduction of the initial Pd^{II} species into $Pd^{0}(L4X)_2$ and organic aryl containing fragments; a process that is in accordance with our previous findings using the similar phosphane ligand 'L3X' (see Chapter 4).

AV.3. Procedure to estimate Gibbs free energy differences

To estimate the Gibbs free energy differences of the complexes that can be involved in the nitrobenzene deoxygenation process (Scheme 6.5), it is necessary to estimate both the enthalpy and the entropy of formation of all the molecules involved in its formation. The enthalpy of formation for a certain palladium complex can be estimated by a simple geometry optimization computation with density functional theory (see experimental for details). Thus, by taking $L_2Pd(CO)_2$ (**C0**) as a reference, the enthalpies of formation of (**C1** – **C7**) could easily be obtained. The gain or loss in entropy at a given temperature relative to **C0** can be estimated using the standard molar entropies for each molecule involved (S° in $J.mol^{-1}.K^{-1}$, available from the handbook of chemistry and physics). These values are obviously unknown for the palladium complexes. It must be noted however, that although the molecular entropy consists out of a translational, rotational, vibrational and an electronic component, it is generally accepted[3] that the latter two (vibrations and electronics) are negligibly small compared to the former two (translation and rotation). It is thus reasonable to assume that the entropy contribution of the palladium complexes is, by approximation, constant. For example, when a palladium complex is carbonylated, the loss is entropy is mainly caused by the inability of the 'frozen' CO molecule to translate and rotate, while the vibrational and electronic differences can be marginalized, and for our rough approximation even neglected. The standard molar entropies of gas-phase CO and CO_2 are 197.60 and 213.79 $J.mol^{-1}.K^{-1}$ respectively. The value of S° for liquid nitrobenzene is unknown, but a value of 220 $J.mol^{-1}.K^{-1}$ may be assumed as this is roughly the S° value for molecules of similar structure (i.e.: 216.7 (benzyl alcohol); 219.2 (bromobenzene); 222.8 (benzenethiol); 221.2 (benzaldehyde) $J.mol^{-1}.K^{-1}$). Thus, the Gibbs free energy ('ΔG') for a certain complex can be estimated, for example for **C6** *versus* **C0**, as follows. The net reaction to go from **C0** to **C6** is given by: **C0** + $PhNO_2$ → **C6** + CO_2. Hence, the Gibbs free energy can be calculated using Equation 1:

$$'\Delta G'_{C0\rightarrow C6} = \Delta H_{C0\rightarrow C6} - \left(\Delta S_{C0\rightarrow C6} \times T\right) =$$

$$\left(H°_{C6} + H°_{CO_2} - H°_{C0} - H°_{PhNO_2}\right) - \left(\frac{\left[S°_{C0} + S°_{CO_2} - S°_{C6} - S°_{PhNO_2}\right] \times T}{4186.8}\right) \quad \text{Eq. 1}$$

This can be re-written numerically for phen as the supporting ligand at 130 °C (i.e., 403 K) reaction temperature by Equation 2, and for L4X as the supporting ligand at 110 °C (i.e., 383 K) by Equation 3:

$$'\Delta G'_{C0\rightarrow C6\ (phen)} = (-34.6) - \left(\frac{[213.79 - 220.00] \times 403}{4186.8}\right) = -34.0 \text{ kcal.mol}^{-1} \quad \text{Eq. 2}$$

$$'\Delta G'_{C0\rightarrow C6\ (L4X)} = (-34.2) - \left(\frac{[213.79 - 220.00] \times 383}{4186.8}\right) = -33.6 \text{ kcal.mol}^{-1} \quad \text{Eq. 3}$$

In this manner, the numerical data shown in Scheme 6.5 was computed.

AV.4. Validation of the procedure to estimate Gibbs free energy differences

The validity of the above approximation was assed by applying the method to two known reactions. First the hydratation of 1-butene to 1-butanol at 25 °C, which is known to be a thermodynamic equilibrium reaction. Secondly the hydroformylation of ethene to pronanal was considered at 110 °C; this reaction must clearly be exothermic, while the entropy contribution must be energetically highly unfavourable. Table AV.2 lists the relevant literature values of H° and S° for the molecules involved in these reactions, together with the estimated Gibbs free energy values computed using Equation 1. As can be seen form the table, the formation of 1-butanol at 25 °C is indeed estimated to be thermodynamically neutral ('ΔG' = +0.17 kcal.mol^{-1}), whereas the formation of propanal at 110 °C is estimated to be thermodynamically favourable ('ΔG' = –8.1 kcal.mol^{-1}).

Table AV.2. Literature data for selected molecules and selected thermodynamic data derived from them.

	1-butene	H_2O	1-butanol		Δ
H° (kcal.mol^{-1})	–4.97	–68.27	–78.17		–4.93
S° (J.K^{-1}.mol^{-1})	+224.0 (l)	+69.95 (l)	+225.8 (l)		
$S°_{25\ °C}$ (kcal.mol^{-1})	+16.2	+5.0	+16.1		–5.1
$S°_{110\ °C}$ (kcal.mol^{-1})					
'ΔG' (kcal.mol^{-1})[a]					+0.17
	propene	**CO**	**H_2**	**propanal**	**Δ**
H° (kcal.mol^{-1})	+12.5	–26.40	0.00	–44.3	–30.4
S° (J.K^{-1}.mol^{-1})	+219.30 (g)	+197.66 (g)	+130.68 (g)	+304.5 (g)	
$S°_{25\ °C}$ (kcal.mol^{-1})					
$S°_{110\ °C}$ (kcal.mol^{-1})	+20.1	+18.1	+12.0	+27.9	–22.3
'ΔG' (kcal.mol^{-1})[a]					–8.1

[a] computed using Equation 1.

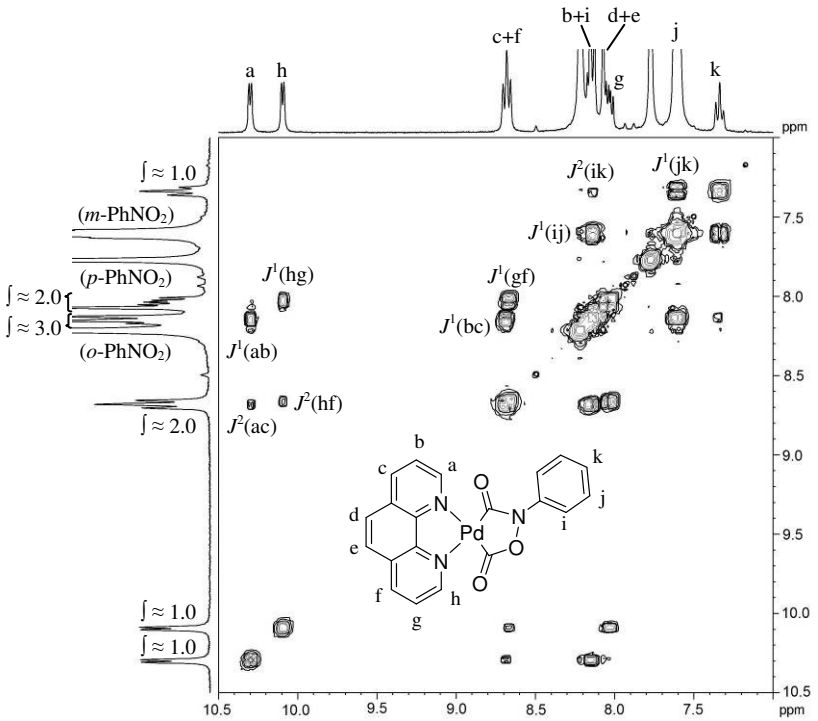

Figure AV.3. ^{1}H–^{1}H–COSY–NMR spectrum and assignments of 'phen–palladacycle' (see inset figure) recorded at 300 MHz in deuterated nitrobenzene.

References

[1] A. S. o Santi, B. Milani, G. Mestroni, E. Zangrando, L. Randaccio, *J. Organomet. Chem.* **1997**, *546*, 89.

[2] P. Leconte, F. Metz, A. Mortreux, J. A. Osborn, F. Paul, F. Petit, A. Pillot, *J. Chem. Soc.-Chem. Commun.* **1990**, 1616.

[3] W. J. Moore, *Physical Chemistry*, 5 ed., Longman, London, **1963**.

Appendix VI

Supporting Information of Chapter 7

-Weight, ^{1}H-NMR, GLC-MS, and HPLC-UV/MS analysis of reaction mixtures-

AVI.1. Weight, ^{1}H-NMR and GLC-MS analysis of a reaction mixture.

An overview of the results obtained from a weight, ^{1}H-NMR, and GLC-MS analysis obtained from the five fractions obtained by column separation of a reation mixture is shown in Table AVI.1. Compounds that have to be present (phen, *p*-cresyl phenyl carbamate (CPCam), *p*-cresol and azoxybenzene) were clearly found back in the various fractions by their characteristic ^{1}H-NMR spectrum and m/z ratios. However, none of the fractions appeared to consist of a single, pure compound (^{1}H-NMR); in all fractions unidentified aryl-containing products were present (also in the GLC-MS analysis).

Table AVI.1. Overview of ^{1}H-NMR, GLC-MS and weight analysis of separate fractions obtained by chromatographic workup of the reaction mixture employing $[Pd(phen)_2](OTs)_2$ as catalyst precursor.[a]

Fraction (R_f)[b]	GC-MS (m/z)	^{1}H-NMR	Weight of fraction (g)	
			Identified	Unidentified
1 **(1.0)**	180 phen 154, 212 (n.i.)	77% phen 23% (n.i.)	0.06	0.06
2 **(0.3)**	119 PhNCO 108 *p*-cresol 108, 253 (n.i.)	36% CPCam 64% *p*-cresol 0.7% (n.i.)	0.01	0.01
3 **(0.2)**	119 PhNCO 108 *p*-cresol 198 Azoxy 154,108, 212 (n.i.)	22% CPCam 75% *p*-cresol 1% Azoxy 2% (n.i.)	3.35	0.11
4 **(0.1)**	108, 154 n.i.	n.i., several Ph-rings	0.78	0.01
5 **(0.0)**	198 n.i.	n.i., two Ph-rings	0.83	0.19
Total:			5.03	0.38

[a] n.i. = 'not identified'. [b] The retention factor (R_f) is the ratio of the distance travelled by the compound divided by the distance travelled by the solvent, and was determined with TLC

The amounts of known, and the amount of unidentified products was estimated from the total weight of the fraction and the intensity of aromatic ^{1}H-NMR resonances relative to the total amount of observed aromatic resonances. The combined estimated mass of the unidentified compounds was 0.38 g (see Table AVI.1). Moreover, the silica column used for the purification was darkly colored after the separation and of the 5.95 g concentrated reaction mixture (before column), only (5.03+0.38=) 5.41 g was recovered. This means that (5.95–5.41=) 0.54 g of reaction mixture has retained on the column, which might well comprise either very polar molecules or oligomers/polymers. When combining this amount of 0.54 g with the 0.38 g 'unknowns', and assuming a molar weight comparable to that of *p*-cresol (because of the phenyl rings that were visible on the NMR spectra and *p*-cresol being the suspected H-source), the amount of aryl rings can be estimated; thus, $(0.38+0.54)/108\times10^3 \approx 8.5$ mmol of unidentified compounds is present, presumably originating from *p*-cresol.

AVI.2. HPLC-UV(and MS) analysis of reaction mixture

Shown in Figure AVI.1 are the HPLC-UV chromatograms (200 nm, see experimental of Chapter 6 for details) of a mixture of pure reference compounds (a, top) and the reaction mixture (b, bottom). The Figure also shows the most prominent molecular weights that were measured for a given peak.

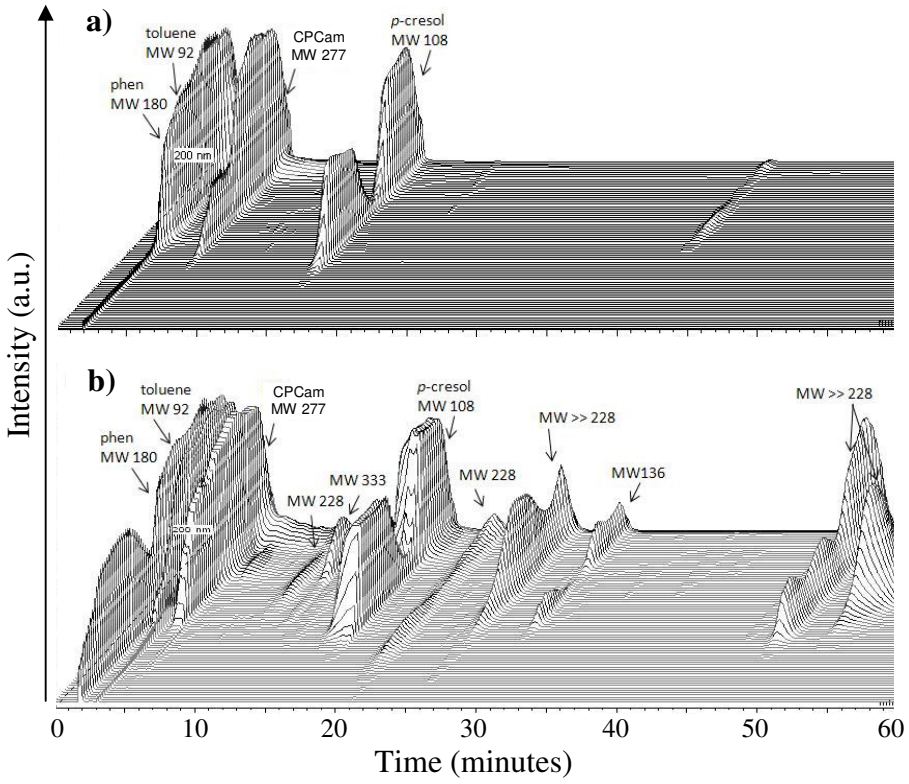

Figure AVI.1. HPLC-UV chromatograms of: a) a mixture of phen, CPCam, and *p*-cresol in toluene (reference compounds) and b) a reaction sample.

The reference compounds used are toluene (solvent), *p*-cresyl phenylcarbamate (CPCam, reaction product), *p*-cresol (reactant), and 1,10-phenanthroline (phen, ligand). Azoxybenzene was not considered, as this product was not detected with GLC-FID analysis of this particular reaction mixture. Likewise, DPU was not considered, as this product is insoluble in toluene. Phen has the same retention time as toluene, and is thus obscured by the abundance of this solvent. CPCam and *p*-cresol are clearly separated with retention times (t_R) of about 5 and 15 minutes respectively. The small impurity around t_R = 40 minutes may originate from any of the reference compounds, but is considered too small to be important.

In the HPLC-UV chromatogram of the reaction mixture shown in Figure AVI.1b, the reference compounds are clearly identified at t_R = 2 (toluene/phen), 5 (CPCam), and 15 (*p*-cresol) minutes. Additionally, there are multiple peaks which cannot be identified as reference compounds. As can be anticipated, neither the mass of azoxybenzene (198) nor that of DPU (212) is observed. Instead, the prominent peaks at t_R = 1.5, 10, 20, 25, 30, 48, and 50 minutes, all consist of some other

compound(s) with a molecular weight higher than that of a single *p*-cresol molecule. In fact, mass spectrometry analysis indicates that those products could indeed be dehydrogenation or oxidation products of *p*-cresol.

Notably, for the compounds with a very high retention time (t_R = 48 and 50 minutes), higher mass fragments were detected, together with a mass of 228 m/z, which is also present in many other peaks (e.g. t_R = 20 and 25 minutes). It is thus likely that some oligomeric compound with a mass of 228 g/mol forms the basis for further polymerization reactions, although at this point it is unclear what exactly this compound could be.

Samenvatting

Algemene introductie; alternatieve routes naar TDI and MDI (H 1)

Het eerste hoofdstuk bevat een samenvatting van de conventionele en bekende alternatieve strategieën om aromatische isocyanaten, zoals tolueendiisocyanaat (TDI) en methyleendifenylisocyanaat (MDI), op een grote schaal te synthetiseren. In de momenteel toegepaste productie van TDI en MDI wordt fosgeen gebruikt als carbonyleringsreagens voor aromatische amines. Fosgeen is echter niet alleen extreem toxisch, maar gebruik ervan resulteert ook in stoichiometrische hoeveelheden van het corrosieve zoutzuur; dit zuur kan de reactor aantasten en leiden tot gechloreerde bijproducten die moeilijk van het gewenste product zijn te scheiden. Ondanks deze nadelen wordt de 'fosgeen-route' vandaag de dag nog op de megaton-schaal toegepast, omdat het nog steeds de meest (kosten-)effectieve methode is. Over de jaren heen zijn verschillende alternatieven voor dit proces voorgesteld en de meest veelbelovende optie is gebruik te maken van CO als reductie- en carbonyleringsreagens in de door overgangsmetalen gekatalyseerde reductieve carbonylering van nitroaromatische verbindingen. In de gerapporteerde studies over dit onderwerp wordt nitrobenzeen ($PhNO_2$) meestal gebruikt als modelsubstraat. Het toepassen van palladium als overgangsmetaal heeft geleid tot de meest effectieve katalytische systemen. De katalytische carbonylering van nitrobenzeen wordt over het algemeen gedaan in methanol als het oplosmiddel met gebruikmaking van homogene palladiumcomplexen met bidentate N- of P-donor liganden. In een methanolische omgeving is methylfenylcarbamaat (MPC) het product (in plaats van fenylisocyanaat). Dit kan –in principe– worden gepyroliseerd tot fenylisocyanaat, terwijl methanol wordt teruggewonnen. Gebruikmaking van het N-donor ligand 1,10-fenanthroline (fen) in combinatie met een zuur als co-katalysator resulteerde in relatief actieve en selectieve katalytische systemen. Ten gevolge van deze eerste bevindingen heeft de academische gemeenschap zich voornamelijk toegelegd op het bestuderen van dit $Pd/fen/CH_3OH/H^+$ en aanverwante katalytische systemen, met als resultaat dat '*turnover numbers*' (mol/mol) tot wel ~10^5 zijn gerapporteerd. Deze studies ten spijt, is er nog steeds geen algemeen geaccepteerd mechanistisch beeld naar voren gekomen voor deze reactie. Er zijn over de jaren heen veel voorstellen gedaan

waarin palladacyclische verbindingen meestal een sleutelrol spelen, maar het gebrek aan empirische data om deze voorstellen te ondersteunen heeft hun acceptatie tot op heden in de weg gestaan. Eén van de belangrijkste paradigma's binnen het vakgebied van de homogene katalyse is echter, dat voor het ontwikkelen van commercieel toepasbare katalysatoren voor een bepaalde reactie een gedegen begrip van het onderliggende moleculaire mechanisme van essentieel belang is.

Een hoofddoel van de studie in deze dissertatie is dan ook om een mechanistisch begrip te ontwikkelen van de palladium-gekatalyseerde reductieve carbonylering van nitrobenzeen in methanol. Voor deze studies werden bidentate fosfaanliganden gekozen om palladium te ondersteunen; het Pd/difosfaan/CH_3OH systeem is niet alleen uitermate zelden bestudeerd, het is ook bekend dat difosfaanliganden betere liganden zijn voor palladium dan N-donorliganden, zoals fenantroline, in het bijzonder als het om laag-valent Pd of Pd^0 gaat. Daarenboven kunnen de sterische en elektronische eigenschappen van fosfaanliganden veel gemakkelijker worden aangepast dan die van aromatische N-donorliganden. De verwachting is dat de moleculaire relatie tussen de stereo-elektronische eigenschappen van de katalytische complexen en hun katalytische prestaties zal leiden tot een beter begrip van het onderliggende moleculaire mechanisme; een begrip dat essentieel is voor de verdere ontwikkeling van actieve en selectieve katalysatoren voor een duurzame, fosgeenvrije synthese van aromatische isocyanaten.

De vorming en structuur van katalysator-precursorcomplexen (H 2)

Veel van de katalytische reacties die in deze dissertatie zijn gerapporteerd, zijn uitgevoerd met katalysator-precursorcomplexen van het type [Pd(ligand)$(anion)_2$], waarin het ligand een bidentaat diarylfosfaan is. Dergelijke katalysatorprecursors worden over het algemeen *in situ* bereid, voordat het katalytische experiment wordt gestart. Voor een correcte interpretatie van de gegevens die uit dergelijke katalytische experimenten voortvloeien, is het echter van cruciaal belang om te weten of het verwachte complex ook daadwerkelijk is gevormd. Daarnaast is intieme (gedetailleerde) structurele kennis vereist om de prestaties van een bepaalde katalysator te relateren aan zijn structuur.

In het tweede hoofdstuk wordt hiertoe de syntheseroute naar [Pd(ligand)(anion)$_2$] en [Pd(ligand)$_2$](anion)$_2$ complexen beschreven; achttien verschillende liganden zijn gebruikt in combinatie met sterk coördinerende (acetaat, OAc^-) of zwak coördinerende (tosylaat, OTs^-) anionen. Van enkele representatieve complexen is de structuur in de vaste fase bepaald met behulp van röntgendiffractie-kristallografie. Het werd aangetoond dat de complexen hun vaste-fase-structuur volledig behouden als ze in oplossing zijn en dat de axiale posities van palladium sterisch worden afgeschermd als het ligand in het complex is gefunctionaliseerd met ortho-methoxy-substituenten.

De vorming van complexen van het type [Pd(ligand)(anion)$_2$] is gedetailleerd bestudeerd met behulp van ^{1}H- en ^{31}P-NMR-spectroscopie. Afhankelijk van de structuur van het ligand, vormt het [Pd(ligand)(anion)$_2$] complex zich instantaan, *via* een polynucleair complex, of wordt het in zijn geheel niet gevormd. Er is ook aangetoond dat het kinetische en/of het thermodynamische product kan worden veranderd, wanneer anionen worden gebruikt met verschillende coördinatiesterkte.

Welk type complex daadwerkelijk in oplossing wordt gevormd, is afhankelijk van de lengte en de rigiditeit van de brug die de twee donoratomen in het ligand met elkaar verbindt (de 'backbone') en afhankelijk van de sterische bulk in de *ortho*-positie van de fenylringen aan fosfor. De vorming van het gewenste complex is trager naarmate de sterische bulk in de *orhto*-positie van de fenylringen aan fosfor wordt vergroot en in sommige gevallen wordt het gewenste complex helemaal niet gevormd. Deze vertragende werking kan in zijn geheel teniet gedaan worden door de 'backbone' van het ligand meer rigide te maken, hetgeen altijd tot resultaat heeft dat het gewenste [Pd(ligand)(anion)$_2$] complex zich instantaan vormt in methanol.

Een onverwacht complex netwerk van katalytische reacties, gecentreerd rondom een Pd-imido-intermediair (H 3)

In het derde hoofdstuk wordt de katalytische activiteit beschreven van palladiumverbindingen van bidentaat diarylfosfaanliganden in de reactie van nitrobenzeen met CO in methanol. De vier liganden die werden gebruikt zijn voor

een deel geselecteerd op basis van hun rigide 'backbone', waardoor een instantane vorming van het gewenste complex is gegarandeerd (Hoofdstuk 2).

Een zorgvuldige analyse van de reactiemengsels laat zien dat naast de normaliter gerapporteerde nitrobenzeen reductieproducten (MPC, *N,N*'-difenylureum (DPU), aniline ($PhNH_2$), azobenzeen (Azo) en azoxybenzeen (Azoxy)), er ook grote hoeveelheden methanol-oxidatieproducten zijn geproduceerd (dimethylcarbonaat (DMC), dimethyloxalaat (DMO), methylformiaat (MF), H_2O, en CO). Door middel van een gedetailleerde *kwantitatieve analyse* van de verscheidene waargenomen reactieproducten, kan worden geconcludeerd dat er verschillende katalytische processen tegelijkertijd operationeel moeten zijn, welke gekoppeld zijn *via* gemeenschappelijke katalytische intermediairen. Door de waargenomen productdistributies te simuleren met theoretisch afgeleide reactiestoichiometriën, bleek het mogelijk om het relatieve belang en de samenhang van de verschillende katalytische processen te bepalen. Er is voorgesteld dat de katalytische cycli een complex reactienetwerk vormen, dat is gecentreerd rondom een palladium-imido-intermediair ('P_2Pd^{II}=NPh'), zoals schematisch is weergegeven in Schema S.1.

Beginnend met een *in situ* gevormde P_2Pd^0-verbinding, kan de oxidatie tot een palladium-imido-verbinding 'P_2Pd^{II}=NPh' geschieden middels de *deoxygenering* van nitrobenzeen *via* drie verschillende reactiepaden (Schema S.1, links): (a) met twee moleculen CO; (b) met twee moleculen CO en de zure protonen van twee methanolmoleculen; (c) met alle vier de waterstofatomen van één enkel methanolmolecuul.

Na de vorming van het imido intermediair kan deze worden geprotoneerd tot $P_2Pd^{II}(OCH_3)NHPh$ (Schema S.1, rechts boven), of met nitrobenzeen reageren *via* een 'disproportioneringsreactie' tot Azoxy en 'P_2Pd=O' (Schema S.1, rechts onder). Beide intermediairen kunnen worden gecarbonyleerd tot respectievelijk MPC (rechts boven in Schema S.1) of CO_2 (rechts onder in Schema S.1) en daarmee het P_2Pd^0-deeltje vormen, waardoor deze reacties katalytisch kunnen verlopen. Beide intermediairen kunnen echter ook worden geprotoneerd tot een $P_2Pd^{II}(OCH_3)_2$-intermediair en aniline (rechts boven in Schema S.1) of water (rechts onder in Schema S.1). De carconylering van dit $P_2Pd^{II}(OCH_3)_2$-complex zal dan DMC/DMO produceren (rechts in het midden in Schema S.1) en wederom het P_2Pd^0-deeltje vormen, zodat ook deze reacties katalytisch kunnen verlopen.

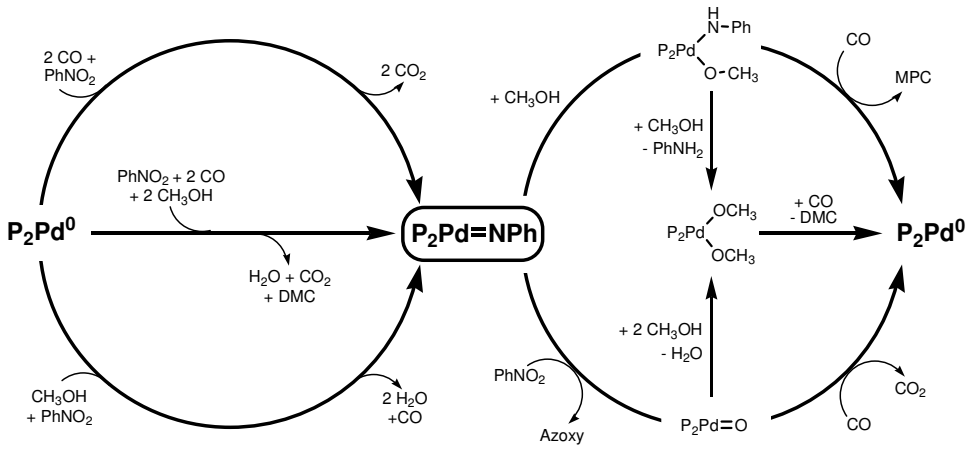

Schema S.1. Algemeen mechanistisch voorstel gecentreerd rondom een palladium-imido-intermediair, voor de katalytische koppeling tussen nitrobenzeenreductie- and methanoloxidatiechemie gekatalyseerd door het Pd/difosfaan/CH_3OH-systeem.

Het wordt daarom voorgesteld dat het Pd-imido-deeltje een centraal sleutelintermediair is, dat alle reductieproducten van nitrobenzeen en alle oxidatieproducten van methanol aan elkaar kan koppelen door middel van één verenigd en relatief eenvoudig mechanistisch schema. Het wordt daarnaast aangetoond dat het relatieve belang van de verschillende katalytische processen afhankelijk is van de stereo-elektronische eigenschappen van de katalysator, zoals deze zijn gepredestineerd door de stereo-elektronische eigenschappen van het ligand.

Een palladium-imido-complex als het centrale productvormende deeltje (H 4)

In de mechanistische studie zoals beschreven in het vierde hoofdstuk werd een variëteit aan *in situ* gevormde palladiumcomplexen met bidentaat diarylfosfaanliganden toegepast als katalysator-precursor in de carbonylering van nitrobenzeen. Variatie in de lengte en de rigiditeit van de brug die de twee donoratomen in het ligand met elkaar verbindt (de 'backbone'), en door de arylringen van sommigen van deze liganden uit te rusten met methoxy-substituenten, kon onderscheid worden gemaakt tussen de elektronische en sterische effecten die het ligand in de katalysator heeft op de kwantitatieve productsamenstelling. Additionele mechanistische informatie werd vergaard door

de effecten te bestuderen van verschillende reactiecondities op de productsamenstelling.

Er is vastgesteld dat meer carbonyleringsproducten (MPC en DPU) worden gevormd, relatief ten opzichte van hydrogeneringsproducten ($PhNH_2$ en DPU), wanneer een ligand wordt gebruikt met een kleinere *bite–angle* (C_3–'backbone'), of wanneer het ligand is uitgerust met *ortho*–methoxygroepen. Er wordt tot wel 73% van de koppelingsproducten (Azo(xy)) gevormd wanneer een ligand wordt gebruikt met een grotere *bite–angle* (C_4–'backbone'). Gebaseerd op deze observaties, en op de waargenomen afhankelijkheid van de productdistributie van de concentraties van de reactanten ($PhNO_2$, CO), is voorgesteld dat – in lijn met het mechanistische voorstel geïntroduceerd in Hoofdstuk 3 – de vorming van de arylbevattende producten een competitie behelst voor hetzelfde palladium-imido-complex (P_2Pd^{II}=NPh).

Een palladacyclische verbinding die vaak wordt voorgesteld als het productvormende intermediair in het Pd/fen/CH_3OH katalytische systeem (**I** in Schema S.2) werd ook onder de loep genomen als een mogelijk intermediair in het Pd/difosfaan/CH_3OH systeem (**II** in Schema S.2). Echter, zoals is samengevat in Schema S.2, een liganduitwisselingsreactie van de stabiele fen-palladacyclus **I** met difosfaanliganden (bestudeerd met $^{31}P\{^1H\}$–NMR en ESI-MS) laat zien dat de gevormde difosfaan-palladacyclus **II** snel uit elkaar valt onder milde condities, middels uitdrijving van een CO in plaats van een molecuul CO_2. Dit proces leidt uiteindelijk (waarschijnlijk) tot het P_2Pd^{II}=NPh-intermediair (**V**), in plaats van tot de verwachte carbonyleringsproducten (isocyanaat of MPC) na decarboxylering van palladacyclus **II**; dit tweede proces heeft dus blijkbaar een hogere activeringsbarrière.

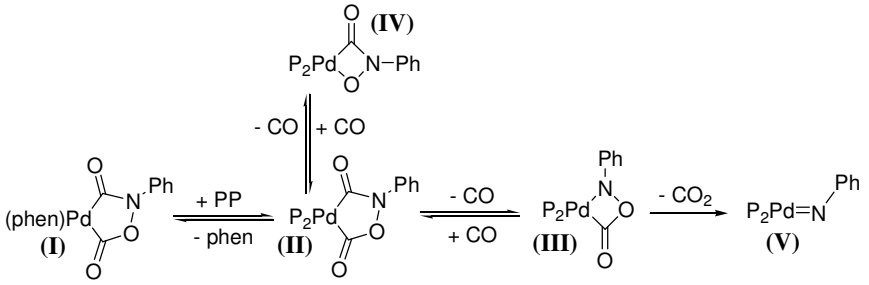

Schema S.2. Voorgestelde reactie van liganduitwisseling tussen palladacyclus **I** en een fosfaanligand, gevolgd door de ontleding van **II** naar het imidocomplex **V** middels initiële uitdrijving van CO.

DFT-berekeningen suggereren dat verbinding **II** minder stabiel is dan **I**, en klaarblijkelijk als een gevolg daarvan snel uit elkaar valt (middels decarbonylering). De waargenome afname in ontledingssnelheid van palladacyclus **II** in een atmosfeer van CO, suggereert dat de decarbonylering van deze verbinding middels een *reversibele* carbonylering/decarbonyleringsreactie verloopt, welke een lage reactiebarrière heeft. Onder sommige liganduitwisselingscondities werden meerdere $^{31}P\{^{1}H\}$–NMR-resonanties waargenomen, welke het meest waarschijnlijk zijn toe te schrijven aan palladacyclus **III**, welke waarschijnlijk wordt gevormd middels een decarbonylering van palladacyclus **II**.

Een logische gevolgtrekking van deze waarnemingen is dat de palladacycli **II**, **III** en **IV**, weergegeven in Schema S.2, alle onderling verbonden zijn door reversibele carbonylering/ decarbonyleringsreacties. De *irreversibele ontsnapping* uit deze onderling geëquilibreerde palladacycli kan slechts geschieden door middel van de decarboxylering (–CO_2) van intermediair **III** tot het imido-complex **V**. Tot nu toe kon **V** echter niet spectroscopisch worden gekarakteriseerd en dit deeltje blijft dus ongrijpbaar. Dit komt waarschijnlijk doordat de verdere ontleding snel verloopt onder de a-protische, drukloze reactiecondities van de liganduitwisseling-sexperimenten, resulterende in het waargenomen Pd^{0}(difosfaan)$_2$-complex en voornamelijk ongeïdentificeerde organische producten die het ‘NPh’-fragment moeten bevatten.

Bewijs van het mogelijke *bestaan en de reactiviteit* van een P_2Pd^{II}=NPh–type complex komt van een gecombineerde $^{31}P\{^{1}H\}$NMR- en ESI–MS-analyse van de reactie tussen een P_2Pd^{0}-verbinding bestaande uit een sterisch heel erg omvangrijk difosfaan (1,3-bis(1,3,5,7-tetramethyl-4,6,8-trisoxa-2-fosfaadamantyl)propaan), en mesityl-azide, tot wat zeer waarschijnlijk een P_2Pd-imido complex is (sterisch beschermd tegen een te snelle thermische ontleding). Dit complex reageert inderdaad met CO en methanol tot methylmesitylcarbamaat, zelfs onder zeer milde condities.

Er is voorgesteld dat onder de daadwerkelijke hoge druk CO katalytische nitrobenzeen-carbonyleringscondities in methanol als oplosmiddel, reactie van het palladium-imido-complex **V** kan leiden tot respectievelijk: i) MPC en DPU (door een methoxy- of amino-carbonylering); ii) Azoxy en Azo (door een

'disproportionering' met nitrobenzeen of nitrosobenzeen); iii) $PhNH_2$ (door protonering met methanol) en gekoppelde DMC/DMO-vorming door carbonylering van methanol.

De gecombineerde katalytische en organometaal-experimentele data wijzen dus gezamenlijk zeer sterk naar een P_2Pd^{II}=NPh-complex als het *meest waarschijnlijke, productvormende* intermediaire deeltje onder nitrobenzeen carbonyleringscondities.

Oxidatieve carbonylering van methanol (H 5)

Zoals uiteengezet in Hoofdstuk 3 is nitrobenzeen reductiechemie katalytisch gekoppeld aan methanol-oxidatiechemie, wanneer wordt gewerkt met het Pd/difosfaan/CH_3OH-systeem. De moleculaire details van deze gekoppelde reacties zijn gedetailleerd beschreven in Hoofdstuk 4, gezien vanuit het perspectief van nitrobenzeen reductiechemie. In het vijfde hoofdstuk is een soortgelijke studie beschreven, maar nu vanuit het perspectief van methanol oxidatiechemie. Het systeem is beschouwd vanuit het perspectief om de industriëel belangrijke methanol carbonyleringsproducten DMC en DMO te maken, waarin nitrobenzeen dan als uiteindelijk oxidant fungeert. Het algemene mechanistische inzicht, verkregen bij de bestudering van de carbonyleringschemie van nitrobenzeen (Hoofdstuk 3 en 4), blijkt direct toepasbaar op het algemene mechanisme voor de vorming van oxidatieve carbonyleringsproducten van methanol. In feite is het algemeen mechanistische schema, zoals dat in Schema S.1 is weergegeven, direct toe te passen; dit schema laat namelijk direct zien op welke manier methanol-oxidatiechemie is gekoppeld met nitrobenzeen-reductiechemie. Er bestaan twee beslissende intermediaire stadia in deze katalytische cyclus; in elk van deze stadia kan één equivalent DMC/O worden geproduceerd per gereduceerde $PhNO_2$.

In het 'eerste' stadium, beginnend bij P_2Pd^0, is de oxidatieve carbonylering van CH_3OH gekoppeld aan de reductie van $PhNO_2$ om het eerste equivalent DMC/DMO samen met een 'P_2Pd=NPh'-complex te produceren (links in het midden in Schema S.1). De vorming van DMC/O in dit stadium kan worden voorkomen wanneer alleen CO als reductant fungeert (links boven in Schema

S.1), of wanneer $PhNO_2$-reductie is gekoppeld met oxidatieve dehydrogenering van CH_3OH tot CO (of MF; links onder in Schema S.1).

In het 'tweede' stadium (rechts in Schema S.1) kan het P_2Pd^{II}=NPh-complex op twee soortgelijke manieren reageren om uiteindelijk respectivelijk aniline (rechts boven in Schema S.1) dan wel azoxy (rechts onder in Schema S.1) te produceren, samen met de tweede equivalent DMC/DMO. Beide routes verlopen *via* hetzelfde $P_2Pd^{II}(OCH_3)_2$-complex (richts in het midden in Schema S.1). De $PhNH_2$/DMC/O-route (rechts boven in Schema S.1) verloopt eerst *via* een $P_2Pd^{II}(OCH_3)$NHPh-complex; hier kan de productie van DMC/O worden voorkomen door $P_2Pd^{II}(OCH_3)$NHPh te carbonyleren tot MPC. De Azoxy/H2O/DMC/O-route (rechts onder in Schema S.1) verloopt eerst *via* een P_2Pd^{II}=O complex; hier kan de productie van DMC/O worden voorkomen door P_2Pd^{II}=O te carbonyleren tot CO_2. Al deze processen zijn katalytisch omdat het P_2Pd^0-complex waarmee het eerste stadium begon wordt teruggevormd als 'PhN'-houdende producten worden gemaakt.

Er is voorgesteld dat de selectiviteit voor DMC ten opzichte van DMO wordt bepaald in een complex van het type $[P_2PdC(O)OCH_3(R)]$; de DMC/DMO-ratio kan worden verhoogd door een hogere CO druk toe te passen, zuur toe te voegen, of door een ligand te gebruiken met een relatief grote '*bite-angle*'.

Gebaseerd op de bovenstaande resultaten werd geconcludeerd dat een ideale katalysator voor de oxidatieve carbonylering een relatief zuur palladiumcentrum moet hebben, maar ook sterisch ongehinderd in de axiale posities en sterisch gehinderd in de equatoriale posities can palladium.

Het palladiumcomplex bis(difenylfospfanyl)-ferroceen voldoet aan deze criteria en gebruikt nitrobenzeen het meest efficient van alle geteste katalysatorprecursor-complexen als oxidant voor de oxidatieve carbonylering van methanol . Dat wil zeggen, met ongeveer 50% efficiëntie ten onzichte van het theoretische maximum van een 2:1 ratio tussen DMC/O en gereduceerde nitrobenzeen.

Vergelijkende studie van difosfaan- en fen-gestabiliseerde palladium complexen (H 6)

Tijdens de studies beschreven in Hoofdstuk 3 en 4, werd ontdekt dat de reactiviteit van katalytische palladiumsystemen ondersteund door fen of het bidentaat fosfaanligand 'L4X' opmerkelijk gelijk is. Beide zijn ongeveer 70% selectief voor de 'PhN-bevattende' koppelingsproducten Azo(xy), maar produceren ook carbonyleringsproducten (MPC en DPU) en hydrogeneringsproducten ($PhNH_2$ en DPU). Contrasterend met deze overeenstemming voor nitrobenzeen-reductieproducten is de vinding dat alleen het Pd/L4X-systeem de oxidatie van methanol katalyseert (vorming van DMC, DMO, MF, CO en H_2O).

Voor beide systemen werd gevonden dat Azoxy niet kan worden gevormd door een condensatiereactie van aniline met nitrobenzeen; ook is geen Azoxy gevormd uit 'vrij' aanwezig nitrosobenzeen. In plaats daarvan is het waarschijnlijker dat azoxy ontstaat door de disproportionering van nitrobenzeen met een $L_2Pd{=}NPh$ intermediair, omdat de hoeveelheid gevormd azoxy afhankelijk is van de concentratie van nitrobenzeen. De mogelijke aanwezigheid van een dergelijk imido-intermediair tijdens de daarwerkelijke carbonyleringsreactie wordt bevestigd door het "vangen" van het 'PhN'-fragment in deze verbinding met cyclohexeen, hetgeen resulteert in de, met GLC-MS waargenomen, corresponderende azaridine.

Het palladium-imido-complex $L_2Pd{=}NPh$ en de palladacyclus **I/II** (zie Schema S.2) werden nader overwogen als mogelijke *carbonylerings*productvormende complexen, wanneer gebruik wordt gemaakt van fen of L4X als het ondersteunende ligand.

Uit het ESI-MS-spectrum van 'fen–palladacyclus', een liganduitwisselingsreactie van 'fen–palladacyclus' met L4X, en een theoretische (DFT) studie van nitrobenzeen de-oxygenering tot $L_2Pd{=}NPh$, blijkt echter dat deze palladacyclus *niet* het belangrijkste carbonyleringsproduct-vormende intermediair is; de barrière voor decarbonylering (–CO) is lager dan decarboxylering ($–CO_2$). Als gevolg daarvan is de palladacyclus slechts onderdeel van meerdere CO-geëquilibreerde palladacycli, die samen fungeren als tijdelijk 'NPh-reservoir', net zoals eerder was gevonden voor de difosfaan-systemen in Hoofdstuk 4. Echter, onder zure

omstandigheden wordt de decarboxyleringsbarrière ($-CO_2$) verlaagd; voor de 'fen-palladacyclus' tot het punt waar CO_2-extrusie het wint van CO-uitdrijving (zoals eerder gerapporteerd door Osborn).[1] Voor 'L4X-palladacyclus' is de barrière voor CO extrusie echter nog steeds lager dan die voor CO_2 extrusie, waarschijnlijk doordat dit grotere ligand een destabiliserende werking heeft op dergelijke palladacycli.

Zoals ook is geïllustreerd in Schema S.3, werd geconcludeerd dat: i) met katalysatoren die worden ondersteund door een fen-ligand de de-oxygenering van nitrobenzeen, in tegenstelling tot katalysatoren ondersteund door L4X, vrijwel uitsluitend door CO geschiedt; ii) in afwezigheid van zuur is het $L_2Pd{=}NPh$ complex het dominante 'PhN'-product-vormende intermediair, zowel voor op fen- als voor op difosfaan gebaseerde katalysatoren; iii) *alleen* onder zure condities kan de palladacyclus I – afhankelijk van het ligand – een carbonylerings-productvormend intermediair worden. Door toevoeging van slechts substoichiometrische hoeveelheden zuur (ten opzichte van Pd) als co-katalysator, kan de decarboxyleringsbarrière worden verlaagd, waarschijnlijk aanvankelijk door een protonering van het N-atoom van de palladacyclus.

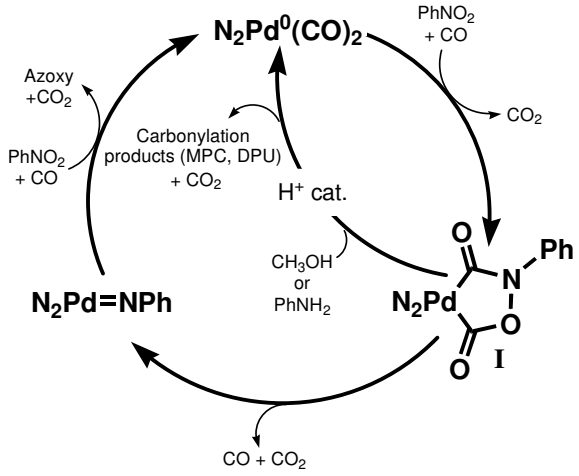

Schema S.3. Voorgesteld mechanisme voor de nitrobenzeen-reductieve carbonyleringschemie in het Pd/fen/CH_3OH(/H^+)-systeem. N_2 = fen.

Het is opmerkelijk te noemen, dat het mechanistische voorstel zoals weergegeven in Schema S.3 zeer sterk overeenkomt met – maar ook cruciaal verschilt van –

een recent voorstel van Ragaini en zijn medewerkers voor het Pd/fen/CH_3OH/H^+-systeem.[2, 3] Volgens dit voorstel wordt nitrobenzeen eerst volledig gereduceerd tot aniline en een (fen)Pd$(C(O)OCH_3)_2$-complex (*via* een onbekende en niet-becommentarieerde route), welke vervolgens zou reageren met aniline tot MPC. Het mechanistische voorstel ontwikkeld in dit hoofdstuk is fundamenteel anders, in die zin, dat een voorloper van aniline (namelijk het imido-complex of de palladacyclus), de directe antecedent is van MPC; onder zuurvrije condities wordt het Pd-imido-complex direct gemethoxycarbonyleerd tot MPC, terwijl onder licht-zure omstandigheden de palladaclyclus reageert tot MPC.

Het (fen)Pd$(C(O)OCH_3)_2$-complex kan daarom beter worden gezien als DMC/DMO-precursor-complex *via* de (anilinevormende) dubbele protonering van het imido-intermediair. DMC en DMO werden inderdaad waargenomen, zij het in kleine hoeveelheden, wanneer onder zuurvrije omstandigheden werd gewerkt. DMC en DMO bleken echter (in lijn met de data gerapporteerd door Ragaini) geheel afwezig, wanneer onder zure omstandigheden wordt gewerkt; dit suggereert sterk dat een dergelijk complex niet eens gevormd wordt onder die omstandigheden.

Gebruikmaking van andere nucleofielen dan methanol (H 7)

Zoals uiteengezet in Hoofdstuk 3–5, heeft de katalytische koppeling tussen nitrobenzeen-reductiechemie en methanol-oxidatiechemie in het Pd/difosfaan /CH_3OH-systeem een aantal unieke en duidelijke hints kunnen geven waarmee de moleculaire details van deze reacties – tot op zekere hoogte – konden worden ontrafeld. Vanuit een meer praktisch oogpunt maakt deze koppeling de Pd/difosfaan/CH_3OH-systemen echter onpraktisch ingewikkeld. Voordat het werk beschreven in de eerste hoofdstukken van deze dissertatie kan leiden tot een echte toepassing in de duurzame synthese van aromatische isocyanaten, is het daarom nodig om de carbonyleringsproducten (een carbamaat of ureum) met een veel hogere selectiviteit te produceren.

In het zevende hoofdstuk worden enige voorlopige studies gerapporteerd waarin methanol werd vervangen door respectievelijk *p*-cresol, *i*-propanol, 2,2,2-trifluoroethanol (TFE) en aniline, met als doel het voorkomen van de vorming van oxidatieproducten van het gebruikte nucleofiel. Daarnaast werden deze

nucleofielen geselecteerd op basis van hun grotere omvang (relatief ten opzichte van methanol) in de hoop de vorming van carbonaat en/of oxalaat te blokkeren. *p*-Cresol en TFE werden ook geselecteerd op basis van hun lagere nucleofiliciteit, om zo een carbamaat te verkrijgen dat gemakkelijker pyroliseerbaar is. Aniline werd onder andere gekozen omdat eventueel oxidatieve carbonyleringsreacties van aniline, net als de reductieve carbonylering van nitrobenzene, DPU als nuttig product kan opleveren.
Er is echter ontdekt dat wanneer *p*-cresol werd gebruikt – onder strikt watervrije condities – er wederom significante hoeveelheden van de H-bevattende nitrobenzeen-reductieproducten aniline en DPU werden gevormd, wanneer gebruik werd gemaakt van typische op palladium gebaseerde katalytische precursor-complexen, zoals $(L3)Pd(OAc)_2$ of $[Pd(fen)_2](OTs)_2$. Op basis deze bevinding, samen met een kwantitatieve en kwalitatieve analyse (massaspectrometrie, ^{1}H-NMR en GLC-MS) van een door middel van kolomchromatografie in fracties gescheiden reactiemengsel, en een HPLC-UV/MS-analyse van een reactiemengsel, is geconcludeerd dat *p*-cresol oxidatief wordt gedehydrogeneerd tot voornamelijk ongeïdentificeerde producten (mogelijk oligomere cresyleen oxides).

Gebruikmaking van *i*-propanol als nucleofiel reagens en oplosmiddel in de carbonylering van nitrobenzeen is onderzocht met $(oMeOL3X)Pd(OAc)_2$ en $(L3X)Pd(OAc)_2$ als katalysator-precursorcomplexen. Met $(oMeOL3X)Pd(OAc)_2$ kan *i*-propanol zeer efficiënt worden gebruikt als H-donor *via* de oxidatieve dehydrogenering van *i*-propanol tot aceton, terwijl nitrobenzeen selectief wordt gehydrogeneerd tot aniline. Met $(L3X)Pd(OAc)_2$ fungeert *i*-propanol ook als een goede H-donor, maar nu voornamelijk *via* de oxidatieve carbonylering.

Wanneer TFE als zwak nucleofiel reagens en tevens oplosmiddel werd gebruikt, kon een ongeëvenaarde, selectiviteit van 95% tot de carbamaat worden bereikt bij een 90% nitrobenzeen-conversie met $(L3X)Pd(OAc)_2$ als katalysator-precursorcomplex. Daarenboven, trifluoroethylfenylcarbamaat pyrolyseert gemakkelijk naar fenylisocyanaat bij relatief lage temperaturen van 200-250 °C.

Het gebruik van aniline als nucleofiel en oplosmiddel, in combinatie met diverse Pd-difosfaansystemen resulteerde veelal in volledige conversie met excellente selectiviteit foor DPU. Het is noemenswaardig dat wanneer $(L3X)Pd(OAc)_2$ werd

gebruikt als katalysator-precursorcomplex onder de transamideringstemperatuur van 70-80 °C, 3-methylnitrobenzeen volledig werd geconverteerd tot 3-methylaniline, terwijl ook een stoichiometrische hoeveelheid carbonyleringsproduct werd gevormd (90% DPU, 10% DPO). Op basis hiervan, en de volledige afwezigheid van de niet-symmetrische ureum en *N,N*'-di(3-methylfenyl)ureum, is geconcludeerd dat 3-methylnitrobenzeen omgezet wordt tot 3-methylaniline *via* een liganduitwisseling op de Pd-katalysator. De moleculaire mechanistische details van dit proces, samen met die van de nitroareen-de-oxygenering en de vorming van DPU/DPO, zijn voorgesteld als zijnde analoog aan de nitrobenzeen carbonylerings- en methanol oxidatieprocessen zoals beschreven in Hoofdstuk 3–5 voor de Pd/difosfaan/CH_3OH-systemen.

Gebaseerd op bovenstaande bevindingen, werd geconcludeerd dat *p*-cresol and *i*-propanol geen geschikte vervangers zijn van methanol. Aniline kan een veelbelovend alternatief zijn, maar de moeilijkheid waarmee DPU pyrolyseert (relatief ten opzichte van carbamaten met een goede vertrekkende groep) kan dit alternatief serieus in de weg staan. TFE daarentegen is een zeer veelbelovend (zwak) nucleofiel reagens om door Pd/difosfaan gekatalyseerde nitrobenzeen-carbonylerings-reacties mee uit te voeren; niet alleen kan de carbamaat zeer selectief worden gevormd bij een hoge nitrobenzeen conversie, de carbamaat pyrolyseert ook relatief gemakkelijk.

Referenties

[1] P. Leconte, F. Metz, A. Mortreux, J. A. Osborn, F. Paul, F. Petit, A. Pillot, *J. Chem. Soc.-Chem. Commun.* **1990**, 1616.
[2] F. Ragaini, M. Gasperini, S. Cenini, L. Arnera, A. Caselli, P. Macchi, N. Casati, *Chem. Eur. J.* **2009**, *15*, 8064.
[3] F. Ragaini, *Dalton Trans.* **2009**, 6251.

List of publications

17) **Mechanistic study of the nickel-diphosphane catalyzed hydrogenation and isomerization of 1-octene;** T. J. Mooibroek, E. C. M. Wenker, W. Smit, E. Bouwman, E. Drent, **2011**, in preparation.

16) **Mechanistic study of the palladium-diphosphane catalyzed oxidative carbonylation of methanol, using nitrobenzene as oxidant;** T. J. Mooibroek, E. Bouwman, E. Drent, **2011**, to be submitted.

15) **Mechanistic study of the L_2Pd catalyzed reduction of nitrobenzene with CO in methanol; a comparative study between diphosphane and 1,10-phenanthroline complexes;** T. J. Mooibroek, E. Bouwman, E. Drent, *Organometallics*, **2011**, submitted.

14) **Mechanistic study of the palladium–bidentate diarylphosphane catalysed carbonylation of nitrobenzene in methanol; a palladium-imido complex as the central product-releasing species;** T. J. Mooibroek, W. Smit, E. Bouwman, E. Drent, **2011**, to be submitted.

13) **Carbonylation of nitrobenzene in methanol with palladium bidentate phosphane complexes: an unexpectedly complex network of catalytic reactions, centred around a Pd-imido intermediate;** T. J. Mooibroek, L. Schoon, E. Bouwman, E. Drent, *Chem. Eur. J.*, **2011**, DOI: 10.1002/chem.201100923.

12) **Anion– and lone pair–arene interactions are directional;** T. J. Mooibroek, P. Gamez, *Cryst. Eng. Comm.*, **2011**, DOI: 10.1039/C1CE05946G.

11) **Putting Anion–π Interactions Into Perspective;** A. Frontera, P. Gamez, M. Mascal, T. J. Mooibroek, J. Reedijk, *Angew. Chem.*, **2011**, 50, *41*, 9564.

10) **Structure elucidation of the unprecedented asymmetric bis-chelate complex [Pd(1,3-bis(di(*o*-methoxy-*m*-methylphenyl)phosphino)-propane)$_2$]$^{2+}$ in the solid state and in solution;** T. J. Mooibroek, M. Lutz, A. L. Spek, E. Bouwman, *Dalton Trans.*, **2010**, *45*, 11027.

9) **Efficient, stable, tunable, and easy to synthesize, handle and recycle luminescent materials: $[H_2NMe_2]_3[Ln(III)(2,6\text{-dipicolinolate})_3]$ (Ln = Eu, Tb, or its solid solutions);** T. J. Mooibroek, A. Pevec, M. Kasunič, B. Kozlevčar, W. T. Fu, P. Gamez, Jan Reedijk, *Dalton Trans.*, **2010**, *28*, 6483.

8) **NMR studies of palladium(II) complexes of bidentate diphenylphosphane ligands with acetate and tosylate anions: complex formation and structures;** T. J. Mooibroek, E. Bouwman, M. Lutz, A. L. Spek, E. Drent, , *Eur. J. Inorg. Chem.*, **2009**, *2*, 298.

7) **A Mixed-Valent Pentanuclear $Cu^{II}4Cu^{I}$ Compound Containing a Radical-Anion Ligand;** T. J. Mooibroek, G. Aromi, M. Quesada, O. Roubeau, P. Gamez, S. DeBeer George, J. van Slageren, S. Yasin, E. Ruiz, J. Reedijk, *Inorg. Chem.*, **2009**, *48*, 10643.

6) **Lone pair-π interactions: a new supramolecular bond?;** T. J. Mooibroek, P. Gamez, J. Reedijk, *Cryst. Eng. Comm.*, **2008**, *11*, 1501.

5) **What's new in the realm of anion-π binding interactions? Putting the anion-π interaction in perspective;** T. J. Mooibroek, C. A. Black, P. Gamez, J. Reedijk, *Cryst. Growth Des.,* **2008**, *4*, 1082.

4) **Anion binding involving π-acidic heteroaromatic rings;** P. Gamez, T. J. Mooibroek, S. J. Teat, J. Reedijk, *, Acc. Chem. Res.,* **2007**, *40*, 435.

3) **The s-Triazine ring, a remarkable unit to generate supramolucular interactions;** T. J. Mooibroek, P. Gamez, *Inorg. Chim. Acta.,* **2007**, *360*, 381.

2) **Luminescent lanthanide complexes;** T. J. Mooibroek, P. Gamez, W. T. Fu, J. Reedijk, *U.S. Patent N^o 2008221328),* **2007**.

1) **Crystallographic and Theoretical Evidence of Acetonitrile-pi Interactions with the Electron-Deficient 1,3,5-Triazine Ring;** T. J. Mooibroek, S. J. Teat, C. Massera, P. Gamez, J. Reedijk, *Cryst. Growth Des.,* **2006**, *6*, 1569.

Curriculum Vitae

The author of this thesis was born in Delft, the Netherlands, on the 12th of March 1982 and baptized as Tiddo Jonathan Mooibroek. After obtaining his MAVO diploma from the CSG Aquamarijn in Vlaardingen in 1998, he started an education for chemical technician (MLO) at the 'Mon3aan Onderwijsgroep' in Delft. After receiving his diploma in 2002, he continued his studies at the 'Hogeschool Leiden', where he graduated *cum laude* (2005) for his bachelor degree, following both the organic and analytical chemistry track. His final training period for this education was performed in the group of prof. Jan Reedijk (Leiden University), where he worked with prof. Patrick Gamez on functional materials based on the *s*-triazine building block. He then pursued his MSc at the University of Leiden, also in the group of prof. Jan Reedijk, during which he worked with: dr. Wen-Tian Fu on the development of new luminescent materials; with prof. Patrick Gamez on studying the anion/lone-pair-π interaction; and with prof. Elisabeth Bouwman on studying the palladium-diphosphane complex formation with multinuclear dynamic NMR techniques. In 2007 he obtained his MSc degree in Chemistry, for which he was awarded the '*Oosterhof award*'.

The author then pursued a PhD in industrial homogeneous catalysis under the guidance of prof. Eite Drent and prof. Elisabeth Bouwman, leading to the work described in this thesis. The expertise of safely performing high pressure experiments with carbon monoxide was acquired during a short stay at Shell Global Solutions B.V. (Amsterdam) under the guidance of Lodi Schoon. As part of has PhD training, the author supervised three BSc and three MSc students, was involved in the development of the new practical course that is currently taught to MST freshmen students in Leiden with dr. Frans Hulsbergen, and has been assistant at several such courses over the years.

Parts of this thesis and results of other inquiries have been published in scientific journals (see pages 295-296). As is listed below in descending chronological order, the author also communicated his findings to peers more directly with posters (18) and oral presentations (9) during several international conferences (10) and symposia (7). He also attended four postgraduate courses as part of his PhD training. Notably, the author has received five poster prizes over the year and obtained an MA degree in the philosophy of science from the University of

Leiden, and an MA degree in Christian studies of science and society from the Free University of Amsterdam (both in 2011).

He currently works with prof. Anthony P. Davis (Bristol, U.K.) as a postdoctoral researcher on the synthesis and evaluation of synthetic sugar receptors.

2011: H.E.L. conference on flow and batch processes, Cambridge, UK (invited lecture); Christian Philosophy Conference 2011, Amsterdam, NL (lecture);

2010: 11th Netherlands' Catalysis and Chemistry Conference (NCCC), Noordwijk, NL (lecture, and poster); 17th International Symposium on Homogeneous Catalysis, Poznan, Poland (poster prize);

2009: Holland Research School on Molecular Chemistry (HRSMC) Symposium, NL (poster); 10th NCCC, Noordwijk, NL (two posters); Gratama symposium, Delft, NL (poster); 18th European Conference on Organometallic Chemistry, Gothenburg, Sweden (poster prize);

2008: HRSMC Symposium, Amsterdam, NL (poster prize); 9th NCCC, Noordwijk, NL (poster); 4th European Chemical and Molecular Science Conference, Garmisch-Partenkirchen, Germany (presentation); HRSMC course in molecular modelling, Amsterdam, NL; Lecture at Shell Global solutions B.V., Amsterdam, the Netherlands; Lecture at the University of Budapest, Hungary; Lecture at the University van Vienna, Austria;

2007: HRSMC symposium, Amsterdam, NL (poster prize); 8th NCCC conference, Noordwijk, NL (poster); Conference 'Academic freedom and Religious freedom', Leiden, NL; 6th International School of Organometallic Chemistry, Camerino, Italy (poster);

2006: P.A.C. symposium, Amsterdam, NL (poster prize); 7th NCCC conference, Noordwijk, NL (KNCV grant, poster); Netherlands' Institute for Catalysis Research Course 'Catalysis, an integrated approach', Schiermonnikoog, NL; HRSMC summer school molecular chemistry, Amsterdam, NL; Lecture series 'medical calculus', academic medical centre Leiden, NL; Invited lecture coordination chemistry, Polytechnical school Leiden, NL;

2005: PAC symposium, Amsterdam, NL (poster); 6th NCCC conference, Noordijk, NL (KNCV grant, poster); Invited lecture coordination chemistry, Polytechnical school Leiden, NL.

Nawoord

Aan het eind van een boekje als dit, behoren uiteraard een aantal mensen bedankt te worden. Eigenlijk zou zo'n pagina aan het begin moeten staan, omdat het totstandkomen van dit werkje simpelweg onmogelijk zou zijn geweest zonder jullie.

Om te beginnen wil ik de Bachelor- en Masterstudenten, Bart van Limburg, Elwin Molenbroek, Ruud Kortlever, Erica Wenker, Wietse Smit en Hanneke Muilwijk bedanken: bedankt dat jullie je bijdrage hebben geleverd aan het uitwerken, dan wel het sluiten van onderzoekstakken. Leuk ook dat we nog even collega's konden zijn Erica.

Over collega's gesproken: beter een goede collega dan een verre vriend. Mart**H**a, Jimmy, Joris, and Raja: you ensured that it was always a party to go to the lab, thank you for that. Ik denk ook aan andere collega's en vakgroepgenoten: Saeed, Prassad, Paul, Geoff, Erik, Wen Tian, Gé, Sylvestre, Stefania, Corry, Guillem, Sebastiaan, Katja, Susmit, Sudeshna, Ariadna, Ira, José, Laurent, Nuria, Tiger, Karlijn, Eva, Anna, Elena, Tom, en natuurlijk Yvonne en Ingrid. Frans, Trudie, Arjan en Paul, jullie wil ik bedanken voor de mooie tijd tijdens de praktica.

Veel van de data in dit boekje zijn tot stand gekomen met de onmisbare hulp van Jos, John, Olga, Jopie, Alex, Fons, Kees en Karthick; ik zal jullie hulp missen. Jos, enorme ruiker, zonder jou en Olga waren de injecties in de GLC nooit gelukt. Ik hoop dat je nog lang kan blijven darten John. Fons en Kees, ik heb me altijd welkom gevoeld op julie afdeling en genoten van de tijd dat 'we' al grappend een probleem met één van de NMR apparaten oplosten. Martin Lutz en Anthony Spek wil ik bedanken voor hun hulp met de kristalstrukturen, Andreas Ehlers voor zijn hulp met de DFT berekeningen en René, Stuart, Hades en Keith voor de prettige contacten en goede hulp met de 'polyblock' systemen. Patrick; I have enjoyed our contact over the years, and also our collaborative efforts which will hopefully endure. Lodi, ik heb een leuke en leerzame tijd gehad bij Shell en ik kom snel nog eens een biertje drinken in De Pont.

Als laatste zijn er natuurlijk mijn familie en vrienden; wanneer ik de goede en soms minder goede kanten van het leven niet met met jullie had mogen delen was

het promotietraject voor mij een stuk minder aangenaam geweest; bedankt daarvoor.

Met name wil ik hier Allard en Persijn bedanken voor hun vriendschap over de jaren en natuurlijk ook dat jullie paranimf wilden zijn. Ma, heel erg bedankt voor alles wat je me hebt geleerd en het is erg jammer dat we je moeten missen; je zou trots op me zijn geweest en me een dikke knuffel hebben gegeven. Pa, Tiddo, jij ook bedankt voor alles in de afgelopen jaren en vooral ook je advies om eerst scheikunde en dan wellicht filosofie te studeren; dat was het beste advies dat ik ooit heb gehad. Elly, jij ook bedankt voor je goede zorgen. Harmen en Annemarie, Marten en Nadine, Cesar en Annemarie, we hebben geweldige tijden met elkaar doorgebracht; we moeten snel weer eens een avondje plannen; lijkt Bristol jullie iets?

Tot slot aan Lauranne, mijn verloofde: wat een eer en geluk is het om met jou door het leven te mogen gaan. Bedankt voor je geduld, *merci pour toi patience*.

Tiddo J. Mooibroek